



 **haematologica**

Journal of the Ferrata Storti Foundation

**XVIII Congress of the Italian Society of Experimental Hematology
Firenze, Italy, March 7-9 2024**

ABSTRACT BOOK

ISSN 0390-6078

Volume 109

**MARCH
2024 - S1**

www.haematologica.org

XVIII Congress of the Italian Society of Experimental Hematology

COMITATO SCIENTIFICO

Alessandro Maria Vannucchi, *Presidente*
Maria Paola Martelli, *Vice Presidente*
Maria Teresa Voso, *Past President*
Matteo Della Porta
Paola Guglielmelli
Simona Soverini
Carolina Terragna
Luca Arcaini, *Rappresentante Haematologica*
Chiara Paoli, *Segretario Generale*
Stefano Sacchi, *Tesoriere*

SEGRETERIA SIES

Via De' Poeti 1/7 - 40124 Bologna
Tel. 051 6390906 - Fax 051 4219534
E-mail: segreteriasies@ercongressi.it
www.siesonline.it

SEGRETERIA ORGANIZZATIVA

Studio E.R. Congressi
Via De' Poeti 1/7 - 40124 Bologna
Tel. 051 4210559 - Fax 051 4210174
E-mail: ercongressi@ercongressi.it
www.ercongressi.it

ABSTRACT BOOK

XVIII Congress of the Italian Society of Experimental Hematology

Main Program

.....	1
-------	---

Best Abstracts

.....	9
-------	---

Oral Communications

Session 1.	C001-C008	Acute Leukemias 1	15
Session 2.	C009-C016	Monoclonal Gammopathies and Multiple Myeloma 1	19
Session 3.	C017-C024	Myelodysplastic Syndromes.....	23
Session 4.	C025-C032	Monoclonal Gammopathies and Multiple Myeloma 2.....	26
Session 5.	C033-C040	Acute Leukemias 2	30
Session 6.	C041-C048	Lymphomas	35
Session 7.	C049-C056	Chronic Myeloproliferative Disorders	39
Session 8.	C057-C064	Immunotherapy and Cell Therapy.....	44
Session 9.	C065-C072	Chronic Lymphoproliferative Disorders.....	49

Posters

Session 1.	P001	Stem Cells Signaling and Microenviroment	55
Session 2.	P002-P004	Omic and Multiomic Analysis	56
Session 3.	P005-P017	Myelodysplastic Syndromes	58
Session 4.	P018-P023	Chronic Myeloid Leukemia	66
Session 5.	P024-P029	Myelodysplastic Syndromes	69
Session 6.	P030-P067	Acute Leukemia	72
Session 7.	P068-P078	Chronic Lymphocytic Leukemia and Chronic Lymphoproliferative Disorders	91
Session 8.	P079-P093	Lymphomas.....	97
Session 9.	P094-P111	Monoclonal Gammopathies and Multiple Myeloma	105
Session 10.	P112-P113	Stem Cell Transplantation.....	114
Session 11.	P114-P118	Immunotherapy and Cell Therapy	116
Session 12.	P119-P123	Benign Hematology (Red Cell Disease Thrombosis and Hemostasis).....	118
Session 13.	P124-P125	Susceptibility and Pathogenesis of Hematologic Malignancies	121

Authors Index

.....	i
-------	---

XVIII Congress of the Italian Society of Experimental Hematology

MAIN PROGRAM

CLONAL HEMATOPOIESIS OF INDETERMINATE POTENTIAL (CHIP): INSTRUCTIONS (FOR USE)

L. Malcovati

Department of Molecular Medicine, University of Pavia, Pavia, Italy & Department of Hematology, Fondazione IRCCS Policlinico S. Matteo, Pavia, Italy

High throughput DNA sequencing studies have contributed to unveil the genomic landscape of myeloid neoplasms and to identify relevant precursor states, including Clonal Hematopoiesis of Indeterminate Potential (CHIP), Clonal Cytopenia of Undetermined Significance (CCUS) and Clonal Monocytosis of Undetermined Significance (CMUS) (Table 1).¹⁻³ Population-based studies first provided evidence of CHIP in up to 10-20% of persons 60 years of age or older.¹ Individuals with CHIP were found to have a significantly higher risk of hematologic cancers, as well as of therapy-related myeloid neoplasms. Carrying a mutation was also associated with higher risk of cardiovascular morbidity and mortality and of inflammatory or autoimmune disorders.⁴ From both biological and clinical standpoints, inspecting clonal hematopoiesis is potentially useful in patients with unexplained peripheral blood abnormalities and suspected hematologic neoplasm. In fact, the number of somatic mutations, the size of the mutant clone and the driver mutation(s) had high predictive values to recognize or rule out a myeloid neoplasm.² Notwithstanding, the clinical context remains critical to inform the correct interpretation of detectable hematopoietic clones. To describe patients carrying somatic mutation(s) in whom a diagnosis of myeloid neoplasm is not proven, the term of CCUS has been introduced.^{2,3} Notably, specific mutation patterns, i.e. *SF3B1* mutation and biallelic *TP53* lesions, have been recognized recently as disease-defining irrespective of morphologic co-criteria.⁵ Mutation analysis has been also proven of value in the diagnostic work-up of peripheral blood monocytosis,⁶ and the category of CMUS has been introduced to identify cases not fulfilling criteria for myeloid neoplasm.⁵ Recent studies embracing the whole spectrum of clonal hematopoiesis developed risk scores distinguishing individuals with higher risk for progression into myeloid neoplasm, as well as enabling prediction of the likelihood of developing different types of malignancy.^{7,8} Persistent clonal hematopoiesis may complicate the determination of minimal residual disease in patients with acute myeloid leukemia (AML). While the presence of AML-related mutations has been shown to be an indicator of relapse, the significance of other types of clonal hematopoiesis is less well understood.⁹ CHIP can also arise in allogeneic hematopoietic stem cell transplantation recipients with different mechanisms, involving transfer of the clone from the donor, de novo occurrence of a clone from donor cells or expansion of an existing clone in the host.¹⁰ In summary, the available evidence has proven the utility of somatic mutational analysis in patients with suspected myeloid neoplasm, enabling the identification of clinically meaningful precursor states. Furthermore, the access to a minimally invasive assessment is paving the way for screening programs of clonal hematopoiesis in individuals with mild or absent hematologic phenotype.

Table 1. Current definitions of clonal hematopoiesis in the clinical context

<p><i>Clonal Hematopoiesis of Indeterminate Potential (CHIP)</i></p> <ul style="list-style-type: none">• Presence of a somatic mutation associated with hematologic neoplasm, at a variant allele frequency of at least 2%;• Absence of persistent peripheral blood cytopenia and dysplasia;• Exclusion of other underlying conditions as primary reason for the observed mutation(s).
<p><i>Clonal Cytopenia of Undetermined Significance (CCUS)</i></p> <ul style="list-style-type: none">• One or more somatic mutations otherwise found in patients with myeloid neoplasms detected in bone marrow or peripheral blood cells with an allele burden of $\geq 2\%$;• Persistent cytopenia (≥ 4 months) in one or more peripheral blood cell lineages;• Diagnostic criteria of myeloid neoplasm not fulfilled;• All other causes of cytopenia and molecular aberration excluded.
<p><i>Clonal Monocytosis of Undetermined Significance (CMUS)</i></p> <ul style="list-style-type: none">• Persistent absolute peripheral blood monocytosis $\geq 0.5 \times 10^9/L$ and relative monocytosis of $\geq 10\%$ of circulating peripheral blood leukocytes;• Absence or presence of peripheral blood cytopenia;• Presence of at least one myeloid neoplasm associated mutation at a variant allele frequency of at least 2%;• No significant dysplasia, increased blasts or morphologic findings of chronic myelomonocytic leukemia on bone marrow examination;• No criteria for a myeloid or other hematopoietic neoplasm are fulfilled;• No reactive condition that would explain a monocytosis is detected.

References

1. Jaiswal S, Fontanillas P, Flannick J, et al. Age-related clonal hematopoiesis associated with adverse outcomes. *N Engl J Med.* 2014;371(26):2488-98.
2. Malcovati L, Galli A, Travaglini E, et al. Clinical significance of somatic mutation in unexplained blood cytopenia. *Blood.* 2017;129(25):3371-8.
3. Galli A, Todisco G, Catamo E, et al. Relationship between clone metrics and clinical outcome in clonal cytopenia. *Blood.* 2021;138(11):965-76.
4. Jaiswal S, Natarajan P, Silver AJ, et al. Clonal Hematopoiesis and Risk of Atherosclerotic Cardiovascular Disease. *N Engl J Med.* 2017;377(2):111-21.
5. Arber DA, Orazi A, Hasserjian RP, et al. International Consensus Classification of Myeloid Neoplasms and Acute Leukemias: integrating morphologic, clinical, and genomic data. *Blood.* 2022;140(11):1200-28.
6. Cargo C, Cullen M, Taylor J, et al. The use of targeted sequencing and flow cytometry to identify patients with a clinically significant monocytosis. *Blood.* 2019.
7. Weeks LD, Niroula A, Neuberg D, et al. Prediction of risk for myeloid malignancy in clonal hematopoiesis. *NEJM Evid.* 2023;2(5).

8. Gu M, Kovilakam SC, Dunn WG, et al. Multiparameter prediction of myeloid neoplasia risk. *Nat Genet.* 2023;55(9):1523-30.
9. Jongen-Lavrencic M, Grob T, Hanekamp D, et al. Molecular Minimal Residual Disease in Acute Myeloid Leukemia. *N Engl J Med.* 2018;378(13):1189-99.
10. Frick M, Chan W, Arends CM, et al. Role of Donor Clonal Hematopoiesis in Allogeneic Hematopoietic Stem-Cell Transplantation. *J Clin Oncol.* 2019;37(5):375-85.

VEXAS: A NOVEL HEMATO-INFLAMMATORY DISORDER

C. Gurnari^{1,2}, M. Pascale¹, T. Ottone¹, G. Falconi¹, E. Galossi¹, M.T. Voso¹

¹Department of Biomedicine and Prevention, University of Rome Tor Vergata, Rome, Italy; ²Translational Hematology and Oncology Research Department, Taussig Cancer Center, Cleveland Clinic, Cleveland, OH, USA

VEXAS (Vacuoles, E1 enzyme, X-linked, Autoinflammatory, Somatic) is a novel hemato-inflammatory disorder juxtaposing in a unique nosological entity previously unconnected autoinflammatory and hematological disorders.¹ Somatic mutations of the X-linked gene *UBA1* are the pathogenetic events leading to an alteration of ubiquitination processes and a condition of hypercytokinemia.² The latter is mainly responsible for the extremely diverse clinical manifestations of the disease, ranging from the universal presence of bone marrow (BM) vacuoles and macrocytic anemia to varied organ (skin, lung, joints) involvement, chondritis, thrombosis, myelodysplastic syndromes (MDS), and plasma cell dyscrasias.^{3,4} MDS is present in up to 40-70% of cases, typically showing normal karyotype and lower risk profile according to current prognostic risk schemes. Indeed, MDS/VEXAS cases have a low mutational burden with, when present, classical age-related mutations (ARCH), e.g. *DNMT3A* and *TET2*, often occurring also in cases without frank MDS.⁵

In an attempt to categorize such a multitude of clinical phenotypes, the French VEXAS group analyzed 116 patients identifying 3 clusters with diverse prognosis and survival: cluster 1 (47% of cases) characterized by mild-to-moderate disease; cluster 2 (16% of cases) characterized by underlying MDS and higher mortality rates; and cluster 3 (37% of cases) with constitutional manifestations, higher C-reactive protein levels and less frequent chondritis.⁶ From a therapeutic standpoint, no guidelines exist, patients tend to be refractory to multiple lines of treatment, often becoming steroid-dependent, and show high morbidity/mortality due to disease-specific autoinflammatory manifestations. Being a multifaceted syndrome, the hypothesized approaches aim either to: i) target the clone (with hypomethylating agents e.g., azacitidine-AZA, or allogeneic stem cell transplant, allo-HCT), ii) block the cytokines storm responsible for the clinical picture (with steroids or a plethora of anti-interleukins), iii) supportive treatment (transfusions, thrombotic and infectious prophylaxis).⁷ Given the common MDS association, AZA treatment has been reported to be effective in VEXAS/MDS cases, being also able to lower steroids requirements.⁸ Another promising approach seems to be represented by Jak-inhibitors, particularly ruxolitinib.⁹ However, the only therapy with curative potential is allo-HCT. So far, anecdotal cases have been described gathering < 20 allografted patients, and trials are ongoing (NCT05027945). Most patients were allografted with reduced-intensity conditioning regimens and matched unrelated donors, and clinical and molecular remission was described in some cases.^{4,10} In conclusion, VEXAS is another of the big masqueraders, whereby clinical acumen is crucial to establish a prompt diagnosis and cascade multidisciplinary evaluation to tailor the best therapeutic strategy.

References

1. Gurnari C, Visconte V. From bone marrow failure syndromes to VEXAS: Disentangling clonal hematopoiesis, immune system, and molecular drivers. *Leuk Res.* 2023;127:107038.
2. Beck DB, Ferrada MA, Sikora KA, et al. Somatic Mutations in UBA1 and Severe Adult-Onset Autoinflammatory Disease. *N Engl J Med.* 2020;383(27):2628-2638.
3. Gurnari C, Pagliuca S, Durkin L, et al. Vacuolization of hematopoietic precursors: an enigma with multiple etiologies. *Blood.* 2021;137(26):3685-3689.
4. Gurnari C, Pascale MR, Vitale A, et al. Diagnostic capabilities, clinical features, and longitudinal UBA1 clonal dynamics of a nationwide VEXAS cohort. *Am J Hematol.* 2023.
5. Gutierrez-Rodriguez F, Kusne Y, Fernandez J, et al. Spectrum of clonal hematopoiesis in VEXAS syndrome. *Blood.* 2023;142(3):244-259.
6. Georjgin-Lavialle S, Terrier B, Guedon AF, et al. Further characterization of clinical and laboratory features in VEXAS syndrome: large-scale analysis of a multicentre case series of 116 French patients. *Br J Dermatol.* 2022;186(3):564-574.
7. Heiblig M, Patel BA, Groarke EM, Bourbon E, Sujobert P. Toward a pathophysiology inspired treatment of VEXAS syndrome. *Semin Hematol.* 2021;58(4):239-246.
8. Comont T, Heiblig M, Rivière E, et al. Azacitidine for patients with Vacuoles, E1 Enzyme, X-linked, Autoinflammatory, Somatic syndrome (VEXAS) and myelodysplastic syndrome: data from the French VEXAS registry. *Br J Haematol.* 2022;196(4):969-974.
9. Heiblig M, Ferrada MA, Koster MJ, et al. Ruxolitinib is more effective than other JAK inhibitors to treat VEXAS syndrome: a retrospective multicenter study. *Blood.* 2022;140(8):927-931.
10. Gurnari C, McLornan DP. Update on VEXAS and role of allogeneic bone marrow transplant: Considerations on behalf of the Chronic Malignancies Working Party of the EBMT. *Bone Marrow Transplant.* 2022;57(11):1642-1648.

BEYOND CONVENTIONAL LIMITS: SINGLE-CELL TECHNOLOGY FOR CLONAL HETEROGENEITY AND MEASURABLE RESIDUAL DISEASE DETECTION IN ACUTE LEUKEMIAS

I. Iacobucci

Department of Pathology, St. Jude Children's Research Hospital, Memphis (TN), USA

The integration of clinical features and genetic alterations is important to precisely classify patients with acute leukemias (AL), assess risk factors and determine eligibility to targeted therapies.^{1,2} However, despite progress in understanding disease biology and advances in therapeutic options, prognosis remains poor for most patients with AL. This dismal outcome is in part promoted by the dynamic and complex genetic heterogeneity of leukemic cells with expansion of resistant clones hampering disease eradication. Alongside genetic alterations, leukemia cell hierarchy composition play a role in determining vulnerability to therapeutic treatments.³ While conventional diagnostic approaches fail in examining intratumor genetic heterogeneity or inferring leukemia cellular origins, single-cell sequencing (sc-seq) technologies enable to explore inter- and intratumor genomic and transcriptional heterogeneity,⁴ determine leukemia cell type composition⁵ and assess measurable residual disease (MRD).⁶

Single-cell RNA-sequencing (scRNA-seq) has been instrumental to precisely annotate leukemia cell hierarchy by projecting data from leukemia samples on a single cell reference atlas of bone marrow hematopoiesis (Figure 1A). The abundance of specific cell type popula-

tions in leukemic samples has been found associated with functional, genomic and clinical features. For example, in acute myeloid leukemia (AML), abundance of primitive stem cell hierarchies has been associated with worse outcomes while abundance of granulocyte-monocyte progenitors has been associated with better outcomes.⁷ In B-cell acute lymphoblastic leukemia (B-ALL), enrichment of early lymphoid developmental stages was found to be associated with age at diagnosis (infants and adults), higher MRD levels and worse overall survival compared to samples with enrichment of cells with a pro-B and pre-B phenotype.⁵

Single-cell DNA-sequencing (scDNA-seq) has provided insights into clonal genetic evolution, overcoming the limit of conventional MRD tools in discriminating residual leukemic clones from clonal hematopoiesis/preleukemic clones that do not invariably lead to relapse (Figure 1B). Recently, multiomic scDNA-seq and cell surface marker analysis combined with flow cytometric enrichment of AML precursor/blast populations demonstrated high MRD sensitivity of approximately 0.01% and enabled both deconvolution of clonal genetic architecture and clone-specific immunophenotypic characterization⁶. These findings improve our understanding of mechanisms favoring MRD persistence and provide guidance for therapeutic approaches able to prevent and/or overcome relapse. In conclusion, despite persisting challenges, such as high costs and throughput limitations, sc-seq has demonstrated the power to implement and enhance current approaches for monitoring MRD and identifying early relapse clones.

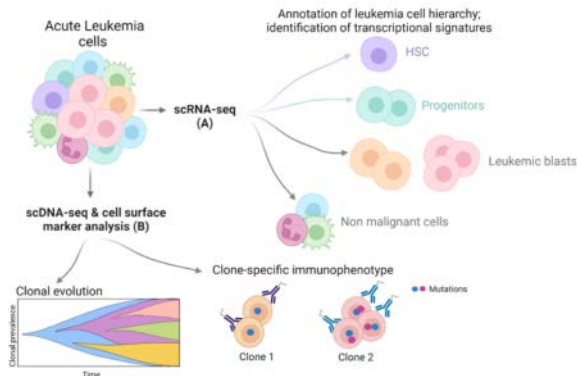


Figure 1. Schematic representation of applications of sc-sequencing in acute leukemia. A) scRNA-seq enables precise annotation of leukemia cell hierarchy and identification of transcriptional signatures accounting for transcriptional heterogeneity. B) single-cell genotypic and phenotypic analysis enables dissection of clonal genetic architecture and elucidation of clone-specific immunophenotype patterns. Created with Biorender.com.

DEVELOPMENT AND EVOLUTION OF 3D MODELS FOR PRECLINICAL RESEARCH

M. Rossi¹, F. Alviano², P. Marrazzo¹, S. Righi¹, G. Motta³, F. Paris¹, V. Pizzuti¹, C. Bertuzzi³, E. Sabbatini³, C. Agostinelli^{1,3}

¹Department of Medical and Surgical Sciences, University of Bologna, Bologna, Italy; ²Department of Biomedical and Neuromotor Sciences, University of Bologna, Bologna, Italy; ³Haematopathology Unit, IRCCS Azienda Ospedaliero-Universitaria di Bologna, Bologna, Italy

Three dimensional (3D) *in vitro* models are progressively being applied to investigate tumor cell biology and can significantly mimic the complexity of neoplastic architecture and physiology compared to traditional 2D models, which lack cell-to-cell and cell-extracellular matrix (ECM) signaling occurring *in vivo*.¹ The introduction of a third dimension not only influences cell spatial organization but also the cellular morphological and physiological characteristics.² The interaction of cancer cells with tumor microenvironment non-neoplastic cells, ECM and inflammatory mediators allows to create a realistic environment, thus representing a potential bridge between standard *in vitro* cultures and *in vivo* experimental models.^{3,4} In the last years, different methods (mainly

divided into scaffold-free or scaffold-based methods) have been developed to create spheroids, organoids, tumorspheres and tumoroids which differ by cell source (cell lines or patient-derived cells), size, complexity of cellular architecture and tumor microenvironment. Each technique has advantages and limitations also based on individual research needs and tools.⁵ Understanding the differences among 3D-systems allows the optimal choice, which must consider similarity to *in vivo* tissue and tumor architecture, ease of applications in high-throughput scenarios and costs.⁶ Three dimensional models in solid tumors have been widely used and studied and their advantages have been recognized for many years.⁷ In contrast to solid cancers, significant 3D models for lymphoma and leukemia are poorly described. The application of 3D models in the hematological field represents a demanding challenge for researchers precisely due to the nature of blood tumor cells which are non-adherent and the techniques commonly used for solid tumors have highlighted some critical issues when applied to hematological models [8]. The creation of a lymphoid or bone marrow niche in three dimensional structures highlights the importance of the effective interactions between neoplastic and tumor microenvironment cells to better understand the complex pathogenetic and chemoresistance mechanisms of the disease. This approach is particularly important to deepen the field of preclinical research and personalized medicine, bridging the gap between 2D *in vitro* assessment and clinical oncology, accelerating and facilitating the translation of basic advances into innovative treatments.

References

- Breslin S, O'Driscoll L (2013) Three-dimensional cell-culture: the missing link in drug discovery. *Drug Discov Today*. 18(5-6):240-9. doi: 10.1016/j.drudis.2012.10.003.
- Riedl A, Schleiderer M, Pudelko K, Stadler M, Walter S, Unterleuthner D, Unger C, Kramer N, Hengstschläger M, Kenner L et al. (2017) Comparison of cancer cells in 2D vs 3D culture reveals differences in AKT-mTOR-S6K signaling and drug responses. *J Cell Sci* (1):203-218. doi: 10.1242/jcs.188102.
- Yamada KM, Cukierman E (2007) Modeling tissue morphogenesis and cancer in 3D. *Cell* 130(4):601-10. doi: 10.1016/j.cell.2007.08.006
- Jackson EL, Lu H (2016) Three-dimensional models for studying development and disease: moving on from organisms to organs-on-a-chip and organoids. *Integr Biol (Camb)* 8(6):672-83. doi: 10.1039/c6ib00039h.
- Langhans SA (2018) Three-Dimensional *In Vitro* Cell Culture Models in Drug Discovery and Drug Repositioning. *Front Pharmacol* 9:6. doi: 10.3389/fphar.2018.00006.
- Atat OE, Farzaneh Z, Pourhamzeh M, Taki F, Abi-Habib R, Vosough M, El-Sibai M. (2022) 3D modeling in cancer studies. *Hum Cell*. 2022 Jan;35(1):23-36. doi: 10.1007/s13577-021-00642-9.
- Marsee A, Roos FJM, Verstegen MMA; HPB Organoid Consortium; Gehart H, de Koning E, Lemaigre F, Forbes SJ, Peng WC, Huch M, Takebe T, Vallier L, Clevers H, van der Laan LJW, Spee B. Building consensus on definition and nomenclature of hepatic, pancreatic, and biliary organoids. *Cell Stem Cell*. 2021 May 6;28(5):816-832. doi: 10.1016/j.stem.2021.04.005.
- Rossi M, Alviano F, Righi S, Sabbatini E, Agostinelli C. (2022) Three-dimensional models: a novel approach for lymphoma research. *J Cancer Res Clin Oncol*. 148(4):753-765. doi: 10.1007/s00432-021-03897-9.

HARNESSING THERAPY-INDUCED SENESENCE TO STIMULATE IMMUNE RESPONSES AGAINST ACUTE MYELOID

A. Santoro,¹ A. Zangari,¹ S. Fusco,¹ T. Tavella,¹ D. Gilioli,¹ E. Carsana,¹ K. Giannetti,¹ S. Feola,^{2,3,4} S. Russo,^{2,3,4} L. Passerini,¹ I. Merelli,¹ F. Aletti,^{5,6} M. Carrabba,^{5,6} V. Cerullo,^{2,3,4} S. Gregori,¹ C. Lo Celso,^{8,9} L. Vago,^{5,6,7}, R. Di Micco¹

¹San Raffaele Telethon Institute for Gene Therapy, Milan, Italy; ²Drug Research Program (DRP) ImmunoViroTherapy Lab (IVT), Division of Pharmaceutical Biosciences, Faculty of Pharmacy, University of Helsinki, Helsinki, Finland; ³Helsinki Institute of Life Science (HiLIFE), University of Helsinki, Helsinki, Finland; ⁴Translational Immunology Program (TRIMM), Faculty of Medicine Helsinki University, University of Helsinki, Helsinki, Finland; ⁵Unit of Immunogenetics, Leukemia Genomics and Immunobiology, Division of Immunology, Transplantation, and Infectious Disease, IRCCS San Raffaele Scientific Institute, Milan, Italy; ⁶Hematology and Bone Marrow Transplantation Unit, IRCCS San Raffaele Scientific Institute, Milan, Italy; ⁷San Raffaele Vita-Salute University, Milan, Italy; ⁸Department of Life Sciences, Imperial College London, London, UK; ⁹The Francis Crick Institute, London, UK

Acute myeloid leukemia (AML) is an aggressive hematological malignancy. First line therapeutic treatment relies on cycles of intensive chemotherapy including cytarabine and anthracycline drugs. Nonetheless, early treatment failure is frequent, leading to disease relapse and dismal outcome.¹⁻⁴ Therapy-evoked stress induces the activation of a senescence program characterized by a DNA Damage Response (DDR)-mediated growth arrest. While senescence may be beneficial at halting proliferation of cancer cells shortly after therapy it may be detrimental in the long term, due to the persistence of proinflammatory secretory phenotype (SASP) and the activation of stemness-like reprogramming, ultimately causing disease relapse.⁵ However, recent evidence in solid tumours supports the idea that the activation of therapy induced senescence (TIS) may in turn stimulate the innate and adaptive immune system for cancer cell eradication.^{7,8} Recent findings, including our own, suggest that cytarabine treatment induces a senescence-like state in AML.^{5,9} Specifically, using state of the art *in vitro* models for human AML, we uncovered increased antigenicity of senescent AML cells in response to chemotherapy and activation of T cell responses. Because we observed increased immunogenicity of senescent AML by expression of HLA I and HLAII, we hypothesized that they may present specific immunogenic peptides which in turn trigger T cell activation. Mass Spectrometry analyses of HLA-I bound peptides from *in vitro* chemotherapy treated human AML samples revealed a high number of peptides only in AML cells undergoing TIS. From a total of 6000 peptides across three patients, we identified 69 peptides associated with senescence, metabolic pathway activation and, more interestingly, immune cells activation. We will adopt *in vitro* culture systems to assess their immunogenicity and ability to trigger T cell activation and their potential use for cancer vaccination purposes by using preclinical *in vivo* models. Due to the high cytotoxicity and low tolerability of chemotherapy, elderly patients are now more frequently treated with hypomethylating drugs, such as Decitabine or Azacitidine,¹⁰ which can reverse DNA methylation that aberrantly occurs in leukemic blasts, leading to the silencing of critical tumour suppressor genes involved in cancer-related pathways. Nevertheless, such treatments may still cause relapse.¹¹ We hypothesised that also such treatments may cause TIS. Our preliminary data show that treated THP1 cell lines show a slower proliferation and accumulation of senescence associated β -Galactosidase. Future work will elucidate the senescence phenotype and evaluate the downstream immune system responses. Conclusively, we identify novel triggers as well as common features of therapy induced senescence and show a new set of mechanisms controlling the crosstalk between leukemic cells and the immune system. These findings will

provide the bases for novel therapeutic options for patients with AML and beyond.

References

1. Tallman, M. S., Gilliland, D. G. & Rowe, J. M. Drug therapy for acute myeloid leukemia. *Blood* 106, 1154–1163 (2005).
2. Burnett, A., Wetzler, M. & Löwenberg, B. Therapeutic advances in acute myeloid leukemia. *J. Clin. Oncol. Off. J. Am. Soc. Clin. Oncol.* 29, 487–494 (2011).
3. Gurnari, C., Pagliuca, S. & Visconte, V. Deciphering the Therapeutic Resistance in Acute Myeloid Leukemia. *Int. J. Mol. Sci.* 21, 8505 (2020).
4. van Gils, N., Denkers, F. & Smit, L. Escape From Treatment; the Different Faces of Leukemic Stem Cells and Therapy Resistance in Acute Myeloid Leukemia. *Front. Oncol.* 11, (2021).
5. Duy, C. et al. Chemotherapy Induces Senescence-Like Resilient Cells Capable of Initiating AML Recurrence. *Cancer Discov.* 11, 1542–1561 (2021).
6. Milanovic, M. et al. Senescence-associated reprogramming promotes cancer stemness. *Nature* 553, 96–100 (2018).
7. Chen, H.-A. et al. Senescence Rewires Microenvironment Sensing to Facilitate Antitumor Immunity. *Cancer Discov.* 13, 432–453 (2023).
8. Marin, I. et al. Cellular Senescence Is Immunogenic and Promotes Antitumor Immunity. *Cancer Discov.* 13, 410–431 (2023).
9. Gilioli, D. et al. Therapy-induced senescence upregulates antigen presentation machinery and triggers anti-tumor immunity in Acute Myeloid Leukemia. 2022.11.17.515658 Preprint at <https://doi.org/10.1101/2022.11.17.515658> (2022).
10. Zhang, R.-J. et al. Hypomethylating agents for elderly patients with acute myeloid leukemia: a PRISMA systematic review and meta-analysis. *Eur. Rev. Med. Pharmacol. Sci.* 25, 2577–2590 (2021).
11. Prébet, T. et al. Outcome of high-risk myelodysplastic syndrome after azacitidine treatment failure. *J. Clin. Oncol. Off. J. Am. Soc. Clin. Oncol.* 29, 3322–3327 (2011).

COMPUTER VISION E DIGITAL PATHOLOGY: APPLICAZIONI IN EMATOLOGIA

S. D'amico

IRCCS Humanitas Research Hospital, Rozzano, Milan, Italy

Myeloid Neoplasms (MNs) represent a spectrum of blood disorders characterized by abnormal proliferation and differentiation of myeloid cells within the bone marrow. Accurate diagnosis and classification of MNs are paramount for guiding optimal patient care and treatment strategies. Currently, the gold standard for MN diagnosis is histopathological analysis of bone marrow biopsies and aspirates. However, this traditional approach is time-intensive, subject to interpretation biases, and susceptible to inter-observer variability. Recent advancements in image analysis and deep learning methodologies offer a promising avenue for enhancing the precision and efficiency of histopathological diagnosis. By leveraging automated segmentation and feature extraction techniques rooted in artificial intelligence (AI), clinicians can identify and quantify specific cellular and tissue components, allowing for more objective and reproducible analysis. This integration of AI into hematological clinical practice holds the potential to improve the classification and prognostic stratification of myeloid neoplasms. The potential of this opportunity lies in the application of deep learning algorithms for image analysis, particularly in tasks such as image segmentation and classification. Moreover, establishing a correlation between histomorphometric data extracted

from image analysis, genomic insights, and clinical parameters could pave the way for novel approaches to classifying and prognosticating myeloid malignancies. This comprehensive analysis may reveal new insights into disease progression, response to treatment, and patient outcomes. Artificial intelligence techniques applied to digital pathology can provide clinicians with a reliable and efficient tool for the diagnosis and classification of myeloid neoplasms. The integration of deep learning-based image analysis with multimodal data can lead to improved accuracy, reproducibility, and predictive capabilities in the field of myeloid neoplasia diagnosis, resulting in patient benefits through more personalized and effective treatment strategies. To validate the clinical utility of AI models, a collaborative framework involving both clinical and technical experts is indispensable. The validation process entails leveraging active learning methodologies to iteratively refine the models based on clinically validated information. Crucially, these implementations must adhere to principles of Explainable and Trustworthy AI to foster the development of a reliable and validated technology poised for seamless integration into clinical practice.

DIAGNOSTIC AND MOLECULAR FEATURES OF GRAY ZONE LYMPHOMA

A. Di Napoli,¹ C. Agostinelli,² E. Sabattini²

¹Department of clinical and molecular medicine, Sant'Andrea University Hospital, Sapienza University of Rome; ²Haematopathology Unit, IRCCS Azienda Ospedaliero-Universitaria di Bologna, S Orsola Malpighi, Bologna, Italy

Gray zone lymphomas (GZL) are a group of rare and aggressive B-cell lymphomas with overlapping morphological, immunophenotypic, and genetic features of both classical Hodgkin lymphoma (CHL) and diffuse large B-cell lymphoma (DLBCL), that may not respond to standard treatments used for either CHL or DLBCL.^{1,2} Both the 5th edition of the WHO classification of haematolymphoid tumours and the International Consensus Classification of lymphomas limited GZL to neoplasms presenting as a localized anterior mediastinal mass with/without supraclavicular lymph nodes involvement (MGZL). GZL with primary extra-mediastinal disseminated disease are classified as DLBCL because of different gene expression profiles (GEP) and genomic alterations.³⁻⁵ MGZL characterize by discordant morphology and immunophenotype, ranging from cases with CHL-like morphology but full B-cell phenotype and cases with DLBCL-like morphology but negativity for B cell markers and diffuse, strong CD30 and/or CD15 expression.⁶ Composite or sequential CHL and primary mediastinal large B cell lymphoma (PMBL) are not classified as MGZL, since both components show coherent morphology and immunophenotype underlying a poorly understood cellular plasticity.^{7,8} MGZL diagnosis is challenging, especially in bioptic material, and should be made only after careful exclusion of CHL and PMBL. In a study promoted by the Italian Lymphoma Foundation (FIL) 50% of the 38 Italian MGZL cases were not confirmed upon central review by expert haematopathologists. Extra-mediastinal GZL, composite CHL/PMBL, EBV-infected lymphomas, and transformed follicular lymphomas were also among the unconfirmed cases (unpublished data). Similar studies reported a rate of confirmed GZL diagnoses ranging from 38% to 55% (9,6). MGZL show recurrent mutations in SOCS1, B2M, TNFAIP3, GNA13, LRRN3, and NFKBIA genes resembling both CHL and PMBL.⁴ Consistently, on GEP MGZL cluster either closer to CHL or to PMBL, but with a stronger NF-κB signature and a prominent regulatory tumor microenvironment (TME) with expression of immune checkpoint molecules (LAG3, PD1, and PD-L1) and predominance of tumor-associated macrophages.^{3,10} The GEP-based Lymph3Cx assay, which discriminates between DLBCL and PMBL, classified 12 MGZL, submitted to the 20th meeting of the European Association for

Haematopathology, as PMBL-like in 75% of the cases (6 CHL-like/intermediate and 3 PMBL-like morphology) whereas reporting an unclear signature in the remaining 25% (all CHL-like morphology).¹¹ More recently, a 168 tumor- and TME-related gene signature categorized 24 MGZL into 19 CHL (7 CHL-like, 7 PMBL-like, 5 intermediate morphology) and 5 PMBL (1 CHL-like, 3 PMBL-like, 1 intermediate morphology) (abstract SIES n.98 Ciavarella *et al.*). These data further underline the dyscrasia between histological and molecular profiles and the need of addition studies addressing the utility of a combined approach for the diagnosis and treatment choice of MGZL.

References

- Alaggio, R.; Amador, C.; Anagnostopoulos, I.; et al. The 5th edition of the World Health Organization Classification of Haematolymphoid Tumours: Lymphoid Neoplasms. *Leukemia* 2022, 36, 1720–1748.
- Campo, E.; Jaffe, E.S.; Cook, J.R.; et al. The International Consensus Classification of Mature Lymphoid Neoplasms: A report from the Clinical Advisory Committee. *Blood* 2022, 140, 1229–1253.
- Sarkozy, C.; Chong, L.; Takata, K.; et al. Gene expression profiling of gray zone lymphoma. *Blood Adv.* 2020, 4, 2523–2535.
- Sarkozy C, Hung SS, Chavez EA, et al. Mutational landscape of gray zone lymphoma. *Blood.* 2021;137:1765–1776.
- Gibson SE, Dojcinov S, Dotlic S, et al. Mediastinal large B cell lymphoma and surrounding gray areas: a report of the lymphoma workshop of the 20th meeting of the European Association for Haematopathology. *Virchows Arch.* 2023 Dec;483(6):733-749.
- Sarkozy, C.; Copie-Bergman, C.; Damotte, D.; et al. Gray-zone Lymphoma Between cHL and Large B-Cell Lymphoma: A Histopathologic Series From the LYSA. *Am. J. Surg. Pathol.* 2019, 43, 341–351.
- Aussedat, G.; Traverse-Glehen, A.; Stamatoullas, A.; et al. Composite and sequential lymphoma between classical Hodgkin lymphoma and primary mediastinal lymphoma/diffuse large B-cell lymphoma, a clinico-pathological series of 25 cases. *Br. J. Haematol.* 2020, 189, 244–256.
- Traverse-Glehen, A.; Pittaluga, S.; Gaulard, P.; et al. Mediastinal gray zone lymphoma: The missing link between classic Hodgkin's lymphoma and mediastinal large B-cell lymphoma. *Am. J. Surg. Pathol.* 2005, 29, 1411–1421.
- Pilichowska, M.; Pittaluga, S.; Ferry, J.A.; et al. Clinicopathologic consensus study of grey zone lymphoma with features intermediate between DLBCL and classical HL. *Blood Adv.* 2017, 1, 2600–2609.
- Pittaluga S, Nicolae A, Wright GW, et al. Gene Expression Profiling of Mediastinal Gray Zone Lymphoma and Its Relationship to Primary Mediastinal B-cell Lymphoma and Classical Hodgkin Lymphoma. *Blood Cancer Discov.* 2020;1(2):155-161.
- Gibson SE, Dojcinov S, Dotlic S, et al. Mediastinal large B cell lymphoma and surrounding gray areas: a report of the lymphoma workshop of the 20th meeting of the European Association for Haematopathology. *Virchows Arch.* 2023 Dec;483(6):733-749.

THROMBOTIC THROMBOCYTOPENIC PURPURA

L. Fianchi^{1,2}

¹Dipartimento di Diagnostica per Immagini, Radioterapia Oncologica ed Ematologia; ²Fondazione Policlinico Universitario A. Gemelli, IRCCS- Roma 2 Università Cattolica del Sacro Cuore- Roma, Italy

Thrombotic thrombocytopenic purpura (TTP) is a life-threatening thrombotic microangiopathy characterized by microangiopathic hemolytic anemia, consumptive thrombocytopenia, and ischemic end-organ dam-

age. This is caused by a hereditary (cTTP) or immune-mediated deficiency (iTTP) of ADAMTS13 (a disintegrin and metalloproteinase with a thrombospondin type 1 motif, member 13), a proteolytic enzyme that specifically degrades high molecular weight multimers of von Willebrand factor (HMW-vWF). ADAMTS13 deficiency leads to impaired proteolytic processing of HMW-VWF, which avidly interacts with platelets and subendothelial collagen and promotes tissue and multiorgan ischemia. In iTTP, anti-ADAMTS13 autoantibodies include inhibitory (that inhibit the proteolytic activity of ADAMTS13) and non-inhibitory antibodies, which bind to ADAMTS13 and increase its circulatory clearance. Recently, an open ADAMTS13 conformation was found during the acute phase of iTTP, and autoantibodies were revealed to mediate this conformational change. Untreated, TTP has a high mortality due to neurological and cardiac dysfunction, so early diagnosis and treatment are essential to reduce the mortality. Recently ISTH and SIE guidelines for diagnosis and treatment of thrombotic thrombocytopenic purpura have been published. A plasma ADAMTS13 activity of less than 10 IU/dL (often referred to as 10% of normal ADAMTS13 activity) is the hallmark of TTP. Front-line therapy includes daily plasma exchange (PEX) with fresh frozen plasma replacement and immunosuppression with corticosteroids. Caplacizumab, a nanobody that binds to the A1 domain of vWF and inhibits spontaneous platelet adhesion preventing microthrombi formation, has been shown to reduce mortality due to ischemic events, refractoriness and exacerbations after PEX discontinuation. The drug should be considered for patients with a high ($\geq 90\%$) pretest probability of TTP, according to clinical parameters (eg, PLASMIC score or French score), if ADAMTS13 test results are expected within 72 hours. In refractory or relapsing disease the addition of rituximab is suggested, as well as for patients with iTTP who are in remission without clinical signs/symptoms, but with persistent low plasma ADAMTS13 activity. SIE guidelines recommend monitoring ADAMTS13 in patients in remission: monthly for the first 3 months, subsequently every 3 months in the first year, and every 6-12 months if stable. ADAMTS13 activity during clinical remission has emerged as an important targetable risk factor for iTTP relapse and other outcomes including stroke and all-cause mortality. The improvement of survival of acute iTTP might lead in the future to focus on optimizing outcomes in survivors, who are at risk of multiple adverse health outcomes including increased rates of stroke and other cardiovascular diseases and higher rates of morbidities such as obesity, hypertension, autoimmune disorders, neurocognitive impairment, depression, and reduced quality of life.

References

- Joly BS, Coppo P, Veyradier A. Thrombotic thrombocytopenic purpura. *Blood*. 2017 May 25;129(21):2836-2846.
- Roose E, Schelpe AS, Tellier E et al. Open ADAMTS13, induced by antibodies, is a biomarker for subclinical immune-mediated thrombotic thrombocytopenic purpura. *Blood* 2020, 136, 353–361.
- F_o_d_i_l_S, Zafrani L. Severe Thrombotic Thrombocytopenic Purpura (TTP) with Organ Failure in Critically Ill Patients *J Clin Med* . 2022;11(4):1103.
- Zheng XL, Vesely SK, Cataland SR, Coppo P, Geldziler B, Iorio A, Matsumoto M, Mustafa RA, Pai M, Rock G, Russell L, Tarawneh R, Valdes J, Peyvandi F. ISTH guidelines for the diagnosis of thrombotic thrombocytopenic purpura. *J Thromb Haemost*. 2020 Oct;18(10):2486-2495.
- Zheng XL, Vesely SK, Cataland SR, Coppo P, Geldziler B, Iorio A, Matsumoto M, Mustafa RA, Pai M, Rock G, Russell L, Tarawneh R, Valdes J, Peyvandi F. ISTH guidelines for treatment of thrombotic thrombocytopenic purpura. *J Thromb Haemost*. 2020 Oct;18(10):2496-2502
- Bendapudi PK, Hurwitz S, Fry A, Marques MB, Waldo SW, Li A, Sun L, Upadhyay V, Hamdan A, Brunner AM, Gansner JM, Viswanathan S, Kaufman RM, Uhl L, Stowell CP, Dzik WH, Makar RS. Derivation and external validation of the PLASMIC score for rapid assessment of adults with thrombotic microangiopathies: a cohort study. *Lancet Haematol*. 2017 Apr;4(4):e157-e164.
- Peyvandi F, Scully M, Hovinga JA, Cataland S, Knöbl P, Wu H, et al. Caplacizumab for acquired thrombotic thrombocytopenic purpura. *N Engl J Med*. (2016) 374:511–22. doi: 10.1056/NEJMoa1505533
- Scully, M, Cataland, SR, Peyvandi, F, et al. Caplacizumab treatment for acquired thrombotic thrombocytopenic purpura. *NEJM* 2019; 380 :335-346
- Doyle AJ, Stubbs MJ, Dutt T, et al. Long-term risk of relapse in immune-mediated thrombotic thrombocytopenic purpura and the role of anti-CD20 therapy. *Blood*. 2023; 141:285-294.
- Selvakumar S, Liu A, Chaturvedi S. Immune thrombotic thrombocytopenic purpura: Spotlight on long-term outcomes and survivorship. *Front Med (Lausanne)*. 2023 Feb 28;10:1137019.

BLASTIC PLASMACYTOID DENDRITIC CELL NEOPLASM

C. Papayannidis, C. Sartor, G. Cristiano, J. Nanni, A. Curti

IRCCS, Azienda Ospedaliero Universitaria di Bologna, Istituto di Ematologia "Seragnoli", Bologna, Italy

Blastic plasmacytoid dendritic cell neoplasm (BPDCN) is a rare disease originating from precursors of plasmacytoid dendritic cells (pDCs), and accounting for less than 1% of hematological neoplasms. pDCs, also known as professional type 1 interferon producing cells or plasmacytoid monocytes, produce high amounts of interferon- α in response to viruses and play a role in the innate immune system. Nevertheless, no known pathogenetic association to any virus has been demonstrated so far. The nomenclature of this neoplasm has been modified in the past due to its unknown origin, thus leading to underestimated incidence and delayed disease recognition. In 2008 WHO classification, BPDCN was defined as a type of acute myeloid leukemia (AML), but in the 2016 revision it was for the first time described as its own entity. Diagnosis of BPDCN is challenging, due to the extreme heterogeneity of clinical signs, symptoms as well as molecular and cytogenetics alterations which can be identified at disease onset. It can occur at any age, but it is most common in the elderly, with a median age at diagnosis in the mid to late 60s, with a male to female ratio of 3:1.

Table 1. Highlights on BPDCN

BPDCN has an estimated incidence of 1,000 to 1,400 annually in the US and Europe combined.
While BPDCN can occur at any age, the median age at diagnosis is in the mid-60s, with approximately 75% of cases occurring in men.
Accurate diagnosis requires a biopsy showing the morphology of plasmacytoid dendritic blast cells and immunophenotypic criteria established by either immunohistochemistry or flow cytometry.
Immunohistochemical criteria for BPDCN include positivity for CD123, CD4, CD56 and TCL1 in the absence of myeloperoxidase and lysozyme.
Historically, initial response to combination chemotherapy has been high, but patients usually relapse with a median overall survival of approximately 1 year. These regimens are often associated with significant side effects and poor tolerability.
Tagraxofusp is a therapy directed to CD123 (IL-3R), a cell surface receptor highly expressed in BPDCN. The drug is approved as monotherapy by AIFA for the frontline treatment of adult BPDCN patients.
Additional therapies are currently under investigation within clinical trials for the treatment of BPDCN.

About 80-90% of patients have skin involvement at disease presentation, including solitary, localized or generalized plaques or tumors, frequently asymptomatic. In about 30% to 50% of cases only skin involvement is detected at diagnosis; however, lymphadenopathy, bone marrow and peripheral blood involvement are also frequently reported (in 40%-60% and 60%-90% respectively). The central nervous system (CNS) can be involved in about 10% of newly diagnosed cases of BPDCN, and in about 30% at relapse. The definitive diagnosis of BPDCN relies on the immunohistochemical results, including the expression of CD4, CD56 and the pDC-specific markers CD123, TCL1 and BDCA-2/CD303 and lack of lymphoid and myeloid markers. However, some cases are negative for typical markers and positive for atypical ones, making the diagnosis more challenging. Therefore, a multidisciplinary approach, including hematologist, dermatologist and pathologist involvement is strictly required, from diagnosis and through all the patient's therapeutic path, to integrate all clinical and laboratory data and to define the most appropriate treatment. The prognosis of BPDCN is very poor, with a median overall survival (OS) of ~12-14 months. Due to its rarity, for many years treatment relied on standard chemotherapy and allogeneic stem cell transplantation (HSCT), without innovative approaches. Such an intensive program, whose effectiveness in the long run is unfortunately still unsatisfactory, can be offered only to young and fit patients, thus excluding elderly and frail populations. The recent introduction of Tagraxofusp, a recombinant human IL-3 fused to a truncated diphtheria toxin payload, has opened a new era of precision medicine in the treatment of BPDCN, enriched with innovative and promising experimental approaches, currently in clinical development (Table 2).

Table 2. Ongoing clinical trials in BPDCN

Clinicaltrials.gov	Phase	Agent(s)	Mechanism of action	Eligible patients
NCT03599960	II	Methotrexate, L-asparaginase, Idarubicin, Dexamethasone	Combination chemotherapy	Newly diagnosed BPDCN
NCT03485547	I	Venetoclax	Anti-Bcl2	BPDCN
NCT03386513	I/II	IMG632	Anti-CD123	BPDCN
NCT03113643	I	Tagraxofusp, Azacitidine, Venetoclax	Anti-CD123, HMA, anti-Bcl2	BPDCN
NCT04216524	II	Tagraxofusp, Venetoclax, chemotherapy	Anti-CD123, anti-Bcl2, multiple	BPDCN
NCT04230265	I	UniCAR02-T-CD123	Anti-CD123 CAR T cell	BPDCN
NCT06006403	I/II	CD123 CAR-NK	Anti-CD123 CAR-NK cell	BPDCN
NCT05086315	I	SAR443579	CD123 NK Cell Engager	BPDCN
NCT04013685	I	Orca-T	Engineered donor grafts	BPDCN after HSCT

References

- Recent Advances in the Biology and CD123-Directed Treatment of Blastic Plasmacytoid Dendritic Cell Neoplasm. Pemmaraju N, Deconinck E, Mehta P. et al. Clin Lymphoma Myeloma Leuk. 2023 Dec 20;S2152-2650(23)02198-5.
- Plasmacytoid dendritic cell expansion in myeloid neoplasms: A novel distinct subset of myeloid neoplasm? Peng J, He S, Yang X et al. Crit Rev Oncol Hematol. 2023 Dec;192:104186.
- Blastic plasmacytoid dendritic cell neoplasm: emerging developments and special considerations for 2023. Pemmaraju N, Kantarjian H. Clin Adv Hematol Oncol. 2023 May;21(5):257-264.
- Tagraxofusp for blastic plasmacytoid dendritic cell neoplasm. Luskin MR, Lane AA. Haematologica. 2024 Jan 1;109(1):44-52.
- Unmet Clinical Needs and Management Recommendations for Blastic Plasmacytoid Dendritic Cell Neoplasm: A Consensus-based Position Paper From an Ad Hoc International Expert Panel. Pagano L, Zinzani PL, Pileri S et al. Hemasphere. 2023 Feb 21;7(3):e841.
- Tagraxofusp in Blastic Plasmacytoid Dendritic-Cell Neoplasm. Naveen Pemmaraju, Andrew A Lane, Kendra L Sweet et al. N Engl J Med 2019 Apr 25;380(17):1628-1637.

PATIENT-DERIVED-XENOGRAFT (PDX): MODELLI DI STUDIO DELLA CELLULA STAMINALE LEUCEMICA E DI TARGET THERAPY

T. Ottone^{1,2}, S. Travaglini³, D.F. Angelini⁴, G. Silvestrini⁵, M. Serra⁶, M. Mattei⁶, M. Divona¹, C. Gurnari^{1,7}, M.T. Voso¹⁻²

¹Department of Biomedicine and Prevention, Tor Vergata University, Rome, Italy; ²Santa Lucia Foundation, I.R.C.C.S., Neuro-Oncohematology, Rome, Italy; ³Department of Experimental Medicine, University of Rome Tor Vergata, Rome, Italy; ⁴Santa Lucia Foundation, I.R.C.C.S., Neuroimmunology Unit, Rome, Italy; ⁵Department of Biomedicine and Prevention, PhD in Immunology, Molecular Medicine and Applied Biotechnology, University of Rome Tor Vergata, Rome, Italy; ⁶Interdepartmental Service Centre-Station for Animal Technology, University of Rome "Tor Vergata", Rome, Italy; ⁷Translational Hematology and Oncology Research Department, Taussig Cancer Center, Cleveland Clinic, Cleveland, OH 44106

Despite recent advances in the understanding of pathogenesis and the molecular heterogeneity, AML remains a prognostically adverse disease, with 5-year survival rates of only 30%-40%,¹ due to the high frequency of relapse due to the persistence of chemoresistant leukemic clones. Several studies have demonstrated that subclonal heterogeneity, and the subsistence of leukemic stem cells (LSCs) and their progeny may be responsible for AML recurrence.²⁻⁴ In recent decades, there has been increasing interest in LSCs and their biology. It is now widely acknowledged that effectively targeting this subpopulation is crucial to achieve cure in patients with AML. The characterization of surface markers that reliably identify LSCs is a central objective to monitor the disease clinical course and to develop novel strategies targeting LSCs.⁵ Although initial studies suggested that the CD34+/CD38-/lineage- phenotype could pinpoint LSCs, later studies demonstrated that this phenotype was more complex and heterogeneous.⁶ Xenograft AML mouse models, based on the injection of patient-derived leukemic cells (PDXs) in immunodeficient mice, represent valuable tools to recapitulate AML course, identify chemo-resistant subclonal populations,⁷ and to test LSCs targeted drugs. Among surface markers, CD123 and CD25 have been identified as representative LSCs markers. PDX *in vivo* model proved that CD123+/CD25+ clones were capable of initiating leukemic development in NSG mice, and were characterized by a quiescent cell cycle and by chemo-resistance *in vivo*. This is reflected by the significantly poorer

prognosis of AML with CD25 expression exceeding 10%, which is associated with OS and RFS as compared to AML with lower to negative CD25 expression.^{8,9} In multivariate analysis, CD25 expression represents an independent adverse factor for OS and RFS, particularly in *FLT3*-ITD positive AML. The negative prognostic impact of *FLT3*-ITD mutations has long been reported, being associated with reduced overall survival due to a high rate of disease recurrence, partly due to the persistence of *FLT3*-ITD-expressing LSCs after first-line treatment. Particularly, we previously reported that the presence of CD34/CD123/CD25/CD99+ leukemic precursor cells (LPCs) phenotype at diagnosis predicts for *FLT3*-ITD mutation and disease recurrence⁸⁻¹⁰. Indeed, the *FLT3*-ITD mutation load was significantly higher in these LPCs, versus the bulk AML population. To confirm their stem cell potential, we sorted CD34/CD123/CD25/CD99+ cells purified from *FLT3*-ITD mutated AML samples, and transplanted this cell population into conditioned NSG mice. LPCs showed higher potential to engraft NSG mice and induce AML as compared to paired blasts, confirming the self-renew and leukemia-initiating capacity. Interestingly, after sequential passages, the LSCs phenotype, showed an expansion in the CD34+/CD123+/CD25+/CD99+/CD38- compartment, potentially indicating that serial transplantation may unveil the ancestral leukemic precursor cells (unpublished). Furthermore, we demonstrated that Dasatinib/Gilteritinib combinations were able to target LSCs and could be used to eradicate residual leukemic cells harbinger of relapse. In conclusion, PDXs are the most valuable tool to study AML pathogenesis and development, in order to optimize preclinical drug testing, based on the potential to retain the genetic diversity and phenotypic heterogeneity of the original tumor.

References

1. Ding L, Ley TJ, Larson DE, et al. Clonal evolution in relapsed acute myeloid leukaemia revealed by whole-genome sequencing. *Nature*. 2012;481(7382):506–510.

2. van Galen P, Hovestadt V, Wadsworth II MH, et al. Single-Cell RNA-Seq Reveals AML Hierarchies Relevant to Disease Progression and Immunity. *Cell*. 2019;176(6):1265-1281.e24.
3. Boyd AL, Aslostovar L, Reid J, et al. Identification of Chemotherapy-Induced Leukemic-Regenerating Cells Reveals a Transient Vulnerability of Human AML Recurrence. *Cancer Cell*. 2018;34(3):483-498.e5.
4. Hope KJ, Jin L, Dick JE. Acute myeloid leukemia originates from a hierarchy of leukemic stem cell classes that differ in self-renewal capacity. *Nat Immunol*. 2004;5(7):738–743.
5. Ding Y, Gao H, Zhang Q. The biomarkers of leukemia stem cells in acute myeloid leukemia. *Stem Cell Investig*. 2017;4(3):19–19.
6. Taussig DC, Vargaftig J, Miraki-Moud F, et al. Leukemia-initiating cells from some acute myeloid leukemia patients with mutated nucleophosmin reside in the CD34- fraction. *Blood*. 2010;115(10):1976–1984.
7. Ishikawa F, Yoshida S, Saito Y, et al. Chemotherapy-resistant human AML stem cells home to and engraft within the bone-marrow endosteal region. *Nat Biotechnol*. 2007;25(11):1315–1321.
8. Angelini DF, Ottone T, Guerrera G, et al. A leukemia-associated CD34/CD123/CD25/CD99+ immunophenotype identifies *FLT3*-mutated clones in acute myeloid Leukemia. *Clinical Cancer Research*. 2015;21(17):3977–3985.
9. Travaglini S, Angelini DF, Alfonso V, et al. Characterization of *FLT3*-ITD^{mut} acute myeloid leukemia: molecular profiling of leukemic precursor cells. *Blood Cancer J*. 2020;10(8):.
10. Travaglini S, Ottone T, Angelini DF, et al. CD99 as a novel therapeutic target on leukemic progenitor cells in *FLT3*-ITD^{mut} AML. *Leukemia*. 2022;36(6):1685–1688.

BEST ABSTRACTS

B01

INFLAMMATION SHAPES THE TRANSCRIPTIONAL LANDSCAPE OF THE BONE MARROW MICROENVIRONMENT IN POST-TRANSPLANTATION LEUKEMIA RELAPSES

P.E. Rovatti^{1,2}, M. Punta^{1,3}, G. Orofino^{1,2,4}, M.M. Naldini⁵, M.G. Carrabba⁴, M. Bernardi⁴, J. Peccatori⁴, B. Gentner^{4,5}, F. Ciceri^{2,4}, L. Vago^{1,2,4}, C. Toffalori^{1,2}

¹Unit of Immunogenetics, Leukemia Genomics and Immunobiology, Division of Immunology, Transplantation and Infectious Disease, IRCCS San Raffaele Scientific Institute; ²San Raffaele Vita-Salute University; ³Unit of Immunogenomics, Center for Omics Sciences, IRCCS San Raffaele Scientific Institute; ⁴Unit of Hematology and Bone Marrow Transplantation, IRCCS San Raffaele Scientific Institute; ⁵Translational Stem Cell and Leukemia Unit, San Raffaele Telethon Institute for Gene Therapy (SR-TIGET), IRCCS San Raffaele Scientific Institute, Italy

Introduction. Allogeneic Hematopoietic Cell Transplantation (allo-HCT) represents the most successful therapeutic option for many patients with Acute Myeloid Leukemia (AML). Nevertheless, leukemic cells often find means to evade control from the donor-derived immune system and re-emerge, such as by reducing antigen presentation or by dampening effector responses via inhibitory checkpoint molecules. Here we investigate how immune subsets from the bone marrow microenvironment (TME) are rewired upon relapse.

Methods. We leveraged on single-cell RNA-sequencing (scRNA-seq) to detail the quantitative and qualitative changes that occur in the bone marrow of patients at AML relapse after allo-HCT. By 10x 5'-sequencing were profiled: 145,420 cells from 25 AML patients with different mechanisms of leukemia relapse, including downregulation of HLA class II (n=5), upregulation of inhibitory ligands (n=4), and genomic loss of incompatible HLAs, "HLA loss" (n=10); 56,831 cells from 5 post-transplant patients in complete remission (CR), at two timepoints (+90 and +365 days) and 45,279 cells from 6 healthy controls (HC).

Results. First, we were able to recapitulate the distinguishing features of each relapse modality. Moreover, combining genotype and Copy Number Variation (CNV) inference algorithms, malignant cells were separated from their healthy counterparts. Interestingly, HLA loss relapses exhibited a more immature profile, with a significantly high leukemia stem cell signature (LSC17) (P<0.0001), hinting that the hematopoietic cell of origin impacts on the type of post-HCT relapse. AML cells also featured a high inflammation-associated gene score (iScore), as also evident in non-malignant HSPCs from relapsed patients, which showed an increased IFN α signature compared to HC and CR. However, AML samples that couldn't be categorized by a known mechanism of relapse displayed a significantly lower iScore, suggesting that escape in these patients might not have had an immune-related driver. In parallel, we annotated CD56^{dim} and CD56^{bright} Natural Killer (NK) cell clusters, confirming at a transcriptional level an inverse correlation between the percentage of CD56^{bright} NK cells and time to transplantation. Moreover, we observed a smaller subset of immature CD56^{bright} NK cells with high expression of IFN-related genes and exhaustion markers, defined as inflamed NK. This cluster was more represented in patients with upregulation of T cell inhibitory ligands compared to other relapsed ones (5.97% vs 0.91%, adjusted P<0.05, respectively), suggesting a shared mechanism of dysfunction between T and NK cell that may favor leukemia immune evasion

Conclusions. Findings from this study provide new insights on

how leukemic cells exploit their TME to escape immune surveillance in the different patients, and identify new subsets and phenotypes that may be targeted for personalized therapeutic approaches.

B02

DECIPHERING GENETIC SIGNATURES ASSOCIATED WITH OUTCOMES TO ERYTHROPOIESIS STIMULATING AGENTS IN LOWER RISK MYELODYSPLASTIC NEOPLASMS, A MULTICENTRIC EUROPEAN STUDY

M.G. Raddi¹, A. Consagra¹, L. Rigodanza¹, C. Amato¹, A. Sanna², G. Mattiuz¹, S.J.M. De Pourcq¹, E. Tofacchi¹, M. Diez Campelo³, J.C. Berrocal⁴, S. Park⁵, M. Meunier⁵, C. Orlando⁵, M. Fontenay⁶, O. Kosmider⁶, N. Chapuis⁶, M. Sebert⁷, L. Adès⁷, U. Platzbecker⁸, K. Atharina Zoldan⁸, A. Kubasch⁸, V. Santini¹

¹MDS Unit, DMSC, AOU Careggi, University of Florence; ²AOU Careggi, Hematology department; ³Hospital Universitario de Salamanca; ⁴Hospital Clínico de Valladolid; ⁵Grenoble Alpes Hospital, University Grenoble Alpes, Hematology Department, Team Epigenetics regulation, Institute for Advanced Biosciences; ⁶Université Paris Cité and Assistance Publique-Hôpitaux de Paris. Centre, Hôpital Cochin, Laboratory of Hematology; ⁷Institut de Recherche Saint-Louis (IRSL), Université Paris Cité, Clinical Hematology Departments, Saint-Louis Hospital, Assistance Publique-Hôpitaux de Paris; ⁸Department of Hematology, Cellular Therapy, Hemostaseology and Infectious Diseases, University Medical Center Leipzig

Introduction and aim. Myelodysplastic neoplasms (MDS) are genetically heterogeneous myeloid disorders defined as lower risk (LR-MDS) by an IPSS-R score below 3.5. Anemia is the most common cytopenia of LR-MDS and it is primarily treated with erythropoiesis stimulating agents (ESAs) when sEPO is <200mU/mL. However, primary resistance occurs in around 40% of eligible LR-MDS patients. Genes recurrently mutated in MDS are integrated into new classificatory (WHO and ICC both published in 2022) and prognostic systems (IPSS-M). Despite studies trying to validate these molecular models, their application does not currently guides treatment. In this study, we investigated the role of mutations and IPSS-M in determining ESA response in a large European cohort (Italy, France, Spain, Germany), focusing on specific molecular subgroups.

Methods. Baseline mutations of 483 LR-MDS were evaluated from 15 different European centers with next generation sequencing panels (t-NGS). Next, we correlated genetic MDS groups per latest WHO and IPSS-M with ESA response assessed by IWG criteria and performed hierarchical clustering analysis based on mutations and Log2(VAF) of common genes (n=32).

Results. BM blasts, sEPO, transfusion dependence (TD), IPSS-R and IPSS-M, but not mutations number, correlated with ESA response (Table 1). MDS SF3B1 cases (n=166) were more often TD compared to the rest of MDS (58% vs 49.2% respectively, p=0,004), however both sEPO and ORR were similar (mean 61,6 vs 78,09 mU/mL, and 58% vs 56,5%). 5,4% had mono- (n=21) or bi- (n=6) allelic inactivation of TP53 without BM blasts increase nor complex karyotype and had an ORR of 62 and 66% respectively, both higher than ORR of MDS TP53WT (56%, p=0,056 and 0,047). Responders had more frequently 0-2 mutations mostly occurring in DNMT3A, ASXL1, TET2 (DAT genes) at low VAF and were more often females with low sEPO. Non-responders were more frequently U2AF1 or EZH2 mutated male cases presenting with TD, despite lower sEPO. Finally, isolated ZRSR2 and IDH2 \pm SF3B1 mutations also characterized non-responders (Figure 1).

Conclusions. Our study highlights the importance of mutations in ESA response and their correlations with sEPO and TD. IPSS-M score, evaluating the prognostic weight of single mutations, shows a

strong correlation with response, unlike the number of mutations. MDS SF3B1 response was comparable to other categories, while MDS with TP53 inactivation seems to have better ORR in case of not advanced disease, likely due to the anti-apoptotic effect of TP53 loss. No or isolated mutations linked to clonal hematopoiesis (DAT) are associated with better ESA outcomes, while non-SF3B1 splicing mutations together with IDH2 and EZH2 characterize resistant cases irrespective of sEPO levels. Integrating molecular information might thus serve as a valuable tool to guide future treatment beyond sEPO levels, especially in the era of emerging therapies for the frontline setting like luspatcept.

Table 1.

Table 1. Study population characteristics according to ESA response. ESA = erythropoiesis stimulating agents, Hb = hemoglobin, BM = bone marrow, sEPO = serum erythropoietin, TD = transfusion-dependent (*transfusion history available for 332/483 cases). VL = very low, L = low, I = intermediate, ML = moderate low, MH = moderate high, H = high, VH = very high.

Parameter (unit)	ESA responders n=273 (56.2%)	ESA non-responders n=210 (43.8%)	p
Age (yrs)	75.2 ± 10.26	72.7 ± 11.16	ns
Male	140 (51.3)	120 (57.1)	
Female	133 (48.7)	90 (42.9)	
Hb (g/dL)	9.7 ± 1.35	9.38 ± 1.3	ns
Ferritin (ng/mL)	480 ± 431	690.7 ± 1202	ns
BM blasts (%)	2 ± 1.9	1.97 ± 2.1	0.037
sEPO (mU/mL)	119.3 ± 218.26	262.2 ± 394.7	<0.0001
TD per IWG*	79 (44)	94 (63.5)	0.004
IPSS-R score	2.14 ± 0.9	2.54 ± 0.94	<0.0001
VL	64 (23.7)	33 (16)	
L	178 (65.9)	125 (60.7)	
I	28 (10.4)	48 (23.3)	
IPSS-M score	-0.9 ± 0.75	-0.5 ± 0.87	<0.0001
VL	58 (21.6)	18 (8.7)	
L	147 (54.9)	109 (52.9)	
ML	31 (11.7)	33 (16)	
MH	17 (6.3)	21 (10.3)	
H	13 (4.8)	20 (9.7)	
VH	2 (0.7)	5 (2.4)	

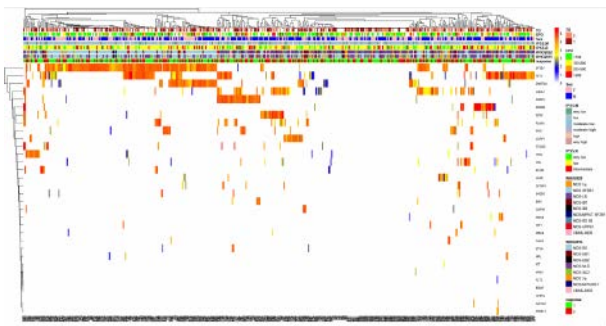


Figure 1. Genetic clusters of 483 LR-MDS. Hierarchical clustering analysis was based on 32 genes and corresponding $\text{Log}_2(\text{VAF})$ and was correlated with ESA response, WHO classifications, IPSS-R and IPSS-M categories, sex, EPO levels and transfusion dependence (TD).

B03

PREVALENCE AND CLINICAL IMPACT OF CLONAL HEMATOPOIESIS OF INDETERMINATE POTENTIAL (CHIP) IN CHRONIC LYMPHOCYTIC LEUKEMIA

C. Cosentino, D. Talotta, M. Almasri, S. Mouhssine, R. Dondolin, M. Bellia, S. Rasi, E. Secomandi, S. Kogila, J. Ghanej, G. Gaidano, R. Moia

Division of Hematology, Department of Translational Medicine, Università del Piemonte Orientale, Italy

Introduction. Clonal Hematopoiesis of Indeterminate Potential (CHIP) is an aging-related condition characterized by the accumulation of somatic mutations in hematopoietic stem cells (HSCs). CHIP is defined as the presence of mutations in myeloid genes with a variant allele frequency (VAF) of at least 2%. The most frequently mutated genes include *DNMT3A*, *TET2*, and *ASXL1*, which provide a fitness advantage to HSCs. CHIP is associated with a variety of different diseases but its role in the pathogenesis and prognosis of lymphoid neoplasms remains unclear.

Methods. Tumor genomic DNA were extracted from granulocytes from CLL patients (N=271) referring at our institution. Samples were analyzed by targeted next-generation sequencing (NGS), employing a custom panel of recurrently mutated genes in CHIP (N=28) and sequenced by MiSeq and NextSeq550 platforms (Illumina). Statistical analyses were performed using R studio and SPSS software v24.

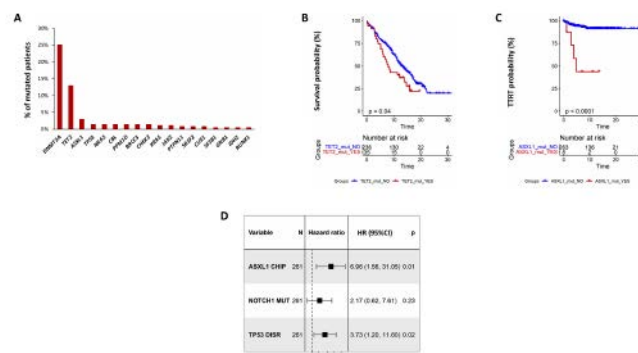


Figure 1.

Results. The median age at diagnosis was 69,1 years, 152 patients (56,1%) were male and 119 (43,9%) were female. The median lymphocyte count was $9,2 \times 10^3/\mu\text{L}$, median Hb level was 13,8 g/dL, and median PLT count was $207 \times 10^3/\mu\text{L}$. A total of 123 (43,4%) patients showed at least 1 CHIP mutation. The most frequently mutated genes were *DNMT3A* in 68 (25,0%) patients, followed by *TET2* in 35 (12,9%) and *ASXL1* in 8 (2,9%) (Figure 1A). As expected, the presence of at least 1 CHIP mutation significantly correlated with older age ($p=0,004$). The potential clinical impact of CHIP in terms of overall survival (OS) and time to first treatment (TTFT) was investigated. At the current follow-up, no differences in OS and TTFT were observed between CHIP+ and CHIP- patients. By analyzing the clinical impact of individual CHIP genes, however, *TET2* mutated patients showed a decreased OS compared to *TET2*-wild type patients ($p=0,04$) (Figure 1B). The potential contribution of CHIP in Richter transformation (RT) was also assessed. At the current follow-up, 22 patients experienced RT and the presence of any CHIP mutations did not correlate with a reduced time to Richter transformation (TRT). Conversely, by analyzing the impact of each gene, *ASXL1*-mutated patients showed a shorter TRT compared to those with wild-type *ASXL1* ($p<0,0001$) (Figure 1C). Remarkably, in mul-

tivariate analysis *ASXL1* mutations maintained an independent association with shorter TTRT (HR 6,96, 95% CI 1,56-31,05, $p=0,01$) when adjusted for *TP53* disruption and *NOTCH1* mutations (Figure 1D). Subsequently, the clonal evolution of CHIP following therapy was assessed. This longitudinal analysis showed that chemoimmunotherapy (CIT) lead to an increase in the number of CHIP mutations and in an increase in the VAF of pre-existing mutations ($p=0,004$).

Conclusions. This study suggests that CHIP may harbor potential clinical relevance in CLL and in Richter transformation. Molecular analysis in sorted myeloid cells and CLL cells is ongoing to evaluate the interplay between CHIP and CLL.

B04

INVESTIGATING THE FUNCTIONAL AND CLINICAL IMPACT OF CLONAL HEMATOPOIESIS OF INDETERMINATE POTENTIAL IN MULTIPLE MYELOMA PATHOGENESIS

M. Lionetti¹, M. Scopetti¹, A. Matera², A. Maeda¹, A. Marella², F. Lazzaroni¹, G. Castellano¹, S. Fabris¹, S. Pioggia¹, S. Lonati², A. Cattaneo³, M. Tornese³, C. De Magistris^{1,2}, L. Pettine¹, M.C. Da Vià¹, F. Passamonti^{1,2}, N. Bolli^{1,2}

¹Hematology Unit, Fondazione IRCCS Ca' Granda Ospedale Maggiore Policlinico di Milano; ²Department of Oncology and Hemato-Oncology, University of Milan; ³Flow Cytometry Laboratory, Clinical Pathology Unit, Fondazione IRCCS Ca' Granda Ospedale Maggiore Policlinico di Milano, Italy

Introduction. Multiple myeloma (MM) is a plasma cell (PC) malignancy whose progression is driven by genetic and phenotypic features of different cell subpopulations and changes in the tumor microenvironment (TME). Clonal hematopoiesis of indeterminate potential (CHIP) refers to hematopoietic stem cells' clonal expansion supported by somatic mutations in leukemia-driver genes in otherwise healthy individuals. In MM, the presence of CHIP has been associated with poorer clinical outcomes after autologous transplant, partially mitigated by IMiD maintenance.

Methods. To evaluate the potential interrelationships between MM and CHIP we assessed by targeted DNA NGS the prevalence and clinical correlates of CHIP in peripheral blood of 40 prospectively collected newly diagnosed MM patients, 7 of whom also sampled after induction therapy. Furthermore, to assess possible CHIP-induced changes in TME we performed single cell RNA-seq (scRNA-seq) in non-malignant bone marrow (BM) cells from 4 CHIP-pos and of 4 CHIP-neg cases.

Results. We identified 14 CHIP mutations in 22.5% of the cohort at diagnosis. The most frequently mutated genes were TET2, ASXL1 and SF3B1. In 1 patient a branching evolution pattern of CHIP mutations was found, with loss of a subclone and gain of a novel one while on lenalidomide treatment. We found significant correlations between CHIP and higher R-ISS stage. Noticeable trends for lower hemoglobin levels, higher β 2-microglobulin and increased BM PC infiltration were observed in CHIP carriers. Adverse clinical outcomes, including cytopenias at diagnosis and after treatment, and CD34+ cells yield after mobilization for transplant were similar between carriers and non-carriers. ScRNA-seq of 34.283 non-malignant BM cells from 8 cases revealed notable differences in the composition of TME between CHIP-pos and CHIP-neg. Specifically, there was a significant increase in regulatory T cells and a trend towards decreased levels of naïve CD8+/CD4+ T cells in CHIP carriers. These composition changes were accompanied by increased expression of cytotoxic and exhaustion markers (e.g. LAG3, TIGIT, and XCL2) in effector T cells of CHIP+ pts. This exhaustion of T cell compartment could have an impact on T cell engagers

immunotherapy. Additionally, we observed an increase in RBC progenitors, potentially indicating ineffective hematopoiesis. Furthermore, CHIP+ CD14+/CD16+ monocytes exhibited a significant upregulation of MHC class II genes. Pathway analysis indicated increased activation of IFN α/γ responses, as well as pro-inflammatory cytokine signaling pathways in activated monocytes and T cell subsets from CHIP carriers.

Conclusions. Our study provided valuable insights into the clinical implications of CHIP in MM. ScRNA-seq revealed a pro-inflammatory TME in CHIP patients, with potential for immune dysregulation similar to what observed in advanced MM. Our results also have potential implications for response prediction of novel immunotherapies.

B05

THE INTEGRATION OF GENOMIC AND TRANSCRIPTOMIC DATA IMPROVES CLINICAL OUTCOME PREDICTION IN MYELODYSPLASTIC SYNDROMES

E. Sauta¹, M. Zampini¹, C. Sala², D. Dall'olio², L. Lanino¹, S. D'amico¹, G. Asti¹, C.A. Tentori¹, G. Maggioni¹, L. Dall'olio³, E. Mosca⁴, M. Ubezio¹, A. Campagna¹, E. Riva¹, M. Bicchieri¹, V. Savevski¹, A. Santoro^{1,5}, S. Kordasti⁶, V. Santini⁷, M.D. Campelo⁸, A.S. Kubasch⁹, U. Platzbecker⁹, P. Fenaux¹⁰, L. P. Zhao¹⁰, A.M. Zeidan¹¹, T. Haferlach¹², G. Castellani², M.G. Della Porta^{1,5}

¹Humanitas Clinical and Research Center IRCCS; ²Department of Experimental, Diagnostic and Specialty Medicine, DIMES; ³Data Science and Bioinformatics Laboratory, IRCCS, Institute of Neurological Sciences; ⁴Institute of Biomedical Technologies, National Research Council (CNR); ⁵Department of Biomedical Sciences, Humanitas University; ⁶Haematology, Guy's Hospital & Comprehensive Cancer Centre, King's College; ⁷Azienda Ospedaliero-Universitaria Careggi; ⁸Hematology Department, Hospital Universitario de Salamanca; ⁹Medical Clinic and Policlinic 1, Hematology and Cellular Therapy, University Hospital; ¹⁰Department of Hematology and Bone Marrow Transplantation, Hôpital Saint-Louis/Assistance Publique-Hôpitaux de Paris; ¹¹Section of Hematology, Department of Internal Medicine, Yale School of Medicine and Yale Cancer Center; ¹²MLL Munich Leukemia Laboratory

Introduction. Myelodysplastic syndromes (MDS) comprises a heterogeneous group of myeloid malignancies characterized by ineffective hematopoiesis, genetic instability, and risk of progression to acute myeloid leukemia (AML). Their heterogeneity in clinical courses makes prognostic stratification of crucial importance in clinical decision making. Recently, the genomic screening integration (by Molecular International Prognostic Scoring System, IPSS-M) into patient assessment has significantly improved clinical outcomes prediction compared to the conventional prognostic score (Revised IPSS, IPSS-R). Evaluating the prognostic impact of integrating additional -omics data with the clinical information may facilitate their inclusion within current MDS classification systems, leading to an individual risk assessment and tailored treatment decisions. The aim of this study led by GenoMed4All and Synthema EU consortia is to link genomic and transcriptomic data to enhance the accuracy of clinical outcomes prediction in MDS patients.

Methods. Clinical, cytogenetic, genomic (somatic mutations screening of 31 target genes) and transcriptomic (bulk RNA-seq of CD34+ bone marrow cells) data were collected at diagnosis from 389 MDS patients. Transcriptomic and genomic profiles were processed and analyzed using dimensionality reduction techniques to mine the interdependency of recurrent genomic alterations and gene expression perturbation. Prognostic impacts of cytogenetic, transcriptomic, genomic, clinical and demographic features were assessed

using a penalized Cox's proportional hazards model [Gerstung M et al, Nat. Commun. 2015] focusing on Overall Survival (OS). A five-fold cross-validating (CV) scheme controlled risk estimation bias, with model accuracy evaluated by Harrell's C-index. Independent validation on 202 patients was planned.

Results. Each data layer was processed, uninformative variables removed and quantitative ones scaled. Selected features included recurrent genomic and cytogenetic abnormalities, platelets, hemoglobin, bone marrow blasts, age and sex as covariates, 20 principal components (explaining 42% of the total transcriptomic variability). Our integrative model achieved a predictive accuracy of 0.83 for OS, with a marked improvement to the conventional IPSS-R (0.68) and IPSS-M (0.76) scores. Analyzing the contribution of each feature data category to the OS probability (Figure 1), the relative impact in term of explained variance is 40% for transcriptomics, 24% for genomic and cytogenetic features, 20% and 15% for demographics and clinical features. Independent validation is currently underway.

Conclusions. The integration of genomic, transcriptomic, and diagnostic clinical variables effectively enhances clinical outcome prediction in MDS patients, as demonstrated by the improved C-index. Risk stratification can be further refined using additional –omic layers that we are currently testing through advanced multimodal techniques.

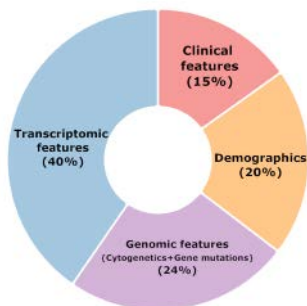


Figure 1.

B06

MYELOID NEOPLASM-ASSOCIATED GENE MUTATIONS DO NOT PREVENT CLINICAL AND MOLECULAR RESPONSE TO ROPEGINTERFERON IN THE LOW-PV STUDY

P. Guglielmelli, A. Carobbio, A. Ghirardi, G. Carioli, F. Gesullo, F. Vanderwert, E. Rossi, A. Masciulli, F. Ciceri, M. Bonifacio, A. Iurlo, F. Palandri, G. Benevolo, F. Pane, A. Ricco, G. Carli, M. Caramella, D. Rapezzi, C. Musolino, S. Siragusa, E. Rumi, A. Patriarca, N. Cascavilla, B. Mora, E. Cacciola, G.G. Loscocco, S. Betti, F. Lunghi, L. Scaffidi, C. Bucelli, N. Vianelli, M. Bellini, M.C. Finazzi, G. Tognoni, V. De Stefano, A. Rambaldi, T. Barbui, A.M. Vannucchi

¹CRIMM, Center for Research and Innovation of Myeloproliferative Neoplasms, AOU Careggi, University of Florence; ²FROM Research Foundation Ospedale di Bergamo; ³Hematology unit, Dep. of Radiological and Hematological Sciences, Catholic University, Fondazione Policlinico A Gemelli, IRCCS; ⁴Università Vita-Salute San Raffaele and Istituto di Ricovero e Cura a Carattere Scientifico Ospedale San Raffaele, Dep. of Onco-Hematology; ⁵Department of Medicine, Section of Hematology, University of Verona and Azienda Ospedaliera Universitaria Integrata; ⁶Hematology Division, Fondazione IRCCS Ca' Granda Ospedale Maggiore Policlinico; ⁷IRCCS Azienda Ospedaliera Universitaria di Bologna, Istituto di Ematologia "Seragnoli"; ⁸Hematology Division, Città della Salute e della

Scienza Hospital; ⁹Azienda Ospedaliera Universitaria Federico II; ¹⁰Hematology and Stem Cell Transplantation Unit, AOUC Policlinico; ¹¹Hematology Department, Ospedale San Bortolo; ¹²Department of Hematology, ASST Grande Ospedale Metropolitano Niguarda; ¹³S. C. Ematologia, ASO S. Croce e Carle; ¹⁴Divisione di Ematologia - Policlinico Universitario; ¹⁵Department of Health Promotion, Mother and Child Care, Internal Medicine and Medical Specialties (PRO. MI. SE), University of Palermo; ¹⁶Department of Molecular Medicine, University of Pavia; ¹⁷Azienda Ospedaliera Universitaria Maggiore della Carità di Novara SCU Ematologia; ¹⁸Division of Hematology, IRCCS Casa Sollievo Della Sofferenza Hospital; ¹⁹Hematology, University Hospital "Ospedale di Circolo e Fondazione Macchi" - ASST Sette Laghi, University of Insubria; ²⁰Hemostasis/Hematology Unit, Dep. of Medical, Surgical and Advance Technologies Sciences "G. . F. Ingrassia", University of Catania, Italy

Background. The Low-PV phase II randomized trial (NCT030030025) tested the safety and efficacy of Ropeginterferon alfa-2b (Ropeg) versus phlebotomy-only (standard therapy, STD) in low-risk patients (pts) with polycythemia vera (PV), with crossover to Ropeg at 1y in non-responders. The composite primary endpoint (maintaining median HCT values $\leq 45\%$ over 12 mo, in the absence of progressive disease was achieved in 81% ropeg vs 51% s in STD arm; superiority (83% vs 59%) was confirmed at 2yr (study extension). Aim. To study the impact of mutations in myeloid neoplasm-associated genes (myelo) on the achievement of primary response and JAK2V617F molecular response in the Low-PV study.

Methods. JAK2V617F VAF was determined by droplet PCR in granulocytes at baseline (BL), at study endpoint (1y) and at 2y. A panel of 27 myelo genes were sequenced by NGS at BL and 2y. Germline polymorphisms at interferon lambda 4 locus (IFNL4) were evaluated by real-time PCR. Partial molecular response (PMR) was defined according to ELN criteria.

Results. At baseline (BL) and 1y, samples were available for 99 pts, 45 randomized to STD and 54 to Ropeg arm; 44 samples were available at 2y, 27 Ropeg and 11 pts crossed over to Ropeg (STD>Ropeg). Mutated myelo genes at BL was TET2 (28.7%), DNMT3A (14.8%), ASXL1 (7%), SH2B3 (3.2%); other mutations occurred in 2 (IDH1, RUNX1, SETBP1, CSF3R) and 1 pt (SF3B1, CUX1, CBL, PTPN11, TP53, ZRSR2). At least 1 mut myelo gene was found in 37.9% STD and 42. 6% Ropeg pts; 2 pts in each arm (0.4%) had 2 mutations. At 2y, an additional mut myelo gene was acquired by 14. 8% Ropeg arm and 16. 2% STD>Ropeg. Disappearance of a BL mut myelo gene was observed in 2 pts (1 in each group). As concerned the attainment of study primary endpoint, 17/43 Ropeg pts with >1 myelo mut gene (73. 9%) obtained endpoint as compared to 26/43 (86. 7%) without mutation (p=0.20); at 2y, figures were 63.6% vs 73. 3% (p=0.33). The primary endpoint at 1y, and maintained at 2y, was also achieved by 4 Ropeg pts who acquired new variant from BL and in 1 of 2 STD>Ropeg pts. Mean JAK2V617F VAF reduced from 39.0 ± 25.4 to 28.7 ± 22.4 in Ropeg arm (p<0. 01) at 1y, and to 17.3 ± 18.9 (p<0. 001) at 2y. As regarded the impact of BL mut myelo genes on achievement of PMR at 1y, 28. 6% mutated pts in ropeg arm achieved PMR vs 39. 3% without mut myelo (p=0.31). Figures at 2y were 42. 9% PMR vs 52.3% (p=0.42). Finally, we examined the impact of 2 germline SNPs at IFNL4 locus, rs368234815/rs117648444, previously reported to affect molecular response to Ropeg. However, we found no correlation between each single SNP or diplotype SNPs and molecular response at 1y and 2y in Low-PV pts.

Conclusions. In pts enrolled in the Low-PV trial, presence of any mutation(s) in myeloid-neoplasm associated genes did not prevent achievement of study primary endpoint nor of JAK2V617F partial molecular remission.

B07

LONG-TERM OUTCOME OF A LARGE COHORT OF PATIENTS WITH ACUTE PROMYELOCYTIC LEUKEMIA FROM THE HARMONY PROJECT

L. Guarnera^{1,2}, S. Lehmann³, K. Döhner⁴, H. Döhner⁴, U. Platzbecker⁵, N.H. Russell⁶, R. Dillon⁷, I. Thomas⁸, G. Ossenkoppele⁹, M. Vignetti¹⁰, E. La Sala¹⁰, A. Piciocchi¹⁰, A. Villaverde Ramiro¹¹, L. Tur¹², C. Gurnari^{1,2}, L. Bullinger¹³, J.M. Hernández-rivas¹⁴, M.T. Voso^{1,15}.

¹Department of Biomedicine and Prevention, University of Rome "Tor Vergata"; ²Department of Translational Hematology and Oncology Research, Taussig Cancer Institute, Cleveland Clinic; ³Department of Medical Sciences, Hematology, Uppsala University, University Hospital Uppsala; ⁴Department of Internal Medicine III, University Hospital of Ulm; ⁵Medical Clinic and Policlinic I, Hematology and Cellular Therapy, University Hospital Leipzig; ⁶Guy's & St Thomas' NHS Foundation Trust; ⁷Guy's Hospital and King's College; ⁸Cardiff University; ⁹Department of Hematology, Amsterdam UMC location Vrije Universiteit Amsterdam; ¹⁰GIMEMA Foundation, Data Center and Health Outcomes Research Unit; ¹¹University of Salamanca, IBSAL, IBMCC, CSIC, Cancer Research Center, Department of Hematology - Hospital Universitario de Salamanca; ¹²GMV Innovating Solutions; ¹³Department of Hematology, Oncology, and Cancer Immunology, Charité – Universitätsmedizin Berlin, corporate member of Freie Universität Berlin, Humboldt Universität zu Berlin, and Berlin Institute of Health; ¹⁴Institute of Biomedical Research of Salamanca (IBSAL); ¹⁵Neuro-Oncohematology Unit, Istituto di Ricovero e Cura a Carattere Scientifico (IRCCS) Fondazione Santa Lucia, Italy

Introduction. Acute promyelocytic leukemia (APL), is now curable in 75-90% of patients using targeted agents [All-transretinoic acid (ATRA)/Arsenic Trioxide (ATO) or ATRA combined with chemotherapy (ATRA+Idarubicin, AIDA-based)]. Despite significant advances, many questions remain unanswered, such as the optimal setting of chemo-free regimens and the prevention of long-term relapses.

Methods. We analyzed a large cohort of newly diagnosed patients with APL included in the HARMONY Platform (derived from APL0406 and AML17 clinical trials, and Study Alliance Leukemia, Swedish Cooperative Group or AML study Group registries). After acquisition from the sources, data were harmonized and transformed using an Observational Medical Outcomes Partnership Common Data Model, and registered in the HARMONY Platform.

Results. Of 1296 patients (pts), 562 were treated with ATRA-ATO (median age 51y, range 16-94; M 50%), and 605 with AIDA (median age 50y, range 17-86; M 50% ratio 1). 250 pts (44%) were low-risk (LR) according to Sanz risk score, 258 (46%) intermediate-risk (IR), and 50 (9%) high-risk (HR) in the ATRA-ATO cohort. The AIDA cohort included 191 LR (31.5%), 235 IR (39%), and 171 HR (28%) pts (p for risk groups according to treatment <0.001). Treatment data not available in 8 pts (1%). The 10-year overall survival (OS) was 90% and 77% in ATRA-ATO vs AIDA cohorts, respectively (p<0.001, Figure 1), while event-free survival (EFS) was 86% and 67%, respectively (p<0.001). At a median follow-up of 4.5 y (range 0.02–10.2), OS and EFS in pts treated with ATRA-ATO was consistent across the three Sanz-risk classes (OSI LR 95%, IR 91%, HR 86%, p=0.233, EFSI LR 93%, IR 89%, HR 86%, p=0.319). Pts treated with AIDA, at a median follow-up of 6y (range 0-14.2) presented an OS of 88% in LR, 83% in IR, and 75% in HR (p=0.004), while EFS was 72% in LR, 75% in IR, and 67% in HR (p=0.102). Age was significantly correlated with OS and EFS both p<0.001). Pts treated outside the clinical trial context had inferior outcomes when compared to clinical trials in both AIDA (8-year OSI 74% vs 88%, p<0.001, EFSI 69% vs 72%, p=0.291) and ATRA-ATO cohorts (8-year

OSI 88% vs 93%, p=0.010, EFSI 81% vs 92%, p<0.001). The multivariate analysis for OS showed that age (50-69 vs <50 y, p<0.001, HR4.2; >70 vs <50y p<0.001, HR8.9), Sanz-risk score (High vs Low/Intermediate p<0.001, HR2), treatment type (AIDA vs ATRA-ATO p=0.001, HR1.9) and treatment context (clinical trial vs non-clinical trial p=0.005, HR1.7) were independent predictors of OS. The multivariate analysis for EFS showed an independent correlation with type of treatment (AIDA vs ATRA-ATO, p<0.001 HR2.6), age (50-69 vs <50 y, p<0.001, HR2.1; >70 vs <50y p<0.001, HR4.8) and Sanz-risk score (High vs Low/Intermediate p=0.005, HR1.5).

Conclusions. The analysis of the HARMONY APL registry at long-term, showed a survival advantage in pts treated with ATRA-ATO vs AIDA regimens, irrespective of Sanz-risk score

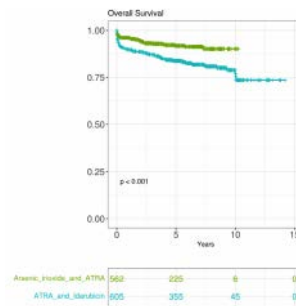


Figure 1. Overall survival of newly diagnosed APL patients according to treatment.

B08

TP53, NOTCH1/2 AND CD36 MUTATIONS PREDICT POOR OUTCOME IN MANTLE CELL LYMPHOMA; MOLECULAR ANALYSIS OF THE FIL V-RBAC PHASE 2 TRIAL

R. Moia¹, D. Talotta¹, C. Cosentino¹, M. Almasri¹, V. Tabanelli², G. Motta², F. Melle², M.V. Sacchi³, A. Evangelista⁴, I. Ferrarini⁵, M.C. Tisi⁵, A. Merli⁶, S. Fiori², A. Re⁷, C. Castellino⁸, V.R. Zilioli⁹, F. Piazza¹⁰, P. Corradini¹¹, S. Hohaus¹², G. Musuraca¹³, F.G. Rossi¹⁴, B. Puccini¹⁵, F. Cavallo¹⁶, F. Ballerini¹⁷, R. Sciarra¹⁸, A. Di Rocco¹⁹, A. Arcari²⁰, C. Boccomini²¹, F. Merli²², G. Gini²³, M. Tani²⁴, R. Bruna¹, V. Pavone²⁵, M. Ladetto²⁶, S. Galimberti²⁷, R. Bomben²⁸, I. Del Giudice¹⁹, S. Ferrero¹⁶, S. Pileri², M. Balzarotti²⁹, G. Gaidano¹, C. Visco³⁰

¹Division of Hematology, Department of Translational Medicine, Università del Piemonte Orientale; ²IEO, Istituto Europeo di Oncologia IRCCS - Haematopathology Division; ³Fondazione Italiana Linfomi, Onlus; ⁴Azienda Ospedaliera Città della Salute e della Scienza - Unit of Clinical Epidemiology; ⁵Hematology Unit, San Bortolo Hospital, AULSS 8 Berica; ⁶Ospedale degli Infermi di Rimini - U. O. di Ematologia; ⁷ASST Spedali Civili di Brescia - Ematologia; ⁸A. O. S. Croce e Carle - S. C. di Ematologia e Trapianto di Midollo Osseo; ⁹ASST Grande Ospedale Metropolitano Niguarda - SC Ematologia; ¹⁰AOU di Padova - Ematologia; ¹¹Fondazione IRCCS Istituto Nazionale dei Tumori di Milano - Ematologia; ¹²Fondazione Policlinico Universitario Agostino Gemelli IRCCS; ¹³IRCCS Istituto Romagnolo per lo studio dei Tumori "Dino Amadori" - IRST S. R. L. - Ematologia; ¹⁴Ospedale Maggiore Policlinico - Fondazione IRCCS Ca Granda - Ematologia; ¹⁵Azienda Ospedaliera Universitaria Careggi - Unit funzionale di Ematologia; ¹⁶Division of Hematology, University of Torino; ¹⁷Ospedale Policlinico San Martino S. S. R. L. - IRCCS per l'Oncologia - U. O. Clinica Ematologica; ¹⁸IRCCS Policlinico S. Matteo di Pavia - Div. di Ematologia; ¹⁹Policlinico Umberto I - Università "La Sapienza" - Istituto Ematologia - Dipartimento di Medicina Traslazionale e di Precisione; ²⁰Ospedale

Guglielmo da Saliceto - U. O. Ematologia; ²¹A. O. U. Città della Salute e della Scienza di Torino - S. C. Ematologia; ²²Azienda Unit Sanitaria Locale-IRCCS - Arcispedale Santa Maria Nuova – Ematologia; ²³AOU Ospedali Riuniti - Clinica di Ematologia; ²⁴Ospedale delle Croci – Ematologia; ²⁵A. O. C. Panico - U. O. C Ematologia e Trapianto; ²⁶A. O. SS. Antonio e Biagio e Cesare Arrigo - S. C. Ematologia; ²⁷Department of Clinical and Experimental Medicine, Section of Hematology, University of Pisa; ²⁸Clinical and Experimental Onco-Hematology Unit, CRO-Aviano National Cancer Institute, IRCCS; ²⁹Department of Medical Oncology and Hematology, Humanitas Clinical Research Hospital-IRCCS; ²⁹Department of Engineering for Innovation Medicine, Section of Hematology, University of Verona, Italy

Introduction. The FIL V-RBAC trial (EudraCT: 2017-004628-31) is a phase 2 study which enrolled patients with previously untreated mantle cell lymphoma (MCL), stratifying them at initial diagnosis depending on risk factors. Patients with high-risk (HR) features (defined as Ki67 \geq 30% and/or blastoid variant and/or TP53 disruption) were treated differently from standard risk patients (i.e. abbreviated course of R-BAC followed by consolidation and maintenance with venetoclax). The aim of the present project was to evaluate the prognostic role MCL gene mutations in patients enrolled in the FIL V-RBAC trial.

Methods. Patients enrolled in the V-RBAC trial with available gDNA extracted from lymph node biopsy were included in this mutational analysis. The CAPP-Seq assay including 146 genes relevant in MCL pathogenesis was used coupled with a robust and previously validated bioinformatic pipeline. The primary endpoint was progression-free survival (PFS) according to mutational pattern.

Results. Among the 140 patients enrolled in the V-RBAC trial, 96 were analyzed (41 high risk and 55 standard risk). The median age of analyzed patients was 72 years, 75% were male, 13.5% had the blastoid variant, and 29.2% had Ki67 \geq 30%. The median follow-up was 32.0 months. The prognostic markers of MCL, namely blastoid variant (HR 5.64, 95% CI 2.31-15.58, p<0.001), Ki67 \geq 30% (HR 3.35, 95% CI 1.41-7.95, p=0.006), and MIPI-c (HR 2.29, 95% CI 1.50-3.51, p<0.001) significantly associated with PFS. The mutational analysis recapitulated the mutational landscape of MCL and identified *ATM* as the most frequently mutated gene (51.0%, N=49), followed by *KMT2D* (20.8%, N=20), *TP53* (24.0%, N=23), *WHSC1* (14.6%, N=14), and *BIRC3* (11.5%, N=11) (Fig.1A). As expected, *TP53* mutations were significantly associated with an inferior PFS compared to *TP53* unmutated patients (2-years PFS 48.6% versus 89.1%, p<0.001). The clinical impact of *TP53* mutations was maintained in the HR group (i.e. patients receiving venetoclax consolidation and maintenance). Among the other genes analyzed, *NOTCH1/2* mutations, and *CD36* mutations were significantly associated with inferior PFS. Importantly, *NOTCH1/2* and *CD36* mutations independently predicted shorter PFS when adjusted for *TP53* mutations (Figure 1B). Overall, *NOTCH1/2* and/or *CD36* mutated patients presented a poor outcome superimposable to *TP53* mutated cases (Figure 1C). Among standard risk patients, *ATM* mutations were associated with excellent outcome with a 2-years PFS of 100% versus 84.0% in unmutated standard risk patients (p=0.017). Non-negative matrix factorization based on gene mutations identified 4 different clusters characterized by different molecular composition and with clinical relevance (Figure 1A,D).

Conclusions. Initial evidence from the molecular analysis of the FIL V-RBAC trial suggests that *TP53*, *NOTCH1/2* and *CD36* mutations identify MCL patients with unfavorable outcomes.

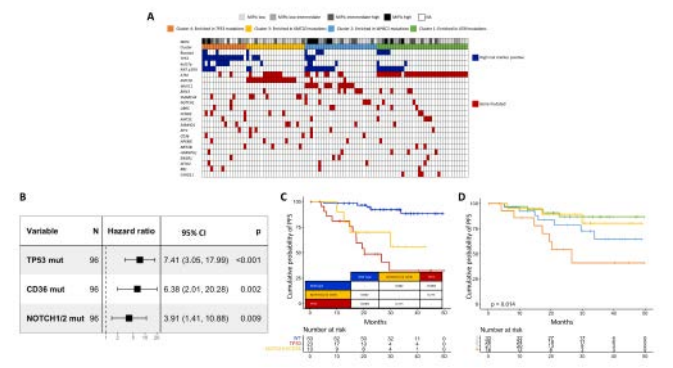


Figure 1.

ORAL COMMUNICATIONS

Acute Leukemias 1

C01

FUNCTIONAL OMICS IN HIGH-RISK T-CELL ACUTE LYMPHOBLASTIC LEUKEMIA

M. Giaimo^{1,2,3}, L. Pagliaro^{1,2,3}, R. Zamponi^{1,2}, L. Moron Dalla Tor^{1,2}, K. Tragni², A. Montanaro^{1,2}, B. Cambò³, M. Messina⁴, V. Bardelli⁵, R. La Starza⁵, C. Mecucci⁵, G. Roti^{1,2,3}

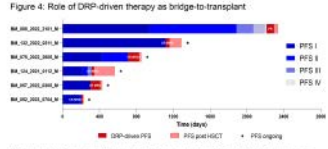
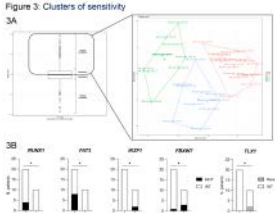
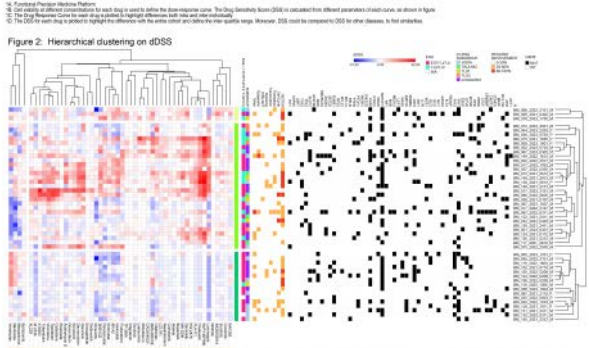
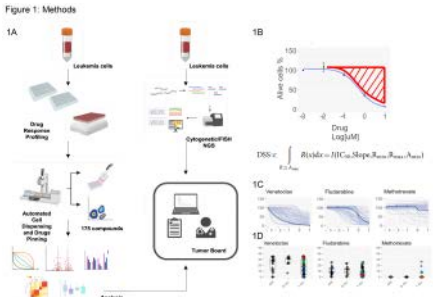
¹Department of Medicine and Surgery, University of Parma; ²Translational Hematology and Chemogenomics Laboratory, University of Parma; ³Department of General and Specialist Medicine, Complex Operational Unit of Hematology and Hematopoietic stem cell transplant, AOU of Parma; ⁴GIMEMA Foundation; ⁵Department of Medicine and Surgery, Cytogenetics and Molecular Medicine Laboratory, University of Perugia, Italy

Introduction. Acute lymphoblastic leukemia (ALL) has seen improvements in prognosis over the last decades. However certain subgroups like T-ALL, still present an unmet clinical need due to their poor prognosis and the absence of alternative therapies (tx) for relapsed/refractory (RR) patients (pts). A promising strategy involves functional precision medicine (FPM), which relies on information obtained through *ex-vivo* chemogenomic profiling. Our study aims to develop a chemogenomic FPM platform for identifying new actionable targets and guiding tx.

Table 1. Patients' characteristics.

	Patient cohort (n = 45)
DRP available	48
Age	
Median	41
Range	14-74
Sex (%)	
Male	33 (73.3)
Female	11 (24.4)
N/A	1 (2.2)
M:F ratio	3:1
Disease status at DRP (%)	
Diagnosis	11 (22.9)
Relapse/Refractory	37 (77.1)
Number of Prior lines (%)	
Median	2
Range	0-6
1	11 (22.9)
2	9 (18.8)
3	7 (14.6)
≥4	9 (18.8)
N/A	1 (2.1)
Sample source (%)	
Bone Marrow	36 (75)
Peripheral Blood	10 (20.8)
Pleural Effusion	2 (4.2)
Phenotypic subgroup	
Immature (ETP; EGIL T-I/II)	31 (64.5)
Typical (EGIL T-III/IV)	15 (31.3)
N/A	2 (4.2)
Genetic subgroup, n. patients (%)	
HOXA	12 (25)
TAL/LMO	5 (10.4)
TLX1	5 (10.4)
TLX3	4 (8.3)
Unclassified	22 (45.8)
Genomic profile, number of aberrations (%)	
Median n. aberrations	10
Range	2-24
DRP-FISH combined report	
Median time	7
Range	3-18

Methods. We enrolled pts with new diagnoses or RR T-ALL. Leukemic cells were isolated from either bone marrow or peripheral blood samples, and pleural effusion was used for pts with mediastinal bulky disease. We used a library of 77 molecules for drug response profiling (DRP). The compounds were dispensed in duplicate at 4 different concentrations, and cell viability was assessed after 72 hours of incubation. To identify resistance and sensitivity profiles, we used the drug sensitivity score (DSS), which is calculated based on the half-maximal inhibitory concentration and the area under the curve. The inter-individual analysis was based on the difference between each pt's DSS and the median DSS of the entire cohort (dDSS) for each drug. For each pt we collected data on their genomic profile through a Combined Interphase FISH and a customized panel of recurrently mutated genes used for Next Generation Sequencing (Figure 1).



Figures 1, 2, 3, 4.

Results. We collected a total of 79 samples from 76 pts. 27 pts participated in the GIMEMA trial ALL2720 (NCT04582487), and the DRP was assessable in 94% of cases. Genomic and functional characterization was conducted for 45 pts, including 3 individuals who experienced 2 different relapses, resulting in a total of 48 fully characterized samples (Table 1). Based on the DRP, we identified 3 response patterns according to dDSS (Figure 2).

Pts exhibiting the highest sensitivity were subjected to an agglomerative clustering approach. Cluster1 (C1) mainly consisted of immature T-ALL with chemoresistance and sensitivity to antiapoptotic and kinase inhibitors, whereas C2 and C3 primarily featured a mature phenotype, with medium to high chemosensitivity and increasing resistance to kinase inhibitors (Figure 3). A significant difference in the expression of gene mutations and cytogenetic aberrations was observed when comparing C1 and C2 (Figure 4). From a translational

perspective, 13 pts underwent tx guided by DRP. Of these, 76% achieved a response, including 9 CR, 5 of which achieved MRD negativity, and 1 PR. 6 responders successfully proceeded to allogeneic hematopoietic transplantation (Figure 4).

Conclusions Our data indicate that FMP is an innovative strategy for identifying new response patterns and druggable targets in high-risk T-ALL. Additionally, the chemogenomic approach represents a promising tool for guiding tx in these pts, particularly for achieving a deep response in transplant-eligible individuals.

C02

ABSTRACT NOT PUBLISHABLE

C03

ONCOGENOMICS TO PINPOINT TARGETABLE ALTERATIONS IN ACUTE T-CELL LYMPHOBLASTIC LEUKEMIA

V. Bardelli¹, S. Arniani¹, V. Pierini¹, C. Nardelli¹, A.G. Lema Fernandez¹, S. Sica², F. Giglio³, S. Mastaglio⁴, M. Dargenio⁵, S. Mohamed⁶, E. Todisco⁷, C. Papayanidis⁸, M. Cimminiello⁹, P. Salutati¹⁰, M. Defina¹¹, M. Leoncin¹², M. Piccini¹³, P. Zappasodi¹⁴, C. Mecucci¹, R. La Starza¹

¹Hematology and Bone Marrow Transplantation Unit, Department of Medicine and Surgery, University of Perugia; ²Section of Hematology, Department of Radiological and Hematological Sciences, Catholic University of the Sacred Heart; ³OncoHematology Division, European Institute of Oncology; ⁴Hematology and Bone Marrow Transplantation Unit, IRCCS Ospedale San Raffaele; ⁵Hematology and Stem Cell Transplantation Unit, Vito Fazzi Hospital; ⁶UCO Ematologia, Azienda Sanitaria Universitaria Giuliano Isontina; ⁷Ospedale di Busto Arsizio, ASST Valle Olona; ⁸IRCCS Azienda Ospedaliero-Universitaria di Bologna, Istituto di Ematologia "Seràgnoli"; ⁹Dipartimento Oncologico, U. O. C. di Ematologia-Centro Trapianti di Cellule Staminali, Azienda Ospedaliera Regionale "San Carlo" di Potenza; ¹⁰Hematology Unit, Department of Oncology and Hematology, Spirito Santo Hospital; ¹¹Hematology Unit, University of Siena, Azienda Ospedaliera Universitaria Senese; ¹²UOC Ematologia, Azienda ULSS 3 Serenissima, Ospedale Dell'Angelo; ¹³SODc Ematologia, Azienda Ospedaliera Universitaria Careggi; ¹⁴Department of Hematology Oncology, Division of Hematology, Fondazione IRCCS Policlinico San Matteo, Italy

Introduction. Acute T-cell lymphoblastic leukemia (T-ALL) belongs to the most aggressive forms of hematologic cancers. Prognosis is particularly severe in cases with refractory disease/early relapse. Unlike B-cell ALLs, for which cytogenetic-molecular markers have been introduced into the diagnostic classification, T-ALLs are still "orphan" even though their genomic background has been deeply elucidated and clinically relevant events, such as *NOTCH1/FBXW7* and *N/K RAS* mutations and *PTEN* alterations, have been identified. Furthermore, genetic markers are essential to guide tailored treatments.

Aim. Comprehensive molecular-cytogenetic studies provide predictive and prognostic biomarkers to improve clinical management of T-ALL.

Methods. The study was conducted on a selected cohort of 165 T-ALL (21 children, 144 adults), including 103 immature and 62 typical cases, which were genetically classified as *TAL/LMO* (=12), *HOXA* (=40), *TLX3* (=12), *TLX1* (=18), *SPI.1* (=2), *BCL11B-a* (=6), or undetermined (=75). Gene variants were studied with a custom targeted NGS exploring hot-spot or the full coding region of *AKT1*, *ATM*, *BCL11B*, *BRAF*, *CND3*, *CNOT3*, *CREBBP*, *CTCF*, *DNM2*, *EED*, *EP300*, *ETV6*, *EZH2*, *FAT1*, *FAT3*, *FBXW7*, *FLT3*, *GATA3*,

GLI1, *GLI2*, *GLI3*, *IKZF1*, *IL2RB*, *IL7R*, *JAK1*, *JAK3*, *KDM6A*, *KMT2D*, *KRAS*, *LEF1*, *LMO1*, *LMO2*, *MED12*, *MYB*, *NF1*, *NOTCH1*, *NRAS*, *NT5C2*, *PHF6*, *PIK3CD*, *PIK3R1*, *PTCH1*, *PTEN*, *RELN*, *RPL10*, *RPL22*, *RPL5*, *RUNX1*, *SETD2*, *SH2B3*, *SMARCA4*, *SMO*, *STAT5B*, *SUZ12*, *TALI*, *TP53*, *TYK2*, *USP7*, *USP9X*, and *WT1*. NGS was flanked by CI-FISH and SNPα to detect gene rearrangements.

Results. Overall, 746 pathogenic, likely pathogenic, or variants of uncertain significance were found (median 6.5; range 1-12). Putative molecular targets were detected in 144 cases and were distributed according to phenotype and genetic subgroups. Namely, *NOTCH1/FBXW7* mutations (111 cases) and activation of the PI3K-AKT signaling (33 cases) (*AKT1*=2; *PTEN*=20; *PIK3R1*=8; *PIK3CD*=4) were significantly associated with a typical phenotype (Chi-square test, p=0.005 and p=0.039). The former, a favorable prognostic marker, was mainly found in the *TLX1/3* subgroups, while the latter, a high-risk marker, was enriched within *TAL/LMO*. RAS alterations (*BRAF*=2; *N/KRAS*=23; *NF1*=10), were detected in 33 cases and were found to be significantly associated with an immature phenotype (p=0.024). In immature cases we also observed a high incidence of *FLT3* (p=0.03), *RUNX1* (p<0.001) and *ETV6* (p=0.029) mutations. Variants affecting JAK/STAT members (48 *JAK1/3*; 7 *IL7R*; 26 *DNM2*; 5 *SH2B3*; 6 *STAT5B*), identified in 62 cases, mainly occurred in homeobox related subgroups.

Conclusion. Our comprehensive study implements genomic profiling of T-ALLs and identifies known prognostic markers whose distribution correlates with leukemia differentiation and genetic subgroups, thereby fine-tuning risk stratification of patients. It also provides valuable targets that can be exploited to guide personalized treatments, in more than 85% of cases.

C04

GENERATION OF A RNA INTERFERENCE IN VIVO MODEL TO TARGET MUSASHI- 2 IN KMT2AR INFANT ALL PRIMARY PATIENTS' CELLS

L. Valsecchi¹, S. Procopio¹, S. Naso¹, F. Klein², M. Carlet², I. Jeremias², A. Biondi^{3,4}, G. Cazzaniga^{1,5}, M. Bardini¹

¹Tettamanti Center, Fondazione IRCCS San Gerardo dei Tintori; ²Research Unit Apoptosis in Hematopoietic Stem Cells, Helmholtz Center Munich, German Center for Environmental Health (HMGU); ³Pediatrics, Fondazione IRCCS San Gerardo dei Tintori; ⁴School of Medicine and Surgery, University of Milano-Bicocca; ⁵Medical Genetics, Department of Medicine, University of Milano-Bicocca, Italy

Introduction. Acute Lymphoblastic Leukemia occurring in infants and carrying the rearrangement of *KMT2A* (*KMT2Ar* infant ALL) is a rare but very aggressive leukemia, associated with poor outcome and infant patients are typically resistant to conventional therapy and prone to relapse. In our previous study, by using a CRISPR-edited cell line model, we demonstrated that the RNA binding protein *MSI2* sustains the growth and the leukemogenic potential of *KMT2Ar* ALL, and it is involved in Glucocorticoids (GCs) resistance.

Methods. To study the functional role of *MSI2*, we generated a Knock Down (KD) using a lentiviral vector system to abrogate the expression of *MSI2* in patient-derived xenograft (PDX) samples derived from *KMT2Ar* infant ALL patients. In parallel we also generated a *KMT2A*||*AFF1*+ ALL cell line model with *MSI2* KD, in which we performed validation experiments (WB, qPCR and long term competitive assays *in vitro*) as a proof of principle for the efficacy of our shRNA lentiviral system.

Results. Eight different 110-mer oligonucleotides shRNA anti *MSI2* constructs were screened in order to select the three best per-

forming. Then we co-infected a KMT2A||AFF1+ ALL cell line (SEM) with two viruses (Figure 1A) the dsRED/miR30 vector in which the shRNA anti-MSI2 or the shRNA CNTRL constructs were cloned (Figure 1B) and the virus containing the Gaussia Luciferase (GLuc) and the mtagBFP fluorescent marker, or the Firefly Luciferase (eFFly) and the eGFP fluorescent marker. This co-infection with Luciferase plasmids allow to discriminate MSI2 KD cells and CNTRL cells and to track the engraftment in mice by *in vivo* imaging. The validation experiments confirmed the efficacy of the shRNA lentiviral system and we successfully generated SEM MSI2 KD cells in which the expression of MSI2 was strongly silenced compared to SEM CNTRL cells. In a long-term competitive assay *in vitro*, in which we mixed the SEM MSI2 KD with the CNTRL cells at the initial ratio of 90/10 or 50/50 KDCNTRL, we observed that the MSI2 KD cells slowly but progressively diminished throughout the passages (from p0 to p40), while the CNTRL cells slightly but consistently increased. Interestingly, the administration of Dexametasonone or the glucose inhibitor 2-DG to the co-culture promoted a more rapid outgrowth of CNTRL cells. Finally, we co-infected PDXs derived from three KMT2Ar infant ALL with the same plasmids and we successfully generated three MSI2 KD PDXs in which the expression of MSI2 was strongly silenced and CNTRL PDXs.

Conclusions. Our data clearly show that the absence of MSI2 confers a proliferation disadvantage to SEM cells and sensitize leukemic cells to GC-treatment and also glycolysis inhibition; thus uncover novel functions of MSI2, in the response to corticosteroid treatment and metabolic plasticity of leukemia. In the future we will use our MSI2 KD PDXs to corroborate the essential role of MSI2 *in vivo* and to validate MSI2 as a therapeutic target in KMT2Ar infant ALL patients.

C05

ABSTRACT NOT PUBLISHABLE

C06

THE COMBINATION OF SILMITASERTIB WITH EITHER VENETOCLAX OR PALBOCICLIB ARE PROMISING THERAPEUTIC STRATEGIES AGAINST A NOVEL SUBGROUP OF ADULT PH-LIKE B-CELL ACUTE LYMPHOBLASTIC LEUKEMIA CHARACTERIZED BY HIGH CRLF2, CTGF AND CD200 EXPRESSION

F. Lo Schiavo¹, A. Ghelli Luserna Di Rorà², L. Ledda¹, M. Paganelli¹, G. Capirossi¹, C. Salvesi¹, E. Fonzi³, C. Papayannidis⁴, P. Salutari⁵, M. Rondoni⁶, A.M. Mianulli⁷, B. Giannini⁸, F. Giglio⁹, C. Pasciolla¹⁰, M. Fumagalli¹¹, A. Imovilli¹², M. Endri¹³, S. Galimberti¹⁴, G. Martinelli¹⁵, G. Simonetti¹, A. Ferrari¹

¹Biosciences Laboratory, IRCCS Istituto Romagnolo per lo Studio dei Tumori (IRST) "Dino Amadori"; ²Fondazione Pisana per Scienza ONLUS; ³Unit of Biostatistics and Clinical Trials, IRCCS Istituto Romagnolo per lo Studio dei Tumori (IRST) "Dino Amadori"; ⁴IRCCS Azienda Ospedaliero-Universitaria di Bologna, Istituto di Ematologia "Seràgnoli"; ⁵Dipartimento Oncologia Ematologia, Ospedale Civile Santo Spirito; ⁶Hematology Unit & Romagna Transplant Network, Ravenna Hospital; ⁷Hematology Infermi Hospital; ⁸Laboratorio Unico-AUSL della Romagna Pievesestina di Cesena; ⁹Hematology and Bone Marrow Transplantation Unit, IRCCS San Raffaele Scientific Institute; ¹⁰Hematology and Bone Marrow Transplantation Unit, Istituto Oncologico IRCCS "Giovanni Paolo II"; ¹¹Hematology Unit, Ospedale San Gerardo; ¹²Hematology Azienda USL-IRCCS Reggio Emilia; ¹³UOC Ematologia Ospedale Ca' Foncello Azienda ULSS Marca Trevigiana; ¹⁴Hematology Unit AOUP Santa Chiara; ¹⁵Scientific Directorate, IRCCS Istituto Romagnolo per lo Studio dei Tumori (IRST) "Dino Amadori", Italy

Introduction. Adult patients (pts) with B-cell acute lymphoblastic leukemia (B-ALL) lacking the most common rearrangements are collectively referred to as "triple-negative" (Ph^{-/-}) ALL. *CRLF2* is frequently altered in adult B-ALL (50-75% of cases), especially in Ph-like pts (20.4% of adult B-ALL), a subgroup of Ph^{-/-}. *CRLF2* alterations generally lead to overexpression that associates with poor outcome in adult pts.

Aims: Dissecting the transcriptional program of *CRLF2*^{high} Ph^{-/-} B-ALL and testing novel specific therapeutic strategies.

Methods. Gene Expression Profiling (GEP) was performed on 60 Ph^{-/-} ALL, 30 Ph+ B-ALL and mononuclear cells from 7 healthy donors (HTA 2.0, Thermo Fisher Scientific). *In vitro* studies were conducted on cell lines representative of Ph^{-/-} (MUTZ5, MHH-CALL4, NALM6, NALM19) and other B-ALL subgroups: RS4;11 (t4;11), KOPN8 (t11;19), 697 (t1;19), REH (t12;21), SUPB15 (Ph+) and BV173 (Ph+). *CRLF2*, *CTGF*, and *CD200* levels were assessed by flow cytometry and immunometric assay (Ella, BioTechne). Cell response to drugs was evaluated by RealTime-Glo assay. Drug effects on phagocytosis and T-cell cytotoxicity, were assessed by flow cytometry after co-culture of B-ALL cell lines with healthy M1-M2 polarized macrophages and lymphocytes, respectively.

Results. By GEP we identified in Ph^{-/-} a new 10-genes signature, related to *CRLF2* expression, that defined 2 clusters (Gr1 and Gr2; Figure 1A). Gr2 represents 12.2% of all B-ALL, resembled Ph+, suggesting that it could contain Ph-like cases and it is characterized by high expression of *CRLF2*, *CTGF* and *CD200* (3C-UP; Figure 1B). Among B-ALL tested cell lines, MUTZ5 and MHH-CALL4 co-express the three markers and release CTGF in the medium (Figure 1C-D), making them suitable *in vitro* models to study specific therapeutic strategies. We selected drugs targeting the three markers or their pathways (Figure 1E): JAK inhibitor (i) Ruxolitinib, mTORi

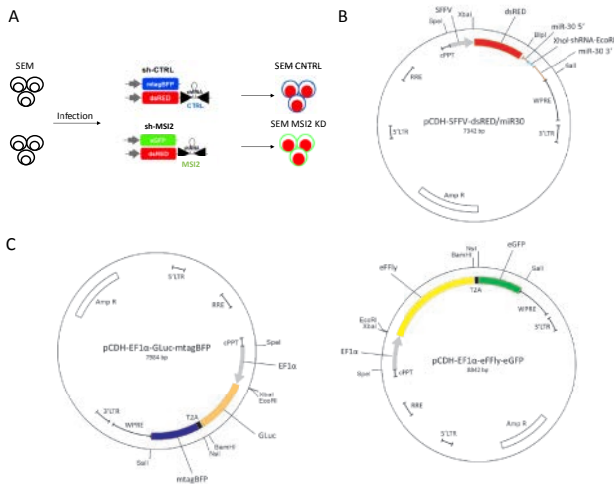


Figure 1.

Rapamycin, CDK4/6i Palbociclib, BCL2i Venetoclax, CK2i Silmitasertib, anti-CD200 and anti-CTGF antibodies (Samalizumab & Pamrevlumab, respectively). Single agent small molecules treatment resulted in good sensitivity of MHH-CALL4, while MUTZ5 were resistant. Preliminary data suggests that anti-CD200 does not significantly increase phagocytosis and cytotoxicity when KOPN8 cells (CD200^{high}) were co-cultured with macrophages and lymphocytes, respectively. Anti-CTGF treatment does not inhibit 3C-UP cell growth in monocultures. However, the combination of BCL2i and CK2i showed synergy in MUTZ5, additivity in MHH-CALL4 and a milder effect in RS4;11 (Figure 1F). Accordingly, the combination of CK2i and CDK4/6i resulted in an additive effect in MHH-CALL4 and MUTZ5, while showing antagonism in the REH model (Fig.1G).

Conclusions. 3C-UP represents a novel targetable B-ALL subgroups. In particular, the combinations of Silmitasertib with either Venetoclax or Palbociclib are novel potential selective therapeutic options for these pts. Thanks to MoH L3P1946.

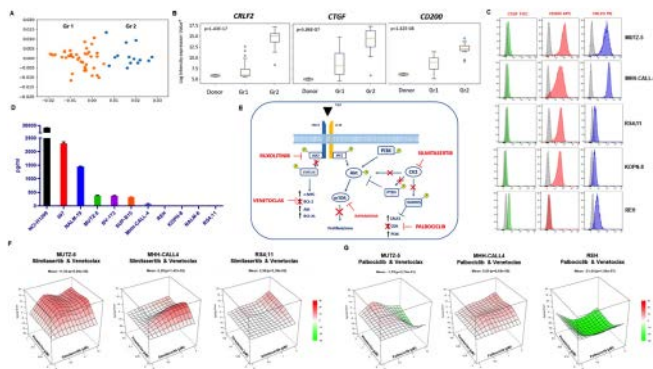


Fig.1 (A): K-means clustering of 2 components PCA of 10 selected genes in Ph⁺/⁻ B-ALL samples. (B): Results of GEP analysis: gene expression profiles are distributed into two groups, and group 2, in particular, is characterized by higher expression of the genes CRLF2, CD200, and CTGF. (C): Expression of CRLF2, CRLF2, and CD200 in MUTZ5, MHH-CALL4, RS4;11, KOPN8 and REH cell lines analyzed by flow cytometry. MUTZ5 and MHH-CALL4 are both positive for CRLF2 and CD200, but not CTGF. RS4;11 and KOPN8 cell lines are positive only for CD200, and REH cells are positive only for CRLF2. The graph was generated from three independent experiments and showed as mean. (D): Analysis of CTGF release using ELISA (Automated Immunoassay (concentration expressed in pg/ml) in the culture medium of the analyzed cell lines. The NCI-H299 cell line (non-small cell human lung carcinoma) was used as a positive control. (E): Pathways upstream and downstream CRLF2. CD200 and CTGF and their inhibitors. (F): Effect of the combination of Silmitasertib and Venetoclax on MUTZ5, MHH-CALL4, and RS4;11 cell lines, and (G) the combination of Silmitasertib and Palbociclib on MUTZ5, MHH-CALL4, and REH cell lines, expressed using the Bliss Synergy Score (SynergyFinder+). green represents antagonism, red represents synergy, and white represents additivity. The graphs were generated from three independent experiments and showed as mean.

Figure 1.

C07
GENOMIC CHARACTERIZATION OF PH- B-LINEAGE ACUTE LYMPHOBLASTIC LEUKEMIA PATIENTS ENROLLED IN THE GIMEMA LAL2317 TRIAL

D. Cardinali¹, M. Beldinanzi¹, M. Ansuinelli¹, I. Della Starza^{1,2}, M. Piccini³, F. Ferrara⁴, P. Zappasodi⁵, E. Borlenghi⁶, M. Bocchia⁷, M. Messina⁸, A. Piciocchi⁸, M. Di Trani¹, A. Rambaldi⁹, S. Chiaretti¹, R. Bassan¹⁰, R. Foà¹

¹Ematologia, Dipartimento di Medicina Traslazionale e di Precisione, Sapienza Università di Roma; ²AIL Roma; ³AOU Careggi; ⁴AORN Cardarelli; ⁵Struttura Complessa di Ematologia, Fondazione IRCCS Policlinico S. Matteo; ⁶Dipartimento di Ematologia, ASST Spedali Civili di Brescia; ⁷Unità Operativa Complessa di Ematologia, AO Senese Policlinico Le Scotte; ⁸Fondazione GIMEMA; ⁹Struttura Complessa di Ematologia, AO Papa Giovanni XXIII e Dipartimento di Oncologia ed Ematologia, Università di Milano; ¹⁰Unità di Ematologia, Ospedale dell'Angelo, Italy

The outcome of adult patients with Philadelphia-negative B-lineage acute lymphoblastic leukemia (Ph- ALL) has improved markedly in the last decade, due to the use of intensive pediatric-inspired regimens, minimal residual disease (MRD)-driven allogeneic stem cell transplantation (HCT) and, more recently, immunotherapy. In this

context, the identification of genomic alterations is pivotal to optimize the management of ALL patients and to identify biologically defined prognostic subgroups. Aim of this study was to conduct an extensive genomic characterization to identify nucleotide substitutions, insertion/deletion mutations, copy number aberrations (CNAs) and gene rearrangements in patients enrolled in the phase II GIMEMA LAL2317 trial¹ - designed for newly diagnosed B-lineage Ph- ALL - based on the administration of intensive chemotherapy and the addition of two cycles of the bispecific monoclonal antibody blinatumomab in the consolidation phase.

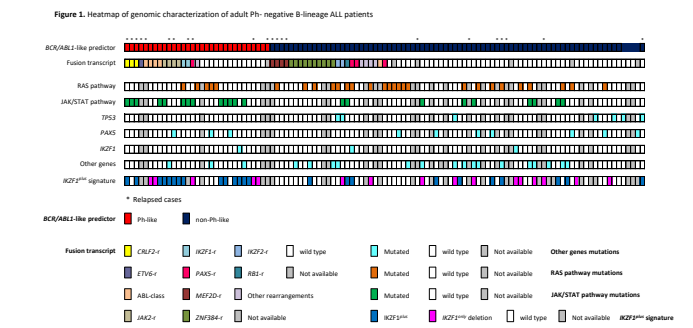


Figure 1.

Patients enrolled in the trial without major molecular aberrations (*KMT2A-r* and *TCF3::PBX1*) were evaluated at diagnosis for the presence of the Ph-like signature, genomic lesions by targeted DNA/RNA sequencing and CNAs by Multiplex Ligation-dependent Probe Amplification (MLPA). Of the 149 cases enrolled in the trial, 111 were evaluated for the *BCR/ABL1*-like predictor² and 31 (28%) proved to be Ph-like. Within Ph-like cases, targeted RNA sequencing, performed in 106 patients, showed that 41 (39%) had a fusion transcript involving ABL-class genes in 4 (*PDGFRB* in 2 cases and *ABL1* and *CSF1R* in 1 case each), *JAK2* in 4, *CRLF2* in 3, *IKZF1* in 2, *ETV6* and *PAX5* in 1 case each, while 1 case had a non-recurrent aberration. Within non-Ph-like cases, *ZNF384* rearrangement was found in 10, *MEF2D* in 4, *IKZF2* in 2, *PAX5* in 3, *PDGFRB* and *RBI* in 1 case each, with 5 cases carrying non-recurrent rearrangements. Targeted DNA sequencing analysis was carried out in 85 patients and highlighted the presence of JAK/STAT mutations in 22 cases, RAS pathway mutations in 28, *TP53* in 7, *PAX5* in 10, *IKZF1* in 3 and other mutations in different genes in 19 cases. Finally, MLPA analysis revealed the *IKZF1*^{plus} signature in 24/84 (29%) patients evaluated. The Ph-like ALL subset was overrepresented in relapsed cases (11/22 evaluated cases, 50%), with 9 displaying a gene rearrangement, 4 a *IKZF1*^{plus} signature, and 5 a JAK/STAT pathway mutation. In cases not displaying a Ph-like signature, the presence of *MEF2D*, detected in 4 relapsed cases (4/4 *MEF2D* rearranged cases), was associated with a particularly poor outcome. At variance, no events were recorded in *ZNF384* rearranged cases (Figure 1).

This extensive genomic characterization confirms the genomic complexity of Ph- B-lineage ALL, with more than 50% of cases displaying more than 1 lesion. Clinical correlate analysis confirms the negative impact of the Ph-like signature, and, with the caveat of the small patient size, also of *MEF2D* rearrangements.

References

1. Bassan R et al, EHA 2021
2. Chiaretti S et al, BJH 2018

C08

NOTCH1 TRANSLOCATIONS ARE THE HALLMARK OF A NEW SUBTYPE OF HIGH-RISK CORTICAL T-CELL LYMPHOMA/ LYMPHOBLASTIC LEUKEMIA

S. Arniani¹, V. Bardelli¹, V. Pierini¹, S. Mastaglio², S. Trappolini³, M. Piccini⁴, C. Pasciolla⁵, L. Brunetti³, F. Giglio⁶, M. Crocioni¹, D. Beacci¹, C. Nardelli¹, A.G. Lema Fernandez¹, F. Ciceri², C. Mecucci¹, R. La Starza¹

¹Hematology and Bone Marrow Transplantation Unit, Department of Medicine and Surgery, University of Perugia, Perugia; ²Hematology and Bone Marrow Transplantation Unit, IRCCS San Raffaele Hospital, Milano; ³Hematology Clinic, AOU Marche, Ancona; ⁴SODc Haematology, AOU Careggi, University of Florence, Florence; ⁵Haematology Unit, IRCCS Istituto Tumori "Giovanni Paolo II", Bari; ⁶OncoHematology Division, European Institute of Oncology, Milan, Italy

Introduction. *NOTCH1* is one of the most recurrently affected genes in T-ALL/LBL as it undergoes gain-of-function mutations in more than 50% of cases. Its in T-ALL/LBL was initially identified by cloning an extremely rare translocation, the t(7;9)(q34;q34) and later on the t(9;14)(q34;q11). So far, these alterations have been considered as alternative mechanisms of NOTCH signaling activation.

Aim. To delineate the genetic landscape of T-ALL/LBL cases without subtype-defining oncogenetic events to pinpoint as yet unknown entities.

Materials and Methods. To pinpoint new genetic subtypes among T-ALL/LBL, we performed Whole transcriptome expression array (WTEa) (ClariomS Assay human, Affymetrix/ThermoFisher Scientific). Supervised analysis was done by "Expression gene" type analysis; unsupervised analysis by "Exploratory Grouping Analysis" using a previously defined dataset of 312 probes. CI-FISH, SNPa and custom target NGS provided a comprehensive genomic characterization of cases. The study was carried out in 249 cases (231 T-ALL and 18 T-LBL); 159 had genomic features typical of HOXA (=60), TAL/LMO (=24), TLX1/NKX2.1 (=38), TLX3 (=21), BCL11B (=14), or SPI1 (=2) subgroup, while 90 cases had no subtype-defining alterations. Among the latter, there were five cortical cases, 1 T-ALL and 4 T-LBL, with *NOTCH1* translocations (*NOTCH1-t*) with *TRB* (=2), *TRAD* (=2), or *IKZF2* (=1) genes. The study was therefore extended to the SUPT1 cell line which presents *TRB*||*NOTCH1* rearrangement.

Results. Overall, cluster plot distributed cases into 9 subgroups, with 71/90 of undetermined cases scattered in 4 distinct clusters. One of them included the 5 cases with *NOTCH1-t* plus 1 case undetermined at genomic level. An additional unsupervised analysis, including relapse samples (n=3) and the SUPT1 cell line confirmed clustering of all samples with *NOTCH1* rearrangements. Transcriptomic signature of *NOTCH1-t* cases was characterized by 677 differentially expressed genes (DEGs), 53 of which were represented by *NOTCH1* targets, i.e. 27 up- (*DTX1*, *HEY1*, *HES4*, *NOTCH3*, etc. .) and 26 down-regulated (*ETS2*, *KDM2A*, *RUNX1*, *NR3C1*). Remarkably, 34 of them were deregulated in *NOTCH1-t* cases but not in cases with *NOTCH1* mutations. Other DEGs were cell surface molecules (*CD40LG*, *CD52*, *CD1C*, *CD8*, *TLR7*, *CD72*, *ESR2*, and *IRAK4*), transcription factors (*TCF12*, *IKZF3*, *KLF12*, and *LMO7*), chemokines (*IGFBP2*, *CXCL9*, *IL9*), genes involved in signaling (*TIAMI*, *STAT5B*), and immune modulators (*IDO1*, *PDCD1*).

Conclusion. The distinct gene expression profile, leukemia cell immunophenotype, and clinical presentation of *NOTCH1-t* T-ALL/LBL, suggest they represent a distinct subtype of leukemias. Indeed, *NOTCH1* rearrangements mark a rare but extremely aggressive subtype of T-LBL/ALL, typically characterized by mediastinal bulk, pleural effusion, and bone lesions. The specificity of DEGs indicates that different types of *NOTCH1* alterations exert their oncogenic activity through different sets of downstream *NOTCH1* effectors.

Monoclonal Gammopathies and Multiple Myeloma 1

C09

FUNCTIONAL DISSECTION OF THE SINGLE CELL TRANSCRIPTOMIC LANDSCAPE OF GENOTYPICALLY-IDENTIFIED POLYCLONAL PLASMACELLS IN MULTIPLE MYELOMA MICROENVIRONMENT

M.C. Da Vià¹, F. Lazzaroni¹, A. Matera², A. Marella², A. Maeda¹, A. Marchetti², S. Fabris¹, S. Pioggia¹, I. Silvestris¹, D. Ronchetti², S. Lonati², G. Fabbiano¹, V. Traini¹, E. Taiana¹, G. Castellano¹, C. De Magistris^{1,2}, M. Scopetti², N. Puccio³, F. Torricelli³, M. Barbieri¹, L. Pettine¹, A. Neri⁴, M. Lionetti², F. Passamonti^{1,2}, N. Bolli^{1,2}

¹Hematology Unit, Fondazione IRCCS Ca' Granda Ospedale Maggiore Policlinico; ²Department of Oncology and Hemato-Oncology, University of Milan; ³Laboratory of Translational Research, Azienda USL-IRCCS di Reggio Emilia; ⁴Scientific Directorate, Azienda USL-IRCCS di Reggio Emilia, Italy

Introduction. Multiple Myeloma (MM) is a plasma cell (PC) dyscrasia usually preceded by asymptomatic stages defined as Monoclonal Gammopathy of Undetermined Significance (MGUS) or Smoldering MM (SMM). Progression is driven by cell-intrinsic factors in the clonal PCs population as well as by changes in the tumorigenic microenvironment (TME). Even if the role of immune and non-immune cells has been extensively studied, the disruption of polyclonal PCs and their role in contributing to TME dysregulation has never been deeply studied. Taking advantage of single-cell B-cell receptor (BCR) genotyping and scRNAseq in the same single cells, we aimed to dissect the transcriptional landscape and role of polyclonal PCs in asymptomatic PC dyscrasia progression.

Methods. We performed scRNAseq and scBCR analysis to unequivocally identify polyclonal PCs within the CD138pos population in a cohort of n=7 MGUS, n=16 SMM and n=23 newly diagnosed (ND)MM patients. Cells derived from healthy donors (HDs) sourced both locally (n=1) and from publicly available repositories (n=17) were used as controls. InferCNV and MultinicheNET tools were applied to study the copy number alterations (CNA) and the PCs-TME interactions, respectively.

Results. A total of n=213,146 CD138pos PCs were analyzed, revealing the presence n=170,428 clonal and n=42,718 polyclonal cells (Figure 1A) in patients with PC dyscrasias. The polyclonal nature of the latter group was confirmed by lack of identity with the clonal BCR sequence at nucleotide level and by the lack of CNAs. As compared to PCs from HDs, polyclonal PCs from patients showed a peculiar transcriptomic profile across different stages (Figure 1B). The supervised marker genes expression analysis revealed the upregulation of genes of TME and inflammation (i.e. *ICAM1*, *TIMP1*, *ITGB7*), autophagy (i.e. *P62*) and interferon pathway (i.e. *IFI6*, *IFITM1*) in polyclonal PCs derived from patients, as well as *HLA-DPA1* and *HLA-DOB*, that are fundamental modulators of immune response (Figure 1C). Gene Set Enrichment Analysis showed a climax of increasing inflammatory status from HD to NDMM. The HALLMARK TNF SIGNALING VIA NFkB was the only upregulated pathway in HD PCs, compared to the MGUS, SMM and NDMM ones. Inflammatory pathways as HALLMARK ALLOGRAFT REJECTION, HALLMARK INFLAMMATORY RESPONSE, IFN related pathways, resulted overexpressed in MGUS, SMM and NDMM (Figure 1D) as compared to HDs. Finally, we performed a network analysis between polyclonal PCs and TME in each patient, highlighting an increased suppressive interaction between polyclonal PCs and effector CD8 T cells, mainly in NDMM.

Conclusions. Overall, our findings shed some light for the first

time on the transcriptomic landscape of corrupted polyclonal PCs in patients with asymptomatic and symptomatic PCs dyscrasias, showing functional disruptions that may contribute to disease pathogenesis through promoting an inflammatory milieu, as well as explain the typical immunoparesis seen upon progression.

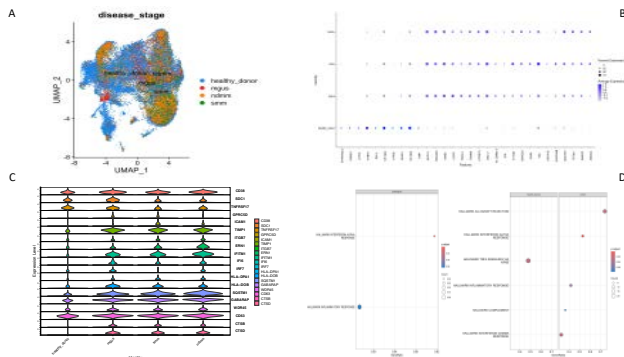


Figure 1.

C10

CIRCULATING MULTIPLE MYELOMA CELLS (CMMCS) COUNT IDENTIFIES TWO DIFFERENT DYNAMICS IN MM PATIENTS UNDER TREATMENT BY THE COMMSTANT INDEX

I. Vigliotta^{1,2}, V. Solli^{1,2}, A. Kanapari^{1,2}, S. Armuzzi^{1,2}, G. Mazzocchetti^{1,2}, A. Poletti^{1,2}, B. Taurisano¹, I. Pistis², E. Borsi^{1,2}, M. Martello^{1,2}, L. Pantani¹, I. Rizzello¹, G. Marzocchi², N. Testoni², E. Zamagni^{1,2}, M. Terracciano³, V. Del Monaco³, M. Garonzi³, N. Manaresi³, M. Cavo^{1,2}, C. Terragna¹

¹IRCCS Azienda Ospedaliero-Universitaria di Bologna, Seràgnoli Institute of Hematology; ²Dipartimento di Scienze Mediche e Chirurgiche - Università di Bologna; ³Menarini Silicon Biosystems SpA, Italy

Aim of the study was to analyze circulating multiple myeloma cells (CMMCs) in newly diagnosed MM patients (pts), by CELLSEARCH system[®], to correlate CMMCs amount with bone marrow (BM) baseline tumor burden and with its dynamics under treatment. 94 peripheral blood (PB) samples were collected every 3 months (m) during treatment, from a cohort of 44 pts (median follow-up 6m, range 0-18m). In 18/44 pts, PB samples were collected also at diagnosis. In 4 pts, single cell (sc) DNA analysis was performed to study the Copy Number Alterations (CNAs) profile of CMMCs persisting after therapy. At diagnosis, a median of 349 CMMCs was counted (range 1-39940); overall, the amount of CMMCs significantly correlated with albumin, C-reactive protein, calcium, and monoclonal component ($p < 0.05$), suggesting more aggressive disease characteristics in pts with higher CMMCs counts. Under induction therapy, a median of 2 CMMCs (range 0 to 5432) were counted in 40/44 MM patients (42 samples), whereas at pre-maintenance a median of 0 CMMCs (range 0-180) was counted in 38/44 pts (52 samples). According to CMMCs count dynamics across these two phases, a coMMstant index was proposed, equal to 1 when CMMCs resulted enumerable both under induction therapy and at pre-maintenance, or equal to 0, when CMMCs resulted continuously undetectable. Overall, 15/40 (37%) and 25/40 (63%) pts had coMMstant index=1 and =0, respectively. In pts with coMMstant index=1, high quality response rates (\geq VGPR and \geq CR) were significantly lower, as compared to those of pts with coMMstant index=0 ($p=0.019$ and 0.002 , for response rates \geq VGPR and \geq CR, respec-

tively). BM-MRD measurements, as assessed by Next Generation Sequencing at a sensitivity of 10^{-5} , were positive in 8/10 (80%) pts with coMMstant index=1 and in 9/23 (39%) pts with coMMstant index=0 ($p=0.05$). Moreover, pts with coMMstant index=1 had 4.5 times higher risk of progression and 7.8 times higher risk of death ($p=0.07$), as compared to pts with coMMstant index=0, suggesting that either the persistence or the continuous release of CMMCs correlates to poor prognosis. Notably, neither the CMMCs counts at diagnosis nor the ISS or R-ISS stages were different in pts with coMMstant index=1 or =0, supporting the relevance of CMMCs dynamics under treatment in defining pts' prognosis. Finally, the genomic analysis of residual CMMCs collected from 4 pts after therapy showed that CMMCs CNAs profiles mirrored the baseline BM-PCs one, though minutely disclosing its sub-clonal composition and highlighting putative emerging and/or resistant sub-clones after therapy. In conclusion, CMMCs dynamics observed in MM pts under treatment, independently from their baseline characteristics, not only reflects pts' disease dynamics, but might also predict their disease outcome. Although the pts' cohort was small, these results support the benefit of CMMCs count under treatment, to assess pts' dynamic risk.

Thanks to AIRC19-IG22059, AIL Bologna ODV, RC 000599/22

C11

ABSTRACT NOT PUBLISHABLE

C12

ABSTRACT NOT PUBLISHABLE

C13

SINGLE CELL TRANSCRIPTOMICS OF BONE MICROENVIRONMENT CELLS REVEALED ALTERED FEATURES IN MULTIPLE MYELOMA PATIENTS COMPARED TO PRE-MALIGNANT MONOCLONAL GAMMOPATHIES

P. Storti¹, T. Torelli², C. Manferdini³, D. Toscani¹, A. Guidi², R. Vescovini¹, N.T. Iannozzi¹, B. Dalla Palma⁴, M. Scita⁴, F. Librale⁴, M. Bernardi⁴, S. Ricci⁴, V. Raimondi¹, O. Lungu¹, V. Marchica¹, J. Burroughs-garcia⁴, G. Todaro⁴, G. Sammarelli⁴, E. Aleo⁵, G. Lisignoli³, L. Agnelli², N. Giuliani^{1,4}

¹Dipartimento di Medicina e Chirurgia, Università di Parma; ²Dipartimento di Diagnostica Innovativa, IRCCS Istituto Nazionale dei Tumori; ³Laboratorio di Immunoreumatologia e Rigenerazione Tissutale, IRCCS Istituto Ortopedico Rizzoli; ⁴U. O. Ematologia e CTMO, Azienda Ospedaliero-Universitaria di Parma Programma Dipartimentale Mieloma Multiplo e Gammopatie Monoclonali; ⁵IGA Technology Services

Introduction. Multiple myeloma (MM) can be preceded by monoclonal gammopathy of undetermined significance (MGUS) and smoldering MM (SMM). However, how the bone microenvironment (BME) changes and contributes to tumoral progression in MM remains unresolved. Published data on BME are mainly produced *in vitro* and few data are on MGUS/SMM patients. Up to date, no single-cell RNA sequencing database of the BME cells has been described in MM. The aim of this project was to characterize for the first time at single cell level, the BME in patients with newly diagnosed MM (MMD) and MGUS/SMM to identify alterations involved in tumoral progression.

Methods. From 15 bone biopsies of MMD, MGUS and SMM

patients, to enrich the rare BME non-hemopoietic cells, we depleted CD235a⁺, CD45⁺, CD31⁺, and CD138⁺ cells. The CD45⁻CD31⁻CD235a⁻CD138⁻ cells were analyzed by scRNAseq. Data were generated on Chromium 10X Genomics. Cellranger and Seurat pipeline in R software has been used. Cell identities were assigned by manual curation. The trajectory analysis has been made by Monocle3. Decouple R and FindMarkers were used to compare pathways, and differential gene expression (DGE) of the samples throughout the different conditions.

Results. A total of 35723 cells were profiled. We identified 13 BME cell type clusters | 7 mesenchymal stromal cell (MSC) clusters (proliferating MSC, MSC DDK-OPG-, MSC DKK+, MSC RUNX2, MSC OPG+, MSC Osteogenic, Perivascular MSC) and 6 osteoblasts (OBs) clusters (OB precursor, OB precursor LEPR+, OB BGLAP+, OB SPP1+, OB NFkB+, OB late). Pseudotime analyses highlighted a complex trajectory of differentiation from more immature cell clusters (proliferating MSC) to late OB cluster, confirming the ability of the dataset to snapshot the *in vivo* complexity of BME. We highlighted an alteration of the MSCs clusters trajectories starting in SMM samples till a disruption in MM, especially from MSCs OPG+ and OB precursors LEPR+ to OB NFkB+. In MMD compared to MGUS/SMM, pathway analyses revealed an upregulation of VEGF activity in immature MSCs and of PI3K activity in proliferating MSC, perivascular MSC and OB clusters. In MGUS, TRAIL pathway activity, known to suppress MM cell proliferation, was upregulated in MSC osteogenic and OB BGLAP+. Finally, DGE analyses revealed the modulation of different genes, several not described in MM. MGUS MSCs clusters showed an upregulation of *FBLN1*, *SERPINF1* and MMD MSCs clusters dramatically downregulated *WISP2* and upregulated *SRGN*, involved in MM cell proliferation. Interestingly, in SMM samples, we reported an upregulation of genes involved both in the promotion of osteoblastogenesis (*CHI3LI*, *SCARA3*, *SPON2*) and inhibition (*GREM1*), likely underling the attempt to contrast the establishment of altered BME, characteristic of MM.

Conclusions. Our approach is able to dissect the complex organization of the BME and to highlight at single cells level the alterations of the BME in patients with MM compared to MGUS and SMM.

C14

HIGH LEVEL OF CIRCULATING TUMOUR DNA AT DIAGNOSIS CORRELATES WITH DISEASE SPREADING AND DEFINES MULTIPLE MYELOMA PATIENTS WITH POOR PROGNOSIS

M. Martello^{1,2}, V. Solli^{1,2}, G. Mazzocchetti^{1,2}, A. Solimando³, D. Bezzi⁴, B. Taurisano^{1,2}, A. Kanapari^{1,2}, A. Poletti^{1,2}, E. Borsi^{1,2}, S. Armuzzi^{1,2}, I. Vigliotta^{1,2}, I. Pistis¹, V. Desantis³, I. Rizzello^{1,2}, L. Pantani¹, K. Mancuso^{1,2}, P. Tacchetti¹, C. Nanni⁴, M. Cavo^{1,2}, E. Zamagni^{1,2}, C. Terragna¹

¹IRCCS Azienda Ospedaliero-Universitaria di Bologna, Istituto di Ematologia "Seràgnoli"; ²Department of Medical and Surgical Sciences, University of Bologna; ³Azienda Ospedaliera Policlinico di Bari- Università degli Studi di Bari "Aldo Moro"; ⁴Nuclear Medicine, IRCCS Azienda Ospedaliero-Universitaria di Bologna, Italy

Background. Multiple Myeloma (MM) is a plasma cell (PC) disorder characterized by the presence of skeletal involvement at the time of diagnosis. Recently, cell-free DNA (cfDNA) has been proven to resume the heterogeneity of spatially distributed clones.

Aims. To evaluate the prognostic role of cfDNA at diagnosis in correlation with imaging data and bone marrow (BM) microenvironment features, and the possibility to integrate this liquid biopsy approach with molecular bone marrow and whole-body residual disease assessment.

Methods. A total of 162 newly diagnosed MM patients underwent baseline screening with 18F-FDG PET/CT and molecular assessment by Ultra Low Pass-Whole Genome Sequencing (ULP-WGS). For each pts, ULP-WGS was used to characterize both the neoplastic PC clone(s) in the BM (gDNA) and the cfDNA.

Results. Genomic profile comparison between cfDNA and BM revealed an overall concordance (56/62 = 90.3%) strictly dependent from the cfDNA tumor fraction (TF). Interestingly, high cfDNA TF levels (ROC-determined cut-off > 12% cfDNA TF values; range 4.4-84.3%) correlate with different MM tumor mass markers, particularly for b2-microglobulin (p<0.001), albumin (p=0.006) and total bone marrow plasma cells (p<0.001). Strikingly, patients with high cfDNA TF were more likely to present with paraskelatal (PS) and extramedullary (EM) lesions as compared to pts with low TF (PS lesions | 13/27 vs 13/69, p=0.005; PS Deauville score (DS) ≥ 4 | 11/27 vs 10/69, p=0.003; PS SUV MAX | p=0.007. EM lesions | 4/27 vs 3/69, p=0.09; EM lesions DS ≥ 4 | 4/27 vs 3/69, p=0.067; EM SUV MAX | p=0.008). The tumor-homing in its surrounding microenvironment is critical for the release of cfDNA into the bloodstream. Indeed, we demonstrate that a Cancer-associated Fibroblasts (CAFs)-mediated inflammatory state might correlate to a high cfDNA level, which likely contributes to aggressive disease progression. Interestingly, high cfDNA TF at diagnosis predicted for poorer prognosis as compared with low cfDNA TF (PFS at 20 months | 67% vs 86%, p=0.001; OS at 20 months | 90% vs 100%, p=0.04), independently from R-ISS III and Iq amplification. Finally, including cfDNA > 12% in the current R-ISS risk score enables better identification of that patient at a higher risk of progression.

Conclusions. We provide evidence that cfDNA can be a reliable and less invasive marker for disease characterization. Moreover, if evaluated with PET/CT and with BM for R-ISS, it can refine and/or better define the patients' risk. In addition, the analysis of cfDNA allows - with a single assay - both to capture the patient's whole genomic profile and to quantify the tumor fraction, which is finally correlated with patients' risk of progression.

C15

PYG02 IS OVEREXPRESSED IN MULTIPLE MYELOMA PATIENTS WITH 1Q21 AMPLIFICATION AND IT IS A POSSIBLE NEW DRUGGABLE TARGET INVOLVED IN CARFILZOMIB RESISTANCE

N.T. Iannozzi¹, P. Storti¹, J. Burroughs Garcia², V. Marchica¹, V. Franceschi², D. Toscani¹, R. Vescovini¹, V. Raimondi¹, O. Lungu¹, M. Scita², F. Librale², B. Dalla Palma², G. Todaro², G. Sammarelli², L. Agnelli⁴, G. Pruneri⁴, G. Donofrio³, N. Giuliani^{1,2}

¹Dipartimento di Medicina e Chirurgia, Università di Parma; ²U. O. Ematologia e CTMO, Azienda Ospedaliero-Universitaria di Parma, Programma Dipartimentale, Mieloma Multiplo e Gammapatie Monoclonali; ³Dipartimento di Scienze Medico Veterinarie, Università di Parma; ⁴Istituto Nazionale dei Tumori, Italy

Introduction | Multiple myeloma (MM) is a plasma cells (PCs) dyscrasia characterized by an accumulation of malignant PCs in the bone marrow (BM). Gain and/or amplification of 1q21 (1q21+) is one of the most frequent secondary cytogenetic events in MM patients. 1q21+ is a poor prognostic factor and it is associated to a shorter progression free survival in MM patients treated with carfilzomib (CFZ)-based regimens. Therefore, identify possible target genes in the 1q21 region is an emerging unmet medical need in MM patients. *PYGOPUS2* (*PYG02*) is a gene in chromosomal region 1q21 involved in Wnt signaling. In literature, *PYG02* upregulation is implicated in progression of multiple cancers and drug resistance by promoting one of its downstream targets, the drug resistance

polypeptide 1 (*MDR1*). The expression profile of *PYGO2* in 1q21+ MM patients and its possible role in CFZ resistance are still unknown and were explored in this study.

Methods. We purified CD138+ PCs from BM samples from 18 newly diagnosed MM (MMD) and 11 smoldering MM (SMM) patients. Fluorescent in situ hybridization (FISH) analysis was performed on purified CD138+ PCs to access copy number alteration in the region 1q21. The expression profile of all 29 samples was generated using GeneChip ClariomD Arrays (Affymetrix Inc.). The Sam R package was used to identify differentially expressed genes between 1q21+ and control samples. We evaluated *PYGO2* and *MDR1* mRNA expression levels by RT-PCR in PCs from 16 MMD, 13 relapsed myeloma (MMR) with or without 1q21+ and in CFZ-resistant (CFZ-R) human myeloma cell lines (HMCLs). Finally, we generated a *PYGO2*-knockdown (KD) in JLN3, a 1q21+ MM cell line, using shRNA lentivectors. Cell viability and gene expression profile were assessed.

Results. In our analysis on CD138+ cells database, *PYGO2* was significant upregulated in 1q21+ patients compared to controls, and there was a significant positive correlation between *PYGO2* and the copy number of 1q21 region. We also found the *PYGO2* overexpression in 1q21+ MMD and MMR patients compared to controls (MMD no 1q21). There was a significant upregulation of *MDR1* expression in 1q21+ MMD that increased in 1q21+ MMR patients, highlighting a possible relationship between *MDR1* and drug resistance. Interestingly, we found a positive significant correlation between the expression levels of *PYGO2* and *MDR1* in both MMD and MMR patients. In parallel, in CFZ-R HMCLs, we observed a significant upregulation of both genes compared to the CFZ-sensible ones. Finally, we generated a *PYGO2*-KD JLN3 cell line and downregulation of *PYGO2* resulted in decreased cell viability and in a significant reduced *MDR1* expression.

Conclusion. These results showed, for the first time, that *PYGO2* is overexpressed in 1q21+ MM patients and that the *PYGO2*-*MDR1* axis can be involved in CFZ resistance in MM cells, suggesting that *PYGO2* could be a potential drug target for MM patients with 1q21+.

C16

BIOLOGICAL AND MOLECULAR CHARACTERIZATION OF *IN SILICO* IDENTIFIED PUTATIVE INHIBITORS OF PARASPECKLE ASSEMBLY WITH POTENTIAL ANTI-MULTIPLE MYELOMA ACTIVITY

V. Traini¹, G. Fabbiano², D. Ronchetti¹, I. Silvestris¹, N. Puccio^{3,4}, S. Erratico^{5,6}, D. Giannandrea⁷, T. Laurenzi⁸, L. Palazzolo⁸, A. Ciarrocchi³, Y. Torrente⁶, R. Chiaramonte⁷, I. Eberini^{8,9}, N. Bolli^{1,2}, A. Neri¹⁰, E. Taiana²

¹Department of Oncology and Hemato-Oncology, University of Milan; ²Hematology Section, Fondazione IRCCS Ca' Granda Ospedale Maggiore Policlinico; ³Laboratory of Translational Research, Azienda USL-IRCCS Reggio Emilia; ⁴Clinical and Experimental Medicine PhD Program, University of Modena and Reggio Emilia; ⁵Novystem Spa; ⁶Stem Cell Laboratory, Department of Pathophysiology and Transplantation, University of Milan; ⁷Department of Health Sciences, University of Milan; ⁸Department of Pharmacological and Biomolecular Sciences, University of Milan; ⁹Data Science Research Center (DSRC), University of Milan; ¹⁰Scientific Directorate, Azienda USL-IRCCS Reggio Emilia, Italy

Introduction. Paraspeckles (PSs) are membraneless nuclear bodies, assembled through the interaction between the lncRNA NEAT1 and PS proteins (PSPs), among which NONO and SFPQ. We reported that NEAT1 is significantly overexpressed in plasma cells of multiple myeloma (MM) patients, and that its silencing leads to PSs dis-

assembly, negatively regulating MM cells proliferation and viability. On these bases we hypothesized that PSs may represent a novel vulnerability in MM, which remains an incurable disease. Here, we assess *in vitro* the activity of the top 6 hit compounds resulting from an *in silico* screening of small molecules targeting interaction points of NONO/SFPQ, potentially leading to PSs loss, thus mimicking the effect of NEAT1 silencing.

Methods. The biological activity of the 6 small molecules was evaluated in a panel of 6 MM cell lines (HMCLs), 4 haematological non-HMCLs and 6 healthy donors-derived PBMC samples. The IC50 values of the inhibitors were determined from dose-response curves based on Trypan Blue exclusion counts and confirmed by CellTiter-Glo assay. Confocal microscopy of combined NEAT1 RNA-FISH and NONO IF was used to evaluate modification of PSs number upon treatment. Clonogenic potential modulation was investigated through methylcellulose assay. Cell cycle and apoptosis were investigated by FACS analysis. WB was used to assess PSPs levels. Transcriptome analysis was conducted by means of Clariom™ D arrays.

Results. 2 of the 6 compounds led to a significant reduction of the number of viable cells upon treatment in all tested HMCLs but not in non-MM cells, highlighting a specific anti-MM activity. Confocal microscopy analysis showed a ~45% decrease in the number of PSs/cell in treated HMCLs, validating the expected loss of PS integrity and the on-target activity of both molecules. In line with the reduced viability, cell cycle analysis of treated HMCLs revealed a significant 2-fold increase of the cellular population in the Sub-G0/G1 phase, and a downregulation of the frequency of cells distributed in the S phase. Treatment also caused a reduced clonogenic potential, with a median of 50 colonies for vehicle vs 9 and 13 upon treatment with the 2 inhibitors. Flow cytometry analysis revealed a dose-dependent reduction of the % of viable cells and a concomitant increase of early and late apoptotic cells in treated HMCLs (2/5-fold increase, depending on the cell line), suggesting a pro-apoptotic effect exerted by both the molecules. Furthermore, WB results highlighted decreased core PSPs levels after treatment in all the HMCLs tested, but not in non-HMCLs. As expected from literature, transcriptomic analysis performed on treated HMCLs revealed the negative modulation of pathways associated with tumorigenic processes and circadian rhythm regulation.

Conclusions. 2 molecules targeting PSs essential interaction points exhibit an anti-MM specific activity, suggesting PS targeting as possible new druggable vulnerability in MM.

Myelodysplastic Syndromes

C17

ABSTRACT NOT PUBLISHABLE

C18

ABSTRACT NOT PUBLISHABLE

C19

THE POTENTIAL ROLE OF UBE2O IN THE TREATMENT OF INEFFECTIVE ERYTHROPOIESIS IN PATIENTS WITH MYELODYSPLASTIC SYNDROME

B. Maffeo¹, C. Panuzzo¹, F. Itri¹, A. Moraca¹, A. Savi¹, M. Armenio¹, V. Bonuomo¹, S. Marini¹, M.T. Voso², E. Bracco³, B. Pergolizzi¹, D. Cilloni¹

¹Department of Clinical and Biological Sciences of University of Turin; ²Department of Biomedicine and Prevention of University of Rome Tor Vergata; ³Department of Oncology of University of Turin, Italy

Introduction. Erythropoiesis is a tightly-regulated and complex process originating in the bone marrow from a multipotent stem cell and terminating in mature erythrocytes. In the last steps of erythropoiesis, the ubiquitin-proteasome system (UPS) allows to degrade most of the proteins, except for globin, to generate mature red blood cells. The ubiquitin-conjugating enzyme E2O (UBE2O) has been observed to be involved in the proteome remodeling under physiological conditions. Therefore, we hypothesized that it could be implied in the ineffective erythropoiesis characterizing myelodysplastic syndromes (MDS) pathogenesis. Ineffective erythropoiesis and anemia are the main features of low risk MDS. Therefore, new therapies have been developed to reduce or avoid red blood cell transfusion requirement, including Luspatercept which leads to an increase in the transcriptional factor GATA-1 by the inhibition of SMAD pathway.

Methods. We analyzed UBE2O expression levels in bone marrow (BM) samples collected from 70 MDS patients and 8 healthy controls. Then, we induced erythroid differentiation with erythropoietin treatment, and we evaluated UBE2O and GATA-1 mRNA and protein levels and UBE2O expression by immunofluorescent staining, in leukemic cell line (K562) and in patients' samples. In addition, we tested 10 BM samples after Luspatercept treatment.

Results. We observed a downregulation of UBE2O in MDS patients, compared to healthy controls and we demonstrated that the induction of erythropoiesis promotes UBE2O upregulation in patients' samples and in leukemic cells (K562). Moreover, we observed a significative positive correlation between UBE2O and GATA-1, thus validating the involvement of UBE2O in erythropoiesis. Consistently, we demonstrated that UBE2O and GATA-1 expressions are upregulated in MDS with ring sideroblasts (MDS-RS) after *in vivo* treatment with Luspatercept with a significative positive correlation, suggesting that GATA-1 could be a transcriptional factor of UBE2O during erythropoiesis.

Conclusions. Our data indicate that UBE2O may be a player in the erythroid maturation defect of MDS. Erythropoiesis induction is associated with an increase in UBE2O expression which is positively correlated with the expression of GATA-1, considered the master transcriptional factor of erythropoiesis. Finally, our data suggest that

Luspatercept treatment could restore a normal red cell maturation by upregulating UBE2O. Although further studies are needed to establish the role of UBE2O in MDS, and its correlation with GATA-1, this ubiquitination process seems a promising target to improve erythropoiesis in MDS.

C20

SPLICING ALTERATIONS IN LOW RISK MYELODYSPLASTIC SYNDROME, TGF-B PATHWAY DEREGLATION IN SF3B1 MUTATED PATIENTS

H. Hajrullaj¹, A. Onorato¹, M. Valenzuela¹, A. Cristiano¹, G. Silvestrini¹, M. Pieraccioli², E. Galossi¹, G. Falconi¹, S. Hutter³, N. Nadarajah³, R. Latagliata⁴, T. Haferlach³, P. Bielli¹, M.T. Voso¹, E. Fabiani^{1,5}

¹Department of Biomedicine and Prevention, University of Tor Vergata; ²Università Cattolica del Sacro Cuore; ³MLL Munich Leukemia Laboratory; ⁴Unità Operativa Complessa (UOC) Ematologia, Ospedale Belcolle and Division of Cellular Biotechnology and Hematology, Sapienza University; ⁵UniCamillus-Saint Camillus International University of Health Sciences

Low-risk myelodysplastic syndromes (LR-MDS), defined as MDS with a Revised International Prognostic Scoring System (IPSS-R) score ≤ 3 . 5 are a heterogeneous group of clonal disorders characterized by good prognosis. However, patients harboring mutations of some splicing factor genes, such as SRSF2, U2AF1 and ZRSR2 are characterized by poor prognosis as compared to SF3B1^{mut} patients. In this work we aim to identify transcriptome alterations implicated in clinical outcome of splicing factors mutated patients. For this purpose, from an initial cohort of 300 MDS, of which we had paired DNA and RNA BM-MNCs collected at the time of diagnosis and classified according to their mutational profile (t-NGS), we selected a study cohort of 50 LR-MDS (30 male and 20 female, median age 75 years, range 40-91) enriched for mutations in splicing factors (SF) genes. Bone marrow samples from 64 non-hematological patients were used as a control group. Whole exome sequencing (WES) was performed to identify additional non canonical mutations in SF genes (SF double mutated and ZRSR2^{mut} patients were excluded by the analysis). Principal component analysis (PCA) from RNA-seq data revealed distinct clusters between LR-MDS and non-hematological patients (differentially expressed genes, DEGs 4221; 3921 down- and 300 up-regulated). Subgrouping LR-MDS patients according to their specific SF mutation (SF3B1, SRSF2 or U2AF1), SF3B1^{mut} patients showed the higher number of DEGs (622; 10 down- and 612 up-regulated), while SRSF2^{mut} and U2AF1^{mut} patients displayed an expression profile similar to SF^{wt} LR-MDS patients (DEGs 13 and 4, respectively). Gene Ontology (GO) analysis (padj < 0.05 and log2 FC ≥ 2 and ≤ -2) identified TGF- β pathway as one of the most deregulated in SF3B1^{mut} patients. The analysis of alternative splicing (AS) was performed using rMATS to recognize aberrant splicing events in SF3B1-, SRSF2- and U2AF1-mutated patients. The percentage of genes subjected to AS regulation was high in all subgroups as compared to SF^{wt} patients (SF3B1^{mut} 25.7%, SRSF2^{mut} 20.92% and U2AF1^{mut} 13.16%). Most common AS events were "mutually exclusive" and "exon skipping" (SF3B1^{mut} 25% and 28%, SRSF2^{mut} 9% and 54% and U2AF1^{mut} 11% and 57%, respectively). Functional annotation of AS events in SF^{mut} patients identified iron metabolism, heme and coenzyme A synthesis among the most deregulated pathways. Of note, SF3B1^{mut} patients showed AS in genes belonging to TGF- β pathway (TGFB1, TGFB3, MAP3K7, FKBP12, etc.), suggesting that not only differentially expressed but also aberrant spliced genes may have a role in the pathogenesis of SF3B1^{mut} LR-MDS patients.

Since genes belonging to TGF- β pathway may be targeted by novel therapies (TGF ligand traps, anti TGF- β ligand antibodies, TGF- β receptor kinase inhibitors, antisense oligonucleotides, etc.), the identification of specific transcriptomic biomarkers predictive of response or disease evolution may be useful in the context of personalized therapy.

C21

ABSTRACT NOT PUBLISHABLE

C22

NATURAL LANGUAGE PROCESSING DRIVEN CLUSTERING OF PATIENTS WITH MYELOID NEOPLASMS USING CLINICAL TEXT REPORTS

G. Asti¹, E. Sauta¹, N. Curti², G. Carlini², L. Dall’olio³, L. Lanino⁴, G. Maggioni¹, A. Campagna¹, M. Ubezio¹, A. Russo¹, G. Todisco¹, C.A. Tentori¹, P. Morandini¹, M. Bicchieri¹, M.C. Grondelli¹, M. Zampini¹, E. Travaglino¹, V. Savevski¹, N.R. Derus², D. Dall’olio², C. Sala², L. Zhao⁵, A. Santoro¹, S. Kordasti⁶, V. Santini⁷, A.S. Kubasch⁸, U. Platzbecker⁸, M. Diez-campelo⁹, P. Fenaux⁵, A.M. Zeidan¹⁰, T. Haferlach¹¹, G. Castellani², M. Della Porta¹, S. D’amico¹

¹Humanitas Clinical and Research Center, IRCCS; ²University of Bologna; ³Data Science and Bioinformatics Laboratory, IRCCS, Institute of Neurological Sciences of Bologna; ⁴Humanitas Clinical and Research Center, IRCCS; ⁵Saint Louis hospital APHP; ⁶Comprehensive Cancer Center, King’s College London; ⁷MDS Unit, DMSC Hematology, University of Florence, AOUC; ⁸Medical Clinic and Policlinic 1, Hematology and Cellular Therapy, University Hospital Leipzig; ⁹Department of Hematology, Salamanca-IBSAL University Hospital; ¹⁰Section of Hematology, Department of Internal Medicine, Yale School of Medicine and Yale Cancer Center; ¹¹MLL Munich Leukemia Laboratory.

Introduction. This project was conducted by GenoMed4all and Synthema EU consortia. Clinical reports are the main form of data recording in healthcare, providing crucial information on diseases, patient’s status and clinical decisions. Leveraging new Natural Language Processing (NLP) Artificial Intelligence (AI) models it is possible to extract information from this unstructured data layer and use them in multimodal clinical solutions to perform personalized or precision medicine.

Methods. A NLP model was domain-adapted on hematological clinical reports of patients with myeloproliferative neoplasms (MPN), myelodysplastic syndrome (MDS) and acute myeloid leukemia (AML). We converted texts into embeddings, using a bidirectional encoder representations from transformers (BERT) model. Patients were stratified with HDBSCAN clustering on embeddings encoded by BERT (HematoBERT). Clusters were validated by assessing patients’ diagnosis and survival probability. HematoBERT’s performances were compared to pre-trained non-contextualized models.

Results. HematoBERT was fine-tuned by performing Masked Language Modeling (MLM) with the base-multilingual-uncased version of BERT on hematological reports of 1,328 patients. We then stratified a validation set of 360 patients’ reports and identified 7 clusters, defined by similar context. A brief description for each group of patients was obtained by summarizing the most important concepts of each cluster (Figure 1). Two clusters included MDS patients with excess blasts and MDS patients without excess blasts with ring sideroblasts and del5q. One cluster included MDS patients with excess blasts and MDS/MPN. Two clusters included MPN

patients with primary and secondary myelofibrosis, and MPN patients most including subject affected with polycythemia vera and essential thrombocytemia. Two clusters included patients with AML from MDS and therapy-related AML, and patients with de novo AML. Patients’ diagnoses resulted compatible with the cluster assignment (Figure 1). Frequency of gene mutations (assessed by targeted Next-Generation Sequencing) in each cluster reflected the genotypic-phenotypic associations in MDS, MPN and AML. Kaplan-Maier curves showed significant risk stratification in clusters in terms of survival probability, similar to stratifications performed on clinical and genomic data.

Finally, we evaluated the domain adaptation by comparing HematoBERT to other language models using Pseudo perplexity score (PPS), Accuracy and F1 score on a validation set of patients. HematoBERT outperformed the other models.

Conclusions. NLP domain-adapted language models can understand text representations and correlations between clinical reports and can be used to extract relevant features from clinical reports. The textual data layer is relevant to perform disease stratification of patients based on clinical and genomic information and could be integrated into next-generation multimodal models of personalized medicine.

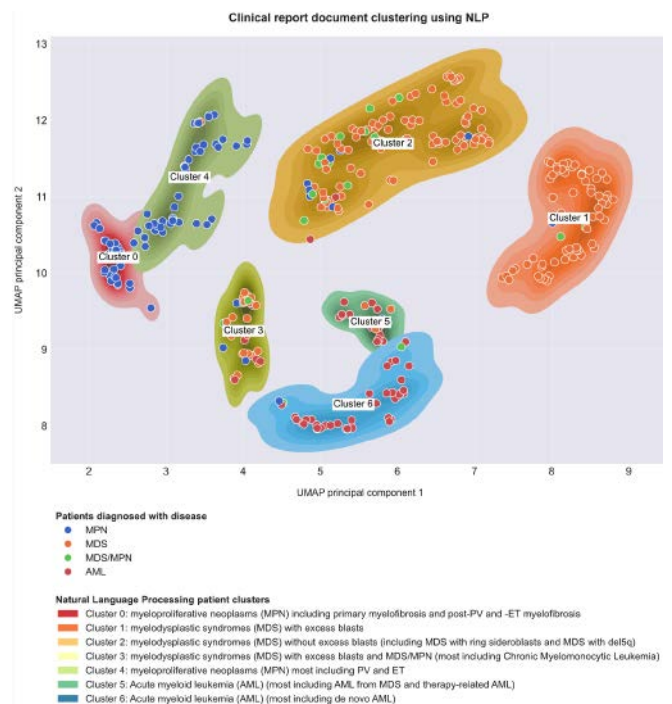


Figure 1.

C23

IMPROVING HEMATOLOGY RESEARCH AND CLINICAL OUTCOMES THROUGH SYNTHETIC HISTOPATHOLOGICAL IMAGES GENERATION

G. Asti¹, S. D'amico¹, N. Curti^{2,3}, G. Carlini^{2,3}, E. Sauta¹, N.R. Derus², D. Dall'olio², C. Sala², L. Dall'olio^{3,4}, L. Lanino⁵, G. Maggioni¹, A. Campagna¹, M. Ubezio¹, A. Russo¹, G. Todisco¹, C.A. Tentori¹, P. Morandini¹, M. Bicchieri¹, M.C. Grondelli¹, M. Zampini¹, V. Savevski¹, A. Santoro^{6,7}, S. Kordasti⁸, V. Santini⁹, A.S. Kubasch¹⁰, U. Platzbecker¹⁰, M. Diez-campelo¹¹, P. Fenauz¹², L. Zhao¹², A.M. Zeidan¹³, T. Haferlach¹⁴, G. Castellani², M. Della Porta^{1,15}

¹Humanitas Clinical and Research Center, IRCCS; ²University of Bologna; ³Data Science and Bioninformatics Laboratory, IRCCS, Institute of Neurological Sciences of Bologna; ⁴Department of Physics and Astronomy, University of Bologna; ⁵Humanitas Clinical and Research Center, IRCCS; ⁶Oncology Unit, Humanitas Cancer Center; ⁷Humanitas University; ⁸Comprehensive Cancer Centre, King's College London; ⁹MDS Unit, DMSC, Hematology, University of Florence, AOUC; ¹⁰Medical Clinic and Policlinic 1, Hematology and Cellular Therapy, University Hospital Leipzig; ¹¹Department of Hematology, Salamanca-IBSAL University hospital, Salamanca, Spain; ¹²Saint Louis Hospital APHP; ¹³Section of Hematology, Department of Internal Medicine, Yale School of Medicine and Yale Cancer Center; ¹⁴MLL Munich Leukemia Laboratory; ¹⁵Department of Biomedical Sciences, Humanitas University

Introduction. This project was conducted by GenoMed4all and Synthema EU consortia. Multimodal data (ranging from clinical and genomic information to imaging) are required to perform precision medicine when facing the rarity and complexity of Hematological malignancies. Unfortunately, collecting these data layers is challenging, in particular when collecting histological images from bone marrow (BM) biopsies. These issues can now be circumvented thanks to Synthetic data generation by Artificial Intelligence (AI), in fact, synthetic images can now be generated from textual inputs (e.g. pathologists' reports), thus allowing datasets enrichment, boosting translational research and improving precision medicine.

Methods. Use cases were patients affected by Myelodysplastic Syndrome (MDS), Acute Myeloid Leukemia (AML) and Myeloproliferative Neoplasm (MPN). We fine-tuned a Stable Diffusion (SD) generative model on hematological data to generate Hematoxylin and Eosin (H&E) images of myeloid neoplasms (MN) patients, conditioning the generation from text with a domain-adapted language model (HematoBERT). The morphological features extracted from real and synthetic images were compared using Synthetic Images Validation Framework (SIVF). Clinical validation was performed on disease classification and survival probability prediction, using real and synthetic images features (Figure 1).

Results. We trained the SD model on 200 patients. We applied SIVF to compare the extracted morphological features between synthetic and real images of 55 patients of the validation set, which resulted similar under distributions and correlations. We then implemented 3 XGBOOST models for MN classification. The classifiers were trained and validated on the morphological features of a real set of patients, a synthetic group and a mixed dataset. Data augmentation improved classification performance by 10% (F1 Score) when tested on the 3 validation sets. Finally, demographics, clinical and genomic features were included as covariates with the morphological ones of the BM biopsies in L1 penalized Cox's proportional hazards models, considering Overall Survival as primary endpoint. Models were fitted on two different cohorts of real patients (n=182, n=294). Both sets were enriched with 112 synthetic patients and the models refitted. We observed an improvement in performances of >10% (C-

Index) for both cases, with morphological features being selected among the best predictors. Results confirmed that synthetic data augmentation improves the models capability to capture clinical outcomes at individual patient level.

Conclusions. AI generated images preserve properties of real-world images, replicating cells morphological features relevant to identify hematological diseases and their status. This approach based on available textual data allows effective data augmentation and effortless data sharing, thus accelerating and improving precision medicine research in hematology.

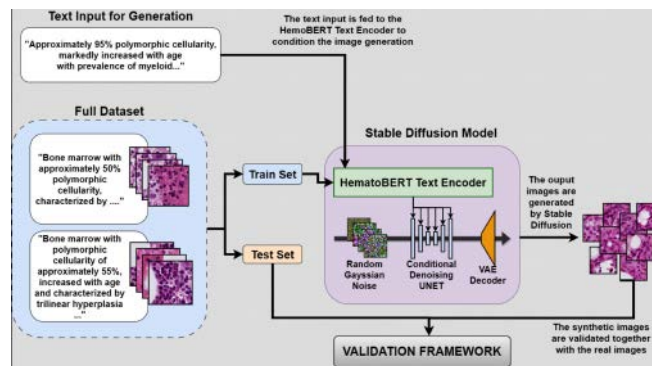


Figure 1.

C24

ABSTRACT NOT PUBLISHABLE

Monoclonal Gammopathies and Multiple Myeloma 2

C25

DRP1-MEDIATED MITOCHONDRIAL FISSION IS A THERAPEUTIC VULNERABILITY IN MULTIPLE MYELOMA

M.E. Gallo Cantafio¹, R. Torcasio¹, L. Ganino¹, I. Valentino¹, A. Gallo², I. Perrotta³, M. Gentile⁴, D. Tibullo⁵, C. Giallongo⁵, G. Viglietto¹, F. Di Raimondo⁵, A. Neri⁶, N. Amodio¹

¹Department of Experimental and Clinical Medicine, Magna Graecia University of Catanzaro; ²Fondazione Ri. MED; ³Department of Biology, Ecology and Earth Sciences, Centre for Microscopy and Microanalysis, University of Calabria; ⁴Department of Pharmacy, Health and Nutritional Science, University of Calabria; ⁵Department of Biomedical and Biotechnological Sciences, University of Catania; ⁶Scientific Directorate, IRCCS di Reggio Emilia, Italy

Introduction. Changes in mitochondrial dynamics, consisting in a continuum between fission and fusion events, impact on various tumor phenotypes, but their role in multiple myeloma (MM) pathobiology remains unclear. Herein, we have analyzed the biological significance of mitochondrial dynamics using *in vitro* and *in vivo* models of MM.

Methods. Mitochondrial architecture was assessed by transmission electron microscopy (TEM) analysis. Mitochondrial dynamics regulators' expression was evaluated by qRT-PCR and western blotting (WB). Cell viability was assessed by CTG assay, while apoptosis by Annexin V/7-AAD. ROS and mitochondrial superoxide species were determined by H2DCFDA and MITOSOX red staining, while lipid peroxides by BODIPY C11 FACS-analysis. NOD-SCID mice bearing proteasome-inhibitor (PI) resistant MM xenografts were used to test the anti-MM effects of Drp1 inhibitors *in vivo*.

Results. Morphological assessment of mitochondria by TEM evidenced peculiar mitochondrial patterns, with smaller mitochondria particularly evident in PI-resistant cell lines and primary PCs from RRMM patients. Upregulation of mitochondrial fission drivers, namely the GTPase Drp1, its active S616 phosphorylated form, the Drp1-receptor MFF, along with down-regulation of fusion promoter MFN2, was observed in different PI-resistant, but not in DEXA-resistant, MM cell lines. In three public datasets (GSE5900, GSE13591 and GSE2658), the DNM1L mRNA, encoding Drp1, was found upregulated in MM as compared to healthy plasma cells, and high DNM1L correlated with worse overall survival of patients undergoing PI-regimens within the CoMMpass dataset. These data underscore a mitochondrial dynamics shift towards fragmentation, which accompanies the acquisition of PI resistance. Targeting mitochondrial fission with mDIVI-1, an established inhibitor of Drp1, or with a novel ellipticine derivative, reduced the viability of primary MM cells or cell lines, even co-cultured with patient-derived bone marrow stromal cells, increased ROS and mitochondrial superoxide species and enhanced bortezomib activity, while was not cytotoxic to healthy PBMCs. RNA seq analysis highlighted an upregulation of apoptotic and ferroptotic pathways in PI-resistant cells upon Drp1 pharmacological inhibition, together with decreased expression of transcription factors prompting de novo lipogenesis and ferroptosis resistance (c-MYC, SREBF1/2); consistently, reduced levels of saturated and mono-unsaturated fatty acids were observed upon Drp1 pharmacological inhibition, as determined by targeted lipidomics. *in vivo*, inducible knock-down of DNM1L, as well as Drp1 pharmacological inhibition with two different drugs, reduced the growth of PI-resistant MM xenografts and prolonged animal survival.

Conclusion. These findings shed light on unbalanced mitochondrial dynamics associating with PI resistance, highlighting novel mitochondrial vulnerabilities with therapeutic significance.

C26

NAD+ METABOLISM RESTRICTION BOOSTS HIGH-DOSE MELPHANAN EFFICACY IN MULTIPLE MYELOMA PATIENTS

D. Soncini¹, P. Becherini², S. Ravera³, A. Chedera⁴, D. Truffelli², E. Gelli⁵, F. Ladisa^{2,6}, C. Martinuzzi¹, G. Giorgetti^{2,6}, F. Piacente³, F. Guolo^{1,2}, M. Garibotto², S. Aquino⁷, S. Bruzzone³, A. Bellotti⁸, M. Duschosal⁸, A. Nahimana⁸, E. Angelucci⁷, N. Chandra⁴, A. Nencioni^{1,9}, R.M. Lemoli^{1,2}, M. Cea^{1,2}

¹IRCCS Ospedale Policlinico San Martino; ²Clinic of Hematology, Department of Internal Medicine and Medical Specialties (DiMI), University of Genoa; ³Department of Experimental Medicine (DIMES), University of Genoa; ⁴Department of Biochemistry, Biological Science Division, Indian Institute of Science, Bengaluru; ⁵Genetics and Epigenetics of Behavior Laboratory, Fondazione Istituto Italiano di Tecnologia (IIT); ⁶Jerome Lipper Multiple Myeloma Center, Department of Medical Oncology, Dana Farber Cancer Institute, Harvard Medical School; ⁷Hematology and Hematopoietic Stem Cell Transplantation Unit, IRCCS Ospedale Policlinico San Martino; ⁸Central Laboratory of Hematology, Department of Medical Laboratory and Pathology, Lausanne University Hospital and University of Lausanne; ⁹Geriatrics Clinic, Department of Internal Medicine and Medical Specialties (DIMI), University of Genoa, Italy

Introduction. We previously reported pervasive nicotinamide adenine dinucleotide (NAD+) dysregulation in Multiple Myeloma (MM) cells associated with NAMPT enzyme thus supporting its druggability. Unfortunately, clinical utility of this strategy is hampered by alternative NAD+ production routes that confer resistance to NAMPT inhibitors. For young fit MM patients, the standard of care consists of high-dose melphalan (HDM) followed by autologous stem cell transplantation (ASCT), which still remains the most effective option to achieve deep response and long-term remission.

Methods. The NAD+-biosynthetic landscape of MM was investigated by measuring transcript levels of NADome signature in 787 MM patients of the CoMMpass dataset and in a proprietary cohort of 20 NDMM patients. The clinical impact [i]n terms of OS and PFS) of this signature and the genomic aberrations of enzymes involved in NAD+ synthesis were also analyzed. A quantitative kinetic model of the NAD+-biosynthetic landscape (NADnet) of MM cells was built using mathematical modeling by integrating transcriptome and biochemical data; next, chemical and genetic (shRNAs and CRISPR-Cas9 Knock-Out) targeting approaches were used. Detailed functional analyses using qPCR, western blot, immunofluorescence, biochemical- and FACS-based assays were performed. Translational relevance of these results was confirmed by focusing on CD138+ primary tumor cells and using a mouse model xenografted with MM engineered cells. Finally, clinical benefits of our study were tested by analyzing gut microbiota status of 80 MM patients undergoing HDM followed by ASCT.

Results. A comprehensive metabolic landscape analysis revealed Preiss-Handler (PH) and salvage pathways as the predominant NAD+ sources for MM cells with their expression affecting clinical outcome of these patients. By integrating transcriptional data of CD138+ and CD138- fractions derived from CoMMpass dataset with specific biochemical parameters of MM cells, we built a quantitative kinetic model of NAD+ biosynthetic pathway (NADnet) which reveals that PH pathway significantly sustains NAD+-synthesis through NAPRT1. Accordingly, we found that NAPRT1 confers resistance to NAD+ depleting agents but dual NAMPT/NAPRT1 inhibition represents an effective anti-MM strategy. Bioenergetic profiling of NAPRT1 KO cells revealed increased oxidative stress, weakened endogenous antioxidant defenses, and enhanced genomic instability; NAMPT inhibitors further improve these findings with NAD+- comprehensive restriction sensitizing MM cells to genotoxic

stress. In a clinical setting, we show that interfering with NAD⁺-boosting effects of gut-microbiome enhances HDM regimens benefit in ASCT-eligible MM patients with NAD⁺ complete starvation further improving its effectiveness.

Conclusion. Overall, our results propose metabolic restriction as promising strategy to be tested in randomized clinical trials involving transplant eligible MM patients.

C27

GLUTAMATE METABOLISM AFFECTS OSTEOCLAST DIFFERENTIATION IN MULTIPLE MYELOMA PATIENTS| NOVEL THERAPEUTIC TARGET FOR MYELOMA BONE DISEASE

O. Lungu¹, D. Toscani¹, V. Raimondi¹, N.T. Iannozzi¹, M. Chiu², A.B. Dalla Palma³, S. Ricci³, M. Scita³, O. Bussolati², P. Storti¹, N. Giuliani^{1,3}

¹Laboratorio di Ematologia, Dipartimento di Medicina e Chirurgia, Università di Parma; ²Patologia Generale, Dipartimento di Medicina e Chirurgia, Università di Parma; ³U. O. Ematologia e CTMO, Azienda Ospedaliero-Universitaria di Parma, Programma Dipartimentale Mieloma Multiplo e Gammopatie Monoclonali, Italy

Introduction. Multiple myeloma (MM) cells are Glutamine (Gln)-addicted and MM-dependent Gln-exhausted niche impairs osteoblast differentiation. We demonstrated that MM patients are characterized by lower Gln and higher levels of its main metabolite Glutamate (Glu) as compared with Smoldering MM (SMM) and Monoclonal Gammopathy of Uncertain Significance (MGUS) patients. Based on this evidence, we hypothesized that high Glu levels may have a significant impact on osteoclast (OCL) formation and thereby contribute to the development of osteolytic lesions.

Methods. The bone resorption marker C-terminal telopeptide of collagen type I (CTX-I) and Glu levels were measured on a cohort of 97 serum samples (20 MGUS, 32 SMM and 45 newly diagnosed MM). CD14⁺ monocytes were isolated from bone marrow (BM) aspirates and incubated in osteoclastogenic medium in the presence or absence of Glu. Amino acid uptake and amino acid content have been assessed by radiolabeled amino acids and liquid chromatography coupled with tandem mass spectrometry (LC-MS/MS), respectively.

Results. MM patients have higher levels of BM CTX-I compared with MGUS and SMM patients reflecting the increased OCL activity typical of MM patients. There is a positive correlation in MM patients between CTX-I and Glu suggesting that high Glu levels characterize patients with high bone turnover. The presence of Glu increased the number of OCLs generated from MGUS/SMM CD14⁺ compared with cells differentiated in the absence of the amino acid. In these patients, Glu increased the expression of NF- κ B and NFATc1 pointing to a stimulatory effect on osteoclastogenic pathway. On the contrary, CD14⁺ obtained from MM patients have a lower response to Glu probably as a consequence of the high Glu microenvironment imposed by MM cells. The analysis of intracellular amino acids performed on pre-malignant CD14⁺ cells indicated that Glu content significantly increases after 8 days of differentiation while decreasing after 14 days pointing to a fast accumulation of Glu upon differentiation. Consistently, the activity of the Glu transporter EAAT1 increases already after 3 days of incubation in differentiating medium without Glu, with a further increase in the presence of the amino acid. In contrast, in MM CD14⁺ cells Glu does not stimulate neither Glu uptake nor intracellular content. Selective inhibitors of EAAT1, D-Aspartate (D-ASP) and TFB-TBOA completely blocked the formation of multinucleated OCLs in the presence of Glu.

Conclusions. OCLs formation is characterized by increased activity of EAAT1 transporter and Glu content during the early phase of differentiation, while the inhibition of EAAT1 markedly blocks OCL

formation. A different sensitivity to Glu was observed in patients with MGUS and SMM compared to MM due to the high Glu level found in MM bone niche. Overall, our data suggest that glutamate metabolism could be a possible target for MM-induced osteoclastic bone destruction in MM patients.

C28

CD56 EXPRESSION ENHANCES THE EFFICACY OF DARATUMUMAB-BASED TREATMENT STRATEGIES IN MYELOMA CELLS BY REDUCING INTRACELLULAR NAD⁺ AND INCREASING CD38 EXPRESSION LEVELS

G. Giorgetti^{1,2}, P. Becherini¹, E. Maroto-martin^{2,3}, D. Fenoglio^{4,5}, D. Soncini¹, C. Martinuzzi⁴, S. Bruzzzone⁶, F. Ladisa^{1,2}, I. Traverso¹, A. Nahimana⁷, C.R.M. Uras⁸, A. Schavgoulidze^{2,9}, J. Fong Ng², N.C. Munshi^{2,3,10}, R.M. Lemoli^{1,4}, M. Fulciniti^{2,3}, M. Cea^{1,4}

¹Clinic of Hematology, Department of Internal Medicine and Medical Specialties (DiMI), University of Genoa; ²Department of Medical Oncology, Jerome Lipper Multiple Myeloma Center, Dana-Farber Cancer Institute; ³Harvard Medical School; ⁴IRCCS Ospedale Policlinico San Martino; ⁵Centre of Excellence for Biomedical Research and Department of Internal Medicine, University of Genoa; ⁶Department of Experimental Medicine (DIMES), University of Genoa; ⁷Central Laboratory of Hematology, Department of Medical Laboratory and Pathology, Lausanne University Hospital and University of Lausanne; ⁸Department of Experimental Medicine, Centre of Excellence for Biomedical Research, University of Genoa; ⁹Toulouse Cancer Research Center-Oncopole, Toulouse University; ¹⁰VA Boston Healthcare System

High levels of CD56 are observed on tumor plasma cells of 70% of Multiple Myeloma (MM) patients. This molecule has several functions including tumor growth, adhesion and response to therapy. However, an extensive analysis of the specific landscape underlying its expression and its role as prognostic biomarker is lacking, especially in MM. CD56 and CD38 surface levels were evaluated by FACS analysis on CD138POS cells collected from 136 newly diagnosed MM patients at Clinic of Hematology of San Martino Hospital (Genoa, Italy), between 2015 and 2022, by MFI. Isogenic MM cell lines, control and stable CD56-overexpressing or silenced cells, were generated by lentiviral transduction. Metabolic profiling triggered by CD56 handling was investigated using different assays including NAD⁺ fluorometric assay and CD38 enzymatic activity (cyclase activity assay). *Ex vivo* ADCC assays, using NK from healthy donors, were also employed to quantify MM cell lysis triggered by anti-CD38 antibody (1 μ g/mL Daratumumab). We found that low CD56 surface expression significantly correlates with extramedullary disease (EMD) (p=.016) while high CD56 levels are associated with a lower risk of disease progression or death (p=.003) in our cohort of MM patients. Surprisingly, a positive correlation between CD56 and CD38 levels (p<.0001) was observed and it was also replicated in a panel of MM cell lines with different genomic background. As result, we hypothesized that CD56 expression affects Daratumumab (DARA)-mediated ADCC. Indeed, MM cell lines with high expression of CD56 were more sensitive to DARA-mediated NK cell killing (p=.004 at ratio 1:1 EIT) than those carrying lower levels of CD56 on their surface. Consistently, MM patients with higher CD56 levels had better overall response rates from DARA-based therapies compared to others. Since CD38 is a critical enzyme for breaking down NAD⁺ in cells, we next tested the hypothesis that CD56 modulates CD38 levels by affecting intracellular NAD⁺ pathway. The ectopic expression of CD56 led to lower intracellular NAD⁺, increase CD38 enzymatic activity and increase MM cells' sensitivity to NAMPT inhibitors agents. Indeed, CD56-overexpressing MM cells were more

vulnerable to these molecules, including next-generation inhibitors; by contrast, CD56 silencing made MM cells more resistant. Our data suggest CD56 level is an important determinant for DARA-based therapies and further support its role as biomarker for selecting the most appropriate anti-MM strategies. Moreover, we identify NAMPT inhibitors as an innovative strategy to be offered mainly to CD56-over-expressing MM patients.

C29

A SINGLE MRD NEGATIVITY DETECTION BY NEXT GENERATION FLOW (NGF) 10-6 RESULTS IN A SIGNIFICANT PROLONGED PFS IN THE DART4MM STUDY (DARATUMUMAB AS FIXED CONSOLIDATION THERAPY IN MULTIPLE MYELOMA PATIENTS IN >VGPR/MRD POSITIVE AFTER A FIRST LINE THERAPY)

A. Gozzetti¹, P. Pacelli¹, D. Raspadori¹, F. Caroni¹, E. Bestoso¹, E. Antonioli², G. Buda³, S. Ciofini¹, A. Santoni¹, L. Puccetti¹, P. Galieni⁵, F. Bacchiari¹, M. Staderini², D. Tocci¹, I. Attucci², M.L. Del Giudice³, V. Candi⁵, V. Sammartano¹, A. Lombardo, A.M. Liberati⁴, A. Sicuranza¹, M. Ruggieri, U. Occhini⁵, S. Galimberti³, A.M. Vannucchi², M. Bocchia¹

¹Hematology, University of Siena; ²Hematology, University of Florence, Florence; ³Hematology, University of Pisa; ⁴Hematology, University of Perugia; ⁵Hematology, Ascoli Piceno; ⁵Hematology, Arezzo, Italy

Introduction. Although multiple myeloma (MM) patients have experienced many progresses in survivals in latest years, the disease is still incurable. Novel drugs can give deeper responses respect to the past, and CR achievement is not sufficient anymore to testify a durable response. MRD status measured both by Euro-FLOW or NGS is a consolidated new prognostic parameter in MM trials (threshold at 10-5 according to IMWG guidelines). A consolidation therapy with VTD after Autologous Stem cell Transplant (ASCT) has been reported in a randomized trial to increase the level of MRD responses measured by NGS. Daratumumab is an IgG/k monoclonal antibody that binds selectively to CD38 on MM plasma cells and is now part of the standard of care therapy. However, little is known about Daratumumab efficacy as consolidation therapy after a first line of therapy and about its MM eradication potential as means of MRD negativity and PFS, especially if used in a very good responder group of patients after ASCT.

Methods. Bone marrow aspirates from MM patients, achieving >VGPR after a fixed first line of therapy were collected from 5 centers for MRD positivity in the DART4MM study (Co-financed by Janssen). NGF was centralized at the Hematology University of Siena and measured according to Euro Flow consortium guidelines with 2 height colors tubes (BD OneFLOW Tm PCST e BD OneFLOW Tm PCD. BD BioSciences). MRD detection was set at 10-6 in all samples analyzed. Clinical and biological data as well as molecular cytogenetics information was collected. In particular PET/CT at screening and every 6 months for 24 months; ISS status and presence of high-risk features (del17p, t(4;14) or t(14;16) ampl 1q by FISH). Daratumumab was given according to monotherapy schedule weekly for 8 times and then every two weeks for 8 times. Primary endpoint was set at 6 months MRD negative patients stopped the drug, MRD positive patients continued once a month until 24 months total. MRD was measured at 2, 6, 12, 18, 24 months (MRD2, 6, 12, 18, 24). PFS and OS were measured and analyzed related to MRD status, FISH risk, ISS in univariate analysis (MED CALC, Belgium).

Results. Between December 2018 and March 2022, 110 MM patients were screened. 53 patients resulted MRD positive, 3 with-

drawn consent and 50 were enrolled. Median age was 61 (range 40-77); male/female 27/23; IgG (K/Lambda) 33(21/12); IgA 6 (3/3); BJ 9(5/4); IgD lambda1; NS 1. ISS 3 was present in 16% of the patients. High risk cytogenetics in 9/50 (8%) of the patients (del 17p in 2, t(4;14) in 1; amp 1q in 4, 1 patient had a double-hit MM (amp 1q and t(4;14) and 1 patient had a triple hit (del17p, t(4;14) and amp1q). 45 patients received an ASCT (1 ASCT 34; 2 ASCT 11) and 5 patients were after VMP treatment. enrolled after >VGPR (Seventeen (34%) patients were judged in CR and 33 (66%) in VGPR at the enrollment. At the primary endpoint 15/50 (30%) patients were MRD negative at 10-6. Interestingly other 8 patients became MRD negative for the first time after 6 months and during daratumumab therapy between month 6 and 24 and 2 patients had a MRD negativity detection at month 2 but unsustainable later. Totally 27/50 (54%) MM patients had at least one MRD negativity detection. At a median follow up of 42 months (range, 13-55), 23 (46%) patients relapsed (15 before 24 months). Median PFS is not reached, and OS is not reached. In particular achieving at least one MRD negativity is statistically significant vs not reaching MRD negativity (NR vs 24 months, p=0,001). Particularly, MRD6 negativity is not significant (44 vs 39 months, p=0,44) but MRD12 it is (NR vs 42 months, p=0,0001). FISH did not correlate with PFS or OS.

Discussion. MRD negativity confirm to be a prognostic parameter in MM. This is the longest follow up ever of an MRD based study in MM

C30

COMBINATORIAL STRATEGIES TARGETING NEAT1 AND AURKA AS NEW POTENTIAL THERAPEUTIC OPTIONS FOR MULTIPLE MYELOMA

N. Puccio^{1,2}, E. Taiana³, G. Manzotti¹, F. Torricelli¹, E. Mereu⁴, D. Ronchetti^{3,5}, C. Bandini⁴, I. Craparotta⁶, M. Bolis⁶, V. Manicardi¹, V. Fragiasso¹, N. Bolli^{3,5}, R. Piva⁴, A. Ciarrocchi¹, A. Neri⁷

¹Laboratory of Translational Research, Azienda Unità Sanitaria Locale-IRCCS Reggio Emilia; ²Clinical and Experimental Medicine PhD Program, University of Modena and Reggio Emilia; ³Hematology, Fondazione Cà Granda IRCCS Policlinico; ⁴Department of Molecular Biotechnology and Health Sciences, University of Turin; ⁵Department of Oncology and Hemato-oncology, University of Milan; ⁶Computational Oncology Unit, Oncology Department, Mario Negri IRCCS; ⁷Scientific Directorate, Azienda Unità Sanitaria Locale-IRCCS Reggio Emilia, Italy

Introduction. Multiple myeloma (MM) patients show a severe de-regulation of long non-coding RNAs (lncRNAs) that influence disease progression and therapy resistance. NEAT1 is a lncRNA essential for nuclear paraspeckles and is involved in gene expression regulation. We showed that NEAT1 supports the proliferation of MM cells *in vitro* and *in vivo*, making this lncRNA an attractive candidate for therapeutic intervention. Herein, we aim to identify targeting strategies that could synergize with NEAT1 inhibition in restraining MM growth and progression.

Methods. We used a combinatorial approach that integrates computational tools with functional screening. RNA-seq analysis was performed in NEAT1 silenced (KD) and relative control (SCR) AMO-1 MM cell line and the output was used to query the Connectivity Map database (cMAP) to find targeting drugs that mimic the transcriptional effect of NEAT1 KD. 320 inhibitors were screened through a high-throughput (HT) approach in both KD and SCR AMO-1 cells. Validation of HT results was performed on a panel of three MM cell lines with live-imaging system. Rescue experiments were performed using a CRISPRa NEAT1 overexpressing AMO-1 cell system. *In vivo* validation was performed using the MMRF CoMMpass dataset.

Results. RNA-seq analysis resulted in 752 down-regulated and 957 up-regulated genes in NEAT1 KD AMO-1 cell line. cMAP query reveals 14 drug categories mimicking NEAT1KD transcriptional effect. Aurora kinase A (AURKA) inhibitors were identified as top-scoring molecules. HT screening identified 19 different compounds showing synergistic activity with NEAT1 KD. In line with the in-silico prediction, two different AURKA inhibitors were found within this list. An in depth-validation was performed on a panel of three MM cell lines, confirming the synergistic activity. At the biological level, we demonstrated that the combination of NEAT1 and AURKA inhibition caused severe nuclei and cytoskeleton alterations with evidently enlarged cell nuclei and actin mislocalization, indicative of impaired cytokinesis and enhanced cellular stress. Noticeably, over-expression of NEAT1 determined a significant reduction of MM cells' sensitivity to both AURKA inhibitors, confirming the interplay between AURKA and NEAT1 in this context. Analysis of the CoMM-pass dataset showed that AURKA expression is strongly associated with reduced progression-free ($p < 0.0001$) and overall survival probability ($p < 0.0001$) in MM and that, patients displaying high levels of both NEAT1 and AURKA have a worse clinical outcome, as compared with the other categories.

Conclusion. Our results demonstrated for the first time a functional cooperation between AURKA and NEAT1, paving the way for the development of a combinatorial therapeutic strategy targeting AURKA and NEAT1 in MM.

C31

USE OF BOVINE HERPES VIRUS TYPE 1 (BOHV-1) AS ALTERNATIVE TOOL IN MULTIPLE MYELOMA ONCOLYTIC VIROTHERAPY

V. Raimondi¹, P. Storti¹, V. Marchica¹, V. Franceschi², R. Vescovini¹, D. Toscani¹, N.T. Iannozzi¹, O. Lungu¹, A.B. Dalla Palma³, M. Bernardi³, M. Scita³, G. Pozzi¹, P. Mirandola¹, G. Donofrio², N. Giuliani^{1,3}

¹Dipartimento di Medicina e Chirurgia, Università di Parma;

²Dipartimento di Scienze Medico Veterinarie, Università di Parma;

³U. O. Ematologia e CTMO, Azienda Ospedaliero-Universitaria di Parma, Programma Dipartimentale, Mieloma Multiplo e Gammopatie Monoclonali, Italy

Introduction. Oncolytic viruses (OVs) represent a new anti-cancer strategy. Several studies reported that, in multiple myeloma (MM), the OVs act through tumor-specific oncolysis and generation of an anti-tumor immune response increasing the anti-MM effect of T and NK cells. The main tested viruses are of human origin; however, this approach is highly restricted by pre-existing anti-virus humoral immunity that neutralizes the anti-tumor effect of OVs. Recently, the use of non-human viruses, non-pathogen for humans, has been under consideration for a direct anti-MM oncolytic effect. To increase the possible spectrum of non-human oncolytic viruses, in this study we aim to evaluate the role of the Bovine Herpes Virus type 1 (BoHV-1) as anti-MM treatment investigating both its direct and indirect immune-therapeutic effects.

Methods. Firstly, we evaluated the expression of BoHV1 entry putative receptors (CD111, CD155 and CD138) on human myeloma cell lines (HMCLs) by flow cytometry. Thereafter we treated JJN3 and MM1.S cell lines with BoHV-1 at 1 and 2 multiplicity of infection (MOI) for 24, 48 and 72h. Besides, BoHV-1 pre-treated JJN3 were co-cultured with NK-92 cells and the NK-mediated cytotoxicity was assessed. Moreover, we evaluated the expression of BoHV-1 entry receptors on primary MM plasma cells (PCs) from bone marrow (BM) mononuclear cells (MNCs) of a cohort of relapsed/refractory MM patients. In parallel, BM MNCs were infected with BoHV-

1, at 1 and 2 MOI, for 48, 72 and 96h and the oncolytic effect was evaluated. The activation of NK cells, CD8⁺ T cells and monocytes was determined by CD69 surface expression analysis; while CD107a, as degranulation marker, were assessed on NK and CD8⁺ T cell.

Results. We observed that HMCLs express high levels of BoHV1 entry receptors and we found a significant increase of HMCLs death after 48h and 72h of BoHV1 infection. This BoHV-1 cytotoxic effect was associated to a significant increased expression of the apoptotic marker Apo2.7. Interestingly, BoHV-1 pre-treatment of JJN3 significantly increased the cytotoxic effect of NK-92 in a 4h co-culture assay. Next, we studied the *ex vivo* effect of BoHV-1 treatment on patients' BM MNCs. We detected variable BoHV1 entry receptors expression on MM PCs and a significant decrease of viable CD138⁺CD38⁺ cells after 48h of BoHV-1 infection at both 1 MOI and 2 MOI. Additionally, we investigated whether BoHV-1 treatment could modulate activation markers on immune effector cells *ex vivo*. BoHV-1-treated BM MNCs showed a significant upregulation of CD69 expression on NK, CD8⁺ T cells and monocytes and a significant increase of CD107a expression on NK and CD8⁺ T cells.

Conclusions. Overall, our data indicate that BoHV-1 has a direct effect against malignant PCs and can also act indirectly involving the immune-microenvironment cells in the generation of an anti-tumor immune response. This study suggests the use of BoHV-1 as a novel alternative anti-MM virotherapy strategy.

C32

DYSFUNCTIONAL BONE MARROW AND CIRCULATING $\gamma\delta$ T CELLS PREDICT A HIGH RISK OF PROGRESSION FROM PRE-MALIGNANT PLASMA CELL DYSCRASIAS TO SYMPTOMATIC MULTIPLE MYELOMA

A.M. Corsale^{1,2}, M. Shekarkar Azgomi^{1,3}, F. Plano², M. Di Simone¹, C. Perez⁴, E. Gigliotta², M. Speciale², C. Aquilina², C. Vullo², F. Garofano², G. Camarda², C. Rotolo², M. Santoro², N. Caccamo^{1,3}, B. Paiva⁴, S. Siragusa², F. Dieli^{1,3}, S. Meraviglia^{1,3}, C. Botta²

¹Central Laboratory of Advanced Diagnosis and Biomedical Research (CLADIBIOR), University of Palermo; ²Department of Health Promotion, Mother and Child Care, Internal Medicine and Medical Specialties (ProMISE), University of Palermo; ³Department of Biomedicine, Neuroscience and Advanced Diagnosis (Bi. N. D.), University of Palermo; ⁴Centro de Investigacion Medica Aplicada, Instituto de Investigacion Sanitaria de Navarra Hematology Unit, Clinica Universidad de Navarra, Centro de Investigacion Biomedica en Red, Cancer Hematology Unit, Italy

Introduction. The interplay between clonal plasma cells and the bone marrow (BM) microenvironment plays a crucial role in the development of multiple myeloma (MM). Therefore, understanding this relationship is crucial for identifying and effectively managing patients at a high risk of neoplastic progression, ultimately improving clinical outcomes. $\gamma\delta$ T cells, functioning as a link between the innate and adaptive immune systems, contribute to immune responses during cancer progression. However, their role in MM and its early phases, such as monoclonal gammopathy of undetermined significance (MGUS) or smoldering MM (SMM), remains unclear. Thus, the purpose of this study was to determine the role of $\gamma\delta$ T cells in the immunopathogenesis of MM and its preneoplastic stages.

Methods. We conducted scRNAseq analysis on BM CD3⁺ cells from 3 healthy donors (HD), 5 MGUS/SMM patients, and 9 MM patients, analyzing a total of 12527 $\gamma\delta$ T cells. Next, we performed flow cytometric analysis on 11 HD, 13 MGUS, and 29 MM patients to assess their frequency, differentiation/exhaustion profile, and effector functions. We functionally validated our results by co-culturing PBMCs or sorted $\gamma\delta$ T cells from HD with MM cell lines.

Results. Through scRNAseq analysis, we identified 7 $\gamma\delta$ T cell clusters! 2 naive subpopulations (CD4-/CD8- and CD4+), 3 GZMB effector/terminally differentiated (CD8+/TIGIT+/LAG3+, TIM3+/CD27- and GNLY+/FTH1+) and 2 GZMK memory subpopulations (GZMK+ and CXCR3+). Moreover, as MM progressed, we observed a decrease in naive $\gamma\delta$ T cells ($p<0.05$) followed by an increase in TIM3 expression. No significant differences were observed in the frequencies of circulating and BM V δ 1+ and V δ 2+ T cells. However, effector memory V δ 2+ cells increased in MM patients compared to preneoplastic conditions and HD, where naive and central memory populations predominated ($p<0.05$). Co-culture with the cell line U266 confirmed the expansion in effector memory V δ 2+ T cells ($p<0.01$) and a decrease in central memory phenotype ($p<0.001$), indicating a MM-dependent induced phenotypic alteration. Circulating and BM $\gamma\delta$ T cells acquired an exhausted phenotype as MM progressed, mainly demonstrated by the co-expression of TIM3 and PD1. ($p<0.05$). This altered phenotype was associated with impaired functions of V δ 1+ and V δ 2+ T cell subsets, as evidenced by reduced TNF- α and IFN- γ expression upon *in vitro* stimulation, along with overexpression of the CD69 molecule ($p<0.05$). Notably, lower percentages of circulating and BM PD1+ V δ 2+, as well as BM effector memory V δ 2+ T cells (MGUS/SMM-like profile) were associated with improved patients' 1-year progression-free survival ($p<0.05$).

Conclusions. $\gamma\delta$ T cells acquire a dysfunctional phenotype during MM progression, which significantly impacts patient prognosis. Circulating $\gamma\delta$ T cells, which mimic the BM milieu, may serve as a potentially less invasive means for follow up and prognostication of patients affected by monoclonal gammopathies.

Acute Leukemias 2

C33

ABSTRACT NOT PUBLISHABLE

C34

THE NPM1 MUTANT IS EXPRESSED IN CAJAL BODIES AND LOST DURING DIFFERENTIATION IMPLICATION FOR THE PATHOGENESIS OF NPM1-MUTATED AML

B. Falini¹, T. Marafioti², A. Marra¹, F. Facchetti^{3,4}, B. Bigerna¹, D. Sorcini¹, V. Perriello¹, E. Tiacci¹, P. Sportoletti¹, M.P. Martelli¹, B.T. Gjertsen⁵, V. Andresen⁵

¹Department of Medicine and Surgery, Institute of Hematology and Center for Hemato-Oncology Research (CREO), University of Perugia, Santa Maria della Misericordia Hospital, Perugia, Italy; ²University College, London, UK; ³University of Brescia School of Medicine, Brescia, Italy; ⁴Hematopathology Unit, IRCCS Azienda Ospedaliero-Universitaria di Bologna, Italy; ⁵Centre for Cancer Biomarkers (CCBio), Department of Clinical Science, University of Bergen, Norway

Background. NPM1-mutated AML shows unique clinical and molecular features, including cytoplasmic expression of the NPM1 mutant that is critical for leukemogenesis and can be detected by immunohistochemistry.

Aims. We generated a tumor specific monoclonal antibody (mA[b] UBE recognizing the NPM1 mutant, to study the expression of NPM1 mutant at subcellular level and during maturation of the leukemic clone.

Methods. Single e double immunostainings with the specific mAb UBE were performed according to standard procedures.

Results. The NPM1 mutant was consistently and strongly expressed in the cytoplasmic of leukemic cells but about 40-50% of NPM1-mutated AML cases showed also nuclear positivity that was mainly found in the nucleoli (more strongly in leukemic proerythroblasts) and in other smaller subnuclear dots of leukemic cells (Figure 1A). To further investigate the nature of the smaller subnuclear dots, we performed double immunostainings for UBE and PML, speckles probe or coilin and found that the NPM1 mutant co-localizes with coilin in the so-called Cajal bodies that are involved in the processing of small nuclear ribonuclear proteins (snRNPs) and small nucleolar RNA (snoRNAs). The possible nature of the partner to which the NPM1 mutant binds in the Cajal bodies is discussed. Immunostaining of 60 NPM1-mutated AML cases of M4-M5 FAB subtype showed that the expression on the NPM1 mutant was usually lost in the terminal phases of differentiation of the leukemic clone, whilst that of the NPM1 wild-type was retained, suggesting that the NPM1 mutant may be degraded during maturation more rapidly than the NPM1 wild-type protein. Because the NPM1 mutant protein is not expressed in the most mature cells [i]ncluding starry sky macrophages), this probe cannot be used to establish whether they belong or not to the leukemic clone. To track clonality, we focused our analysis on AML cases co-mutated for NPM1 and IDH1 R132H. Immunostaining, with a specific anti-IDH1 R132H mAb revealed strong positivity of the NPM1-mutant negative mature macrophages for the IDH1 mutant, clearly demonstrating for the first time that these cells belong to the leukemic clone (Figure 1B).

Conclusions. Our results point for the first time to a role of the nuclear expression of NPM1 mutant (nucleoli and Cajal bodies) in the pathogenesis of AML and highlight a new assay to track clonality in this common leukemic entity.

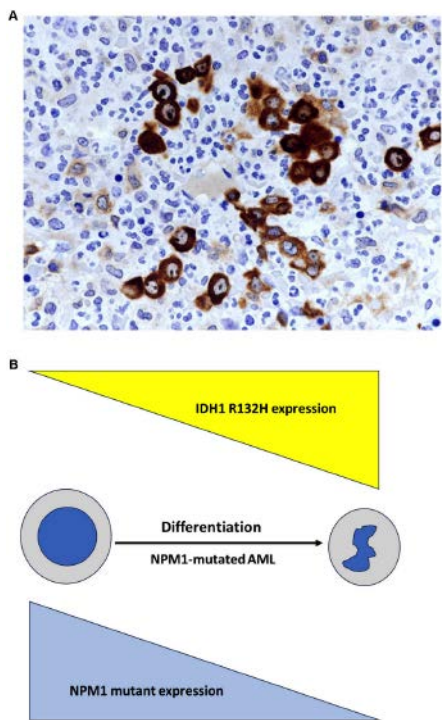


Figure 1.

C35
UNRAVELING THE IMPACT OF THE DIAGNOSTIC QUALIFIERS IN SECONDARY ACUTE MYELOID LEUKEMIA ACCORDING TO 2022 CLASSIFICATIONS

E. Attardi¹, A. Savi², B. Borsellino¹, M. Cipriani^{3,4}, A. Piciocchi³, F. Mallegni⁵, F. Moretti⁵, G. Silvestrini¹, H. Awada⁶, A. Durmaz⁶, V. Visconte⁶, M.G. Della Porta⁷, A. Venditti⁵, J.P. Maciejewski⁶, C. Gurnari^{5,6}, M.T. Voso⁵

¹Department of Biomedicine and Prevention, PhD in Immunology, Molecular Medicine and Applied Biotechnology, University of Rome Tor Vergata; ²Department of Clinical and Biological Sciences, University of Turin; ³Italian Group for Adult Hematologic Diseases (GIMEMA) Foundation; ⁴Department of Statistical Sciences, University of Rome La Sapienza; ⁵Department of Biomedicine and Prevention, University of Rome Tor Vergata; ⁶Translational Hematology and Oncology Research Department, Taussig Cancer Center, Cleveland Clinic; ⁷IRCCS Humanitas Clinical & Research Center and Department of Biomedical Sciences, Humanitas University, Italy

In 2022, 2 new acute myeloid leukemia (AML) classifications (World Health Organization, WHO and International Consensus Classification, ICC) and a new edition of the European LeukemiaNet (ELN) prognostic system have been released. Although important similarities, the different approach to define AML ontogenesis (primary vs secondary) remains a central issue of the classification discrepancy. While for the WHO 2022 a prior diagnosis of myelodysplastic syndrome (MDS) or MDS/myeloproliferative neoplasm (MPN) is enough to define AML myelodysplasia-related (MR), the ICC no longer recognizes the AML arising from MDS (sAML) as a disease entity, and instead introduces a list of “diagnostic qualifiers”, also including therapy-related AML (tAML). Nevertheless, whether these “diagnostic qualifiers” impact on prognosis and outcome is not well defined. We studied a cohort of 936 AML patients collected across 5 academic centers. An integration of clinical and cyto-

ic/molecular data was used to apply the WHO 2016, WHO 2022 and ICC diagnostic classifications and the ELN 2017 and 2022 editions.

Overall, 220 cases were classified as secondary AML (155 sAML and 65 tAML). As per the 2016 and 2022 WHO, the majority of sAML cases, accounting for 98,1% and 95,5% respectively, fell into the myelodysplasia-related changes (MRC) AML and AML-MR categories due to the “disease defining” presence of an antecedent MDS or MDS/MPN. According to the ICC, 81,9% of sAML cases were defined by the presence of a MDS-related genetic profile, belonging to AML with mutated *TP53* (AML-*TP53*) and AML with MDS-related gene mutations / cytogenetic abnormalities subcategories. TAML showed a greater heterogeneity, with a higher frequency of *KMT2A*-related categories (10,8% and 7,7% according to WHO 2022 and ICC, respectively) and AML-*TP53* for the ICC (21,5%, Figure 1A). In terms of outcomes, according to the ELN 2022 risk classification the sAML and tAML groups were classified into favorable risk 5,8% and 13,9%, intermediate 12,3% and 36,9%, and adverse 81,9% and 49,2%, respectively. Notably, while the ELN 2022 edition was effective in stratifying the group of tAML patients receiving conventional treatment (p=0,002), no statistically significant differences were noticed in sAML stratification according to ELN 2022 (Figure 1B).

We demonstrated the overarching importance of the biological ontogenetic profile in AML (>80% of sAML presented an MDS-related profile) and of the risk stratification according to ELN 2022 (>80% of sAML belonged to adverse risk). As to outcomes, ELN 2022 confirmed its stratification capability for tAML, while sAML were not adequately stratified. This evidence supports the idea that tAML should be acknowledged as “second” neoplasms, rather than being categorized as secondary AML. Considering the overlap in AML of MDS-related profile, these cases could potentially benefit from treatments specifically tailored for MDS-related conditions or secondary AML, such as CPX-351.

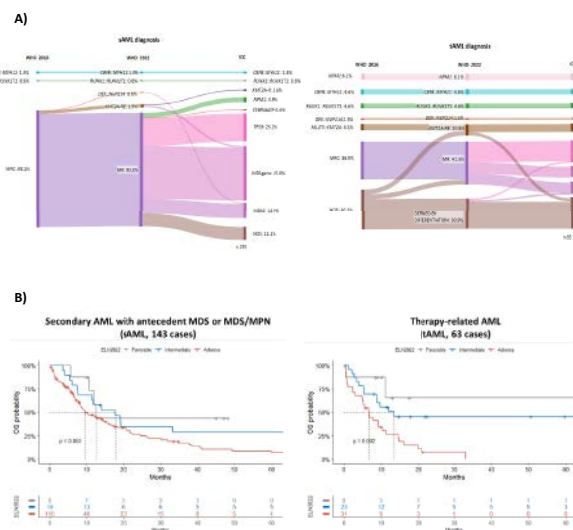


Figure 1.

36
ABSTRACT NOT PUBLISHABLE

C37

THE INTERSECTION OF PROTEOGENOMIC APPROACHES IDENTIFIES PA2G4 AS A NEW TARGET IN 3Q26 AML

E. Simoncini^{1,2}, M. Marchesini^{1,2,3}, A. Gherli^{1,2}, L. Moron Dalla Tor^{1,2}, A. Montanaro^{1,2}, F. Vento^{2,5}, L. Pagliaro^{1,2}, R. Zamponi^{1,2}, R. La Starza⁷, C. Mecucci⁷, F. Quaini¹, S. Colla⁴, G. Roti^{1,2,6}

¹Department of Medicine and Surgery, University of Parma; ²Translational Hematology and Chemogenomics Laboratory, University of Parma; ³IRCCS Istituto Romagnolo per lo Studio dei Tumori (IRST) "Dino Amadori"; ⁴Department of Leukemia, The University of Texas MD Anderson Cancer Center; ⁵Department of Medical Science, University of Ferrara; ⁶Hematology and BMT Unit, Azienda Ospedaliero-Universitaria di Parma; ⁷Department of Medicine and Surgery, Hematology and Clinical Immunology, University of Perugia, Italy

Introduction. Despite advancements in next-generation technologies, progresses in treating subtypes of acute myeloid leukemia (AML) driven by aberrantly activated transcription factors (TFs) have been limited. However, the integration of orthogonal omics led to the identification of drugs for "undruggable" TFs. Here, we sought to discover modulators of *EVII/MECOM* gene, the most lethal oncogenic TF, hyper expressed in AML carrying chromosome 3q26 abnormalities.

tures we defined an *EVII* "on" and "off" state and used Connectivity Map to identify inducers of an *EVII* "off" status. To investigate the *EVII* co-transcriptional complex, we performed rapid immunoprecipitation mass spectrometry of endogenous proteins (RIME). Then, target hits were validated *in vitro*, *in vivo* with studies in 3q26 patient-derived AML xenografts models and in humans through an N-of-1 clinical trial.

Results. Histone deacetylase inhibitors (HDAC[i]) emerged as the top class of compounds able to repress leukemia proliferation by suppressing *EVII*. HDACi induced apoptosis and reduced *EVII* in AML models, while the *EVII* expression sensitizes cells to HDACi. We translated these results in a clinical trial proposing entinostat in association with azacytidine to 3q26 AML patients. *EVII* expression decreased in blasts 6 hours after entinostat administration and *EVII* depletion paralleled clinical improvements. To exclude for a contribution of azacytidine in our trial, we completed an *in vivo* study and we demonstrated a reduction of AML blasts in mice treated with entinostat but not with azacytidine. Longitudinal single-cell RNA sequencing of 3q26 AML blasts of patients treated with azacytidine-entinostat revealed an inhibitory effect on Myc target genes as observed in cell lines treated with HDACi suggesting that multiple HDACi regulates the *Evi1*-Myc axis in 3q26 AML. HDACi-mediated or genetic silencing of *EVII* led to a direct decrement of MYC. To dissect the *EVII* co-transcriptional complex and explain the modulation of Myc signaling, we performed a RIME. Eleven *EVII* interactors were targets of Myc signaling, including PA2G4, a protein modulated by HDACi. *PA2G4* silencing or inhibition (WS6) depleted MYC protein levels recapitulating the effect of HDACi and WS6 reduced leukemic growth *in vivo* by suppressing an *EVII*-MYC signature suggesting that *PA2G4* is a druggable mediator of *EVII* complex.

Conclusions. In conclusion, we propose a clinical treatment strategy that capitalizes on the *EVII*-suppressing capacity of HDACis in 3q26 AML patients who lack biomarker-directed treatment approaches. Furthermore, based on the mechanism driving efficacy upon HDAC inhibition, our work positions *PA2G4* as a druggable target for 3q26 AML patients.

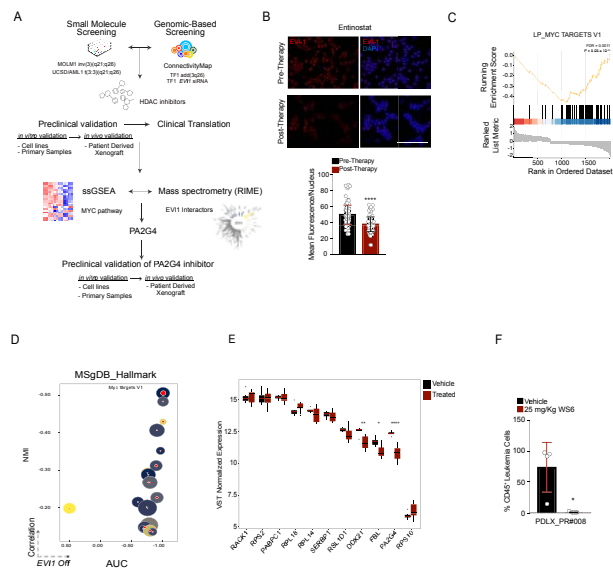


Figure 1: A) This research project uses phenotypic and *in silico* gene-expression-based screening approaches to identify Histone Deacetylase Inhibitors (HDACi) as modulators of the *EVII* gene, with a focus on turning off its expression. Genome-based and proteomic methods reveal *PA2G4* as a link between *EVII* and the MYC pathway, and preclinical validation supports its role as a mediator of the effects of HDAC inhibitors. B) Effect of entinostat on *EVII* nuclear localization (in red) following 6h of treatment in a 3q26 AML patient. The nuclei were stained with DAPI (blue). The histogram shows quantification of *EVII* nuclear content. C) GSEA running score plot of the top enriched MYC targets V1 pathway in leukemic population (Adj.P = 0.0011) of 3q26 AML patient after entinostat-azacytidine treatment. The graph indicates the running enrichment score (ES) of the pathway (top), the location of single genes of the gene set in the ranking (central), and the distribution of the ranking metric (bottom). D) Bubble plot showing the intersection of ssGSEA enrichment of the Molecular Signatures Database (MSigDB) and RIME of 3q26 AML cells. The x axis represents the area under the curve (AUC) and the y axis the normalized mutual information (NMI) y axis. The bubble size indicates the number of genes in each pathway of dataset, and the color scale indicates the level of statistical significance (+P). The inner red dots show *EVII* interactors, identified by RIME, that are common in the genes contained in each pathway. Their size represents the number of *EVII*-interacting proteins. E) Histograms show the normalized gene expression levels of eleven *EVII* interactor genes that are targets of Myc signalling, following 16 hr of 0.5 μ M AR-42, 2 μ M entinostat in UCSD/AML1, or 0.8 μ M AR-42 and 4 μ M entinostat in MOLM1 compared to vehicle. F) *In vivo* antileukemic effect of WS6. Mice (PDLX_PRL008, Patient Derived Xenograft of 3q26 AML patient) were treated at 25mg/kg for 15 days. Histogram indicates the percentage of bone marrow hCD45⁺ cells at the end of treatment.

Figure 1.

Methods. We intersected phenotypic, gene expression-based, proteomic approaches to identify modulators of *EVII*. We screened and scored 5294 compounds on their ability to suppress proliferation of 3q26 AML models (*EVII*^{high}). From *EVII*^{null} transcriptional signa-

C38

REDOX SYSTEM. A NEW THERAPEUTIC TARGET IN PLZF/RARA POSITIVE APL PATIENTS

A. Zaza^{2,5}, G. Catalano^{1,2}, S. Travaglini^{1,2}, E. Fabiani¹, D.F. Angelini³, M. Divona⁴, T. Ottone^{1,2}, E. De Marinis⁵, M. Gentile⁵, A. Venditti¹, M.T. Voso^{1,2}, C. Nervi⁵, N.I. Noguera^{1,2}

¹Department of Biomedicine and Prevention; University of Rome Tor Vergata; ²Neuro-oncology Units, Santa Lucia Foundation; ³Neuroimmunology and Flow Cytometry Units, Santa Lucia Foundation, IRCCS; ⁴Policlinico di Tor Vergata; ⁵Department of Medical-Surgical Sciences and Biotechnologies, La Sapienza University of Rome, Polo Pontino, Italy

PLZF/RARa (ZBTB16-RARa) fusion gene causes a rare variant of acute promyelocytic leukemia (APL), suppressing transcription of genes essential for myeloid maturation. Antioxidant activity is fundamental in normal hematopoiesis. NRF2, erythroid 2-related factor 2, is the master regulators of cellular resistance to oxidative stress. Glucose-6-phosphate dehydrogenase (G6PD) is the rate-limiting enzyme in the pentose phosphate pathway and a major source of NADPH. The aim of this work is to study the antioxidant system in cells expressing the PLZF/RARa fusion protein in order to individuate new therapeutic targets. The role of PLZF/RARa on oxidative stress was investigated in primary blasts from PLZF/RARa positive patients in normal bone marrow cells (NBM) and in the ZnSO₄-inducible PLZF/RARa [U937-B412(B)/control U937-MT(M)] cell

C39

CLUSTER ANALYSIS BASED ON IMMUNOPHENOTYPIC FEATURES OF NPM1-MUTATED ACUTE MYELOID LEUKEMIA IDENTIFIES THREE DIFFERENT PHENOTYPIC SUBSETS WITH DISTINCT MOLECULAR AND CLINICAL PROFILES

M. Piccini¹, S. Bencini², G. Ciolli³, F. Mannelli^{3,5}, L. Fasano³, B. Peruzzi², R. Palmieri⁴, M.I. Consalvo⁴, G. Gianfaldoni¹, B. Scappini¹, R. Caporale², G. Rotunno⁵, F. Pancani⁵, L. Signori⁵, C. Maccari⁵, A. Pasquini³, F. Crupi³, E. Quinti³, J. Caroprese³, I.V. Paradiso³, F. Vanderwert⁵, P. Guglielmelli^{3,5}, A. Venditti⁴, F. Annunziato², F. Buccisano⁴, A.M. Vannucchi^{3,5}

¹SOD Ematologia, Azienda Ospedaliera Universitaria Careggi; ²Centro Diagnostico Citofluorimetria e Immunoterapia, Azienda Ospedaliera Universitaria Careggi; ³Università degli Studi di Firenze, Dipartimento di Medicina Sperimentale e Clinica; ⁴Dipartimento di Biomedicina e Prevenzione, Università Tor Vergata; ⁵CRIMM, Centro Ricerca e Innovazione per le Malattie Mieloproliferative, Italy

Introduction. Mutations in the *NPM1* gene are found in 20-30% of adult acute myeloid leukemia (AML) and identify a distinct biological entity. However, *NPM1*mut AML displays remarkable immunophenotypic heterogeneity and its clinical behavior has been shown to be modulated by concomitant mutations, most notably *FLT3* internal tandem duplications (ITD). The correlation between immunophenotypic (IF) patterns, co-mutations and outcomes have not been extensively investigated in *NPM1*mut AML. In order to address this issue, we performed a cluster analysis based on IF features on a large series of *NPM1*mut AML patients.

Methods. The learning cohort (LC) included 80 *NPM1*mut AML pts from AOU Careggi, Firenze; the validation (VC) cohort included 33 pts from AOU Careggi and 41 pts treated at Policlinico Tor Vergata. Patients were treated between 2011 and 2023. Flow cytometry was performed on BM samples in order to define the IF profiles of leukemic populations within the CD45dim SSClow blast area. Data were collected on the pattern of expression (percentage of positive events; MFI) of seven antigens (HLA-DR, CD34, CD117, CD45, CD25, CD13, CD7) within the blast area. Cluster analysis based on IF data was performed separately on both cohorts. NGS data were available for 83/154 (54%) pts.

Results. Cluster analysis reproducibly identified three distinct IF clusters (C1, C2, C3) with recurrent molecular and clinical features in both the LC and VC. C1 was characterized by the CD34-, CD117+, HLA-DR- profile, mutations in *IDH1* or *IDH2* or *TET2*, older age, higher WBC counts and intermediate outcome (EFS| LC, 8.5 months; VC, not reached; OS| LC, 19.4 months; VC, nr). C2 was characterized by aberrant CD7 and CD25 expression, enrichment in *DNMT3A* R882+ and/or *FLT3-ITD*+ pts, high rate of early events and an overall unfavorable outcome (EFS| LC, 3.7 months; VC, 6.7 months; OS| LC, 10.1 months; VC, nr). C3 identified patients with monocytic differentiation, lower WBC counts, trend towards higher frequency of *RAS* mutations and an excellent outcome. While *FLT3-ITD* mutations were enriched in C1 and C2 compared to C3, median allelic ratio was higher in C2 compared to C1 (LC, 0.783 vs 0.294, $p < 0.001$; VC, 0.700 vs 0.375; $p = 0.076$). When pooling all *FLT3-ITD*+ pts ($n = 79$), OS and EFS differed between clusters (EFS| C1, 8.5 months; C2, 3.6 months; C3, nr, $p = 0.002$; OS| C1, 13.0; C2, 11.4 months, C3 nr; $p = 0.076$). In multivariate analysis, C2, *FLT3-ITD*+ and older age were independently associated with refractory disease and very short CR duration (< 6 months) in both cohorts. In the LC, C2, *FLT3-ITD*+ and older age were independently associated with shortened EFS and OS, while in the validation cohort only *FLT3-ITD*+ retained an independent detrimental impact on OS and only C2 and older age were

lines. We used MitoSOX-based assays to measure ROS levels; Western blot and qRT-PCR to evaluate expression of NRF2, and its target genes (HO-1, NQO-1) and of G6PD; Immunofluorescence to visualize the localization of NRF2; co-immunoprecipitation and Duolink proximity assay (PLA) to study protein interaction. Images were acquired using confocal microscopy. Apoptosis was evaluated using annexin and live/dead exclusion assay and flow cytometry in cells treated with Ascorbate (ASC, 1 and 3 mM) for two days. PLZF/RARa expression interferes with antioxidant defenses. Increased ROS levels were observed in B412 compared with control cells, after the addition of ASC 3mM (ROS inductor) (B412| 8460 vs MT| 4631) and Rotenone-Antimycin (positive control) (B412| 39390 vs MT| 17636), indicating that enhanced ROS production is associated with PLZF/RARa expression (Figure 1A). PLZF/RARa induction increases NRF2 nuclear translocation (MT 6hl 0.4±0.2 vs B412 6hl 0.9±0.42) ($p = 0.03$) but reduces the expression of NRF2 target genes HO-1 (MT 6hl 3.6±0.6 vs B412 6hl 1.7±0.1) ($p = 0.002$) e NQO1 (MT 6hl 4.9±1 vs B412 6hl 2.8±0.9) ($p = 0.03$), suggesting a functional interference. Immunofluorescence analysis revealed that PLZF/RARa co-localizes with NRF2. Co-immunoprecipitation demonstrated an interaction between the two proteins, confirmed by PLA assay (Figure 1C). Blasts from 5 PLZF/RARa positive patients show a reduced expression of G6PD than primary t(15;17) APL and AML blasts and NBM (APL PLZF/RARa $n = 5$ | 0.6±0.2); (vs APL $n = 10$ | 3.7±2.6, $p = 0.02$); (vs AML $n = 13$ | 2.5±1.8, $p = 0.03$); (vs NBM $n = 2$ | 1.6±0.8) (Figure 1B). Finally primary blasts from one APL PLZF/RARa positive patient assayed for annexin and live/dead exclusion by flow cytometry showed a dose-dependent apoptotic response in the presence of ASC (Ctrl 14%, ASC 1mM 47%, ASC 3 mM 99%), a potent pro-oxidant (Fig.1D). PLZF/RARa expression led to a reduction in antioxidant defense capacity of AML cells' suggesting that redox system represents a new therapeutic target in PLZF/RARa positive AML patients. Moreover, pro-oxidant drugs, as ASC, at high doses could be an innovative therapeutic option for this incurable disease.

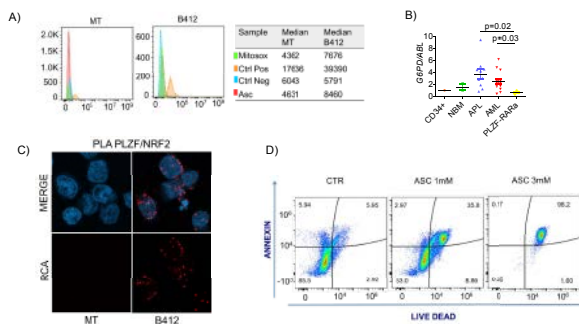


Figure 1. (A) Flow cytometry measurement of ROS in MT and B412 cells using MitoSOX assay after treatment with 3 mM Ascorbate (ASC); ctrl neg, Azacitidine; ctrl positive, rotenone/antimycin. (B) qRT-PCR on G6PD mRNA in 5 PLZF/RARa positive APL patients, AML blasts and NBM samples. (C) PLZF-NRF2 protein interaction by proximity ligation assay (PLA) in MT and B412 cells. (D) Apoptosis in APL PLZF/RARa primary blast cells treated with Ascorbate (ASC, 1 and 3 mM) for two days.

shown to independently impact EFS.

Conclusions. Our data shed light on the recurrent immunophenotypic patterns of *NPM1*mut AML and their correlation with co-mutational patterns and clinical outcomes.

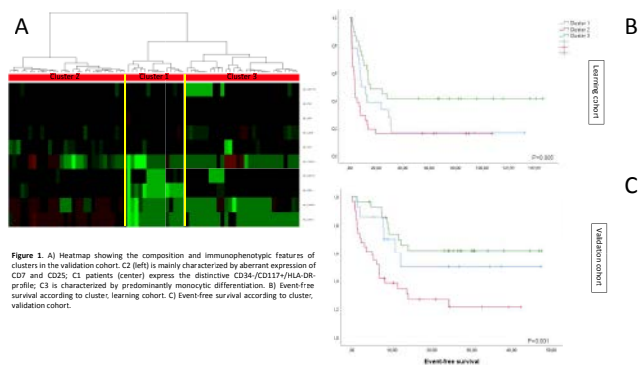


Figure 1.

C40

FINAL ANALYSIS FOR THE PRIMARY END-POINT OF GIMEMA AML1718, A SAFETY RUN-IN AND PHASE 2 STUDY OF VENETOCLAX, FLUDARABINE, IDARUBICIN AND CYTARABINE (V-FLAI) IN THE INDUCTION THERAPY OF NON LOW-RISK ACUTE MYELOID LEUKEMIA

G. Martinelli¹, A. Piciocchi², E. Audisio³, C. Papayannidis⁴, F. Guolo^{5,6}, M. Cerrano³, V. Arena², S. Capria⁷, M. Rondoni⁸, M.G. Della Porta⁹, G. Beltrami¹⁰, M. Bocchia¹¹, A. Lico¹², L. Giaccone¹³, M. Rossi¹⁴, C. Califano¹⁵, M.G. Carrabba¹⁶, C. Cattaneo¹⁷, M. Frigeni¹⁸, M.C. Di Chio¹⁹, B. Serio²⁰, R. Freilone³, A. Curti⁴, P. Minetto⁵, G. Marsili², C. Minotti⁷, B.A. Zannetti⁸, F. Cotugno², J. Nanni⁴, G. Simonetti¹, M.T. Bochicchio¹, S. Rosellini⁵, E. Tedone⁵, A. Venditti²¹, R.M. Lemoli^{3,6}, M. Vignetti², P. Fazi², G. Marconi¹

¹IRCCS Istituto Romagnolo per lo Studio dei Tumori “Dino Amadori” - IRST S. r. l.; ²Fondazione GIMEMA; ³SC Ematologia - AOU Città della Salute e della Scienza di Torino; ⁴IRCCS Azienda Ospedaliero-Universitaria di Bologna, Istituto di Ematologia “Seràgnoli”; ⁵Clinic Of Hematology, Department Of Internal Medicine (Dim[i], University Of Genoa; ⁶IRCCS San Martino Hospital; ⁷UOC Ematologia- AOU Policlinico Umberto I; ⁸AUSL Della Romagna, Ospedale Santa Maria Delle Croci; ⁹Humanitas Clinical and Research Center – IRCCS & Humanitas University, Department of Biomedical Sciences; ¹⁰Ematologia E Terapie Cellulari, Irccs Ospedale Policlinico San Martino; ¹¹AOU Senese, Università Di Siena - Uoc Ematologia; ¹²AULSS 8 Berica - Ospedale Di Vicenza; ¹³Allogeneic Transplant and Cell Therapies Unit, Division of Hematology, Department of Molecular Biotechnology and Health Sciences, University of Torino; ¹⁴Division of Hematology, Fondazione IRCCS Policlinico San Matteo; ¹⁵UOC Ematologia P. O. Pagani; ¹⁶IRCCS Ospedale S. Raffaele; ¹⁷ASST Degli Spedali Civili Di Brescia; ¹⁸ASST Papa Giovanni XXIII; ¹⁹Fondazione IRCCS Istituto Nazionale Tumori; ²⁰AOU Ematologia San Giovanni Di Dio E Ruggi D’Aragona; ²¹Dipartimento Di Biomedicina E Prevenzione, Università Tor Vergata, Italy

Introduction. The management of Acute Myeloid Leukemia (AML) has been a persistent challenge, especially in the intermediate and high-risk categories. Traditional treatments have offered limited success, with complete remission (CR) rates of just 40-50%.

Methods. The GIMEMA AML1718 phase 1/2 multicenter trial

(NCT03455504) evaluates the safety and efficacy of 21+ days of venetoclax (VEN) in combination with FLAI (fludarabine, cytarabine, and idarubicin) for treating newly diagnosed ELN intermediate or high-risk AML patients. The trial followed a modified two-stage Simon’s design, incorporating a safety run-in (SR), a part 1 (P1) with the randomized evaluation of different dosages of VEN (400 or 600 mg), and a confirmatory cohort (part 2, P2). In P2, the trial extended the lower effective dose of VEN (400 mg) and had a centralized measurable residual disease (MRD) assessment in part 2.

Results. A total of 124 participants were enrolled: 12 in SR, 45 in P1, and 67 in P2. Of these, 95 received a 400 mg daily dosage of VEN in combination with FLAI (V-FLAI 400), whereas 29 patients V-FLAI 600 mg. Patients had a median age of 55 years- (range 18 – 66). Males constituted 56% (70 patients) of the population. Risk stratification according to the ELN 2017 indicated that 54% (67 patients) were of intermediate risk, while 46% (57 patients) were classified as high-risk. Additionally, 16 patients (13%) had a secondary form of AML. The study’s primary endpoint—Composite Complete Remission (CCR)—was achieved by 75% (93 out of 124) of patients following their first treatment course. One patient, initially in partial remission, transitioned to complete remission post the second V-FLAI induction cycle. In part 2, 47 out of 67 achieved CCR, amounting to 70.0%; 9 patients in this cohort await testing. Notably, centralized MRD analysis revealed that 31 out of 48 tested subjects (64. 5%) achieved MRD negativity by day 28 of the first course, as determined by flow cytometry with a 0.1% threshold. During a median 10-month follow-up, 49% of patients (60 individuals) proceeded to hematopoietic stem cell transplant (55 in CR1). The median overall survival rate was 22. 4 months, with a 12-month survival probability of 64% (Figure 1). Disease-free survival at 12 months was equally promising at 64%. Overall, only five induction-related deaths were reported (4 %), and the 60-day mortality rate was recorded at 6%, which includes deaths attributable to disease progression. Infections were the most frequent grade 3+ adverse events. The safety profile remained consistent with established AML induction protocols. Among HSCT recipients, no instances of graft failure or elevated graft-versus-host disease were noted. No notable differences in outcomes were found between the V-FLAI 400 and 600 mg dosage groups.

Conclusions. The V-FLAI regimen shows remarkable efficacy and safety. The high CCR rates and MRD-negativity rates warrant further exploration.

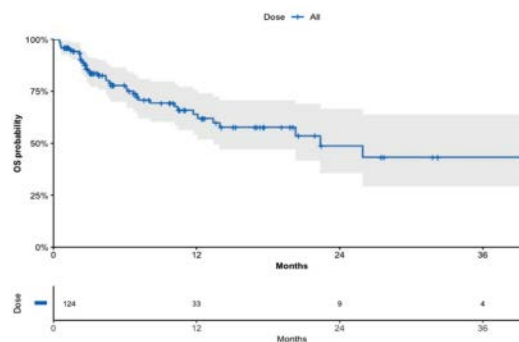


Figure 1.

Lymphomas

C41

FRAGMENTOMICS COMPLEMENTS MOLECULAR CLUSTERING ON CTDNA TO IMPROVE OUTCOME PREDICTION IN DIFFUSE LARGE B-CELL LYMPHOMA

M. Almasri¹, R. Moia¹, D. Talotta¹, C. Cosentino¹, R. Dondolin¹, R. Bruna¹, I. D. Starza², R. Soscia², A. Brusca³, L. Terzi Di Bergamo³, M. Salehi³, A. Andorno⁴, F. Mercalli⁴, R. Bomben⁵, T. Bittolo⁵, F. Vit⁵, P. Bulian⁵, F. Melle⁶, G. Motta⁶, M. Leutner⁷, A. Mahmoud¹, C. Deambrogio¹, S. Rasi¹, S. Mouhssine¹, M.T. Petrucci², R. Boldorini⁴, A. Di Rocco², I. Del Giudice², M. Spina⁸, V. Canzonieri⁹, M. Martelli², S. Pileri⁶, V. Gattei⁵, D. Rossi³, R. Foà², G. Gaidano¹

¹Division of Hematology, Department of Translational Medicine, Università del Piemonte Orientale; ²Institute of Hematology, Hematology Unit, Department of Translational and Precision Medicine, 'Sapienza' University; ³Laboratory of Experimental Hematology, Institute of Oncology Research; ⁴Division of Pathology, Department of Health Sciences, Università del Piemonte Orientale; ⁵Clinical and Experimental Onco-Hematology Unit, Centro di Riferimento Oncologico di Aviano (CRO), IRCCS; ⁶Haematopathology Division, European Institute of Oncology (IEO) Istituto di Ricovero e Cura a Carattere Scientifico (IRCCS); ⁷Division on Pathology, Azienda Sanitaria Locale del VCO; ⁸Division of Medical Oncology and Immune-related Tumors, Centro di Riferimento Oncologico di Aviano (CRO) IRCCS; ⁹Pathology Unit, CRO Aviano National Cancer Institute, Italy

Introduction. Diffuse large B-cell lymphoma (DLBCL), the most common lymphoma in adults, exhibits genetic and clinical heterogeneity. Recent studies identified different molecular clusters based on mutational analysis. Cell-free DNA (cfDNA) analysis on the liquid biopsy recapitulates DLBCL genetics and the levels of circulating tumor DNA (ctDNA) are a powerful prognostic marker. In addition, the analysis of cfDNA fragment size, known as fragmentomics, represents a novel prognostic marker. On these grounds, ctDNA may provide complementary information to improve outcome prediction in DLBCL patients.

Methods. This study involved 166 newly diagnosed DLBCL patients in two real-life cohorts using a training-validation approach. The training group was provided with tumor gDNA from lymph node (LN) biopsies, ctDNA from plasma, and germline gDNA from granulocytes. The validation cohort was provided with ctDNA and granulocyte gDNA. CAPP-Seq was used to genotype these biological samples, and the LymphGen tool to identify molecular clusters. Fragment size data was extracted from cfDNA BAM files.

Results. The training cohort included 77 DLBCL patients treated with R-CHOP. The median age was 67,5 years, PFS and OS at 40 months were 68,2% and 85,2%, respectively. Using the LymphGen tool, 46,5% of cases were assigned to a specific molecular cluster on the LN biopsy, and 40,3% on liquid biopsy. Patients with ST2 or BN2 cluster had better PFS in both ctDNA and LN with a 40-months PFS and OS of 100%. To validate these findings, a validation cohort composed of 89 patients was collected. Also, in the validation cohort BN2 and ST2 patients showed a very good outcome with a 40-months OS of 88,4%. By combining the training and the validation cohort we evaluated the fragmentomic profile of cfDNA in 166 DLBCL cases. Two different clusters with distinct fragmentation patterns were identified. The nucleosomal (N) cfDNA cluster included 122 patients and the median fragment length was 197bp that is similar to healthy donors. The remaining 44 DLBCL cases had shorter median fragment length (175bp) and were named as sub-nucleosomal (SN) cluster (Figure 1A, B). The fragmentation profile can improve out-

come prediction in patients not assigned to any molecular cluster or without any gene mutations identified. In these patients (N=107) the SN cfDNA group had poorer outcomes compared to N cfDNA patients with a 40-months PFS of 74,9% and 28,2% respectively (Figure 1C). The prognostic impact of SN cfDNA fragmentomic profile remained significant in multivariate analysis when adjusted for ctDNA levels and for mutated allele frequency (Fig 1D).

Conclusions. Molecular clustering on the liquid biopsy reflects in most cases the molecular subtype and the prognostic impact of clusters identified in the tissue biopsy. The fragmentomic profile of cfDNA further stratifies patients not assigned to a specific molecular cluster independent of ctDNA levels.

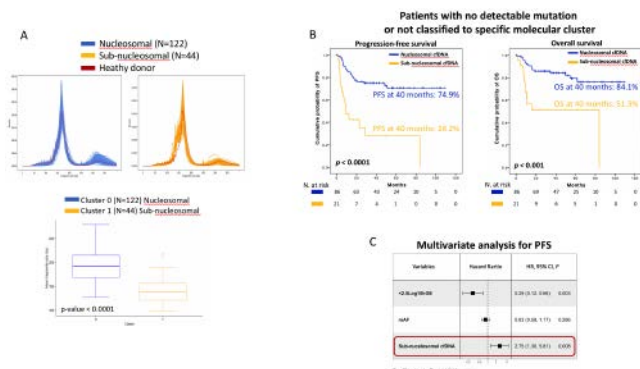


Figure 1.

C42

PRE-TREATMENT CELL-FREE DNA CONCENTRATION AS PREDICTOR OF SURVIVAL IN NEWLY DIAGNOSED PERIPHERAL T-CELL LYMPHOMAS

G. Zanirato¹, E. Fardella², M. Magni¹, N. Caldarelli^{1,2}, A. Chiappella¹, A. Doderò¹, S. Ljevar³, L. Orsucci⁴, A. Re⁵, S.V. Usai⁶, V. Stefoni⁷, C. Castellino⁸, F.G. Rossi⁹, A. Pinto¹⁰, C. Carniti¹, P. Corradini^{1,2}

¹Division of Hematology and Stem Cell Transplantation, Fondazione IRCCS Istituto Nazionale dei Tumori; ²University of Milan; ³Department of Clinical Epidemiology and Trial Organization, Fondazione IRCCS Istituto Nazionale dei Tumori; ⁴Division of Hematology, Azienda Ospedaliera e Universitaria Città della Salute e della Scienza; ⁵Hematology Division, ASST Spedali Civili di Brescia; ⁶Hematology Unit, Ospedale Oncologico Armando Businco; ⁷Institute of Hematology Seràgnoli, University of Bologna; ⁸Division of Hematology, Azienda Ospedaliera S. Croce e Carle; ⁹Division of Hematology, Fondazione IRCCS Cà Granda, Ospedale Maggiore Policlinico; ¹⁰Hematology-Oncology & Stem Cell Transplantation Unit, IRCCS Istituto Nazionale Tumori, Fondazione G. Pascale, Italy

Introduction. Peripheral T-cell lymphomas (PTCLs) are a heterogeneous group of non-Hodgkin lymphomas characterized by poor prognosis. Given the lack of predictive biomarkers of response, we aimed to explore the role of cell-free DNA (cfDNA) in 75 patients (pts) enrolled in the PTCL13 prospective study (NCT02223208), including newly diagnosed Peripheral T-cell Lymphoma, Not Otherwise specified (PTCL-NOS, n=30), nodular T follicular helper lymphoma (nTFHL, n=26) and Anaplastic Lymphoma Kinase negative Anaplastic Large Cell Lymphoma (ALK-ALCL, n=19).

Methods. Cell-free DNA was extracted using the Maxwell[®] RSC LV cfDNA Kit (Promega) from plasma samples and quantified with Qubit[®] 2.0 fluorometer (Invitrogen). Statistical analysis was performed by GraphPad Prism (version 9.3.1) and R (version 4.1.2).

Results. Pre-treatment cfDNA concentration was significantly increased in presence of high-risk clinical parameters, such as disease-related risk factors (increased lactate dehydrogenase levels, $p < 0.0001$; presence of extranodal disease $p = 0.04$), prognostic scores used in PTCLs (International prognostic Index > 2 , $p < 0.0001$; prognostic Index for T-cell lymphoma > 1 , $p = 0.0006$), and patient condition (poor performance status, $p = 0.0003$). Moreover, higher baseline cfDNA concentration was found in pts who progressed compared with those who achieved a response at the end of 6 chemotherapy cycles ($p = 0.0303$). Importantly, pre-treatment cfDNA level had a negative impact on both progression-free survival (PFS, Univariate Cox linear model, $p = 0.0001$) and overall survival (OS, Univariate Cox nonlinear model, $p = 0.0105$). Multivariate analysis confirmed a significant influence of cfDNA on PFS [Multivariate Cox Model, HR 1.34, 95% Confidence Interval (CI) 1.14-1.58, $p = 0.0004$ and HR 1.28, 95% CI 1.11-1.48, $p = 0.0006$] greater than that of IPI and PIT scores, LDH, performance status, and extranodal disease. Through an analysis by receiver operating characteristic (ROC) curve was identified a specific pre-treatment cfDNA concentration cut-off associated with a worse prognosis. Above 42.78 ng/mL PFS and OS are significantly reduced (log-rank test $p = 0.0177$ and < 0.0001). Multivariate analysis confirmed a significant effect on survival when cfDNA above or below 42.78 ng/mL were tested with IPI, LDH and ECOG (HR 2.76, 95% CI 1.24-6.16, $p = 0.0128$ for PFS; HR 9.45, 95% CI 3.10-28.81, $p = 0.0001$ for OS). When tested together with PIT, ECOG and extranodal disease, both cfDNA and PIT score were associated with OS (HR 9.30, 95% CI 3.22-26.87, $p < 0.0001$ and HR 0.34, 95% CI 0.12-0.94, $p = 0.037$ respectively), while no significant correlations with PFS were found (cfDNA \geq vs < 42.78 ng/mL, HR 1.83, 95% CI 0.86-3.91, $p = 0.1178$).

Conclusion. Pre-treatment cfDNA concentration has a strong prognostic impact in PTCLs and represents a superior predictor of shorter survival and an inexpensive assessable biomarker that can quickly provide prognostic information in the real-world PTCLs scenario.

C43

MRD MONITORING BY EUROCLONALITY IGH BASED NGS APPROACH PROVIDES OUTCOME PREDICTION IN FOLLICULAR LYMPHOMA PATIENTS LACKING A CONVENTIONAL BCL2||IGH MARKER| BIOLOGICAL RESULTS FROM THE FONDAZIONE ITALIANA LINFOMI (FIL) FOLL12 TRIAL

E. Genuardi¹, B. Alessandria¹, I. Della Starza^{2,3}, F. Guerrini⁴, R. Bomben⁵, D. Drandi¹, M. Ferrante¹, C. Bono⁴, R. Soscia², T. Bittolo⁵, S. Ragaini^{1,6}, S. Mancuso⁷, E. Cencini⁸, N. Di Renzo⁹, C. Mannarella¹⁰, M. Murineddu¹¹, V. Stefoni¹², R. Centurioni¹³, L. Baldini¹⁴, A.M. Civita¹, V. Gattei⁵, S. Galimberti⁴, I. Del Giudice², B. Bruno^{1,6}, M. Federico¹⁵, M. Ladetto¹⁶, C. Pott^{16,18}, S. Luminari^{19,20}, S. Ferrero^{1,6}

¹Divisione di Ematologia, Dipartimento di Biotecnologie Molecolari e Scienze per la Salute, Università di Torino; ²Ematologia, Dipartimento di Medicina Traslazionale e di Precisione, Università La Sapienza; ³AIL Roma ODV; ⁴Ematologia, Dipartimento di Medicina Clinica e Sperimentale, Università di Pisa; ⁵Unità di Onco-Ematologia, CRO; ⁶Divisione di Ematologia e Trapianto cellule staminali, AOU Città della Salute e della Scienza; ⁷Unità di Ematologia, Dipartimento di Promozione della Salute, Materno-Infantile (ProMISE), Policlinico Paolo Giaccone, Università di Palermo; ⁸Ematologia, Azienda Ospedaliera Universitaria Senese e Università di Siena, Siena, Italy; ⁹Dipartimento di Ematologia, Ospedale Vito Fazzi; ¹⁰Unità di Ematologia, Ospedale Madonna delle Grazie; ¹¹Unità di Ematologia e Trapianto di Midollo Osseo, Ospedale San

Francesco; ¹²Dipartimento di Scienze Mediche e Chirurgiche, Università di Bologna; ¹³U. O. C. Medicina Interna Civitanova Marche; ¹⁴Dipartimento di Oncologia e Emato- Oncologia, Università di Milano; ¹⁵Dipartimento CHIMOMO, Università di Modena e Reggio Emilia; ¹⁶Dipartimento di Medicina Traslazionale, Università del Piemonte Orientale, SCUD Ematologia AO SS Antonio e Biagio e Cesare Arrigo; ¹⁷EuroClonality-NGS Working Group; ¹⁸Second Medical Department, University Hospital Schleswig-Holstein, Campus Kiel; ¹⁹Dipartimento di Clinica e Salute Pubblica "Arcispedale S. Maria Nuova", Università of Modena e Reggio Emilia; ²⁰Divisione di Ematologia, Dipartimento di Medicina Diagnostica, Italy

Background. Despite durable clinical responses achieved by chemo-immunotherapy in follicular lymphoma (FL) patients, most of them eventually relapse. Actually, minimal residual disease (MRD) analysis based on the detection of BCL2||IGH rearrangement by PCR is able to early identify patients at high risk of relapse. Nevertheless, this tool fails in up to 45% of FL cases. The improvement of next- generation sequencing (NGS) allowed to introduce these novel tools that are still scant in the context of FL MRD monitoring. Therefore, we tested the feasibility of the EuroClonality (EC) IGH-based NGS approach to identify novel molecular markers for MRD monitoring in the context of the large prospective trial "FOLL12" (EudraCT1 2012-003170-60) by the Fondazione Italiana Linfomi. Methods| In FOLL12 clinical trial, bone marrow (BM) samples were centralized to the FIL MRD Network for standardized MRD analysis. Baseline and follow up (FU) gDNA of "BCL2||IGH no marker" patients were analysed by EC IGH-based NGS approach. The identification of baseline clonotypes and MRD clones was performed by ARRest/Interrogate tool. Results| 124/343 lacked a conventional BCL2||IGH marker (77%) showed morphologic BM lymphoma infiltration with an available baseline sample were included in the analysis.

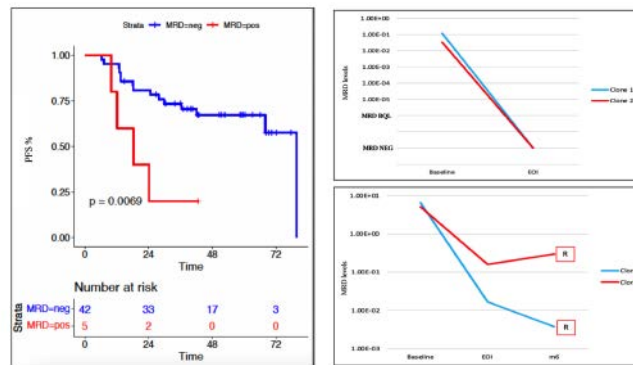


Figure 1. PFS stratified on MRD status in BM at end of induction by EC-IGH based NGS analysis. MRD, minimal residual disease; EOJ, end of induction; 6M, six months after EOJ; CL, clinical relapse.

Figure 1.

Overall, IGH clonotypes were identified in 75/124 patients (60%), of which 73 were mono-clonal and 2 bi-allelic. In this series, MRD analysis, performed in only 47 patients with a centralized BM sample at EOJ, showed 89% of MRD negativity rate. Interestingly, the 5 patients who scored MRD+ showed statistically significant worse PFS at 3 years than MRD- cases (22% vs 73%, respectively, $p = 0.0069$, Figure 1). Notably, 4 out of 5 MRD+ patients experienced POD24. Focusing on bi-allelic cases, one presented superimposable MRD trends between clones [b]oth achieving MRD negativity), while in the other both clones remained MRD positive but showing one Log difference between them. Interestingly, only one of the two clones showed a MRD increase in the following timepoint (6 months after end of induction), heralding the clinical relapse subsequently occurred at month 12 (Figure 2). Conclusions| The first data of NGS-based tools in FL patients lacking a conventional BCL2||IGH marker

for MRD enrolled in a prospective clinical trial, showed that the EC IGH-based NGS approach was able to provide a new molecular marker in 60% of patients with evidence of BM infiltration (that means about the 28% of “no marker” FL patients); importantly, this approach was predictive of worse PFS for MRD+ cases. Overall, these data are promising for the wide employment of novel, effective MRD monitoring tools, and so, by combining conventional and NGS-based techniques, they potentially rise the percentage of MRD evaluable cases up to at least 70%.

C44

ABSTRACT NOT PUBLISHABLE

C45

ABSTRACT NOT PUBLISHABLE

C46

A DIGITAL GENE-EXPRESSION SIGNATURE FOR MEDIASTINAL GRAY ZONE LYMPHOMA STRATIFICATION WITHIN CLASSICAL HODGKIN OR PRIMARY MEDIASTINAL LYMPHOMA

S. Ciavarella², G. Gargano^{1,2}, M.C. Vegliante², S.A. Pappagallo², F. Esposito¹, G. Opinto², G. Zaccaria³, P. Mondelli², G. Loseto², A. Scattone⁴, E. Sabattini⁵, C. Agostinelli⁵, V. Tabanelli⁶, S.A. Pileri⁶, L. Nassi⁷, N. Del Buono¹, A. Guarini²

¹Department of Mathematics, University of Bari ‘Aldo Moro’; ²Hematology and Cell Therapy Unit, IRCCS-Istituto Tumori ‘Giovanni Paolo II’; ³Department of Electrical and Information Engineering (DEI), Polytechnic University of Bari; ⁴Pathology Department, IRCCS-Istituto Tumori ‘Giovanni Paolo II’; ⁵Haematopathology Unit, IRCCS Azienda Ospedaliero-Universitaria di Bologna and Department of Experimental, Diagnostic and Specialty Medicine, University of Bologna; ⁶Division of Hematopathology, European Institute of Oncology IRCCS; ⁷Department of Hematology, Careggi Hospital and University of Florence, Italy

Introduction. Mediastinal non-Hodgkin lymphomas with intermediate features between primary Mediastinal B-cell lymphoma (PMBL) and classical Hodgkin lymphoma (CHL) - also known as mediastinal gray zone lymphomas (MGZL) - represent a unique, diagnostically challenging entity (Khoury et al., Leukemia 2022). They typically exhibit discordant morpho-phenotypical characteristics between CHL and PMBL, a high rate of diagnostic reclassification and consequent poorer therapeutic outcomes. While a comprehensive biological picture of this entity remains to be fully deciphered, recent gene expression profiles (GEP) of MGZL confirmed their molecular straddling between CHL and PMBL (Pittaluga et al., Blood Cancer Discov., 2020; Sarkozy et al., Blood Adv., 2020). However, the diagnosis of MGZL is still challenging and largely based on fulfilling morphological and immunophenotypic criteria. Therefore, there is a need for practical tools exploiting additional molecular traits of MGZL to facilitate their stratification between CHL or PMBL, and selection of proper treatment.

Methods. We applied CIBERSORTx (Newman et al., Nat. Biotechnol., 2019) to public GEP of a training set comprising 50 CHL (GSE17920) and 31 PMBL (GSE11318). We thus purified GEP of both tumor and microenvironment (TME) and used non-negative matrix factorization (NMF) to select genes with high discriminating capacity between the two lymphoma subtypes. After further feature selection, a 168-gene final signature was tested in silico on an inde-

pendent series of 34 CHL (GSE17920) and 20 PMBL (GSE87371), and finally validated (NanoString Technology) on a real-life (RL) cohort including 18 CHL, 19 PMBL and 24 MGZL samples. The latter, collected by a multicenter retrospective study, underwent central pathological revision by a panel of expert hematopathologists and classified according to the Sarkozy’s subgroups and morphological, cytoarchitectural and phenotypical criteria.

Results. Beyond producing a successful clustering of CHL or PMBL cases in all analyzed cohorts, our gene panel allowed a transcriptional stratification of MGZL within either CHL or PMBL cluster. In particular, 5 out of 24 cases broke down into the molecular PMBL subgroup, whereas the majority of MGZL (n=19) located within the CHL cluster, although being pathologically annotated as at intermediate (n=5), CHL-like (n=7), or PMBL-like (n=7) morpho-phenotype. Moreover, a speculative analysis on clinical data, available for 14 MGZL, indicated poorer outcomes for 5 cases whose treatment - typically based on pathological annotation - resulted discordant with their transcriptomic stratification.

Conclusions. In conclusion, we provided proof of concept for a NanoString-based gene signature enabling a transcriptomic stratification of MGZL, adding up to their morpho-phenotypical categorization. If validated on larger cohorts, our approach might prompt the design of a new molecular assay to be usefully transferred into the routine clinical practice.

C47

MOLECULAR CHARACTERIZATION OF DIFFUSE LARGE B-CELL LYMPHOMA ASSOCIATED TO HEPATITIS C VIRUS INFECTION

C. Varraso¹, R. Sciarra^{1,2}, M. Merli³, C. Cristinelli², M. Lucioni^{2,4}, S. Zibellini¹, R. Riboni⁴, D. Furlan⁵, S. Uccella^{6,7}, C. Zerbi^{1,2}, B. Bianchi⁸, M. Gotti¹, V.V. Ferretti⁹, S. Fraticelli^{2,4}, T. Lazic², I. Defrancesco^{1,10}, B. Mora³, L. Libera⁵, A. Mazzacane², F. Carpi², M. Berliner², G. Neri², E. Rizzo¹¹, F. De Paoli¹¹, F. Sessa⁵, F. Passamonti^{3,12}, M. Paulli^{2,4}, L. Arcaini^{1,2}

¹Division of Hematology, Fondazione IRCCS Policlinico San Matteo; ²Department of Molecular Medicine, University of Pavia; ³Division of Hematology, Fondazione IRCCS Cà Granda Ospedale Maggiore Policlinico; ⁴Anatomic Pathology Unit, Fondazione IRCCS Policlinico San Matteo; ⁵Anatomic Pathology Unit, University of Insubria, Ospedale di Circolo; ⁶Department of Biomedical Sciences, Humanitas University; ⁷Pathology Service, IRCCS, Humanitas Research Hospital; ⁸Division of Hematology, University Hospital Ospedale di Circolo e Fondazione Macchi-ASST Sette Laghi, University of Insubria; ⁹Biostatistics and Clinical Trial Center, Fondazione IRCCS Policlinico San Matteo; ¹⁰Department of Medical, Surgical, Diagnostic and Pediatric Sciences, University of Pavia; ¹¹enGenome s. r. l.; ¹²University of Milan, Italy

Introduction. HCV-positive DLBCL displays typical clinical and histological features compared to its negative counterpart, such as older age, extranodal involvement, elevated serum lactate dehydrogenase, high International Prognostic Index and a higher proportion of tumors “transformed” from a low grade lymphoma. However, data regarding molecular characteristics of HCV-positive DLBCL remains limited.

Methods. In this bicentric study, we investigated the clinico-pathological and molecular features of 54 patients with HCV-positive DLBCL. With Illumina HiSeq 2500, we applied targeted next generation sequencing (NGS) of 184 genes on DNA extracted from archived formaline fixed paraffin embedded tissue. We applied fluorescence in-situ hybridisation (FISH) for the detection of *MYC*, *BCL2* and *BCL6* rearrangements and Lymph2Cx assay (Nanostring)

for cell-of-origin determination. We performed cluster analysis with the LymphGen genetic classifier.

Table 1. Baseline clinical characteristics of 54 HCV-positive patients affected with diffuse large B-cell lymphoma.

	Patients, N	Total data available
Age, median (range)	71 (33-84) (IQR: 61.9-77)	54
Sex (M/F)	27/27 (50%/50%)	54
Involved site		54
Nodal	32 (59.3%)	
Extranodal	4 (7.4%)	
Nodal and extranodal	18 (33.3%)	
Spleen involvement	22 (40.7%)	54
Bone marrow involvement	6 (16.2%)	36
B symptoms	23 (42.6%)	54
Stage		54
I	6 (11.1%)	
II	14 (25.9%)	
III	18 (33.3%)	
IV	16 (29.7%)	
ECOG PS		54
0-1	14 (25.9%)	
2-4	40 (74.1%)	
IPI score		51
Low	12 (23.5%)	
Low-intermediate	10 (19.6%)	
Hihj-intermediate	18 (35.3%)	
High	11 (21.6%)	
R-IPI score		54
Good	2 (3.7%)	
Intermediate	22 (40.7%)	
Poor	30 (55.6%)	
LDH > UNL	36 (66.6%)	54
β ₂ -microglobulin > UNL	36 (66.6%)	54
ALT > UNL	19 (35.8%)	53
Albumin < 3.5 g/dl	11 (23.9%)	46
HCV genotype		30
1	10 (33.3%)	
2	16 (53.4%)	
3	4 (13.3%)	
HPS		46
low	11 (23.9%)	
intermediate	18 (39.1%)	
high	17 (37.0%)	
Anti-HBc positive	15 (28.3%)	53
Cryoglobulins	5 (21.7%)	23
First line therapy		50
R-CHOP-like	28 (56.0%)	
CHOP-like	19 (38.0%)	
Other (VACOP-B, IPAD)	4 (8.0%)	
First line response		50
CR	32 (64.0%)	
PR	2 (4.0%)	
SD/PD	14 (28.0%)	
Death during therapy (toxicity)	2 (4.0%)	

* Abbreviations: ECOG= Eastern Cooperative Oncology Group; IPI = International Prognostic Index; LDH= Lactate Dehydrogenase; ALT= alanine transaminase; UNL= Upper Normal Limit; HPS = Hepatitis C Prognostic Score; CR= Complete Response; PR= Partial Response; SD= stable disease; PD= Progressive Disease

Results. Clinical, histological and virological features are reported in Table 1. FISH analysis showed rearrangements involving *BCL6* in 50.9% of patients, *MYC* in 11.3% and *BCL2* in 3.7%. Hans algorithm was applied to 45 tumors, classifying 22 (48.9%) cases as Germinal Center B cell (GCB) and 23 (51.1%) as non-GCB. Lymph2Cx-based assay was successful in 38 cases (70.4%) of which 16 (42.1%) were classified as Activated B cell (ABC), 16 (42.1%) as GCB and 6 (15.8%) as unclassified. Concordance between these two methods was 60%. NGS showed mutations in 158/184 evaluated genes (Figure 1). All patients harbored at least one oncogenic variant with a median of 13 mutated genes per case (2-26; IQR 9-16). The most frequently mutated genes were *KMT2D* (42.6%), *SETD1B* (33.3%), *RERE* (29.4%), *FAS* and *PIM1* (27.8%), *TBL1XR1* (25.9%). Mutated pathways involved the epigenetic regulation (94.4%), cell cycle or apoptosis (75.9%), BCR/NFκB signaling (70.4%), immune regulation (56%) and the NOTCH pathway (25.9%). Twenty-nine patients (53.7%) were classified into defined clusters using the LymphGen tool, including 14 in BN2 (48.2%), 7 in ST2 (24.1%), 4 each in MCD and EZB subtype (13.8%). Using NanoString analysis, patients with GCB or unclassified COO showed a trend toward a better OS compared to patients with ABC (HR=0.5, 95%CI 0.2-1.1, p=0.089).

Conclusions. This study confirmed the scarcity of *BCL2* translocations and showed that nearly 40% of cases present the ABC signature, which is associated with poorer outcome. We identified a set of genes recurrently mutated at a higher frequency compared to those in the HCV-negative DLBCL series (*SETD1B*, *RERE*, *BCL11A*, *TBL1XR1* and *ZFP36L1*) and therefore probably involved in HCV-

promoted lymphomagenesis. Finally, about a quarter of cases involve NOTCH pathway signaling. The prevalence of the BN2 cluster suggests that a consistent subgroup of HCV-positive DLBCL cases have a preferential marginal zone origin. These findings may have potential implications for molecularly targeted therapies.

C48

ABSTRACT NOT PUBLISHABLE

Chronic Myeloproliferative Disorders

C49

CIRCNAOME VARIATION IN AN *IN VITRO* MODEL OF JAK-INHIBITOR RESISTANT MPN DISCLOSED BY LONG-READ SEQUENCING

E. Gaffo^{1§}, R. Merlo^{1§}, D. Tarantino^{2§}, M. Balliu², S. Romagnoli², A. Enderti², I. Glogovitis¹, N. Bartalucci^{2*}, S. Bortoluzzi^{1*}, A.M. Vannucchi^{2*}

¹Computational Genomics Group, Department of Molecular Medicine, University of Padua; ²CRIMM, Center Research and Innovation of Myeloproliferative Neoplasms, University of Florence, AOU Careggi; [§]These authors equally contributed as first authors, *These authors equally share the senior authorship

Introduction. The hyperactivation of the JAK/STAT pathway is the mechanistic hallmark of Myeloproliferative Neoplasms (MPN). The JAK-inhibitor Ruxolitinib (RUX) improves systemic symptoms and splenomegaly, however it fails to eradicate the pathologic clone, with a gradual waning of the initial therapeutic benefit, associated with drug resistance, and eventually disease progression. The mechanisms underlying the loss of response to RUX are still an area for further investigation. In this scenario, we leveraged a new sequencing technology based on long-reads to characterize the circular RNA (circRNA) expression profile of two RUX-resistant JAK2V617F mutant cell lines.

Methods. Drug-resistant SET2 and HEL were generated by repeated treatment with increasing concentrations of RUX (0.1 to 2.5 μ M). Resistant clones with a growth reduction to <10% relative to the parental (P) line in presence of the RUX LD50 (0.25 and 1 μ M for SET2 and HEL, respectively) were selected. RNA from P, RUX-resistant (R) and RUX-treated (T) SET2 and HEL cells underwent RNase R treatment, to enrich circRNAs, and sequencing by long-read Oxford Nanopore Technology (ONT). RNA-seq data were analyzed by CIRI-long and custom R scripts, differential expression with DESeq2 ($\text{padj} \leq 0.01$).

Results. The proliferation assay on the SET2 T and R cells showed reduced cell growth to 60% ($P=0.0015$) and 4.5% ($P=0.02$), respectively, compared to the P cells. Figures for HEL were similar. Overall, we detected 25,681 individual circRNA isoforms expressed from 7,848 genes. In this group of circRNAs, 25,213 different backsplice junctions were represented, indicating that also circRNAs with different exon composition (linear isoforms) can be distinguished by ONT. Next, we focused on the most expressed circRNAs, which included circARID1A, circCDYL, circGSE1, circRUNX1, circETV6 and, notably, circRNAs derived from mitochondrial genes (meccRNAs). In line with their different genetic background, the unsupervised and differential expression analyses showed that the circRNAs expression profile of P SET2 and HEL were different. Both R cell lines displayed a different circRNAome compared to P cells. The treatment with RUX had a marked effect on circRNA expression, particularly in SET2.

Conclusions. The established ONT-based protocol allows the detection and quantification of circRNAs, to obtain the complete sequence of the circular molecules, discriminating isoforms with the same backsplice but different internal sequences. We disclosed that resistant clones present a peculiar circRNAome and that circRNA expression is modulated upon JAK-inhibition in MPN *in vitro*. CircRNAs with expression levels significantly different in resistant cells, and affected by the treatment, are undergoing further study to clarify their involvement in resistance mechanisms. For this purpose, the knowledge of the whole circRNA sequence is precious to model their involvement in targetable regulatory axes.

C50

CYTOTOXIC T CELLS FROM MYELOFIBROSIS PATIENTS SHOW EARLY EXHAUSTED FEATURES TARGETABLE BY CTLA-4 INHIBITION *IN VIVO* IN A PDX MOUSE MODEL

L. Tavernari^{1,2}, S. Rontauroli^{1,3}, R. Norfo^{1,3}, M. Mirabile^{1,2}, M. Maccaferri⁴, B. Mora⁵, E. Genovese^{1,3}, S. Parenti^{1,3}, C. Carretta^{1,3}, E. Bianchi^{1,2}, M. Bertesi^{1,2}, F. Pedrazzi^{1,2}, P. Guglielmelli^{6,7}, L. Fabbiani⁸, C. Colasante⁹, L. Losi¹⁰, L. Potenza⁹, F. Passamonti^{11,12}, E. Tagliafico^{9,13}, M. Luppi⁹, A.M. Vannucchi^{6,7}, R. Manfredini^{1,3}

¹Interdepartmental Centre for Stem Cells and Regenerative Medicine, University of Modena and Reggio Emilia; ²Department of Life Sciences, University of Modena and Reggio Emilia; ³Department of Biomedical, Metabolic and Neural Sciences, University of Modena and Reggio Emilia; ⁴Department of Laboratory Medicine and Pathology, Diagnostic Hematology and Clinical Genomics AUSLAOU Policlinico; ⁵Department of Oncology, Ospedale ASST Sette Laghi; ⁶Center Research and Innovation of Myeloproliferative Neoplasms (CRIMM), Azienda Ospedaliera Universitaria Careggi; ⁷Department of Experimental and Clinical Medicine, University of Florence; ⁸Department of Medical and Surgical Sciences of Children & Adults, Pathology Unit, University of Modena and Reggio Emilia; ⁹Department of Medical and Surgical Sciences, University of Modena and Reggio Emilia, AOU Policlinico; ¹⁰Department of Life Sciences, Pathology Unit, University of Modena and Reggio Emilia; ¹¹Hematology Foundation IRCCS Ca'Granda Ospedale Maggiore, Policlinico Milan; ¹²Department of Oncology and Haemato-Oncology, University of Milan; ¹³Center for Genome Research, University of Modena and Reggio Emilia, Italy

Introduction. Myelofibrosis (MF), either primary or secondary, belongs to Philadelphia-negative myeloproliferative neoplasms (MPN) and is characterized by bone marrow fibrosis, hematopoietic stem cell mobilization and extramedullary haematopoiesis. Persistent antigen stimulation in the tumour microenvironment can differentiate T effector cells into terminally exhausted T cells, a functional state characterized by decrease in proliferation, cytotoxicity, and cytokine production. Even in myeloid neoplasms such as MF, T cells are showing dysfunctional features; thus, we investigated T cell exhaustion in MF to assess the possibility of immune checkpoint inhibition as a new effective therapy.

Methods. Peripheral blood mononuclear cells (PBMCs) were isolated from 50 MF patients and 22 healthy donors (HD). CD3+CD8+ T cells were characterized by multicolour flow cytometry to assess surface expression of inhibitory receptors (IRs) like PD-1, CTLA-4 and others. Results were correlated with patient's clinical features. Residual cytokines production was assessed via intracellular flow cytometry staining. IRs-ligands expression was evaluated on monocytes and granulocytes by multiparametric flow cytometry. A co-culture system was established to investigate the immunosuppressive interplay between the dysfunctional T cells and the cells from the neoplastic clone and to test anti-CTLA-4 inhibition *in vitro*. Patient-Derived-Xenograft (PDX) mice were established by transplanting CD34+ MF cells to test the effect of anti-CTLA-4 treatment *in vivo*.

Results. Increased expression of IRs like CTLA-4 was observed on cytotoxic T cells from MF patients together with a decreased secretion of IFN γ and TNF α . Correlation analysis evidenced a more severe disease in patients with higher IRs expression on cytotoxic T cells. IR-ligands like CD80 and CD86 were increased on MF granulocytes and monocytes. While cytotoxic T cells from HDs were effectively activated either alone or in co-culture with myeloid cells, the activation of cytotoxic T cells from MF patients was attenuated in presence of myeloid cells and restored when T cells were cultured alone or treated with anti-CTLA-4. Anti-CTLA-4 treatment *in vivo* reduced myeloid engraftment, preferentially targeted granulocytes

and monocytes and expanded T cells.

Conclusions. Our data evidenced in MF patients the presence of an impaired population of cytotoxic T cells expressing multiple IRs and with reduced cytokine production. An immunosuppressive interplay between the myeloid neoplastic clone and T cells was reported and partially reverted by anti-CTLA-4 treatment *in vitro*. Moreover, anti-CTLA-4 *in vivo* treatment in PDX mice preferentially targeted malignant cells and expanded the lymphoid compartment. Taken together this data highlights an exhausted state likely implicated in immune escape that could be targeted and potentially reverted by immune checkpoint inhibitions.

C51

TRANSCRIPTIONAL AND PHOSPHO-PROTEOMIC PROFILING OF CALR+/- MICE REVEALS THE DEREGULATION OF SIGNALING PATHWAYS INVOLVED IN CALCIUM HOMEOSTASIS, CELL-TO-CELL INTERACTION AND VESICLE TRAFFICKING

N. Bartalucci¹, A. Enderti¹, S. Romagnoli¹, L. Calabresi¹, M. Balliu¹, D. Tarantino¹, M. Lomi¹, F. Arciprete², C. Di Buduo³, M. Zingariello², A. Balduini³, A.R. Migliaccio⁴, P. Guglielmelli¹, A.M. Vannucchi¹

¹CRIMM, Center Research and Innovation of Myeloproliferative Neoplasms, University of Florence, AOU Careggi; ²Unit of Microscopic and Ultrastructural Anatomy, Dept of Medicine, University Campus Bio-Medico Roma; ³University of Pavia; ⁴Medicine and Surgery, University Campus Bio-Medico, Italy

Introduction. Calreticulin (CALR) mutations are known to drive Myeloproliferative Neoplasm (MPN). CALR mutated cells share with JAK2 and MPL mutant an enhanced JAK/STAT signaling and cytokine independence, nevertheless they are characterized by a wide spectrum of deregulation reflecting the numerous cellular processes involving the protein. Accumulating evidence hints the role of CALR in hemopoiesis, however the mechanism through which CALR shapes the MPN phenotype remains an area of robust investigations. Here we present the results emerging from the transcriptional and phospho-proteomic profiling of the hemopoietic-restricted Calr+/mouse model.

Methods. Calr+/- colony were generated by crossing Calr+/floxed with Vav-Cre mice. Transcriptomic analysis of Calr+/- and Calr+/floxed (control) LSK was accomplished by DESeq2 and DOSE to obtain differentially expressed (DE) RNAs and enrichment analysis, respectively. Phospho-proteomic data were generated by LC-MS/MS after phospho-peptides enrichment of BM myeloid cells. Differentially phosphorylated (DP) sites were retrieved by PhosR and used for enrichment analysis and to predict kinase-substrate interactions. A $P\text{-adj} \leq 0.01$ was used as threshold for all the analysis. **RESULTS** Calr+/- mice resembled a MPN phenotype, characterized by increased platelet count (range 1156-1986x10⁹/L, +1.5 fold, $P=0.007$), enhanced megakaryopoiesis (Mk progenitors) +1.6 fold, $P=0.048$, splenomegaly (spleen index) +1.35 fold, $P=0.039$, BM focal fibrosis, and the expansion of stem cell compartment (+2 fold, $P=0.008$), compared to controls. Calr+/- showed 714 DE-RNAs (increased $n=373$, decreased $n=341$) enriched in signaling pathways regulating intracellular Ca²⁺, cell adhesion and vesicles trafficking. The DP-residues of Calr+/- myeloid cells ($n=262$) identified 170 DP-proteins (67 up, 103 down) that were enriched in gene-sets belonging to the category of cell adhesion and Ca²⁺ homeostasis. Among the DP-proteins, 142 entered in the signaling pathway analysis and were grouped into 6 clusters as predicted substrates of the following upstream kinases: MAPK, CDK, mTOR, ABL1, AuroraKb and PRKAA1. To further compare Calr haploinsufficient and CALR mutant features, we matched transcriptomic data from Calr+/- mice with available data from CALRdel52 and Ins5 UT7 cells. Interest-

ingly, CALR mutant UT7 shared the same spectrum of deregulations with Calr+/- mice involving the stress of endoplasmic reticulum (GOI0006874), augmented vesicles trafficking (GOI0006887) and the deregulated expression of adhesion molecules regulating cell-to-cell interaction (GOI1903039).

Conclusions. The results obtained from Calr haploinsufficient mice, further integrated with data from CALR mutant UT7, pointed to specific molecular signatures potentially underlying the development of the MPN phenotype. The validation of identified molecular players is ongoing in CALR knock-out models and CALR mutated patients and these results will be presented at the meeting.

C52

BCR-ABL1 TRANSCRIPT LEVEL IN SMALL EXTRACELLULAR VESICLES FROM ADULT CML PATIENTS' PLASMA; AN INSIGHT ON PHYSICAL FEATURES AND CORRELATION WITH CLINICAL AND BIOLOGICAL PARAMETERS

S. Mutti^{1,2}, S. Bernardi^{1,2}, A. Cavalleri^{1,2}, B. Xhahysa^{1,2}, M. Farina¹, A. Leoni^{1,2}, L. Garuffo^{1,2}, C. Ielo³, A. Radeghieri⁴, V. Mangolini⁴, C. Bonvicini⁵, E. Morello¹, V. Radici¹, E. Accorsi Buttini¹, N. Polverelli¹, M. Malagola¹, E. Abruzzese⁶, M. Breccia³, D. Russo¹

¹Department of Clinical and Experimental Sciences, University of Brescia, Unit of Blood Diseases and Bone Marrow Transplant, ASST Spedali Civili of Brescia; ²Centro di Ricerca Emato-Oncologica AIL (CREA), ASST Spedali Civili of Brescia; ³Umberto I Policlinic, La Sapienza University; ⁴Department of Molecular and Translational medicine, University of Brescia; ⁵Molecular Markers Laboratory, IRCCS Istituto Centro San Giovanni Di Dio Fatebenefratelli; ⁶Hematology, S. Eugenio Hospital, ASL Roma 2, Italy

Introduction. Small extracellular vesicles (EVs) recently emerged as useful liquid biopsy tools in Chronic Myeloid Leukemia (CML). Studies on vesicular BCR-ABL1 transcript (BCR-ABL1-EVs), may result in an easier and stronger technique for CML monitoring, particularly for detection of non-circulating residual leukemic cells resident in the bone marrow (BM-LSCs). The clinical-biological insight that BCR-ABL1-EVs conceals are unknown. This study aims to characterize CML-EVs isolated in patients' plasma and correlate disease status and clinical features to BCR-ABL1-EVs level.

Methods. EVs were isolated via commercial kit from 104 plasma samples of adult CML patients. Among them, 18/104 (17%) were in MMR and 86/104 (83%) in DMR following IS. At sampling, 21/104 (20%) patients were treated with imatinib (IMA), 21/104 (20%) with 2nd generation TKIs (2ndTKI), 27/104 (26%) with intermittent TKIs therapy (INT), and 24/104 (23%) were in treatment free remission (TFR). EVs were characterized via Atomic Force Microscopy (AFM), Western Blot (WB) and quantified by Nanoparticle Tracking Analysis. BCR-ABL1-EVs was quantified by digital PCR (dPCR). BCR-ABL1 was evaluated by dPCR also on peripheral blood cells (PB).

Results. EVs presence was confirmed in the isolated precipitate via CD63 and FLOT1 surface markers detection whilst AFM analysis confirmed EVs' size (Figure 1A-B). Compared to PB cells, EVs shuttle a higher overall amount of BCR-ABL1 transcript, suggesting that EVs carry markers also from BM-LSCs ($p=.0052$) (Figure 1C). Despite the amount of EVs is not influenced by MR classes, BCR-ABL1-EVs correlates with the MR classes, with statistical difference between MR3 and MR4, MR4, 5, MR5 ($p=.0354$, $p=.01$ and $p=.0051$, respectively) (Figure 1D). The significance is preserved if samples are grouped after MMR and DMR definition ($p=.0017$) (Figure 1E). In terms of therapy, patients under IMA show the lowest BCR-ABL1-EVs levels, whereas those on INT or TFR show the

highest (Figure 1F). Notably, patients under 2ndTKI have higher BCR-ABL1-EVs level than those under IMA, albeit without statistical significance. When considering the transcript type, no statistical difference is detected in BCR-ABL1 levels (Figure 1G).

Conclusions. This is the first time that BCR-ABL1-EVs is correlated with several clinical and biological features in a cohort of adult CML patients. WB and AFM confirmed the vesicular origin of the detected BCR-ABL1 transcript in CML-patient plasma. The high sensitivity of this approach allows the detection of BCR-ABL1 shuttled by EVs presumably released by BM-LSCs. BCR-ABL1-EVs level reflects the MRD level and discriminates the MR classes. Moreover, BCR-ABL1-EVs correlates with the ongoing therapy and future functional study will clarify the differences between IMA and 2ndTKI, as well as the high levels detected in patients under INT or TFR. These findings expose dPCR and EVs combination as an unrivalled method to detect BM-LSCs in a non-invasive manner.

C53

CHROMOSOME 9P DUPLICATION INDUCES T-CELL EXHAUSTION AND PROMOTES STEM CELL CLONOGENICITY IN JAK2-MUTANT CHRONIC MYELOPROLIFERATIVE NEOPLASMS

R. Norfo^{1,2}, C. Carretta^{1,2}, S. Parenti^{1,2}, F. Badii³, M. Bertesi^{2,4}, S. Rontautoli^{1,2}, L. Tavernari^{2,4}, E. Genovese^{1,2}, S. Sperduti^{5,6}, E. Enzo^{2,4}, M. Mirabile^{2,4}, F. Pedrazzi^{2,4}, C. Pessina⁷, I. Colugnat⁷, B. Mora⁸, M. Maccaferri⁹, E. Tenedini^{9,19}, S. Martinelli¹⁰, E. Bianchi^{2,4}, L. Casarini^{5,6}, L. Potenza¹⁰, M. Luppi¹⁰, E. Tagliafico¹⁰, P. Guglielmelli^{11,12}, M. Simoni^{5,6}, F. Passamonti^{13,14}, A.M. Vannucchi^{11,12}, R. Manfredini^{1,2}

¹Department of Biomedical, Metabolic and Neural Sciences, University of Modena and Reggio Emilia; ²Interdepartmental Centre for Stem Cells and Regenerative Medicine; University of Modena and Reggio Emilia; ³Department of Cancer Biology, Thomas Jefferson University and Sidney Kimmel Cancer Center; ⁴Department of Life Sciences, University of Modena and Reggio Emilia; ⁵Unit of Endocrinology, Department of Biomedical, Metabolic and Neural Sciences, University of Modena and Reggio Emilia; ⁶Center for Genome Research, University of Modena and Reggio Emilia; ⁷SMEL Citogenetica e Genetica Medica, ASST Sette Laghi; ⁸Division of Hematology, Ospedale ASST Sette Laghi, University of Insubria; ⁹Department of Laboratory Medicine and Pathology, Diagnostic Hematology and Clinical Genomics Unit, Modena University Hospital; ¹⁰Department of Medical and Surgical Sciences, University of Modena and Reggio Emilia, AUSL/AOU Policlinico; ¹¹Department of Experimental and Clinical Medicine, University of Florence; ¹²Center Research and Innovation of Myeloproliferative Neoplasms (CRIMM), Azienda Ospedaliera Universitaria Careggi; ¹³Hematology Unit, Fondazione IRCCS Ca' Granda Ospedale Maggiore Policlinico; ¹⁴Department of Oncology and Hemato-Oncology, University of Milan, Italy

Introduction. Myeloproliferative Neoplasms (MPNs) are a group of blood cancers originating from a single hematopoietic stem cell, characterized by an excessive production of mature blood cells. The most common mutation is a gain-of-function point mutation in the JAK2 gene, known as JAK2V617F, which leads to overgrowth of MPN cells. Alongside many other described genetic mutations, chromosome 9 amplification is a commonly reported genetic lesion. As the JAK2 gene is located on the short arm of this chromosome, we hypothesized that chromosome 9 copy number abnormalities may confer different clinical phenotypes in JAK2V617F-mutant MPN patients.

Methods. To characterize the effects of chromosome 9 copy number aberrations on JAK2-mutated MPN cells, we analyzed monocytes and granulocytes from 32 MPN patients through next-generation sequencing, multiplex ligation-dependent probe amplification and immunofluorescence, while CD34+ cells were cultured in semisolid media and colony DNA was used to perform droplet digital PCR. Finally, T cells were analyzed through flow cytometry.

Results. In-depth analysis of JAK2-amplified patients revealed that the amplification involved the entire chromosome 9p (hereafter called +9p), thus including other gene loci like CD274, which encodes programmed death-ligand 1 (PD-L1). Further investigation of the clonal hierarchies through droplet digital PCR on CD34+ cell-derived colonies showed that most CD34+ cells carried two JAK2 mutant alleles and a wild-type allele, with JAK2V617F mutation being the first genetic lesion occurring in these cells, followed by +9p. Functionally, CD34+ cells from +9p patients displayed high clonogenicity with a greater number of primitive colonies. As JAK2V617F protein had been previously reported to promote PD-L1 expression, we investigated the possibility of combinatorial effects in +9p patients. Our analysis showed that PD-L1 expression

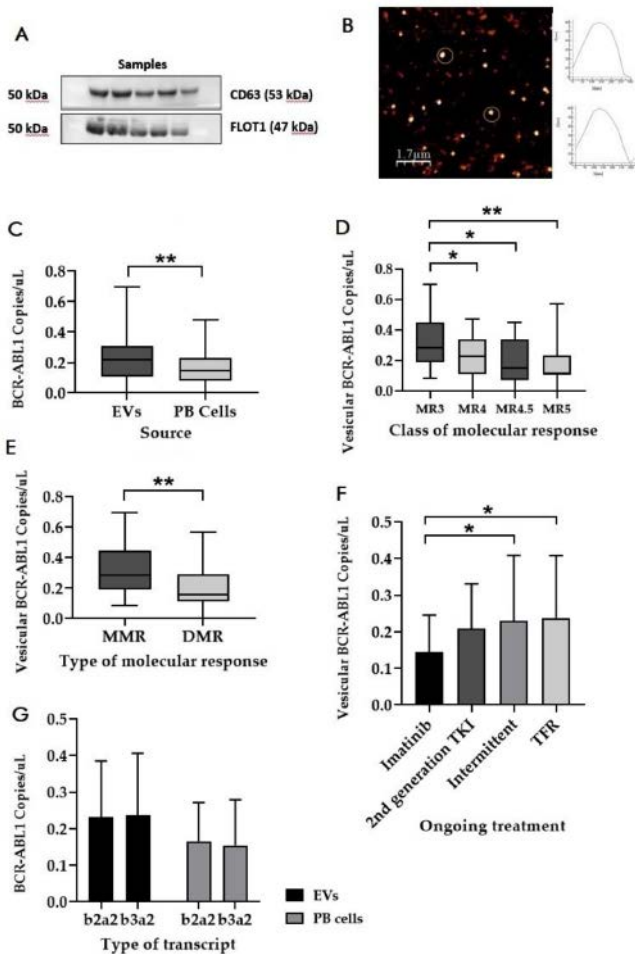


Figure 1.

was increased in monocytes from +9p patients compared to diploid cells from patients and healthy donors and was positively correlated with JAK2 mutational burden. Moreover, PD-L1 protein was mainly intracellular in diploid patients, while it was mostly located on the cell membrane in +9p patients. Finally, as PD-L1 is an immune checkpoint known to dampen T cell activation, we carried out an immunophenotypic analysis of the T cell compartment that revealed increased levels of PD1+ exhausted cytotoxic T cells, suggesting the activation of PD-1/PD-L1 immune escape axis.

Conclusions. these results suggest a combined effect of +9p and JAK2 mutations in increasing PD-L1 expression, promoting its exposure on the cell surface and subsequently enhancing PD-L1/PD-1 axis activation, leading to T cell exhaustion. Moreover, this genetic asset impacts on the clonogenic activity and stemness of MPN CD34+ cells, favoring the shift towards a primitive phenotype.

C54

EXPLORING PROGNOSTIC FACTORS IN MYELOPROLIFERATIVE NEOPLASMS-ASSOCIATED SPLANCHNIC VEIN THROMBOSIS

E. Torre^{1,2,3}, N. Curto-Garcia¹, A. Duminuco^{1,4}, A. Santaolalla², S. Kordasti², C. Harrison¹

¹Department of Haematology, Guy's and St Thomas' NHS Foundation Trust; ²King's College London; ³Hematology Department, AOU delle Marche; ⁴Division of Hematology, AOU "Policlinico G. Rodolico-San Marco", Italy

Introduction. Myeloproliferative Neoplasms (MPN) represents the main underlying cause of Splanchnic Vein Thrombosis (SVT) leading to significant morbidity and mortality. The clinical course is heterogeneous, and as a result, the impact of SVT on MPN patient's survival remains debated.

Methods. A total of 85 patients diagnosed with MPN-SVT referred to Guy's Hospital were retrospectively analysed in this study, and 171 MPNs, were used as controls, matched for the MPN subtype. Demographic, clinical, and outcome data were collected and reported.

Results. Overall, 85 patients with MPN-SVT were analysed with a median follow-up of 7.7 years (range, 0.3-30). Female patients (50/85, 58.8%) were prevalent with a median age at MPN diagnosis of 44 years (range, 13-70). MPN and SVT diagnoses were coincident (within 3 months) in 56 patients (65.9%), and in 21 (24.7%) an SVT index event occurred after the diagnosis of MPN by a median of 4 years (range, 0.3-14.7). In the remaining 8 (9.4%) an SVT index preceded the diagnosis of MPN by a median of 4.4 years (range, 0.4-9). The most common site of thrombosis was the portal vein (PT) which occurred in 60 patients (70.6%), followed by splenic thrombosis (ST) in 22 (26%) and mesenteric vein (MT) in 20 (23.5%). Budd-Chiari Syndrome (BCS) was also experienced in 10 patients (11.8%). The main clinical and laboratory findings are summarised in Table 1. From univariate Cox models we found that age, haemoglobin, cardiovascular risk factors, and splenomegaly at diagnosis were predictive factors of SVT. The incidence of recurrences was 16.5% with a median time to recurrence of 4.5 years (range, 0.2-16.5). Conversely, major haemorrhages were experienced in 20% of patients. Overall, 13/85 (15.3%) and 3/85 (3.5%) progressed to secondary MF and acute leukaemia, respectively. Patients who had not progressed (69/85, 81.2%) had a lower median age at MPN diagnosis (41, range 13-70) than patients who experienced a progression disease (49, range 36-69) (p=0.006). The overall survival (OS) at last follow-up was 89.4%. The most frequent cause of death resulted from acute leukaemia transformation in four patients. Finally, the univariate Cox models, confirmed a negative influence of age at diagnosis (HR 1.08, 95% CI 1.01-1.16, p=0.025) and history of previous thrombosis

(OR 4.46, 95% CI 1.1-18, p=0.036).

Conclusion. We confirmed a consistent association, between SVT and a specific MPN phenotype, which mainly affects young females diagnosed with PV with a low JAK2 allele burden (24% vs 49%, p=0.015). This rare entity remains challenging to manage clinically due to the considerable risk of subsequent vascular events. Furthermore, we discovered that the outcomes for MPN-SVT patients are influenced by their history of previous thrombosis and age at diagnosis. In the future, gaining a more comprehensive understanding of MPN-SVT is crucial for enhanced risk stratification.

Table 1. Clinical and laboratory findings of MPN-SVT and control population.

	MPN-SVT (85)	Controls (171)	p
Age at MPN diagnosis (years), median (range)	44 (13-70)	50 (15-84)	<0.001
Gender (M/F), n	35/50	87/84	0.147
Hb at MPN diagnosis (g/dL), median (range)	13.5 (8-20.9)	15.4 (8.7-22.6)	<0.001
WBC at MPN diagnosis (x10 ⁹ /L), median (range)	8 (4-41.9)	9.4 (3.2-23.7)	0.019
PLT at MPN diagnosis (x10 ⁹ /L), median (range)	389 (130-1800)	591 (41-2095)	0.004
NLR at MPN diagnosis, median (range)	3.6 (1.6-14.9)	3.5 (0.9-15.2)	0.404
PCV at MPN diagnosis, median (range)	0.44 (0.25-0.65)	0.45 (0.29-0.59)	0.068
Constitutional symptoms at MPN diagnosis, n (%)	46 (54.1)	91 (53.2)	0.896
Splenomegaly at MPN diagnosis, n (%)	63 (74.1)	47 (27.5)	<0.001
JAK2V617F, n (%)	79 (92.9)	144 (84.2)	0.083
JAK2V617F allele burden (%), median (range)	25 (4-91)	42 (0.1-97)	0.05
N evaluable (SVT/controls=34/71)			
CALR, n (%)	3 (3.5)	18 (10.5)	0.088
MPL, n (%)	0 (0)	5 (2.9)	0.173
Abnormal karyotype, n (%)	5 (20)	11 (15.5)	0.755
N evaluable (SVT/controls=25/71)			
CV risk factor, n (%)	62 (72.9)	82 (48)	<0.001
Thrombosis recurrence, n (%)	14 (16.5)	0 (0)	0.043
History of previous thrombosis, n (%)	9 (10.6)	12 (7)	0.341
Haemorrhages, n (%)	17 (20)	4 (2.3)	0.783
Myelofibrosis progression, n (%)	13 (17.3)	14 (8.2)	0.079
Leukemic evolution, n (%)	3 (3.5)	2 (1.2)	0.184
Death, n (%)	9 (10.6)	4 (2.3)	0.004
Follow-up from MPN diagnosis (months), median (range)	93 (3-358)	74 (2-486)	0.02

C55

P210 PEPTIDE-DERIVED VACCINATIONS IN CHRONIC MYELOID LEUKEMIA PATIENTS DURING IMATINIB TREATMENT| LONG-TERM OUTCOMES OF GIMEMA CML0206 AND SI0207 STUDIES

A. Sicuranza¹, M. Breccia², F. Iuliano³, G. Gugliotta⁴, F. Castagnetti⁴, M. Lunghi⁵, A. Patriarca⁵, T. Intermesoli⁶, L. Luciano⁷, A. Russo Rossi⁸, G. Rege Cambrin⁹, V. Vucinic¹⁰, D. Russo¹¹, M. Malagola¹¹, A. Malato¹², E. Abruzzese¹³, M. D'adda¹⁴, S. Galimberti¹⁵, M. Defina¹, V. Sammartano¹, C. Cafarelli¹, G. D'alfonso¹⁶, A. Piciocchi¹⁶, M. Bocchia¹

¹Hematology Unit, Azienda Ospedaliera Universitaria Senese, University of Siena; ²Department of Translational and Precision Medicine, Sapienza University; ³Presidio Ospedaliero N. Giannetasio - Azienda ASL 3; ⁴Institute of Hematology "L. and A. Seràgnoli", Department of Experimental, Diagnostic and Specialty Medicine, "S. Orsola-Malpighi" University Hospital, University of Bologna; ⁵Division of Hematology, Department of Translational Medicine, University of Eastern Piedmont and AOU Maggiore della Carità; ⁶Struttura Complessa Ematologia, Ospedale di Bergamo, ASST Papa Giovanni XXIII; ⁷Hematology Unit "Federico II", University of

Naples; ⁸Department of Precision and Regenerative Medicine and Ionian Area (DiMePRE-J) - Hematology and Stem Cell Transplantation Unit - University of Bari "Aldo Moro"; ⁹Division of Internal Medicine and Hematology, San Luigi Gonzaga Hospital; ¹⁰Klinik und Poliklinik für Hämatologie, Zelltherapie und Hämostaseologie, University Hospital Leipzig; ¹¹Unit of Blood Diseases and Bone Marrow Transplantation, Cell Therapies and Hematology Research Program, Department of Clinical and Experimental Sciences, University of Brescia, ASST Spedali Civili di Brescia; ¹²Hematology, Cervello Hospital; ¹³Division of Hematology, S. Eugenio Hospital; ¹⁴Hematology Division, Department of Oncology, ASST Spedali Civili di Brescia; ¹⁵Section of Hematology, Department of Clinical and Experimental Medicine, University of Pisa; ¹⁶GIMEMA Foundation

Nowadays the ambitious goal of hematologists for chronic myeloid leukemia (CML) patients (pts) is the achievement of a stable treatment free remission (TFR). Yet only a minority of pts achieve the molecular response prerequisites to attempt a TFR approach and ultimately about half of them experience a molecular relapse and need to restart TKI treatment. We and others investigated the potential involvement of immune system in CML control, and immunotherapeutic strategies have been proposed. Peptide-derived antitumor vaccines have been developed to obtain a specific antitumor response able to control and eradicate residual disease. We previously showed that peptides encompassing b3a2 or b2a2 breakpoint p210 aminoacid sequence induced peptide-specific T cell responses in CML pts. Thus, an alternative peptide vaccine-based target therapy was hypothesized to further reduce residual disease in imatinib (IMA) treated CML pts. We conducted 2 multicenter peptide vaccine phase-II studies, GIMEMA CML0206 and SI0207 enrolling 109 chronic phase CML pts (68 b3a2 and 41 b2a2) with persistence of cytogenetic a/o molecular disease during IMA. We present the outcome of these pts vaccinated with p210 specific peptide-vaccine after a median observation time of 10 ys (3-14 ys). All pts completed vaccination schedule with no significant short- or long-term toxicity. After vaccinations, peptide-specific CD4+ T-cell response was documented at least once in about 80.8% of b3a2 and 78% of b2a2 pts. In the short terms 30% of vaccinated pts achieved a reduction of BCR/ABL1 transcript while the majority showed stable molecular disease with fluctuations (58%). At present, median follow-up since diagnosis and last vaccination are 18 ys and 10 ys respectively, with an overall survival (OS) rate at 18 ys of 89%. 97/109 (89%) pts are alive and 12/109 (11%) died of CML-unrelated reasons. 55/109 (50%) pts discontinued IMA the most reason was discontinuation for TFR (24.7%) followed by resistance (22%), enrollment in a clinical trial (2.7%) or second neoplasia (0.9%); 27/109 (24.7%) received a second TKI 8/27 pts (29.6%) dasatinib and 19/27 pts (70.4%) nilotinib. Overall, 34/109 (31%) pts attempted TFR after a median time of 40.5 mos from last vaccination. 20/34 (59%) pts maintained molecular response and are still in TFR, 18/27 (66%) pts after IMA and 2/4 (50%) after nilotinib. Median IMA treatment duration before discontinuation was 151 mos and median TFR time was 46 mos. Long-term results of b2a2 and b3a2 peptide vaccinations showed feasibility and safety of this approach and allow us to speculate about the introduction of this strategy in CML pts with low-level molecular residual disease to increase the depth of response and successful TFR. Alternatively, breakpoint peptide vaccination could be used after TKI discontinuation, to stimulate the immunological compartment against the residual disease again with the aim to increase the rate of success after stopping treatment.

C56

BCR-ABL1 POSITIVE CHRONIC MYELOID LEUKAEMIA (CML) TRANSGENIC ZEBRAFISH| AN EFFECTIVE MODEL FOR A RAPID AND RELIABLE TEST OF DIFFERENT TYROSINE KINASE INHIBITORS (TKIS) AND TO STUDY THE PATHOGENESIS OF THE DISEASE

S. Bernardi^{1,2}, D. Zizioli³, A. Cavalleri^{1,2}, S. Mutti^{1,2}, M. Farina¹, B. Xhahysa^{1,2}, L. Mignani³, A. Leoni^{1,2}, L. Garuffo^{1,2}, F. Re^{1,2}, F. Trenta^{1,2}, V. Radici¹, E. Morello¹, N. Polverelli¹, E. Accorsi Buttini¹, E. Monti³, G. Borsani⁴, M. Malagola¹, D. Russo¹

¹Unit of Hematology, Department of Clinical and Experimental Sciences, University of Brescia, Bone Marrow Transplant Unit, ASST Spedali Civili of Brescia; ²Centro di Ricerca Emato-Oncologica AIL (CREA), ASST Spedali Civili of Brescia; ³Unit of Biotechnology, Department of Molecular and Translational Medicine, University of Brescia; ⁴Unit of Biology and Genetic, Department of Molecular and Translational Medicine, University of Brescia, Italy

Introduction. Zebrafish (*Danio rerio*) has proven to be an effectiveness animal model that can be easily genetically manipulated to understand several diseases' mechanisms. The blood system and the hematopoiesis are very similar and conserved in mammals and in zebrafish, and specific leukemia types are generatable. Recently, a zebrafish model resembling a CML-like disease has been reported. While considering the remarkable results, the unique CML zebrafish model requires multiple activations of BCR-ABL1 expression, thus it cannot be excluded a forced phenotype of the disease. For this reason, we generated a new zebrafish model constitutively expressing human BCR-ABL1.

Methods. We generated a zebrafish CML model by using a GAL4/UAS/hsp70 system named tg(BCR-ABL1pUASICFP/hsp70-Gal4). This transgenic system regulates gene expression in a cell-specific and temporally restricted manner and provides a powerful tool to trace transgene expression. To test the robustness of the model, the transgenic fishes (tgBCR-ABL1) were treated with TKIs [i]matinib, dasatinib, nilotinib, bosutinib, ponatinib [b] and asciminib, after establishment of optimal dose. Artery blood flow, heart beats and heart morphology were considered to evaluate the recapitulation of the know cardiac side effects. In situ hybridization was used to evaluate the expression of hematopoietic markers (pu1, L-plastin and mpx) during embryonic development. The angiogenesis was evaluated analyzing cell activity via phosphatase assay. Immunofluorescence targeting Hystone H3 and digital PCR were used to assess cell proliferation and BCR-ABL1 transcript, respectively. Wild type fishes served as control.

Results. tgBCR-ABL1 resume the CML phenotype by presenting altered expression of hematopoietic markers during embryonic development compared to controls. Moreover, tgBCR-ABL1 show high proliferating hematopoietic cells in the caudal hematopoietic tissue. All tested TKIs induce morphological effects with the presence of cardiac edema, significance alteration of cardiac parameters (Figure 1A-B), and anti-angiogenic affects (Figure 1C), similarly to what observed in human. Treated tgBCR-ABL1 show a significant down-regulation of all hematopoietic markers and the proliferation rate compared to controls and untreated tgBCR-ABL1, suggesting the capability of the model to resume the response to the treatment (Figure 1D). This observation is confirmed by the significant decreased BCR-ABL1 transcript level observed in treated tgBCR-ABL1 compared to untreated tgBCR-ABL1.

Conclusions. Considering that the presented zebrafish model well recapitulates both the disease phenotype, and the treatment effects (efficacy and toxicity), it represents a reliable model to explore different combinations of compounds for new therapeutic strategies assessment. Moreover, combining the stability of the presented model

with the feature of zebrafish as disease model, it will be also a useful tool for further investigations on CML pathogenesis.

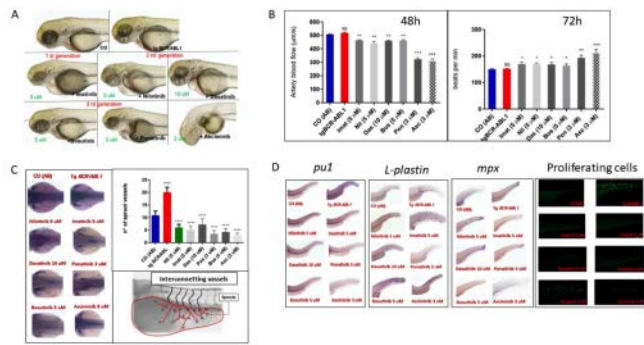


Figure 1.

Immunotherapy and Cell Therapy

C57

DEFINING THE ROLE OF MONOCYTES IN MEDIATING RESPONSE TO COMMERCIAL ANTI-CD19 CAR T-CELL THERAPY IN RELAPSED/REFRACTORY DIFFUSE LARGE B-CELL LYMPHOMA PATIENTS

M. Magni¹, N. Caldarelli^{1,2}, T. Torelli^{3,4}, L. Agnelli^{3,4}, G. Zanirato¹, S. Jonnalagadda², A. Rigamonti², A. Chiappella¹, A. Bermema¹, P. Corradini^{1,2}, C. Carniti¹

¹Hematology division, Fondazione IRCCS Istituto Nazionale dei Tumori; ²Università degli Studi di Milano; ³Department of Diagnostic Innovation, Fondazione IRCCS Istituto Nazionale dei Tumori; ⁴Department of Molecular Oncology 1, Fondazione IRCCS Istituto Nazionale dei Tumori, Italy

Introduction. Despite the unparalleled efficacy of commercial anti-CD19 chimeric antigen receptor (CAR) T-cell therapy for relapsed/refractory (R/R) large B-cell lymphoma patients (LBCL), durable responses were observed only in 40% of patients. Mechanisms of resistance are not well defined and many of the clinical and biological parameters used to date to predict CAR T success were generated at the time of or after CAR T infusion.

Methods. The study included 95 patients treated with tisagenlecleucel (Tisa-cel) and axicabtagene ciloleucel (Axi-cel). Prospectively collected pre-manufacturing leukapheresis products (LK) were characterized at the mRNA and protein level. For transcriptomic analysis, RNA of sorted CD3+ cells was analyzed using the nCounter 780-gene CAR-T Characterization Panel (NanoString). For flow cytometry, thawed LK and fresh peripheral blood samples - collected pre and post CAR T infusion - were stained with CD3, CD19, CD20, CD56, CD14, CD16, HLA-DR, CD33, CD15, CD11b, CD192, CX3CR1 and VISTA antibodies, to study monocyte subsets and myeloid derived suppressor cells (MDSCs). Circulating CAR T-cell expansion was longitudinally monitored using the CD19 CAR FMC63 antibody (Miltenyi biotec). Cell acquisition was performed on a MACSQuant Analyzer MQ16 (Miltenyi biotec) and data analyzed using the MACSQuantify Software and FlowJo software. Statistical analyses were performed by GraphPad Prism v9.00 and R v4.1.2.

Results. By transcriptomic analyses we identified a 4-gene myeloid signature able to stratify patients characterized by shorter progression free survival (PFS, $p < 0,0001$) and less likely to respond ($p < 0,01$). This myeloid signature is the result of monocyte-T cell complexes present in LK, positive for both CD3 and CD14, which are more abundant in patients expressing the signature (median 0,5% vs 0,2%, $p = 0,0005$). Patients expressing the 4-gene signature also display higher levels of monocytes in the LK at cell count (median 22,7% vs 16,8%, $p = 0,0015$), of intermediate monocytes (CD14+CD16+) (median 12,5% vs 8,5%, $p = 0,02$) and of intermediate monocytes expressing CD192 (median 52,1% vs 33,4%, $p = 0,0054$). Given the unexpected role of monocytes in LK, we then investigated the impact of myeloid populations on CAR T-cell expansion *in vivo*, which is a surrogate of response (Monfrini et al, 2022). We used the median concentration of CAR T cells at the time of maximal expansion (Cmax) to dichotomize patients into expanders and poor expanders and we observed that poor expanders have higher levels of circulating monocytes (median 23,5% vs 14,9%, $p = 0,04$), of intermediate monocytes and of monocytic MDSCs at peak expansion. Additionally, poor expanders display higher levels of monocyte-CAR T cell complexes when compared to expanders ($p = 0,004$).

Conclusions. Collectively our data point to a role of monocytes in affecting CAR T efficacy in LBCL patients, both at the time of leukapheresis and after CAR T infusion.

C58

TREGS-DERIVED EXTRACELLULAR VESICLES AS A NEW TOOL FOR IMMUNOMODULATING THERAPIES

P. Simeone¹, S. Veschi², I. Villanova³, B. Di Francesco³, G. Catitti¹, A. Piro², F. Guardalupi¹, G. Corradi¹, L. Ruggeri⁴, A. Cama², P. Lanuti¹, M. Di Ianni^{1,3}

¹Department of Medicine and Aging Sciences, University "G. d'Annunzio" Chieti-Pescara; ²Department of Pharmacy, University "G. d'Annunzio" Chieti-Pescara; ³Hematology Unit, Pescara Hospital; ⁴Department of Medicine and Surgery, University of Perugia, Italy

Background. In HLA-haploidentical transplantation, T regulatory cells (Tregs) co-infused with conventional T cells (Tcons), protect against graft-versus-host disease (GvHD) while maintaining the graft versus leukemia effect (GvL) [Di Ianni *et al.*, Blood 2011]. We have also demonstrated that GMP-grade expanded Tregs, that display phenotypic and functional Treg characteristics, can be obtained using a fully automated system [Ulbar *et al.*, BBMT 2020]. Recently, extracellular vesicles (EVs), released by various cell types, emerged as an alternative tool for cellular-mediated therapies. Here we isolated Tregs-derived EVs for the first time and characterized them for their *in vitro* activities.

Methods. Immunoselected Tregs (CD4+CD25+ 94.5%±6.3; FoxP3+ 63.7%±11.5; CD127+ 20%±3; suppressive activity 60%±7) were activated with anti CD3/CD28 beads and expanded in the presence of Rapamycin and IL-2. Tregs-derived EVs were studied using a flow cytometry method (patent n. EP19164567A), and isolated by cell sorting. A shotgun proteomics approach was used for the proteomic analysis. Flow cytometry, morphological (nanotracking analysis, NTA, atomic force microscopy), western blotting, and proteomic analyses were carried out with the aim of ascertaining their vesicular nature, while their inhibition potential was assessed by the *in vitro* suppression assay, on the related autologous T effector cells.

Results. The NTA characterization of Treg-derived EVs revealed that their size was in the range of small EVs (50-150nm). Atomic force microscopy results confirmed those data. The suppression assay (n=3) carried out on activated autologous T effector cells revealed that the optimal EV concentration to achieve the best results in terms of suppression (97-98%) was between 3-6x10⁶ EVs/1x10⁵ cells after 24 hours of treatment. FACS-purified EVs displayed a 3-fold higher inhibition ability compared to the ultracentrifuged ones. Furthermore, the inhibition effects of Treg EVs were comparable to those induced by the related parental cells (p<0.05). The immunomodulatory functions of EVs stemming from expanded Tregs were confirmed by the functional analysis of their protein cargo.

Conclusions. We demonstrated that Treg-derived EVs have strong immunomodulatory functions and their well-known low toxicity points out their potential as new therapeutic agents in GvHD prevention.

C59

CD19-CAR REDIRECTED NK CELLS SHOW ANTI-LEUKEMIC ACTIVITY AND PRODUCE CYTOTOXIC EXTRACELLULAR VESICLES EXPRESSING CAR MOLECULES

G. Corradi¹, F. Guardalupi¹, S. Vespa^{1,2}, P. Simeone^{1,2}, P. Del Boccio^{2,3}, D. Pieragostino^{2,4}, S. Veschi³, S. Baldoni⁵, B. Fabi⁵, A. Cama³, L. Ruggeri⁶, I. Caruana⁷, P. Lanuti^{1,2}, M. Di Ianni^{1,5}

¹Department of Medicine and Aging Sciences, University "G. D'Annunzio" of Chieti-Pescara; ²Center for Advanced Studies and Technology (CAST), University "G. D'Annunzio" of Chieti-Pescara; ³Department of Pharmacy, University "G. D'Annunzio" of Chieti-Pescara; ⁴Department of Innovative Technologies in Medicine and Dentistry, University "G. D'Annunzio" of Chieti-Pescara; ⁵Department of Oncology Hematology, Pescara Hospital; ⁶Department of Medicine and Surgery, University of Perugia; ⁷Department of Pediatric Hematology, Oncology and Stem Cell Transplantation, University Hospital Würzburg

Background. NK cells expressing a CD19. CAR showed encouraging results in early-phase clinical trials, representing an attractive alternative to CAR-T, due to their potential to overcome some of the limitations of the CAR-T therapy. Recently, extracellular vesicles (EVs), released by various cell type, emerged as new tool for monitoring the disease status and therapy response. However, the therapeutic efficacy of EVs for immunotherapy is still under investigation.

Methods. CD3⁺/CD56⁺ NK cells were isolated from healthy donors, activated with IL-2/IL-15/IL-1 β and transduced with a CD19. CAR vector. CAR⁺ cells were then enriched by sorting and *in vitro* expanded with IL-2/IL-15. From CAR-NK supernatants, EVs were characterized by a flow cytometry method (patent n. EP19164567A), isolated by cell sorting and lastly concentrated by PEG. A shotgun proteomics approach was then used for their molecular characterization.

Results. In the first part of the study, we focused on the expansion and transduction of primary NK cells reaching a transduction efficiency of 9,75±3,23%. Then, CAR-NK cells were sorted obtaining a purity of 91,41±2,37%. CAR-NK were functional and displayed a potent anti-tumor activity against the CD19⁺ cell lines, HG-3 and/or SUP-B15. Indeed, CAR-NK showed a significantly increased killing of target cells compared to untransduced NK cells (HG-3: 67,46±10,05 vs 31,77±7,03 p<0,05; SUP-B15: 83,13±13 vs 23,17±9,96 p<0,01; ratio NK:target 5:1). Furthermore, CAR-NK were also able to kill primary tumor cells of B-cell-acute lymphoblastic leukemia in a dose dependent manner, contrary to untransduced NK cells. In the second part of the study, we analysed the CAR-NK derived EVs CAR-NK cells produce a high amount of EVs (□4000 EVs/microliter), with a diameter of 117,1 nm+47,1 (small EVs), which strongly expressed CAR-CD19 (MFI Ratio>1.5). The analysis of protein cargo showed an enrichment of proteins associated with the "vesicle-mediated transport" (FDR = 1,31x10⁻¹⁷), the "leukocyte mediated immunity" (FDR = 2,231x10⁻²⁰), the "immune effector process" (FDR = 3,10x10⁻¹⁹), the "immune system process" (FDR = 1,33x10⁻²⁰) and the "programmed cell death" (FDR = 2,69x10⁻⁶) functions. Interestingly, CAR-NK EVs efficiently killed the HG-3 cells to a higher extent compared to EVs obtained from untransduced NK cells (37% ± 6,4 vs 22,3%±1,9; ratio EVs:HG-3 15:1, p<0.05). In order to investigate the mechanism of action of these EVs, we investigated the presence of NK-mediated killing proteins detecting in all the analyzed EVs significant high level of both granzyme B and perforin.

Conclusions. We were able to generate a population of CD19. CAR-NK cells capable to produce high amount of EVs, which showed a potent anti-leukemic activity, like the parental CAR-NK.

Our data provide the rationale to consider the EVs as new immunotherapeutic agents alone or in combination with their parental cells, to potentiate their function.

C60

TARGETING NPM1-MUTATED ACUTE MYELOID LEUKEMIA BY A DUAL TARGETING STRATEGY OF CHIMERIC ANTIGEN RECEPTOR (CAR) ENGINEERED CELLS

M. Capurro, N. Martarelli, M. Gentili, R. Rossi, E. Longetti, M.P. Martelli, E. Tiacchi, B. Falini, V.M. Perriello

Institute of Hematology and Center for Hemato-Oncology Research

Introduction. CAR-T cell therapy has been revolutionizing the treatment of blood malignancies, but its translation in AML is hindered by the absence of specific leukemic antigens lacking in normal tissues. NPM1-mutated AML offers an ideal model for CAR-T cell development, since the mutant NPM1 protein is uniquely expressed in leukemic cells and generates a neopeptide presented via HLA-A*020111 allele in 50% of the population. A novel CAR-T targeting NPM1mut neopeptide in complex with HLA-A*0201 was already designed but the low NPM1 neopeptide antigen density limits its efficacy. To overcome this issue, we probe a dual CAR-T cell model co-expressing anti-NPM1mut/HLA-A2 CAR and an anti-CD123 costimulatory receptor (CCR) lacking activation domains. This approach aims to improve affinity and activity for leukemic cells, avoiding off target toxicities.

Methods. Second generation CD8hinge. NPM1 CAR and dual CD8hinge. NPM1/ CD28hinge. CD123 CCR were cloned into a lentiviral backbone. CAR-T cells were generated after CD4/CD8 enrichment from healthy donors' PBMC, activated for 24 h before viral transduction and then cultured for 10 days. *In vitro* studies were performed co-culturing NPM1mut/HLA-A2+ AML3 cell line with single and dual CAR-T cells. Cytotoxicity assay was performed by luminescence assay after 24, 48 and 72 h at E:T ratio 1:1. A 96 hours cytotoxicity flow cytometry evaluation at unfavourable E:T ratio was further assessed for killing and CAR-T cell proliferation using precision counting beads. Cytokine assay at E:T 1:3 quantitatively measures the secretion of Th1 cytokines in co-cultures supernatants after 24 h.

Results. A novel anti-CD123 CAR developed from single chain fragment variable (scFv) of a newly generated mAb at the Haemato-Oncology Research Center of Perugia was validated for activity and specificity (Figure 1a,b). Hence, the anti-CD123 scFv was used to develop a dual targeting CAR-T cell strategy together with the anti-NPM1/HLA-A2 CAR to enhance target cell affinity. Preliminary cytotoxicity data indicate that dual NPM1/CD123 CAR-T cells exhibited higher targeted anti-leukemic activity *in vitro* compared to single targeting NPM1 CAR at 24, 48 and 72 h (Figure 1c). Absolute counting beads reveal that dual CAR-T cells reduce the number of tumour cells and enhance CAR-T cell proliferation after antigen encounter (Figure 1d). Furthermore, dual CAR-T cells exhibit the release of key pro-inflammatory cytokines (GM-CSF, IFN- γ , TNF- α), aligning with increased killing efficiency (Figure 1e).

Conclusions. The proposed dual targeting strategy suggests that the addition of an anti-CD123 CCR to the NPM1/HLA-A2 CAR may contribute to overcome the low antigen density of the NPM1mut neoantigen and thus may enhance the specific anti-leukemic activity. Further investigations are required to corroborate these findings and confirm the absence of on-target off-tumour effects on CD123+ Hematopoietic Stem Cells (HSCs) and endothelial cells.

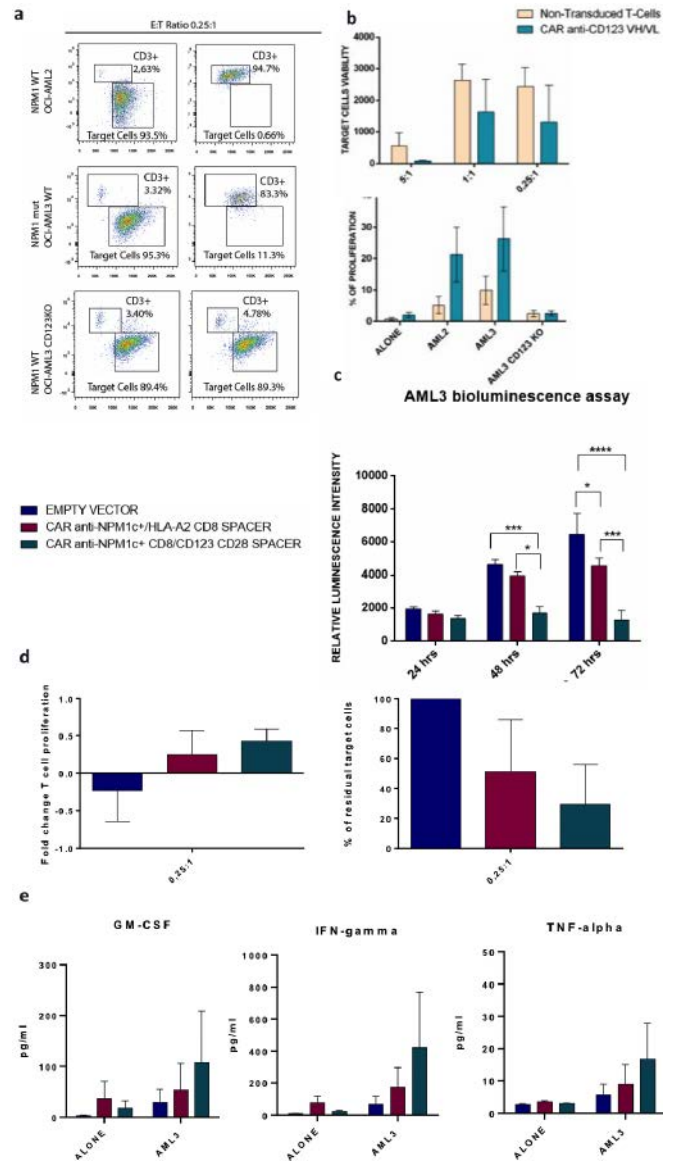


Figure 1.

C61

CD161+TREGS EXHIBITED REDUCED SUPPRESSION ACTIVITY WHILE PERMITTING THE TCON-MEDIATED ANTI-LEUKEMIC EFFECT

F. Guardalupi¹, G. Corradi¹, I. Villanova², B. Di Francesco², S. Scardi², S. Baldoni², B. Fabi², L. Ruggeri³, P. Lanuti¹, M. Di Ianni^{1,2}

¹Department of Medicine and Aging Sciences, University of Chieti-Pescara; ²Department of Oncology Hematology, Pescara Hospital; ³Department of Medicine and Surgery, University of Perugia, Italy

Introduction. In HLA-haploidentical transplantation, T regulatory cells (Tregs) co-infused with conventional T cells (Tcons), protect against graft-versus-host disease (GvHD) while maintaining the graft versus leukemia effect (GvL) [Di Ianni *et al.*, Blood 2011]. GvHD prevention associated with a powerful GvL effect could be linked to the ability of Tregs to reduce T cell expansion without dampening their activation [Edinger *et al.*, Nature Medicine 2003]. Recently, we described the preferential localization of the pro-inflammatory

CD161⁺Tregs in the bone marrow of Treg transplanted patients, where they can enhance the anti-leukemic activity of Tcons [Guardalupi *et al.*, Leukemia 2023]. This study aims to explore the potential in-vitro mechanisms of action of CD161⁺Tregs on Tcons.

Methods. Immunoselected Tregs were isolated from peripheral blood of healthy donors and cultured for 14 days using two different stimulation protocols to generate CD161⁺Tregs (TexMACSTM, 5% AB serum, IL-2, IL-6, TGF-B and TransActTM) and expanded Tregs (ExpTregs) as a control (TexMACSTM, 5% AB serum, IL-2, Rapamycin and TransActTM). After 14 days of culture, functional assays were made and flow cytometry analysis on CD161⁺Tregs/ExpTregs and Tcons co-cultures was performed. Lastly, cytokines profile of CD161⁺Tregs/ExpTregs after stimulation with PMA/Ionomycin and Monensin were evaluated.

Results. The suppression assay demonstrated that CD161⁺Tregs had a lower suppressive activity compared to ExpTregs (28.7%±2.1 vs 17.3%±3.8; p<0.0001) while cytotoxicity assay revealed increased Tcon-mediated tumor lysis in the presence of CD161⁺Tregs compared to ExpTregs (28.6±4.4 vs 15.7±2.5, p<0.05). Flow cytometry analysis revealed, when CD161⁺Tregs/Tcons and K562 co-culture were analyzed, a reduced inhibition of NOTCH-1 and Granzyme B (GZB) expression in Tcons compartment compared to ExpTregs (59.1±5.3 vs 38.5±4.3, 85.5±3.6 vs 68.9±6.2, p<0.05). However, CD161⁺Tregs expressed higher levels of CD39, Perforin, and GZB compared to ExpTregs (83.9%±4.1 vs 27.9%±4.0, 68.4%±9.2 vs 40.4%±7.6, 89.5%±4.9 vs 59.2%±12.4; p<0.05). Cytokines profile of CD161⁺Tregs displayed higher levels of IL-10, IL-35, IL-17A and IFN-γ compared to ExpTregs. Finally, the analysis of transcription factors reveals high levels of T-BET and RORγt in CD161⁺Tregs.

Conclusions. In this study, CD161⁺Tregs showed reduced suppression activity but permissive Tcon-mediated anti-leukemic effect. Infact, the cytokine profile of CD161⁺Tregs displayed a unique pattern with elevated levels of immunomodulatory cytokines (IL-10 and IL-35) as well as pro-inflammatory factors (IL-17A, IFN-γ, GZB, Perforin) with a Th1-17 hybrid phenotype. These results collectively suggest a distinct role of CD161⁺Tregs in balancing immune suppression while promoting a T-con mediated antileukemic effect that in the setting of Treg transplantation could enable GvHD prevention associated with a powerful GvL effect.

and 231) while the other one was already commercially validated (clone BER-H2). Results of such computational analysis were compared to conventional methods to investigate mAb binding affinity as surface plasmon resonance (SPR) and *in vitro* and *in vivo* CAR-T cell efficacy studies.

Methods. AlphaFold2, a deep learning-based method, predicted the 3D structure of both antibody clones and CD30 antigen. Molecular Dynamics simulations using Coarse Grained (CG) Sterred Molecular Dynamics (SMD) and Umbrella Sampling (US) identified the most stable complex and calculated the energy required to dissociate the antibody-antigen binding. All these data were compared to SPR analysis and conventional *in vitro* assays by means of cytotoxicity, cell proliferation and cytokine release co-culturing HL cell line HD-LM2 with CD30 CAR-T cells developed from each mAb clone. *In vivo* CAR-T cell activity was measured by tumor BLI signal after NSG mice s.c. injection of luciferase positive HD-LM2 HL cell line.

Results. Molecular docking from the AI-predicted 3D complex conformation indicated that clone 142 mAb requires the highest peak force and the maximum energy for CD30/mAb complex displacement, suggesting a higher affinity as compared to clones 231 and BER-H2 (Figure 1A). Binding association and dissociation rates determined by SPR confirmed *in silico* results (Figure 1B). Clone 142-derived CD30 CAR-T cells displayed an *in vitro* higher cytotoxic activity (E:T ratios 1:1 and 0,25:1) and 72h cell proliferation and main release of pro-inflammatory cytokines when co-cultured with HD-LM2 HL cell line, compared to CD30 CAR-T cells from 231 and BER-H2 scFv (Figure 1C). As a further confirm of high anti-tumor activity, clone 142-derived CD30 CAR-T cells eradicate HD-LM2 cells s.c. injected in NSG mice 2 weeks after CAR-T cell infusion and remains in remission even subsequent tumor rechallenge at day 65 (Figure 1D).

Conclusions. The proposed prediction analysis of AI-assisted molecular docking showed comparable results to SPR and conventional *in vitro* and *in vivo* CD30 CAR-T cell assays, highlighting the potential to streamline the scFv selection from mAbs and advance CAR constructs development, with a substantial impact on reducing time, costs and the need for laboratory animal use.

C62

ARTIFICIAL INTELLIGENCE-POWERED MOLECULAR DOCKING FOR PROPER SCFV SELECTION OF ANTI-CD30 CHIMERIC ANTIGEN RECEPTOR (CAR)

N. Martarelli¹, M. Capurro¹, G. Erol³, R. Vassoughi¹, R. Rossi¹, E. Longetti¹, A. Rosseto¹, R. Rossi¹, B. Bigerna¹, C. Argentati¹, C. Emiliani¹, S. Martino¹, M. Gentili¹, A. Stella¹, M. Gobbi³, E. Tiacci¹, B. Falini¹, F. Morena², V.M. Perriello¹

¹Institute of Hematology and Center for Hemato-Oncology Research; ²Department of Chemistry Biology and Biotechnologies, ³Mario Negri Institute of Pharmacological research, Italy

Introduction. The selection of monoclonal antibody (mAb)-derived single chain fragment variable (scFv) is a fundamental step for Chimeric Antigen Receptor (CAR) construction, to ensure accurate and effective CAR signaling towards tumor antigen binding. Conventional approaches to compare different scFv-derived CARs may be expensive and labor-intensive. In this study, innovative artificial intelligence (AI) tools were exploited to investigate molecular antigen-antibody interactions of 3 different anti-CD30 mAbs with the aim to predict the best scFv affinity for CD30 CAR-T cell development against Hodgkin's lymphoma (HL). Two of these anti-CD30 mAbs were newly generated at CREO, Perugia (called clones 142

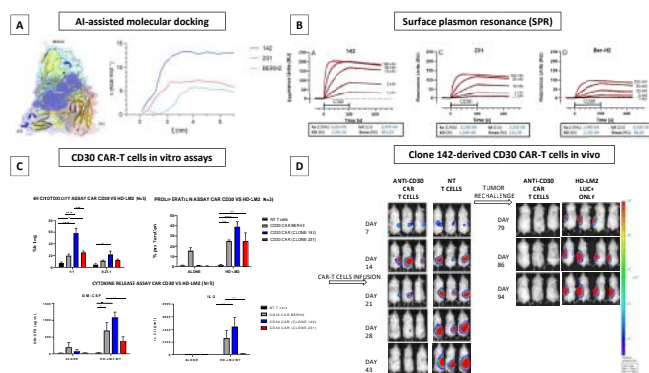


Figure 1.

C63

PROTEIN KINASE CK2 IS A KEY REGULATOR OF ERYTHROPOIESIS

L. Quotti Tubi^{1,2}, S. Canovas Nunes^{2,3}, E. Mandato^{2,4}, M. Pizzi⁵, N. Vitulo⁶, M. D'agnolo⁷, R. Colombatti⁷, M. Martella⁷, M.P. Boaro⁷, E. Doriguzzi Breatta^{1,2}, A. Fregnani^{1,2}, Z. Spinello^{1,2}, M. Nabergoj⁸, O. Filho⁹, B. Boldyreff¹⁰, M. Albiero^{11,12}, G.P. Fadini^{12,13}, C. Gurrieri^{1,2}, F. Vianello^{1,2}, G. Semenzato², S. Manni^{1,2}, L. Trentin¹, F. Piazza^{1,2}

¹Department of Medicine, Division of Hematology, University of Padova; ²Laboratory of Normal and Malignant Hematopoiesis and Pathobiology of Myeloma and Lymphoma. Veneto Institute of Molecular Medicine (VIMM); ³Current affiliation Division of Hematology/Oncology, Boston Children's Hospital; ⁴Current affiliation Department of Medical Oncology, Dana-Farber Cancer Institute; ⁵Department of Medicine, Cytopathology and Surgical Pathology Unit; ⁶Department of Biotechnology, University of Verona; ⁷Department of Women's and Child's Health, University of Padova; ⁸Hematology Service, Institut Central des Hôpitaux (ICH), Hôpital du Valais; ⁹Institut National de la Santé Et de la Recherche Médicale (INSERM) U1036, Institute de Reserches en Technologies et Sciences pour le Vivant/Biologie du Cancer et de l'Infection; ¹⁰Kinase Detect; ¹¹Department of Surgery, Oncology and Gastroenterology, University of Padova; ¹²Veneto Institute of Molecular Medicine, Experimental Diabetology Lab; ¹³Department of Medicine, University of Padova

Introduction. The Ser-Thr kinase CK2 is well-known for its involvement in hematologic malignancies since it sustains cell survival and proliferation. It usually acts as a tetramer composed of two catalytic (α) and two regulatory (β) subunits, however, the α and β subunits can also function independently. We have recently demonstrated the involvement of CK2 in B cell maturation, nevertheless, its role in the development of other hematopoietic cells is still undefined. To fill this gap, we have generated a conditional knockout (KO) mouse model for CK2 β in the whole hematopoietic system. Since CK2 β loss caused lethality at the embryonic level, the investigations were performed during gestation. We focused here on the erythroid development that was markedly depleted and altered upon CK2 β deletion.

Methods. Mice were generated through Cre/loxP system with the Cre recombinase under the control of Vav-1 promoter. G1E-ER cells (mouse proerythroblasts bearing a β -estradiol-inducible form of GATA1), were treated with β -estradiol with or without CK2 inhibitor CX-4945 or siRNA against CK2 β ; bortezomib or the caspase inhibitor ZVAD were added to determine GATA1 turnover. We used FACS to study erythroid differentiation, enucleation, cell cycle and viability. Deformability assay on fetal erythrocytes was performed through ektacytometer. Erythropoietin was quantified through ELISA. mRNA expression levels were evaluated by RNA sequencing and by RT-PCR. WB was performed to assess protein amounts; immunofluorescence to investigate GATA1, CK2 β and HSP70 cell localization and Proximity Ligation Assay to establish the interaction of these proteins.

Results. CK2 β loss caused a reduction of mature erythroid cells, that were morphologically altered, displayed a reduced deformability capacity and showed higher levels of apoptosis. Heterozygous mice were not anemic since they compensated with ectopic erythropoiesis in the spleen. At the molecular level, the more immature Ter119⁻ red cell population displayed a decrease of cKit expression and in the activation ERK and AKT downstream effectors. The Ter119⁺ mature counterpart showed a reduced activation of AKT and downregulation of STAT5 and GATA1 factors with impairment of their transcriptional activity. The nuclear distribution of GATA1 changed upon CK2 β silencing or CK2 inhibition. Treatment with Bortezomib or

ZVAD restored GATA1 levels. Since HSP70 binds to GATA1 protecting it from degradation and it is a phosphorylation target of CK2, we postulated a possible indirect role of CK2 in the control of GATA1 protein turnover. CK2 β silencing reduced HSP70 protein levels, while CK2 inhibition caused the disassembly of GATA1 from HSP70. Although CK2 did not physically interact with GATA1 and HSP70, it co-localized with them, thus CK2 seems important in regulating somehow HSP70-GATA1 binding likely not through HSP70 direct phosphorylation.

Conclusions. CK2 β is essential for erythroid maturation, regulating cKIT, STAT5 and GATA1.

C64

RANKL CYTOKINE IN THE BONE MARROW HEMATOPOIETIC NICHE - A NOVEL SUPPORTIVE SIGNAL

L. Crisafulli^{1,2}, M.L. Schiavone¹, D. Strina^{1,2}, F.S. Colombo^{1,3}, G. De Simone¹, C. Sobacchi^{1,2}, F. Ficara^{1,2}

¹IRCCS Humanitas Research Hospital; ²Milan Unit, CNR-Istituto di Ricerca Genetica e Biomedica; ³Presente Fondazione IRCCS Ca' Granda Ospedale Maggiore Policlinico, Italy

Introduction. RANKL (Receptor activator of nuclear factor kappa-B ligand) is a pleiotropic cytokine belonging to the tumor necrosis factor superfamily involved in the regulation of skeletal homeostasis, immune system, reproductive system, and mammary gland function. In the bone, it is the essential pro-osteoclastogenic signal. However, recent studies have proposed a novel pro-osteogenic and pro-clonogenic role of RANKL in bone marrow (BM) mesenchymal stromal cells (MSC). Since MSC are crucial components of the hematopoietic stem cell (HSC) niche, we asked whether RANKL is also involved in their HSC supporting ability. This is clinically relevant since RANKL inhibitors have been developed for the treatment of common pathological conditions with excessive bone loss like osteoporosis or metastatic breast cancer.

Methods. To assess the role of RANKL in the HSC niche, we took advantage of the RANKL knockout (KO) murine model. We performed a phenotypic and functional characterization of RANKL KO HSC and progenitors, including FACS analysis, gene expression, *in vitro* culture, and *in vivo* transplantation assays.

Results. The proportion of LKS cells, which include both stem and progenitor cells, is higher in the BM of RANKL KO mice compared to WT. A detailed analysis of HSC and of the multi-potent progenitor (MPP) fractions within LKS shows an expansion of the MPP1 myeloid-prone fraction at the expenses of HSC and of lymphoid-prone MPP3. Short-term liquid culture of purified HSC reveals a premature loss of stem cell markers, associated with a more rapid myeloid differentiation and proliferation. On the other hand, RANKL KO BM displays a reduced proportion of common lymphoid progenitors (CLP), which are less clonogenic; accordingly, RANKL KO MPP3 have reduced ability to differentiate into CD19⁺ cells compared to WT. Gene expression studies confirm a defect in lineage priming that starts at the HSC developmental stage. We then performed BM long-term reconstitution assays in WT recipients by transplanting RANKL KO BM cells in competition with WT BM. Chimerism, multilineage reconstitution, CLP and HSC maintenance were similar in WT or RANKL KO donor cells, suggesting that the hematopoietic defects observed in the RANKL KO mice are not cell autonomous. Moreover, the hematopoietic defects are peculiar to the BM, since they are not present in the spleen nor in the fetal liver. MSC and HSC co-culture experiments are ongoing to further demonstrate that the impaired lineage skewing of RANKL KO stem and progenitor cells is driven by lack of support from RANKL KO stromal cells.

Conclusions. RANKL expression within the BM microenvironment is crucial to maintain the MSC HSC-supporting ability. Due to the chronic nature of osteoporosis and the ever-increasing aging of the population, already prone to clonal hematopoiesis and BM microenvironment alterations, the consequences of prolonged inhibition of RANKL signaling must be studied.

Chronic Lymphoproliferative Disorders

C65

THE GENE EXPRESSION PROFILE HELPS TO UNDERSTAND THE NEGATIVE PROGNOSIS OF PATIENTS WITH CHRONIC LYMPHOCYTIC LEUKEMIA CARRYING T(14;19) AND TO SELECT THE BEST TREATMENT. AN ITALIAN CAMPUS CLL AND ERIC STUDY

A. Visentin¹⁺, E. Gaffo²⁺, M. Furstenau³⁺, J.A. Woyach⁴⁺, P. Baliakas⁵, K.A. Rogers⁴, C. Miller⁴, C. Haferlach⁶, K. Plevova⁷, D. Oscier⁸, Z. Davis⁸, F. Nguyen-khac⁹, E. Roncaglia², G.M. Rigolin¹⁰, A. Athanasiadou¹¹, F. Baran-marszak¹², A. Valiente¹³, M.J. Terol¹⁴, P. Abrisqueta¹⁵, B. Espinet¹⁶, A. Puiggros¹⁶, A. Martines¹⁷, L. Bonaldi¹⁷, F.R. Mauro¹⁸, L. Scarfò^{19,20}, T. Chatzikonstantinou²⁰, E. Tausch²¹, K.A. Kreuzer³, A. Kater²³, F. Bosch¹⁵, M. Doubek⁷, P. Panagiotidis²⁴, O. Kalashnikova²⁵, F. Frezzato¹, M. Facco¹, V. Ruocco¹, A. Buratin², S. Orsi², A. Cellini¹, F. Angotzi¹, C.A. Cavarretta¹, I. Zatta¹, A. Serafin¹, R. Foà¹⁸, B. Eichhorst³, A. Cuneo^{10°}, K. Stamatopoulos^{21°}, P. Ghia^{19,20°}, S. Bortoluzzi^{2°}, L. Trentin^{1°}

¹Hematology Unit, Department of Medicine, University of Padua; ²Computational Genomics Group, Department of Molecular Medicine, University of Padua; ³Department I of Internal Medicine, University of Cologne; ⁴The Ohio State University Comprehensive Cancer Center; ⁵Department of Immunology, Genetics and Pathology, Science for Life Laboratory, Uppsala University; ⁶MLL Munich Leukemia Laboratory; ⁷Department of Internal Medicine, Hematology and Oncology, University Hospital Brno and Faculty of Medicine, Masaryk University-University Hospital Brno; ⁸Molecular Pathology, University Hospitals Dorset, Royal Bournemouth Hospital; ⁹Hôpital Pitié-Salpêtrière, Service d'Hématologie Biologique; ¹⁰Hematology Section, Department of Medical Sciences, Azienda Ospedaliera-Universitaria, Arcispedale S. Anna, University of Ferrara; ¹¹Hematology Department and HCT Unit, G. Papanicolaou Hospital; ¹²Laboratoire d'hématologie, Hopital Avicenne, Assistance Publique-Hôpitaux de Paris; ¹³Servicio de Genética, Hospital Universitario de Navarra; ¹⁴Servicio de Hematología y Oncología Médica, Hospital Clínico Universitario de Valencia; ¹⁵Department of Hematology, Vall d'Hebron Institute of Oncology (VHIO), Hospital Universitari Vall d'Hebron; ¹⁶Laboratori de Citogenètica Molecular, Servei de Patologia, Hospital del Mar; ¹⁷Immunology and Molecular Oncology Unit, Veneto Institute of Oncology IOV-IRCCS; ¹⁸Department of Translational and Precision Medicine, Hematology unit, 'Sapienza' University; ¹⁹Università Vita-Salute San Raffaele; ²⁰Division of Experimental Oncology, IRCCS Ospedale San Raffaele; ²¹Institute of Applied Biosciences, Center for Research and Technology Hellas; ²²Ulm University; ²³Department of Hematology, Cancer Center Amsterdam and Lymphoma and Myeloma Center Amsterdam, The Netherlands; ²⁴First Department of Propedeutics, University of Athens; ²⁵Federal State Budgetary Educational Institution of Higher Education Academician I. P. Pavlov First St. Petersburg State Medical University of the Ministry of Healthcare of Russian Federation; ⁺these authors equally contributed as first authors. [°] these authors equally share the senior authorship.

Introduction. Previous studies reported that t(14;19)(q32;q13), which involves IGH:BCL3, can be identified in almost 1% of chronic lymphocytic leukemias (CLL) and associates with an adverse outcome. We aimed at better understanding the clinical-molecular features of CLL with t(14;19).

Methods. CLL with the t(14;19) were collected from the Italian Campus CLL, European Research Initiative on CLL (ERIC), German

CLL study group (GCLLSG) and Ohio State University, and compared to 520 CLL without t(14;19). For RNA sequencing (RNA-seq), RNA was extracted from 106 purified cells from 25 t(14;19) CLL patients, 22 CLL with normal karyotype/FISH or trisomy 12 (+12), and B cells from 9 healthy volunteers and sequenced by Illumina (120x10⁶ reads/sample). After analysis with CirCompara2, differential expression was assessed with DESeq2 and GSEA was used for pathway enrichment analysis. Treatment-free survival (TFS), time to next treatment (TTNT) and overall survival (OS) were analyzed.

Results. We identified 88 CLL patients with t(14;19), 52% were males, 32% were <50y old at diagnosis, 93% (68/73) had an unmutated IGHV status [U-IGHV, including 25% (9/35) stereotyped subset #8], 60% carried +12, 52% a complex karyotype (CK, 54% ≥3 rearrangements, 19% ≥5), 39% an atypical phenotype and 15% TP53 abnormalities. Compared to patients without t(14;19), they were younger and enriched for U-IGHV, subset #8, +12 and CK (p<0.01). By RNA-seq, we found 708 upregulated and 1,230 downregulated genes between CLL with and without t(14;19). BCL3, CD79b (confirming their atypical phenotype) and disruption of immune checkpoint genes (LAG3, TIGIT and PD-L1) appeared among the most deregulated. In addition, t(14;19) CLL was characterized by higher levels of BTK and a downregulation of BCL2L11 (coding for the pro-apoptotic protein BIM). By GSEA we found the downregulation of several pathway including immune processes, chemotaxis and cytokine signaling in t(14;19) CLL. After a median follow-up of 7.6 years, the median TFS and OS were 2yy vs 7yy and 12.6yy vs not reached for patients with and without t(14;19), respectively (p<0.0001). Regarding the first-line therapy of t(14;19) patients, 28 received FCR/BR, 6 VEN (5 within the GAIA/CLL13 trial), 12 BTKi, and 34 other treatments (OTs). At 3-years 59%, 67%, 100% and 35% of patients treated with FCR/BR, VEN, BTKi and OTs did not require further therapy. Indeed, t(14;19) had a negative impact on the TTNT after FCR/BR chemoimmunotherapy (HR 2.19, p=0.0029), venetoclax-based therapy (VEN) (HR 20.5, p=0.0316), but not after BTKi (HR 1.23, p=0.6857). A trend for a longer TTNT was also observed in the relapse setting with BTKi (29 BTKi, 11 VEN, 32 others, 3-yy TTNT 64% vs 16% vs 44%, p=0.05).

Conclusions. We report that patients with t(14;19) are young, enriched for +12, CK, U-IGHV, and BCR subset #8, and have a distinct gene expression profile. While acknowledging the limitations of a retrospective analysis, BTKi appeared to be more effective in this aggressive CLL subgroup.

C66

MUTATION STATUS OF KAPPA AND LAMBDA LIGHT CHAIN GENES INDEPENDENTLY PREDICTS TIME TO FIRST TREATMENT IN EARLY-STAGE CHRONIC LYMPHOCYTIC LEUKEMIA

J. Nabki*, B. Al Deeban*, A. Mehari Sium*, M. Bellia, R. Dondolin, D. Talotta, M. Almasri, C. Cosentino, S. Mouhssine, E. Secomandi, S. Kogila, J. Ghanej, S. Rasi, R. Moia, F. Gaidano

*Division of Hematology, Department of Translational Medicine, Università del Piemonte Orientale. *Equally contributed*

Introduction. The mutation status of the immunoglobulin heavy chain variable region genes (IGHV) represents a pivotal prognostic marker in chronic lymphocytic leukemia (CLL). Conversely, the clinical impact of the mutation status of light chain genes has not been extensively investigated in CLL. Here we aimed at investigating the repertoire and the prognostic role of light chain genes in CLL.

Methods. Tumor genomic DNA was extracted from peripheral blood mononuclear cells of 567 CLL patients prospectively followed at our institution. Light chain rearrangements were identified using

Sanger sequencing. The primary endpoint was time to first treatment (TTFT) in Binet A CLL.

Results. The median age of CLL patients was 70 years, 58.1% were male, the median lymphocyte count was 10000/μl, 46.9% had del13q, 11.9% had TP53 aberrations, and 38.5% had unmutated (UM)-IGHV. Kappa light chain was expressed in 324 (66.1%) patients and lambda light chain in 166 (33.8%). The median follow-up of the studied cohort was 11.6 years. Among the 567 CLL patients, 490 cases were successfully sequenced and a total of 529 productive rearrangements were identified. For kappa chains, the most frequently rearranged gene was IGKV4-1 in 21.27% of patients followed by IGKV3-20 in 14.92% and IGKV1-39 in 11.05%. For lambda chains, the most frequently rearranged gene was IGLV3-21 in 17.96% followed by IGLV2-14 in 16.17% and IGLV3-25 in 7.19% (Figure 1A). As expected, UM-IGHV (using the standard 98% cut-off of homology) was associated with poorer survival (HR=1.85, 95% CI 1.42-2.40, p<0.001) and shorter TTFT (HR=3.22, 95% CI 2.45-4.22, p<0.001) compared to mutated IGHV. Since no validated cut-off has been established for light chain genes, the maxstat statistics was used to identify the best cut-off that predicts TTFT in Binet A CLL (N=381). For kappa chain genes, the best cut-off was 99.28% and for lambda chain genes, it was 98.57%. Using the new cut-offs, UM-kappa patients presented a worse TTFT with a 10-year TTFT of 44.9% compared to 74.9% for mutated patients (p<0.0001) (Figure 1B). Similarly, also UM-lambda patients presented a 10-year TTFT of 28.8% compared to 81.4% for mutated cases (p<0.0001)(Figure 1C). Importantly, in kappa expressing CLL, both UM-kappa (HR=1.90, 95% CI 1.16-3.09, p=0.01) and UM-IGHV (HR=2.14, 95% CI 1.30-3.50, p=0.003) maintained an independent TTFT association (Figure 1D). Remarkably, in lambda expressing CLL, the independent prognostic value of UM-IGHV was lost (HR=1.28, 95% CI 0.60-2.77, p=0.522), while UM-lambda independently associated with shorter TTFT (HR=4.06, 95% CI 1.85-8.93, p<0.001)(Figure 1E).

Conclusions. The light chain genes analysis in this real-life cohort of CLL patients referring at our institution suggests that light chain genes analysis improves TTFT prediction compared to IGHV alone in early-stage CLL. Further analyses are ongoing to evaluate the impact of kappa and lambda mutation status on response to therapy and Richter transformation.

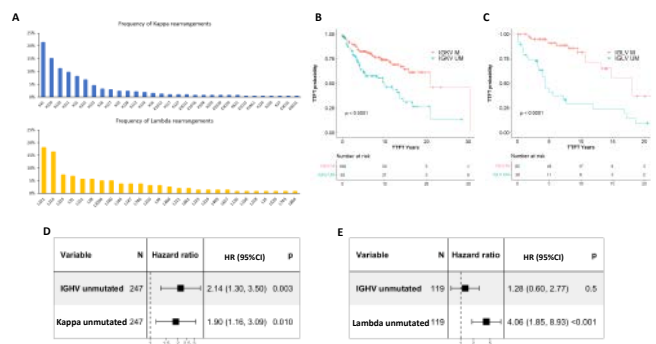


Figure 1.

C67

EXPLORING THE POTENTIAL OF HIGH-THROUGHPUT SCREENING AND DRUG REPURPOSING FOR NOVEL THERAPEUTIC APPLICATIONS IN CHRONIC LYMPHOCYTIC LEUKEMIA. INSIGHTS INTO NOTCH1 SIGNALING

E. Dorillo¹, C. Rompietti¹, E.C. Silva Barcelos¹, F. De Falco¹, F.M. Adamo¹, D. Sorcini¹, A. Stella¹, B. Del Papa¹, S. Baldoni¹, A. Esposito¹, C. Geraci¹, R. Arcaleni¹, L. Moretti¹, M.G. Mameli¹, E. Rosati², G. Roti³, P. Sportoletti¹

¹Department of Medicine and Surgery, Institute of Hematology and Center for Hemato-Oncology Research (CREO), University of Perugia; ²Department of Medicine and Surgery University of Perugia; ³Department of Medicine and Surgery, University of Parma, Italy

Introduction. Targeted therapies have revolutionized Chronic Lymphocytic Leukemia (CLL) treatment. However, drug resistance and toxicity remain challenges in this disease. Addressing molecular heterogeneity through pathway-centered approaches still represents an opportunity for a tailored therapy in CLL. NOTCH1 has gained growing attention in CLL after the identification of deregulated pathway and high-risk mutations, to which we provided a pivotal contribution. Here, we explored the potential of a gene expression based high-throughput screening (GE-HTS) approach and drug repurposing for therapeutic uses targeting the NOTCH1 pathway.

Methods. HST was performed on the PGA1 CLL cell line using two compound libraries: MicroSource Spectrum FDA approved (2000 compounds) and Selleck Anticancer Library (349 compounds). Cells were treated with 1 μ M drugs for 72 hours. Viability was assessed using the CellTiter-Glo[®] Luminescent Assay. The NanoString nCounter Elements protocol was used to custom a NOTCH1 signature. Compounds inducing a NOTCH1-off signature were identified using a weighted summed score that weights each gene based on the signal-to-noise ratio determined from the Notch “On” positive and Notch “off” negative controls. Validation was done on PGA1 and primary CLL assessing cell viability, NOTCH1 activity and targets. *In vivo* studies were conducted with C57BL/6 mice transplanted with frozen splenocytes from E μ -TCL.

Results. After conducting an HTS assay in the PGA-1 cell line, we identified 262 molecules that met the criteria CellTiter-Glo percentage over control <50% (CTG. poc). From these, 68 compounds were selected for Nanostring analysis. The subsequent Nanostring assay on treated PGA1 cells aimed to assess whether the chosen compounds modulate the NOTCH1 signature. By establishing a threshold based on the gene expression profile of GSI treated cells, we performed a weighted summed score analysis, which revealed five potential NOTCH1 inhibitors: TW-37, obatoclax mesylate, geldanamycin, axitinib, and elesclomol. In PGA-1 cells and primary CLL cells, elesclomol, TW-37 and geldanamycin significantly reduced viability after 72hr. Geldanamycin significantly decreased the levels of both NICD and transmembrane/intracellular region (NTM), while elesclomol reduced the expression of the NTM only. Elesclomol and geldanamycin treatments significantly downregulated *HES1*, *C-MYC* and *DTX1* mRNA levels. *In vivo* studies showed that the number of splenic CD19+/CD5+ cells was decreased in mice treated with elesclomol and geldanamycin compared to the vehicle. WB analysis, performed in CD19+/CD5+ cells of the spleen from elesclomol-treated mice showed a reduction in NICD levels compared with vehicle.

Conclusions. Our study successfully integrated GE-HTS and drug repurposing to identify geldanamycin and elesclomol as anti-CLL drugs targeting NOTCH1. These findings advance the development of targeted therapies for resistant or intolerant CLL.

C68

T-CELL PROLYMPHOCYTIC LEUKEMIA TRANSCRIPTOME ABERRANCIES AND GENOTYPE/PHENOTYPE LINKS DISCLOSED BY A MULTI-OMICS APPROACH

S. Orsi^{1,2§}, V.R. Gasparini^{3,4§}, A. Buratin^{1§}, E. Rampazzo^{3,4}, G. Calabretto^{3,4}, A. Teramo^{3,4}, E. Gaffo¹, M. Facco^{3,4}, L. Trentin⁴, G. Semenzato^{3,4}, R. Zambello^{3,4*}, S. Bortoluzzi^{1*}

¹Department of Molecular Medicine, University of Padova; ²Department of Biology, University of Padova; ³Veneto Institute of Molecular Medicine (VIMM); ⁴Department of Medicine, Hematology and Clinical Immunology Branch, University of Padova; [§]these authors equally contributed as first authors; ^{*}these authors equally share the senior authorship.

Introduction. T-cell prolymphocytic leukemia (T-PLL) is a fast-growing chemoresistant cancer that primarily affects older individuals. It is associated with excessive lymphocytosis, splenomegaly, B symptoms, and lymphadenopathy. Leukemic cells, mostly CD4+, in T-PLL display complex chromosomal aberrations, particularly on chromosomes 14 and 8, along with gene mutations mainly related to the JAK/STAT pathway. The transcriptomic profiling of T-PLL, including long non-coding (lncRNAs) and circular RNAs (circRNAs), remain poorly understood due to limited and scattered data.

Methods. Peripheral blood mononuclear cells (PBMC) of 10 T-PLL patients from Padua University Hospital's Hematology Unit, and purified CD4+ of 5 healthy controls were collected and underwent Ribodepleted Illumina RNA-seq. Expressed Single Nucleotide Variants (SNVs) have been detected using a custom made pipeline based on the gold standard procedure of Genome Analysis Toolkit v4.2.4 for variant calling from RNA-seq data. The expression profile of both linear and circular RNAs has been extracted using CirComPara2 tool and normalized using edgeR.

Results. The genomic analysis of our T-PLL cohort identified SNVs and small InDels in well-established driver genes like KMT2C, STAT5B, JAK3, and ATM, and in novel genes. Driver gene variants showed either mutually exclusive patterns or, when coexistent, displayed alternating clonal or subclonal behavior. Notably, we observed the activation of cancer-related pathways, such as the Wnt signaling pathway and an overexpression of genes involved in cell cycle regulation and anti-apoptotic mechanisms. Conversely, essential pathways for healthy T-cell function were suppressed. Of novelty, we disclosed non coding RNAs with expression altered in T-PLL and circRNAome aberrancies in this malignancy. Oncogenic lncRNAs like XIST, FIRRE, and TERC overexpressed in T-PLL could contribute to the malignant cell phenotype. CircKMT2C and circHAT1 were too abundantly expressed in T-PLL, whereas circSIRT5 was markedly downregulated. Further, we used a multi-omics approach to characterize the impact of key lesions on gene expression and pathway activation in T-PLL. Leveraging Machine Learning techniques we disclosed strong correlations between genetic lesions and gene expression profiles. A deeper investigation involving the lesions recurrent in the cohort, unmasks the peculiar transcriptome and pathways activation readout of each lesion, revealing similarities and differences between T-PLL with distinct genetic makeup.

Conclusions. We provided new transcriptomic data about genes, lncRNAs and circRNAs altered in T-PLL. Motivated by the aggressive nature of T-PLL and the complex molecular landscape of malignant cells with several concurrent lesions, multi-level data integration is revealing the impact of different lesions on malignant cell phenotype in a personalized medicine perspective.

IRF4 CONTROLS CELL POSITIONING INSIDE PROLIFERATION CENTER BY REGULATING CXCR4 AND CXCR5 IN CHRONIC LYMPHOCTIC LEUKEMIA

R. Maffei¹, C.G. Atene², N. Mesini², S. Martinelli¹, B. Conte¹, G. Debbia², F. Pilato¹, F. Giacobbi¹, G. Corradini¹, A. Paolini¹, D. Bernabei¹, G. Riva¹, V. Nasillo¹, F. Forghieri², A. Candoni², M. Morselli², L. Potenza², D. Giusti², E. Colaci², F. Bettelli², P. Bresciani², A. Cuoghi², A. Gilioli², A. Messerotti², V. Pioli², M. Maccaferri², G. Leonardi², M. Luppi², T. Trenti¹, E. Tagliafico¹, R. Marasca²

¹Department of Laboratory Medicine and Pathology, Diagnostic Hematology and Clinical Genomics, Azienda Ospedaliero-Universitaria, Policlinico; ²Hematology Unit, Department of Medical and Surgical Sciences, University of Modena and Reggio Emilia, Azienda Ospedaliero-Universitaria, Policlinico, Italy

Introduction. The germinal center (GC) is the functional district devoted to production of high-affinity antibodies during adaptive immune response and is composed of a “dark zone” of proliferative centroblasts and a “light zone” of small resting centrocytes. Chemokine gradients discriminate these two B cell compartments, being CXCR4/CXCL12 signal needed for positioning B cells into the dark zone of GC whereas the CXCR5/CXCL13 pair controls the transit of rapidly dividing centroblasts to nondividing centrocytes in light zone. IRF4 is expressed at low levels inside the proliferative compartment of centroblasts but increased in CXCR4-negative centrocytes inside light zone. Chronic lymphocytic leukemia (CLL) is characterized by the clonal expansion of CD5+CD19+ malignant B cells, that are located within specific structures in lymph nodes, resembling proliferation centers, otherwise known as pseudofollicles. Signals that restrain leukemic cells inside the proliferative structures blocking the physiological trajectory of neoplastic B cells towards the natural terminal fate are relevant for CLL progression. In the present study, we investigate the ability of IRF4 to regulate chemotactic properties of CLL cells, pointing our attention on CXCR4 and CXCR5 signaling.

Methods. CLL cells were transfected using IRF4 plasmid vector in a Nucleofector instrument. CXCR4 levels on the surface of CLL cells were inspected by flow cytometry in CD5+CD19+ alive cells. Migration assay was performed by using Transwell. Akt activation was inspected by western blot.

Results. Transfecting cells with IRF4 plasmid vector, we observed a reduction of CXCR4 expression from 82.6% to 58.6% (p=0.002). Accordingly, the up-regulation of IRF4 in CLL, lowering the percentage of CXCR4-expressing cells, reduced the migration of leukemic cells towards CXCL12 cytokine (p<0.05). Moreover, BCR stimulation in CLL cells promotes IRF4 up-regulation while reducing CXCR4 expression. In CLL cells transfected with IRF4 vector, we detected an inhibition of Akt activation upon CXCL12 stimulation (p<0.05). The vitamin A metabolite ATRA increases IRF4 expression in normal human B cells, thus promoting plasma cell differentiation. We treated CLL cells with ATRA for 48 hours, inducing IRF4 expression. CLL cells up-regulated CD38 at 24h and 48h, particularly when BCR activation was concomitantly induced with anti-IgM (p<0.05). No differences in CLL survival were detected upon ATRA treatment. Furthermore, CLL cells treated with ATRA increased the expression of CXCR5, while reducing CXCR4.

Conclusions. Our data implies that low IRF4 levels observed in CLL cells contribute to maintain a CXCR4^{high}/CXCR5^{low} profile promoting leukemic cell compartmentalization inside proliferative centers and restraining cells in an activated phenotype. Increasing IRF4 expression by treating cells with retinoic acid allows the down-regulation of CXCR4 with a concomitant induction of CXCR5, implying a role of IRF4 in CLL trafficking.

IDENTIFICATION OF A PLASMA EXTRACELLULAR VESICLE SIGNATURE RELATED TO DISEASE AGGRESSIVENESS IN HAIRY CELL LEUKEMIA

F. Maltoni¹, G. Narimanfar¹, P. Coppola¹, D. Forte¹, F. Caicci², L. Argani¹, A. Broccoli^{1,3}, P.L. Zinzani^{1,3}, L. Catani^{1,3}

¹Institute of Hematology “L. e A. Seràgnoli”, Department of Medical and Surgical Sciences, University of Bologna; ²Department of Biology, University of Padova; ³IRCCS Azienda Ospedaliero-Universitaria di Bologna, Italy

Introduction. Classic Hairy Cell Leukemia (cHCL) is a rare indolent but still incurable clonal B-cell malignancy. cHCL patients present bone marrow (BM) fibrosis, splenomegaly, pancytopenia, and defective immunity. Clinical features are frequent relapses and susceptibility to infections. No disease-specific biomarkers have yet penetrated clinical practice to guide treatment strategy selection and patient stratification. Along with *BRAFV600E* mutation, cHCL is characterized by infiltration of hairy cells (HCs; with hairy projections) within BM, liver and spleen. A strong dependence of HCs on the tumor microenvironment (TME) has been described. Extracellular vesicles (EVs) are small particles involved in intercellular communication that, based on size and biogenesis, can be divided into Small (S-; 30-200 nm) and Large (L-; 0.2-10 μm) EVs. Thanks to their cargo of nucleic acids, proteins and lipids, EVs are recognized as key players of the TME. However, their role in cHCL has never been explored.

Methods. EVs were isolated from platelet-free plasma of cHCL patients (n=7) at diagnosis and healthy donors (HD; n=7) by differential ultracentrifugation (20.000g for L-EVs and 100.000g for S-EVs). EV size, concentration and morphology were analyzed through tunable resistive pulse sensing (TRPS) analysis and transmission electron microscopy (TEM). Thirtyseven surface EV antigens were characterized by high dimensional flow cytometry.

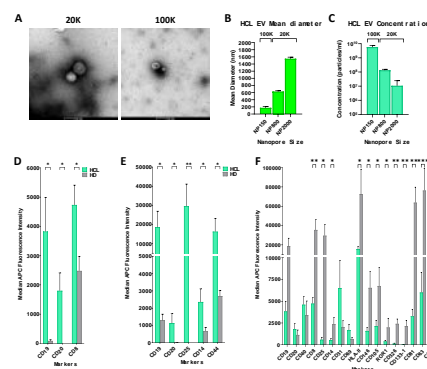


Figure 1. Transmission Electron Microscopy images of 20K L-EVs and 100K S-EVs isolated from plasma of HCL patients. **Figure B and C.** Tunable Resistive Pulse Sensing (TRPS) analysis (by EXO200 instrument) of 20K L-EVs and 100K S-EVs from plasma of HCL patients using NP150, NP800 and NP200 membrane pores. Histograms show particles mean diameter (B) and concentration (C). **Figure D, E and F.** MACSPlex analysis of EVs isolated from HCL and HD plasma samples. The histograms show the comparison of the expression of most relevant EV surface proteins between HCL and HD L-EVs (D), HCL and HD S-EVs (E), and HCL L- and S-EVs (F).

Figure 1.

Results. TRPS analysis and TEM confirmed the isolation of both S- and L-EVs. The morphology, size and concentration of cHCL EVs were superimposable to HD EVs. Comparing cHCL and HD EVs, both HCL S- and L-EVs overexpress the B cell markers CD19 and CD20. Moreover, while L-EVs were CD8-enriched, S-EVs were enriched in CD25, a well-known HC-associated marker, CD14, a key molecule in the activation of innate immunity, and CD44, an adhesion-related molecule. Of note, CD44 is expressed on HCs and, as a receptor for hyaluronan, has been described to be involved in the mechanisms contributing to cHCL-associated fibrosis. Comparing cHCL S- and L-EVs, the former resulted enriched in immune markers (CD8, CD14, CD25, HLA-II), cancer/stem cell markers

(ROR1, CD326 and CD133-1), EV markers (CD9, CD63 and CD81) and endothelial markers (CD105 and CD146), while the latter resulted slightly enriched in immune markers CD20, CD40, CD31, CD69. Interestingly, the expression of CD14, CD63, CD9 and CD29 on HCL S-EVs positively correlated with the absolute number of white blood cells, lymphocytes and monocytes.

Conclusions. Here we report for the first time that circulating EVs from cHCL patients display a tumor-related signature associated to disease biology and aggressiveness according to cytopenia. Moreover, the EV-based liquid biopsy provides pathogenesis-related and clinically-relevant information on cHCL TME which can be exploited as disease biomarker for diagnostic and prognostic purposes.

C71

THE RS 1001179 SNP WITHIN CATALASE PROMOTER IDENTIFIES AN AGGRESSIVE CLINICAL BEHAVIOR IN CHRONIC LYMPHOCYTIC LEUKEMIA

M. Galasso¹, V. Mozzo², E. Lovato³, S. Gambino³, O. Lovato⁴, F.M. Quaglia⁵, M. Krampera³, I. Ferrarini³, O. Perbellini^{6,7}, C. Visco³, M.T. Scupoli^{1,4}

¹Department of Neurosciences, Biomedicine and Movement Sciences, University of Verona; ²Veneto Institute of Oncology IOV - IRCCS; ³Department of Engineering for Innovation Medicine, Section of Hematology, University of Verona; ⁴Research Center LURM, Interdepartmental Laboratory of Medical Research, University of Verona; ⁵Department of Medicine, Section of Hematology, Azienda Ospedaliera Universitaria Integrata Verona; ⁶UOC di Ematologia - Azienda ULSS - Berica; ⁷UOSD Diagnostica Genetica e Genomica - Azienda ULSS - Berica, Italy

Chronic lymphocytic leukemia (CLL) is an incurable disease characterized by a highly variable clinical course, with some patients having indolent disease and others experiencing a more accelerated course, treatment resistance and a dismal outcome. We have recently identified low catalase (CAT) expression as a major antioxidant element that identifies an indolent clinical behavior in CLL. In contrast, high CAT expression is associated with a more aggressive disease course. Moreover, we have shown that CLL cells harboring the rs1001179 single nucleotide polymorphism (SNP) T allele in the CAT promoter exhibit a significantly higher CAT expression compared with cells bearing the CC genotype.

The objective of this study was to investigate the prognostic significance of the CAT rs1001179 SNP in CLL. We studied 235 patients with CLL and 123 healthy donors (HDs). Genotyping was assessed by restriction fragment length polymorphism (RFLP)-PCR. Time to first treatment (TTFT) curves were estimated using the Kaplan-Meier method and compared using the log-rank test.

The distribution of genotypes was consistent with the Hardy-Weinberg equilibrium among CLL patients and HDs ($\chi^2=0.156$, $P>0.05$; $\chi^2=0.099$, $P>0.05$; respectively), and no significant differences in genotype frequencies was found. The mutant homozygous TT genotype identified a subgroup of CLL patients with a more aggressive disease and a shorter TTFT whereas the CC and CT genotypes were associated with an indolent disease course (CC/CT vs TT $P=0.0096$). Furthermore, TT genotype refines risk stratification in patients with indolent disease, defined by low ZAP70 expression (CC/CT vs TT $P<0.0001$), favorable/neutral cytogenetics (CC/CT vs TT $P=0.0004$) and Binet A stage (CC/CT vs TT $P=0.0383$). Consistently, we have documented that patients bearing the TT genotype were characterized by a higher % of lymphocytes; a lower count of red blood cells, hemoglobin, and platelets at diagnosis compared with patients bearing the CC/CT genotype. Remarkably, the TT genotype identified a subgroup of CLL patients with a faster clinical progression within

early-stage disease subgroups of patients characterized by lower CD38 expression and wild-type p53 (CC/CT vs TT $P=0.0514$; CC/CT vs TT $P=0.0560$; respectively). Moreover, in bivariate analysis the TT genotype combined with age at diagnosis, Binet stage B/C risk, ZAP70 positivity, unmutated IGHV, mutated TP53, unfavorable cytogenetic predicted shorter TTFT.

This study shows for the first time that the TT genotype of CAT rs1001179 SNP identifies CLL patients with a poor prognosis and provides prognostic information on disease progression in patients with early-stage disease.

C72

CIRCULAR AND LONG NON-CODING RNAs AS POTENTIAL BIOMARKERS AND THERAPEUTIC TARGETS FOR T-LGL LEUKEMIA

A. Teramo^{1,2}, G. Calabretto^{1,2}, C. Vicenzetto³, B. Mariotti⁴, A. Buratin^{5,6}, V.R. Gasparini^{1,2}, E. Rampazzo^{1,2}, G. Barilà^{1,2*}, E. Roncaglia⁵, E. Gaffo⁵, E. Buson^{1,2}, M. Facco¹, L. Trentin¹, G. Semenzato^{1,2}, F. Bazzoni⁴, R. Zambello^{1,2°}, S. Bortoluzzi^{5°}

¹Department of Medicine, Hematology and Clinical Immunology Unit, University of Padova; ²Veneto Institute of Molecular Medicine (VIMM); ³Cardiology, Department of Cardiac Thoracic Vascular Sciences and Public Health, University of Padova; ⁴Department of Medicine, Division of General Pathology, University of Verona; ⁵Department of Molecular Medicine, University of Padova; ⁶Department of Biology, University of Padova; * Present affiliation Hematology Unit, Vicenza Hospital; °Co-last Authors

Introduction. T large granular lymphocyte leukemia (T-LGL) is a rare lymphoproliferative disease with cytopenias, particularly neutropenia, mostly impacting patients' quality of life and survival. Neutropenic patients often exhibit activating mutations in transcription factor STAT3, while those with an indolent clinical course have wild-type STAT3 gene, occasionally carrying mutations in STAT5B gene. T-LGL pathogenesis remains incompletely understood and a curative therapy is yet to be discovered. Therefore, understanding the underlying causes of this disease is essential for developing novel and effective treatments. Despite the increasing interest in circular RNAs (circRNAs) and long non-coding RNAs (lncRNAs) for their involvement in cancer development, no data are currently available on their role in T-LGL.

Methods. Twenty T-LGL cases, including both neutropenic and not neutropenic cases, were recruited for RNA sequencing (RNA-seq), together with 5 healthy donors (HD). Total RNA from purified LGLs was sequenced using a HiSeq3000 high-throughput seq system (Illumina). CircRNAs and lncRNAs were identified and quantified by CirComPara2. Differential expression was assessed by DESeq2 and edgeR. RT-qPCR and Sanger sequencing were performed from an independent validation cohort of 20 patients and 6 HD to confirm RNA-seq results PVT1 expression modulation was evaluated after patients' cell culture treated with Stattic 5 μ M for 6h.

Results. Principal component analysis of the RNA-seq expression profiles showed a distinct separation between T-LGL patients and HD. Neutropenic patients also significantly differed from asymptomatic cases. Overall, a total of 3,164 differentially expressed lncRNAs and 5,948 circRNAs ($p\text{-adj}<0.05$) were identified. Focusing on neutropenic patients, 238 lncRNAs and 358 circRNAs were differentially expressed as compared to the other patients. Several of these, including CRNDE, GLIDR, NALT1, CYTOR, PVT1, circSETBP1, circBNC2, and circZBTB46, were overexpressed and negatively correlated with patients' absolute neutrophil count (ANC). Special attention was paid to PVT1, already known to promote oncogenic mechanisms in other hematological malignancies. It has been found to be

up-regulated both in its long and circular form of ncRNA. Next, we observed that the deregulation of ncRNAs could also be due to the presence of STAT3 mutations in neutropenic patients, as a substantial number of circRNAs are derived from STAT3-target genes. The STAT3-dependency of the PVT1 oncogene transcription was also confirmed by observing the restoration of normal PVT1 expression in neutropenic patients' primary samples treated with Stattic, a selective STAT3 inhibitor.

Conclusions. Our results show that discrete circular and long non-coding RNAs characterize the subset of T-LGLL patients with neutropenia and suggest that they might contribute to its development. Among these, PVT1 deserves further investigation as a promising new therapeutic target.

POSTERS

Stem Cells Signaling and Microenvironment

P001

MESENCHYMAL STROMAL CELL-DEPENDENT ADHESION PATHWAYS AFFECT THE SENSITIVITY OF ACUTE MYELOID LEUKEMIA CELLS TO VENETOCLAX TREATMENTM. Ciciarello^{1,4,5}, G. Corradi², K. Volkava¹, S. Bruno¹, J. Nanni¹, S. Squarzonzi^{4,5}, M. Cavo^{1,3}, A. Curti³

¹Dipartimento di Scienze Mediche e Chirurgiche, Università di Bologna; ²Dipartimento di Medicina e Scienze dell'Invecchiamento, Università di Chieti-Pescara; ³IRCCS Azienda Ospedaliero-Universitaria di Bologna, Istituto di Ematologia "Seràgnoli"; ⁴CNR Institute of Molecular Genetics "Luigi Luca Cavalli-Sforza", Unit of Bologna; ⁵IRCCS Istituto Ortopedico Rizzoli, Italy

Background. Acute myeloid leukemia (AML) patients have a poor prognosis with standard treatments due to a high relapse rate. Recently, Venetoclax (VEN), the first B-cell lymphoma 2 (BCL-2) selective inhibitor to enter the clinics, has shown a breaking-through effect in combination with demethylating agents in unfit-to-chemotherapy patients with treatment-naïve AML. However, resistance mechanisms have been described. It has been proposed that the bone marrow microenvironment, in general, and Mesenchymal stromal cells (MSCs), in particular, may favor a protective niche, thus playing a crucial role in drug sensitivity in hematological disorders, including AML.

Aim. Our study aims to investigate the mechanisms of MSC-mediated VEN resistance in AML.

Methods. We performed MSC/AML cell co-culture experiments

using the VEN-sensitive AML cell line MV4-11. We optimized an MSC/leukemic cell co-culture model to separate VEN-sensitive from VEN-resistant leukemic cells. We sorted VEN-sensitive from VEN-resistant leukemic cells and compared Gene Expression Profiling (GEP).

Results. We found that MSCs significantly reduced MV4-11 apoptosis after VEN exposure. Furthermore, when we cultured MV4-11 cells in direct contact with MSCs, we were able to distinguish, among leukemic cells, a cell population that remained floating in the supernatant and a cell population that kept adherent to MSCs and could be collected by trypsin detachment only. The electron microscopy observation highlighted a close physical interaction between MSCs and AML cells with a consequent reciprocal morphology remodeling. Interestingly, MSCs protected the adherent but not the floating cells from VEN-induced apoptosis, suggesting a central role of a close adhesion in the MSC-driven resistance to VEN. GEP of adherent vs floating MV4-11 cells revealed 159 differential expressed genes (DEGs). Interestingly, the principal component analysis suggested that the GEP of floating cells was more similar to the GEP of MV4-11 cells cultured without MSCs and compared to that of adherent cells. Enrichment analysis showed that DEGs were involved in cell adhesion migration and proliferation pathways. Among DEGs, we found that CD90/Thy-1, an adhesion molecule whose expression correlated with unfavorable karyotypes and shorter survival in AML, was significantly up-regulated in adherent MV4-11 cells. Flow cytometry confirmed that the adherent, compared to the floating MV4-11 cells, showed a higher expression of CD90. Finally, adding an anti-CD90 inactivating antibody to the co-cultures decreases the MSC-protective effect of VEN on adherent, but not on floating AML cells.

Conclusions. Our study demonstrates that MSCs protect AML cells from VEN-induced apoptosis through a complex mechanism involving tight adhesion, including a CD90-mediated pathway. Further clarifying these interactions can shed light on putative targets to counteract MSC-mediated VEN resistance, which may translate into increased overall response.

Omic and Multiomic Analysis

P002

A SYSTEMS-THINKING MODEL TO CAPTURE PLASMA CELLS METABOLISM AND COMPETITION UNDER MAXIMUM POWER CONSTRAINTS TO EXPLORE MULTIPLE MYELOMA EVOLUTION TRAJECTORIES

A. Romano, L. Conte, F. Surra, A. Giansanti, A. Kleidon, F. Gonella
Università degli Studi di Catania, Università Ca' Foscari, Italy

Background. Multiple myeloma (MM) is a challenging blood cancer that often requires patients to progress through multiple lines of therapy. MM clinical behavior arises from a complex system, where neoplastic, normal, immune and structural cells, proteins and soluble factors of the host interact together at different hierarchical levels, conveying emergent properties, not yet identified by current deterministic and probabilistic approaches. Taking advantage of Systems-thinking diagrams, pre-clinical models, multi-omics in primary samples obtained from patients affected by relapsed and refractory multiple myeloma, and mathematical modelling principles of system dynamics, we aim to capture the evolution trajectories of multiple MM players, e. g. normal and neoplastic plasma cells in response to internal and external triggers. In this work, we show a preliminary minimal ecological approach that encompasses growth, adaptation and survival of cell populations to model cell metabolisms and competition under energetic constraints, applied to MM as a proof-of-concept.

Methods. The stationary states that model the metabolisms of normal and neoplastic plasma cell populations can be described by differential equations derived from a systems-thinking mini model. The parameters are estimated through reported indirect measures of intrinsic growth rates and proteome turnover times of plasma cells. The carrying capacity is estimated from the average number of cells which can be plasma cells in the bone marrow, measured in ATPeq. The efficiency of ATP production is estimated accounting for the pathway of oxidative phosphorylation.

Results. Increases in growth rates lead to higher stock values that have access to higher power inflows corresponding to higher dissipative heat flows. These states are more stable the greater the stock value, according to the logistic growth model. Among all phenotypes of plasma cells (PCs), normal PCs occupy the steady state corresponding to the smallest stock value, the lowest ATP production flow, the lowest dissipative heat flow, and the least stability, as compared to neoplastic PCs in shades of red. In neoplastic PCs genetic mutations create the conditions for the system to access states of uncontrolled proliferation by perturbing the stationary states of normal cells converting the primary energy inflow into useful power to grow population structure, which corresponds, in the model, to more dissipative and stable metabolisms. We identified a class of regime shifts to more dissipative states for selectively advantaged malignant plasma cells, reflecting a breakdown of self-regulation in the bone marrow, lead to the extinction of normal plasma cells. The transition times obtained from the simulations range from years to decades consistently with clinical observations of survival times of patients. This irreversible dynamical behavior represents a possible description of the incurable nature of myelomas based on the ecological interactions between plasma cells and the microenvironment, embedded in a larger complex system.

Conclusions. Unfolding the role of the competitive interaction between normal, cancerous cell populations and the micro-environment by quantifying the energetic constraints operating on them is of key relevance in MM evolution.

P003

OPTICAL GENOME MAPPING IN MULTIPLE MYELOMA| A PILOT STUDY TO ASSESS FEASIBILITY IN THE CLINICAL SETTING

F. Restuccia^{1,2}, A. Mohamedali³, Le Anh Luong³, F. Aldridge³, I. Sa³, E. Liscano³, R. Dunn³, R. Benjamin^{2,4}

¹Dipartimento di Medicina e Scienza dell'Invecchiamento, Scuola Superiore "G. d'Annunzio"; ²School of Cancer and Pharmaceutical Sciences, King's College London; ³South-East Haematological Malignancy Diagnostic Service (SE-HMDS) at King's College Hospital; ⁴Department of Haematology, King's College Hospital

Introduction. Multiple Myeloma (MM) is a heterogeneous malignancy associated with many genetic abnormalities. The standard-of-care (SOC) prognostic score in MM is the Revised International Staging System (R-ISS), which stratifies the risk according to serum markers and high-risk cytogenetic abnormalities detected by fluorescence in situ hybridization (FISH). R-ISS clearly identifies the low- and high-risk patients, however, most of the patients are characterised as an intermediate-risk disease, with a wide heterogeneity in terms of survival. Detection of genomic aberrations is required and is solely carried out through FISH, with cytogenetic techniques not been reconsidered for decades. Optical genome mapping (OGM) is a novel cytogenetic technology that visualises ultralong DNA molecules, allowing large-scale structural and copy number evaluation of the genome. OGM has already been validated in Acute Myeloid Leukaemia, matching the current SOC methods, and expanding important clinical information.

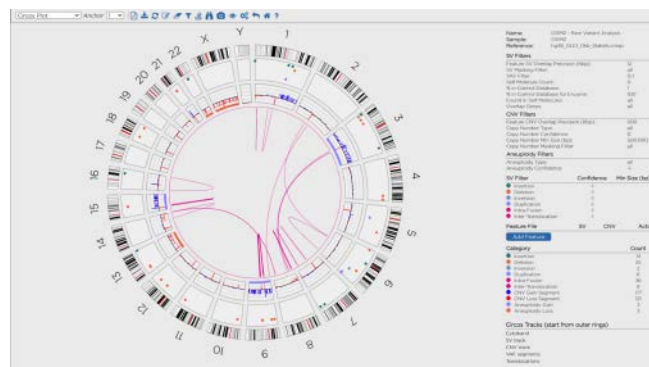


Figure 1.

Methods. The aim of this project is to demonstrate the benefits of OGM in MM. This will be carried out by analysing bone marrow samples of MM patients with either newly diagnosed or relapsed/refractory disease, to assess the feasibility of the methodology and the quality of the data, and consequently compare results with FISH. Ultra-High Molecular Weight genomic DNA is extracted from CD138 automatically selected plasma cells, and the samples are then labelled allowing the generation of highly contiguous genome maps. The genomic material is subsequently loaded onto the Bionano Saphyr chip to initiate the run.

Results. The OGM analysis performed on a single sample showed a gain of 1 copy of the 1q21.3 region, confirmed by FISH analysis, and also showed an IGH||MYC rearrangement, which was initially not detectable by the MYC probe that is usually used for SOC testing, however, further investigation through FISH was able to confirm the rearrangement.

Conclusions. To further validate our study and results, more samples need to be processed. Although OGM analysis did not match

the whole FISH reading, was able to demonstrate its potential by finding a rearrangement that would have not been found otherwise, possibly due to the limitation of the standard probe to cover the interest region or because of the insertion of the IGH locus into the MYC region. The technology of OGM is still accompanied by some limitations, including the difficulty of reading critical regions such as centromeres and telomeres, which was highlighted by a loss of chromosome 17 centromere not detected by OGM but found through FISH, as well as the non-high-throughput methodology. The latter is soon to be resolved as the company is releasing a fully automated and high-throughput version of the existing OGM.

P004

COMMON REQUIREMENTS IN NEXT GENERATION SEQUENCING ANALYSIS REPORT IN ONCOLOGICAL GENETICS

E. Ronda¹, E. Borotti¹, A. Ubiali³, S. Trubini³, A. Schena³, D. Vallisa², A. Zangrandi³, A. Rossi¹

¹UOC Biologia dei trapianti diagnostica molecolare e manipolazione cellule staminali emopoietiche AUSL di Piacenza; ²UOC Ematologia AUSL di Piacenza; ³UOC Anatomia Patologica AUSL di Piacenza, Italy

Introduction. In the heterogeneous panorama of instrumental platforms, multigenic panels, several chemistry and algorithms, a standardized NGS report based on common requirements through different disciplines is still challenging. The aim of this abstract is to start a debate in the scientific community to establish guidelines for the analysis and the interpretation of somatic profile in patients with neoplastic disorders, standardise the reporting of low allelic frequency or unknown clinical significance variants, and to define the ones of possible germinal origin.

Methods. We propose a reporting model according to Italian Soci-

ety of Human Genetics, European Society for Medical Oncology, Italian Association of Medical Oncology and Italian Society of Pathological Anatomy recommendations.

Results. In addition to generic information (*e.g.* personal data, sample's type and traceability), it is proposed to include additional attributes such as clinical data, diagnostic questions, time point, method description and limitations. The integration of this kind of information allows to provide a correct variants classification which can respond to diagnostic and prognostic questions or assess therapy efficacy, defining specific allelic frequency cut-offs. Given the continuous updating of pathology-related genes and the all-exons sequencing analysis, it is frequent to find variants that are difficult to interpret and have an unknown meaning. The anamnestic-family history of the patient can represent a valid support for a better interpretation of the result and consider the possible risk of identifying germline variants. Finally, it is suggested to provide a short qualitative report with information on the reliability of the result, such as the list of genes, read depth, coverage of the regions of interest and limits of the method.

Conclusions. It is worth providing a report containing a brief interpretation which can support clinical/diagnostic decisions, as well as the list of variants identified. Despite the cited guidelines, the aim remains to provide a complete reporting showing a simple and unique interpretation and an appropriate management of germinal variants. However, it is difficult to understand how to identify tumor variants of presumed germline origin. This limit may lead to an unnecessary genetic counselling or, conversely, to the loss of important results with familial and hereditary implications if laboratories fail to undertake a successful germline analysis. In the context of germline follow-up of tumor-only sequencing, it is useful to define a shared subset of 'most actionable' genes (such as *BRCA1*, *BRCA2*, *DDX41*, *ETV6*, *GATA2*, *MLH1*, *MSH2*, *MSH6*, *PALB2*, *TP53*, *RUNX1*, etc.). Multi-gene analysis represents the support for personalized and preventive medicine, therefore continuous collaboration between clinical geneticists, oncologists, hematologists and biologists is always necessary.

Myeloproliferative Disorders

P005

JAK2 IMPACT ON THROMBOTIC RISK IN ESSENTIAL THROMBOCYTHEMIA; TIME TO CONSIDER QUANTITATIVE DATA?

L. Tosoni¹, G. Morelli¹, C. Magagnotto², R. Mullai¹, A. Strazimiri², L. Scaffidi², M.E. Zannier¹, D. Damiani^{1,3}, M. Krampera², R. Fanin^{1,3}, M. Bonifacio², M. Tiribelli^{1,3}

¹Division of Hematology and Bone Marrow Transplantation, Azienda Sanitaria Universitaria Friuli Centrale; ²Department of Engineering for Innovation Medicine, Section of Innovation Biomedicine, Hematology Area, University of Verona; ³Department of Medical Area (DAME), University of Udine, Italy

Introduction Thrombosis represent the leading cause of mortality and morbidity of patients affected by Essential Thrombocythemia (ET). Thrombotic risk is defined by IPSET-t and r-IPSET-t scores. JAK2 mutation correlates with thrombosis occurrence, compared to other driver mutations and triple-negatives (TN), and is included in risk score calculation. Still, JAK2 variant allele frequency (VAF) impact on thrombosis remains a matter of debate. Aim of the study was to analyze incidence and main features connected to thrombosis in ET patients, focusing on molecular status, including JAK2 VAF.

Methods. We retrospectively analyzed 439 patients diagnosed with ET between 2000 and 2022 at the Divisions of Hematology of Udine and Verona, treated according to the current international guidelines. Molecular status was defined as soon as analysis were available, and a VAF cut-off 5% was arbitrarily set to distinguish high and low burden of JAK2 mutation.

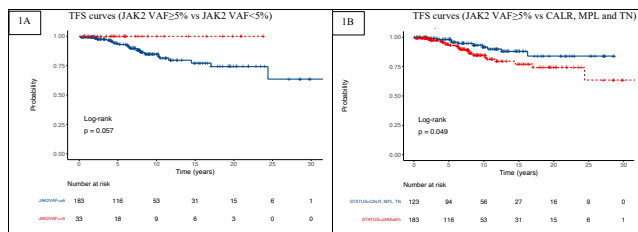


Figure 1. A. TFS at 10 years was 100% and 85% in JAK2 VAF<5% and JAK2 VAF_≥5%, respectively (p=0.057). None of the 33 patients with JAK2 VAF<5% experienced a thrombosis. **B.** JAK2 VAF_≥5% had a shorter TFS compared to CALR, MPL and TN at 10 years (85.0% vs 91.8%) and 20 years (74.2% vs 84.0%), respectively (p=0.049).

Results. Median age at diagnosis was 58 yrs (range: 14-87), with a slight female prevalence (55.1%). Median follow up was 97 months (range: 1-264). According to molecular analysis, 298 patients (67.9%) were JAK2+, 78 (17.8%) CALR+, 16 (3.6%) MPL+, 29 (6.6%) TN, and in 18 (4.1%) mutational status was not evaluable (NE). Within 298 JAK2+ patients, 216 (72.5%) had VAF measurement (median: 16.1%; range: 0.14-92.0%) and 183 (84.7%) had VAF_≥5%: these patients had higher Hct (p<.001) and Hb (p<.001) at diagnosis, compared to VAF<5%, while other clinical features were similar in the two cohorts. Based on r-IPSET-t, 193 patients (44.0%) were at high, 47 (10.7%) at intermediate, 118 (26.9%) at low, and 78 (17.7%) at very low risk, respectively; r-IPSET-t was NE in 3 cases. IPSET-t and r-IPSET-t both resulted significant predictors of thrombosis in the entire cohort (p=0.003). No significant difference emerged between JAK2 and other mutation or TN in terms of thrombosis-free survival (TFS), but a strong correlation between JAK2 VAF and thrombosis was noted: among 183 patients with

VAF_≥5%, 24 (13.1%) experienced at least one thrombotic event during ET course, whereas no event was recorded among the remaining 33 with VAF<5% (p=0.027); TFS at 10 years was 100% in VAF<5% and 85% in VAF_≥5% (p=0.057 - Figure 1A). Excluding VAF<5% patients from analysis, we found that VAF_≥5% JAK2 TFS resulted to be significantly shorter than other driver mutation and TN (p=0.049 -Figure 1B).

Conclusions Our results confirm IPSET-t and r-IPSET-t scores as strong predictors of thrombosis in ET patients. We found that VAF_≥5% JAK2 had higher thrombotic risk, compared to VAF<5% or other molecular abnormalities. Remarkably, none of the 33 patients with VAF<5% experienced thrombosis. We conclude that JAK2 contribution to thrombotic risk may be not only qualitative, but also quantitative, and risk-dependent indication for cytoreduction might be reappraised in low-burden JAK2+ patients, though the role of molecular signature still needs to be fully elucidated.

P006

ASSESSMENT OF DROPLET DIGITAL POLYMERASE CHAIN REACTION (DDPCR) AND REAL TIME PCR-BASED ASSAY PERFORMANCE FOR THE DETECTION OF KIT D816V MUTATION IN SYSTEMIC MASTOCYTOSIS| A NATIONWIDE PILOT STUDY BY THE RIMA (RETE ITALIANA MASTOCITOSI) ASSOCIATION

C. Monaldi¹, S. De Santis¹, M. Mancini², D. Pietra³, G. De Matteis⁴, S. Fabris⁵, N. Bolli^{5,6}, S. Errichiello⁷, B. Izzo⁸, F. Gesullo⁹, P. Guglielmelli⁹, G. Minnella¹⁰, P. Chiusolo^{10,11}, C. Papayannidis², C. Sartor^{1,2}, S. Bruno¹, C. Elena³, I. Tanasi⁴, M. Bonifacio⁴, F. Irene Grifoni⁵, M. Sciumè⁵, F. Mannelli⁹, L. Pagano^{10,11}, A.M. Vannucchi⁹, N.C.P. Cross¹², R. Zanotti⁴, M. Cavo^{1,2}, S. Soverini¹

¹Dipartimento di Scienze Mediche e Chirurgiche (DIMEC), Università di Bologna; ²IRCCS Azienda Ospedaliero-Universitaria di Bologna, Istituto di Ematologia "Seràgnoli"; ³U. O. C. Ematologia, Fondazione IRCCS Policlinico San Matteo; ⁴Azienda Ospedaliera Universitaria Integrata di Verona; ⁵U. O. C. Ematologia, Fondazione Cà Granda IRCCS Policlinico; ⁶Dipartimento di Oncologia ed Emato-Oncologia, Università di Milano; ⁷CEINGE Biotecnologie Avanzate "Franco Salvatore"; ⁸Dipartimento di Medicina Molecolare e Biotecnologie Mediche, Università degli Studi di Napoli "Federico II"; ⁹Center for Research and Innovation of Myeloproliferative Neoplasms (CRIMM), Azienda Ospedaliero-Universitaria Careggi di Firenze; ¹⁰Dipartimento di Diagnostica per Immagini, Radioterapia Oncologica ed Ematologia, IRCCS Fondazione Policlinico Universitario Agostino Gemelli; ¹¹Università Cattolica del Sacro Cuore; ¹²University of Southampton

Introduction. Detection of the activating D816V KIT mutation in the bone marrow is one of the minor criteria for the diagnosis of Systemic Mastocytosis (SM) and requires sensitive PCR-based methods, such as Allele-Specific Oligonucleotide-Real Time Quantitative PCR (ASO-qPCR) or ddPCR. To date, a map of labs across Italy offering KIT D816V testing with adequate sensitivity is lacking, nor have cooperative efforts aimed to check lab performance and reproducibility of diagnostic results ever been performed. Therefore, RIMA undertook, with the sponsorship of the GIMEMA Working Party on Chronic Myeloproliferative Neoplasms, a project aimed to create a nationwide network of competent reference laboratories performing KIT D816V mutation testing, promote harmonization of local procedures and ensure adequate proficiency and cross-comparability of results.

Methods. KIT D816V-mutated and wild-type genomic DNA obtained from HMC-1. 2 and HL60 cell lines, respectively, were

mixed in order to mimic different allele burdens (AB), from 10% down to 0,01%. Seven labs (L) (Bologna, Verona, Pavia, Milan, Florence, Rome and Naples) were involved in this pilot phase. The D816V KIT mutation was assessed according to local protocols 5 labs (L2-L6) used a commercial ddPCR assay (KIT p. D816V c. 2447A>T, Assay ID dHsaCP2000023; Bio-Rad); one lab (L7) used a home brew ASO-qPCR assay; one lab (L1) used a commercial semi-quantitative real time PCR-based assay (PlentiPlex Mastocytosis D816V kit; Pentabase).

Results. Dilutions were externally validated by the UK Wessex Genomics Laboratory Service (WGLS), using an accredited ddPCR assay. Of note, the 6th dilution (D6) was scored as slightly below their limit of detection (LoD) (0.008%; 3 positive droplets only). Identical batches of blinded vials were then distributed and analyzed in parallel by the 7 participating labs. Positivity/negativity as scored by L1-7 and AB values as scored by L2-7 are detailed in Table 1. All the evaluated methods proved highly accurate in the detection and, for ddPCR and ASO-qPCR, in the quantitation of the KIT D816V. A very high degree of agreement was achieved for the first 5 dilutions across different labs and methods, with coefficients of variation (CV) between 0.07 and 0.2. D6 was called borderline positive with the semi-quantitative real time PCR-based assay performed by L1 and positive by L2-L7, with a slightly greater CV (0.79) as compared to the other dilutions. Overall, however, accuracy and concordance of results between laboratories were deemed satisfactory.

Conclusions. This preliminary experience shows that PCR-based methods may yield accurate and comparable results for the detection and quantification of KIT D816V. Involvement of additional laboratories is planned.

Table 1.

DILUTIONS	Expected AB	WGLS	L1	L2	L3	L4	L5	L6	L7	AVERAGE	SD	CV
D1	10%	9.99	Pos	11.60	12.26	12.30	11.76	12.19	7.14	11.208	1.838	0.164
D2	1%	1.27	Pos	1.64	1.67	1.70	1.47	1.64	1.42	1.590	0.106	0.066
D3	0.50%	0.73	Pos	0.95	0.81	1.01	0.88	0.90	0.82	0.895	0.070	0.078
D4	0.10%	0.11	Pos	0.15	0.15	0.17	0.17	0.13	0.12	0.148	0.019	0.126
D5	0.05%	0.04	Pos	0.08	0.07	0.09	0.08	0.07	0.04	0.072	0.016	0.219
D6	0.01%	0.008	Borderline	0.04	0.01	0.04	0.01	0.01	0.004	0.019	0.015	0.789

KIT D816V mutation burden and summary statistics (average, standard deviation [SD], coefficient of variation [CV]) of results obtained by the Wessex Genomics Laboratory Service (WGLS) and the seven participating laboratories.

P007

RELATIONS BETWEEN GENETIC DETERMINANTS AND GLOBAL COAGULATION ASSAYS IN MYELOPROLIFERATIVE NEOPLASMS| FURTHER MOLECULAR AND FUNCTIONAL EVIDENCE OF THE “BIOLOGICAL CONTINUUM”

A. Lucchesi¹, G. Micucci¹, M. Poggiaspalla¹, G. Musuraca¹, G. Martinelli², F. Frabetti³, F. Foca³, G. Simonetti⁴, L. Catani⁵, G. Giordano⁶, M. Napolitano⁷

¹Hematology Unit, IRCCS Istituto Romagnolo per lo Studio dei Tumori (IRST) “Dino Amadori”; ²Scientific Directorate, IRCCS Istituto Romagnolo per lo Studio dei Tumori (IRST) “Dino Amadori”; ³Unit of Biostatistics and Clinical Trials, IRCCS Istituto Romagnolo per lo Studio dei Tumori (IRST) “Dino Amadori”; ⁴Biosciences Laboratory, IRCCS Istituto Romagnolo per lo Studio dei Tumori (IRST) “Dino Amadori”; ⁵Istituto di Ricovero e Cura a Carattere Scientifico (IRCCS) Azienda Ospedaliero-Universitaria di Bologna, Istituto di Ematologia “Seràgnoli”, Dipartimento di Medicina Specialistica, Diagnostica e Sperimentale, Università di Bologna; ⁶Division of Internal Medicine, Hematology Service, Regional Hospital “A. Cardarelli”; ⁷Department of Health Promotion, Mother and Child Care, Internal Medicine and Medical Specialties (PROMISE), University of Palermo, Reference Regional Center for Thrombosis and Hemostasis, Hematology Unit

Introduction. Within the realm of myeloproliferative neoplasms (MPNs), there is significant variability across hemostatic balance alterations and hypercoagulation tendencies, revealing the biological complexities that characterize these disorders. Moreover, the link between coagulation abnormalities and fibrotic progression still retains several unresolved dilemmas. Through a mixture of genetic analysis and functional assays, this study shows distinct patterns in coagulation pathways among classical MPNs.

Methods. A cohort of 53 MPN patients, naïve to therapy except for ASA, was scrutinized. A 30-gene panel (SOPHiA Myeloid Solution™) and cytofluorimetric determination of Platelet Function Receptors (PFRs) were performed. Rotational thromboelastometry (ROTEM® Delta) was used for INTEM, EXTEM, and FIBTEM measurements.

Results. ROTEM parameters revealed distinct coagulation profiles across MPNs. Essential thrombocythemia (ET) patients, especially those with CALR mutations, exhibited a balanced coagulation system with adequately contracted clot formation times (CFT) in both intrinsic and extrinsic pathways. Polycythemia vera (PV) patients have longer CFT (EXTEM 114 sec, p=0.008, INTEM 82 sec, p=0.027), but at the same time a selective contraction of the intrinsic pathway parameters (INTEM) for higher cell counts. Primary myelofibrosis (PMF) depicted a unique coagulation pattern confirming our ‘circulating wound’ model. This highlighted a propensity for the extrinsic pathway, likely driven by elevated tissue factor (TF) levels, establishing a link to systemic inflammation and fibrosis. Multivariate analysis affirmed the importance of hemoglobin levels in PV, while the role of platelet count resulted more relevant in PMF and ET. Mutational analysis unveiled the impact of specific genetic determinants on ROTEM parameters. For instance, DNMT3A mutations were linked to reduced clotting time (CT) in EXTEM, while ASXL1 mutations correlated with decreased maximum lysis (ML). Notably, mutations in EZH2 were found to be responsible for CFT elongations in INTEM assays. We further identified CBL mutations in 9.4% of our cohort. Despite similar ROTEM parameters as non-mutated patients, CBL mutated MPNs showed a phenotype characterized by aspirin (ASA)-resistant microcirculatory issues and a propensity for hemorrhagic events.

Conclusions. Our results corroborate Dameshek’s 1959 theory of a biological continuum within MPNs, extended here to the realm of coagulation. Each MPN subtype seems to have its own “coagulopathic personality,” justifying individualized therapeutic approaches. We introduce the concept of a ‘circulating wound’ in PMF, highlighting its unique coagulation dynamics and hinting at inflammation-fibrosis crosstalk. The presence of specific mutations further nuanced these coagulopathic profiles. Our findings illuminate the need for a stratified approach in the management of coagulation in MPNs and introduce new variables for future research.

P008

EXPLORING THE ROLE OF MEDIATOR COMPLEX SUBUNIT 12-LIKE (MED12L) IN MYELOPROLIFERATIVE NEOPLASMS

M. Brindisi^{1,2}, M. Liturri^{1,3}, L. Crisafulli^{1,2}, M. Zampini¹, E. Saba¹, E. Riva¹, D. Strina^{1,2}, L. Susani^{1,2}, M. Balliu⁴, P. Guglielmelli⁴, A. Vannucchi⁴, M.G. Della Porta^{1,5}, F. Ficara^{1,2}

¹IRCCS Humanitas Research Hospital; ²Milan Unit, CNR-Istituto di Ricerca Genetica e Biomedica; ³Università di Pavia; ⁴Centro di ricerca ed Innovazione per le Malattie Mieloproliferative (CRIMM), Azienda ospedaliera universitaria Careggi, Università degli studi di Firenze; ⁵Humanitas University, Italy

Introduction. Myeloproliferative neoplasms (MPN) are heterogeneous diseases characterized by excessive production of platelets,

as in the Essential Thrombocytemia (ET) subtype, or of erythrocytes, as in Polycytemia Vera (PV). MPN patients have increased risk of thrombotic events and evolution to acute myeloid leukemia (AML). A frequent feature of MPN is the somatic mutation V617F in the JAK2 gene, present in patient's hematopoietic stem and progenitor cells (HSPC). The JAK2V617F mutation and thrombocytemia are typical also of the MDS/MPN subgroup of myelodysplastic syndromes (MDS). In conditional JAK2V617F knockin mice in which the stem cell transcription factor Pbx1 has been deleted, we showed that thrombocytemia does not develop, and erythrocytosis disappear with time. One of the genes downregulated in the absence of PBX1 is Med12L, which codes for a component of the Mediator complex. MED12L is highly expressed in normal HSPC and megakaryocyte (Mk) precursors and it is upregulated in Mk-Erythroid progenitors of two independent MPN murine models. We hypothesize that MED12L is involved in HSPC function and in Mk priming, and that its dysregulation, secondary to an established driver mutation, contribute to the phenotype of hematological malignancies with thrombocytemia.

Methods. To assess the role of MED12L in normal HSPC we are taking advantage of Med12L knockout (KO) mice. To analyze a potential contribution of MED12L in myeloid neoplasms, we are studying MED12L expression in HSPC from MPN and MDS patients and the outcome of its inhibition in human MPN cell lines. Finally, we generated a novel mouse model (named JM) by crossing MED12L KO with JAK2V617F knockin mice, to analyze the consequences of MED12L absence *in vivo* in an MPN model.

Results. RNA sequencing of CD34+ HSPCs from MDS patients indicate that, in a portion of high-risk (HR) subjects, the expression of MED12L is higher compared to that found in normal controls (NC), while it is significantly lower in patients who underwent AML evolution. We found a positive correlation between MED12L expression and platelet counts, especially in the low-risk MDS subgroup, and with hemoglobin level mainly in HR-MDS. In ET and PV patients, MED12L expression is higher in CD34+ compared to CD34- cells; correlation with VAF, disease type, thrombocytemia or erythrocytemia and comparison with NC is forthcoming. We successfully performed CRISPR/Cas9-mediated deletion of MED12L in Set-2 and HEL cell lines with the aim of analyzing colony formation, proliferation, apoptosis and metabolic state compared to WT cells. Preliminary analysis of Med12L KO mice shows increased platelet volume; expansion of the JM mouse line is ongoing.

Conclusions. If the hypothesis of a role for MED12L in MPN and MDS subtypes is confirmed, this protein might represent a novel biomarker to further stratifying these heterogeneous patients and personalize their therapeutic approach or highlight a new oncogenic pathway to be targeted.

P009

THE INHIBITION OF CD14+ AND CD34+ CELL MIGRATION WITH AN ANTI-CD44 ANTIBODY COULD COUNTERACT EXTRAMEDULLARY HEMATOPOIESIS IN MYELOFIBROSIS PATIENTS

M. Mirabile^{1,2}, L. Tavernari^{1,2}, S. Rontautoli^{1,3}, R. Norfo^{1,3}, M. Maccaferri⁴, S. Parenti^{1,3}, C. Carretta^{1,3}, E. Bianchi^{1,2}, M. Bertesi^{1,2}, F. Pedrazzi^{1,2}, P. Guglielmelli^{5,6}, L. Potenza⁷, E. Tagliafico^{7,8}, M. Luppi⁷, A.M. Vannucchi^{5,6}, R. Manfredini^{1,3}

¹Interdepartmental Centre for Stem Cells and Regenerative Medicine, University of Modena and Reggio Emilia; ²Department of Life Sciences, University of Modena and Reggio Emilia; ³Department of Biomedical, Metabolic and Neural Sciences, University of Modena and Reggio Emilia; ⁴Department of Laboratory Medicine and Pathology, Diagnostic Hematology and Clinical Genomics AUSL/AOU Policlinico; ⁵Center Research and Innovation of Myeloproliferative Neoplasms (CRIMM), Azienda Ospedaliera Universitaria Careggi; ⁶Department of Experimental and Clinical Medicine, University of Florence; ⁷Department of Medical and Surgical Sciences, University of Modena and Reggio Emilia, AOU Policlinico; ⁸Center for Genome Research, University of Modena and Reggio Emilia, Italy

Introduction. Myelofibrosis (MF) is a chronic myeloproliferative neoplasm characterized by inflammation, bone marrow fibrosis, stem cell mobilization and extramedullary haematopoiesis (EMH). In MF EMH often results in splenomegaly, which affects life quality and supports systemic spreading. Despite the clinical need, little is known about EMH. However, the removal of macrophages in a JAK2 mutated mouse model resulted in a reduction of splenomegaly. Mutated monocytes, migrating from peripheral blood into the spleen, create an inflammatory milieu that recruits CD34+ hematopoietic stem and progenitor cells. Therefore, the aim of this study is to block the extravasation of monocytes and then CD34+ cells to reduce EMH.

Methods. We generated an *in vitro* model of extravasation with a transwell system and an endothelial layer with HUVEC (human umbilical vein endothelial cells). HUVEC are seeded on a upside down transwell and leaved overnight with the pro-inflammatory stimuli TNF- α to create *in vitro* an activated endothelial layer. CD14+ or CD34+ cells are seeded on the transwell with HUVEC; after an overnight incubation, the cells in the down side of the system were collected and counted by means of flow cytometer.

Results. An anti-CD44 antibody and, to a lesser extent, an anti- $\alpha 4\beta 1$ antibody significantly reduce migration of healthy donor (HD) monocytes. At the highest dose, the anti-CD44 antibody caused a complete inhibition of migration. The reduction in migration is always greater in presence of the endothelium, supporting the idea that an anti-CD44 antibody inhibits not only the extravasation of monocytes but also the recall by the inflamed endothelium. Regarding CD34+ cells, a small reduction in migration is observed on HD cells, but the effect is very evident on MF CD34+ cells, with a 25% reduction at the highest dose. Furthermore, the comparison between the reduction in migration for HD cells and MF cells is statistically significant, indicating that MF CD34+ cells are more sensitive to inhibition by the anti-CD44.

Conclusion. An anti-CD44 antibody is able to reduce the migration of CD14+ and CD34+ cells. To a lesser extent, an antibody against $\alpha 4\beta 1$ was also able to reduce the migration of CD14+ cells; interestingly, this integrin is capable of physical coupling to CD44. These results pave the way for *in vivo* testing of the anti-CD44 antibody. Preliminary data show that Ruxolitinib is unable to reduce cell migration in this *in vitro* model; therefore, the inhibition of splenomegaly observed in the patients by Ruxolitinib treatment would be due to different mechanism, probably linked to the reduction of inflammatory cytokines. Therefore, this CD44-based

approach could be considered in JAK2-inhibitor resistant patients. Moreover, antibodies against CD44 would then be easily translated into the clinic because two clinical trials demonstrated the safety of anti-CD44 antibodies in acute myeloid leukemia and in solid tumors.

P010

CLINICAL-PATHOLOGICAL CHARACTERIZATION OF MYELOPROLIFERATIVE AND MYELODEPLETIVE PHENOTYPES OF PRIMARY AND SECONDARY MYELOFIBROSIS

S. Zoletto¹, R. Biancotti², V. Fabiano², L. Trentin¹, A.P. Dei Tos², G. Binotto¹, M. Pizzi²

¹Unità di Ematologia e Immunologia Clinica, Dipartimento di Medicina-DIMED, Università degli Studi di Padova; ²Unità di Anatomia Patologica e Citopatologia, Dipartimento di Medicina-DIMED, Università degli Studi di Padova, Italy

Introduction. Primary Myelofibrosis (PMF), Polycythemia Vera (PV), and Essential Thrombocythemia (ET) are hematopoietic stem cell disorders, belonging to the group of classic Myeloproliferative Neoplasms. Of these, PMF and post-ET/post-PV Myelofibrosis (*aka* secondary Myelofibrosis [SMF]) are heterogeneous diseases, with variable clinical and biological features. Recently, two clinical phenotypes of PMF/SMF have been described, i. myelodepletive (MD) PMF/SMF, characterized by severe cytopenia; and ii. myeloproliferative (MP) PMF/SMF, featuring elevated white blood cell (WBC) and/or platelet (PLTs) counts. The histological correlates of such phenotypes and their prognostic impact are poorly understood. To address these issues, we conducted a retrospective clinical-pathological study on a large series of PMF/SMF.

Methods. This study considered a consecutive series of 94 cases of PMF/SMF, diagnosed at Padua University Hospital (Padua – Italy) over a 5-year period (2017-2022). Inclusion criteria included i. age >18 years; ii. clinical-pathological diagnosis of PMF or SMF; iii. availability of clinical/therapeutic data; iv. follow-up ≥ 3 months; and v. availability of adequate bone marrow (BM) specimens. For each case, clinical-laboratory and prognostic data, as well as BM histological features were collected. Segregation into clinical phenotypes was made by Coltro's definition of MD phenotype (*id est* no increase in WBC/PLTs counts and at least one among Hb <10 g/dL for women/<11 g/dL for men, PLTs <100x10⁹/L, WBC <4x10⁹/L). Comparative analyses were conducted by T/Mann-Whitney tests (quantitative variables) and Chi-square/Fisher exact tests (qualitative variables). Survival analyses were performed using Cox regression, log-rank test and Kaplan-Meier curves. Differences between groups were considered statistically significant for p<0.05.

Results. The study population included 65 patients with PMF and 29 patients with SMF. The mean age at diagnosis was 60.5 years, with a M/F ratio of 1.61 and a median follow-up of 42 months. Overall, 25/94 (27%) patients had MD and 69/94 (73%) non-MD (*id est* MP) phenotype. Histological evaluation disclosed more severe fibrosis and higher frequency of dysplastic megakaryocytes (*id est* micromegakaryocytes; megakaryocytes with separated and/or 5q- nuclei) in MD as compared to MP cases (p<0.001). Prognostic correlations showed a trend toward worse prognosis for MD phenotype (HR 1.96; p=0.11). Megakaryocytic dysplasia impacted on outcome (HR 3.8; p<0.001), added to IPSS-based patient stratification and was an independent prognostic factor in multivariate analyses considering cytopenia, age >65 and previous treatments (Cox regression p=0.04).

Conclusions. MD and MP PMF/SMF exhibit distinct BM histology, likely subtending differences in their biological features. The assessment of megakaryocytic dysplasia may represent a new, independent prognostic factor, improving patient stratification and clinical management.

P011

GLUTAMATE ACCUMULATION IN MYELOFIBROSIS TUMOR MICROENVIRONMENT TRIGGERS MESENCHYMAL STROMAL CELLS SENESCENCE BY INDUCING FUMARATE OVERPRODUCTION

S. Giallongo¹, L. Longhitano², J. Ferrigno², E. Tropea², C. Giallongo¹, A. Romano³, A.M. Amorini², G. Lazzarino², F. Di Raimondo³, G. Li Volti², G.A. Palumbo¹, D. Tibullo²

¹Department of Scienze Mediche, Chirurgiche e Tecnologie Avanzate "G. F. Ingrassia", University of Catania; ²Department of Biomedical and Biotechnological Sciences, University of Catania; ³Division of Hematology, Azienda Ospedaliero Universitaria Policlinico "G.Rodolico -San Marco", Italy

Introduction. Primary myelofibrosis (PMF) is a clonal stem cell disorder clinically displaying anemia, splenomegaly, leukoerythroblastosis and constitutional symptoms. In this context, the malignant clone progression is regulated by tumor microenvironment (TME), where mesenchymal stromal cells (MSCs) are located. The latter are usually senescent, releasing proinflammatory cytokines as part of senescence associated secretory phenotype (SASP), therefore enhancing the inflammatory status already characterizing PMF-TME. Moreover, it is also enriched in several metabolites including glutamate (Glu). Of note, alterations of its metabolism have been reported in senescence establishment, prompting us to investigate its regulation within MF-TME.

Methods. HLPC analysis has been performed. HS-5, used as healthy-MSC model, were treated with Glu and dimethyl-Fumarate (DMF). Whole proteins and histone fraction were isolated. Western blot was performed against H3K36me2, Col1A1, phospho-p53. Flow cytometry was used to assess ROS and DNA damage. SASP gene expression profile was assayed by qPCR. B-Galactosidase activity was evaluated. Immunofluorescence was performed to assess 5-methyl Cytosine (5mC).

Results. To assess the accumulation of several metabolites within MF-TME, we performed HPLC analysis on healthy and PMF sera, eventually showing an accumulation of Glu. Since glutaminolysis leads to fumarate accumulation, we detected the accumulation of this metabolite in HS-5 cells after treatment with Glu, as further corroborated by western blot analysis showing an increase in fumarate accumulation marker H3K36me2. Interestingly, the fumarate accumulation was confirmed in MF sera. Therefore, we next used DMF to assess the impact of fumarate accumulation on MSC compartment. We found a significant enhancement of ROS in HS-5 cells upon Glu and DMF treatment compared to untreated cells. In agreement, we also observed increased DNA damage after treatment. These data prompted us to perform B-Galactosidase assay, eventually displaying an increased enzymatic activity upon Glu and DMF addition. The senescent profile was corroborated by IL6, TFN, and TGFB upregulation, along with phospho-p53. Furthermore, senescent HS-5 accumulated 5mC, as mirrored on primary PMF-MSCs. Finally, Glu and DMF supplementation increased COL1A1 levels, therefore suggesting a contribution of these metabolites in fibrosis, one of the PMF hallmarks.

Conclusions. Our data define the essential role covered by Glu metabolism in remodeling of tumor microenvironment in PMF. Its uptake and conversion in fumarate are indeed crucial for the establishment of MSC senescent profile, eventually also promoting the fibrotic state characterizing PMF bone marrow. Therefore, further studies will be needed to counteract MSC Glu uptake, possibly unveiling a novel therapeutic strategy against PMF.

P012

JAKNET NETWORK UNDER THE LENS, RESULTS OF THE LABORATORY 2023 QUALITY CONTROL

F. Gesullo, M. Messina, R. Cucci, A. Piciocchi, M. Vignetti, T. Barbui, G. Barosi, V. De Stefano, U. Gianelli, F. Pane, F. Passamonti, A.M. Vannucchi, P. Guglielmelli

¹CRIMM, Centro di ricerca ed Innovazione per le Malattie Mieloproliferative, Azienda Ospedaliera-Universitaria Careggi, Università Degli Studi di Firenze; ²Fondazione GIMEMA, Roma; ³Foundation of Clinical Research-FROM, Ospedale Papa Giovanni XXIII; ⁴Centro per lo Studio e la Cura della Mielofibrosi, Fondazione IRCCS Policlinico San Matteo; ⁵Fondazione Policlinico Universitario Agostino Gemelli IRCCS; ⁶SC Anatomia Patologica, ASST Santi Paolo e Carlo; ⁷AOU Federico II, UOC Ematologia; ⁸Ematologia, Fondazione I. R. C. C. S. Ca' Granda, Ospedale Maggiore Policlinico, Italy

Introduction. In 2018, GIMEMA – thanks to an unconditional grant from Novartis – generated a network (JakNet) connecting several Italian hematology centers with reference laboratories (HUB la[b]) qualified to evaluate the JAK2V617F. The ability to accurately measure JAK2V617F variant allele frequency (VAF) is of great interest given the diagnostic relevance to MPNs. Forty-four laboratories, distributed across Italy, are currently part of the network. The HUB labs elaborated a list of recommendations (R. I. L. v 1.0) and shared a guideline. Though the Scientific Board does not impose a specific assay, in order to ensure a standardized diagnostic/prognostic workup, HUB labs must undergo quality controls (QC) every year. In the current report, we present the results of the 2023 QC.

Methods. Forty-four laboratories took part to the 2023 QC and the proficiency test was based on the analysis of the 1st Panel JAK2V617F NIBSC. This panel comprises 7 individually coded ampoules, each containing freeze-dried purified genomic DNA extracted from human cell lines. Each primary standard has a different value for JAK2 V617F as a percentage of total JAK2 (0%-0.03%-1%-10.8%-29.6%-89.5%-100%). To quantify JAK2 V617F VAF, laboratories used either quantitative PCR (Q-PCR) or digital-droplet PCR (ddPCR). As reported in the RIL, a grid of acceptable values was elaborated and the laboratories were evaluated in terms of data accuracy. From December 2022 we collected and centrally analyzed the results. Laboratories were defined as “compliant” when all the values were included in the acceptable intervals, “active non-compliant” when the discrepancies detected did not impact on the negative/positive classification, “non-compliant” if the discrepancies were in the crucial standards 0-1% interfering with the negative/positive definition.

Results. To perform the proficiency test, the majority of laboratories – *i. e.* (31, 70%) used Q-PCR; roughly half of them (N=17,55%) performed the experiments by using the Qiagen Rotorgene; 10 laboratories (32%) used the 7500/7900/Step One Plus Applied Biosystem instruments; the remaining laboratories used other platforms. The preferred assay was the Ipsogen JAK2 Mutaquant kit (Qiagen) used by 27/31 (87%) laboratories. Thirteen laboratories (29%) used ddPCR and were prevalently run on the QX2000 instrument by employing the ddPCR Mutation Detection Assay FAM+HEX (BioRad). All the laboratories ran 3 independent experiments and used duplicates. The analysis of the proficiency test revealed that 36 laboratories (82%) were “compliant”, 5 laboratories were defined “active but non-compliant” and 3 laboratories resulted “non-compliant”. Of note, though being a minority, all the ddPCR users were compliant.

Conclusions. The 2023 QC carried out by the JakNet laboratories on the 1st Panel JAK2V617F NIBSC showed an overall good performance. Indeed, 93% of laboratories were enabled to perform the

test within the network. DdPCR users increased since 2016 and ddPCR showed a high accuracy.

P013

THE INFLAMMASOME NEGATIVELY REGULATES HEME OXYGENASE 1 PROMPTING BONE MARROW FIBROSIS IN PRIMARY MYELOFIBROSIS

L. Longhitano, D. Tibullo, S. Giallongo, E. La Spina, G. Li Volti, A. Duminuco, A. Romano, R. Caltabiano, L. Salvatorelli, A. Liso, F. Di Raimondo, C. Giallongo, G.A. Palumbo

¹Dipartimento di Scienze Biomediche e Biotecnologiche, Università degli studi di Catania; ²Dipartimento di Scienze Medice, Chirurgiche e Tecnologie Avanzate “Ingrassia”, Università degli Studi di Catania; ³Dipartimento di Specialità Medico-Chirurgiche, CHIRMED, Sezione di Ematologia, University of Catania; ⁴Divisione di Ematologia e Unità di Trapianto di Midollo Osseo, Azienda Ospedaliero Universitaria Policlinico “G. Rodolico-San Marco”; ⁵Dipartimento di Scienze Medice e Chirurgiche, Università di Foggia, Italy

Introduction. Primary myelofibrosis (PMF) is a myeloproliferative neoplasm (MPN) characterized by stem cell-derived clonal myeloproliferation with several disease feature including a fibrotic tumor microenvironment (TME) and aberrant inflammation. In this context, mesenchymal stromal cells (MSCs) are reprogrammed to promote malignant clone proliferation, eventually also triggering bone marrow fibrosis. Moreover, it has been reported that NLR family pyrin domain containing 3 (NLRP3) inflammasome has a crucial role in fibrotic events leading to the chronic release of inflammatory molecules such as IL-1 β and IL-18. As hyperinflammation is prompted by an impairment of the anti-inflammatory system, we here investigated the interplay between NLRP3 inflammasome and the antioxidant protein HO-1 in PMF.

Methods. HS-5 cells were used as model of healthy MSCs. Inflammasome stimulation was achieved by the addition of 2 μ g/mL LPS for 4h, followed by 45 minutes 5mM ATP. Western blot and qPCR analysis were performed to assess NLRP3, pro-Caspase1, Caspase 1, IL1 β , IL18, COL1A1, alpha-SMA, and HO-1 accumulation. MSCs were treated with conditioned media derived from PMF cell line (HEL). HO-1 induction was achieved either by Hemin or CORMA1. Immunofluorescence assay was used to investigate HO-1 and Nrf2 accumulation. The fibrosis was tested by performing the Mallory staining and collagen immunoassaying. Immunocytochemistry was performed on healthy and PMF biopsies to investigate HO-1 expression.

Results. Activation of inflammasome in HS-5 cells was corroborated by a marked increase in NLRP3, Caspase1, IL1 β , IL18 mRNA expression. Interestingly, primed inflammasome cells showed overexpression of fibrotic markers such as COL1A1 and α -SMA. Of note, HO-1 was decreased in this context. Inflammasome activation and fibrosis were also detected following HS-5 treatment with HEL-conditioned media. Therefore, we sought to induce HO-1 expression either by CORMA1 or Hemin, as reported by qPCR and immunofluorescence, also showing an increased nuclear translocation of its transcription factor Nrf2. Interestingly, HO-1 induction recovered the fibrotic phenotype detected in HS-5 upon treatment with HEL-conditioned media, as demonstrated by decreased expression of HEL-induced COL1A1 and α -SMA accumulation. These data were also confirmed by Mallory staining. In agreement with *in vitro* data, HO-1 accumulation was significantly decreased in PMF biopsies but not in healthy counterpart.

Conclusions. Overall our data unveil the crucial interplay between NLRP3 inflammasome and HO-1. Its decrease in this context might be a driver in the establishment of the typical PMF TME, as corrob-

samples, 25/45 (47%) NGS laboratories processes more than 20 samples per month. Their activity is mainly focused on Acute myeloid leukemia, Myeloproliferative disorders, Myelodysplastic syndromes and to a lesser extent on lymphoproliferative disorders. With regards to the method, the survey showed that [i/i] the preferred platform was Illumina, used by 33 (73%) of laboratories, followed by Ion Torrent; [i/i] libraries are usually prepared manually, as 32 (71%) laboratories declared; [i/i] 64% of NGS users prefer commercial to custom panels. Data analysis, a challenging step in NGS pipeline, is mainly performed (84% of laboratories) by using commercially available software. This is partly ascribable to the low number of centers (N=15) that can count on Bioinformatician's expertise.

Conclusions. This report provides a picture of the current use of NGS in Italy. It highlights that NGS data are widely used to guide diagnostic/prognostic decisions, however only half of the Italian Hematology Centers can count on an in-house instrument. Moreover, though a preferred platform/method emerged, we documented a certain degree of heterogeneity. These data indicate that it is crucial to identify hub NGS centers and coordinate the flow of samples as well as align and standardize NGS techniques and analysis.

P016

MYELOID NEOPLASMS WITH ALK REARRANGEMENT, A RARE ENTITY WITH AGGRESSIVE COURSE| A NEW CASE REPORT

M.I. Nasuto¹, G. Todaro¹, B. Cambò¹, G. Sammarelli¹, F. Arienzo³, C. Giordano³, M. Giaimo^{1,2}, A. Rinaldi¹, L. Prezioso¹, S. Bonomini¹, R. Segreto¹, L. Craviotto^{1,2}, G. Roti^{1,2}

¹UOC Ematologia e CTMO, Azienda Ospedaliero-Universitaria di Parma; ²Dipartimento di Medicina e Chirurgia, Università di Parma; ³Dipartimento di Scienze Radiologiche, Oncologiche e Anatomico-Patologiche, Sapienza Università di Roma, Italy

Introduction. Myeloid neoplasms (MN) with oncogenic ALK fusion are extremely rare, with only ten cases reported in the literature, mostly AML. We report a peculiar case with unusual presentation of MDS/MPN with extramedullary involvement(EI) and ALK rearrangement.

Methods. A 25 y. o. man, with family history of MN, was referred to our Center due to asthenia, splenomegaly, lymphadenopathies and tonsillar hypertrophy. CBC showed WBC 53,000/mm³ with monocytosis, Hb 6 g/dL, PLT 73,000/mm³. PB smear confirmed monocytosis(25%) and displayed dysplastic features in granulocytes, with 2% blasts. 18FDG CT-PET scan revealed hypermetabolism in palatine tonsils, lymph nodes(LN), spleen, and BM. BM biopsy showed cellularity >98%, with hyperplastic and dysplastic granulopoiesis. BM cytology indicated granulocytic dysplasia and increase in monocytes with 10% promonocytes and myeloid blasts. Flow cytometry confirmed monocytosis and 1.7% CD34+CD13+CD117+HLA-DR+ blasts. Thus a diagnosis of MDS/MPN Chronic Myelomonocytic Leukemia type-2 (CMML-2) was made, Düsseldorf score 4(high). Diagnostic work-up included conventional cytogenetic (CC), FISH, RT-PCR and NGS analysis(Myeloid Solution). Additionally, a LN biopsy was performed with sections stained with hematoxylin-eosin and used for immunohistochemistry(MPO, e-cadherin, CD61, CD117, CD34). FISH was also employed to evaluate ALK(2p23).

Results. RT-PCR results were negative for mutations in BCR||ABL, NPM1, FLT3 ITD/TKD, IDH1-2, and JAK2V617F. NGS also yielded negative results. Interestingly, CC revealed a karyotype 46,XY[1]/46,XY,inv(2)(p23;q13)?[27]/45,XY,inv(2)(p23;q13)?,-7[2]. FISH ALK(2p23) dual-color break-apart and D7S486/CEP7 probes confirmed ALK rearrangement in 90% and -7 in 33% of nuclei. Metaphase FISH indicated that ALK rearrange-

ment was a result of a pericentric inversion, inv(2)(p23;q13), suggesting RANBP2 as partner gene. As a result, CPSS score was high, and CPSS-Mol int-2. LN biopsy showed proliferation of myeloid cells with E-cadherin+ and CD34+ elements. These findings were consistent with EI by MDS/MPN. The presence of ALK rearrangement was also confirmed. Due to the patient's age, good performance status and unusual presentation of the disease with distinctive genetic signature, treatment approach included an AML-like regimen, with FLA-IDA induction, followed by consolidation with high dose of cytarabine, serving as a bridge to HSCT. After induction, disease evaluation revealed morphological CR with hematological recovery and cytogenetic remission.

Conclusions. MDS/MPN with ALK rearrangement is an exceptionally rare condition with aggressive course. Our case suggests that an intensive approach may be the optimal choice for certain patients, enhancing the chances of achieving CR. Moreover, the identification of these rare ALK fusions in myeloid neoplasms not only contributes to a better understanding of the disease but also opens up the possibility of benefiting from innovative ALK-targeted therapies.

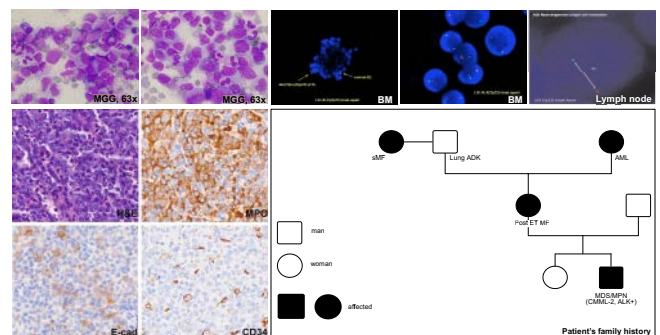


Figure 1.

P017

AGGRESSIVE SYSTEMIC MASTOCYTOSIS WITH THE CO-OCCURRENCE OF PRKG2:PDGFRB, KAT6A:NCOA2, AND RXRA:NOTCH1 FUSION TRANSCRIPTS AND A HETEROZYGOUS RUNX1 FRAMESHIFT MUTATION

D. Tolomeo¹, M. Poscente², A. Arshadi¹, A. Agostini^{3*}, A. L'abbate⁴, A.G. Solimando³, O. Palumbo⁵, M. Carella⁵, P. Palumbo⁵, T. González⁶, J.M. Hernández-rivas⁶, L. Bassi², R. Isidori², M. Dell'aquila⁷, G. Trapè⁸, R. Latagliata⁸, G. Pessina², F. Natoni², C.T. Storlazzi¹

¹Department of Biosciences, Biotechnology and Environment, University of Bari Aldo Moro; ²UOSD Laboratorio di Genetica Medica, Ospedale Belcolle; ³Department of Precision and Regenerative Medicine and Ionian Area, Unit of Internal Medicine and Clinical Oncology, University of Bari Aldo Moro; ⁴Istituto di Biomembrane, Bioenergetica e Biotecnologie Molecolari (IBIOM), Consiglio Nazionale delle Ricerche; ⁵Division of Medical Genetics, Fondazione IRCCS-Casa Sollievo della Sofferenza; ⁶Department of Medicine, Universidad de Salamanca, Department of Hematology, Hospital Universitario de Salamanca, IBSAL, IBMCC-Centro de Investigación del Cáncer (USALCSIC); ⁷UOC Anatomia Patologica, Ospedale Belcolle; ⁸UOC Ematologia, Ospedale Belcolle; *present address| Department of Translational Medicine and Surgery, Università Cattolica del Sacro Cuore, Italy

Introduction. Systemic mastocytosis (SM) is a myeloproliferative

neoplasm displaying abnormal mast cell proliferation. It is subdivided into different forms, including aggressive systemic mastocytosis (ASM) and systemic mastocytosis with an associated hematologic neoplasm. Oncogenic alterations include point mutations, mainly the KIT D816V and JAK2 V617F, conferring poor prognosis and therapy resistance; and fusion genes, with those involving *PDGFRA/PDGRFB* as the most recurrent events.

Methods. We here describe an SM case, rapidly evolved towards SM associated with acute myeloid leukemia (SM-AML). Cytogenetic (karyotyping and fluorescence in situ hybridization (FISH) assays) and molecular (chromosome microarray analysis, DNA targeted-deep sequencing, RNA-Seq, RT-PCR, and Sanger sequencing) analyses were performed on patient bone marrow (BM)/peripheral blood samples collected from the diagnosis to the SM-AML evolution and patient death.

Results. The patient at diagnosis was negative to the KIT D816V and JAK2 V617F alterations but showed a *RUNX1* frameshift heterozygous mutation (Variant Allele Frequency: 11.4%) and the co-occurrence of three fusion transcripts. The first one, *PRKG2::PDGRFB*, was generated by a balanced t(4;5)(q24;q32) translocation as the sole abnormality, identified by karyotyping the BM cells. Other two novel chimeras, *KAT6A::NCOA2* and *RXRA::NOTCH1*, detected by RNA-Seq analysis and validated by

RT-PCR/Sanger sequencing, probably originated from cryptic intrachromosomal abnormalities, since neither karyotype or FISH analyses detected them. The evolution towards SM-AML was characterized by the occurrence of a complex karyotype showing multiple chromosome losses and gains and the presence of an extra copy of the der(5)t(4;5)(q24;q34) chromosome, leading to the persistence and increased expression of the *PRKG2::PDGRFB* chimera. Moreover, an increase in the *RUNX1* mutation allelic frequency (Variant Allele Frequency: 44%) was reported. Whereas *KAT6A::NCOA2* and *RXRA::NOTCH1* fusions were not detected, at least considering the sensitivity limits of the used techniques.

Conclusions. Here, we analyze an interesting SM case showing multiple fusion transcripts involving relevant genes in hematological malignancies: *PRKG2::PDGRFB*, occurring from patient diagnosis to death and already reported in SM; and *KAT6A::NCOA2/RXRA::NOTCH1* detected in the ASM phase and possibly having a role in the rapid disease evolution towards SM-AML. The pathogenic *RUNX1* frameshift mutation was also relevant for ASM disease evolution, as it is considered poor-risk alterations in ASM patients. Overall, our results indicated that the transcriptional landscape and the mutational profile of SM deserve attention to predict the evolution and prognosis of this complex disease, whose classification criteria are still a matter of debate.

Chronic Myeloid Leukemia

P018

POLYCOMB GENES IN CHRONIC MYELOID LEUKEMIA. A POSSIBLE MARKER OF RESISTANCE

C. Bono¹, F. Guerrini¹, C. Baratè², M. Franciosa¹, I. Santo¹, A. Votto¹, F. Ricci², A. Sicuranza³, D. Raspadori⁴, I. Tusa⁵, E. Rovida⁵, P. Dello Sbarba⁴, M. Bocchia^{3,4}, S. Galimberti^{1,2}

¹Dipartimento di Medicina Clinica e Sperimentale, Università di Pisa; ²Azienda Ospedaliero-Universitaria Pisana, Pisa; ³Dipartimento di Scienze Mediche, Chirurgiche e Neuroscienze, Università di Siena; ⁴Azienda Ospedaliero-Universitaria Senese, Siena; ⁵Dipartimento di Scienze Biomediche, Sperimentali e Cliniche, Università di Firenze, Italy

Introduction. Chronic myeloid leukemia is defined by a genetic abnormality known as the Philadelphia chromosome, which is caused by a translocation between the long arms of chromosomes 9 and 22. This results in the formation of the BCR||ABL1 fusion protein, which not only converts hematopoietic stem cells (HSC) into leukemic stem cells (LSC), but also induces epigenetic reprogramming. Polycomb Repressive Complexes (PRCs), which include EZH2 and BMI1, are a group of epigenetic regulators that are known to be dysregulated in CML LSC.

Aim. The aim of this study was to evaluate the expression of BMI1 and EZH2 in 47 CML samples from 9 patients at four time points (diagnosis, three, six, and twelve months after the introduction of TKI). We wished to investigate potential correlations between the Polycomb genes and BCR||ABL1 transcript and evaluate the prognostic significance of these genes.

Methods. To measure gene expression, we developed a novel digital droplet PCR (ddPCR) method capable of simultaneously analyzing three genes (BMI1, EZH2, and GAPD), with the last chosen as the reference gene. We utilized the Droplet Generator and Droplet Reader instruments (BioRad, QX200, Italy) for multiplex ddPCR. Using the QuantaSoft™ Pro Software (BioRad, Italy), the concentration (copies/microliter) and relative expression of each gene of interest (geneX/GAPDH) were determined.

Results. We observed reduced BMI1 levels at diagnosis ($p < 0.001$) compared to all other timepoints. Statistically, EZH2 expression was significantly lower at diagnosis than at 12 months ($p = 0.024$). We observed a significant direct correlation between BMI1 and EZH2 expression levels at diagnosis (Pearson's $r = 0.99$, $p < 0.001$). At 6-month, the analysis revealed a direct correlation between BMI1 and BCR||ABL1 levels ($p = 0.001$), as well as a trend between EZH2 and BCR||ABL1 and EZH2 and BMI1. Three of nine patients exhibited increased levels of BCR||ABL1 after 12 months; in all these cases BMI1 also increased vs the previous timepoint; in 2 of them also EZH2 expression increased.

Conclusion. Although the role of BMI1 and EZH2 as prognostic markers has been established in other malignancies, it remains unclear in CML. The expression of BMI1 increases after 3 months of treatment, which appears to correlate with potential TKI resistance. After 6 months of treatment, the correlation between BMI1 and BCR||ABL1 is confirmed; after 12 months, the simultaneous increase of BCR||ABL1, BMI1, and EZH2 suggests a potential prognostic function for these epigenetic genes. The correlation between expression of BMI1 and EZH2 observed at diagnosis might be explained, as observed in other solid tumors, by the action of EZH2 that, by deregulating the mi-200c, seems to be able to sustain the expression of BMI1. Future studies with a larger cohort are obviously needed to confirm the data.

This study has been performed in the context of the project Bando Salute 2018 "StemCMLCure" PI Prof. Bocchia.

P019

MEK1/2 KINASES DISABLE THE TUMOR SUPPRESSOR FUNCTIONS OF NATIVE BCR AND ABL1 KINASES TO IMPAIR ANTICANCER DRUGS' RESPONSIVENESS IN TKI-RESISTANT PHILADELPHIA POSITIVE LEUKEMIAS

L. Mazzer^{1,2}, M. Abeltino², G. Lombardi¹, A.M. Cantoni³, S. Jottini³, A. Corradi³, M. Ricca¹, E. Rossetti^{2,4}, F. Armando^{3,5}, A. Peli⁶, A. Ferrari⁷, G. Martinelli^{7,8}, M.T. Scupoli⁹, C. Visco¹⁰, M. Bonifacio¹⁰, A. Ripamonti^{11,12}, C. Gambacorti-Passerini^{11,12}, A. Bonati², R. Perris^{13,14}, P. Lunghi^{13,14*}

¹Istituto Zooprofilattico Sperimentale della Lombardia e dell'Emilia Romagna "Bruno Ubertini"; ²Dipartimento di Medicina e Chirurgia, Università di Parma; ³Dipartimento di Scienze Veterinarie, Università di Parma; ⁴Servizio Sanitario Nazionale ASL Piacenza; ⁵University of Veterinary Medicine Hannover, Foundation; ⁶Dipartimento per gli studi sulla qualità della vita Alma Mater Studiorum, Università di Bologna; ⁷IRCCS Istituto Romagnolo per lo Studio dei Tumori (IRST) "Dino Amadori"; ⁸Istituto di Ematologia "L. e A. Seragnoli", Dipartimento di Medicina Sperimentale, Diagnostica e Specialistica, Università di Bologna; ⁹Dipartimento di Neuroscienze, Biomedicina e Scienze del Movimento, Università degli Studi di Verona; ¹⁰Dipartimento di Ingegneria per l'Innovazione Medica, Sezione di Ematologia - Università degli Studi di Verona; ¹¹Dipartimento di Medicina e Chirurgia, Università degli Studi di Milano-Bicocca; ¹²Ematologia, IRCCS San Gerardo; ¹³Dipartimento di Scienze Chimiche, della Vita e della Sostenibilità Ambientale, Università di Parma; ¹⁴Centro Interdipartimentale di Ricerca di Oncologia Molecolare e Translazionale, Università di Parma, Italy

Introduction. Despite the recent development of novel and effective inhibitors, including the novel class of STAMP inhibitors, tyrosine kinase inhibitors (TKI) resistance remains a clinically relevant topic in the management of chronic myeloid leukemia. In addition, clinical responses to TKI drugs are short lived in advanced phases of the disease or in Philadelphia positive (Ph+) acute lymphoblastic leukemia, and therefore new treatment strategies are needed for the subset of patients who fail to respond or develop resistance to treatments with these targeted agents.

Methods. *In vitro* and *in vivo* loss- or gain-of-function approaches on model cell lines and patient-derived leukemic samples were exploited to unveil an unprecedented role of MEK1/2 in sustaining and potentiating the oncogenic and pro-survival effects of BCR::ABL1, and hindering the tumor suppressor functions of native BCR and ABL1 kinases.

Results. We demonstrated that activated MEK1/2 kinases assemble into a pentameric complex with BCR::ABL1, BCR and ABL1 to induce phosphorylation of BCR and BCR::ABL1 at Tyr360 and Tyr177, and ABL1, at Thr735 and Tyr412 residues thus provoking loss of BCR's tumor-suppression functions, enhanced oncogenic activity of BCR::ABL1, cytoplasmic retention of ABL1 and consequently drug resistance. Coherently, pharmacological blockade of MEK1/2 induces dissociation of the pentameric MEK1/2/BCR::ABL1/BCR/ABL1 complex and causes a concurrent BCR^{Y360/Y177}, BCR::ABL1^{Y360/Y177} and cytoplasmic ABL1^{Y412/T735} dephosphorylation thereby provoking the rescue of the BCR's anti-oncogenic activities, nuclear accumulation of ABL1 with tumor-suppressive functions and consequently, growth inhibition of the leukemic cells and an Arsenic trioxide (ATO) sensitization via BCR-MYC and ABL1-p73 signaling axes activation. Indeed, by leveraging on the capability of the MEK1/2 inhibitors to promote native ABL1 nuclear translocation, the subcellular compartment where it can exert its tumor suppressor functions, we could also demonstrate that the allosteric activation of nuclear ABL1 kinase activity by DPH significantly potentiates the anti-leukemic effects of the MEK1/2 inhibitor

Mirdametinib on model leukemic cell lines and patient-derived leukemic blasts. Lastly, the Mirdametinib/ATO combination significantly prolonged the survival of mice bearing BCR::ABL1^{T3151}-induced leukemia.

Conclusions. Our findings reveal a novel oncogenic functional interplay between MEK1/2, ABL1 and BCR signaling kinases, which if pharmacologically disabled by antagonizing MEK1/2 actions renders leukemia cells vulnerable to the ABL1 allosteric activators or antitumor agent ATO with consequent implications for the treatment of TKI-resistant Ph+ leukemias. In fact, our data indicate that repurposing FDA-approved MEK1/2 inhibitors in combination with ATO may represent a novel alternative strategy for the subset of patients who fail to respond and/or develop resistance to standard-of-care TKIs treatments.

P020

SETD2 LOSS CONTRIBUTES TO CHRONIC MYELOID LEUKEMIA PROGRESSION AFFECTING DNA INTEGRITY AND EPIGENETIC LANDSCAPE

M. Mancini¹, S. De Santis², C. Monaldi², S. Bruno², A.C. Taccini², F. Castagnetti², G. Gugliotta¹, A. Iurlo³, M. Cerrano⁴, S. Galimberti⁵, S. Balducci⁵, M. Cavo^{1,2}, S. Soverini¹

¹IRCCS Azienda Ospedaliero-Universitaria di Bologna, Istituto di Ematologia "Seràgnoli"; ²Dipartimento di Scienze Mediche e Chirurgiche, Università di Bologna; ³UO Onco-ematologia, Fondazione IRCCS Ca' Granda - Ospedale Policlinico; ⁴A. O. U. Città della Salute e della Scienza di Torino; ⁵Clinical and Experimental Medicine, Hematology, University of Pisa, Italy

Introduction. SETD2 is a tumor suppressor which trimethylates histone H3 at Lys36 (H3K36Me3), a key mark for transcription and DNA damage repair (DDR). We have previously reported SETD2 non-genomic loss of function in blast crisis (BC)-CML, but not in chronic phase at diagnosis. Aim of this study was to assess in CML models whether the contribution of SETD2 loss to disease progression may occur through the impairment of DDR fidelity and the perturbation of the epigenetic landscape.

Methods. SETD2 knock-down and SETD2 forced expression in LAMA84 (SETD2-proficient) and KCL22 (SETD2-deficient) cells were performed by RNAi and nucleofection, respectively. DDR activation was assessed by Western blotting and immunofluorescence. An integrated multi-omics approach of RNA-seq and ChIP-seq for H3K36Me3 and RNA Polymerase (RNAPolII) was performed in SETD2-proficient vs -deficient cells.

Results. To investigate the activation and proficiency of homologous recombination (HR) of double strand breaks (DSB) and of mismatch repair (MMR), we used chronic exposure to UV rays or a single exposure to hydrogen peroxide. Both induced DNA damage in SETD2 siRNA-depleted LAMA 84 cells. Compared to parental cells, cells silenced for SETD2 lost the ability to activate the ATM-dependent repair pathway. We also found that ATM inactivation impaired H2AX localization to the sites of DNA damage *in vitro*, and prevents the formation of RAD51 (HR) and MSH6 (MMR) repair foci. As a confirmation, SETD2 forced expression in KCL22 cells was able to restore DDR, as demonstrated by ATM and H2AX phosphorylation and RAD51 and RAD54 expression after either UV or hydrogen peroxide exposure. ChIP-seq showed that forced SETD2 re-expression rescued H3K36Me3 in coding sequences but not promoters, as expected, and identified a series of genes that are targeted by SETD2 trimethylation in CML (*e.g.*, NOTCH2) and may thus be more prone to DSBs and mutations *in vivo*. In addition, H3K36Me3/RNAPolII colocalization identified genes whose transcription is SETD2/H3K36Me3-dependent (*e.g.*, SRSF9, ZNF668, ZNF888,

ZNF414, SMARCC1, involved in DNA binding/transcription factor activity; IL21R, STRADA, CCNO, CEP170 and LRRFIP1, involved in cell cycle regulation and apoptosis; USP21 and SMURF2, involved in ubiquitination; BAZ2B, involved in epigenetic modification). Accordingly, significant changes in expression of the same genes were detected in our SETD2 on/off models by RNA-seq.

Conclusions. We have dissected some potential roles for SETD2 loss of function in CML transformation. We have demonstrated that SETD2/H3K36Me3 deficiency is a novel, BCR/ABL1-independent mechanism of genetic instability in CML. Moreover, we have shown that SETD2/H3K36Me3 loss perturbs that expression of key cellular genes, including known oncogenes and tumor suppressors, and may compromise their sequence integrity after DNA damage.

Supported by AIRC IG 2019 grant (23001) and by Italian Ministry of Health, project GR-2016-02364880.

P021

DIFFERENT IN VITRO MODELS OF CHRONIC MYELOID LEUKEMIA HAVE DIFFERENT RESPONSES TO THE SAME TREATMENTS

A. Cavalleri^{1,2}, S. Bernardi^{1,2}, S. Mutti^{1,2}, B. Xhahysa^{1,2}, M. Farina¹, A. Leoni^{1,2}, L. Garuffo^{1,2}, R.M. Ferraro³, E. Morello¹, V. Radici¹, E. Accorsi Buttini¹, N. Polverelli¹, M. Malagola¹, D. Russo¹

¹Department of Clinical and Experimental Sciences, University of Brescia, Unit of Blood Diseases and Bone Marrow Transplant, ASST Spedali Civili of Brescia; ²Centro di Ricerca Emato-Oncologica AIL (CREA), ASST Spedali Civili of Brescia; ³Department of Molecular and Translational medicine, University of Brescia, "Angelo Nocivelli" Institute for molecular medicine, ASST Spedali Civili of Brescia, Italy

Introduction. In the field of Chronic Myeloid Leukemia (CML), several *in vitro* models are available and recognized to be equivalent biological replicates. To date, no study has been conducted to define the unique characteristics of distinct CML cell lines and how they can affect the results of the experiments. This study aims to compare 3 *in vitro* CML models (K562, LAMA84, and KCL22 cell lines) treated with 5 tyrosine kinase inhibitors (TKIs) through a multiparametric approach.

Methods. K562, LAMA84 and KCL22 cells were treated for 48h with 5 TKIs: imatinib (IMA), nilotinib (NILO), dasatinib (DASA), bosutinib (BOSU), ponatinib (PONA). Untreated K562, LAMA 84, KCL22 and cells treated with DMSO served as controls (CTR). Morphological differences were evaluated by light microscopy. Commercial kits were used to test enzymatic activity, cell viability, and intake of glutamate (GLU) as metabolic activity. The transcript levels of disease (BCR-ABL1) and myeloid (CD33 and CD11[b] markers) were assessed by digital PCR (dPCR). A total of 63 conditions were considered (21/line).

Results. Untreated cell lines exhibit a round morphology and intact membranes. Cells concentrate in the central part of the well, forming small clusters and high-density areas, especially for K562 and KCL22, while LAMA84 present a higher variable shape. TKIs induce a visible reduction in cell number in all 3 lines, especially under NILO, DASA, and BOSU, while IMA has the lowest impact in cell morphology. In contrast, all TKIs significantly affect LAMA84 morphology. In general, TKIs therapy reduces the enzymatic activity. Comparing the models, no significant variation is found in CTR, BOSU and PONA groups, whilst substantial differences emerge in DMSO, IMA, NILO and DASA ones (Figure 1A). Similarly, cell viability decreases following TKIs therapy with significant inter-model differences in IMA and BOSU groups (Figure 1B). The overall amount of extracellular GLU decreases in all cell lines post-treat-

ment, suggesting an increased GLU intake favoured by TKIs. Inter-model variations are appreciated among single TKIs group (Figure 1C). As expected, TKIs administration strongly reduces BCR-ABL1 levels with inter-models differences appreciable in IMA and NILO (Figure 1D). The same decreasing trend is observed for CD33 and CD11b for all TKI treatments without differences between the cell models, even if strong variables are appreciable in the CTR due to vary basal expression levels.

Conclusions. This is the first time that 3 different CML cell lines are compared in terms of several biological aspects. These data demonstrate that each CML cell lines, given the different origin, is morphologically, phenotypically, and metabolically singular and emphasize the importance of using more than one cell line to generate more robust results. Different disease *in vitro* models cannot be considered as equal biological replicates for every type of experiments and reflect the variability observed between patients.

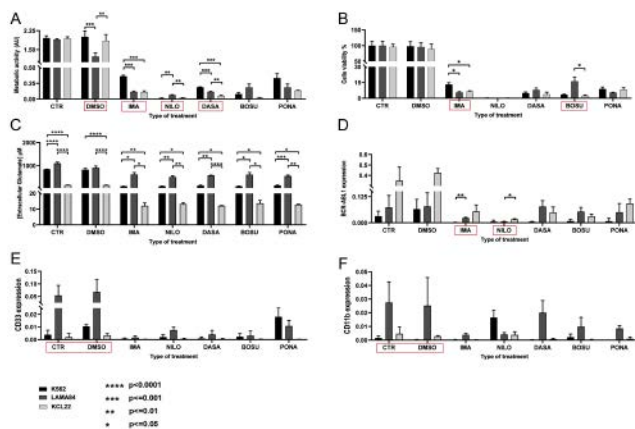


Figure 1.

P022

THE FTO RNA DEMETHYLASE INHIBITOR FB23-2 IMPAIRS CML CELLS PROLIFERATION BY DISRUPTING PYRIMIDINE SYNTHESIS VIA AN UNCHARACTERIZED INHIBITION OF DIHYDROOROTATE DEHYDROGENASE

M. Tarullo¹, G. Fernandez Rodriguez¹, A. Iaiza¹, B. Cesaro¹, S. Masciarelli², E. Bochenkova⁵, M. Giorgis⁴, D. Rotili³, A. Mai³, A. Cafilisch⁵, M. Lolli⁴, F. Fazi², A. Fatica¹

¹Dipartimento di Biologia e Biotecnologie “Charles Darwin”, Sapienza Università di Roma; ²Dipartimento di Medicina Anatomica, Istologica e Forense e Scienze Ortopediche, sezione di Embriologia Istologica e Medica, Sapienza Università di Roma; ³Dipartimento di Chimica e Tecnologie del Farmaco, Sapienza Università di Roma; ⁴Dipartimento di Scienza e Tecnologia del Farmaco, Università di Torino; ⁵Department of Biochemistry, University of Zurich

Introduction. FTO, an RNA N6-methyladenosine (m⁶A) demethylase, has been reported to promote leukemogenesis and resistance to tyrosine kinase inhibitors. To explore the therapeutic potential of targeting FTO in chronic myeloid leukemia (CML), we tested two newly characterized FTO inhibitors, FB23-2 and CS2, which have shown antitumor activity in acute myeloid leukemia (AML) pre-clinical models.

Methods. CML cells were treated with FB23-2 and CS2, evaluating the impact on proliferation and cell cycle. Liquid chromatography–mass spectrometry (LC–MS) was performed to measure m⁶A levels and evaluate the inhibitor impact on FTO activity. To identify

the molecular pathways affected by FTO catalytic inhibition, we investigated the effects of the inhibitors on the transcriptome and metabolome, by RNA-sequencing (RNA-seq) and gas chromatography–mass spectrometry (GC-MS), respectively.

Results. Treatment with FB23-2 and CS2 CML cells significantly decreased proliferation potential and induced a notable cell cycle arrest, particularly in the S and G2/M phases. RNA-seq analysis revealed the downregulation of several amino acid receptors upon FB23-2 treatment. One of the most significantly modulated receptors we identified was SLC7A5 (LAT1), involved in leucine import and, subsequently, in the activation of the mTORC1 pathway. However, metabolomic analysis using GC-MS indicated significant changes in amino acid levels for glutamate, aspartate, and proline exclusively. Notably, we observed a substantial accumulation of dihydroorotate (DHO) in FB23-2 treated conditions. DHO serves as an intermediate in pyrimidine synthesis, converted into orotate through the action of dihydroorotate dehydrogenase (DHODH), an enzyme located in the mitochondrial intermembrane space. The pronounced DHO accumulation suggested a potential FB23-2-mediated inhibition of DHODH, as further confirmed by docking analysis. Furthermore, CS2, also known as Brequinar, has previously been developed as a potent and highly specific inhibitor of DHODH. Therefore, we analyzed the proliferation potential of various leukemic cell lines (CML and AML) treated with FB23-2 and CS2, both with and without uridine, a molecule capable of restoring pyrimidine biosynthesis by bypassing orotate deficiency. Uridine fully compensated for the effects of both inhibitors at lower doses and partially at very high doses of FTO inhibitors. Additionally, the measurement of m⁶A levels by LC-MS/MS demonstrated non-significant changes even at doses where anti-proliferative effects of the inhibitors were evident.

Conclusions. Our data suggest that the previously described FTO inhibitors, FB23-2 and CS2, primarily target DHODH, leading to their anti-tumoral effects, which are predominantly linked to nucleotide deprivation, rather than an increase in m⁶A levels.

P023

THE SURPRISING EFFECTS OF LITHIUM IN COMBINATION OR NOT WITH TKIS ON DIFFERENT CHRONIC MYELOID LEUKEMIA *IN VITRO* MODELS

A. Cavalleri^{1,2}, S. Bernardi^{1,2}, S. Mutti^{1,2}, B. Xhahysa^{1,2}, M. Farina¹, A. Leoni^{1,2}, L. Garuffo^{1,2}, R.M. Ferraro³, E. Morello¹, V. Radici¹, E. Accorsi Buttini¹, N. Polverelli¹, M. Malagola¹, D. Russo¹

¹Department of Clinical and Experimental Sciences, University of Brescia, Unit of Blood Diseases and Bone Marrow Transplant, ASST Spedali Civili of Brescia; ²Centro di Ricerca Emato-Oncologica AIL (CREA), ASST Spedali Civili of Brescia; ³Department of Molecular and Translational medicine, University of Brescia, “Angelo Nocivelli” Institute for molecular medicine, ASST Spedali Civili of Brescia, Italy

Introduction. Lithium (LI) has been known to have hematological effects since the 1980s. However, in the context of Chronic Myeloid Leukemia (CML), just one study investigated the interaction between LI and nilotinib on a single *in vitro* model. No additional study has been reported on the effects of LI used alone or with other TKIs. Thus, we conducted a multiparametric analysis employing 3 *in vitro* CML models (K562, LAMA84, and KCL22 cells) cultured with different TKIs combinations +/- LI.

Methods. Cells were treated with LI alone or with 5 TKIs, namely imatinib, nilotinib, dasatinib, bosutinib, and ponatinib. LI was added for 96 h, to replicate the effects of a chronic administration, while TKIs for 48 h. Cells treated with DMSO and untreated K562, LAMA84 and KCL22 served as controls. Light microscopy was used

Myelodysplastic Syndromes

P024

ABSTRACT NOT PUBLISHABLE

P025

INFLAMMAGING VERSUS INFLAMMATION IN MDS. IS AGING A PRE-MDS STATE?

E. Tofacchi^{1,2}, G. Mattiuzi¹, M.G. Raddi^{1,3}, S.J.M. De Pourcq^{1,2}, M. Cassari¹, C. Amato^{1,3}, A. Consagra^{1,3}, L. Rigodanza^{1,3}, S. Bandinelli⁴, M. Tantarli⁵, S. Kordasti^{6,7}, L. Ferrucci⁸, V. Santini^{1,3}

¹Laboratorio sindromi mielodisplastiche, University of Florence; ²Medical biotechnology, University of Siena; ³MDS-Unit, hematology, AOU Careggi; ⁴Geriatric Unit, Azienda Toscana Centro; ⁵Department of Experimental and clinical medicine, University of Florence; ⁶System Cancer Immunology, Comprehensive Cancer Centre, King's College London; ⁷Hematology Department & Stem Cell Transplant Unit, DISCLIMO-Università Politecnica delle Marche; ⁸National Institute of Aging

Introduction. Myelodysplastic neoplasms (MDS) encompass a heterogeneous group of hematopoietic disorders, mainly affecting elderly individuals (median age 73y), characterized by hematopoietic inefficiencies and a proclivity for the transformation into acute myeloid leukemia (AML). Elderly healthy subjects share many characteristics with LR-MDS patients including inflammation state and compromised T cells expansion and activation. For these reasons, diagnosis of MDS may be often challenging. In this study we analyzed the inflammatory cytokines in LR-MDS vs elderly subjects, and we assessed the effect of the most significant ones on PBMCs isolated from LR-MDS patients and healthy controls.

Methods. MDS patients were selected based on age, WHO classification and IPSS-R criteria (Intermediate, Low and very low) referred to MDS Unit, Florence. Healthy subjects were evaluated in the InChinaty study, but those <60 years old with known inflammatory comorbidities or treated with anti-inflammatory drugs were excluded from evaluation. The 2 analyzed cohorts consisted of 60 cases each. We then measured 36 pro-inflammatory cytokine serum levels by Bioplex assay. Peripheral blood mononuclear cells (PBMCs) from 3 healthy donors and 2 LR-MDS patients (median age=79y; MDS-RS; very low) were stimulated with cytokine cocktails specific to LR-MDS or healthy subjects. T cell subpopulation (CD3+, CD8+, CD4+, CD25+, CD127+) were assessed at different time points (0, 3, 5, and 7 days).

Results. We identified 9 cytokines that statistically differ between the two cohorts. Specifically, CCL2, CCL11, CXCL4, IL-6, IFN γ and IFN α were more present in healthy subject samples (HC-C), whereas IL1 β , IL2 and IL15 were increased in LR-MDS samples (MDS-C) (Figure 1). We also observed that LR-MDS PBMCs stimulated with MDS-C showed a trend to gradual increase in CD8+, and Treg expansion. Healthy PBMCs cells treated with MDS-C revealed a time-dependent increase in CD8+ cells and decrease in Treg population (Figure 2a-2c). In LR-MDS cells exposed to HC-C present a decreased in CD8+ and Treg cell expansion (Figure 2b-2d).

Conclusion. We determined that LR MDS and healthy subjects are characterized by different production of proinflammatory cytokines (MDS-C and HC-C). These specific signatures differentially influence Tregs and the CD8+ population. MDS-C promote a cytotoxic environment by enhancing CD8+ expansion in both isolated PBMCs. This observation could elucidate some aspects of LR-

to assess cells' morphology. Using 3 *in vitro* kits, metabolic activity, cell viability, and glutamate intake (GLU) were measured. Digital PCR was applied to quantify the transcripts of the BCR-ABL1 and CD33/CD11b as disease and myeloid differentiation markers, respectively. A total of 72 conditions were considered (24/line).

Results. Untreated cell lines have round form and intact membrane. They concentrate in the middle of the well to create high-density regions and small clusters. In all models, LI alone impacts the cell numbers. Cells are rich in cytoplasmic granules, variable in shape and with altered membrane structure. These characteristics are amplified in LI+TKIs conditions. LI causes a significant reduction in metabolic activity in every cell line, that is exacerbated when TKIs are added. When comparing LI and LI+TKIs, this decrease is as well significant (Figure 1A). Similarly, the cell viability is decreased by LI in every model, with higher reduction by LI+TKIs and the comparison of 2 treatments is still significant (Figure 1B). The analysis of GLU, affected by CML pathogenesis as well as LI, reveals an increase of GLU intake supported by LI, more so when combined with TKIs in K562 and LAMA84 (Figure 1C). Conversely, in KCL22 GLU retention increases only when LI is administered with TKIs. Then, LI and LI+TKIs have a similar impact on the expression of BCR-ABL1, resulted reduced in all models (Figure 1D). In K562 and LAMA84, which constitutively express both CD33 and CD11b, LI alone causes a decrease in those markers in both. When LI is combined with TKIs, the transcripts rose variably in these 2 lines. In KCL22, which don't basally present CD33 and CD11b, LI induces their increment, lower in combination with TKIs (Figure 1E-F).

Conclusions. This study is the first to examine the effects of LI both by itself and in combination with 5 TKIs currently used in clinical practice. It suggests that LI, +/- TKIs, affects vitality, metabolic activity and differentiation in CML cells. Future research on *in vivo* and *ex vivo* models will clarify the biological mechanisms of LI effects and the hypothetical additive effect of the molecules' combination.

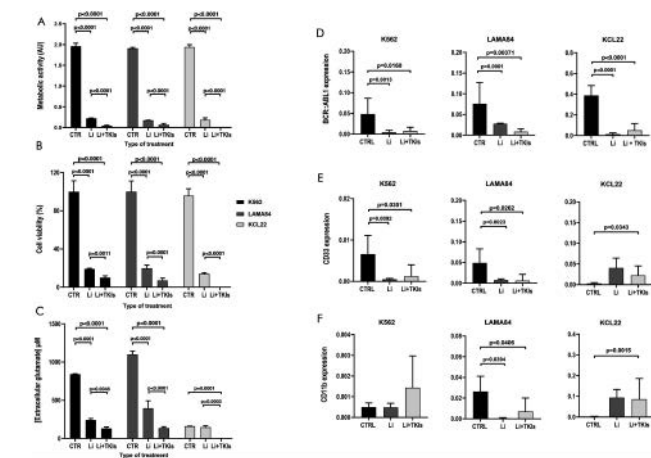


Figure 1.

MDS biology. From our data, we may hypothesize that chronic exposure to an inflammatory environment may trigger Treg-mediated response although insufficient to limit CD8+ cells expansion in LR-MDS.

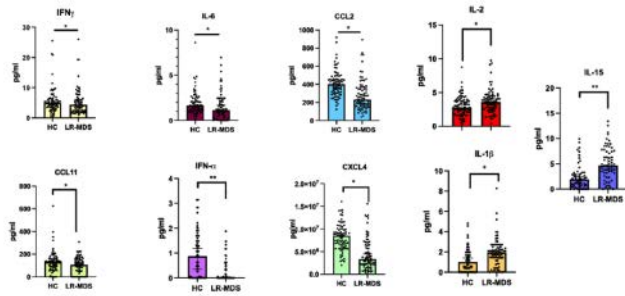


Figure 1. Cytokines level detected in serum collected from LR-MDS patients and healthy elderly donors.

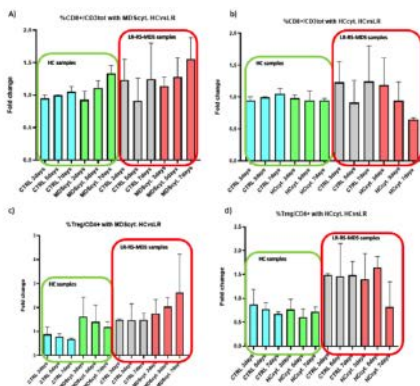


Figure 2. Impact of MDS and HC Cytokines on T cells subpopulation expansion.

Figures 1 and 2.

P026

UNVEILING THE ROLE OF APOPTOTIC AND PLCS-RELATED PATHWAYS IN MYELODYSPLASTIC SYNDROMES (MDS) TREATED WITH AZACYTIDINE AND VENETOCLAX

I. Casalin^{1a}, E. Ceneri^{1a}, A. De Stefano^{1*}, A. Cappellini¹, L. Manzoli¹, S. Ratti¹, L. Cocco¹, A. Curti², M. Cavo², L. Zannoni², M. Fogli², G. Cristiano², S. Parisi², S. Paolini², C. Finelli², M.Y. Follo¹

¹Department of Biomedical and Neuromotor Sciences, Cellular Signalling Laboratory, University of Bologna; ²IRCCS Azienda Ospedaliero-Universitaria di Bologna- Istituto di Ematologia “Seràgnoli”, Italy

Introduction. The combination of Venetoclax (VEN) with Azacytidine (AZA) is effective in both AML and high-risk MDS (Bazinet et al, Curr Treat Options Oncol, 2022). Additionally, Phospholipase C (PLC) β 1 has been identified as a direct target of AZA and is associated with a favorable response in high-risk MDS (Cocco et al. J Leuk Biol, 2015), where it can also regulate apoptotic pathways. In this study, we explored the molecular mechanism of AZA+VEN in both high-risk MDS patients and leukemic cell lines.

Methods. Mononuclear cells were obtained from at least 10 higher-risk MDS (RAEB-1, RAEB-2, R-IPSS High or Very High, Com-

plex Karyotype) or secondary AML (sAML) patients, treated with AZA (n=6) and AZA+VEN (n=4) and came from the IRCCS-Institute of Hematology “L e A Seràgnoli” in Bologna. Molecular analyses were carried out both at the time of diagnosis and during the therapy. In addition, THP-1 and MV4-11 leukemic cells, serving respectively as *in vitro* models for VEN resistance and sensitivity, were treated with AZA, VEN and AZA+VEN. After 24-hours, flow cytometry, gene expression and Western Blot analyses were performed to evaluate the effect of the treatments.

Results. Our results revealed a significant increase in PLCB1 gene expression in AZA-responder patients (R) and AZA+VEN-R patients. In the same groups of patients there is a significant change in apoptotic markers expression (BAX increase, BCL-2 decrease). *in vitro* analysis showed a rapid and strong *in vitro* cell death increase in both cell lines (Sub-G0 cell cycle phase increase), as well as a reduction of the G0-G1 cell cycle phase in MV4-11 cells. Annexin V-PI analysis demonstrated an increase in apoptotic cell death following AZA and AZA+VEN in both cell lines, while VEN only heightened cell death in MV4-11 cells. Western blot assays clearly indicate a reduction in the full-length form of Caspase 3 and an increase in the cleaved form of PARP after AZA+VEN, confirming the presence of a caspase-dependent apoptotic mechanism. Expression analysis of anti-apoptotic (BCL-2) and pro-apoptotic (BAX, BIM, PUMA, BAK1) genes unveiled the impact of AZA+VEN on the expression of these markers, especially in THP-1 cells. Moreover, AZA+VEN, early induced PLCB1 and positively affects the expression of myeloid differentiation markers, with a notable effect on the expression of CD14 in both cell lines.

Conclusions. All in all, our results, that must be confirmed in a larger number of patients and other leukemic cell lines, may pave the way to new molecular mechanisms in MDS response to AZA+VEN, suggesting a potential contribution of PLCs regulation and apoptotic pathways. Ongoing analyses are now investigating the implications of intrinsic or extrinsic apoptosis in the cell death mechanism induced by treatment, as well as the involvement of other key players in both inositol signalling, cell proliferation and apoptosis regulation through the combination of VEN with other drugs.

P027

EFFECT OF PLCB1 MODULATION IN MDS/AML CELL AND BONE MARROW MICROENVIRONMENT RESPONSE

E. Ceneri¹, I. Casalin^{1a}, A. De Stefano¹, A. Cappellini¹, L. Manzoli¹, S. Ratti¹, L. Cocco¹, A. Curti², M. Cavo², L. Zannoni², M. Fogli², G. Cristiano², S. Parisi², S. Paolini², C. Finelli², M.Y. Follo¹

¹Department of Biomedical and Neuromotor Sciences, Cellular Signalling Laboratory, University of Bologna; ²IRCCS Azienda Ospedaliero-Universitaria di Bologna- Istituto di Ematologia “Seràgnoli”, Italy

Introduction. Nuclear Phospholipase C (PLC) β 1 is involved in cell cycle and hematopoietic stem cell (HSC) differentiation, even in MDS and AML. HSCs co-exist with mesenchymal stromal cells (MSCs) in the bone marrow (BM) niche. Therefore, here, we aimed to better understand the interactions between MDS/AML cells and MSCs, focusing on the effect of PLC β 1 modulation and the BM response.

Methods. THP-1 monocytic cell line was transfected to obtain overexpressed and silenced PLC β 1 cells, respectively THP-1 OV and THP-1 KD. The effect of PLC β 1 modulation on the expression of specific PLCs (PLC γ 1 and PLC γ 2), differentiation markers (CD33, CD11b, CD14) and cyclins (D3, B1, E1) was analysed by Real-Time PCR on THP-1 cells cultured alone and after 96h of co-culture with HS-5 stromal cells. The effect of PLC β 1 modulation on

the cytokine secretion was analysed through ELISA assay after co-cultures. *Ex vivo* analyses of at least 10 MDS samples (IPSS-R low, intermediate or high) are ongoing: we are analyzing samples at diagnosis and during epigenetic therapy to find out those with increased or reduced PLC β 1 expression, to recapitulate the overexpressed/silenced *in vitro* model. In the same samples we are also analysing the expression of myeloid differentiation markers and cyclins and we are trying to set up the co-cultures.

Results. THP-1 wild-type cells, when co-cultured with HS-5 cells, exhibited an increase in PLC γ 1 expression, a reduction in the late myeloid differentiation markers, and diminished cyclin expression. THP-1 OV cells showed a decrease in myeloid differentiation markers. However, when THP-1 OV cells were co-cultured with HS-5 cells, we continued to observe a decrease in CD11b, but also a slight increase in cyclin B1 expression. Conversely, silencing PLC β 1 and setting up the co-cultures resulted in a reduction of CD14 and diminished cyclin B1 expression, suggesting an inverse relationship between PLC β 1 and cyclin B1 in our THP-1 cells. Both overexpression and silencing of PLC β 1 were correlated with the inhibition of IL-8 secretion, with the addition of a selective secretion of IL-1 β when cells were co-cultured with HS-5. Instead, THP-1 PLC β 1 KD cells in co-culture with HS-5 cells showed an increased secretion of IL-1 α . Among our MDS patients, we found out 4 higher risk MDS patients with high baseline PLC β 1, and ongoing analyses are profiling the other samples. *Ex vivo* MDS cells are also being co-cultured with MSCs to investigate the mechanisms of BM response.

Conclusions. All in all, our results suggest a role for PLC β 1 in leukemic cell differentiation and proliferation, before and after co-culture. Preliminary analyses are now focusing on the effect of PLC β 1 modulation on the mesenchymal counterpart, and we are profiling the expression of all molecules in patients showing an increased/decreased PLC β 1, to better understand PLC β 1 role in MDS/AML progression and pathogenesis.

P028

THE ROLE OF FLOW CYTOMETRY IN THE DIAGNOSIS OF ADVANCED MYELODYSPLASTIC SYNDROMES AREB-1 AND AREB-2

F. Mattioli¹, V. Pezzoni¹, E. Camaioni¹, D. Maravalle¹, F. De Giorgi², A. Bracischi², S. Mattioli¹, S. Angelini¹, P. Galieni¹

¹U.O. C Ematologia, Ospedale C. G. Mazzoni; ²Dipartimento di Anatomia Patologica, Ospedale C. G. Mazzoni, Italy

In recent years, flow cytometric analysis (FCM) is a valuable tool in the workup of Myelodysplastic Syndromes (MDS) and in the evaluation of cytopenic patients, as recommended by the European Leukemia Net 2023 guidelines. Although there is no universal consensus in the literature on the optimal approach of flow cytometry for MDS, the diagnosis by flow cytometry has been the subject of numerous systematic analyses. Due to its speed of execution, flow cytometry analysis complements and adds to routine diagnostic investigations in patients with undiagnosed cytopenia and suspected MDS. The purpose of this work is to illustrate the role of flow cytometric analysis in the diagnostic process of advanced myelodysplastic syndromes such as refractory anemia with excess blasts 1-2 (AREB-1 and AREB-2). From March 2006 to August 2023, 381 patients with suspected MDS at the U. O. C of Hematology and Cellular Therapy Unit of the C. G. Mazzoni hospital of Ascoli Piceno, were enrolled in this study. Of the 381, 102 patients (27%) were diagnosed with myelodysplasia type AREB-1 and AREB-2, according to the 2016 WHO classification. Bone marrow samples were used for osteomedullary biopsy (BOM), Myelobiopsy and flow cytometric analysis to define the percentage of CD34+ blasts. A total of 51 of

102 (50%) showed a percentage of myeloid precursors ranging from 5 to 19% on BOM, myelobiopsy, and FCM. From the correlation of the percentages of blasts found in the 51 patients, a statistically significant difference emerged (Friedman test, $p=0.0006$) from the FCM, myelobiopsy and BOM. In particular, a statistically significant difference was found in the percentages of myeloid precursors between BOM (12%) and FCM (9%) (Wilcoxon signed-rank test, $p=0.0001$) and between Myelobiopsy (11%) and FCM (9%) (Wilcoxon signed-rank test, $p=0.0146$). The percentage of blasts was also correlated between BOM (12%) and myelobiopsy (11%) and there is no statistically significant difference, therefore the data obtained are concordant. In conclusion, from this work it was observed that there is no correlation between flow cytometry analysis, BOM and myelobiopsy on the correct percentage of blasts in patients with MDS. In addition, it has been observed that FCM is very useful to define a dysplastic bone marrow even if it underestimates the percentage of blasts compared to BOM and mybiopsy.

P029

EFFICACY OF LUSPATERCEPT IN MDS/MPN-RS-T. A CASE REPORT

L. Sijoni, M.C. Caparello, F. Facella, I. Rina, I. Santo, F. Ricci, G. Buda, C. Baratè, E. Benedetti, S. Landi, S. Galimberti

AOUP, Italy

The results of “MEDALIST” study, led to approval of luspatercept by the US FDA and the EMA for the treatment of anemia in adults with low-risk MDS-RS requiring ≥ 2 RBC units/8 weeks after ESA failure. We report the case of an 83-year-old man affected by MDS/MPN-RS-T treated by combination of luspatercept and hydroxyurea.

Methods. Patient presented us for normocytic anemia and mild white blood cells reduction but normal PLT. After one month, the blood cell count showed WBC $5.3 \times 10^9/L$, ANC $3.4 \times 10^9/L$, HB 8.6 g/dL, and PLT $524 \times 10^9/L$. Bone marrow examination showed marked signs of dysplasia, with 40% of ring sideroblasts. Diagnosis of MDS-RARS was done. Patient received alpha erythropoietin 40,000 UI/week (sc), with recovery of Hb values up to 12.5 g/dL. After 2 years, Hb was 9.7 g/dL not with standing the continue erythropoietin support, with PLTs in progressive increase. The abdomen US documented spleen longitudinal diameter 155 mm. In April 2021, patient became transfusion-dependent and abdominal US showed further spleen enlargement 164 mm. A new bone marrow examination was performed: ring sideroblasts were 57% and blasts percentage under 5%; JAK2 gene resulted mutated. ASA 100 mg/day was started. In February 2022, HB was 7.9 g/dL and PLT $776 \times 10^9/L$, with spleen further enlargement (190 mm). In October 2022 patient started luspatercept treatment, patient's disease profile showed spleen longitudinal diameter 198 mm, HB 9.1 g/dL, WBC $5.07 \times 10^9/L$, PLT $612 \times 10^9/L$ and a transfusion need up to 6 RBC units/8weeks. 3. Results After 2 dose of luspatercept, the transfusion need reduced to 2 RBC units/8 weeks (reduction of 30%) while PLT increased up to $900 \times 10^9/L$. In December 2022, HB reached 9.8 g/dL without transfusion support, but PLT count resulted in further increase. We added hydroxyurea. In January 2023 the spleen diameter decreased from 198 to 165 mm; the Hb reduced to 8.1 g/dL, therefore luspatercept was increased to 1.33 mg/Kg. The overall transfusion support from October 2022 to August 2023 was 6 RBC units. The abdomen US in August 2023 showed splenomegaly 165 mm. The follow up is still ongoing.

Conclusions. In our patient, luspatercept appeared a good option, in line with results from “MEDALIST” trial. In this study, 23 patients with MDS/MPN RS-T were enrolled. The TI occurred in 83.3% of

cases showing a low transfusion need if treated with luspatercept vs in 50% in the placebo arm, and in half of patients with high-transfusion need vs none in the placebo cohort. The history of our patient confirms these results. In addition, the combination of luspatercept with HU at low dose allowed to control PLTs and spleen dimensions decreased of 16%. The contemporary introduction of luspatercept and HU, the reduction of splenic dimensions and a not yet documented effect of luspatercept on splenomegaly in the literature arises a doubt in the discrimination of the cause of our feedback.

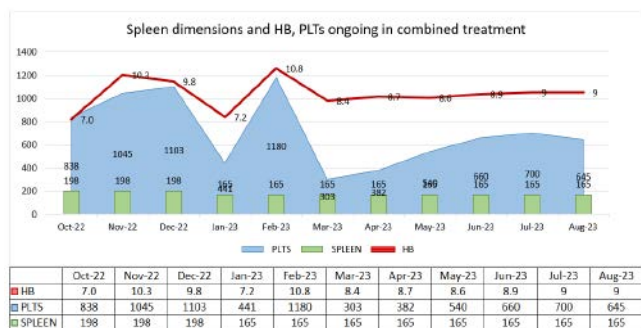


Figure 1.

Acute Leukemia

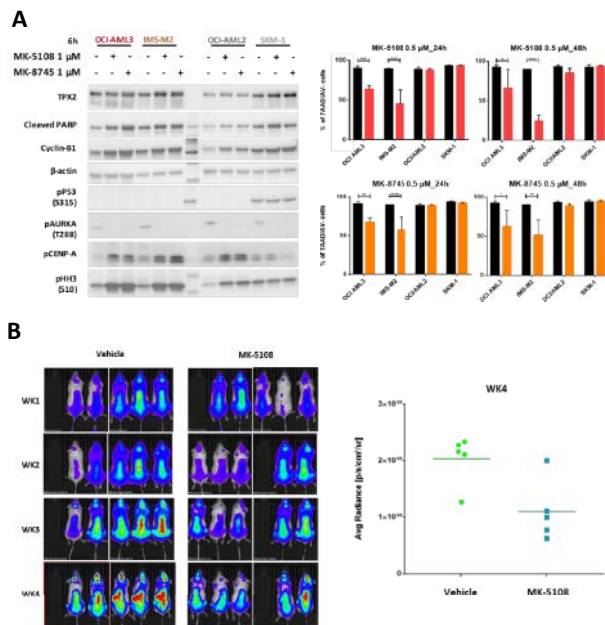
P030

PRECLINICAL VALIDATION OF AURKA-I AND THEIR PROMISING ACTIVITY IN COMBINATORIAL STUDIES AS A NEW TREATMENT STRATEGY IN NPM1-MUTATED AML

R. Ranieri¹, S. Silvestri¹, F. Milano¹, S. Pierangeli¹, S. Donnini¹, S. Cipriani¹, E. Padiglioni¹, V. Tini¹, G. Spinozzi¹, M. Neuenschwander², S. Kleissle², J.P. Von Kries², I. Gionfriddo¹, M.P. Martelli¹

¹Hematology and Clinical Immunology, Department of Medicine and Surgery, University of Perugia; ²Leibniz-Forschungsinstitut für Molekulare Pharmakologie

Introduction. One-third of adult AML patients present the *NPM1* mutation. Despite its high frequency and progress in the treatment of *NPM1*-mut AML, targeted therapy is not yet available. The Ser/Thr kinase Aurora A (AURKA) controls centrosome maturation, bipolar spindle assembly, and cellular mitotic entry explaining its association with oncogenesis. AURKA is frequently overexpressed in AML and is associated with poor clinical outcomes and aggressive tumor phenotypes. AURKA inhibitors emerged from a “designed” high-throughput drug screening (HTS) campaign developed in our lab to find specific active compounds against *NPM1*-mut AML models. Our preliminary data have identified two inhibitors that act selectively on preclinical *NPM1*-mut models (Ranieri R *et al.* Cli Lym Mye Leu. 2022). While preclinical evidence suggests that AURKA kinases are important therapeutic targets, clinical activity as monotherapy has been disappointing to date thus drug combinations could overcome these limits.



A. Western blotting analysis NPM1mut OCI-AML3 and IMS-M2 cells versus NPM1wt OCI-AML2 and SKM1 cells treated for 6h with 1 μM of MK-5108 and MK- 8745. B. NGS mice engrafted with luciferized AML patient cells were treated with MK- 5108 (164 mg/kg, BID/2 days each 14 days). Tumor burden was monitored by bioluminescent imaging

Figure 1. A. Western blotting analysis NPM1mut OCI-AML3 and IMS-M2 cells versus NPM1wt OCI-AML2 and SKM1 cells treated for 6h with 1 μM of MK-5108 and MK- 8745. B. NGS mice engrafted with luciferized AML patient cells were treated with MK- 5108 (164 mg/kg, BID/2 days each 14 days). Tumor burden was monitored by bioluminescent imaging.

Methods. *NPM1*-mut OCI-AML3 and IMS-M2 cells and *NPM1*-

wt OCI-AML2 and SKM-1 cell lines were used and analyzed after AURKAi treatment. Detection of apoptosis was performed using flow cytometry while AURKA protein expression and its cellular localization were evaluated by western blotting and immunofluorescence, respectively. A luciferized *NPM1*-mut AML PDX model for *in vivo* studies was used. For combinatorial experiments AML cell line viability was evaluated with CTB assay; data combination index(CI) values were calculated by the SiCoDEA app, developed by our group(Spinozzi G *et al.* Biomol. 2022).

Results. Our screening strategy led to identifying two structurally related and potent AURKA-selective inhibitors, MK-5108 and MK-8745, that showed the most selective activity in the *NPM1*-mut AML cells compared to wt. Using *in vitro* assays we assessed that AURKA inhibition induces defects in mitotic spindle assembly; in short-term treatment both AURKAi trigger cell cycle perturbations while long-lasting mitotic arrest provokes the formation of monopolar spindle. This results in pronounced cell death in *NPM1*-mut vs *NPM1*-wt cells evaluated by both WB and apoptosis analysis. We also assessed the anti-leukemic effect of MK-5108 inhibitor *in vivo* demonstrating its efficacy in reducing tumor burden in *NPM1*-mut PDX models compared with vehicle-treated mice. Exploiting the SiCoDEA app, we are currently testing AML cells exposed to different drugs combined with the two AURKAi. The preliminary data analysis indicates a synergistic relationship between AURKA inhibition and specific classes of compounds (*i.e.* AKT)in *NPM1*-mut AML cell lines.

Conclusions. AURKAi represents an attractive class of drugs for AML where this kinase is often overexpressed. After demonstrating the selective activity of two AURKAi in preclinical models of *NPM1*-mut AML we are now focusing on combination studies, highlighting the role of AKTi. Our approach will lay the foundation to explore new therapeutic options in *NPM1*-mut AML.

P031

THE NOVEL CHEMO-FREE COMBINATION OMACETAXINE MEPESSUCCINATE PLUS VENETOCLAX SHOWS ANTILEUKEMIC ACTIVITY IN RELAPSED/REFRACTORY NPM1-MUTATED AML WITH MYELOSUPPRESSION AS DOSE LIMITING TOXICITY IN A PHASE 1 ACADEMIC TRIAL

S. Sciolacci, V. Cardinali, S. Pierangeli, S. Donnini, F. Mezzasoma, I. Gionfriddo, F. Milano, A. Ferrari, S. Cipriani, M. Sabino, S. Silvestri, A. Stella, D. Sorcini, V. Tini, G. Spinozzi, B. Falini, P. Sportoletti, G. Martino, M.P. Martelli

Institute of Haematology, Centro Ricerche Emato-Oncologiche (CREO), "Santa Maria Della Misericordia" Hospital, University of Perugia, Italy

Introduction. In NPM1-mutated Acute Myeloid Leukemia (AML), as for other AML entities, there are no effective therapies targeting the disease-defining genetic lesion and its oncoprotein product. The challenge is to define a chemo-free approach, especially for older and relapsed/refractory (R/R) patients. Preclinical experiments in our lab showed a strong synergistic anti-leukemic effect of the combination of omacetaxine mepesuccinate (a protein translation inhibitor, that, beside Mcl-1, we demonstrated to target NPM1 mutant level) and venetoclax, with a very good tolerability and a significant survival benefit in patient-derived xenograft (PDX) murine models (Figure 1A).

Methods. Based on these data, we designed a phase I pilot clinical trial aimed at evaluating the safety and efficacy of the association of subcutaneous administration/14d of omacetaxine and orally administered/21d venetoclax in adult patients with R/R NPM1-mutated AML. Omacetaxine was administered according to a dose-escalation schedule (3+3 design) in order to define the dose limiting toxicities

(DLT) (Figure 1B). Adverse Events were graded according to the NCI CTCAE V5.0.

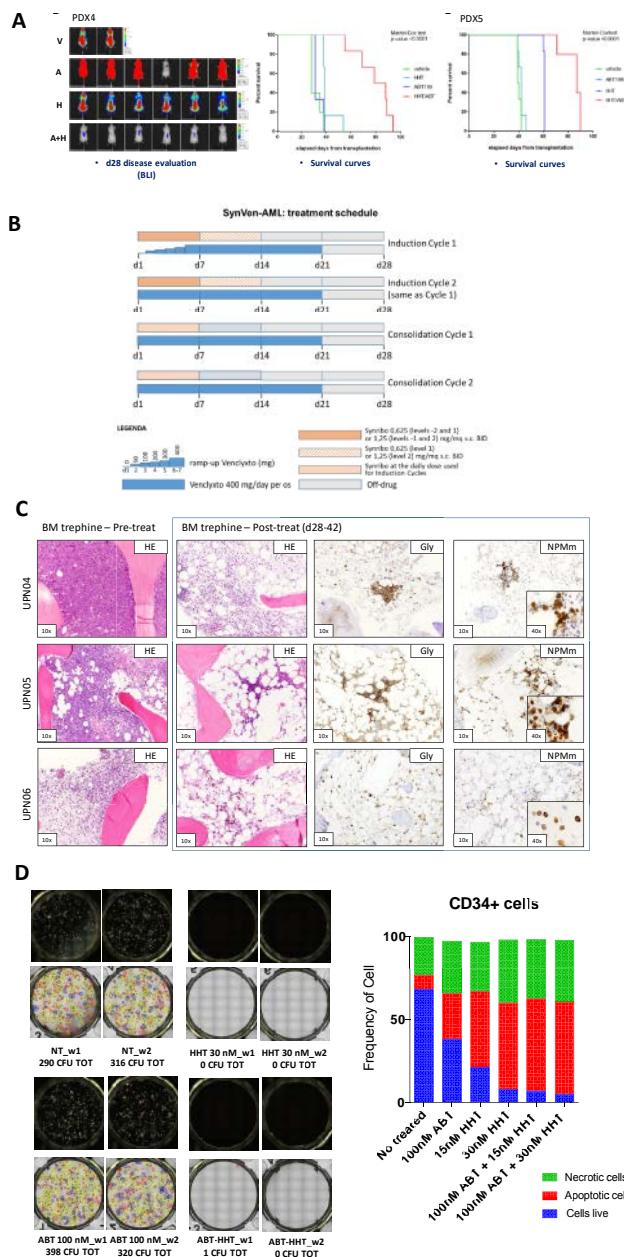


Figure 1.

Results. From June 2021 to June 2023, 6 patients were enrolled. Omacetaxine at dose Level 1 of 0.625 mg/sqm BID/14d and venetoclax/21d induced a partial remission in UPN01 with blasts clearance from 75-80% to 6-10%, and concomitant normal trilineage reconstitution, after the first cycle, whilst only a transient anti-leukemic effect with no response was observed in patients UPN02 and 03. The schedule according to Level 1 was very well tolerated, since no toxicities were registered. The next 3 patients (UPN04, 05 and 06), enrolled in Level 2 cohort, received omacetaxine at 1.25 mg/sqm BID/14d plus venetoclax/21d. In all cases, BM appeared cleared of most leukemic cells, however with little or no recovery of normal cells, raising questions of toxicity (Figure 1C). Indeed, myelosuppression was considered a DLT. Therefore, we focused our studies on toxicity, showing that continuous exposure of normal human hematopoietic stem cell *in vitro* to omacetaxine had a dose-dependent inhibitory effect on

clonogenic ability, providing a partial explanation to the clinical data of bone marrow recovery failure observed in patients (Figure 1D).

Conclusions. It is worth noting that differently from what was described in patients, *in vivo* preclinical studies did not highlight hematological toxicity phenomena in mice. Despite the great efficacy in the human AML PDX models, no survival benefits were otherwise observed in the conditional NPM1-mut AML mouse model. It is unclear whether this evident and striking difference in efficacy and toxicity between these models depends on the cell origin, human vs murine. Considering all, these observations are not only an intriguing subject of investigation, but could also be a clinically relevant issue in consideration of currently active clinical trials in US and China testing omacetaxine/venetoclax in AML patients.

P032

FLT3 ALTERATIONS AND INHIBITION IN TRIPLE NEGATIVE B-CELL ADULT ACUTE LYMPHOBLASTIC LEUKEMIA PATIENTS

A. Ferrari¹, A. Ghelli Luserna Di Rorà², F. Lo Schiavo¹, E. Fonzi³, G. Capirossi¹, C. Salvesi¹, M.T. Bocchicchio¹, L. Ledda¹, C. Servilli¹, M. Paganelli¹, G. Marconi⁴, C. Papayannidis⁵, C. Sartor⁵, M. Rondoni⁶, A.M. Mianulli⁷, B. Giannini⁸, C. Pasciolla⁹, F. Giglio¹⁰, S. Galimberti¹¹, M. Fumagalli¹², P. Salutarì¹³, A. Imovilli¹⁴, M. Endri¹⁵, V. Gaidano¹⁶, G. Martinelli¹⁷, G. Simonetti¹

¹Biosciences Laboratory, IRCCS Istituto Romagnolo per lo Studio dei Tumori (IRST) "Dino Amadori"; ²Fondazione Pisana per la Scienza ONLUS; ³Unit of Biostatistics and Clinical Trials, IRCCS Istituto Romagnolo per lo Studio dei Tumori (IRST) "Dino Amadori"; ⁴Hematology Unit, IRCCS Istituto Romagnolo per lo Studio dei Tumori (IRST) "Dino Amadori"; ⁵IRCCS Azienda Ospedaliero-Universitaria di Bologna, Istituto di Ematologia "Seràgnoli"; ⁶Hematology Unit & Romagna Transplant Network, Ravenna Hospital; ⁷Hematology, Infermi Hospital; ⁸Laboratorio Unico- AUSL della Romagna; ⁹Hematology and Bone Marrow Transplantation Unit, Istituto Oncologico IRCCS "Giovanni Paolo II"; ¹⁰Hematology and Bone Marrow Transplantation Unit, IRCCS San Raffaele Scientific Institute; ¹¹Hematology Unit, AOUNP Santa Chiara; ¹²Hematology Unit, Ospedale San Gerardo; ¹³Dipartimento Oncologia Ematologia, Ospedale Civile Santo Spirito; ¹⁴Hematology, Azienda USL-IRCCS Reggio Emilia; ¹⁵UOC Ematologia Ospedale Ca' Foncello Azienda ULSS 2 Marca Trevigiana; ¹⁶SCDU Ematologia e Terapie cellulari, A. O. Ordine Mauriziano; ¹⁷Scientific Directorate, IRCCS Istituto Romagnolo per lo Studio dei Tumori (IRST) "Dino Amadori", Italy

Introduction. The prognosis of B cell Acute Lymphoblastic Leukemia (B-ALL) patients (pts) relapsing after Hematopoietic Transplant is poor and new drugs are needed. In acute myeloid leukemia, FLT3-inhibitors (FLT3i) are showing promising results in FLT3-mutated (mut) cases. Their potential use in FLT3-mut B-ALL has been poorly investigated.

Methods. We sequenced with a capture based large RNA-seq panel (TruSight RNA Pan-Cancer, Illumina-1385 genes) 183 adult B-ALL [n=52 Positive for Ph or t(4;11) or t(1;19) and n=131 Triple-Negative (TN) pts that are negative for Ph (n=43), t(4;11) and t(1;19) translocations] and 15 donors. To confirm FLT3 mutations, 13 available samples were further sequenced with Extended Myeloid Solution (98 genes; SOPHiA) where FLT3 gene is fully covered. *in vitro* studies using 5 FLT3i [Gilteritinib (Gil), Midostaurin, Crenolanib, Sorafenib and Quizartinib] and Venetoclax (Ven) were conducted on pt primary cells and on TN and other B-ALL cell lines (MUTZ5, MHH-CALL4 Ph-like; NALM6;RS4;11, 697, REH) and 2 AML cell lines (OCI-AML3 FLT3;MV-4-11 FLT3-ITD).

Results. We found 15 FLT3 mut in 14/131 TN B-ALL and in 1/43

Ph+ cases! 43.8% were TKD mut, 3 ITD mut, 3 splicing site mut, 1 N-terminal, 1 juxta-membrane domain and 1 Immunoglobulin-like site (Figure 1A). After pathogenicity interpretation (Clinvar, VarSome, OncoKB) we excluded 3 variants and one mutation was not confirmed at DNA level. Overall 7.6% of TN were mut (Ph+ 2.3%). 81.8% of FLT3mut pts potentially druggable with FLT3i, mainly TKD (63.3%). Targeted NGS revealed the co-occurrence with other mutations (range 2-15), and in particular with CSMD1 (n=4), KDM6A, KMT2D and CREBBP (n=3) alterations. Moreover, 11/13 samples carried copy number alteration (mean 12), mostly amplifications. CDKN2A & IKZF1 were the most frequently altered genes (n=5 and 4 CN-loss). FLT3 expression was increased in 11/15 cases compared to donors and wt pts. To evaluate the effect of FLT3 inhibitors in ALL, we treated *ex vivo* primary leukemic cells of 6 adult ALL patients (FLT3-mut n=4; FLT3-wt n=2) with increasing concentrations of 5 FLT3i for 24, 48 and 72h. We observed a trend towards greater response of FLT3-mut ALL cells compared to wt ones. The average IC50 values in response to the five FLT3i was 1.6 μM and 24.5 μM after 72h of treatment in FLT3-mut and FLT3-wt B-ALL, respectively (Figure 1B). We then evaluated the sensitivity to the 5 Inhs in all cell lines. Interestingly MHH-CALL4 ALL wt were more sensitive to Gil compared to OCI AML3 wt, and showed the same effect compare to MV-4-11 AML mut (Figure 1C). Given the effect of Gil in single agent, we combined it with Ven in wt B-ALL cells at increasing concentrations. Interestingly we noticed a strong additive effect with the higher Gil concentration and all Ven doses (Figure 1D).

Conclusions. FLT3 alterations identify a novel subgroup of TN B-ALL with therapeutic potential also in combination regimens. Thanks to Ricerca Corrente by the Italian MoH L3P1946.

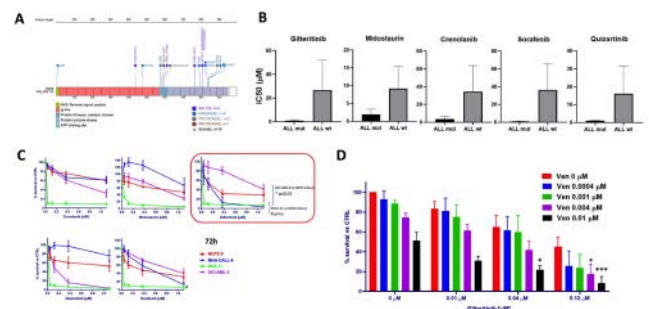


Figure 1. A) FLT3 protein diagrams and mutations in 183 adult B-ALL pts. B) IC50 evaluations with increasing concentrations of 5 FLT3i at 72h in 6 adult ALL pts (FLT3 mut n=4; FLT3 wt n=2). C) IC50 evaluations with increasing concentrations of 5 FLT3i at 72h in 2 FLT3 wt B-ALL cell lines (MHH-CALL4, MUTZ5), OCI-AML3 wt and one FLT3-ITD mut cell line (MV-4-11). D) Viability evaluation of stabilized wt B-ALL cell line treated with Gilteritinib in combination with Venetoclax at different doses (72h).

Figure 1.

P033

DIFFERENCES IN IMMUNE TRANSCRIPTOMIC PROFILE ARE ASSOCIATED WITH RESPONSE TO AZACITIDINE AND VENETOCLAX IN NEWLY DIAGNOSED UNFIT-FOR-CHEMOTHERAPY ACUTE MYELOID LEUKEMIA PATIENTS

L. Zannoni¹, D. Forte¹, C. Sartor¹, G. Cristiano¹, J. Nanni¹, S. Parisi², F. Zingarelli¹, L. Bandini¹, N. Testoni¹, E. Ottaviani², S. Paolini², C. Papayannidis², M. Cavo^{1,3}, S. Rutella³, A. Curti²

¹Dipartimento di Scienze Mediche e Chirurgiche, University of Bologna; ²IRCCS Azienda Ospedaliero-Universitaria di Bologna, Istituto di Ematologia "Seràgnoli"; ³John van Geest Cancer Research Centre, Nottingham Trent University

Introduction. The prognosis of older unfit-for-chemotherapy

patients with Acute Myeloid Leukemia (AML) has significantly improved following introduction into clinical management of the combination of Venetoclax (Ven) and azacitidine (Aza). Nonetheless, the outcome remains dismal. Although the molecular mechanisms of resistance to Ven have been widely investigated, Ven impact on the immunological microenvironment is largely unexplored.

Methods. Twenty seven patients with de novo AML unfit for intensive chemotherapy and treated with Aza-Ven were enrolled. Six patients were refractory to therapy, 21 patients achieved hematological response within cycle 4 and 7 patients relapsed during therapy. A Gene Expression Analysis (NanoString technology) was performed on bone marrow samples collected at diagnosis, at the time of response or refractoriness and at the time of relapse. A paired analysis was also performed on relapsed patients to compare the samples at diagnosis, response and relapse.

Results. The first part of the study aimed to explore the differences between responders and non-responders. An overexpression of genomic pathways related to IFN-dependent adaptive immunity, antigen presentation, priming and T-cell activation was found in responder patients. Refractory patients showed up-regulation of genes related to angiogenesis, tolerogenic inflammation such as TGFB2, and homing regulation such as ITGAV and VCAM. The second part of the study aimed to evaluate differences between patients who maintained response and those who relapsed. The relapse group showed overexpression of genes involved in the control of self-renewal, cell proliferation and differentiation, such as DLL1, FOSL1, LIF and NOTCH, and genes expressed by exhausted CD8+ T lymphocytes, such as CD244. One paired analysis on responder patients at the time of CR compared the genomic profile of those patients who relapsed with that of patients who had durable response. Interestingly, only responder patients who relapsed, and not those who maintained CR, showed at the time of CR the up-regulation of MYC and TP53, which expression has been correlated with immunomodulation of tumor microenvironment, in association with an increased expression of genes related to inflammation, such as IFN-dependent pathways, antigen presentation and T-cell activation. Of note, this profile was also associated with overexpression of genes reflecting immunotolerance, such as FOXP3, TIGIT and effector cell exhaustion, such as CTLA-4 and ICOS.

Conclusions. The study suggests that the immunological microenvironment may play a role in affecting response to Aza-Ven. Gene patterns involved in immune-mediated mechanisms typical of both innate and adaptive responses have been observed. These mechanisms can influence kinetics of AML at different time points, as well as the ability of leukemic cells to create an immune-tolerogenic and inflamed bone marrow niche in response to Aza plus Ven therapy.

P034

THE 3 ADRENERGIC RECEPTOR AS NOVEL TARGET OF METABOLIC PHENOTYPE IN T CELL ACUTE LYMPHOBLASTIC LEUKEMIA AND FLT3 MUTATION ACUTE MYELOID LEUKEMIA

C. Banella¹, G. Mattei², S. Travaglini³, L. Zocca¹, F. Carozzo¹, A. Pasha¹, A. Tondo¹, M. Calvani¹

¹Meyer Children's Hospital IRCCS; ²University of Florence Department of Information Engineering; ³University of Rome Tor Vergata Department of Experimental Medicine, Italy

Introduction. Several recent studies have shown that Beta-adrenergic receptors (β -ARs) sustain the pathogenesis of various malignant cancers. Furthermore emerging evidences demonstrated the potential therapeutic role of a selective β 3-AR antagonist (SR59230A) which exhibits a direct anti tumor activity enhancing apoptosis especially in hypoxic conditions. β 3-AR is also involved in the regulation of

lipid metabolism and glucose homeostasis in cancer cells. Therefore, high levels of β 3-AR in different T-ALL subset and in FLT3-mutated AML cells reveals a promising therapeutic target for not-responder.

Materials and Methods. Cytofluorimetric analysis of β 3-AR level expression was assessed in normal peripheral blood mononuclear cells (PBMCs), T-ALL and FLT3-mutated acute myeloid leukemia (AML) cell models. The metabolic profile after administration of SR59230A, were examined in these cell models utilizing the Seahorse XFe Analyzer. Cell viability was evaluated using MTS assay. Western blot analysis and immunofluorescence was performed for ferroptosis signature and metabolic alteration.

Results. Our findings reveal a significant upregulation of β 3-AR expression in T-ALL Molt-3 (40%), in Molt-4 (63%), in CCRF-CEM (75%) and in FLT3-mutated MV4;11 (92%) cellular models when compared to healthy PBMCs (4-7%). MTS assay detected a decrement of cell viability after administration of SR59230A in a dose dependent manner. Metabolic analysis using Seahorse XFe Analyzer unveiled intriguing differences in metabolic profiles after 72 h treatment with 15 μ M SR59230A for 72 h | no significant metabolic alterations were observed in normal PBMCs. Conversely, in T-ALL cell SR59230A treatment results in a pronounced reduction in both mitochondrial and glycolytic metabolism. Similarly in FLT3-mutated cells, the boost of basal respiration did not correlate with an increment in ATP production, leading to an increment of proton leak and to a decrement in spare reserve capacity. Following the SR 59230A treatment western blot analysis of LC3IIA expression in Jurkat (p=0.0026), Molt-3 (p=0.0001) and MV4;11 (p<0.0001) cell lines, likely mediated by the initiation of autophagy. Conversely western blot analysis revealed a substantial reduction in transferrin receptor (CD71) levels following treatment with SR59230A in MV4;11. Given the implication of CD71 in tumorigenesis and in cancer progression, targeting CD71 could be a viable approach to impede cancer progression.

Conclusions. This finding implies a specific sensitivity of T-ALL cells to β 3-AR modulation, leading to metabolic reprogramming. Furthermore, the different response of T-ALL cells compared to FLT3-mutated AML raises questions about the metabolic implications of such treatment in leukemia therapy.

P035

ABSTRACT NOT PUBLISHABLE

P036

INNOVATIVE APCIN-BASED CDC20 INHIBITORS REGULATING MITOSIS AND CELL DEATH| NOVEL THERAPEUTIC STRATEGIES AGAINST ACUTE LEUKEMIA CELLS

A. Ghelli Luserna Di Rorà^{1,3}, G. Micheletti², A. Marranci¹, F. Olimpico¹, R. Napolitano³, M. Ghetti³, L. Ledda³, M.C. Vinchesi¹, S. Bruno⁴, C. Boga², G. Simonetti³

¹Fondazione Pisana per la Scienza Onlus; ²Department of Industrial Chemistry "Toso Montanari", Alma Mater Studiorum - Università di Bologna; ³Biosciences Laboratory, IRCCS Istituto Romagnolo per lo Studio dei Tumori (IRST) "Dino Amadori"; ⁴Department of Medical and Surgical Sciences (DIMEC), Alma Mater Studiorum - Università di Bologna, Italy

Introduction. CDC20 is a vital part of the mitotic checkpoint, and it is upregulated in high-risk leukemias with complex karyotypes. Various CDC20 inhibitors, including Apcin, have been designed to target cancer cells, however with limited *in vivo* applicability due to the high effective doses. This study assesses the efficacy and mechanism of action of novel Apcin-like compounds in acute myeloid

leukemia (AML) and Philadelphia negative B-acute lymphoblastic leukemia (ALL).

Methods. We produced five structural analogues of Apcin by a multistep approach (Figure 1a). Cell viability was assessed by dose-response curves on four AML (OCI-AML3, KG1, MOLM13, and KASUMI-1) and two ALL cell lines (NALM-6 and HAL-01). We further evaluated the activity of the two most potent molecules, M3 and M4, in terms of apoptosis induction, and cell cycle regulation by flow cytometry and protein expression changes by immunoblotting.

Results. Compared to Apcin, compounds M3 and M4 were the most potent, with significantly lower IC50 values (five to ten-fold reduction)(Figure 1b). Ex vivo studies on M3 compound, also demonstrated that the treatment reduced the clonogenic capacity of patient-derived ALL cells (Figure 1c). Both M3 and M4 induced cell apoptosis even at sub-toxic concentrations, G2/M arrest and activation of the G2/M cell cycle checkpoint, as shown by increased level of phospho-CDK1Tyr15 and Cyclin B1 (Figure 1 d-f). While CDC20 expression was not altered by the treatments, its functionality was inhibited and the levels Securin, a target of the CDC20/anaphase promoting complex/cyclosome, were increased. Interestingly, even using sub-toxic concentrations, both M3 and M4 induced severe DNA damages as showed by the induction of phospho-H2AXSer139. Based on the observed effects on cell cycle checkpoint and mitosis regulation, we tested the combination of M3 or M4 with AZD6738, a specific inhibitor for the G2/M cell cycle checkpoint kinase ATR (Figure 1g) or with mitotic poisons, as vincristine and paclitaxel (Figure 1h-i). We observed a reduction of cell viability in the treated cell lines, with either synergistic or additive effects. Interestingly, no significant differences were seen combining M3 with vincristine (tubulin polymerization inhibitor) or paclitaxel (tubulin stabilizer) in terms of efficacy of the combinations.

Conclusion. We developed two powerful Apcin analogues that effectively inhibit cell viability and induce apoptosis in both AML and ALL cells. The data confirm that CDC20 activity is crucial for the survival of acute leukemia cells. Inhibition of CDC20 synergizes with ATR kinase inhibition, as well as with tubulin polymerization or depolymerization inhibitors.

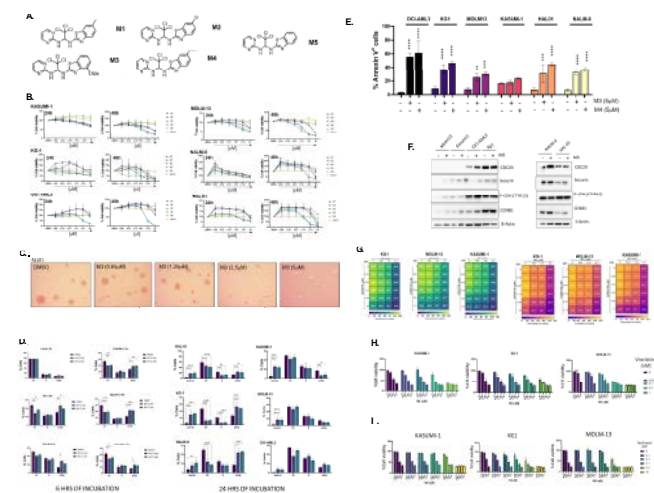


Figure 1.

P037

ABSTRACT NOT PUBLISHABLE

P038

TARGETING NPM1 MUTANT PROTEIN BY HIGH THROUGHPUT MICROSCOPY-BASED DRUG SCREENING

R. Ranieri¹, B. Neumann², C. Tischer², S. Pierangeli¹, S. Donnini¹, V. Tini¹, F. Milano¹, G. Spinozzi¹, S. Cipriani¹, E. Padiglioni¹, M. Neuenschwander³, J.P. Von Kries³, R. Pepperkok², I. Gionfriddo¹, M.P. Martelli¹

¹Hematology and Clinical Immunology, Department of Medicine and Surgery, University of Perugia; ²Advanced Light Microscopy Facility, European Molecular Biology Laboratory (EMBL); ³Leibniz-Forschungsinstitut für Molekulare Pharmakologie, Italy

Introduction. Adult patients harboring *NPM1*-mutated (*NPM1*-mut) AML malignancies have few target treatment options, especially in the setting of progressive disease. Moreover, the identification of effective therapies is hampered by the incomplete understanding of the mutated *NPM1* contribution to the development of AML. The *NPM1* protein is a ubiquitous and abundant protein that shuttles between the nucleus and the cytoplasm thanks to nuclear export signals (NES). In AML, the *NPM1* mutations cause the acquisition of new NES causing a stable cytoplasmic localization of the protein. Mutations are exclusively heterozygous resulting in dimeric *NPM1* / *NPM1*mut proteins with altered functions. Here we describe an image-based drug screening strategy to identify chemical compounds potentially active in directly targeting the *NPM1* mutant, leveraged on a high-throughput microscope technique and image analysis pipeline designed to analyze thousands of compounds.

Methods. To this end, we generated and tested a “fitting” cellular model suitable for microscopy. Using lentiviral infection of HeLa cells, the fluorescent protein eGFP sequence fused at the N-term of the *NPM1* sequence was inserted in pLVX-EF1 α -mCherry vector. A collection of 38,720 compounds belonging to different chemical libraries was sourced from the Leibniz-FMP Screening Unit (Berlin) organized in 384-well plates and screened at 1 μ M for 4 hours. Image data were analyzed with an in-house developed pipeline (CellProfiler software) in order to assess the re-localization of the *NPM1*-mutated protein while ShinyHTM software allows an easy-to-use visualization of each treated plate.

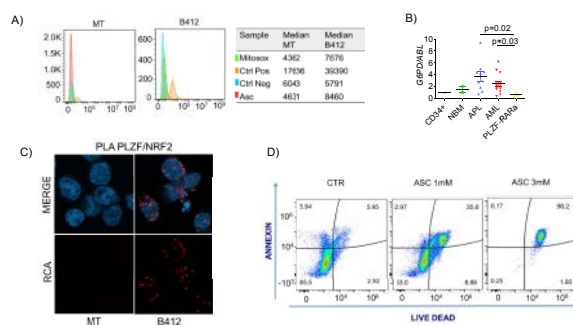


Fig 1: (A) Flow cytometry measurement of ROS in MT and B412 cells using Mitosox assay after treatment with 3 mM Ascorbate (ASC); ctrl neg, Azacitidine; ctrl positive, rtenone/antimycin. (B) qRT-PCR on G6PD mRNA in 5 PLZF/RARA positive APL patients, AML blasts and NEM samples. (C) PLZF-NRF2 protein interaction by proximity ligation assay (PLA) in MT and B412 cells. (D) Apoptosis in APL PLZF/RARA primary blast cells treated with Ascorbate (ASC, 1 and 3 mM) for two days.

Figure 1.

Results. Using an approach based on immunofluorescence, automated microscopy, and image analysis we performed a high-throughput drug screening on a cellular model ‘designed’ for monitoring the *NPM1*-mutated protein subcellular localization. Different libraries divided into 44 plate layouts of 96 well plates were tested on eGFP-*NPM1*mut-HeLa cells and subjected to image analysis. To determine

whether NPM1-mutated protein translocated from the cytoplasmic to the nucleus compartment the N (mean nuclear intensity)/ C (mean cytoplasmic intensity) ratio was obtained from the image segmentation process. The developed workflow allows the accurate identification of fluorescent cells and their cellular features such as counts, intensity, and morphology measurements. The data analysis by revealing compounds already known for their activity in mediating the re-localization of the mutated NPM1 protein (*i.e.* KPT[*i*]) demonstrates its reliability and reproducibility.

Conclusions. Our microscope-based approach taking advantage of high throughput and automatic workflow and using a cellular model expressing NPM1-mutated tagged protein represents a useful tool to identify classes of drugs able to hit NPM1 oncoprotein. Studies are ongoing in order to confirm the activity of the resulting compounds on NPM1-mutated AML cell models.

P039

MOLECULAR CHARACTERIZATION OF *MECP2* IN ACUTE MYELOID LEUKEMIA

A. Javadpoor, S. Rocco, B. Maffeo, A. Moraca, F. Itri, B. Pergolizzi, D. Cilloni, C. Panuzzo

Department of Clinical and Biological Sciences, University of Turin, Italy

Introduction. Acute myeloid leukemia (AML) stems from clonal disorders in hematopoietic stem cells driven by genetic mutations. Alongside genetic changes, epigenetic regulators are also deregulated in AML's onset. Altered expression of methylation-related genes, including *DNMT1*, *DNMT3A*, and *HDAC1* in AML patients, has spurred the use of hypomethylating agents like decitabine and histone deacetylase inhibitors in leukemia therapies. *MECP2*, a prominent epigenetic regulator, binds to methylated CpG DNA sequences, affecting nucleosome remodeling around these sequences. While *MECP2* point mutations are linked to Rett Syndrome, its amplification is seen in *MECP2* duplication syndrome and various cancers, leading to the activation of certain pathways. The role of *MECP2* in leukemogenesis, despite its known affinity for 5-methylcytosine, is not well-understood.

Methods. The study utilized leukemia cell lines MOLM-13, OCI-AML3, and K562, with a non-cancer cell line as a baseline. The focus was on *MECP2* characterization within leukemia. Primers were designed for *MECP2*'s isoforms 1 and 2 to discern differential expression between leukemia and healthy cell lines. We examined *MECP2* expression at RNA and protein levels using qPCR and Western Blot techniques. The intracellular localization of *MECP2* was assessed using immunofluorescence and confocal microscopy. Bioinformatics revealed that the *MeCP2* promoter and transcript were enriched in CpG islands, leading us to treat our specimens with AZA. Using MTT and FACS assays, we determined the optimal AZA concentration and evaluated its effectiveness. qPCR, Western Blot, and confocal microscopy techniques were carried out to investigate *MECP2* changes after treatment. Lastly, to ensure our *in vitro* observations were in alignment with clinical conditions, we expanded our qPCR evaluations to patient samples from AML, CML, MDS, at diagnosis, remission or under treatment with AZA.

Results. Using leukemia cell lines MOLM-13, OCI-AML3, and K562 compared to a normal cell line, we identified a distinct difference in *MECP2* protein levels, with leukemia cells showing substantially reduced *MECP2* mRNA and protein expressions. The *MECP2* protein in leukemia cells predominantly localized in the nucleus, a pattern different from the standard, especially evident during metaphase where it colocalized with tubulin. *MECP2* promoter analysis revealed three CpG islands with higher methylation in leukemia,

suggesting hypermethylation sites potentially modulated by AZA. After a 48-hour AZA treatment, *MECP2* levels in leukemia cells increased, though its localization remained consistent, albeit more pronounced. Examination of *MECP2* in patient samples with AML, CML, MDS revealed lower expression at diagnosis compared to healthy or remission-stage patients, with AZA treatment positively influencing *MECP2* expression.

Conclusion. Our findings spotlight *MECP2* as a promising biomarker and potential target in leukemia research. Such revelations hold the potential to lead to the development of enhanced therapeutic strategies and diagnostic tools for leukemia. By merging molecular, bioinformatics, and clinical approaches, our research accentuates *MECP2*'s multifaceted significance, urging the scientific community to explore its intricate role in oncology, which might redefine its position in therapeutic paradigms.

P040

FROM *IN VITRO* TO *IN VIVO* AND BACK| UNRAVELING TREATMENT RESPONSIVENESS OF AML CELLS UPON THE INTERACTION WITH BONE MARROW NICHE MESENCHYMAL CELLS

F. Liccardo¹, G. Mazzanti¹, M. Marcotulli², G. Cidonio², T. Ottone³, S. Travaglini³, M. Divona³, M.T. Voso³, S. Masciarelli¹, F. Fazi¹

¹Dipartimento di Scienze Anatomiche, Istologiche, Medico-Legali e dell'Apparato Locomotore, Sezione di Istologia ed Embriologia Medica, Sapienza Università di Roma; ²3D Microfluidic Biofabrication Laboratory, Center for Life Nano- & Neuro-Science-CLN2S, Istituto Italiano di Tecnologia (IIT); ³Dipartimento di Biomedicina e Prevenzione, Università degli Studi di Roma Tor Vergata, Italy

Introduction. In the past decade tremendous progress has been achieved in the development and clinical application of molecular targeted therapies for Acute Myeloid Leukemia (AML). However, drug resistance and relapses are still major issues rendering the rate of cure unsatisfying. This is mostly due to the clonal selection and the protective effect of the leukemic bone marrow microenvironment. We previously developed a strategy based on a combination of drugs inducing proteotoxic and oxidative stress and demonstrated that it efficiently leads to cell death of AML cells bearing the mutation FLT3-ITD, both *in vitro* and *in vivo*. Moreover, we investigated the protective mechanisms triggered by the bone marrow niche using a coculture system of AML cells and BM-derived mesenchymal stromal cells (MSCs). We showed that MSCs are able to protect AML cells by reducing the amount of oxidative stress generated by the treatment. Furthermore, we described the contribution of YAP signaling in the crosstalk between stromal cells and AML blasts suggesting a role for mechanotransduction in the protective abilities of MSCs. Now, aiming to optimize the combination of drugs to increase its translational potential, we are evaluating the efficacy of combining induction of proteotoxic stress with different drugs that are at the cutting edge in clinical trials for AML, among which the BCL-2 inhibitor venetoclax.

Methods. We tested the sensitivity of FLT3-ITD+ AML cell lines and primary LSCs to the combined treatment in conditions of both monoculture and coculture with MSCs. In parallel with an *in vivo* orthotopic murine model of AML, we also evaluated treatment efficacy in a 3D bio-printed porous matrix containing MSCs and mimicking bone marrow structure. This 3D model provides new insights into AML-stromal cell interactions upon treatment and MSCs mechanotransduction contribution in AML protection.

Results. The combination of proteotoxic stress and venetoclax is effective against FLT3-ITD+ AML cells *in vitro*, overcoming the protection provided by MSCs in a coculture system. Importantly, MSCs

viability is not affected by the treatment. Moreover, this combined strategy significantly prolongs the life span of a murine model of FLT3-ITD+ AML. Additionally, we confirmed that the coculture model is reliable in predicting *in vivo* treatment responsiveness.

Conclusions. We showed the efficacy of a new combined therapeutic strategy based on proteotoxic stress and the inhibition of the antiapoptotic protein BCL-2. This combination is able to overcome AML protection mediated by the MSCs, hence it could hopefully hinder AML resistance in a clinical setting. Indeed, we demonstrated treatment efficacy *in vivo*. On the other hand, we highlighted the relevance of a 3D coculture model as a critical tool to investigate both the interactions of AML and MSCs within the niche and drug effectiveness in the context of the bone marrow microenvironment.

P041

ABSTRACT NOT PUBLISHABLE

P042

IS IMMUNOGLOBULIN/T-CELL RECEPTOR MEASURABLE RESIDUAL DISEASE MONITORING TRULY INFORMATIVE IN PH+ ACUTE LYMPHOBLASTIC LEUKEMIA?

M. Beldinanzi¹, I. Della Starza^{1,2}, V. Bellomario¹, D. Cardinali¹, L. Elia¹, M. Matarazzo¹, R. Soscia¹, M. Cola¹, M. Di Trani¹, R. Foà¹, S. Chiaretti¹

¹*Ematologia, Dipartimento di Medicina Traslazionale e di Precisione, Università Sapienza di Roma;* ²*AIL Roma, Italy*

Measurable residual disease (MRD) negativity represents a primary goal in adult Ph+ acute lymphoblastic leukemia (ALL) patients' management. MRD assays must be sensitive and specific. Digital droplet PCR (ddPCR) can overcome some RQ-PCR limitations. The aims of the study were to carry out a [i/i] BCR//ABL1-based MRD quantification; i[i/i] comparison of MRD concordance rate between immunoglobulin/T-cell receptor clonal gene rearrangements (IG/TR) and BCR//ABL1; ii[i/i] correlation with biological features.

Samples from 56 adults enrolled in the phase III frontline GIMEMA LAL2820 trial for adult Ph+ ALL were collected at the end of induction (day +70) and during the consolidation (day +133). At diagnosis, patients underwent a screening for the identification of the predominant IG/TR gene rearrangement by PCR and/or NGS, and of the IKZF1plus signature by multiplex ligation-dependent probe amplification. BCR//ABL1-based MRD was performed by RQ-PCR and ddPCR, and by ddPCR for IG/TR. The concordance rate was evaluated comparing the results obtained by RQ-PCR and ddPCR for BCR//ABL1, and by BCR//ABL1 RQ-PCR and IG/TR ddPCR.

BCR//ABL1-based MRD comparison by RQ-PCR and ddPCR showed a correlation degree of $R^2=0.99$ and a concordance of 60%, with discordances falling mostly in cases with low MRD levels. As for IG/TR monitoring, only 47/56 (83.9%) cases were evaluable (lack of a reliable marker for the others). At day +70, the overall concordance was 55.3%| 25/47 (53.1%) cases were BCR//ABL1pos| 10 were IG/TRpos, 1 IG/TRPNQ and 14 IG/TRneg; 18/47 (38.3%) cases were BCR//ABL1neg| 16 were IG/TRneg, and 2 were IG/TRPNQ; finally, 4/47 (8.5%) cases were BCR//ABL1PNQ of which 1 was IG/TRpos and 3 were IG/TRneg. The concordance rate was similar between the experimental (EA) and the control (CA) trial arm (58.1% vs 43.7%), IKZF1plus vs IKZF1 WT/IKZF1 loss (55.5% vs 51.7%), and p190 vs p210-p190/p210 (48.5% vs 64.3%). At day +133, the overall concordance was 44.4%| 13/27 (48.1%) cases were BCR//ABL1pos| 2 were IG/TRpos, 1 IG/TRPNQ and 10 IG/TRneg; 10/27 (37%) cases were BCR//ABL1neg and IG/TRneg; finally, 4/27

(14.9%) cases were BCR//ABL1PNQ and IG/TRneg. Eight/17 (47%) and 4/10 (40%) cases in the EA and in the CA were concordant, respectively| notably, 1/2 IG/TRpos in the CA experienced a hematologic relapse. A lower concordance was observed in the IKZF1plus (33.3%) vs IKZF1 WT/IKZF1 loss (53.3%); contrariwise, at this timepoint, we observed a significantly higher concordance between p190 (62.5%) compared to p210-p190/p210 (18.2%) ($p=0.047$).

The overall good correlation for BCR//ABL1-based MRD evaluation methodologies was confirmed; IG/TR MRD monitoring was feasible in 83.9% of cases. The concordance rate between BCR//ABL1 and IG/TR, though suboptimal, is in line with previous reports; a significant correlation with the fusion type at day +133 was found. The high rate of discordances among the 2 markers suggests that IG/TR may not be a reliable MRD marker in adult Ph+ ALL.

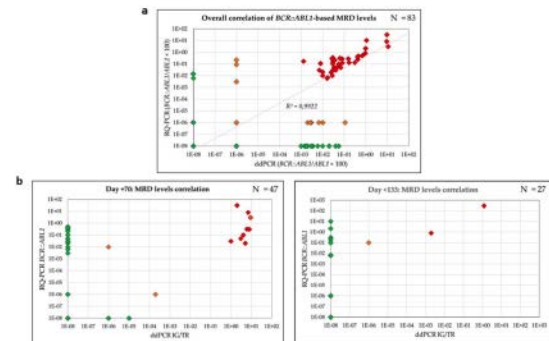


Figure 1. a) Overall BCR//ABL1-based MRD comparison between RQ-PCR and ddPCR; b) MRD comparison between BCR//ABL1 and IG/TR at day +70 and +133.

Figure 1.

P043

OPTICAL GENOME MAPPING| A NOVEL TOOL TO REFINE ROUTINE CYTOGENETIC DIAGNOSIS IN ADULT B-CELL ACUTE LYMPHOBLASTIC LEUKEMIA.

G. Lapietra^{1,2,3}, A. Cisneros^{2,3}, M. Mallo², J. Ribera², F. Solé², N. De Haro², E. Santafé^{2,3}, M.C. Villena^{2,3}, I. Del Giudice¹, S. Chiaretti¹, J.M. Ribera^{2,3}, I. Granada^{2,3}

¹*Dipartimento di Medicina Traslazionale e di Precisione, Sapienza Università di Roma;* ²*Josep Carreras Leukaemia Research Institute (IJC);* ³*Department of Hematology, Institut Català d'Oncologia (ICO), Italy*

Introduction. The genomic landscape of adult B-cell acute lymphoblastic leukemia (B-ALL) is widely heterogeneous. About 10-30% of cases remain unclassifiable by routine cytogenetic diagnostic tests (RT) (chromosomal banding analysis, fluorescence in situ hybridization, chromosomal microarrays). Optical genome mapping (OGM) is a novel high-resolution genome-wide technology revealing both structural (SVs) and copy-number variations (CNVs) in a single assay and could be the ideal candidate for a more extensive assessment of B-ALL genetic background. In our study, we compared OGM with RT in a cohort of newly diagnosed adult B-ALL patients (pts) to evaluate its feasibility and diagnostic value in a real-life setting.

Methods. The study was carried out at the Cytogenetic Unit of Catalan Institute of Oncology-Josep Carreras Leukemia Research Institute (Badalona, ES). For each case, we firstly performed RT. OGM was performed on available leftover bone marrow or peripheral blood cells, following manufacturer's instructions (Bio-

nanoGenomics) ultra-high molecular weight (UHMW) DNA was extracted, labelled with DLE-1 enzyme, loaded onto a chip and run by Saphyr instrument. Data analysis was done through rare variant analysis algorithm on BionanoSolve software, using GRCh37/h19 as genome reference. For the aim of the study, SVs and CNVs ≥ 100 kbp were analysed. Shorter aberrations were considered if overlapping with regions included in locally created BED files for B-ALL.

Results. From May 2023, seven cases were collected. Median age was 31 years (range 18-70). The male/female ratio was 1/1. Based on RT, the cases were classified according to 2022 WHO classification as follows: B-ALL with *KMT2A*-rearrangement (r) 1 pt; B-ALL, *BCR*||*ABL1*-like 3 pts (1 with *JAK2*-r; 2 with *CRLF2*-r); B-ALL, NOS 3 pts [1 with normal karyotype (NK); 1 with marker (mar); 1 with complex karyotype (CK)]. OGM analysis confirmed all alterations, except for *CRLF2*-r, and identified further aberrations: i(9)(p24.1q33.3)/*STRBP*||*JAK2*, as responsible for *JAK2*-r; t(12;16)(p13;p13.3)/*ZNF384*||*CREBBP* in NK (with subsequent re-stratification to the category “with other defined genetic abnormalities”); t(4;20)(q25;p13) with putative involvement of homeostasis regulator *MCUB* in pt with mar; i(17)(q10) without *TP53* loss and t(6;9;11)(q15;p21.3;q14.1) with putative involvement of guanylate kinase coding gene *DLG2* in CK.

Conclusion. In our study, OGM detected most aberrations identified by RT and further alterations with potential influence on prognosis. It provided an accurate description of B-ALL, NOS cases, confirming the need for a more extensive evaluation of this category. Challenging UHMW-DNA extraction, high overall costs and failure to detect *CRLF2*-r for low coverage of chromosomal repeated sequences represented the main limitations. Therefore, OGM could improve cytogenetic diagnosis of adult B-ALL but further experience is needed for its correct placement in the laboratory workflow.

Table 1. Comparison between cytogenetic results obtained by routine testing and by OGM. FISH analysis with commercially available probes was performed based on CBA: if no finding was detected, *CRLF2* rearrangement was still investigated. CMA with HD Cytoscan system by ThermoFisherTM was performed only for patients enrolled in PETHEMA protocol LAL-2019. CBA: chromosomal banding analysis; FISH: fluorescence in situ hybridization; CMA: chromosomal microarrays; OGM: optical genome mapping.

No. of case	Age (years old)	Sex	CBA results	FISH results	CMA results	OGM results
1	55	Male	46,XY,t(14;11)(q21;q23)[20]	NA	-Monoallelic deletion of <i>CDKN2A/B</i> (9p21.3)	-Detection of t(4;11)(q12;q23)/ <i>KMT2A</i> - <i>AF1</i> - Monoallelic deletion of <i>CDKN2A/B</i> (9p21.3)
2	18	Male	46,XY[20]	-Absence of <i>CRLF2</i> (Xp22.33) rearrangement	-Multiple non-pathogenic micro-deletions	-Detection of t(12;16)(p13;p13.3)/ <i>ZNF384</i> - <i>CREBBP</i> -Detection of same non-pathogenic micro-deletions detected by SNP array
3	70	Female	47,XX,+13[5]/46,XX[15]	-Presence of monoallelic <i>CRLF2</i> (Xp22.33) rearrangement -Trisomy of chromosome 13	NA	-Failure to detect <i>CRLF2</i> (Xp22.3) rearrangement -Trisomy of chromosome 13
4	21	Female	46,XX,-20,+mar[5]/46,XX[4]	-Absence of <i>CRLF2</i> (Xp22.33) rearrangement	-Multiple non-pathogenic micro-deletions and micro-gains	-Detection of t(4;20)(q25;p13) -Detection of same non-pathogenic micro-deletions and micro-gains detected by SNP array
5	29	Male	46,XY[20]	-Presence of monoallelic <i>CRLF2</i> (Xp22.33) rearrangement	-Monoallelic deletion of <i>CDKN2A/B</i> (9p21.3) -Monoallelic deletion of <i>AKAP12/MRPS32</i> (13q14.11)	-Failure to detect <i>CRLF2</i> rearrangement -Monoallelic deletion of <i>CDKN2A/B</i> (9p21.3) -Monoallelic deletion of <i>AKAP12/MRPS32</i> (13q14.11)
6	31	Female	46,XX,del(12)(p13),del(16)(q22)[2]/46,XX,del(6)(q21q25),add(9)(p22),del(11)(q21),del(12)(p13),del(16)(q22),t(17)(q10)[8],46,XX[9]	-Absence of <i>CRLF2</i> (Xp22.33) rearrangement -Bistertine monoallelic deletion of <i>TP53</i> (17q13.3) -Monoallelic deletion of <i>ETV6</i> (12p13.2)	-Monoallelic deletion of <i>CDKN2A/B</i> (9p21.3) -Monoallelic deletion of <i>ETV6</i> (12p13.2)	-Detection of t(17)(q10) -Detection of t(6;9;11)(q15;p21.3;q14.1) -Monoallelic deletion of <i>CDKN2A/B</i> (9p21.3) -Monoallelic deletion of <i>ETV6</i> (12p13.2)
7	60	Female	46,XX,inv(9)(p24.1q33.3)[15]/46,XX[5]	-Absence of <i>PAK3</i> (9p24.2) rearrangement -Presence of monoallelic <i>JAK2</i> (9p24.1) rearrangement	NA	-Detection of t(9)(p24.1q33.3)/ <i>STRBP</i> - <i>JAK2</i>

P044

GIMEMA ALL2418| UPDATED INTERIM ANALYSIS OF A PHASE IIA STUDY OF FEASIBILITY AND EFFECTIVENESS OF INOTUZUMAB OZOGAMICIN IN ADULT PATIENTS WITH B-CELL ACUTE LYMPHOBLASTIC LEUKEMIA WITH POSITIVE MINIMAL RESIDUAL DISEASE

G. Martinelli¹, A. Piciocchi², S. Chiaretti³, C. Papayannidis⁴, P. Salutari⁵, A. Olivieri⁶, P. Zappasodi⁷, A. Rambaldi⁸, N. Fracchiolla⁹, M. Cavallari¹⁰, S. Soddu², M. Abbenante¹¹, A. Candoni¹², C. Cattaneo¹³, F. Gigli¹⁴, M.R. Marino², M. Messina², G. Grillo¹⁵, F. Ferrara¹⁶, S. Siragusa¹⁷, P. De Fabritiis¹⁸, A. Lico¹⁹, E. Audisio²⁰, M. Bonifacio²¹, R.M. Lemoli²², D. Mattei²³, M. Lunghi²⁴, D. Cilloni²⁵, A. Ferrari¹, J. Nanni⁴, I. Della Starza³, G. Simonetti¹, M. De Propriis³, M.T. Bochicchio¹, M. Vignetti², P. Fazi², G. Marconi¹

¹IRCCS Istituto Romagnolo per lo Studio dei Tumori “Dino Amadori” - IRST S. r. l.; ²Fondazione GIMEMA; ³Universita’ Degli Studi Di Roma Sapienza-Dipartimento Di Medicina Traslazionale E Di Precisione-U. O. C. Ematologia; ⁴IRCCS Azienda Ospedaliero-Universitaria di Bologna, Istituto di Ematologia “Seragnoli”; ⁵ASL Pescara, Presidio Ospedaliero ‘Spirito Santo’-UOC Ematologia Clinica; ⁶AOU Ospedali Riuniti Umberto I - G. M. Lancisi - G. Salesi - SOD Clinica Ematologica; ⁷Fondazione IRCCS Policlinico San Matteo -UO Ematologia; ⁸ASST Papa Giovanni XXIII - Ospedale Di Bergamo - SC Ematologia; ⁹Fondazione IRCCS Ca’ Granda, Ospedale Maggiore Policlinico – Ematologia; ¹⁰AULSS 3 Serenissima, Ospedale Dell’Angelo - UO Ematologia; ¹¹Ente Ecclesiastico Casa Sollievo Della Sofferenza - Ematologia; ¹²Presidio Ospedaliero Santa Maria Della Misericordia - Clinica Ematologica; ¹³ASST Degli Spedali Civili Di Brescia-UO Ematologia; ¹⁴Istituto Europeo Di Oncologia IRCCS - Divisione Di Oncoematologia; ¹⁵ASST Grande Ospedale Metropolitano Niguarda - SC Ematologia; ¹⁶AO Di Rilievo Nazionale Antonio Cardarelli - UOC Ematologia Con Trapianto Di Midollo; ¹⁷AO Ospedali Riuniti Villa Sofia Cervello - UO Ematologia Con UTMO; ¹⁸ASL ROMA 2, Ospedale S. Eugenio - UOC Ematologia; ¹⁹AULSS 8 Berica - Ospedale di Vicenza - UOC Ematologia; ²⁰AOU Città della Salute e della Scienza, Ospedale S. Giovanni Battista Molinette - SC Ematologia 2; ²¹AOU Integrata di Verona, Policlinico G.B. Rossi - UOC Ematologia; ²²Clinic of Hematology, Department of Internal Medicine (Dim/[i]), University Of Genoa & IRCCS San Martino Hospital; ²³ASO S. Croce e Carle SC Ematologia; ²⁴AOU Maggiore Della Carita’ Di Novara - SCDU Ematologia; ²⁵Ospedale Mauriziano Umberto I - SCDU Ematologia, Italy

Introduction. The presence of minimal residual disease (MRD) is linked to elevated rates of treatment failure in B-cell acute lymphoblastic leukemia (B-ALL). Inotuzumab Ozogamicin (IO), a CD22-targeted antibody-drug conjugate, has displayed notable success in treating overt B-ALL.

Methods. In this phase 2 study (NCT03610438), we are examining the effectiveness of IO in achieving MRD negativity across two groups: 38 patients with Ph+ B-ALL and 38 with Ph- B-ALL. IO was dispensed at a dosage of 0.5 mg/sqm on days 1 - 8 -15 of a 28-day cycle. Those who did not reach MRD negativity following the initial IO cycle had the option to undergo a second cycle at the same dosage. Responding patients were administered low-dose chemotherapy regimens (featuring a rotation of vincristine, cyclophosphamide, prednisone, methotrexate, and 6-mercaptopurine), or tyrosine kinase inhibitors (TKIs) as a bridge to transplant or as a long-term maintenance according to Ph status. The central measurement of MRD was evaluated at baseline, post-course 1, post-course 2, and prior to transplantation, using *BCR-ABL1* or *V(d)J* fusion transcripts. We are presenting an unscheduled interim analysis.

Results. As of now, 68 patients have been screened for eligibility,

with 59 meeting the criteria. Data from the initial 50 patients treated in the study is presented here. The patient pool consisted of 26 individuals with Ph- B-ALL and 24 with Ph+ B-ALL; 26/50 (52%) were male. The median age among participants was 56 (22-84). Among Ph+ B-ALL patients, 39% had the p190 fusion transcript, while 61% had p210. In the Ph- B-ALL cohort, one patient had the ALL1/AF4 fusion transcript, and another had the ALL1/ENL fusion transcript. Most patients had undergone either one (21/50, 44%) or two (22/50, 46%) prior lines of treatment; (7/50) 14% were blinatumomab-resistant, all of whom were Ph- B-ALL. During study treatment, half of the Ph- B-ALL patients (13/26) completed 1 IO cycle, while the other half completed 2. Of note, only 5 patients (10%) met MRD progression criteria during IO courses (4 Ph+ ALL and 1 Ph- ALL). Among Ph+ B-ALL patients, 29% (7/24) had 1 IO cycle and 71% (17/24) had 2. Central MRD monitoring data is currently available for 28 patients (16 Ph- and 12 Ph+ B-ALL), with ongoing monitoring for the rest. Overall, MRD negativity was achieved in 9/28 (32%) patients. Specifically, 7/16 (44%) of the Ph-B-ALL cohort reached MRD negativity, and 3/16 (19%) achieved a low level of MRD positivity (<10⁻⁴). In the Ph+ B-ALL cohort, 2/12 (17%) reached MRD negativity. Among the seven patients pre-treated with blinatumomab, two (28%) achieved MRD negativity. Adverse events during the study were few and generally mild. Of the 50 patients, one experienced veno-occlusive disease (0.5%), which occurred within 20 days of the last IO dose and before any HSCT.

Conclusions. IO treatment showed effectiveness along with a favorable safety profile in the context of MRD-positive B-ALL.

P045

ABSTRACT NOT PUBLISHABLE

P046

MUTANT NPM1 marginally impacts translation in NPM1-mutated AML

L. Brunetti, G. Pianigiani, M. Gundry, M. Goodell, B. Falini

Università Politecnica delle Marche; IRCCS Materno-Infantile Burlo Garofolo; Boston Children's Hospital; Baylor College of Medicine; Università di Perugia, Italy

Background. NPM1-mutated acute myeloid leukemia (AML) is the most frequent AML subtype. As wild-type NPM1 is known to orchestrate ribosome biogenesis, it has been hypothesized that altered translation may contribute to leukemogenesis and leukemia maintenance in NPM1-mutated AML. However, this hypothesis has never been investigated. We reasoned that if mutant NPM1 (NPM1c) directly impacts translation in leukemic cells, loss of NPM1c would result in acute changes of the ribosome footprint.

Methods. We performed ribosome footprint profiling and bulk RNA sequencing in two NPM1-mutated cell lines (OCI-AML3 and IMS-M2), engineered to express endogenous NPM1c fused to the FKBP(F36V) degron tag (hereafter referred as to degron cells). Incubation of degron cells with the small compound dTAG-13 enables highly specific degradation of >85% of NPM1c within 4 hours. The experiments were performed comparing cells treated with either DMSO or dTAG for 6 hours. We chose this timepoint as it guarantees maximal NPM1c degradation and minimal differentiation, which is known to happen shortly after NPM1c loss, influencing translation. We performed one replicate for OCI-AML3 and two replicates for IMS-M2 cells. For differential expression analysis, when two replicates were used, genes that passed a false discovery rate of 5% and with a z-score of ≥ 4 and ≤ -4 were considered regulated, while when one replicate was used, genes with a z-score of ≥ 4 and ≤ -4 were

considered regulated. Efficient NPM1c degradation was confirmed by western blot.

Results. As the impact of NPM1c loss on transcriptional regulation has been already studied, we first analyzed RNA-seq data to confirm the fidelity of our experimental system. In OCI-AML3 13 genes were upregulated and 12 downregulated upon NPM1c loss. In line with NPM1c directly promoting the expression of homeobox (HOX) genes, 11 of the 12 downregulated genes were part of the HOX family, including members of the HOXA and HOXB clusters. In IMS-M2 cells only one gene was upregulated, while none of the downregulated genes had an average z-score of ≤ -4 . However, among the 8 genes with an average z-score of ≤ -3 , 4 were members of the HOXA and HOXB clusters, indicating consistent downregulation of HOX genes. Altogether, these results confirmed that NPM1c drives HOX expression and that our model was reliable. We next focused on Ribo-seq data to infer translational regulation upon loss of NPM1c after adjusting for RNA-seq data. Only one gene (CXCL8) was translationally upregulated and 4 genes (CTC1, C8orf37, FCGR2A, MYNN) were downregulated in OCI-AML3, while none was found to be translationally regulated (any z-score) in IMS-M2 using 5% FDR. These results indicate that NPM1c only marginally impacts translation.

Conclusions. Analysis of transcriptome following NPM1c degradation in two NPM1-mutated cell lines demonstrates that NPM1c only marginally impacts translation. Further efforts are warranted to clarify the role the NPM1c in the cytoplasm.

P047

A NOVEL SYSTEM FOR TESTING DOMAIN ESSENTIALITY IN CANCER

S. Peruzzi¹, A. Gagliardi¹, A. Scialdone¹, L. Brunetti^{1,2}

¹Università degli studi di Perugia; ²Università politecnica delle Marche, Italy

Introduction. The identification of fundamental domains in oncogenic proteins represents a key step to elucidate the molecular mechanism of tumorigenesis and for the development of effective targeted therapies. Degron systems such as the FKBP(F36V) degron tag have enabled fast and specific degradation of proteins of interest, demonstrating the essentiality of specific proteins for cancer maintenance and propagation. We have previously engineered OCI-AML3 cells (an AML cell line bearing NPM1 mutation A) to express endogenous NPM1c fused to the FKBP(F36V) tag (degron cells) and demonstrated that specific degradation of NPM1c causes terminal differentiation and growth arrest. However, differentiation and growth arrest can be rescued by ectopic expression of NPM1c prior to degrading endogenous NPM1c.

Methods. We reasoned that transducing degron cells with ectopic NPM1c variants with single amino acid changes or lacking small aminoacidic stretches would enable testing for domain essentiality up to single-amino acid resolution just by looking at differentiation (CD11b expression, by flow cytometry) and growth arrest (cell counts), following degradation of endogenous NPM1c. Specifically, degron cells transduced with NPM1c variants lacking essential amino acids would undergo differentiation, while cells transduced with variants missing non-essential ones should remain undifferentiated.

Results. To test the feasibility of our strategy, we first transduced degron cells with lentiviruses encoding for either full-length NPM1c (mutation A) or WT NPM1. As expected, following degradation of endogenous NPM1c, cells transduced with WT NPM1 underwent terminal differentiation, while those transduced with NPM1c did not. Expression of ectopic genes was confirmed by western blot. Starting

from previously published data and personal observations, we generated multiple NPM1c variants, including the deletion of the first acidic stretch (AS) and single amino acid mutations in the same region, replacing each of the charged residues with alanine. The AS deletion made NPM1c unable to rescue the leukemic phenotype, confirming that this domain is essential for maintaining the leukemic phenotype. Furthermore, we observed that mutation of the last 4 charged amino acids of the AS resulted in remarkable differentiation compared to the other amino acids tested, indicating this short stretch is critical for NPM1c activity.

Conclusion. Although we optimized this approach on OCI-AML3 cells and specifically NPM1c, our screening strategy can be translated to any cancer context to test domain essentiality of proteins known to be necessary for cancer propagation. We believe that data obtained from the domain essentiality screening represent the starting point for subsequent bioinformatic evaluation of small compounds that interfere with oncogenic protein activity, paving the way for new opportunities for targeted therapy in cancer.

P048

RE-ESTABLISHMENT OF DNMT3A-WT IN OCI-AML2 AND IMS-M2 CARRYING DNMT3A DISRUPTIVE MUTATIONS DOES NOT AFFECT LEUKEMIA SURVIVAL, GROWTH AND RESPONSE TO DRUGS IN VITRO AND IN VIVO

E. Padiglioni¹, F. Milano¹, C. Quadalti¹, L. Albicocco Giovinati¹, S. Pierangeli¹, M. Sabino¹, R. Ranieri¹, S. Donnini¹, I. Gionfriddo¹, S. Silvestri¹, F. Mezzasoma¹, V. Ciauro¹, S. Cipriani¹, V. Tini¹, G. Spinuzzi¹, L. Vago², M.P. Martelli¹

¹Section of Hematology and Clinical Immunology, Department of Medicine and Surgery, University of Perugia; ²Unit of Immunogenetics, Leukemia Genomics and Immunobiology, Vita-Salute San Raffaele University, Italy

Introduction. Acute Myeloid Leukemia (AML) is a heterogeneous malignancy characterized by abnormal clonal hematopoietic stem cell (HSC) expansion. *DNMT3A* mutations are the most prevalent gene alteration observed in patients with AML. These gene mutations are early events during cancer development and seem to confer poor prognosis at least in some genetic subtypes of AML. While it is known that *DNMT3A* mutations have a crucial role in the development of leukemia, their role in the maintenance of the established disease, and therefore its value as a therapeutic target remain elusive. We hypothesized that the maintenance of the AML leukemic state is uncoupled from the presence of the *DNMT3A* mutation and might be dependent on other mechanisms. We previously shown that in OCI-AML3 cell line harbouring *DNMT3A*^{R882C} mutation, correction of the mutation by CRISPR-based genome editing did not affect growth, immunophenotypic profile, colony forming unit (CFU) capacity and engraftment in immunocompromised NSG mice. Here, we aimed at confirming our findings in different fit for purpose models created in our laboratory, and testing how re-established *DNMT3A* wild type (WT) expression affect response to drugs.

Methods IMS-M2 carries a frameshift *DNMT3A* mutation, and OCI-AML2 carries the *R635W* mutation leading to absence of protein expression. Cells were infected with lentiviral vectors containing the *ZsGreen1* gene reporter and the *DNMT3A-WT* gene under the same promoter. After 72h, *ZsGreen*-positive cells were sorted, counted and used either as a bulk population for IMS-M2 or for isolating single colonies for OCI-AML2. Expression of *DNMT3A* was checked by western blot. Cells were studied to evaluate growth, immunophenotype, CFU capacity, engraftment and survival in NSG mice, and response to either chemotherapeutic drugs commonly used in AML treatment or an epigenetic drug library.

Results As previously shown for OCI-AML3_ *DNMT3A*^{wt/wt} colonies, both IMS-M2 and OCI-AML2 re-expressing *DNMT3A-WT*, did not show a significant difference in CFU capacity, growth rate, and engraftment and disease development in NSG mice, as compared to the parental cell line. No significant differences were observed in immunophenotype and intracellular signaling pathways either. Re-expression of *DNMT3A-WT* did not influence response to daunorubicin, doxorubicin, etoposide and Ara-C, and to an array of epigenetic drugs.

Conclusions These findings suggest that AML progression is uncoupled by the influence of *DNMT3A* mutation once the disease is already established, doubting the role of mutated *DNMT3A* as therapeutic target in AML. We are currently carrying out additional experiments in AML cellular models carrying *DNMT3A* mutations to confirm our findings. Moreover, a CRISPR based genome wide screen on OCI-AML3 edited versus unedited clones is ongoing in order to investigate how correction of *DNMT3A* mutation into wild type affects the landscape of genetic dependencies in AML.

P49

ABSTRACT NOT PUBLISHABLE

P050

MULTIPARAMETRIC FLOW CYTOMETRY-MRD ASSAY IN CORE-BINDING FACTOR (CBF) AML. LESSON FROM PHASE II TRAIL REL AML 001

A. Gatti², S.M. Veronese¹⁶, G. Grillo¹, B. Di Camillo^{3,4}, M. Fumagalli⁵, M. Krampera⁶, P. Zappasodi⁷, E. Borlenghi⁸, E. Todisco⁹, M. Ubezio¹⁰, M. Bernardi¹¹, A. Molteni¹², C. Basilio¹³, M. Turrini¹⁴, R. Greco¹, V. Mancini¹, M. Riva¹, G. Magliano¹, M.R. Stefanucci¹⁵, B. Brando², A. Beghini¹⁵, R. Cairoli¹

¹Department of Hematology, ASST Grande Ospedale Metropolitano Niguarda; ²ASST Ovest Milanese, Legnano Hospital; ³Department of Information Engineering, University of Padova; ⁴Department of Comparative Biomedicine and Food Science, University of Padova; ⁵Division of Hematology and Bone Marrow Transplant Unit, Ospedale San Gerardo; ⁶Section of Hematology and Bone Marrow Transplant Unit, Department of Medicine, University of Verona; ⁷Department of Hematology Oncology, Fondazione IRCCS Policlinico San Matteo; ⁸Department of Hematology, ASST Spedali Civili di Brescia; ⁹Division of Hematology, European Institute of Oncology; ¹⁰Cancer Center, IRCCS Humanitas Research Hospital & Humanitas University; ¹¹Hematology and Bone Marrow Transplantation Unit, IRCCS San Raffaele Scientific Institute; ¹²Division of Hematology, ASST Cremona; ¹³Division of Hematology, ASST Settelaghi, Ospedale di Circolo; ¹⁴Section of Hematology, Valduce Hospital; ¹⁵Department of Health Sciences, University of Milan; ¹⁶ Department of Pathology ASST Grande Ospedale Metropolitano Niguarda, Italy

Background. Core-binding factor (CBF) AML with RUNX1/RUNX1T1 (AML1/ETO) and CBF/ MYH11 fusion genes is known as a heterogeneous group, accounting for about 10% to 15% of AML. In the Phase II Trial REL AML 001 (EudraCT Number 2017-002094-18; Clinical Trials ID: NCT 03686345) adult CBF leukemia patients treated with a continuation therapy with Midostaurin were included, and the measurable residual disease (MRD) was performed by molecular MRD assessment (qPCR) and multiparametric flow cytometric-MRD (MCF-MRD) assay. The findings of MCF-MRD assay were compared to qPCR.

Methods. 31 patients with AML1/ETO (n=15) and CBF/ MYH11 (n=16) were evaluated between December 2018 to July 2022 with both techniques. A total of 145 determinations (n. AML1/ETO = 56

and n. CFBF/MYH11= 89) were performed. MCF panel included 2 10-color tubes| CD15 FITC/ CD56 PE/ CD34 PerCP-cy5. 5/ CD117 PE-cy7/ CD7 APC/ CD13 APC-R700/ CD19 APC H7/ HLADR V450/ CD45 V500C/ CD33 BV630, specific for RUNX1/RUNX1T1 cases and CD64 FITC/ CD2 PE/ CD34 PerCP-cy5. 5/ CD117 PE-cy7/ CD200 APC/ CD13 APC-R700/ CD14 APC H7/ HLADR V450/ CD45 V500C/ CD33 BV630, specific for CFBF/MYH11 cases. A mean of 1,733,240 CD45 positive events were acquired, with a mean lower limit of detection (LLOD) of 0.001% (ranging 0.01-0.0003%). In 10 cases (6 RUNX1 and 4 CFBF/MYH11) the molecular and phenotypical features at onset were not available. MCF analyses were performed by Infinicyt™ software and reference image tool was used wherever possible.

Results. We found a concordance of 76% between MCF cases and RUNX1/RUNX1T1 qPCR, and a concordance of 83% between MCF cases and CFBF/MYH11 qPCR (Table 1a and b). In relapsed cases we observed a dynamic and continuous increase of abnormal MCF events, that was not found in cases without clinical relapse although with positive qPCR (Table 2). The HLADR expression evaluated as the geo mean intensity at presentation and/or at relapse resulted higher in RUNX1/RUNX1T1 patients than in CFBF/MYH11 cases (29845 vs 8979, respectively, p=0.0039 Figure 1). Interestingly, we found in a single case with atypical CFBF/MYH11 fusion gene a high value of HLADR geo mean (44522). The down-regulated expression of HLADR in CFBF/MYH11 blasts may be a useful clue to distinguish AML blasts from the scarcely represented normal CD2 positive myeloid precursors, and from the strongly HLADR positive elements that are found in a regenerating bone marrow background.

Conclusion. Although MCF-MRD assay showed lower sensitivity than CBF qPCR, MCF offered interesting information about the dynamics of the abnormal clone size with time, evaluated as the increasing number of MRD clustering events, which may predict an impending relapse.

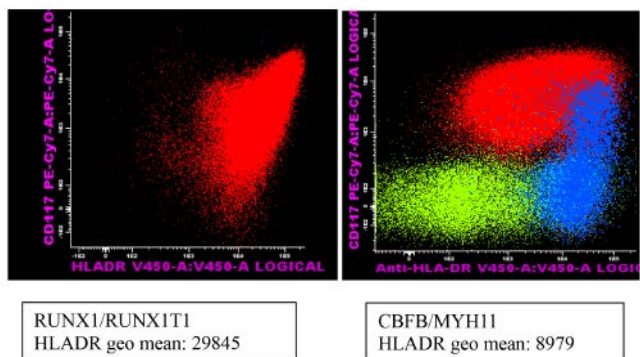


Figure 1. Different HLADR expression in representative RUNX1/RUNX1T1 and CFBF/MYH11 cases, evaluated at presentation. Red= AML blasts; Blue= Monocytes; Green= Lymphocytes.

Table 1. a) Comparison between MCF and qPCR in 56 analyses of RUNX1/RUNX1T1 cases. b) Comparison between MCF and qPCR in 89 analyses of CFBF/MYH11 cases.

a.			b.		
RUNX1/RUNX1T1 (56 analyses)			CFBF/MYH11 (89 analyses)		
	qPCR	MFC		qPCR	MFC
Positive	43	44	Positive	71	66
Negative	13	12	Negative	18	23
<hr/>			<hr/>		
MFC-/qPCR-	6		MFC-/qPCR-	13	
MFC+/qPCR+	37		MFC+/qPCR+	61	
MFC-/qPCR+	6		MFC-/qPCR+	10	
MFC+/qPCR-	7		MFC+/qPCR-	5	
(Concordance 76%)			(Concordance 83%)		

Table 2. a) An example of relapse case in which a continuous increase of abnormal MCF events was detected. b) An example of non-relapsing case without increases of abnormal MCF events.

a)		
qPCR	log	MFC events
5736135,00	6,758619364	139669
3153,2400	3,498757027	547
0,005506	-2,259163793	41
0,000766	-3,11577123	48
0,006900	-2,161150909	32
0,011376	-1,944010417	50
0,021487	-1,667824216	82
9,655100	0,984756776	698
120,22	2,079983949	3284
b)		
qPCR	log	MFC events
0,246	-0,61	50
0,0123	-1,91	11
0,00	0,00	78
0,00	0,00	2
0,00	0,00	9
0,0006	-3,22	0
0,0002	-3,70	3

P51

ABSTRACT NOT PUBLISHABLE

P52

ROLE OF NPM1 MONITORING IN MRD EVALUATION, A FOLLOW UP ON AML1310 PROTOCOL

E.L. Lindfors Rossi¹, R. Palmieri¹, G. Marsili², T. Ottone^{1,3}, M. Divona^{1,4}, L. Maurillo¹, F. Buccisano¹, M. Alfò⁴, V. Arena², A. Piciocchi², M.T. Voso^{1,3}, A. Venditti¹

¹Department of Biomedicine and Prevention, Tor Vergata University; ²GIMEMA Foundation; ³Santa Lucia Foundation, I.R.C.C.S., Neuro-Oncohematology; ⁴Saint Camillus International University of Health Sciences; ⁵Department of Statistical Sciences, Sapienza University of Rome, Italy

NPM1 mutation is the most common mutation in cytogenetically normal (CN) Acute Myeloid Leukemia (AML), and monitoring of measurable residual disease (MRD) in this patient subset is prognostic and can be used to guide therapeutic decisions. We retrospectively performed MRD study on a cohort of patients affected by *de novo* AML, homogeneously treated according to their risk stratification status, to assess whether the detection of NPM1 mutation transcripts in bone marrow samples could predict early relapse. A total of 515 patients were enrolled in GIMEMA AML1310 Study (EudraCT number 2010-023809-36;113 ClinicalTrials. Gov Identifier NCT01452646) between 2012 and 2017 (Venditti *et al.* Blood 2019). All patients gave informed consent according to the declaration of Helsinki. Risk stratification was performed using NCCN 2009 guidelines since later versions were not yet published at time of protocol enrollment. Routine morphologic, cytogenetic and genetic analysis was performed at time of diagnosis at the University of Rome Tor Vergata. Molecular and MFC assessments of MRD are available at post-induction and post-consolidation time points. We performed molecular MRD monitoring by reverse transcriptase-quantitative PCR (RQ-PCR) using primers and probes described by Gorello *et al.* (Leukemia 2006) (type A,B and D). Survival distributions were

estimated using the Kaplan-Meier Product Limit estimator. Cox regression models in univariate and multivariate analysis were conducted after assessment of proportionality of hazards. NPM1 molecular MRD thresholds were established using a survival decision tree approach based on a single binary split and log-rank test as homogeneity criteria. We performed multivariate analysis and observed that post-consolidation MRD status had the most significant impact on the Disease Free Survival (DFS) model. Splitting the DFS analysis according to the risk categories, 2-years DFS was 50% (95% cloglog CI 36-63) for favorable risk patients and 48% (95% cloglog CI 31-64) for poor risk patients. However, when studying the NPM1-alone population, we observed that molecular positivity above 7,58 copies/10⁴ ABL threshold after consolidation was associated with a decreased 2-year-DFS (66% vs 25%), and an improved splitting performance when compared to the zero threshold (p=0.003 vs p=0.049). MRD assessment through MFC (threshold below 0.1) did not play a significant role (p=0.061). Furthermore, we noticed that patients with NPM1-alone AML who were molecular MRD positive post-consolidation phase had a disease progression similar to the poor risk patient category, as shown in Figure 1. Molecular MRD in NPM1-mutated AML at a threshold of 7,58 copies/10⁴ ABL after consolidation treatment may detect a very unfavorable patient group, in need of treatment intensification.

P053

EXTRAMEDULLARY INVOLVEMENT IN PATIENT-DERIVED XENOGRAFT MODELS OF ACUTE MYELOID LEUKEMIA (AML) WITH NUCLEOPHOSMIN (NPM-1) MUTATION

M. Caridi, S. Cipriani*, G. Martino, F. Milano, S. Pierangeli, S. Donnini, E. Padiglioni, R. Ranieri, L. Ruggeri, G. Cimino, I. Gionfriddo*, M.P. Martelli(co-last)

Division of Hematology and Clinical Immunology, Department of Medicine and Surgery, University of Perugia, Italy

Introduction. Acute Myeloid Leukemia (AML) is characterized by a particularly poor prognosis, especially in the elderly and in relapsed/refractory cases. One distinct aggressive feature of AML involves the extramedullary manifestation (EMI) of the disease, notably in the central nervous system (CNS). However, currently there is a limited understanding of underlying mechanisms. Emerging evidence suggests the potential role of leukocyte trafficking mechanisms, selectin and integrin expression, and extracellular matrix-receptor interactions in promoting AML localization within the CNS. Understanding the molecular and cellular pathways that underlie CNS involvement could provide critical insights into the pathogenesis of AML and potentially unveil novel therapeutic targets. Further investigations are warranted to elucidate the complex interplay between leukemic cells and the unique microenvironment of the CNS in the context of AML.

Methods. To address these critical knowledge gaps, we are establishing patient-derived xenograft (PDX) models of AML with EMI by inoculating AML cells from patients at diagnosis or relapse and verifying the engraftment by organs IHC with a human CD45 antibody. PDX models hold pivotal importance in cancer research by faithfully recapitulating the intricate dynamics of the disease within the unique microenvironment of the host.

Results. So far we succeeded in replicating EMI in various organs, including spleen, stomach, liver, intestine, kidneys, pancreas, uterus, tubes and lung. We are now assessing the stability in subsequent passages. We obtained 6 CNS involvement. While 5 are in follow-up, one was consistently maintained in the following passages (n=3); all of them derived from NPMmut blasts and among those, 6 were NPM-mut/FLT3-ITD, a phenotype prone to EMI in patients. Investigating the nature of the CNS involvement, we observed a localization of the disease in the meningeal spaces and associated vessels, both arteries and venules. The encephalus and the parenchymatous structures were mostly spared from the leukemic infiltration. Studies are ongoing to elucidate correlation with NGS scSeq data, transcriptional profiles, and adhesion molecules assets. With particular reference to the engraftments in the CNS, we will investigate metabolic changes to study the metabolic reprogramming through which leukemic cells could survive in the nutrient-poor and oxygen-deprived CNS microenvironment.

Conclusions. These models provide a valuable platform to investigate the mechanisms driving extramedullary manifestations in Acute Myeloid Leukemia, offering a promising tool to enhance our comprehension of this complex facet of the disease. Through PDX models, we aim to bridge the existing knowledge deficit and explore novel strategies for tackling AML with EMI, ultimately improving patient outcomes and therapeutic interventions.

Reference

Ottone, T et al. Leukemia, 10. 1038/s41375-023-02054-0. 6 Oct. 2023.

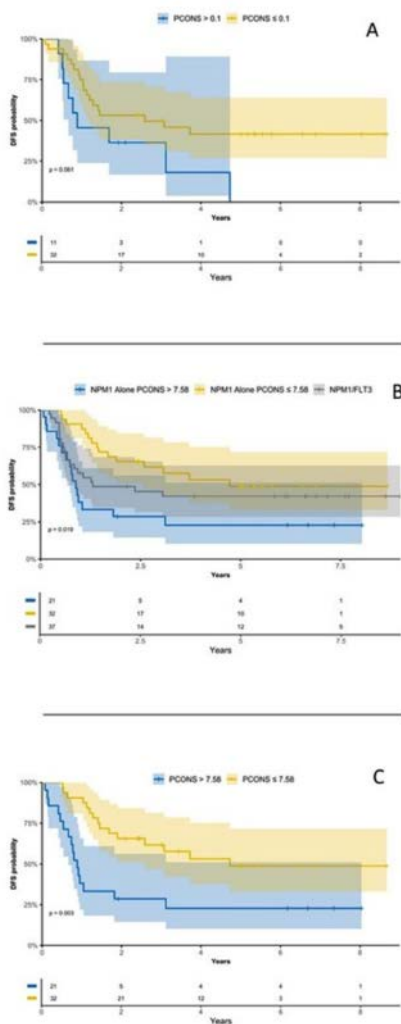


Figure 1. DFS status: A) NPM1-alone patients according to molecular MRD positivity>7,58 copies/10⁴ ABL threshold B) NPM1-alone patients according to MPFC MRD positivity>0.1 threshold C) overall DFS status.

Figure 1.

P54

ABSTRACT NOT PUBLISHABLE

P055

LABNET AML STANDARDIZATION TO ENSURE ACCURATE DIAGNOSIS AND MONITORING OF ACUTE MYELOID LEUKEMIA. EVALUATION OF LABORATORY PERFORMANCE

M. Messina¹, M.D. Divona², T. Ottone², R. Cucci¹, S. Orlando¹, S. Soddu¹, B. Izzo³, S. Errichiello⁴, E. Gottardi¹, E. Giugliano⁵, E. Ottaviani⁶, A. Santoro⁷, A. Piciocchi¹, P. Fazi¹, M. Vignetti¹, B. Falini⁸, F. Pane³, G. Saglio⁹, S. Amadori¹, M.T. Voso²

¹Fondazione GIMEMA; ²AOU Policlinico Tor Vergata, UOC Trapianto Cellule Staminali; ³Dipartimento di Medicina Molecolare e Biotecnologie Mediche, AOU Federico II; ⁴CEINGE Biotecnologie Avanzate “Franco Salvatore”; ⁵AOU San Luigi Gonzaga, SCDU Ematologia Generale e Oncoematologia; ⁶IRCCS AOU di Bologna, Istituto di Ematologia “Seràgnoli”; ⁷AO Ospedali Riuniti Villa Sofia Cervello, UO Ematologia con UTMO; ⁸AO di Perugia, Ospedale S. Maria della Misericordia, Ematologia e Trapianto Midollo Osseo; ⁹Ospedale Mauriziano Umberto I, SCDU Ematologia, Italy

Introduction. Since 2016, GIMEMA – thanks to an unconditional grant from Novartis - guarantees an accurate diagnosis and monitor of AML by the LabNet network that connects Italian hematology centers with reference laboratories, qualified to evaluate the genetic aberrations included in a basic panel, *i.e.* PML/RARA, BCR/ABL1, RUNX1/RUNX1T1, CBFB/MYH11, NPM1, FLT3-ITD and D835 mutations. To ensure a standardized diagnostic/prognostic workup, reference laboratories regularly undergo quality controls (QC). In the current report, we present the results of the last QC Round, the fourth, focused on the quantification of BCR/ABL1 p190 and p210, PML/RARA, CBFB/MYH11. The analysis was aimed at elaborating robust criteria to identify out-of-range data and favor the standardization process.

Methods. Thirty-three laboratories (Figure 1) took part to the 4^o QC Round and analyzed 4 dilutions (10^{-1} , 10^{-2} , 10^{-3} , 10^{-4}) and the undiluted sample for every target. Dilutions were centrally prepared from an undiluted standard (Werfen) and were distributed to laboratories in May 2021. Targets were analyzed by real time quantitative PCR (Q-PCR). Instruments and kits were those in use by the laboratories. For the evaluation of BCR/ABL1 p210 and p190 most widely used kits were: IPSOGEN-QIAGEN, one-step ELITECH, and one-step BIOCLARMA; for the quantification of PML/RARA and CBFB/MYH11 the majority of laboratories adopted the IPSOGEN-QIAGEN kit, or an in-house system. Results were collected from June to September 2021 and centrally analyzed. Data were summarized using Tukey’s Box-and Whiskers plot, a non-parametric method which allows to graphically represent fundamental characteristics of a statistical distribution. Values with a distance greater than $1.5 \times \text{IQR}$ [interquartile range] from the first or third quartile are defined as outliers, while in faroutliers the distance is greater than $3 \times \text{IQR}$. The analysis was carried out using the SAS 9.4 software.

Results. The analysis of BCR/ABL1 p210 – performed by 32 laboratories - identified 9 outlier values in 6 laboratories (18.7%), while that of BCR/ABL1 p190 showed 13 outliers in 6 of the 31 involved laboratories (19.3%). Analysis of PML/RARA - performed by 32 laboratories - lead to the identification of 6 outliers in 2/32 laboratories (6.2%), while that of CBFB/MYH11 – carried out by all the laboratories - lead to the identification of 16 outliers in 4 laboratories (12.1%). Overall, 19 laboratories did not have any out-of-range data and were defined “compliant”; 5 laboratories had 1 outlier value and were defined “active but non-compliant”; 9 laboratories had 1 faroutlier or 2 outliers and were defined “non-compliant”.

Conclusions. The analysis of the 4^o QC Round showed an overall good performance of the participating laboratories. Indeed, roughly 70% of laboratories had none out-of-range data or only 1 outlier. To improve the standardization, “active but non-compliant” and “non-compliant” laboratories were invited to adopt corrective actions in cooperation with the coordinating laboratory.

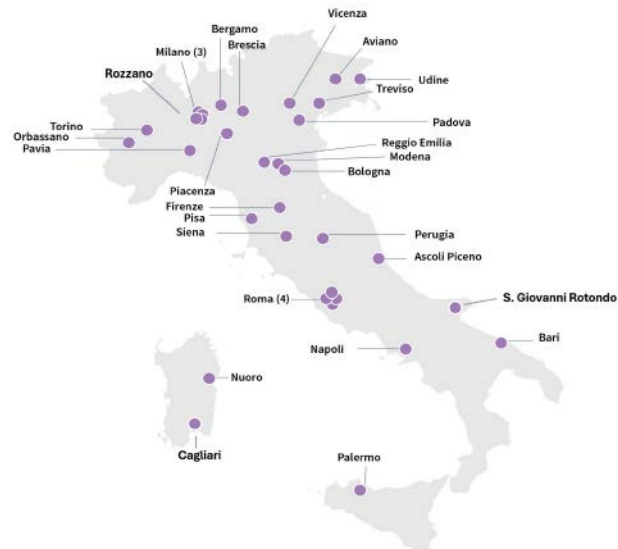


Figure 1. Laboratories participating to the 4^oQC Round.

Figure 1. Participating laboratories.

P056

PRE-EXISTING MYELOID SUBCLONES MAY ACCOUNT FOR A SUBSET OF ACUTE MYELOID LEUKEMIAS AND MYELODYSPLASTIC NEOPLASMS IN PATIENTS WITH PRE-EXISTING OR CONTEMPORARY LYMPHOID DISORDERS

A. Mattei, G. Marconi, S. Ronconi, D. Cangini, M. Ceccolini, C. Cerchione, I. Zacheo, M.B. Giannini, M. Norata, G. Martinelli, A. Ferrari, M.T. Bochicchio, M. Ghetti, M. Marchesini, G. Simonetti, G. Musuraca, D. Nappi

Istituto Romagnolo per lo Studio dei Tumori “Dino Amadori”, Italy

Background. Myelodysplastic neoplasms (MDS) and acute myeloid leukemia (AML) are occasionally observed in association with lymphoid tumors. There is a subset of patients who receive a contemporary diagnosis of myeloid and lymphoid disease, and the myeloid disease may both arise from clonal hematopoiesis substrate or harbor chemotherapy signature (Diamond, Blood 2023). Biological differences justified by the ontogenesis of the myeloid disease may justify prognosis and suggest appropriate intervention methods.

Methods. We searched our patient database for AML and MDS which were diagnosed together with lymphoid diseases. Data was collected under the study NCT04298892, after approval of the ethical committee. Statistics were performed with Kaplan-Meier estimation. Nonparametric tests were used as appropriate.

Results. Out of 164 patients who were referred to our service from May 2021 to Jul 2023 for MDS or AML, 11 patients were diagnosed with AML or MDS together with a concomitant or previous lymphoid disease. The median age at AML or MDS diagnosis was 67 (range 58-82); 9/11 (82%) patients were male. Four out of 11 (36%) patients were diagnosed with AML, 7/11 with MDS. The diagnosis

of myeloid and lymphoid diseases was concomitant in 2 patients (18%) and sequential in 9 patients (82%). The lymphoid diseases were smoldering multiple myeloma (3/11,27%), multiple myeloma (5/11,45%), diffuse large B-cell lymphoma (1/11,9%), mantle cell lymphoma (1/11,9%), marginal zone lymphoma (1/11,9%). Eight out of 11 patients (73%) had a history of chemotherapy before the diagnosis of MDS or AML; 5 patients (45%) were exposed to high-dose alkylating agents, 2 (18%) low-dose alkylating agents, 2 (18%) anthracyclines. Seven patients (64%) were diagnosed while they were receiving lenalidomide (median exposure of 8.8 months). In the 9 patients with consecutive lymphoid and myeloid disease diagnosis, AML or MDS were diagnosed after a median of 23 months. Regarding the AML or MDS, 3/11 patients (27%) had complex karyotype of which 1 had t(3;21)(q26;q22) RUNX1/MECOM rearrangement, 2/11 had TP53 mutation. The remaining patients harbored methylation or splicing mutations and normal karyotype or karyotype single non-high-risk alterations. Patients with complex alterations had similar times of onset from their first tumor and baseline characteristics, but they had an increased risk of death.

Conclusions. The incidence of AML or MDS associated with lymphoid disease is low and the population is heterogeneous. The characteristics and the timing of onset of the disease account for different ontogenesis; some patients have a disease that harbors complex alterations. The most frequent origin of AML and MDS can be researched in pre-existing or contemporary hematopoietic clones, that overall account for a whole bone-marrow disease. The relation between chemotherapy exposition and the biology of the AML or MDS is not univocal. This difference could be therapeutically relevant.

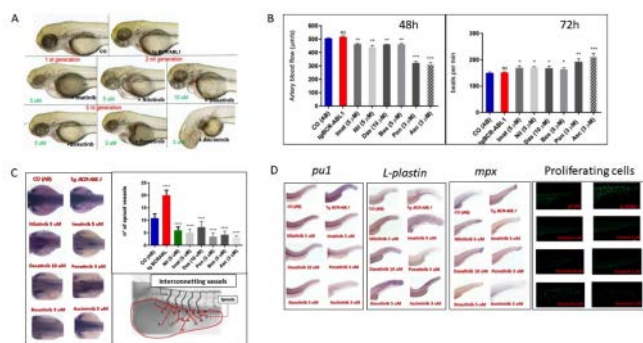


Figure 1.

P057

PROTOCOL GIMEMA AML2220| ROLE OF ADRENOMEDULLIN IN LEUKEMIC ENDOSTEAL/VASCULAR NICHES

R. Di Liddo¹, M. Basso², E. Nexha², G. Ciotti², A. Sperotto², A. Picciocchi³, V. Sargentini³, E. Crea³, A. Venditti⁴, M. Gottardi²

¹Department of Pharmaceutical and Pharmacological Sciences, University of Padova; ²Onco Hematology, Veneto Institute of Oncology, IOV-IRCCS; ³Italian Group for Adult Hematologic Diseases (GIMEMA) Foundation; ⁴Department of Biomedicine and Prevention, Tor Vergata University, Italy

Introduction. In the past decade, the bone marrow (BM) vascular niche has been demonstrated to actively interact with hematopoietic stem cells (HSCs). In acute myeloid leukemia (AML), a growing body of evidence demonstrates that the BM microenvironment is hypervascular and the increased microvessel density correlates with prognosis or reverts to normal conditions at remission. As such, BM

endothelial cells (ECs) and their released factors have recently emerged as an attractive target for therapeutic modulation in hematological cancers and “inflamm-aging”. It is well known that AML cells secrete angiogenic cytokines (e.g., VEGF), express cytokine-related receptors (e.g., VEGFR), and adhesion molecules to mediate physical interaction with ECs (e.g., VLA-4/VCAM-1; CD44/E-selectin) of type H [high CD31/endothelial (Emcn)], or type L (low CD31/Emcn), corresponding to transitional and sinusoidal vessels, respectively. Among vascular regulatory peptides, adrenomedullin (ADM), a 52 amino acid protein belonging to the calcitonin gene-related peptide family, is known to potentially contribute through calcitonin receptor-like receptor (CRLR) and Receptor-Activity-Modifying Proteins (RAMP2/3) to the pathogenesis of solid tumors by modulating the activity of PI3K/Akt and ERK/MAPK signaling pathways.

Methods. We performed preclinical screening of BM and peripheral blood (PB) from eligible and newly diagnosed AML patients (n=38) to study by flow cytometry (FCM) the expression of ADM, RAMP2/3, CRLR, adhesion molecules (CD31, CD38, CD44s, CD44v6) and PD-L1. To define the biological activity of ADM in chemoresistant cells, BM mononuclear cells from an AML patient with hyperleukocytosis (41 years old, > 80% blasts in BM and PB; FLT3 ITD mutated; M0) were treated for 7 days with ADM, and/or its inhibitor (ADM22-52). The expression of PDL-1 and cell viability were assessed by FCM.

Results. In this study, we demonstrated the expression of ADM, RAMP2, RAMP3, and CRLR in the BM and PB of AML patients. The expression pattern was likely correlated with the number of blasts, hyperleukocytosis, and genetic abnormalities. In the FLT3 ITD mutated patient, we observed CD31/CD38 ratio>1 and CD44v6/CD44>1 in BM but a higher expression of RAMP2 and RAMP3 in PB. In contrast, RUNX1 (45 years old; 35% BM blasts; 0% PB blasts; M5) or IDH2 (55 years old; 72% BM blasts; 28.2% PB blasts; M2) mutated patients showed RAMP3 and RAMP2 highly expressed in BM in association with CD31/CD38 ratio>1 and CD44v6/CD44 ratio<1. In the absence of circulating blasts, a lower expression of CRLR and ADM was detected. Upon *in vitro* treatment with ADM, a dose-dependent upregulation of PDL-1 expression together with reduced apoptosis was observed in AML cells with hyperleukocytosis.

Conclusions. These preliminary data offer a rationale for deeply exploring the biological effects of abnormal ADM signaling in the bone marrow and peripheral blood of AML patients.

P058

EVALUATION OF MRD MONITORING IN PERIPHERAL BLOOD VS BONE MARROW SOURCE IN PH-POSITIVE ALL

E. Attardi^{1*}, A. Savi^{3*}, D. Sini^{2*}, C. Conti², A.M. Nardoza², E. Meddi², F. Mallegni², G. Ranucci², E. Buzzatti², T. Ottone^{2,4}, C. Gurnari², M. Divona^{2,5}, M.G. Cefalo⁶, F. Locatelli^{6,7}, M.I. Del Principe², M.T. Voso², *this Symbol Indicates Equal Contribution

¹Department of Biomedicine and Prevention, PhD in Immunology, Molecular Medicine and Applied Biotechnology, University of Rome Tor Vergata; ²Department of Biomedicine and Prevention, University of Rome Tor Vergata; ³Department of Clinical and Biological Sciences, University of Turin; ⁴Santa Lucia Foundation, I. R. C. C. S., Neuro-Oncohematology; ⁵Saint Camillus International University of Health Sciences; ⁶Department of Pediatric Hemato-Oncology and Cell and Gene Therapy, Bambino Gesù Children's Hospital, Scientific Institute for Research and Healthcare (IRCCS); ⁷Department of Life Sciences and Public Health, Catholic University of the Sacred Heart

The Philadelphia (Ph) chromosome is the most common cytogenetic abnormality observed in adult acute lymphoblastic leukemia (ALL), with increasing prevalence with age. Measurable residual disease (MRD) monitoring is carried out in Ph+ ALL by quantitative reverse-transcriptase polymerase chain reaction (qRT-PCR) of *BCR-ABL1* rearrangement, with up to 10^{-6} sensitivity. Recently, the growing use of tyrosine-kinase inhibitors (TK[i]) together with chemotherapy (CHT) increased the importance of MRD monitoring in these patients (pts), to timely predict relapse. In contrast to chronic myeloid leukemia, the preferred source for quantifying MRD in Ph+ ALL is bone marrow (BM) blood.

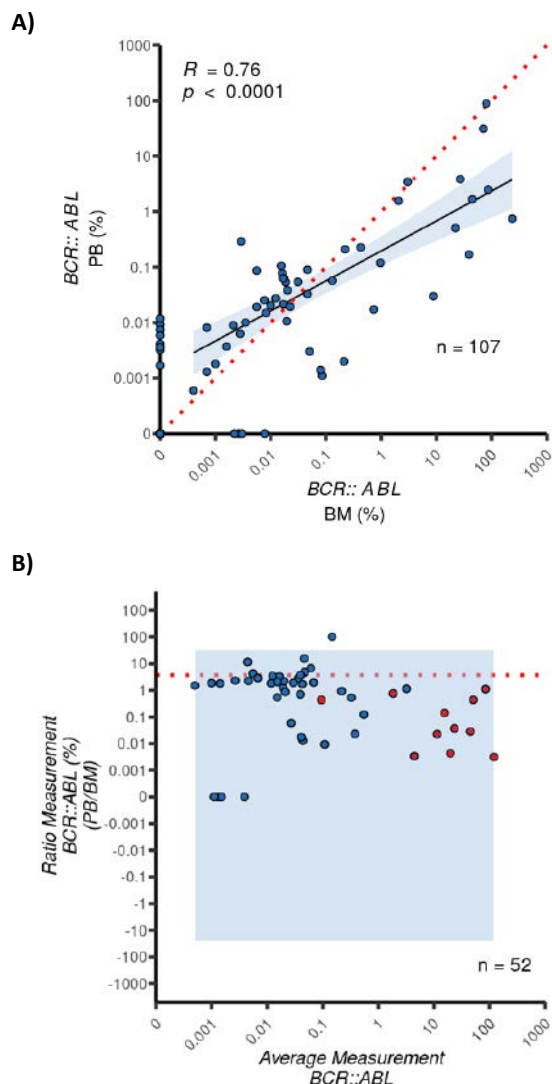


Figure 1.

However, the EuroMRD Consortium guidelines for standardization of the e1a2 *BCR-ABL1* transcript qRT-PCR recommend to consider peripheral blood (PB), along with BM samples, for parallel MRD analysis. We aimed to verify the correlation between levels of *BCR-ABL1* in PB vs BM for MRD monitoring. We examined 107 paired BM and PB samples ($n=214$ total samples) of 34 pts with a Ph+ ALL. Samples were collected at the Lab of Oncohematology at University of Rome Tor Vergata, during a 53-month time period (Jan/2021-Apr/2023), at a median of 13 months (2-73) from ALL diagnosis. Patients' median age was 46 years (range 2-75), with a 1,3 MIF ratio. They were treated with CHT and TKi, and 41% of them received hematopoietic stem cell transplant (14/34). All sam-

ples were analyzed using qRT-PCR for *BCR-ABL1*. Of 34 cases, 26 (76,5%) presented the e1a2 p190, and 8 (23,5%) the p210 b2a2 or b3a2 transcripts. During follow-up, 43,3% of samples became MRD-negative. Mean BM and PB *BCR-ABL1* levels during follow-up were 5,8% (SD 26,8%) and 2,4% (SD 14,6%), respectively ($p=0,74$), with higher p210 vs p190 BM levels, related to the higher frequency of relapse in the latter (3/8 vs 7/26 pts, $p<0,05$). Paired samples were concordant (BM/PB +/- or -/-) in 86,6% of cases, and discordant in 5,2% (BM/PB +/-) and 8,2% (BM/PB -/+). There was a moderate overall concordance of *BCR-ABL1* levels between BM and PB samples ($R=0,76$, $p<0,0001$, Figure 1A), with higher levels in BM at the time of relapse, as expected (red spots, Figure 1B). Significant differences in Δ (BM-PB) *BCR-ABL1* levels were associated with the p190 transcript type (vs p210, $p<0,01$), higher for p210 in BM. Ten of 34 pts experienced disease relapse, and an early increase of PB *BCR-ABL1* transcript levels was observed in 8 pts, 2,5 months prior to clinical relapse. Two pts had an extramedullary relapse, and had one Log higher *BCR-ABL1* levels in PB vs BM.

In summary, our data demonstrate that the correlation between PB and BM levels is not strong enough to suggest complete substitution of BM with PB sources for MRD monitoring in Ph+ ALL. However, our study supports the practice to use PB for long-term monitoring in pts with the e1a2 p190 transcript who achieve the MRD negativity goal, deserving BM evaluation in cases with incipient PB MRD positivity.

P059

VALIDATION STUDY OF ANALYTICAL METHODS FOR MULTICOLOR FLOW CYTOMETRY-BASED MINIMAL RESIDUAL DISEASE ASSESSMENT IN ACUTE MYELOID LEUKEMIA

M. Barone¹, A. Patuelli¹, M. Dicalardo², G. Chirumbolo², L. Bandini², G. Atzeni¹, D. Forte², G. Cristiano², E. Ottaviani¹, A. Curti¹, M. Cavo^{1,2}, L. Catani^{1,2*}, M. Arpinati^{1*}

¹IRCCS Azienda Ospedaliero-Universitaria di Bologna, Istituto di Ematologia "Seràgnoli"; ²Department of Medical and Surgical Sciences, Institute of Hematology "L. and A. Seràgnoli", University of Bologna, Italy; *Equally contributed

Introduction. Measurable residual disease (MRD), assessed by multicolor flow cytometry (MFC), is an important prognostic biomarker in acute myeloid leukemia (AML). However, in contrast to other diagnostic tests for MRD evaluation, the MFC assay suffers from large interlaboratory variations in terms of sample processing and data acquisition and interpretation. Harmonization and standardization of the MFC technique are still limited, as sensitivity and specificity depend on the monoclonal antibody panels used and the discriminatory level of leukemia-associated-immunophenotypes (LAIPs). Taken together, these issues limit the comparability and clinical interpretation of MFC-MRD results. This study aimed to evaluate two different analytical approaches for MFC-MRD based on the concordance of their results with those of RT-qPCR for NPM1 mutations.

Methods. Using the sequential gating technique, we prepared a patient (pt)-specific template analysis at diagnosis. Based on the template analysis, we explored the accuracy of two method for MRD evaluation (1) Template-Method, all cells within the pt-specific template are counted without further gate manipulation; (2) Restricted-Method, only cells positive for LAIP-specific aberrant markers are selected. A total of 125 bone marrow samples from 25 pts with AML were studied for MFC-/molecular-MRD ($n=62$ post-chemotherapy (CHT); $n=58$ post-hypomethylating agents-based regimens (HMA); $n=5$ post-Allogeneic stem cell transplant).

Results. To statistically evaluate the accuracy of the two MFC-

methods we performed a Receiver Operating Characteristic (ROC) analysis based on NPM1-MRD outcomes. ROC curves showed that the restricted-method is more accurate (area under curve (AUC)=0.75; $p<0.0001$) than the template-method (AUC=0.69; $p=0.0014$)(Figure 1A). Furthermore, we determined that the cut-off value for the restricted-method is 0.034% of LAIP+ cells. Next, we evaluated whether different therapies might affect the MFC-MRD. The restricted-method showed a higher AUC than the template-method in both post-CHT/-HMA MRDs. Of note, ROC analysis identified a cut-off of 0.034% for post-CHT MRDs and a cut-off of 0.095% for post-HMA MRDs (Figure 1B-C). We also found different degrees of accuracy based on the LAIP-specific aberrant lineage markers used for MRD assessment. LAIPs harboring markers such as CD25/CD56 may allow an MFC-MRD analysis with high specificity/sensitivity. Conversely, marker such as CD7/CD4 may be less reliable. However, the restricted-method proves to be the best approach.

Conclusions. Our data demonstrate that the restricted-method improves the accuracy of the MFC-MRD and its comparability with molecular MRD results in AML. These results further contribute to redefine and confirm an MFC-MRD analysis approach and threshold, highlighting the importance of subdividing MRD assays according to therapeutic settings and defining a classification of LAIPs based on their specificity/sensitivity.

Founded by RC-2022-2773341.

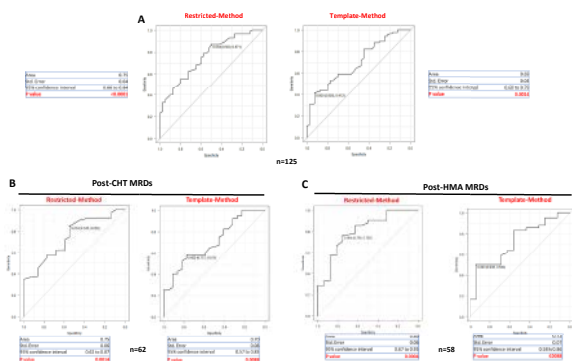


Figure 1.

Methods. We performed a retrospective monocentric analysis in intensively (IC) and non-intensively (NIC) treated AML patients. Effects of altered iron parameters at diagnosis were investigated subdividing patients into an altered (AC) vs a non-altered cohort (NAC). 110 newly diagnosed patients were screened for this study. 62 patients were eligible 46 IC (AC=22 vs NAC=24) and 16 NIC (AC=12 vs NAC=4) patients were analysed. 48 patients were excluded because of previous transfusions, infection or severe comorbidity. We compared the two cohorts in terms of ELN2022 classification, molecular and cytogenetic features. Furthermore, we compared AC vs NAC in terms of OS, CR, measurable residual disease (MRD) negativity, G4 infections and packed red blood cells (PRBC) transfusions rate during induction. ROC analysis was performed to correlate iron values with OS, CR and MRD. Concomitantly, selection bias was assessed.

Results. There was not a significant difference in terms of high-risk subtype frequency between AC vs NAC group in both the IC and NIC population (IC $p=0.39$ /NIC $p=0.29$). The AC group did not significantly differ in both IC and NIC in terms of OS (IC $p=0.16$ /NIC $p=0.62$), post-induction CR rate (IC $p=0.6$ /NIC $p=0.25$) and MRD-negativity rate (IC $p=1$ /NIC $p=1$). In the IC patients with high risk disease, an altered iron profile at diagnosis correlated with a higher need (>10) of PRBC during induction compared to high risk patients with normal iron profile (p -value 0.014). Iron-related lab values at diagnosis were informative in predicting post-induction CR and MRD status in both the IC and NIC population. In the IC population a ferritin cut-off value of 190 ng/ml (AUC 0.625) predicted CR rate while in the NIC population a ferritin cut-off value of 246 ng/ml (AUC 0.772) was informative about MRD negativity rate. Interestingly, in NIC, a ferritin cut-off value of 700 ng/ml predicted OS at 18 months (Figure 1).

Conclusions. Our retrospective study did not find a correlation between a specific ELN2022 AML risk subtype and altered iron lab-values at diagnosis, whereas an association in ELN2022 high risk IC patients regarding PRBC transfused during induction in AC vs NAC was found. Although the AC did not exhibit a shorter OS compared to the NAC in both IC and NIC population, specific cut-off values were informative about disease response to both intensive and non-intensive treatments.

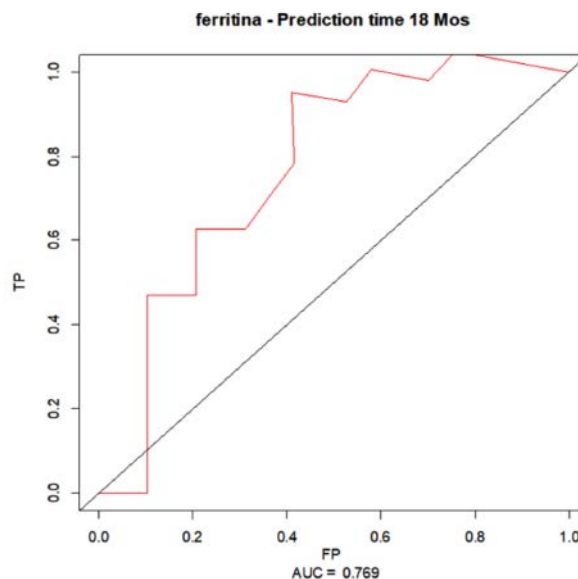


Figure 1: ROC curve analysis, ferritin value (cut-off: 700 ng/ml) in relation to OS (estimator KM) in NIC population (AUC: 0,769)

Figure 1.

P060

IRON-RELATED LABORATORY PROFILE MAY PREDICT DEEPNESS OF RESPONSE, SURVIVAL AND RISK STRATIFICATION IN ACUTE MYELOID LEUKEMIA PATIENTS TREATED WITH INTENSIVE AND NON-INTENSIVE THERAPY REGIMENS

F. Zingarelli¹, G. Cristiano¹, C. Sartor¹, L. Zannoni¹, J. Nanni¹, M. Barone¹, L. Bandini¹, E. Ottaviani², V. Robustelli², N. Testoni^{1,2}, M. Arpinati², C. Papayannidis², M. Cavo^{1,2}, A. Curti²

¹Department of Medical and Surgical Sciences, Institute of Hematology “L. and A. Seràgnoli”, University of Bologna; ²IRCCS Azienda Ospedaliero-Universitaria di Bologna, Istituto di Ematologia “Seràgnoli”, Italy

Introduction. Iron metabolism is deeply related to the pathogenesis of acute myeloid leukemia (AML) and remains largely unexplored as a predictor of response to therapy. There is growing interest towards iron pathobiology in AML since new therapies (i.e. targeting ferroptosis) are being investigated. Nonetheless, no clear association has been established between a specific risk subtype within the new European Leukaemia Net (ELN2022) prognostic classification, post-induction response and a metabolic iron signature at diagnosis.

P61

ABSTRACT NOT PUBLISHABLE

P062

“INTEGRATED DIAGNOSTIC REPORT” FOR MYELOID NEOPLASMS. A MORPHOLOGY-DRIVEN DIAGNOSTIC ALGORITHM

A. Paolini¹, V. Nasillo¹, G. Riva¹, R. Maffei¹, S. Martinelli¹, F. Giacobbi¹, G. Corradini¹, A. Ottomano¹, G. Bergonzini¹, D. Bernabei¹, F. Pilato¹, B. Conte¹, M. Morselli², F. Forghieri², A. Candoni², L. Potenza², R. Marasca², D. Giusti², E. Colaci², F. Bettelli², M. Maccaferri², P. Bresciani², A. Cuoghi², A. Gilioli², A. Messerotti², V. Pioli², G. Leonardi², V. Coluccio², M. Marietta², L. Roncati³, C. Lancellotti³, A. Eccher³, M. Luppi², T. Trenti¹, E. Tonaglia¹

¹*Diagnostic Hematology and Clinical Genomics, Department of Laboratory Medicine and Pathology, AUSL/AOU Modena;* ²*Section of Hematology, Department of Medical and Surgical Sciences, University of Modena and Reggio Emilia, AOU Modena;* ³*Section of Pathology, Department of Laboratory Medicine and Pathology, AOU Modena, Italy*

To uniform diagnostic procedures for the diagnosis of myeloid neoplasms in patients referred to the Departments of AOU and AUSL of the Province of Modena, especially for acute myeloid leukemia, we designed a diagnostic algorithm in which a preliminary diagnosis, established by a skilled morphologist, defines, in the presence of cytopenia(s), cytosis and/or organomegaly (particularly splenomegaly), and after the immunophenotypic characterization, the appropriateness and priority of further investigations leading to a definite diagnosis and preventing unnecessary investigations. Based on preliminary diagnosis of myeloid neoplasm, mainly defined by cyto-histological findings, the cytogenetics, molecular diagnostics and genomic tests are scheduled in terms of priority and panels of execution, according to the algorithm showed in Figure 1.

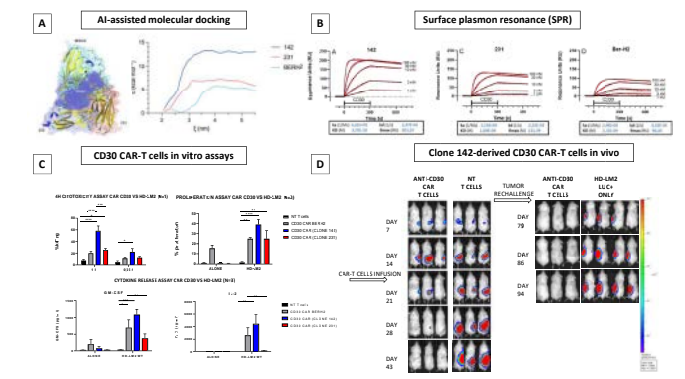


Figure 1.

Upon completion of each cytogenetic (by Fluorescence *in situ* Hybridization and karyotype) and molecular (by targeted PCR and next-generation sequencing) investigation, individual reports will be formulated signed and released by the professionals responsible. Once all the aforementioned data have been obtained, the results will be presented and reviewed during meetings of the staff involved in the Integrated Hematological Diagnostics Area into the Laboratory Medicine and Pathology Department and a summary report (called

“Integrated Diagnostic Report”) including morphological (cyto-histological), immunophenotypic, cytogenetic and molecular data will be provided and signed as a consultancy by the morphologist of the Hemo-lymphopathology Unit. The “Integrated Diagnostic Reports” will provide a detailed and definitive diagnosis according to both the Fifth Edition of the World Health Organization (WHO 5th) and the International Consensus Classifications (ICC) of Myeloid Neoplasms. This final “Integrated Diagnostic Report” will be released and, if necessary, it will be further discussed during periodic meetings with the clinicians, also to help with the divergences between WHO 5th edition and ICC. This integrated reporting has been successfully employed for the diagnosis of 92 cases of myeloid neoplasms, of which 32 acute myeloid leukemias, out of 1300 bone marrow aspirates, in the last 12 months.

P063

DDPCR SPECIFIC ASSAYS APPLICATION FOR THE MOLECULAR ANALYSIS OF IDH1 AND IDH2 GENES MUTATIONS IN ACUTE MYELOID LEUKEMIA

C. Carollo, K. Nikitsenka, E. Novella, A. Tosetto

Laboratorio Interno di Ematologia - U. O. C. Ematologia Ospedale San Bortolo, Italy

Somatic mutations in isocitrate dehydrogenase genes, IDH1 and IDH2, occur in ~5% to 15% and ~7% to 18% respectively of adult Acute Myeloid Leukemia (AML) patients. Molecular characterization of the leukemic clones and possibility of monitoring the minimal residual disease (MRD) offers a refined risk stratification and improved treatment decision making tools in the era of target therapy. In this study, we sought to investigate the prognostic influence of IDH mutations alone and in combination with frequently co-occurring mutation of NPM1-A. The operative procedure was performed optimizing amplification conditions and the Limit of Blank (LoB) and Limit of Detection (LoD) were defined on a panel of 20 wild type patients tested in triplicate for each assay and results of positivity expressed in Fractional Abundance (FA): 0,1 % for IDH2 R140Q, IDH1 R132H, IDH2 R172K mutations, and 0,2% for IDH1 R132C.

The study was performed in 84 samples extracted from peripheral blood and bone marrow related to 4 patients with cytogenetically normal AML, harboring IDH1 or IDH2 plus NPM1 mutations, and 4 patients negative for NPM1, diagnosed between 2019-2023. Three different commercial ddPCR assays for IDH mutations were applied: IDH1 R132H, IDH2 R140Q, IDH2 R132K.

In 8 patients, both in subjects with mutations in IDH genes and in patients with mutations in NPM1-A, it was observed that IDH well correlates with clinic state. In three patients with IDH2 R172K mutated showing at diagnosis FA 28,6%, FA 44. 6%, FA 35. 2% respectively, the IDH clone was no longer quantifiable in ddPCR during follow-up, in accordance with the clinical trend of remission. In one patient harboring IDH2 R140Q mutation, FA was 46,6% at diagnosis, but despite the initial clinical remission, IDH marker was always detectable until the clinical relapse, with IDH increasing FA to 25. 6%. As for patients with both mutated IDH (IDH1 or IDH2) and NPM1-A, it was observed strict correlation between the two markers in study: in three cases both markers have remained detectable in follow up and preceded relapse; in one case IDH resulted undetectable after therapy, NMP1 ratio <4 log and the patient is still maintaining in clinical and molecular remission. ddPCR appears actually the most accurate strategy for detection and quantification of low-abundance nucleic acids which can be applied in combination with RQ PCR and Sanger in laboratory routine. Interpretation and stability of IDH markers are still discussed, but the availability of quantitative molecular assays could be useful to study their prognostic value,

expanding the panel of markers for the MRD monitoring in AML, mainly in those patients where there are no other useful molecular targets.

P064

VENETOCLAX REAL-WORLD OBSERVATIONAL STUDY ON EFFECTIVENESS AND TREATMENT MANAGEMENT IN PATIENTS WITH NEWLY DIAGNOSED AML WHO ARE INELIGIBLE FOR INTENSIVE CHEMOTHERAPY IN ITALY – VERO

M.G. Della Porta¹, P. Volpicelli², M. Caira², S. Malgieri², D. Nucciarelli², G. Gualberti², P. Finsinger²

¹Leukemia Unit, Cancer Center - IRCCS Humanitas Research Hospital & Humanitas University; ²AbbVie srl Campoverde, Italy

Introduction. Venetoclax + Hypomethylating agents (Ven + HMAs) has been approved by EMA based on the VIALE-A study¹, a phase 3 randomized study which demonstrated the superiority of Ven + Azacitidine (Aza) vs Aza monotherapy in terms of deep, durable responses and overall survival in patients with AML who are ineligible for intensive chemotherapy. The international guidelines²⁻³, recently updated, recommend Ven + HMAs as treatment for this setting of patients². Italian physicians have almost 3 years of experience with Ven + HMAs in this setting thanks to the Italian 648/1996 Law, which allowed early access to the combination in 2020. Despite this background, there is still an important need to increase understanding of real-world clinical practice across different hematological centers in Italy. This study aims to collect prospective real-world data on the effectiveness and safety of the combination Ven + Aza, to describe the Ven management pattern in a real-life setting in Italy and the patients' Quality of Life (QoL).

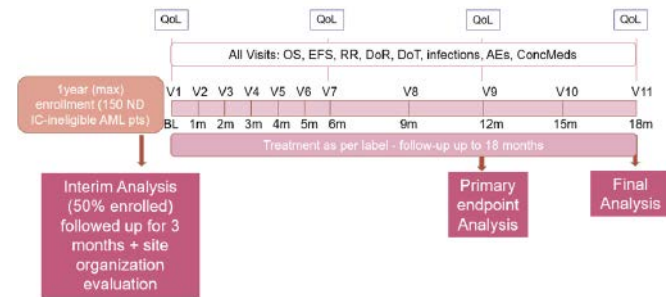


Figure 1. Study schematic.

Methods. This multi-center, prospective, post-marketing observational study will enroll 150 patients with newly diagnosed AML ineligible for intensive chemotherapy, in around 28 hematological centers. The primary endpoint is overall survival with a study follow-up of 18 months. Key secondary endpoints are: event-free survival, response rate, treatment and response duration, time to transfusion independence, proportion of pts with infections, treatment with antifungal prophylaxis and/or granulocyte colony stimulating factors. QoL (exploratory endpoint) will be assessed every 6 months through the EORTC QLQ C-30 and EQ-5D-5L questionnaires (Figure 1). Key inclusion criteria: Adult patients with confirmed diagnosis of primary or secondary AML, who are ineligible for intensive chemotherapy because of age, performance status, comorbidities or any other clinical reason as defined by the treating physician; investigator's decision on patient treatment with Ven + Aza reached prior to and independently of recruitment into the study; treatment prescribed in accordance with the applicable approved label and local regulatory and reimbursement policies.

Results. NA
Conclusions. NA

References

- DiNardo CD, et al. "Azacitidine and Venetoclax in Previously Untreated Acute Myeloid Leukemia". *N Engl J Med.* 2020;383(7): 617-29
- National Comprehensive Cancer Network (NCCN), Version 2. 2023 — March 13, 2023 (<https://www.nccn.org/>)
- Döhner, Hartmut, et al. "Diagnosis and management of AML in adults: 2022 recommendations from an international expert panel on behalf of the ELN." *Blood, The Journal of the American Society of Hematology* 140. 12 (2022): 1345-1377

P065

NON CANONICAL FLT3 MUTATIONS IN ACUTE MYELOID LEUKEMIA (AML) | HOW TO INTERPRET THESE VARIANTS?

E. Borotti¹, E. Ronda¹, A. Schiro¹, P. Cortellazzi¹, N. Codeluppi², E. Follini², L. Pochintesta², A. Rossi¹, D. Vallisa²

¹UO Biologia dei trapianti diagnostica molecolare e manipolazione cellule staminali emopoietiche AUSL di Piacenza; ² UO Ematologia AUSL di Piacenza, Italy

Introduction. Fms-like tyrosine kinase 3 (FLT3) is frequently mutated in haematological malignancies. Routine Next Generation Sequencing (NGS) of all FLT3 exons will lead to identification of rare missense variants. Although canonical FLT3 mutations including internal tandem duplications (ITDs) and tyrosine kinase domain (TKD) have been extensively studied, little is known about the clinical significance of non-canonical FLT3 mutations.

Methods. Analysis of FLT3 gene is performed by fragment analysis (ITD and hot-spot variants in the TKD domain) by LeukoStrat® CDx FLT3 Mutation Assay and by NGS panel of 40 myeloid genes (Ampliseq Myeloid Illumina Panel).

Results. In our Center, among 47 AML patients analyzed by NGS panel between January 2021 and September 2023, we identify 3 ITD variants (confirmed by fragment analysis), 4 mutations affecting D835 codon in the TKD2 domain (1 with variant allele frequency <3%) and 5 missense non-canonical variants in FLT3 gene. The non-canonical missense variants N841K, D839G and Y842S are located in the TKD2 hot-spot protein domain and they can be classified with probably pathogenic significance. The rare K334Q variant is in the Ig-like protein domain and the Y545H variant is in the TMD domain, identified in a patient also carrying the Y842S variant. These variants are therefore classifiable of unknown significance. To date, patients with K334Q and D839G are still in remission until now, after 13 and 7 months; in both patients the molecular profile is characterized by variants in the GATA2, BCOR, SF3B1, WT1 and WT1, NRAS genes respectively. While patients with N841K and Y842S had an aggressive course and died of an infectious complication. In these last cases, genetic analysis highlighted variants in ETV6, STAG2, PHF6, RUNX1 and ASXL1, EZH2, RUNX1, ZRSR2 genes, respectively.

Conclusions. Treatment of AML has been enhanced by the development of several novel agents, including FLT3 inhibitors. During molecular therapies here, determining the efficacy of these agents for patients with AML harbouring atypical driver mutations is still challenging. Clinical reports of non-canonical FLT3-mutated AML are limited, but according to literature variants as N841K, D839G and Y842S seem to be recurrent non-canonical variants with likely pathogenic significance. Therefore, patients carrying these variants could be treated as TKD positive-like patients. In this study, in only one patient a Gilteritinib salvage therapy was employed with initial rapid clearance of the blasts but unfortunately the patient died of septic shock. Prognostics implications of patients with AML harbouring non-canonical FLT3 remain unknown and complex and should be

assessed with other variants in the remaining genes. All-exons molecular investigations allow the identification of rare variants, whose interpretation requires continuous updating, in-depth analysis of medical-scientific studies and careful evaluation of the clinical picture.

P066

CYTOGENETIC ABNORMALITIES IN AML-MYLODYSPLASIA-RELATED CHANGES PATIENTS A MONOCENTRIC EXPERIENCE

C. Fabbricatore, C. Caliendo, G. Malferà, A. Pagano, R. Rosamilio, C. Califano

U. O. C. di Ematologia ed Autotrapianto di Cellule Staminali del P. O. A. Tortora, Italy

Introduction. AML with myelodysplasia-related changes (AML-MRC) represents a subgroup of AML defined by the presence of one or more of the following features: multilineage dysplasia, a history of MDS or MDS/myeloproliferative neoplasm (MPN), and specific MDS-defining cytogenetic abnormalities. AML-MRC portends a worse prognosis than non-MRC AML with both decreased complete remission rate and overall survival. To investigate the genetic and prognostic characteristics of AML-MRC represents a significant challenge to the optimal treatment of patients. Here we reported the study of 25 patients.

Methods. Metaphase cytogenetic analysis was performed in bone marrow (BM) aspirate, which were inoculated into cell culture for 24 h without mitogens. Routinely, 20 metaphases were analyzed for each specimen and the final results were reported by following the 2020 International System for Human Cytogenetics Nomenclature (ISCN 2020) guidelines. The aberrations not appreciated by karyotyping but revealed by FISH. AML FISH analysis typically with LSI CSF1R Spectrum Orange/ D5S23, D5S721 Spectrum Green Probes, LSI D7S486 Spectrum Orange/ CEP 7 Spectrum Green Probes, LSI D20S108 Spectrum Orange Probe and Cep 8 spectrum orange dna probe kit (Abbott Molecular, Des Plaines, IL, USA) was performed in all cases included in this study, which may aid in identifying patients with AML-MRC.

Results. In this study 13 patients (52%) showed chromosomal abnormalities, including +8 2 cases (8%), 5 cases of 5q (20%), 6 cases (24%) of abnormal complex karyotypes (CK) (≥ 5 unrelated chromosomal abnormalities), CK contained chromosomal abnormalities such as +8, 5q-. In 12 patients (48%) was identified no cytogenetic alterations.

Conclusions. The patient's clinical history, cytogenetic analysis, mutational analysis, and morphologic evaluation are all important for the diagnosis and prognosis of AMLMRC, as well as for informing treatment decisions. Since there are now newer initial treatment options for this subset of patients, it is critical for the pathologist to offer the diagnosis of AML-MRC as soon as possible, which may require amending reports after receipt of cytogenetic and molecular genetic results.

References

- "AML with Myelodysplasia-Related Changes| Development, Challenges, and Treatment Advances" Kristin L. Koenig et al. *Genes (Basel)*. 2020 Jul 24;11(8):845.
- "Diagnosis and Treatment of Patients With Acute Myeloid Leukemia With Myelodysplasia-Related Changes (AML-MRC)" Daniel A Arber et al. *Am J Clin Pathol*. 2020 Nov 4;154(6):731-741.

P067

GENETIC MOLECULAR PROFILE IN CHRONIC MYELOMONOCYTIC LEUKEMIA (CMML) PATIENT FROM ONSET TO POST-TRANSPLANT RELAPSE| A CASE REPORT

E. Borotti¹, E. Ronda¹, S. Guidotti¹, A. Scarpa¹, A. Schiro¹, P. Cortellazzi¹, N. Codeluppi², D. Ferrarese¹, L. Pochintesta², E. Follini², D. Vallisa², A. Rossi¹

¹UO Biologia dei trapianti diagnostica molecolare e manipolazione cellule staminali emopoietiche AUSL di Piacenza; ²UO Ematologia AUSL di Piacenza, Italy

Introduction. CMML is a myelodysplastic/myeloproliferative neoplasm with genetic heterogeneity and variable clinical course. We present a case of a 57-year-old female patient with suspected CMML-type MDS/MPN, characterized with advanced molecular biology techniques.

Methods. Hot-spot analysis of FLT3 (ITD, TKD domain variants D835 and I836) and NPM1 (type A, B, D variants) genes, molecular screening of chromosomal rearrangements and NGS analysis (40 myeloid genes) are performed. High resolution HLA typing by NGS and post-transplant chimerism analysis by fragment analysis are also performed.

Results. First analysis reveal an intermediate risk molecular profile (CPPS1 score) positivity for Tier I variants in NRAS (G13V), NPM1 (Type K), DNMT3A (c. 1851+1G>A) genes and a Tier II variant in GATA2 gene (N351K). After the 3^o cycle of Azacitidine, the patient shows leukemia progression with FLT3 ITD variant (allelic ratio 0.09) and an NGS molecular profile overlapping to the onset one. The patient is candidate for an HLA-identical transplant. The 30 days post-transplant evaluation shows negative FLT3 ITD minimal residual disease (MRD), complete chimerism on whole blood and 97% donor on CD3+ cell line. At 60 days post-transplant, the patient shows clinical signs of relapse confirmed by loss of engraftment (8% donor chimerism on whole blood and 3% donor on CD3+) and FLT3 ITD positivity (allelic ratio 3.52). Genetic screening remains negative for chromosomal rearrangements and NGS profiling reveals also a new Tier I variant in WT1 gene (V371Cfs*14). After Gilteritinib therapy, FLT3 ITD is lower (allelic ratio 0.096); so patient is candidate for a second haploidentical transplant, not performed due to patient death.

Conclusions. This case demonstrates the role of molecular analysis to define the dynamic disease architecture and to predict its clinical outcome. The variant in RAS gene identifies an intermediate risk subset which however seems to have a more aggressive phenotype. Her onset molecular profile highlights limitations for MRD evaluation: the rare type K variant in NPM1 gene cannot be monitored by target RT-PCRq method and fragment analysis for FLT3 ITD variant has a sensitivity of 10⁻². Molecular MRD techniques should reach at least a LOD of 10⁻³, more data are required for the use of these molecular markers. In this scenario, the analysis of 30 days post-transplant chimerism can be the only early relapse predictor. The juvenile onset, the aggressive phenotype and the GATA2 likely pathogenic variant suggest a clinical picture compatible with a hereditary form. Although some technical limitations, the methodologies integration and accurate variants interpretation show predictive and prognostic advantages.

Chronic Lymphocytic Leukemia and Chronic Lymphoproliferative Disorders

P068

CHARACTERIZATION OF CD38 EXPRESSION IN T-CELL PROLYMPHOCTIC LEUKEMIA (T-PLL) PATIENTS

E. Buson^{1,2}, G. Calabretto^{1,2}, A. Burattin⁴, V.R. Gasparini^{1,2}, S. Orsi⁴, E. Rampazzo^{1,2}, A. Teramo^{1,2}, V. Trimarco¹, S. Manni^{1,2}, G. Barilà^{1,3}, M. Facco^{1,2}, S. Bortoluzzi⁴, L. Trentin¹, G. Semenzato^{1,2}, R. Zambello^{1,2}

¹Padova University School of Medicine, Department of Medicine, Hematology division; ²Veneto Institute of Molecular Medicine (VIMM); ³Vicenza Hospital, Hematology Division; ⁴University of Padua, Department of Molecular Medicine, Italy

Introduction. T-Cell Prolymphocytic Leukemia (T-PLL) is a rare and aggressive disease characterized by the clonal proliferation of mature CD4+ T-cells that leaves patients with limited therapeutic options and results in a poor outcome. Although gain-of-function mutations in the JAK/STAT pathway of leukemic cells, particularly involving *JAK3* and *STAT5B*, have been reported. The transcriptome perturbances induced by these genetic lesions have not yet been elucidated. Among the downstream targets of JAK/STAT axis, we focused on CD38, a multifunctional ectoenzyme and transmembrane protein often over-expressed in hematological cancers and clinically relevant due to its prognostic significance. Evidence of CD38 expression has recently been provided in a cohort of 7 T-PLL cases, but the impact of *JAK3/STAT5B* mutations on CD38 expression has never been addressed. The aim of this study was to provide new evidence on CD38 expression in T-PLL patients, with the perspective of clinical translation.

Methods. Sixteen patients and 10 healthy donors (HD) were enrolled in the study and provided written informed consent. Mutation analyses were performed using Sanger-seq. CD38 transcription was investigated in a pilot cohort profiled by RNA-seq and in an extended group through RT-qPCR. A multi-color panel was designed for flow cytometry to evaluate CD38 membrane expression. In detail, the anti-human CD3, CD4, CD7, CD26 and CD45 mAbs were combined with CD38 to identify CD38-positive cells (Fluorescence-Minus-One strategy).

Results. Out of 16 T-PLL patients, 63% (10/16) carried at least one mutation in the JAK/STAT axis (N=3 in *STAT5B*, N=4 in *JAK3* and N=3 in both genes). Western blot (WB) analysis revealed different *STAT5B* activation levels in each subgroup, with the highest Tyr694-phosphorylation observed in *STAT5B*-mutated patients, intermediate levels in *JAK3*-mutated patients and low levels in wild-type (WT) cases. CD38 mRNA was first investigated in our RNA-seq pilot cohort (10 T-PLL cases and 5 HD), showing significant up-regulation in pathological CD4+ T-cells ($p < 0.04$) compared to HD. CD38 was subsequently studied in 16 patients (8 of the RNA-seq group and 8 other T-PLL patients) and 6 HD by RT-qPCR. Notably, a CD38 primary transcript up-regulation was found in T-PLL patients and particularly in the *STAT5B*-mutated group, suggesting the occurrence of epigenetic regulation among other mechanisms. In contrast, comparable CD38 levels were observed in *JAK3*-mutated and WT cases (others, OTH). Flow cytometry analysis confirmed a higher expression in *STAT5B*-mutated (mean: $87 \pm 18\%$) compared to OTH T-PLL patients (mean: $26 \pm 9\%$).

Conclusions. Our data provide new evidence on CD38 expression in T-PLL patients, showing a correlation between a high CD38 expression and *STAT5B* mutations/activation. Ongoing analyses are evaluating CD38's prognostic relevance, aiming to improve patient

stratification as well as to explore immune-targeting of CD38 as a novel potential therapeutic strategy.

P069

THE COMBINATION OF DEFACTINIB WITH BTK INHIBITORS AFFECTS CHRONIC LYMPHOCTIC LEUKEMIA CELLS SURVIVAL

G. Capasso, N. Mouawad, E. Ruggeri, A. Visentin, F. Severin, V. Trimarco, A. Tonini, S. Pravato, M. Facco, F. Frezzato, L. Trentin

Hematology and Clinical Immunology Unit, Department of Medicine, University of Padova, Italy

Introduction. Chronic Lymphocytic Leukemia (CLL) is characterized by the accumulation of clonal B lymphocytes in peripheral blood, bone marrow and lymphoid tissues. The mechanisms involved in CLL pathogenesis prompted us to look at Focal Adhesion Kinase (FAK) in this disease. FAK is a 125kDa protein which, upon phosphorylation on tyrosine (Y) 397, is activated thus controlling cellular processes such as adhesion, migration, apoptosis, and proliferation. Several inhibitors have been developed to target FAK kinase, one such inhibitor being defactinib. In CLL, the use of Bruton's tyrosine kinase inhibitors (BTKin) has amazingly changed the clinical history of CLL patients. Nevertheless, an increasing number of patients develop resistance to this treatment. For this reason, alternative therapeutic strategies have necessarily to be explored.

Methods. Freshly isolated leukemic B cells from 10 therapy-free CLL patients were cultured in RPMI1640 supplemented with antibiotics and 2% FBS and treated with $5 \mu\text{M}$ defactinib. $5 \mu\text{M}$ BTKin (ibrutinib, acalabrutinib, zanubrutinib) were added singularly to defactinib-treated cells. In another set of experiments, cells from 4 ibrutinib-resistant CLL patients were cultured with $5 \mu\text{M}$ defactinib. Apoptosis was evaluated after 24 and 48 hours by Annexin V/Propidium iodide (PI) flow cytometry test and by the presence of cleaved PARP in western blotting (WB). The expression level of FAK phosphorylation on Y397, representing its kinase activity, was examined using WB. Calpain, as FAK activator, was also evaluated.

Results. We herein demonstrated that when defactinib is combined with BTKin an increase in PARP cleavage was observed, indicating that defactinib enhances BTKin activity. This finding was further supported by the Annexin V/PI assay, where leukemic B cells showed a significant reduction in their viability when co-treated with both agents (defactinib + BTKin), resulting in an increased apoptosis rate of 33% at 24h and 41% at 48h, compared to either agent alone. Interestingly, calpain expression and FAK phosphorylation were not affected by BTKin alone. However, samples treated with defactinib (alone or in combination) showed a reduction in both calpain expression and FAK phosphorylation, this suggesting that the enhanced apoptosis observed is specifically due to the selective inhibition of FAK. Furthermore, when CLL cells from ibrutinib-resistant patients were treated with defactinib, they underwent apoptosis.

Conclusions. Our findings demonstrate that, *in vitro*, defactinib enhances the cytotoxic effects of BTKin and is effective in ibrutinib-resistant patients, the induced apoptosis being accompanied by decrease of FAK activation. These results highlight FAK as a promising target for the development of novel therapeutic approaches in CLL, particularly for those patients who relapsed after BTKin treatment. The potential clinical relevance of targeting FAK warrants further investigation in clinical settings.

P070

BH3 PROFILING IDENTIFIES BCL-2 AND MCL-1 DEPENDENCIES IN LYMPHOPLASMACYTIC LYMPHOMA

C. Frusteri, M. Paluzzi, E. Lovato, I. Ferrarini

Cancer Research & Cell Biology Laboratory, Section of Hematology, Department of Engineering for Innovation Medicine, University of Verona, Italy

Introduction. Lymphoplasmacytic lymphoma (LPL) is a low-grade B-cell malignancy characterized by the clonal expansion of mature B-cells and related IgM-expressing plasma cells. Despite the efficacy of current treatments, most patients relapse and need novel therapeutic strategies. The mitochondrial pathway of apoptosis has emerged as a successful therapeutic target in cancer. Mitochondrial apoptosis is regulated at the outer mitochondrial membrane by the Bcl-2 protein family. The anti-apoptotic members (Bcl-2, Mcl-1, Bcl-xL and Bfl-1) bind the pro-apoptotic relatives thus preventing the release of cytochrome c (cyt c) from mitochondria. Here, we used BH3 profiling to investigate the apoptotic priming and the anti-apoptotic dependencies of LPL.

Methods. Eleven LPL patients, 9 treatment-naïve (TN) and 2 relapsed, were enrolled. LPL cells were collected from peripheral blood or bone marrow and were subjected to BH3 profiling, a flow-cytometry based assay measuring the percentage of cyt c release from mitochondria after incubation with pro-apoptotic peptides. The promiscuous peptide BIM interrogates the apoptotic priming. Specific peptides (BAD, HRK, MS-1, FS-1) and small molecules (venetoclax, BGB-11417) inform about the anti-apoptotic dependencies of cancer cells. Nine patients with chronic lymphocytic leukemia (CLL), a paradigmatic example of Bcl-2 dependent malignancy, were enrolled as comparison group.

Results. We generated a heatmap (Figure 1A) illustrating the response of LPL cases to all pro-apoptotic stimuli. Each case was analyzed discriminating the lymphoid (Ly, CD19⁺CD138⁻) from the plasma cell (Pc, CD19⁺CD138⁺) component. In patient #5 and #11, only the Ly component could be identified. Burkitt lymphoma cell line DG-75, not expressing Bax and Bak, was used as negative control for cyt c release. Overall, LPL cells were primed for apoptosis, as they released high amount of cyt c in response to BIM peptide, and were highly Bcl-2 and Mcl-1 dependent (Figure 1B).

paring Mcl-1 dependency to Bcl-xL dependency). The apoptotic priming was reduced in the Pc as compared to the Ly component of LPL samples (93.9% vs 74.9%, P<0.05). In contrast, the specific anti-apoptotic dependencies did not differ between the two compartments. To gain further insights on the apoptotic profiles of LPL, we compared TN LPL cases with 9 TN CLL samples. LPL was characterized by lower apoptotic priming and lower Bcl-2 dependency than CLL (P<0.05). Interestingly, non-Bcl-2 anti-apoptotic dependencies, particularly Mcl-1, were higher in LPL as compared to CLL (Figure 1C, P<0.01).

Conclusions. LPL cells are relatively primed for apoptosis and depend mainly on Bcl-2 and Mcl-1 for survival. Dual antagonism of these anti-apoptotic proteins could be explored as a new therapeutic avenue for LPL patients.

P071

REPURPOSING OF THE ANTIMALARIC ATOVAQUONE FOR THE TREATMENT OF PATIENTS AFFECTED BY LARGE GRANULAR LYMPHOCYTE LEUKEMIA

E. Rampazzo^{1,2}, A. Teramo^{1,2}, V.R. Gasparini^{1,2}, G. Calabretto^{1,2}, C. Vicenzetto³, E. Buson^{1,2}, G. Barilà^{1,2}, V. Trimarco¹, M. Facco¹, L. Trentin¹, G. Semenzato^{1,2}, R. Zambello^{1,2}

¹Department of Medicine, Hematology and Clinical Immunology Branch, University of Padova; ²Veneto Institute of Molecular Medicine (VIMM); ³Department of Cardiac, Thoracic, Vascular Sciences and Public Health; University of Padova, Italy

Introduction. Large Granular Lymphocyte Leukemia (LGLL) is a rare lymphoproliferative disorder characterized by clonal expansion of Large Granular Lymphocytes (LGLs). STAT3 activation, whether due to somatic mutations or epigenetic mechanisms, plays a key role in LGLL pathogenesis by triggering the expression of antiapoptotic genes, ultimately resulting in LGLs resistance to the activation induced cell death. LGLL therapy primarily relies on the use of immunosuppressive drugs, whose efficacy is often unsatisfying, therefore finding alternative treatments is mandatory. Atovaquone (ATQ) is an FDA approved drug for the treatment of malaria, known for its minimal collateral effects. A study published in Blood (Xiang *et al.*, 2016) proved its efficacy as a selective STAT3 inhibitor through Gp130 down-modulation. Giving the relevance of STAT3 in the progression of the disease, this study aimed to validate ATQ effect on LGLs survival and to shed a light on its mechanism of action, with the ultimate goal to develop a target approach to treat LGLL patients.

Methods. Peripheral Blood Mononuclear Cells (PBMC) from LGLL patients were cultured with ATQ at a concentration of 25 µM, which is comparable with the levels detected in patients' plasma treated for malaria. By flow cytometry, Annexin V and anti-Gp130 staining were used to assess cell viability and Gp130 expression on LGLs, respectively. ATQ activity was evaluated by analyzing STAT3 phosphorylation and other related pathways by Western Blot; its activity on mitochondrial respiration was assessed on MOTN-1, a LGLL-like cell line, using a staining with CM-H2DCFDA.

Results. The results obtained show a significant cytotoxic activity of ATQ against leukemic LGLs at a concentration of 25µM, evident from 48h of treatment on a cohort of 15 patients. Importantly, the observed efficacy was irrespective of the STAT3 mutational status. In detail, ATQ reduced STAT3 activation mediated by its phosphorylation on Tyr705 (p<0,001) after 24h, confirming its role as a STAT3 inhibitor. Among the other investigated pathways, ERK activation emerged as inhibited by ATQ (p<0,05), suggesting other potential effects of this compound. Unlike Xiang *et al.*, we didn't observe a significant reduction of Gp130 membrane expression on

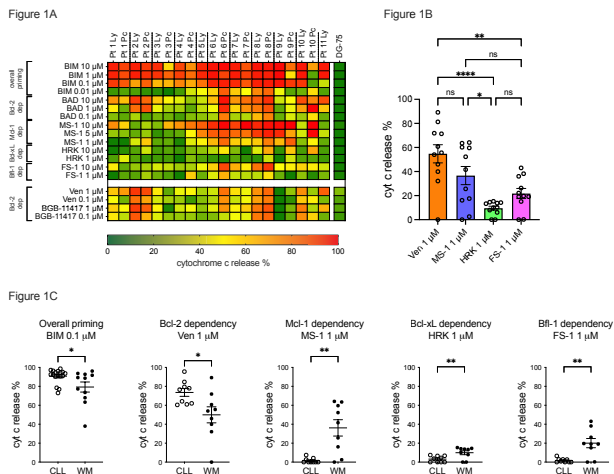


Figure 1.

Instead, Bfl-1 and Bcl-xL played minor roles in the anti-apoptotic defense (P<0.001 and P<0.01 when comparing Bcl-2 dependency with Bcl-xL and Bfl-1 dependency, respectively. P<0.05 when com-

patients' PBMC. So, we focused on a different mechanism of action represented by the inhibition of mitochondrial respiration mediated by ATQ. Functional studies performed on MOTN-1 revealed a trend of increased ROS production after ATQ treatment, supporting its potential impact on the mitochondria. Ongoing analyses are extending this observation to primary LGLL cells.

Conclusions. In conclusion ATQ could be a promising anticancer agent due to its cytotoxicity and antagonistic effect on STAT3 activation. This would represent a more specific therapy for LGLL patients, considering that at present, there are no STAT3 inhibitors available for the clinical treatment.

P072

CD38 IS UP-REGULATED IN SYMPTOMATIC CD8+ STAT3-MUTATED T-LARGE GRANULAR LYMPHOCYTE LEUKEMIA (T-LGLL) PATIENTS

G. Calabretto^{1,2}, E. Buson^{1,2}, B. Mariotti³, V. Trimarco¹, A. Teramo^{1,2}, E. Rampazzo^{1,2}, G. Barilà^{1,2}, S. Manni^{1,2}, M. Facco^{1,2}, F. Bazzoni³, L. Trentin¹, G. Semenzato^{1,2}, R. Zambello^{1,2}

¹Padova University School of Medicine, Department of Medicine, Hematology division; ²Veneto Institute of Molecular Medicine (VIMM); ³Department of Medicine, Division of General Pathology, University of Verona; ⁴Vicenza Hospital, Hematology Division, Italy

Introduction. T-Large Granular Lymphocyte Leukemia (T-LGLL) is a rare lymphoproliferative disorder characterized by the clonal expansion of cytotoxic T-LGL. The disease includes distinct biological and clinical subtypes, distinguishable by immunophenotype into the canonical CD8+ T-LGLL and a CD4+ T-LGLL variant. Additional genetic patient subgroups can be defined by STAT3 activating mutations, which are associated with cytopenias and reduced overall survival. CD38, which is expressed by malignant cells in several hematological diseases, often with prognostic relevance, has not been studied in LGLL. The aim of this work is to investigate CD38 expression in LGLL patients.

Methods. CD38 expression was studied in LGLL from 30 T-LGLL patients and 10 healthy controls (CTR) using flow cytometry (FC). The anti-human CD3, CD4, CD8, CD16, CD45, CD56 and CD57 mAbs were combined with CD38 and CD38+ cells were identified with the Fluorescence-Minus-One strategy. CD38 primary transcript (PT) levels were evaluated through RT-qPCR. H3K27 acetylation was investigated using ChIP-qPCR.

Results. CD38 expression was detected in leukemic T-LGL of 12/30 (40%) patients and it was significantly higher than in the control group. The mean percentage of CD38+ cells was 65±22 in T-LGLL cases vs 24±9 in CTR. A significant difference was also observed in the Mean Fluorescence Intensity (T-LGLL: 818±130 vs CTR: 330±41, p<0.01). Notably, all CD38+ cases fell in the CD8+/CD16+/CD56- T-LGLL subgroup, including 10/12 STAT3-mutated patients, all characterized by increased levels of STAT3 activation compared to other T-LGLL cases. Clinically, CD38+ patients showed a symptomatic disease (neutropenia and/or anemia) requiring treatment. In contrast, CD8+/CD16- (STAT3 wild-type) T-LGLL (N=8) and CD4+ T-LGLL cases (N=10) were negative for CD38 expression and characterized by a more indolent clinical course. Next, to investigate the biological mechanisms of CD38 up-regulation, we evaluated CD38 PT levels. RT-qPCR results confirmed FC data, pointing to increased CD38 transcription in symptomatic CD8+/CD16+/CD56- cases compared to other T-LGLL and CTR (p<0.05), thus suggesting the involvement of epigenetic mechanisms rather than post-transcriptional modifications. Further analyses on CD38 promoter demonstrated increased H3K27 acetylated sites in CD38+ patients and suggested STAT3 recruitment as the most prob-

able factor contributing to CD38 up-regulation.

Conclusions. We herein provide the first evidence of CD38 expression in T-LGLL patients and demonstrate its negative prognostic value. These findings could have clinical impact, enabling prompt identification, through FC, of CD38+ cases warranting a closer follow-up. In addition, our results pave the way for an immune-targeting of CD38 as a novel tailored therapeutic strategy for T-LGLL patients.

P073

IMPLEMENTATION OF MINIMAL MEASURABLE DISEASE ASSESSMENT BY NEXT-GENERATION SEQUENCING IN PATIENTS WITH CLL TREATED WITH VENETOCLAX COMBINATIONS

R. Maffei¹, A. Scarpa², M. Maccaferri³, E. Borotti², G. Debbia³, A. Rossi², A. Paolini¹, S. Martinelli¹, B. Conte¹, F. Giacobbi¹, G. Corradini¹, F. Pilato¹, D. Bernabei¹, G. Riva¹, V. Nasillo¹, C.G. Atene³, N. Mesini³, A. Messerotti³, V. Pioli³, G. Leonardi³, A. Arcari⁴, F. Russo⁵, A. Ferrari⁶, F. Ilariucci⁶, G. Roti⁵, M. Luppi³, T. Trenti¹, E. Tagliafico¹, D. Vallisa⁴, R. Marasca³

¹Department of Laboratory Medicine and Pathology, Diagnostic Hematology and Clinical Genomics, Azienda Ospedaliero-Universitaria, Policlinico; ²UOC Biologia dei Trapianti, AUSL Piacenza; ³Hematology Unit, Department of Medical and Surgical Sciences, University of Modena and Reggio Emilia, Azienda Ospedaliero-Universitaria, Policlinico; ⁴UOC Ematologia e CTMO, AUSL Piacenza; ⁵Azienda Ospedaliero-Universitaria di Parma, UOC Ematologia; ⁶S.C. Ematologia, Dipartimento Oncologico e Tecnologie Avanzate, Azienda USL-IRCCS, Italy

Introduction. In patients with chronic lymphocytic leukemia (CLL), evaluation of measurable residual disease (MRD) after treatment with venetoclax-based therapies is a useful parameter to define treatment efficacy and to stratify patients for time to progression. The optimization of next-generation sequencing (NGS) approach for MRD quantification is the prerequisite to apply MRD in the clinical management of CLL patients treated with venetoclax combinations.

Methods. An NGS approach by using LymphoTrack IGH CE IVD kit was applied for both clonotype identification and MRD evaluation. We designed an optimization plan to improve the applicability of NGS for MRD assessment in a prospective cohort of CLL patients treated with venetoclax-obinotuzumab (VEN-O) as front-line treatment or venetoclax-rituximab (VEN-R) in relapsed/refractory setting.

Results. We prospectively collected 40 patients with CLL treated with venetoclax-based therapies, 12 patients were treated with VEN-O and 28 with VEN-R. Mean age at diagnosis was 64 years (range 40-82). Fifty-three percent of patients had unmutated IGVH genes; TP53 aberrations were detected in 20% of cases. The leukemic clonotype was identified in peripheral blood (PB) sample collected before treatment, and MRD was evaluated in PB at the end of combination (EOCT+2 months) and in PB and bone marrow sample (BM) at the end of treatment (EOT). Data regarding the extent of CD19 positive cells in blood samples were collected to optimize the library preparation. The overall efficiency of NGS test for identification of leukemic clonotype was 100%. We found a predominant unique clonotype in 79% of cases, all were validated comparing results with immunoglobulin gene identified at diagnosis by sanger sequencing. The remaining cases showed multiple clonotypes that were not previously detected by conventional sanger sequencing. DNA obtained at the EOCT and EOT time-points were evaluated for MRD in triplicate, reaching a sensitivity between 10⁻⁴ and 10⁻⁵ in all but one case. Inter-run and intra-run reproducibility was assessed. Library preparation at EOCT was optimized due to B-cell depletion related to effects of therapeutic agents. Patients were divided into 3 subsets

accordingly to MRD data: uMRD-CLL for patients with an undetectable MRD and a sensitivity 10^{-4} , LP (low positive)-MRD-CLL for patients with detectable MRD below 10^{-4} and P-MRD-CLL for patients with detectable MRD above 10^{-4} . Twenty-one patients had samples available at EOCT. Only 9 patients (42%) reached undetectable MRD at the EOCT [u]MRD-CLL). Six CLL were classified as LP-MRD (29%), and 6 were P-MRD. Six CLL patients reached the EOT and persistence of a positive molecular MRD by NGS was found in 3 cases.

Conclusions. Our data describe an optimization approach of NGS test for MRD assessment to improve its application in the management of CLL patients treated with venetoclax combinations.

P074

A MEMBRANE ARRAY HIGHLIGHTS A RELEVANT SHP-1/LYN AXIS PATTERN SHARED BY BOTH IBRUTINIB- AND VENETOCLAX-RESISTANT CHRONIC LYMPHOCYTIC LEUKEMIA CELL LINES

F. Frezzato¹, E. Ruggeri¹, N. Mouawad¹, G. Capasso¹, M.A. Pagano², A. Visentin¹, A.M. Brunati², L. Trentin¹

¹Dipartimento di Medicina; ²Dipartimento di Medicina Molecolare, Italy

Introduction. The Bruton's tyrosine kinase inhibitor ibrutinib and the Bcl-2 inhibitor venetoclax have significantly changed the management of patients with Chronic Lymphocytic Leukemia (CLL) achieving high efficacy even in poor-risk and chemo-refractory patients. Despite this, resistance may develop over time. Besides BTK/PLC γ and Bcl-2 mutations, mechanisms of resistance remain to be clarified. Hence, there is a need to develop a CLL model resistant to ibrutinib or venetoclax that would help in conducting studies aiming at the identification of players or mechanisms involved in drug-resistance. Array studies are particularly suited to this type of investigation.

Methods. The Mec-1 CLL cell line, incubated at 37°C in a humidified atmosphere at 5% CO₂, was cultured in IMDM medium with antibiotics and 10% FBS (wild type, #WT) or with continuous and increasing doses of ibrutinib (#ibr) and venetoclax (#ven) until drug-resistance was verified by ibrutinib and venetoclax IC₅₀s calculation, Annexin V/Propidium Iodide flow cytometry test and the expression of the multi-drug resistance protein MDR-1. The protein profile of resistant cells (#ibr and #ven) was assessed by using membrane-based arrays for multiplexed protein detection from RayBiotech. In particular, the molecules involved in MAPK, AKT/PI3K/mTOR, JAK/STAT, NF- κ B, TGF- β pathways have been analyzed.

Results. In the attempt to create CLL drug-resistant cell lines, we achieved different IC₅₀ values for ibrutinib in Mec-1 #WT (5.14 μ M) vs Mec-1 #ibr (19.88 μ M) and for venetoclax in Mec-1 #WT (2.07 μ M) vs Mec-1 #ven (9.40 μ M) with calculated fold resistance compared to #WT of 3.87 and 4.54, respectively. Resistant cells showed enhanced expression of MDR-1 with respect to #WT. As for phosphorylation pattern, we found that in both Mec-1 #ibr and #ven, with respect to #WT, Src-family kinase Lyn was hyperactivated, whereas its functional counterpart SHP-1 was downregulated. This result highlights an overall activation of Lyn in CLL, known to be responsible of CLL cell enhanced survival. These data have been confirmed by western blotting analysis.

Conclusions. In CLL cells, the Src-family kinase Lyn is atypically expressed contributing to the unbalance between cell survival and pro-apoptotic signals. In Lyn axis, SHP-1 phosphatase has been identified as a novel player in the deranged signaling network and both have been described as potential attractive targets for new therapeutic strategies in CLL. An emerging clinical challenge in CLL research

is represented by new therapeutic strategies to be employed after ibrutinib and/or venetoclax discontinuation following resistance onset or disease progression. In this context, the Lyn/SHP-1 axis could be considered as an emerging therapeutic target in the post-ibrutinib and -venetoclax era.

P075

THE "DEDALUS" PROTOCOL| A COMPARISON OF FLOW CYTOMETRY AND NGS FOR MONITORING MEASURABLE RESIDUAL DISEASE IN CHRONIC LYMPHOCYTIC LEUKEMIA

C. Bono¹, F. Guerrini¹, F. Mavilia¹, F. Facella¹, S. Grassi², G. Tancredi¹, I. Sorgiovanni¹, V. Guerri³, P. Sammuri³, M.R. Metelli³, E. Benedetti³, C. Barattè³, F. Ricci³, S. Galimberti¹⁻²

¹Dipartimento di Medicina Clinica e Sperimentale, Ematologia, Università di Pisa; ²USL Toscana Nord-Ovest, Laboratorio di analisi chimico-clinica, Dipartimento di Diagnostica; ³AOUP, Italy

Introduction. In chronic lymphocytic leukemia (CLL) the therapeutic landscape has changed after introduction of the BTK and BCL2 inhibitors. Venetoclax can eradicate the "measurable residual disease" (MRD) and novel sensitive and accurate imaging and laboratory techniques are today necessary for assessing MRD.

Aim. "Dedalus" protocol was designed to test MRD using 2 different techniques (flow cytometry and NGS) in relapsed CLL patients where the response to rituximab-venetoclax was concomitantly assessed by an advanced ultrasound technique. Until now, 22 patients have been enrolled.

Methods. The flow cytometric analysis was conducted according to the ERIC guidelines, while for NGS we adopted the commercially available NGS panel Lymphotrack (Invivoscribe Technologies, San Diego, CA, USA), able to characterize the clonotypic rearrangement of the immunoglobulin heavy chain (IgH). About 2000 ng of DNA for each of 3 replicates have been used to reach a sensitivity level of at least 10^{-5} , according to the manufacturer's instructions. DNA from a commercial clonal B cell line was added in each reaction as a control spike-in (corresponding to 100 cells) to allow the absolute quantification of tumor clone. Resulting FastQ files were processed using the LymphoTrack Analysis and the LymphoTrack MRD softwares (Invivoscribe Technologies).

Results. The aim of the study was to compare NGS with flow cytometry, both in cases reaching the complete response (CR) and in those remained in partial response (PR). In all cases achieving CR as defined by ultrasound, the two laboratory techniques were superimposable (MRD was undetectable in all subjects by both flow and NGS). In the 2 cases in PR, the NGS mirrored the clinical situation better than flow. Indeed, in the first case, flow was negative while NGS detected the same IgH clone than at diagnosis either after 6 (3 clonal cell equivalents/ 10^6 cells) or 12 cycles (6 clonal cell equivalents/ 10^6 cells). More interestingly, in the second case, when patient was in PR, flow was negative while NGS was still clonal (45 clonal cell equivalents/ 10^6 cells); at CR, both flow and NGS did not detect MRD. Another interesting finding concerns the limit of detection of the 2 methods. For the flow was 10^{-4} in 100% of cases; about NGS, 3 replicates with 2000 ng of DNA were performed for reaching 10^{-5} but, in most cases, we reached 10^{-4} .

Conclusions. The standardized flow cytometry is the technique most frequently used for assessing MRD in CLL because it is quite easy, cheap and reaches the required sensitivity of 10^{-4} . Our results, however, show that NGS is probably more reliable than flow and better correlated with the clinical status, because in 2 cases defined as MRD-undetectable by flow IgH clonality was still detectable by NGS. It will be interesting to investigate if the MRD assessed by dd-PCR for IgH rearrangement on ct-DNA could represent a better non-invasive tool.

P076

INTRODUCTION INTO LABORATORY PRACTICE OF IGH GENE REARRANGEMENTS STUDY BY NEXT GENERATION SEQUENCING IN CHRONIC LYMPHOCYTIC LEUKAEMIA PATIENTS

A. Scarpa¹, E. Borotti¹, V. Scaglia¹, A. Arcari², A. Rossi¹, D. Vallisa²

¹UOC Biologia dei trapianti, Ospedale "G. da Saliceto", AUSL, Piacenza; ²UOC Ematologia e CTMO, Ospedale "G. da Saliceto", AUSL, Piacenza, Italy

Introduction. The assessment of minimal residual disease (MRD) by next-generation sequencing (NGS) in patients with chronic lymphocytic leukaemia (CLL) is becoming established in clinical practice. The use of the IGH-FR1 marker, which is widely used for MRD analysis in ALL and MM, was evaluated alongside the use of the IGH-leader marker, whose identification at disease onset does not require further analysis according to the European Research Initiative on CLL (ERIC) recommendations.

Methods. An NGS approach based on the commercial Lymphotrack Dx IGHV/IGH kit was validated on the Illumina MiSeq platform.

Results. Analytical optimisation of the whole process was carried out from the pre-analytical phase, comparing different approaches to mononuclear cell separation, validated by cytofluorimetric analysis. DNA extraction was validated using haemocytometric data. To assess analytical specificity, CLL samples previously tested by our laboratory and an external ERIC-certified centre for clonotype identification at disease onset by Sanger sequencing were used. Concordance for clonality was 100% between the two centres, and NGS was able to identify a clonal IGHV marker in 100% of patients tested. Scaled-up dilutions of the clonal control in the polyclonal control were performed to assess linearity and limit of detection (LoD), which was confirmed to be 2.5% for clonotype identification as specified by the manufacturer. Scalar dilutions of the internal controls were again used to assess analytical sensitivity for the MRD analysis: the LoDs of the two markers, IGH leader and IGH-FR1, were evaluated by applying the coefficient of determination (R²) to the two data sets obtained, which was 0.9999 for IGH leader and 0.9983 for IGH-FR1. The sensitivity of the method was confirmed at both 10⁻⁴ and 10⁻⁵ with >95% confidence. The diagnostic sensitivity was assessed by analysing 7 peripheral blood samples from CLL patients who had undergone MRD assessment by cytofluorimetry. Partial concordance between the methods was observed, with 44% of samples concordant, of which 33% had undetectable MRD (uMRD) and 11% had detectable MRD (pMRD). The 33% of samples had a discordant uMRD result by cytofluorimetry and pMRD by NGS of which half were 10⁻⁵ positive not cytofluorimetrically detectable. The remaining 23% of samples analysed were classified as NGS fail because the sensitivity of 10⁻⁴ was not achieved. The critical non-compliance was resolved by introducing CD19+ cell counts into the samples for MRD analysis and adjusting the required DNA input in relation to the sample characteristics. Intra- and inter-session repeatability was assessed.

Conclusions. After a successful result obtained in ERIC EPT for clonotype evaluation, the analysis was proposed for diagnostic use. The lack of an EPT for MRD analysis was overcome by an inter-laboratory quality assessment.

P077

COMPLEX KARYOTYPE AS A PROGNOSTIC MARKER IN CHRONIC LYMPHOCYTIC LEUKEMIA PATIENTS DURING TREATMENT WITH CHEMOIMMUNOTHERAPY BTKI AND VENETOCLAX

D. Tocci¹, K. Peccia¹, R. Crupi¹, S. Ciofini¹, M. Bocchia^{1,2}, A. Gozzetti^{1,2}

¹Hematology, Siena University Hospital; ²Department of Medicine, Surgery and Neuroscience, University of Siena, Italy

Introduction. Chronic lymphocytic leukemia (CLL) is a hematological neoplasm characterized by proliferation and accumulation of small mature lymphocytes in the peripheral blood, bone marrow and lymph nodes, that in more than 95% of cases are of B nature. This disease shows remarkable clinical heterogeneity: there are forms of indolent disease with no treatment requirement and there are more aggressive forms that evolve rapidly. The clinical heterogeneity of B-CLL is associated with genetic heterogeneity. The low mitotic index of B cells causes a high failure in conventional cytogenetic analysis in peripheral blood cultures. Thanks to the introduction of new human B-lymphocytes stimulation protocols, the conventional cytogenetic is covering an important prognostic relevance in latest years. The aim of this study was to perform molecular cytogenetics (FISH) and stimulated (karyotype) investigations in B-CLL patients at diagnosis and before starting therapeutic treatment.

Methods. The investigation Cytogenetic tests were performed on peripheral venous blood samples anticoagulated with heparin. For each patient, a stimulated cell culture was set up with the addition of a mixture of oligonucleotides (CpG-Oligonucleotides DSP30) and recombinant human interleukin-2 (IL-2) capable of stimulating *in vitro* the cell division of human B lymphocytes.

Results. The study included a total of 20 patients, 15 males and 5 females, with a median age of 69 years (range 48-84). The results reveal important differences and limitations between the two techniques. The FISH analysis provided an evaluable result in all cases and documented chromosomal alterations in only 9/20 cases (45%). Karyotype analysis was not evaluable in 4/20 cases (20%) and in the remaining 16 cases (80%) evaluable metaphases were obtained which highlighted the presence of structural and numerical chromosomal alterations in 12/16 cases (75%). In 5 cases in which FISH detected chromosomal alterations, the karyotype also showed the same alterations (del13q, +12, del11q and del17p), demonstrating concordance between the two techniques. In 4 cases in which the FISH was normal, the karyotype showed alterations with aberrations in chromosomal regions different from those analyzed using the FISH probes, highlighting that the FISH panels used in clinical practice are not sufficient to highlight all the possible alterations. Furthermore, the analysis of the karyotype in 2 cases with altered FISH revealed the presence of additional chromosomal alterations and therefore, the presence of a complex karyotype, an element which has now been widely demonstrated to represent an independent negative prognostic factor. Those two patients performed badly with BTKi and chemotherapy

Conclusions. Despite the limited number of cases analyzed, the study shows that the stimulated karyotype in B-CLL can detect greater genetic complexity, compared to fish analysis; therefore, the study of karyotype at diagnosis can provide useful information to the hematologist for a better prognostic stratification and therapeutic choice.

P078

ADIPONECTINS SERUM LEVEL CORRELATION WITH KNOWN PROGNOSTIC FACTORS IN B-CELL CHRONIC LYMPHOCYTIC LEUKEMIA

C. Giordano¹, M. Picardi¹, E. Nigro^{2,3}, N. Pugliese¹, F. D'agostino¹, A. Vincenzi¹, L. Esposito¹, D. Lisi¹, A. Scarpa¹, M. Mallardo^{2,3}, A. Daniele^{3,4}, F. Pane¹

¹Department of Clinical Medicine and Surgery, Hematology Unit, Federico II University; ²Dipartimento di Scienze e Tecnologie Ambientali, Biologiche, Farmaceutiche, Università della Campania "Luigi Vanvitelli"; ³CEINGE, Biotecnologie Avanzate Scarl; ⁴Dipartimento di Medicina Molecolare e Biotecnologie Mediche, "Federico II" Università degli Studi di Napoli, Italy

Introduction. Adiponectin is an adipokine with anti-inflammatory properties that has been linked mainly to the risk of myeloid hematological malignancies while there're controversial data regarding its role in the chronic lymphocytic leukemia (CLL). The circulating levels (normal plasma range 2-30 ug/ml) are determined by various genetic, anthropometric, hormonal, inflammatory, dietary, and pharmacological factors. The aim of our study was to prospectively assess serum levels of adiponectin in consecutively admitted patients with treatment naïve CLL to the Hematology department of Federico II University and correlate the values with disease characteristics and known prognostic factors.

Materials and Methods. In this prospective analysis, the level of adiponectin was examined in all adult patients with CLL treatment naïve admitted to the Hematological department of the Federico II University of Naples. Exclusion criteria were any neoplasia other than CLL and concomitant treatment with anti-inflammatory/immunomodulatory drugs. Peripheral blood samples were collected after a 12-hour overnight fasting period. Serum and total adiponectin concentration was analyzed in triplicate by an enzyme-linked immunosorbent assay using a polyclonal antibody produced entirely against a human Adiponectin aminoacid fragment. Routine laboratory studies consisted of complete blood count and blood chemistry, as well as NGS analysis for IGHV (MUT or UNMUT) and TP53 mutational assessment (MUT or WT), karyotype analysis and FISH analysis. Physical examination, chest X-ray, and abdominal ultrasound were performed in all instances to stage patients disease. Biometric data analysis (BMI and waist circumference) and pharmacological anamnesis was also performed. Results are reported as mean \pm SD. Differences were tested for significance by means of the Student t test, the Mann-Whitney U test, and the chi-square test. Correlations between variables of disease and risk disease were tested by means of a 2-tailed Pearson correlation coefficient (analysis of variance).

Results. A total of 20 patients were enrolled with median age 56 (range, 48-72), the 70% (14/20) was male. BMI was under 30 in all patients, median waist circumference was 95 cm (range, 75-112). Six patients were treated for hypercholesterolemia with statins. One patient had diabetes at time of enrolment. Most patients (9/20, 45%) had RAI stage I. The 20% of patients were TP53-MUT and the 55% IGHV-UNMUT. At cytogenetic analysis two patients had del13, one del11 and 4 del17. Overall a total of 7 patients had more or equal to 3 karyotypic alterations. Median white blood cell count at enrolment was 58.390/mm³ (range, 2870-378000/mm³). Overall, a total of 13 patients (65%) had indication to start treatment for either lymphadenomegaly (>10 cm at ultrasound exam) or cytopenia. Adiponectin serum median level was 14.07 ug/mL (range, 5.56-19.29 ug/ml). At t-student test, lower circulating level of adiponectin were found in patients with TP53-MUT versus TP53-WT ($p=0.005$; 95%CI 1.8-8.8), in IGHV-UNMUT versus MUT ($p=0.03$; CI 0.42-6.93) and in patients with indication to start treatment ($p=0.05$; CI 0.10-6.5) versus no indication. No difference were found for sex, age, smoke, drugs, biometrical data and cardiovascular comorbidities. At Pearson correlation, a significant inverse association between adiponectin and absolute peripheral blood lymphocyte count ($r = -0.445$; $p=0.05$) was found, while no correlation with biochemical data (glucose, triglycerides, cholesterol) or other blood cells count was found.

Conclusion. We were able to demonstrate that serum adiponectin is an easy and relatively economic test to perform that inversely correlate with TP53-MUT CLL cells, with IGHV-UNMUT cells and absolute peripheral blood lymphocyte count, all markers of disease severity.

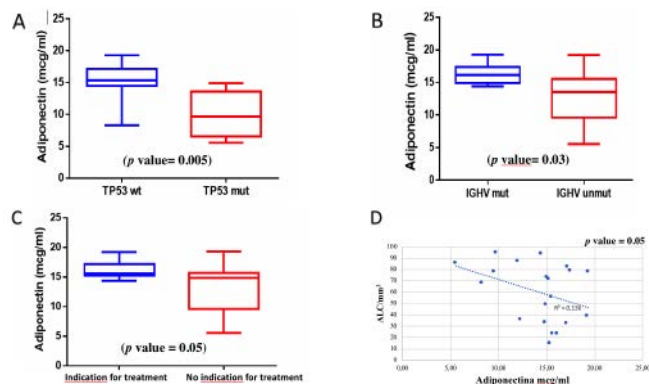


Figure 1.

Lymphomas

P079

PROGNOSTIC AND PREDICTIVE SIGNIFICANCE OF THE B-CELL RECEPTOR SIGNALING IN MANTLE CELL LYMPHOMA

S. Gambino¹, F.M. Quaglia², M. Galasso³, C. Cavallini⁴, R. Chignola⁵, O. Lovato⁶, A. Aparo⁶, I. Ferrarini^{1,2}, R. Giugno⁷, M. Krampera¹, C. Visco^{1,2}, M.T. Scupoli^{3,6}

¹Department of Engineering for Innovation Medicine, Section of Biomedicine of Innovation, Hematology and Bone Marrow Transplant Unit, University of Verona; ²Hematology Unit, Azienda Ospedaliera Universitaria Integrata Verona; ³Department of Neurosciences, Biomedicine and Movement Sciences, University of Verona; ⁴Department of Biosystems Science and Engineering, ETH Zurich; ⁵Department of Biotechnology, University of Verona; ⁶Research Center LURM (Interdepartmental Laboratory of Medical Research), University of Verona; ⁷Department of Computer Science, University of Verona, Italy

Mantle cell lymphoma (MCL) is a rare subtype of Non-Hodgkin lymphoma characterized by the expansion of mature B-cells in the mantle zone of the lymph nodes. MCL presents a high clinical variability, with some patients experiencing an indolent disease while others characterized by an aggressive clinical course. Recent evidence supports that B-cell receptor (BCR) signaling is crucial for MCL initiation and progression and is a target for therapeutic intervention. However, drug resistance inevitably emerges. Therefore, the definition of parameters identifying high-risk patients for aggressive disease and therapy resistance is an unmet need in MCL management. We measured the activation status of 9 BCR signaling kinases (SYK, LCK, BTK, PLC γ 2, p38, ERK1/2, AKT, NF- κ B p65, STAT5) in peripheral blood mononuclear cells (PBMC) from 30 MCL patients and 10 healthy donors, in the basal and anti-IgM modulated conditions, using phospho-specific flow cytometry. To measure phosphorylation statuses as well as responses to external stimulation of the signaling proteins, flow cytometry data were normalized with respect to the controls and subjected to unsupervised hierarchical clustering analysis (HCA). Progression free survival (PFS) and overall survival (OS) curves were estimated using the Kaplan-Meier method and compared using the log-rank test. Univariate and bivariate models for PFS and OS were performed using Cox proportional hazard regression. BCR modulation with anti-IgM determined a heterogeneous activation of the BCR signaling among patients' samples, with identification of two clusters showing differential responses to BCR stimulation. The cluster comprising samples with higher BCR signaling response (HR) was associated with shorter survival than samples grouped in the lower BCR signaling response (LR) cluster ($p=0.042$ and $p=0.041$ for PFS and OS, respectively). This finding was confirmed with time-to-event analyses, which showed that the MCL international prognostic index (MIPI) high-risk category together with high STAT5 response to the stimulation were significant predictors of shorter PFS and OS. In addition, MIPI high-risk category combined with high SYK response predicted shorter OS. While basal BCR activation did not provide prognostic information, higher constitutive activation of AKT was predictive of inferior response to the Bruton's tyrosine kinase inhibitor (BTK[*i*] ibrutinib). In conclusion, we identified BCR signaling activation profiles that were associated with poorer clinical outcome and resistance to ibrutinib. This study highlighted the prognostic and predictive significance of BCR activity in MCL and advanced our understanding of signaling heterogeneity underlying clinical behavior of MCL. A future challenge is the integration of BCR signaling data with genetic signature to predict patient's clinical behavior and drug response for a more personalized

treatment approach. We thank Fondazione Italiana Linfomi (PGR Ed. 2019) for funding support.

P080

RESOLUTION OF R-LOOPS AND DNA DAMAGE REPAIR BY HELLS (LSH) PROMOTE TRANSCRIPTION AND MAINTAIN LYMPHOMA T-CELL VIABILITY

V. Fragliasso¹, S. Mallia¹, A. Tameni¹, V. Manicardi¹, B. Donati¹, F. Torricelli¹, E. Vitale¹², M. Zanelli³, G. Gambarelli¹, S. Ascani⁴, G. Martino⁵, F. Sanguedolce⁶, E. Sauta⁷, I. Tamagnini³, N. Puccio¹², A. Neri⁸, A. Ciarrocchi¹

¹Laboratory of Translational Research, Azienda USL-IRCCS di Reggio Emilia; ²Clinical and Experimental Medicine Ph. D. Program, University of Modena and Reggio Emilia; ³Pathology Unit, Department of Oncology, Azienda Unità Sanitaria Locale - IRCCS di Reggio Emilia; ⁴Pathology Unit, Azienda Ospedaliera Santa Maria di Terni, University of Perugia; ⁵Institute of Hematology and CREO, University of Perugia; ⁶Pathology Unit, Policlinico Riuniti, University of Foggia; ⁷IRCCS Humanitas Clinical and Research Center; ⁸Scientific Directorate, Azienda USL-IRCCS di Reggio Emilia, Italy

Introduction. A high transcriptional rate is required to support cancer cell proliferation, but it is a risky process in which the nascent RNA pairs with its DNA template and forms structures called co-transcriptional R-loops. Their accumulation and persistence alter local chromatin and increase the density of RNA-Polymerases (RNAP) favoring DNA lesions and double-strand breaks (DSBs). DNA helicases operate to ease the evolution of DNA-based processes. Their aberrant activation has been linked to tumor progression but mechanisms by which helicases influence gene expression are unknown. We have recently identified the DNA helicase HELLS as a vulnerability of T cell Lymphomas (TCLs) demonstrating that HELLS orchestrates a transcriptional program impacting on survival of TCLs.

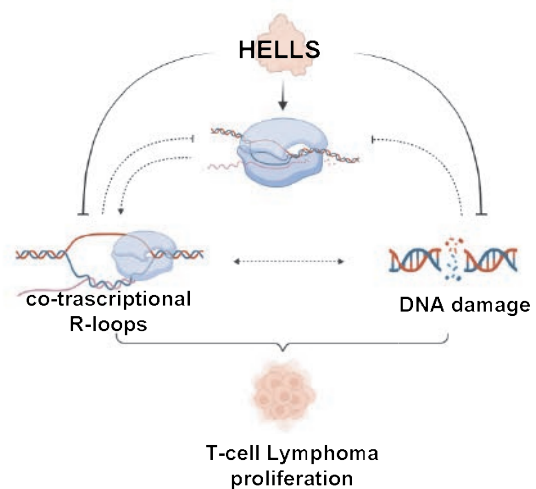


Figure 1.

Methods. RNA-seq, ChIP-seq, and DRIP were performed in TCL cells depleted for HELLS (HELLS KD). GEP of TCL patients was performed by the NCounter platform.

Results. To understand how HELLS coordinates the transcription, we integrated HELLS ChIP-seq analysis with RNA-seq data in TCL HELLS KD and control cells identifying 467 genes directly bound

by HELLS. We termed these genes HELLS-direct genes (HDGs) and we explored their clinical impact in a large cohort of 44 patients with TCLs by NCounter platform validating 60% of genes. To assess the contribution of HELLS to HDG transcription, the distribution of RNAPII was investigated by ChIP-seq. On the 60% of HDGs (n=272), we observed that HELLS KD caused a selective loss of RNAPII signal in the regions downstream of the TSS. Target analysis of ser2P-RNAPII on HELLS HDGs confirmed the accumulation of this marker at the proximal promoter pausing region with a concomitantly decreased signal at the 3' UTR confirming the stall of RNAPII. In the same regions, we also observed a significant increase of R-loops detected by DRIP-qPCR upon HELLS KD. This finding is consistent with R-loops/ser2P-RNAPII immunofluorescence results and strongly suggests that the loss of HELLS leads to co-transcriptional R-loops. After HELLS KD, we also observed a significant increase in the formation of γ H2AX foci in cell lines. This increase was found in R-loops+ cells and was associated with a distinctive pattern of ser2P-RNAPII. Importantly, the loss of HELLS results in decreased NHEJ and MMEJ efficiency without significant effects on the HR system. Thereby, we explored the potential implications of targeting HELLS in TCL. We treated HELLS KD cells with low doses of several chemotherapeutic drugs currently used in the clinic (gemcitabine, cisplatin, etoposide, and cyclophosphamide) and we evaluated cellular proliferation. In all cell lines tested, the loss of HELLS was found to synergize with all compounds, causing a significant synthetic lethality with drugs, compared to the use of drugs alone or control cells.

Conclusions. Our work unveils the role of HELLS in acting as a gatekeeper of TCL genome stability providing a rationale for drug design.

P081

INHIBITION OF PROTEIN KINASE CK2 AND BET PROTEINS. A NOVEL COMBINATION TO INCREASE MANTLE CELL LYMPHOMA CELL DEATH

S. Manni^{1,2}, J. Uddin Dekha^{1,2}, L. Saggin^{1,2}, M. Pesavento^{1,2}, A. Fregnani^{1,2}, A. Yami^{1,2}, L. Quotti Tubi^{1,2}, J. Ceccato^{1,2}, N. Danesin¹, G. Scapinello^{1,2}, A. Visentin¹, F. Vianello^{1,2}, L. Trentin¹, F. Piazza^{1,2}

¹Hematology Unit, Department of Medicine, University of Padova, Padova, ²Veneto Institute of Molecular Medicine, Padova, Italy

Introduction. Mantle Cell Lymphoma (MCL) is characterized by poor prognosis and high relapse rate. The search for new therapeutic targets is therefore mandatory. Bromodomain-containing protein 4 (BRD4) is a member of the Bromodomain (B) and extraterminal (ET) family proteins (BET), which are epigenetic regulators and transcription co-factors. BRD4 regulates the transcription of survival and cell cycle related proteins (*e.g.* P53, and B cell receptor (BCR)-linked prosurvival proteins). BET inhibitors, such as INCB054329 or JQ-1 have been shown to increase ibrutinib sensitivity by perturbing the kinome and signalling involved in tumorigenesis. We previously highlighted the central role of the S/T kinase CK2 in cancer. CK2 sustains MCL growth through chronic BCR activation of survival signals, such as the AKT/PI3K and NF- κ B. CK2 dependent phosphorylation of BRD4 actively promotes the transcription of genes important for cell cycle progression (P53, Myc) or BCR dependent. Therefore, CK2 could potentially be at the crossroad of chromatin remodelling proteins and BCR dependent signaling. The most effective CK2 inhibitor is CX4945 (silmatasertib), but recently the novel CK2 inhibitor, SGC-CK2 has been developed. No data are available on the efficacy of SGC-CK2 in MCL. In this work, we have tested the potential of inhibiting both CK2 and BET proteins to

increase MCL cell apoptosis via deregulation of a common signalling signature.

Methods. MCL cell lines, healthy or MCL patients B cells were treated with CX4945 or SGC-CK2 or with JQ-1 and INCB054329. CK2 gene silencing techniques were also used. Survival, apoptosis, and proliferation were investigated by FACS analysis of Annexin V/PI, detection of PARP cleavage and Mcl1 expression. The synergic action of BET and CK2 inhibitors was analyzed by the Chou-Talalay combination index (CI) method. CK2 expression and survival related signaling components were analyzed by WB and RT-qPCR.

Results. Both CK2 inhibitors caused effective apoptosis and proliferation arrest in MCL cells, with a minimum effect on healthy B cells. A synergistic effect of CK2 and BET inhibitors (CI<1) was observed in all the cell lines tested. The combinatorial administration of CK2 and BET inhibition increased the cytotoxic effect of the single agent also in patients B cells, but not on healthy B cells. The results were confirmed through CK2 gene silencing. CK2 inactivation reduced the expression of c-Myc, Mcl-1 and the activation of NF- κ B and PIK3/AKT signaling pathways. Surprisingly, JQ-1 or INCB054329 increased the expression of Mcl-1, NF- κ B S529 phosphorylation and its target gene TNF α . CK2 inactivation counteracted this effect, neutralizing deleterious BET inhibitors evoked compensatory pathways, that could favor apoptosis resistance.

Conclusions. CK2 and BET inhibition could be an alternative strategy to target survival signalling pathways that promote cancer clonal expansion, being an innovative approach for chemotherapy and BTK inhibitor-resistant MCL.

P082

THE ROLE OF B1 SUBUNIT OF NADH|UBIQUINONE OXIDOREDUCTASE (NDUFB1) AS A POTENTIAL PROGNOSTIC MARKER IN RELAPSED/REFRACTORY DIFFUSE LARGE B CELL LYMPHOMA

G. Scapinello^{1,2}, L. Quotti Tubi^{1,2}, M. Pizzi³, F. Scarmozzino³, L. Mussolin⁴, F. Lovisa⁴, I. Galligani⁴, P. Del Bianco⁵, G. Bonetto¹, M. Carraro¹, N. Danesin¹, A. Branca¹, T. Berno¹, C. Gurrieri¹, F. Lessi¹, A. Visentin^{1,2}, F. Vianello^{1,2}, R. Zambello^{1,2}, L. Trentin^{1,2}, F. Piazza^{1,2}

¹Hematology Unit, Department of Medicine, University Hospital of Padua; ²Veneto Institute of Molecular Medicine; ³Surgical Pathology and Cytopathology Unit, Department of Medicine, University Hospital of Padua; ⁴Pediatric Hematology, Oncology and Stem Cell Transplant Division, University Hospital of Padua; ⁵Veneto Institute of Oncology, Italy

Introduction. Diffuse Large B Cell Lymphoma (DLBCL) is the most common type of non-Hodgkin lymphoma. About two thirds of patients reach stable remission after first line therapy, but 30-40% are primary refractory or relapse (R/R) after an initial response, constituting a group with poor prognosis. Many efforts have been made to identify prognostic factors, able to recognize high-risk patients. However, the currently available scores are often inadequate to this purpose.

Methods. We designed a retrospective study aimed at comparing the clinical and biological features of a cohort of relapsed/refractory patients (R/R, n=140), with those of a cohort of patients not affected by relapse after at least 5 years of follow-up (controls, n=45), selected upon revision of medical charts of cases followed at the Hematology Unit of Padua University Hospital between 2001 and 2023. Gene expression profiling (GEP) analysis was performed on a subgroup of patients (globally 19, 13 relapsed and 6 controls). To further validate GEP results, gene specific expression and protein levels were

tested in DLBCL cell lines and by immunohistochemistry analysis on patients' samples. This latter was performed on slices of formalin-fixed paraffin-embedded tissue biopsies obtained with Galileo TMA CK3500 arrayer; biopsy material was available for about 70 patients. Survival curves were calculated according to Kaplan-Meier method and compared with Log-rank test.

Results. Upon correction for sensitivity thresholds, GEP brought to the identification of B1 subunit of NADH:Ubiquinone Oxidoreductase (NDUFB1) as one of the most differentially expressed genes in R/R patients (log2FC 0.33). We thus evaluated NDUFB1 gene expression in DLBCL cell lines. OCI-Ly1, OCI-Ly18, Pfeiffer, OCI-Ly7, OCI-Ly10, U2932 cell lines displayed elevated NDUFB1 mRNA levels. Next, we performed western blotting analysis that showed a concordant increased expression trend between mRNA and protein in OCI-Ly1, OCI-Ly18 and OCI-Ly10 cell lines, while in Pfeiffer, OCI-Ly7 and U2932 the protein level was not enhanced (Figure 1). Cell lines characterized by high levels of NDUFB1 protein had also elevated replication rate. Immunohistochemistry on patients' samples did not show increased expression in R/R patients vs controls, but NDUFB1 enhanced expression in the R/R cohort was associated with a median PFS disadvantage (4 vs 9 months, p .0005). On the basis of the data from cell lines analysis, we looked for a correlation between NDUFB1 expression and Ki67 value in patients' samples; in 4/9 overexpressing cases it was not available, in 1 it was about 60% and about 70% in the remaining 4 patients.

Conclusions. Our preliminary data show that NDUFB1 enhanced expression in R/R patients may correlate with inferior outcome. These results, if validated in larger cohorts, could aid in the identification of novel biological features to incorporate into new prognostic scores, improving risk-stratification in DLBCL.

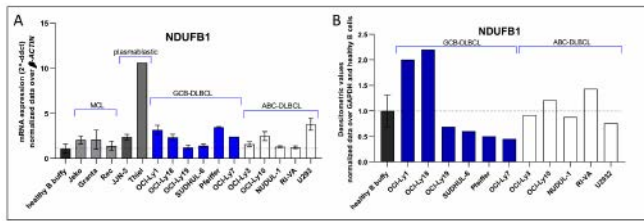


Figure 1.

P083

BONE-BASED 3D TUMOR MICROENVIRONMENT AFFECTS DLBCL GROWTH AND DRUG RESISTANCE

J. Ceccato^{1,2}, M. Piazza^{1,2}, G. Gualtieri^{1,2}, S. Carraro^{1,2}, F. Cinetto³, S. Manni^{1,2}, F. Piazza^{1,2}, G. Semenzato², L. Trentin¹, F. Vianello^{1,2}

¹Department of Medicine, University of Padova; ²Fondazione per la Ricerca Biomedica Avanzata Onlus; Veneto Institute of Molecular Medicine (VIMM); ³Ca' Foncello Hospital, Italy

Introduction. Diffuse large B cell lymphoma (DLBCL) prognosis is negatively affected when bone marrow (BM) is involved, likely owe to the interaction with the microenvironment. We recently demonstrated in a bone-based 3D model that lymphoma cells can adapt and growth as well as take advantage of the interaction with the matrix and the tumor microenvironment (TME), developing chemoresistance to anthracyclines. Ibrutinib, a Bruton's tyrosine kinase inhibitor, has shown anti-tumor effect in a subset of DLBCL patients but underlying mechanisms have not been clearly elucidated. As ibrutinib, by disrupting BCR signalling, leads to the egress of tumor cells from the microenvironment, we sought to explore whether ibrutinib can affect lymphoma cells when growing in a 3D

bone scaffold recapitulating the bone marrow environment.

Methods. The 3D scaffold was developed by the decellularization of human femoral bone fragments, then recellularized with primary human BM-derived mesenchymal stromal cells when required. OCI-LY18 and NU-DUL-1 DLBCL cell lines were used as representative of GCB and ABC DLBCL subtype, respectively. Supernatants after 3D model doxorubicin treatment were analyzed by cytokine array and migration assays were performed to evaluate the chemoattractive capability of lymphoma cells into the TME. Moreover, 3D models underwent Ibrutinib treatment and viability of DLBCL cells was measured by Annexin V assay and compared to canonical cultures.

Results. DLBCL cells, autonomously adhering and dividing onto the 3D model, were also able to exert chemoattraction toward other neoplastic cells. When exposed to ibrutinib, OCI-LY18 GCB-like cells adapted to the 3D structure were more resistant to apoptosis than OCI-LY18 growing in a conventional 2D culture (21.8+5.6%, 43.26+16.8% annexin V positive cells respectively, p=0.0001). On the contrary, the level of ibrutinib-induced apoptosis was higher in NUDUL-1 ABC-like cells growing in the 3D scaffold (67.4+10.1% in the 3D condition, 47.26+10.6% in the 2D control, p=0.047). In this model, the presence of MSC did not influence cells behavior under ibrutinib treatment but co-treatment of 3D NUDUL-1 cells with ibrutinib and doxorubicin seems to overcome the protection given by MSC under doxorubicin treatment. We also found that the 3D environment downmodulates cytokines like IL-6 and IL-8.

Conclusions. A 3D bone scaffold endowed with the ability to promote lymphoma cell growth is also active in protecting non-GC derived B cells from ibrutinib-induced apoptosis. Our results suggest a possible role of BTK pathway in adhesion-mediated chemoprotection of DLBCL and highlight a contrasting behavior of different cell lines not displayed in the standard cultures, emphasizing the relevance of 3D studies. Our model will help to clarify the mechanisms behind drug resistance in r/r DLBCL, to provide new future therapeutic strategies and hopefully to create patient-specific models in order to improve personalized therapies.

P084

CSF EVALUATION IN ORDER TO PREDICT SECONDARY CENTRAL NERVOUS SYSTEM LYMPHOMA | A MONOCENTRIC STUDY ON BIOCHEMICAL ANALYSIS AND FLOW CYTOMETRY

E. Alma¹, R. Ladiana², S. Bellesi¹, E. Maiolo¹, R. Malafronte^{1,2}, F. Bellisario^{1,2}, S. D' Innocenzo¹, A. Toscano¹, F. D'alo^{1,2}, S. Hohaus^{1,2}

¹Dipartimento di Diagnostica per Immagini, Radioterapia Oncologica ed Ematologia, Fondazione Policlinico Universitario A. Gemelli IRCCS; ²Sezione di Ematologia, Dipartimento di Scienze Radiologiche ed Ematologiche, Università Cattolica del Sacro Cuore, Italy

Introduction. Secondary central nervous system lymphoma (SCNSL) is a rare complication of aggressive B-cell lymphoma that can occur early after diagnosis, during therapy or at disease relapse. Given the poor prognosis and therapeutic challenges with SCNSL, early diagnosis of cerebrospinal fluid (CSF) involvement is necessary to improve patient prognosis. In recent years immunophenotyping by flow cytometry (FCM) has demonstrated greater sensitivity, to detect those with occult central nervous system (CNS) disease.

Methods. In our institutional database at Fondazione Policlinico Gemelli, we retrospectively identified 148 patients (pts) diagnosed between January 2015 and May 2022 affected by aggressive B-cell lymphoma without CNS involvement at the diagnosis who received intrathecal CNS prophylaxis as they were considered at risk for CNS progression either due to particular extranodal localization or to high IPI (3-5)/CNS-IPI (>4). At diagnosis, examination of CSF samples

included biochemical analysis, cell count, and FCM. CSF white cell count (WCC), protein and glucose levels were assayed by automated techniques. FCM analyses were performed on fresh samples using an 8-color tube containing the following labelled antibodies: Kappa-V450/CD45-V500/CD20-FITC/CD79b-PE/CD5-PerCy5.5/CD19-PECy7/CD10-APC/Lambda-APC-H7. The data was acquired using BD FACS Canto II and analysed using Diva software (Becton Dickinson). Neoplastic cells were identified through the expression of a clonal light chain. We considered clusters of at least 10 clonal events positive for localization of disease.

Results. Data of 148 pts were analyzed. At diagnosis, multiparameter FCM analysis detected a clonal population in 5 pts of 148 (3%). At a median follow up of 47 months, 38 pts (26%) experienced failure (progressive disease or relapse); 31 pts had systemic progression and 7 pts had CNS relapse (2 pts had a concurrent systemic relapse). Involved CNS area were brain parenchyma in 3 pts and leptomeninges in 4 pts. Of the 5 pts with a positive FCM at diagnosis, none experienced CNS relapse. The 2-year cumulative incidence of CNS progression was 4.7% (95% CI. 1-9) with a median time to progression of 9.8 months (95% CI. 3-30). There was no difference in terms of incidence of CNS relapse considering pts with a positive FCM ($p=0.7$), abnormal protein levels in CSF ($p=0.3$) and abnormal glucose levels in CSF ($p=0.2$).

Conclusions. This monocentric study of a large cohort of patients with aggressive B-cell lymphoma demonstrates that minimal disease detection by FCM in patients receiving i. th. prophylaxis as part of first-line therapy is a rare event and did not improve prediction of CNS relapse. In case of FCM positivity, the continuation of intrathecal prophylaxis seemed to be an option sufficient to prevent CNS progression. However, identifying patients who will face CNS relapse despite intrathecal prophylaxis remains a challenge that needs improvement.

P085

PRESENCE OF A SERUM PARAPROTEIN IN PATIENTS WITH DIFFUSE LARGE B CELL LYMPHOMA (DLBCL) IS ASSOCIATED WITH HIGHER CD79B SURFACE EXPRESSION

E. Maiolo¹, S. Bellesi¹, R. Malafrente¹, C. Iacovelli¹, F. Campana¹, G. Schiaffini¹, Puggioni P.L.¹, S. D'innocenzo¹, A. Toscano¹, E. Alma¹, F. Bellisario¹, A. Bakaks², L.M. Larocca², F. D'alò¹, S. Hohaus¹

¹Dipartimento di Diagnostica per Immagini, Radioterapia Oncologica ed Ematologia Fondazione Policlinico Universitario "A. Gemelli" IRCCS; ²Divisione di Anatomia Patologia e Istologia, Fondazione Policlinico Universitario "A. Gemelli" IRCCS, Italy

Introduction. Evidence from our and other groups indicate that the presence of a serum monoclonal protein (MC) of IgM class is a negative outcome predictor in Diffuse Large B cell Lymphoma (Maiolo *et al.*, 2020). In the current study we were interested whether secretion of MC is associated with surface expression of the Ig-associated CD79b molecule, as this has become a target for an antibody-drug conjugate (Polatumab vedotin).

Methods. We included 94 patients (pts) with aggressive B cell lymphomas: mostly DLBCL-NOS (65 pts: 36 non-GC, 25 GC, 4 not classifiable), 10 G3b/transformed FL, 11 PMBCL, 8 High Grade diagnosed between Dec 2015 and May 2023. 43 were males, 51 females. Median age was 64 (range 22-88). Cell suspensions were generated from fresh lymph node biopsies, prepared by mechanical disaggregation and incubated with 8 surface markers: Kappa-V450, CD45-V500, CD20-FITC, CD79b-PE, CD5-PerCP-Cy5, CD19-PE-Cy7, CD10-APC and Lambda-APC-H7. Data were acquired with

BDFACSCanto for the first 40 and with DXFlex (Beckman Coulter) for other 54 pts. CD79b expression was measured both as percentage of surface positive events considering all pathological B cells, both as intensity of expression defined as Median Fluorescence Intensity respect to negative CD5+ T cells in the sample. Results of serum immune electrophoresis at diagnosis was available for all pts.

Results. Immune electrophoresis showed a MC in 30/94 (32%) cases. The MC subclass was IgM in 15, IgG in 11 and a light-chain MC in 4 cases. Pts with MC resulted more frequently classified as non-GC using the Hans Algorithm ($p=0.02$) and tended to be older, but this difference was not statistically significant ($p=0.07$). CD79b expression was very heterogeneous. Median CD79b MFI was significantly higher in pts with a serum MC vs others, independently from the cytometer used for analysis (Median MFI for BDFACSCanto 14.85 vs 9.5, $p=0.045$ and 16.98 vs 4.5 for DXFlex $p=0.046$) and this difference was even more pronounced comparing only pts with IgM class MC versus pts without MC (BDFACSCanto 23.2 vs 9.5, $p=0.006$). According to the proportion of CD79b surface positivity, we divided cases into low (<20%, 28 pts) and medium-to-high (>20%, 66 pts) expression: CD79B was more often >20% in patients with a serum MC respect to others (26/30 vs 40/64, $p=0.017$) and in general pts with serum MC had significantly higher percentage of surface CD79b (median 86.5% vs 59%, $p=0.03$). Accordingly, only 2/30 pts with a serum MC vs 15/64 pts without a MC showed surface CD79b expression <1% ($p=0.08$). In all cases pts without surface expression displayed CD79b positivity intracytoplasmatically.

Conclusions. The association between the presence of MC in the serum (in particular of IgM class) and higher and most intense CD79B surface expression on pathological CD19+ B cells, could be the rationale to add targeted therapy already in first-line in this group of pts, that are known to have a poor prognosis.

P086

CK2 MODULATES THE T-CELL RECRUITMENT IN HODGKIN LYMPHOMA NICHE

E. Ruggeri¹, N. Mouawad¹, G. Capasso¹, F. Frezzato¹, A. Cellini¹, F. Angotzi¹, L. Quotti Tubi¹, S. Manni¹, M. Facco¹, M. Pizzi², F. Piazza¹, L. Trentin¹, A. Visentin¹

¹Hematology Unit, Department of Medicine, University of Padua; ²General Pathology & Cytopathology Unit, Department of Medicine, University of Padua, Italy

Introduction. Hodgkin and Reed-Sternberg (HRS) cells through the secretion of a multitude of chemokines are typically in close contact with surrounding CD4+ T cells, a phenomenon that is called resetting. We recently identified CK2 as a key protein for the survival of HRS cells and its inhibition trigger apoptosis. In this study, we assess the role of protein CK2 in sustaining T-cells' recruitment in the tumor niche.

Methods. HL cell lines (KM-H2 and HDLM-2) were treated with 0, 5, and 10 μ M of CX-4945 (CX), a CK2 inhibitor, for 24/48h. Apoptosis was quantified by flow cytometry with the Annexin V/Propidium iodide assay. Migration-invasion assays were performed using fibronectin-coated transwells. Conditioned media (CM) from the cell lines, collected after 24/48h treatment, was added to the bottom chamber. T-cells were purified from age-matched healthy donors. A multiplexed array was used to determine the concentration of 27 cytokines from the supernatants. CXCR3 and CCR7 receptors on T-cells was assessed by western blot (WB). For comparison one-way ANOVA test with Dunnett's correction was used.

Results. We observed that the inhibition of CK2 by CX was not able to trigger the apoptosis of T lymphocytes from healthy donors

in 24 or 48 hours of culture ($p>0.05$). We observed that CX-treated HL cell lines generate a conditioned media (CM) with decreased chemoattractant effects on T lymphocytes (Figure 1). The percentage of migrated T lymphocytes toward the CM obtained from HDLM-2 and KM-H2 cells treated with 5 μM CX for 24h decreased by 12.1% and 18%, respectively, compared to untreated conditions. In the presence of C. M. from the cell lines treated with 10 μM CX, a further significant reduction was observed in T cell migration by 25.3% and 34%, respectively, compared to untreated conditions ($p<0.05$). To explore how CK2 influences the cytokines milieu in the CM, we performed an array analysis to identify CK2-related molecules relevant for cHL tumor niche. Among the tested cytokines, IL-6, M-CSF, RANTES, TARC, TGF- β 1, TNF- α , and VEGF, demonstrated a significant CK2 dependence. When HRS cell lines were treated with 10 μM CX, there was a noteworthy reduction of IL-6, TARC, TGF- β 1, TNF- α , and VEGF release ($p<0.0001$). A lower dose, *i. e.* 5 μM CX, was enough to suppress the cytokines released by HDLM-2 cells, while IL-6, TNF- α , and VEGF only impacted in KM-H2 cells. In addition, we found that CM from HL cell lines was able to modulate the expression of the T-cell surface receptor CXCR3 but not CCR7, assessed by WB. T-cell cultured in the presence of CM from HDLM-2 for 24 hours showed an increase of the CXCR3/GAPDH by 1.5 ($p<0.05$), compared the untreated condition.

Conclusions. While we previously showed that CK2 inhibition led to HRS apoptosis, it does not affect T cells survival. Furthermore, CK2 emerged as a novel player in the formation of HL microenvironment by modulating the release of cytokines from HRS cells that favor T cells chemotaxis.

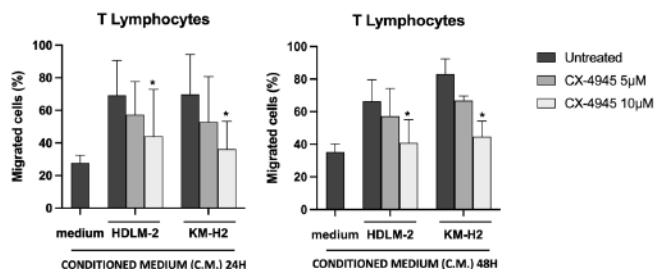


Figure 1. T lymphocyte migration after CK2 inhibition. Histograms depict the percentage levels of T lymphocyte migration across fibronectin-coated membranes in the presence of conditioned medium (CM) collected after 24 and 48 hours of cell cultures. HL cell lines were treated with 0 μM , 5 μM , and 10 μM of CX-4945. * $p<0.05$. One-way ANOVA test.

Figure 1.

P087

SPECIFIC ALTERATIONS IN MEMBRANE LIPID LEVELS AS POTENTIAL BIOMARKERS IN DLBCL PATIENTS

F. Loscocco¹, F. Di Nolfo², A. Isidori¹, A. Sansone³, M. Brunori¹, M. Chiarucci¹, M. Calandrelli¹, G. Visani¹, C. Ferreri³

¹Hematology and Stem Cell Transplant Center, San Salvatore Hospital, AST; ²Laboratorio di Lipidomica Lipinutragen Srl; ³ISOF, Consiglio Nazionale delle Ricerche, Italy

Background. Lipids are essential components of cell membranes and are involved in several cellular processes, including the modulation of immune cells such as T cells and natural killer cells that recognize and eliminate cancer cells. Specific lipids have been implicated in the development or progression of lymphoma. Omega-3 and omega-6 fatty acids are both essential fatty acids that the body needs to function properly. The omega-3 fatty acids, such as eicosapentaenoic acid (EPA) and docosahexaenoic acid (DHA), may have anti-

cancer effects by inhibiting the growth of cancer cells *in vitro* and in animal studies. Arachidonic acid (AA) is an omega-6 polyunsaturated fatty acid involved in the production of several signaling molecules, including eicosanoids, which play a role in inflammation and cancer development. Some studies have suggested that AA levels may be altered in lymphoma and that AA metabolites may serve as potential biomarkers of lymphoma progression and treatment response. However, the relationship between lymphoma and lipids is complex and not fully understood.

Aims. To investigate the lipid profile of patients with diffuse large B cell lymphoma (DLBCL) to identify lipidomic signatures that could become alternative targets for therapy.

Methods. Membrane phospholipids of mature red blood cells (RBCs) were analysed for fatty acid (FA) profiling (GC-MS). Nutritional status was assessed using a validated food frequency questionnaire. The FA panel included 12 representative fatty acids, the unsaturation index (UI), the peroxidation index (PI) and the enzymatic index of the MUFA and PUFA biosynthetic pathways. Samples obtained from fresh blood of DLBCL patients at diagnosis were compared with healthy controls. Data comparison between the two cohorts was performed using the Kruskal-Wallis test. The significance level was set at $p<0.05$. All statistical analyses were performed using Past3 and Power BI for graph spider map.

Results. 38 patients with aggressive B-cells lymphomas (sex= 13F and 18M Age= range 26-90, BMI range 18-34) and 27 healthy controls were investigated (Sex=14F and 13M Age=24-69 range, BMI<25). Lipidomic analysis revealed that several FA species were significantly present in NHL patients, whereas saturated fatty acid (SFA) appeared to be decreased (Figure 1).

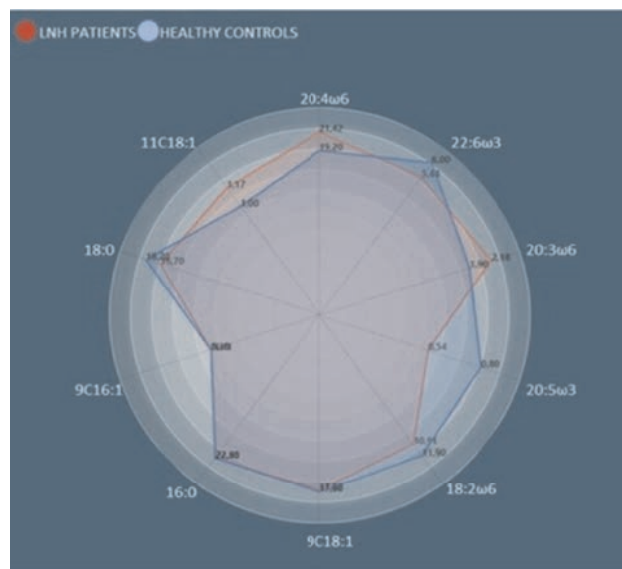


Figure 1.

Looking at specific FA, SFA stearic acid (C18:0) was greatly reduced the lymphoma group, whereas MUFA such as vaccenic acid (C11c18:1) were higher ($p=0.0001$) than in healthy controls. Interestingly, DLBCL patients showed low levels of omega-3 PUFA, EPA (C20:5) and DHA (C22:6) ($p=0.001$ and $p=0.003$) and higher levels of omega-6 PUFA, AA ($p=0.0001$). In terms of enzymatic activity, NHL patients had lower delta-9-desaturase and delta-6-desaturase activity according to the strong reduction of stearic acid and linoleic acid, respectively. Finally, we also found a significant difference in UI and PI between the two groups, explaining changes in fluidity, permeability, oxidative stress and damage.

Summary/Conclusion. Our results showed that patients with DLBCL have a significantly altered lipid profile compared to healthy

donors. Lipidomics has the potential to provide insights into the biology of lymphoma and to identify novel therapeutic targets. Further research is needed to clarify the mechanisms by which lipids may contribute to lymphoma development and progression, and to determine the potential therapeutic implications of targeting lipid metabolism in lymphoma treatment.

Acknowledgments. The study was supported in part by AIL Pesaro Onlus.

P088

PRELIMINARY ANALYSIS OF DNT, DPT, AND NKT-LIKE CELLS IN B-CELL NON-HODGKIN LYMPHOMAS (NHL)

L. Valvano¹, F. D’auria², G. Pietrantonio³, G. Mansueto³, O. Villani³, S. D’agostino³, R. Vilella¹, G. Calice⁴, T. Statuto¹

¹Laboratory of Clinical Research and Advanced Diagnostics, Centro di Riferimento Oncologico della Basilicata (IRCCS-CROB); ²Laboratory of Clinical Pathology, Centro di Riferimento Oncologico della Basilicata (IRCCS-CROB); ³Hematology and Stem Cell Transplantation Unit, Centro di Riferimento Oncologico della Basilicata (IRCCS-CROB); ⁴Laboratory of Preclinical and Translational Research, Centro di Riferimento Oncologico della Basilicata (IRCCS-CROB), Italy

Introduction. A growing interest in minor T-cell subsets such as “double-negative T” (DNT), “double-positive T” (DPT), and “natural killer T” (NKT) cells seems have a relevant role in tumors.

Methods. Seventy-five patients affected by four different subtypes of untreated B-cell non-Hodgkin lymphoma (B-NHL) were identified in this retrospective study: Diffuse large B cell lymphoma (DLBCL), Follicular lymphoma (FL), Mantle cell lymphoma (MCL), and Marginal zone lymphoma (MZL). Percentage values were assessed by using Flow Cytometry in Bone Marrow Aspirates: total lymphocytes was evaluated on the total leukocytes, while each subpopulation was calculated starting from the lymphocyte gate.

and “NKT-like” cells in DLBCL appeared significantly higher than the values found in MCL and MZL (opposite result for B cell). Tc percentages were significantly greater in DLBCL only compared to MZL values. In contrast, Th cells were significantly lower in MCL than in other lymphomas. Total lymphocytes did not differ significantly only between MCL and MZL or DLBCL and FL. Comparison between percentages and staging was possible only in the DLBCL group (among the II, III and IV stages) and MZL (among the III and IV stages). The results showed a significant higher value only for B lymphocytes in DLBCL in stage IV compared to II and III. The remaining populations did not appear to change significantly in relation to staging.

Conclusions. In this study, we analyzed the changes in percentage values in lymphocyte subpopulations in the B-NHL lymphomas. In particular, we focused on small T cell subpopulations, *i.e.*, DNT, DPT, and NKT-like cells, given recent findings on their promising antitumor capacity. A preliminary analysis of our data showed that there was a different trend in the percentages of the subpopulations. Total lymphocytes and B cells were greater in MCL and MZL lymphomas, that presented a lower percentage of disease progression. In contrast, NK and T cells showed higher value in DLBCL and FL lymphomas, that progressed more frequently. The analysis between percentages and staging showed that only B lymphocytes were significantly higher in stage IV compared to stage II and III. These early observations encourage further studies on these minority T subpopulations. Specifically, the different trend of these compared cells could be an interesting object of study to better understand their different functional participation in B-cell NHL.

P089

EFFECTS OF ANTI-CD30 THERAPEUTIC DRUG-ANTIBODIES CONJUGATES ON HODGKIN LYMPHOMA CELLS LINES

S. Matis¹, F. Morelli¹, R. Benelli¹, M.R. Zocchi², A. Poggi¹

¹IRCCS Ospedale Policlinico San Martino, UOSD Oncologia Molecolare e Angiogenesi; ²IRCCS San Raffaele Scientific Institute, Division of Immunology, Transplants and Infectious Diseases, Italy

Introduction. Recently, relevant advances have been made in the management of relapsed/refractory (r/r) Hogkin Lymphomas (HL) with the employment of the anti-CD30 antibody-drug conjugate (ADC) brentuximab vedotin (Bre-Ved). Unfortunately, the large majority of patients will eventually progress, despite the excellent response rates and tolerability. It is well established that the immune host response can play a key role in the anti-HL outcome. In this context, the tumor microenvironment can downregulate the anti-tumor effector immune response to HL cells. Among others, it has been reported that the Vδ2+T cells can efficiently kill HL cells (doi10.1080/2162402X.2015.1123367). More recently, we have shown the aminobiphosphonate zoledronic acid (ZA) conjugated to anti-epidermal growth factor receptor can trigger anti-tumor immune response of autologous Vδ2+T cells against organoids of colorectal cancer (doi10.1136/jitc-2022-005660). This effect is dependent on the metabolic effect of ZA on target cells. Thus, we hypothesize that conjugation of Bre-Ved to the ZA could increase the anti-HL effect of the native Bre-Ved antibody leading to Vδ2+T cell activation.

Methods. The ADC composed of Bre-Ved linked to ZA, termed Bre-Ved-ZA, has been produced by linking the phosphoric group of ZA to the amino groups of Bre-Ved. Inductively coupled plasma-mass spectrometry and matrix assisted laser desorption ionization mass spectrometry analyses confirmed the covalent linkage between the antibody and ZA. The novel ADC has been tested for its reactivity, endocytosis, anti-proliferative and immuno-stimulating effects with HL cell lines (KMH-2, L428, L540, Hs 604, T, HS 445 and

Table 1.

Clinical biological features	Age, median (range)	Males, n (%)	Patients with comorbidities, n (%)	MCL count (x10 ⁹ /L)	Treatment, Treated patients, n (%)	CR, n (%)	PR, n (%)	Disease progression, n (%)	Cell-Mediated Immunity (CMI)	
									CD3, n (%)	DPT, n (%)
n=75										
DLBCL	62	55	11	100	100	100	100	100	100	100
FL	68	60	8	100	100	100	100	100	100	100
MCL	65	58	7	100	100	100	100	100	100	100
MZL	63	56	7	100	100	100	100	100	100	100

Results. In each B-cell NHL subtype (Table 1), we compared B, T, NK, Tc, Th, DNT, DPT, and NKT-like cells. The percentages of total lymphocytes and B cells was found to be higher in MCL and MZL; NK and T values were greater in DLBCL and FL. Comparing the different NHL subtypes, we found a significant percentage difference in each subpopulation, except for DNT and NK cells (however both increased in FL). In particular, the portion of CD3, DPT

RPMI 6666). Reactivity has been assessed by flow cytometry and endocytosis by confocal microscopy and colocalization analysis with markers of endosomes and lysosomes. Proliferation has been assessed by evaluation of ATP content, time lapse imaging and labelling with fluorescent probes for dying cells. Immune stimulation of V δ 2+T cells was assessed by evaluating the cytolysis of HL cell lines in the presence of Bre-Ved-ZA compared to native antibody Bre-Ved.

Results. The Bre-Ved-ZA ADC can react with the HL cell lines more efficiently than the Bre-Ved ADC. Bre-Ved-ZA was found to enter the HL cells co-localizing with EEA1 and LAMP-1 in intracellular vesicles. Also, this ADC exerted a stronger inhibitory (about one Log fold) effect on the proliferation of HL cell lines compared to the native antibody Bre-Ved. Eventually, Bre-Ved-ZA ADC, differently from the native antibody, can trigger the activation of cytolytic activity of V δ 2+T cells against HL cell lines, increasing the anti-HL effect.

Conclusions. We have shown that the novel Bre-Ved-ZA ADC can interfere better than Bre-Ved on HL cell lines proliferation. Also, it triggers the antitumor immune response of V δ 2+T cells. These findings suggest the potential use, in the future, of this ADC to face the management of r/r HL.

P090

OPTICAL GENOME MAPPING REVEALS TP53 DELETION IN A PEDIATRIC PATIENT WITH PERIPHERAL T-CELL LYMPHOMA NOT OTHERWISE SPECIFIED (PTCL-NOS)

S. Russo, V. Alesi, S. Genovese, E. Agolini, M.V. Faggiano, A. Pitisci, L. Martucci, C. Calacci, R. De Vito, A. Novelli, L. Vinti

Ospedale Pediatrico Del Bambino Gesù, Italy

Introduction. Peripheral T-cell lymphoma, not otherwise specified (PTCL-NOS) is a rare molecularly heterogeneous group of lymphoproliferative disorders characterized by a broad cytological spectrum, often with a loss of CD5 and CD7, no typical recurrent mutation and a poor prognosis (5 year OS<30%). As in adult, pediatric PTCL-NOS is an “exclusion diagnosis” among rare mature T-cell lymphomas, with no standardized treatment. Significant improvements have been made in delineating specific biological and prognostic subgroups with gene expression profiling. The Optical Genome Mapping (OGM) could potentially contribute to the discovery of prognostic markers allowing a better classification.

Methods. Ultra-high molecular weight (UHMW) DNA was extracted from frozen tissue (SP Frozen Human Blood DNA Isolation Protocol, Bionano Genomics). Array-CGH analysis was performed by an Agilent 180K oligonucleotide platform and the data were analyzed by means of Cytogenomics v5.3 software. OGM was performed according to the manufacturer’s instructions (Bionano Genomics); reporting and direct visualization of structural variants was done on Bionano Access V1.6.

Results. Here we report a paediatric patient hospitalized for fever, lymphadenopathy, renal infiltration. According to the WHO PTCL classification, a diagnosis of PTCL-NOS was done (immunophenotype CD3+, CD5+, CD7-, CD8+, CD4-, CD30-, ALK-). Cytogenomic analyses performed with array-CGH revealed a 291 kb microdeletion on the short arm of chromosome 17 (17p13.1), including *TP53* gene; OGM showed an adjacent 194.6 kb microinversion. The structural information sheds light on the molecular mechanism that leads to *TP53* inactivation as a result of a multiple breakage event that leads to the simultaneous presence of the microdeletion and the neighbouring inversion.

Conclusions: In this patient, OGM detected a chromosomal rearrangement (inversion of chromosome 17) leading to *TP53* deletion.

This alteration could underlie the pathogenesis of this lymphoma and its refractoriness to treatment as reported in the adult setting. Y. Watatani (Leukemia 2019) identified a previously undescribed molecular subtype characterized by *TP53* mutations and deletions in PTCL-NOS with different prognosis and unique genetic features associated with extensive chromosomal instability. Conversely a pediatric report (RA-Yeung, PBC 2021) did not identify *TP53* variants in 58 children and adolescents with non-anaplastic peripheral T-cell lymphoma. A greater number of patients with PTCL-NOS should be evaluated with OGM in order to compare new techniques and explore the frequency of *TP53* alteration; these results should help to devise a new molecular classification and to exploit new therapeutic strategies in this group of paediatric aggressive malignancies.

P091

ZUMA-23: A GLOBAL, PHASE 3, RANDOMIZED CONTROLLED STUDY OF AXICABTAGENE CILOLEUCEL VERSUS STANDARD OF CARE AS FIRST-LINE THERAPY IN PATIENTS WITH HIGH-RISK LARGE B-CELL LYMPHOMA

A.J.M. Ferreri¹, J.R. Westin², C.A. Jacobson³, J.C. Chavez⁴, A. Sureda⁵, F. Morschhauser⁶, B. Glaß⁷, M. Dickinson⁸, A. Davies⁹, I.W. Flinn¹⁰, D.G. Maloney¹¹, M. Chamuleau¹², M. Tees¹³, B. Schoepf¹⁴, A. Xue¹⁴, S. Shahani¹⁴, O. Nikolajeva¹⁴, J. Kang¹⁴, A. Kaplan¹⁴, M. Schupp¹⁴, H. Miao¹⁴, E.S. Rich¹⁴

¹IRCCS San Raffaele Scientific Institute; ²The University of Texas MD Anderson Cancer Center; ³Dana-Farber Cancer Institute; ⁴Moffitt Cancer Center; ⁵Hematology Department, Institut Català d’Oncologia-Hospitalet; ⁶University of Lille; ⁷Helios Klinikum Berlin-Buch; ⁸Peter MacCallum Cancer Centre, Royal Melbourne Hospital and the University of Melbourne; ⁹Southampton Cancer Research UK/NIHR Experimental Cancer Medicines Centre, University of Southampton; ¹⁰Sarah Cannon Research Institute and Tennessee Oncology; ¹¹Fred Hutchinson Cancer Center; ¹²Amsterdam University Medical Center; ¹³Colorado Blood Cancer Institute; ¹⁴Kite, a Gilead Company

Background. The nearly 40% of patients (pts) with large B-cell lymphoma (LBCL) who are refractory to or relapse after current first-line (1L) standard-of-care (SOC) regimens, such as R-CHOP (rituximab [R] + cyclophosphamide [C], doxorubicin [H], vincristine [O], and prednisone [P]) and DA-EPOCH-R (dose-adjusted etoposide [DA-E]), have poor prognoses. High International Prognostic Index (IPI) score and the subtype of high-grade B-cell lymphoma (HGBL) are associated with shorter progression-free and overall survival (PFS and OS; Nastoupil LJ and Bartlett NL. *J Clin Oncol.* 2023). Strategies to improve outcomes in these subgroups have been largely unsuccessful; therefore, therapeutic options with a different mechanism of action are needed.

Axicabtagene ciloleucel (axi-cel) is an autologous anti-CD19 chimeric antigen receptor (CAR) T-cell therapy approved to treat pts with relapsed/refractory (R/R) LBCL after demonstrating significant clinical benefit as 2L (ZUMA-7; Locke FL, *et al.* *N Engl J Med.* 2022) and \geq 3L (ZUMA-1; Neelapu SS, *et al.* *N Engl J Med.* 2017) therapy. Additionally, in the Phase 2 ZUMA-12 study in pts with refractory 1L LBCL, axi-cel showed a high rate of durable responses with an objective response rate of 89% (complete response rate, 78%) and an ongoing response rate of 73% (median follow-up, 15.9 mo; Neelapu SS, *et al.* *Nat Med.* 2022). ZUMA-23 is the first Phase 3, randomized controlled study to evaluate CAR T-cell therapy as a 1L regimen for any cancer and will assess axi-cel versus SOC in pts with high-risk LBCL, defined as IPI 4-5.

Methods. The Phase 3 trial design will enroll \approx 300 adult pts with high-risk, histologically confirmed LBCL based on the 2016 WHO

classification, including diffuse large B-cell lymphoma (DLBCL), HGBL, and transformed follicular or marginal zone lymphoma (Swerdlow SH, et al. Blood. 2016). Eligible pts will receive 1 cycle of R-chemotherapy and then be randomized 1:1 to receive axi-cel or continue with SOC. Pts in the axi-cel arm will undergo leukapheresis and then receive R-CHOP or DA-EPOCH-R as bridging therapy, followed by lymphodepleting chemotherapy (fludarabine/cyclophosphamide), and a single axi-cel infusion (2×10^6 CAR T cells/kg). Prophylactic corticosteroids may be administered to reduce the incidence and severity of cytokine release syndrome at the investigator's discretion. Pts in the SOC arm will receive 5 additional cycles of R-CHOP or DA-EPOCH-R (investigator's choice). The primary endpoint is event-free survival by blinded central review. Key secondary endpoints are OS and PFS. Safety, quality of life, and pharmacokinetics will also be assessed. Pts with a history of HIV and/or hepatitis B or C and undetectable viral loads may enroll. Key exclusion criteria include LBCL of the central nervous system. ZUMA-23 is open for enrollment (NCT05605899).

P092

ARE SMALL LYMPHOCYTIC LYMPHOMA AND CHRONIC LYMPHOCYTIC LEUKEMIA THE SAME DISEASE? THE UNSOLVED DILEMMA

E. Cencini¹, N. Calomino², A. Sicuranza¹, A. Gozzetti¹, A. Fabbri¹, M. Bocchia¹

¹Unit of Hematology, Azienda Ospedaliera Universitaria Senese & University of Siena; ²Unit of General Surgery and Surgical Oncology, Department of Medicine, Surgery and Neurosciences, University of Siena, Italy

Introduction. The management of small lymphocytic lymphoma (SLL) as chronic lymphocytic leukemia (CLL) or an indolent non-Hodgkin lymphoma is highly debated. SLL is defined by the presence of $<5 \times 10^9$ /L clonal B cells, characterized by an immunophenotype consistent with CLL, together with lymphadenopathy and/or splenomegaly but in the absence of cytopenia. International guidelines recommend to manage these entities with the same therapeutic approach.

Methods. In this single-center, retrospective study, a cohort of 38 consecutive SLL patients managed in daily clinical practice between 2008 and 2022 was evaluated. All patients signed written informed consent in accordance with local Institutional Review Board requirements.

Results. Overall, 26/38 cases (68.4%) needed treatment during disease course, 18/38 (47.4%) were treated at diagnosis, while the remaining 8 cases (21%) received treatment after a period of watch&wait. All but one received CLL concordant therapy, including bendamustine and rituximab (BR) (9/38 cases, with rituximab 500 mg/m² intravenous), fludarabine, cyclophosphamide, rituximab (FCR, 5/38 cases), rituximab and chlorambucil (4/38 cases), BTK inhibitors (7/38 cases) and steroid (1 case, presenting with immune thrombocytopenia). Out of 7 cases receiving BTK inhibitors, ibrutinib and acalabrutinib were administered to 5 and 2 cases, respectively. Treatment response was CR and PR for 2/7 and 5/7 cases. At last follow-up, treatment was ongoing for 5/7 cases, while 2 patients receiving ibrutinib experienced progressive disease (PD) after 12 and 18 months. Patients starting first-line therapy between 2008 and 2018 were more likely to receive chemoimmunotherapy compared to patients treated in 2019-2022, that were more likely to receive BTK inhibitors. Out of 26 SLL cases who received first-line therapy, after a median follow-up of 33 months, the median PFS was 54 months (95% confidence interval 20-54 months), with a 3-y PFS of 58%, while the median OS was not reached, with a 3-y OS of 84%.

Disease relapse was reported in 10/26 cases (38.5%), including 6 patients who evolved to an overt CLL, while no Richter Transformation occurred. All cases had received front-line chemoimmunotherapy and all received novel agents as second-line regimen, including BTK inhibitors and idelalisib. Five cases died, due to sudden death of unknown origin in an elderly case (84 years old), urinary tract infections and PD (2 cases each).

Conclusions. We suggest SLL cases could have a suboptimal outcome if compared to CLL cases enrolled in clinical trials. Due to BTK inhibitors demonstrated prolonged efficacy for CLL/SLL cases, this approach could represent a suitable treatment option. We recommend to enroll SLL patients in clinical trials with the aim of investigating biological predictors of survival, including the study of cytogenetic markers (del17p, trisomy12) and the tumor microenvironment.

P093

LONG-TERM SURVIVAL OF PATIENTS WITH MANTLE CELL LYMPHOMA. A SINGLE-CENTER, RETROSPECTIVE, 15-YEAR REAL-LIFE EXPERIENCE

E. Cencini¹, A. Fabbri¹, A. Dragomir¹, M. Franceschini¹, N. Calomino², M. Bocchia¹

¹Unit of Hematology, Azienda Ospedaliera Universitaria Senese and University of Siena; ²Unit of General Surgery and Surgical Oncology, Department of Medicine, Surgery and Neurosciences, University of Siena, Italy

Introduction. Mantle-cell lymphoma (MCL) prognosis significantly improved since the introduction of rituximab and high-dose cytarabine-based first-line regimens, followed by autologous stem-cell transplantation. Ibrutinib represents an effective regimen for relapsed/refractory (R/R) disease. However, MCL is characterized by multiple relapses and the possible survival benefit of new treatment options in last years should be evaluated, especially for elderly patients.

Methods. We would like to report our 15-year real-life experience, in which we investigated 73 consecutive MCL patients managed at our Institution from 2006 to 2020. Progression-free survival (PFS) was our first end-point. Survival analysis were performed using Kaplan and Meier method and our results were reported as a hazard ratio (HR), with its 95% confidence interval (CI).

Results. First-line therapies included rituximab and bendamustine (26/73 cases), HD cytarabine-based therapies (24/73), R-BAC (9/73), R-CHOP (6/73), fludarabine-based regimens (5/73) and alkylating agents (3/73, with rituximab in 2 cases). For the entire cohort, median PFS was 60 months (95% CI 30-84 months) and we report a 2-year, 5-year and 10-year PFS of 63%, 50% and 32%, respectively. Median OS was not reached and we report a 2-year, 5-year and 10-year OS of 80%, 63% and 51%, respectively. For younger patients <65 years old, median PFS was 72 months and we report a 2-year, 5-year and 10-year PFS of 73%, 62% and 41%; median OS was not reached and we report a 2-year, 5-year and 10-year OS of 88%, 82% and 66%. For patients aged between 65 and 74 years, median PFS was 36 months and we report a 2-year, 5-year and 10-year PFS of 64%, 47% and 23%, respectively; median OS was 84 months and we report a 2-year, 5-year and 10-year OS of 79%, 52% and 34%, respectively. For patients aged 75 years or older, median PFS was 36 months and we report a 2-year, 5-year and 10-year PFS of 52%, 37% and 37%, respectively; median OS was not reached and we report a 2-year, 5-year and 10-year OS of 72%, 55% and 55%, respectively. According to specified treatment periods (2006-2010, 2011-2015, 2016-2020), median PFS was 18 months, 72 months and not reached, respectively. Median PFS was significantly reduced for patients treated between

2006-2010 if compared to patients treated between 2011-2015 (HR 2. 5716, 95% CI 1. 15-5. 7) and between 2016-2020 (HR 1. 6803, 95% CI 0. 72-3. 88) ($p=.04$). Interestingly, there was a trend towards an improved OS for patients treated between 2016-2020 compared to 2006-2010 and 2011-2015 (5-year OS was 91%, 44% and 33%, respectively).

Conclusions. We observed a PFS improvement for MCL patients treated after 2010. This finding could be due to the introduction of BR as 1st line regimen for elderly patients, which demonstrated sustained efficacy. Furthermore, the abovementioned OS benefit during last 5 years for elderly patients could be due to the introduction of ibrutinib as ≥ 2 nd line regimen in Italy.

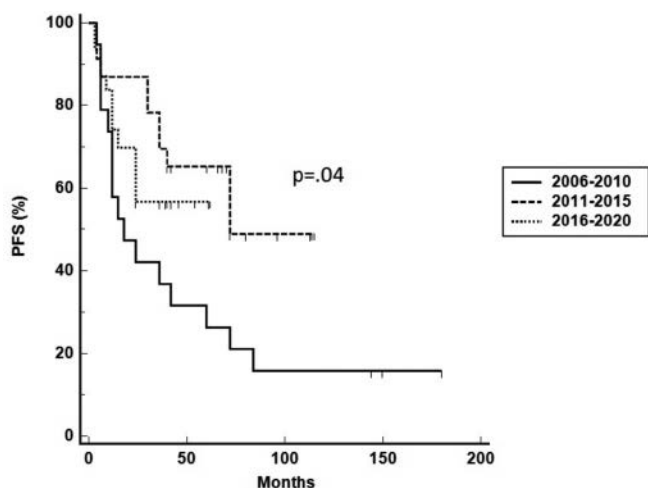


Figure 1.

Monoclonal Gammopathies and Multiple Myeloma

P094

LIPID HANDLING CONVEYS SENSITIVITY TO ANTI-BCMA IMMUNOTHERAPY IN MULTIPLE MYELOMA

E. La Spina¹, A. Romano³, C. Giallongo², D. Tibullo¹, I. Dulcamare, E. Scuderi¹, G. Scandura³, D. Cambria³, S. Cortellino⁵, M. Mecca⁵, S. Picerno⁵, A. Neri⁷, A. Amoresano⁴, G. Pinto⁴, S. Serpico⁴, A. Sgambato⁶, G.A. Palumbo², F. Di Raimondo³

¹Department of Biotechnological and Biomedical Sciences, University of Catania, ²Department of Medical, Surgical Sciences and Advanced Technologies G.F. Ingrassia, University of Catania, ³Department of Surgery and Medical Specialties, University of Catania, ⁴Department of Chemical Sciences, University of Naples Federico II; ⁵Laboratory of Pre-Clinical and Translational Research, IRCCS-CROB, Referral Cancer Center of Basilicata, Italy

Introduction. Lipid metabolic changes in cancer are attracting increased attention. BAFF/APRIL axis is a multifaceted immune regulator of adipose tissue function and an emerging target for anti BCMA therapy in multiple myeloma (MM). Decreased cholesterol levels in MM patients have been previously described, probably representing increased LDL clearance and utilization of neutral lipids and cholesterol by MM cells, however, lipid analyses are scarce in MM onset and response to treatment. Teclistamab (TeCl[i/i] is a bispecific antibody (BsA[b] which target simultaneously BCMA and CD3+ leading to the formation of immunologic synapses with subsequent MM plasmacells (MM PCs) lysis. Although, T cell redirecting BsAbs are showing promising results, drug resistance mechanisms or poor sensitivity to the treatment need to be deeply and molecularly investigated.

Methods. Sera obtained from matched bone marrow and peripheral blood of 9 Relapsed Refractory MM patients at first-MM diagnosis and later at relapse, were evaluated by LS-MS/MS. *in vitro* assays and FACS analysis, were combined to evaluate the response to TeCl[i in human MM cell lines (HMCLs) which were co-incubated with various drug concentrations in the presence of CD3+ T cells from healthy donors at different effector-to-target (E/T) cell ratios. After 24 hours the cocultures were anti-CD138 PE antibody stained and MM-PCs lysis (%) was calculated. BODIPY493/503 was used to quantify cytoplasmatic lipid droplets (CLDs) in surviving CD138+ cells.

Results. String analysis of circulating sera proteins identified crucial pathways including inflammatory response, structural integrity of lipoproteins and lipid transport, with a significant increase of apolipoproteins APO-A1 (key component of HDL particle and cofactor for lecithin-cholesterol acyltransferase (LCAT) which is responsible for the formation of most plasma cholesteryl esters), A2,C2 (which hydrolyzes triglycerides to provide free fatty acids for cells), C3, components of HDL and LDL, confirming a deranged lipid handling in RR-MM patients. Despite no significant differences in BCMA surface expression levels, sensitivity to TeCl[i was largely variable, *in vitro*, outlining a no treatment responding cytotype (OPM2). Conversely, the most sensitive cytotype (U266) showed decreased cell viability in a TeCl[i dose-dependent manner but independent on BCMA expression levels and on E/T ratios. After TeCl[i treatment, BODIPY493/503 highlighted an increase in CLDs in both HMCLs which was partially inhibited by using acipimox as lipolysis inhibitor, which in combination with TeCl[i significantly increased drug sensitivity, also in the no sensitive cytotype with a simultaneous CLDs reduction.

Conclusions. Taken together, our data undoubtedly demonstrated an essential role of CLDs modulation, thus opening a new scenario

about the molecular pathway underlying anti-BCMA immunotherapy sensitivity, independent on BCMA expression but probably favored by a deranged lipid handling in MM.

P095

TARGETING THE NAD⁺ SALVAGE PATHWAY WITH NOVEL NICOTINAMIDE PHOSPHORIBOSYLTRANSFERASE (NAMPT) INHIBITORS UNVEILS METABOLIC DEREGULATION AS EXPLOITABLE VULNERABILITY FOR MYC-DRIVEN MULTIPLE MYELOMA

I. Traverso¹, D. Soncini², P. Becherini¹, D. Truffelli¹, F. Ladisa^{1,3}, G. Giorgetti^{1,3}, F. Guolo^{1,2}, A. Cagnetta^{1,2}, S. Aquino⁴, A. Bellotti⁵, M. Duschosal⁵, A. Nahimana⁵, R.M. Lemoli^{1,2}, M. Cea^{1,2}

¹Clinic of Hematology, Department of Internal Medicine and Medical Specialties (DiMI), University of Genoa; ²IRCCS Ospedale Policlinico San Martino; ³Jerome Lipper Multiple Myeloma Center, Department of Medical Oncology, Dana Farber Cancer Institute, Harvard Medical School; ⁴Hematology and Hematopoietic Stem Cell Transplantation Unit, IRCCS Ospedale Policlinico San Martino; ⁵Central Laboratory of Hematology, Department of Medical Laboratory and Pathology, Lausanne University Hospital and University of Lausanne, Italy

Introduction. Multiple myeloma (MM) is an incurable hematological malignancy in which accumulating evidence suggests altered metabolism as acquired feature for drug resistance occurrence. We previously reported that Nicotinamide Adenine Dinucleotide (NAD⁺), a master regulator of catabolic metabolism and several enzymatic activities, plays a crucial role for MM cells growth; as a result, small molecules targeting the rate-limiting NAD⁺ producer enzyme NAMPT have potent anti-MM activity. Despite their high efficacy in preclinical studies, clinical activity of these molecules was proven to be limited. Here, we report the activity of new NAMPT inhibitors, JJ08, SF183 and FEI199.

Methods. MTT-base assay was used to screen a panel of MM cell lines with different NexGen NAMPT-inhibitors, using the prototype FK866 as reference compound. Statistical models were employed to infer cellular features affecting drug-sensitivity. Chemical and genetic lentiviral-based approaches were both used to test relevance of our findings. Finally, clinical benefits of our findings were accomplished by challenging publicly available datasets on MM patients (CoMMpass).

Results. A broad anti-MM activity of all tested inhibitors was observed, with FEI199 exhibiting higher activity compared with other molecules, including the reference compound FK866. A binomial distribution model of drug-sensitivity screen revealed that MYC amplification status affects the anti-tumor activity of these inhibitors in isogenic cells with MYC-overexpressed resulted particularly sensitive to investigated strategy. As result, gain-of-function models were employed by choosing U266 cell line enforced c-MYC expression enhanced the anti-MM activity of these molecules, thus supporting NAD⁺ metabolism as Achilles heel for MYC-driven tumors. To highlight the translational relevance of these data, FK866-induced transcriptome changes described in GSE96636 were processed to infer MM patients included in the CoMMpass dataset. An enrichment analysis identified a group of patients with an FK866-specific signature (FK866up and FK866dn, respectively) resembling drug-treated cells (FK866 treated-like) reported as sensitive over those with different gene levels. More importantly, clinical analyses revealed that FK-sensitive signature resulted in better outcome among patients with c-MYC amplification (MYCamp). Ongoing mechanistic studies as well as planned *in vivo* studies will help to support these results.

Conclusions. Overall, we identify that NAD⁺-metabolism is an

exploitable vulnerability in MM subgroups overexpressing MYC. Based on these findings, we propose energetic status as novel actionable target for MM, thus providing the framework for testing this approach in clinical trials basically focused on more aggressive diseases.

P096

DECODING TUMOR INTRINSIC AND EXTRINSIC DRIVERS OF DARATUMUMAB ESCAPE IN RELAPSED/REFRACTORY MULTIPLE MYELOMA

C. Giannotta¹, B. Ziccheddu², M. D'agostino³, G. Bertuglia³, E. Saraci⁴, N. Bolli⁵, B. Bruno³, M. Boccadoro⁵, A. Larocca³, F. Maura², M. Massaia^{1,6}.

¹Laboratory of Blood Tumor Immunology, Molecular Biotechnology Center "Guido Tarone", Department of Molecular Biotechnology and Health Sciences, Università di Torino; ²Myeloma Division, University of Miami, Sylvester Comprehensive Cancer Center; ³Division of Hematology, AOU Città della Salute e della Scienza di Torino, University of Torino and Department of Molecular Biotechnology and Health Sciences; ⁴Department of Molecular Biotechnology and Health Sciences, Università di Torino; ⁵Division of Hematology & Stem Cell Transplantation, University of Milano, Fondazione IRCCS; Istituto Nazionale dei Tumori; ⁶SC Ematologia, AO S. Croce e Carle, Italy

Daratumumab (Dara) has become a cornerstone of many triple regimens delivered to naïve and relapsed/refractory Multiple Myeloma (RRMM). Clinical outcome of MM patients has significantly improved with Dara, but there is a small proportion of patients (<10%) who are primary refractory, and, even if Dara is given indefinitely, almost all patients ultimately relapse after an initial response (secondary resistance). At baseline, myeloma cells represent the major target in the tumor microenvironment (TME), whereas other CD38+ immune cells with regulatory or effector activity become the predominant target in responder patients, once myeloma cells have been cleared from the TME. The aim of this work was to investigate tumor-intrinsic and extrinsic mechanisms potentially affecting the efficacy of Dara at baseline and during treatment. To this end, we have investigated and correlated with clinical outcome the genetic and immunological features of 32 RRMM patients treated with Dara, Lenalidomide, and Dexamethasone (D-Rd). Whole genome sequencing (WGS) revealed genomic drivers associated with early progression [high APOBEC mutational activity, chromothripsis events, TP53 deletion, 1p22.1 deletions (RPL5), Structural Variations (SVs) involving MYC locus, and 2 novel deletions involving 16p13.3, and 10p15.3]. Flow cytometry analysis of CD38+ immune cells at baseline (32 paired BM and PB samples) and during treatment (202 PB serial samples in 31 patients) showed modifications in cell subset distribution and CD38+ expression negatively associated with clinical outcome (high levels of CD38+ NK cells at baseline quickly depleted by Dara treatment; the presence and persistence of exhausted CD4+ and CD8+ cells, the expansion of CD38- Tregs). Data integration pointed out the association between specific genomic and immune alterations that negatively affected the clinical outcome. These data indicate that the genomic alterations of myeloma cells and the immune imprinting operated in the TME concurrently hamper the efficacy of Dara treatment.

P097

SOLUBLE B-CELL MATURATION ANTIGEN| ROLE IN SHORT-TERM MONITORING OF DIFFERENTLY TREATED MULTIPLE MYELOMA PATIENTS

M.L. Del Giudice¹, L. Caponi², A. Botti², S. Galimberti¹, G. Buda¹

¹Hematology Division, Pisa University Hospital; ²Department of Translational Research and New Technologies in Medicine and Surgery, Italy

Introduction. The management of multiple myeloma requires accurate ways of assessing disease status. Currently used biomarkers may have limitations (e. g. M protein is not useful in predicting rapid relapse due to the long half-life of Ig; FLC may be affected by renal function and different tests on the same sample may give discordant results; MRD assessment is not routinely performed). Soluble BCMA is released in serum by γ -secretase with a half-life of 24-36 hours. It correlates with the BM plasma cells, with the expression of BCMA on the PC surface and with other clinical features such as immunodeficiency status. sBCMA may also act as a decoy for BCMA-targeted therapies. Based on these assumptions, we are investigating the role of sBCMA in an unselected MM population undergoing different treatments.

Methods. The study is observational and prospective. Patients followed at the Hematology Unit of the University Hospital of Pisa will be assessed for sBCMA using the R&D System® on peripheral blood samples collected at the start of treatment (T0), after 1 month (T1) and after 6 months (T2). Each patient will undergo simultaneous disease assessment with known serum markers, BM and whole-body assessments. The trial has been approved by the EC.

Results. On 6 October 2023, we analyzed data from 55 patients (22 newly diagnosed and 33 after ≥ 1 relapse). sBCMA could be measured in all patients, including those with solitary plasmacytoma and non-secretory disease and those undergoing anti-BCMA target therapies. sBCMA levels at T0 were very heterogeneous. There were no outliers among the 17 samples from patients with renal impairment (eGFR < 40 mL/min per 1.73 m² or Cr > 2 mg/dL). Correlating the median percentage decrease from T0 to T2 with the response to the different treatments, we found a statistically significant correlation (Spearman's $r = -0.5261$; $p < 0.001$). Median T2-T0 was higher after first-line therapy (90.69%) than after salvage therapy (71.09%). In CR/VGPR patients (n=20) it was 91.9%, in PR (n=26) 79.87% and in PD (n=9) -2.53%. When analyzing the percentage decrease at one month (T1-T0), it was 85.13% in newly diagnosed patients and 59% in relapsed patients. The median T1-T0 was 77.37%, 78.6% and 43.5% in CR/VGPR, PR and PD, respectively.

Conclusions. sBCMA was dosable at all study time points. The percentage decrease was more significant in patients who started treatment after initial diagnosis than in those who relapsed. There was a significant correlation between median T2-T0 and the quality of response. The highest median decrease rate was found in newly diagnosed patients and in patients with at least a VGPR. Median T1-T0 was higher in patients who will achieve at least a PR. So, sBCMA seems to be a promising marker of response that changes at a very early stage during treatment. It would allow non-invasive monitoring, especially in patients with non-secretory MM. These reports can be extended but already provide insights into the MM.

P098

IMMUNE SYSTEM, CYTOKINE PROFILES, AND FECAL MICROBIOTA CHANGES INFLUENCE THE PROGRESSION FROM MONOCLONAL GAMMOPATHY OF UNDETERMINED SIGNIFICANCE (MGUS) TO MULTIPLE MYELOMA (MM)

A.M. Corsale^{1,2}, M. Di Simone^{1,3}, M. Shekarkar Azgomi^{1,3}, M. Speciale², E. Gigliotta², F. Garofano², C. Aquilina², C. Vullo², M. Santagati⁴, N. Caccamo^{1,3}, A. Romano⁵, F. Dieli^{1,3}, S. Meraviglia^{1,3}, S. Siragusa², C. Botta²

¹Central Laboratory of Advanced Diagnosis and Biomedical Research (CLADIBIOR), University of Palermo; ²Department of Health Promotion, Mother and Child Care, Internal Medicine, and Medical Specialties (ProMISE), University of Palermo; ³Department of Biomedicine, Neuroscience and Advanced Diagnosis (Bi.N.D.), University of Palermo; ⁴Department of Biomedical and Biotechnological Sciences, Section of Microbiology, University of Catania; ⁵Division of Hematology, AOU Policlinico "G. Rodolico-San Marco", Italy

Introduction. Multiple myeloma (MM) is an incurable blood cancer preceded by monoclonal gammopathy of undetermined significance (MGUS) and smoldering MM (SMM). Understanding the MGUS to MM transition is crucial for better risk assessment and tailored treatments. This study explores immune system changes and fecal microbiota variations during this progression.

Methods. We developed 6 custom panels with 10 different colors and 2 panels with 8 colors for flow cytometry. We analyzed samples from 13 MGUS, 12 SMM, and 63 newly diagnosed MM patients. Additionally, we quantified cytokines and chemokines in both the bone marrow (BM) and peripheral blood using a Luminex plate with 48 analytes. This analysis included 72 samples from the same patients with MGUS, SMM, MM, and four healthy donors. Furthermore, we conducted fecal microbiome profiling in samples from 3 MGUS, 6 SMM, and 9 MM patients to investigate potential links between bacterial composition and MM progression.

Results. Unsupervised analysis of T cells via flow cytometry revealed a significant increase in circulating TEMRA CD8 T cells, primarily CD57+ cells (mean, 7.5% for MGUS vs 20.1% for SMM vs 21.6% for MM; $p < 0.05$). There was also a notable reduction in naive TIGIT+ CD8 T cells (mean, 12.4% for MGUS vs 5.98% for SMM vs 4.16% for MM; $p < 0.001$) and naive TIGIT+ and TIM3+ CD8 T cells (mean, 2.18% for MGUS vs 1.24% for SMM vs 1.17% for MM; $p < 0.001$). Concerning CD4 T cell subsets, a decrease in BM effector memory phenotype was observed as the disease progressed. Interestingly, MM patients' BM CD4 T cells produced more IL17 compared to those with MGUS. In terms of myeloid cell subsets, reductions were observed in circulating non-classical monocytes expressing HLA-DR and CD11c, as well as mature granulocytes as MM progressed. Regarding cytokines and chemokines, a decrease in GM-CSF, IFN- $\alpha 2$, IFN- γ , IL-1 β , IL-2, IL-2Ra, IL-3, IL-10, IL-13, and MCP-1/CCL2 levels within the BM plasma throughout MM progression was noted, supporting a global reduction in myeloid function and T cell effector activity. Finally, there was a general increase in the total abundance of fecal bacteria, with several bacterial genera significantly over-represented in MM patients (e. g., *Bariatricus*, *CAG-83*, *Alistipes*, *Bifidobacterium*, *Streptococcus*, *Ruminococcus D*, *Slackia A*, and *Coprococcus A*), while others were more prevalent in MGUS and SMM patients (e. g., *Parabacteroides B*). The analysis of phyla relative and rare abundance indicated that *Firmicutes D* and *Lactobacillales* were more abundant in MM patients, while *Actinobacteriota* dominated in SMM patients, and *Proteobacteria* and *Bacteroidota* were more prominent in MGUS patients.

Conclusions. In summary, this study has shed light on the changes in both the myeloid and lymphoid components of the immune system

in terms of cellular composition, cytokine production, and control over the fecal microbiome during the transition from pre-cancerous conditions to the onset of MM.

P099

ARGININE REDUCTION PROMOTES THE EMERGENCE OF CANCER STEM-LIKE CELL IN MULTIPLE MYELOMA

G. Scandura¹, C. Giallongo², T. Zuppelli³, I. Dulcamare⁴, E. La Spina³, S. Giallongo⁴, L. Longhitano³, N.L. Parrinello⁵, F. Polito⁶, R. Oteri⁶, M. Aguenouz⁶, N. Vicario³, S. Brunak⁷, J. Xin Hjaltelin⁷, M. Herrera⁷, V. Del Fabro⁵, C. Conticello⁵, G. Li Volti³, G.A. Palumbo^{2,5}, D. Tibullo³, F. Di Raimondo^{4,5}, A. Romano^{4,5}

¹Department of Clinical and Experimental Medicine, University of Catania; ²Department of Medical and Surgical Sciences and Advanced Technologies "G. F. Ingrassia", University of Catania; ³Department of Biomedical and Biotechnological Sciences, University of Catania; ⁴Department of General Surgery and Medical-Surgical Specialties, University of Catania; ⁵Division of Hematology, Azienda Policlinico; ⁶Department of Clinical and Experimental Medicine, University of Messina; ⁷Novo Nordisk Foundation Center for Protein Research, University of Copenhagen

Background. Multiple myeloma (MM) is an incurable haematological cancer characterized by the clonal proliferation of malignant plasma cells (PC) in the bone marrow (BM). Despite the positive effect of several anticancer therapies, patients often relapse. MM progression is supported by the immunosuppressive tumor microenvironment (TME) in the BM, driven mainly by myeloid-derived suppressor cells (MDSCs) releasing arginase-1 (ARG1). Additionally, the TME supports the presence of cancer stem cells (CSCs), a subpopulation of cells characterised by slow-cycling and the unique ability to enter the G0-quiescent cell cycle phase. This confers a reversible dormant state where the cells remain alive but do not proliferate. CSCs play a pivotal role in conferring tumor resistance, underscoring their importance in MM. Previous studies revealed that immortalized human myeloid cells (HMCs) cultured with sera from MM patients exhibit resistance to bortezomib treatment in an ARG1 dependent manner. As such, this study investigates the impact of arginine (Arg) reduction on MM progression and maintenance.

Materials and Methods. We assess the impact of Arg concentration *in vitro* on two HMCs lines (U266, NCI-H929) both short- (48 h) and long-term (10 days). We cultured cells in both complete standard or deprived medium (R_{low}-medium), containing 200 µg/mL or 50 µg/mL of L-Arg, respectively. 50 µg/mL matches with patients' serum concentrations.

Results. At 48h, reduction in Arg concentration in the growth medium did not significantly affect cell viability. However, it slowed proliferation and increased the percentage of cells arrested in the G0-G1 phase. Arg reduction promoted cellular stress, leading to DNA damage, as highlighted by a higher percentage of γH2AX⁺ cells, which is a marker for DNA double-strand breaks. To gain further insights into the cellular response to Arg deprivation, we analysed this change using gene expression profiles and gene set enrichment analysis (GSEA). Cells grew in R_{low}-medium significantly down-regulate pathways related to DNA repair and regulation of chromatid segregation. These findings are closely associated with an increase in genomic instability, which was further corroborated by the presence of a high number of micronuclei. Finally, we assessed the presence of a low-energetic metabolism related to the dormant state of CSCs. GSEA and Seahorse analysis showed a notable reduction in both metabolic pathways, suggesting the acquisition of a senescent-associated secretory phenotype (SASP). This was further

confirmed by the overexpression of the key players of inflammasome activation, including NLRP3, pro-Caspase 1, Caspase 1, interleukin-18 (IL-18) and cleaved IL-1B.

Conclusion. Our results emphasize the role of Arg reduction in promoting genomic instability and inducing a dormant phenotype in MM. This shift, maintained through SASP, might contribute significantly to a resistant phenotype responsible for the persistence of the disease.

P100

SINGLE-CELL RNA SEQUENCING IDENTIFIES NOVEL THERAPEUTIC TARGETS FOR CAR THERAPY IN MULTIPLE MYELOMA

F. Garofano¹, A.M. Corsale², M. Shekarkar Azgomi², M. Di Simone², M. Speciale², C. Aquilina², A. Gulla³, S. Meraviglia², N. Caccamo², F. Dieli², S. Siragusa¹, C. Botta¹

¹Hematology Unit, Policlinico Universitario, University of Palermo; ²University of Palermo; ³Candiolo Cancer Institute FPO- IRCCS, Italy

Introduction. Although recent advances in Chimeric Antigen Receptor T cell (CAR T) therapy have enhanced the survival of multiple myeloma MM patients, challenges persist due to antigen escape and relapse. We harness the power of single-cell (sc) technologies to pinpoint specific surface protein targets for CAR-based therapies at the sc level. This approach holds the potential to pave the way for the development of personalized cellular therapies and treatment protocols.

Methods. Our research involved the analysis of nine publicly available single-cell RNA sequencing (scRNA-seq) datasets (GEO accession numbers: GSE176131, GSE189460, GSE223060, GSE210079, GSE145977, GSE124310, GSE161801, GSE163278, GSE161722) comprising 156 patients: 19 with monoclonal gammopathy of undetermined significance (MGUS), 10 with smoldering MM (SMM), 78 with MM, 25 with relapsed/refractory MM (RRMM) and 24 with normal bone marrow (NBM). We conducted a comprehensive analysis comparing plasma cell PC transcriptomes between MM/RRMM, NBM, MGUS, and SMM patients, delving into cytogenetic-related cell subclusters, and focusing on the top five genes that had not yet advanced to clinical development. Furthermore, we examined various gene profiling datasets (GSE4204, GSE2658, GSE57317, GSE4581, GSE4452, GSE9782, and CoMM-pass study NCT01454297) encompassing around 2000 MM patients.

Results. Our investigation led to the identification of 15 genes overexpressed in PCs that code for surface proteins: TNFRSF17(BCMA), SDCl (CD138), FCRL5 (FCRH5), TNFRSF13B (TACI), CD38, SLAMF7 (CS1), CD59, FCGR2B, FGFR3, SLC44A1 (CTL1), CD320, FCRL2, IL15RA, INSR, and SLAMF1. Many of these genes are already recognized therapeutic targets. In clonal PCs, CD320 was significantly overexpressed as compared with normal PCs. A significant correlation was found between TACI/CD59 expression and increased CCND2 and MAF expression, associated with the t(14;16) chromosomal translocation. Among them, five genes have limited clinical investigation: TNFRSF13B, CD59, FCGR2B, SLC44A1, and CD320. TNFRSF13B, CD59, and FCGR2B expression are correlated with improved patient outcomes; CD320 and SLC44A1 expression are correlated with worse outcomes. The publicly accessible database of the Human Protein Atlas revealed that CD320 is predominantly expressed in adipocytes and PCs, while TNFRSF13B is B-cells and PCs.

Conclusions. We identified a series of novel targets for MM patients which allows each patient to be "screened" to identify the most appropriate target. CD320 and TACI emerge as promising candidate biomarkers for tracking disease progression and predicting patient's outcomes. While additional research is necessary to evaluate

clinical significance, our analysis stands as a notable progression in the exploration of tumor markers. This methodology harbors the capacity for wide-ranging applicability across diverse malignancies, drawing us nearer to the identification of ideal candidates for efficacious CAR therapy.

P101

CIRCULATING CD71+ MYELOID PRECURSORS IN MGUS AND MULTIPLE MYELOMA: A PROSPECTIVE SURVEY

A. Romano, S. Marino, N.L. Parrinello, A. Triolo, G. Scuderi, S. Giannone, V. Del Fabro, G.A. Palumbo, C. Conticello, F. Di Raimondo

Divisione di Ematologia, AOU Policlinico Rodolico San Marco; Dipartimento di Chirurgia e Specialità Medico Chirurgiche, Università degli Studi di Catania, Italy

Our previous work showed that in Multiple Myeloma (MM) high-density of neutrophils are increased, immune suppressive and associated with reduced patient survival, making these cells attractive targets for cancer immunotherapy. In this work, we aimed to quantify the number of neutrophil precursors at different stages of plasma cell dyscrasias. A major comprehension of myeloid compartment and its dynamics may represent a further step to develop a highly accurate immune monitoring in MM. Our study included the evaluation of early myeloid precursors cells (eNeP) in peripheral blood of 93 consecutive individuals including 23 healthy controls, 13 MGUS patients, 57 MM overt disease of which 30 are newly diagnosed (NDMM), 12 patients in continuous therapy and stable disease (CT-MM) and the remaining 15 affected by RRMM (N=15,16%). Whole peripheral blood was collected in EDTA vials and processed within 24 hours after collection. Myeloid precursor cells were performed by multiparameter flow cytometry method with the following panel of 4 monoclonal antibodies: CD71-FITC, CD45-ECD, CD15-PC5, CD117-PC7. The comparison of major demographical, clinical and radiological features between healthy subjects and MM patients did not reveal any significant differences. We distinguished MM patients in three groups, newly diagnosed (NDMM) versus MM stable, versus RRMM. At time for sampling, between NDMM and RRMM there were no significant difference in terms of age, co-morbidity index, biochemistry and haematological findings. The analysis of myeloid precursors revealed a higher value of CD71+ CD117+ cells in MGUS patients than in healthy controls (median CD15+CD71+ CD117+ % 0.004 vs 0.009, p=0.03), with a progressive and significant increase from MGUS through SMM and MM (p<0.001, ANOVA test). In NDMM carrying a standard FISH the median percentage of CD15+CD71+ CD117+ eNeP was 0.07 (range 0.004-0.17), not significantly different compared to patients with a high-risk FISH 0.05% (range 0.004-0.15, p=0.26). Using a cut-off value of 0.05% (equal to the highest percentage plus a standard deviation in healthy subjects), we distinguished MM patients with high or low precursor counts. NDMM patients carrying higher counts of CD15+CD71+ CD117+ % cells showed a lower survival at 18 months (65.1% vs 85.2%, HR 4.7, 95% CI 1.1-20.4, p=0.03). In RR-MM patients with a biochemical relapse the median percentage of CD15+CD71+ CD117+ eNeP was 0.02 (range 0.003-0.08), significantly lower than in patients with a clinical aggressive relapse, 0.06% (range 0.01-0.14, p=0.004).

Conclusions. Our study suggests that eNeP could play a role in the transition from asymptomatic to symptomatic clinical presentation of plasma cell dyscrasias and their quantification in the peripheral blood could play an important biological and clinical role in identifying MM patients with worse outcomes.

P102

[18F]-FLORBETABEN PET/CT IS MORE SENSITIVE FOR CARDIAC AL AMYLOIDOSIS THAN BIOCHEMICAL PARAMETERS

R. Cassano¹, D. Genovesi², G. Vergaro³, A. Aimo³, M.L. Del Giudice¹, S. Galimberti¹, M. Edmin³, G. Buda¹

¹Hematology Unit, Department of Clinical And Experimental Medicine, University of Pisa; ²Division of Nuclear Medicine, Fondazione Toscana Gabriele Monasterio; ³Division of Cardiology and Cardiovascular Medicine, Fondazione Toscana Gabriele Monasterio, Institute of Life Science, Scuola Superiore Sant'Anna, Italy

Introduction. AL amyloidosis is haematological disease characterized by clonal population of plasma cells that produces monoclonal light chains and extracellular deposition of amyloid insoluble fibrils. The misfolded proteins interfere with organs functions, mostly heart and kidney; the involvement could be unknown for years before diagnosis, due to the asymptomatic deposition until disfunction. Different techniques were introduced to detect amyloid deposit like Congo Red staining, immunochemistry, electronic microscopy on Pericardial Fat or on tissues biopsies involved, or cardiac imaging, echocardiography, MRI or PET. Cardiac deposits in amyloidosis are major determinants of clinical presentation and may be present in AL amyloidosis or ATTR amyloidosis; often differential diagnosis is difficult. Concerning ATTR, sensitive diagnostic tool, as diphosphonate scintigraphy, was recently introduced, instead of no imaging approach is as accurate in AL. Cardiac ultrasound and circulating biomarkers may raise the clinical suspicion of AL, but often endomyocardial biopsy remains the only option for diagnosis.

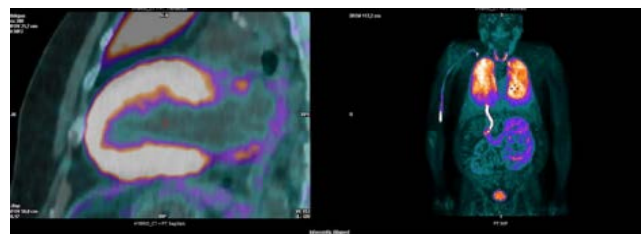


Figure 1. [18F]-florbetaben cardiac positron emission tomography scan in patient with AL amyloidosis. Figure 2. Other localizations of amyloidotic fibrils in the same patient. The [18F]-florbetaben positron emission tomography scan shows pathological positivity in lung and thyroid, histological site of AL detection, and normal hepatic, urinary and intestinal uptake.

	AL patients (n 33)
Male, n	22 (33)
Age, years	65.2 (41-85)
Multiple Myeloma associated to AL amyloidosis, n	20 (33)
creatinine, mg/dL	1.49 (0.54-7.13)
NT-proBNP, ng/L	7944 (537-70000)
hs-Troponin T, ng/L	111.76 (25-203)
FLC ratio	443.89 (1.18-1700)
24h proteinuria, mg/dL	2595 (119-9696)
AL positive Cardiac Biopsy, n	17 (33)
AL positive in Pericardial Fat, n	18 (33)
AL positive Bone Marrow Biopsy, n	10 (33)
AL positive Other Tissues Biopsy, n	8 (33)
[18F]-Florbetaben PET at Diagnosis, n	19 (33)
Previous therapies lines before PET, n	0.6 (0-5)
Therapy after PET:	
Dara-2/BarDec, n	6 (33)
Cy/BarDec, n	13 (33)
Alp/Ida, n	4 (33)
Lu/Idc, n	2 (33)
Others, n	6 (33)
None Therapy, n	2 (33)

TABLE 1. Clinical, Histological and Biomolecular Characteristics of Patients With AL Amyloidosis underwent to [18F]-Florbetaben PET/CT.

Figure 1.

Methods. In this retrospective study, we aimed to explore the sensitivity of 18F-Florbetaben PET/CT respect to common blood tests or POF, cardiac or other tissues biopsies in a cohort of 33 patients, referred to Cardiovascular Unit of Fondazione Monasterio and Haematology Unit in Pisa from July 2016 to January 2023. PET was performed by dynamic reconstruction from list-scan during iv infusion of 18F-Florbetaben, acquiring static cardiac scans 110 min after injection.

Results. PET was performed at time of diagnosis in 19 patients and during the follow up in 11. In our cohort, amyloid fibrils were found in 17/17 endomyocardial biopsies, 18 POF and in 10 BM Biopsies. Blood tests performed at the time of PET showed in 87,8% patient high NT-proBNP and elevated Troponin levels in all study cohort, as a cardiac damage sign, that anyway could be not only related to AL cardiac involvement, but also depends on other cardiological conditions. 24hs Proteinuria could not be considered as a significant parameter in our study, due to low number of patients who collected urine in 24 hours (24,2%); even though the number of patients with renal impairment, creatinine levels in 60,6% of patients with renal involvement were normal. Concerning the most relevant parameter, FLC ratio was normal in 3 patients, suggesting a lower sensitivity of dosing FLC compared to PET. Notably, 18F-Florbetaben PET uptake was also consistent in extra cardiac tissues of amyloid histological deposition.

Conclusions. Earlier diagnosis is challenging in AL amyloidosis with a relevant impact on life expectancy. We demonstrate that 18F-Florbetaben PET positive patients could present normal levels of FLC ratio, suggesting more relevance to perform PET in heart failure patients if AL amyloidosis is suspected, instead of only blood exams or B-Mode US/MRI. Therefore, 18F-Florbetaben PET/CT can be able to explore all sites of amyloid deposits.

P103

CHARACTERIZATION OF THE BIOLOGICAL AND MOLECULAR RELEVANCE OF NONO PROTEIN IN MULTIPLE MYELOMA

G. Fabbiano¹, V. Traini², D. Ronchetti², I. Silvestris², M. Barbieri¹, F. Colombo¹, S. Erratico^{3,4}, V.K. Favasuli⁵, N. Puccio⁶, L. Porretti¹, Y. Torrente⁴, A. Ciarrocchi⁷, A. Neri⁸, N. Bolli^{1,2}, E. Taiana¹

¹Hematology Section, Fondazione IRCCS Ca' Granda Ospedale Maggiore Policlinico; ²Department of Oncology and Hemato-Oncology, University of Milan; ³Novystem Spa; ⁴Stem Cell Laboratory, Department of Pathophysiology and Transplantation, University of Milan; ⁵Dana Farber Cancer Institute, Boston, Massachusetts, United States of America; ⁶Clinical and Experimental Medicine PhD Program, University of Modena and Reggio Emilia; ⁷Laboratory of Translational Research, Azienda USL-IRCCS Reggio Emilia; ⁸Scientific Directorate, Azienda USL-IRCCS Reggio Emilia, Italy

Introduction. Paraspeckles (PSs) are a new class of nuclear ribonucleoprotein organelles, whose relevance in multiple myeloma (MM) pathogenesis has been well documented. PS assembly relies on the binding of the lncRNA NEAT1 with several PS proteins (PSPs), among which NONO. NONO is a multifunctional protein deregulated in many cancer types. Data concerning NONO involvement in MM are virtually absent. We recently reported its overexpression in CD138+ MM cells as compared to healthy plasma cells, also highlighting its correlation with poor outcome in MM patients. Moreover, NONO expression in human MM cell lines (HMCLs) is significantly higher than in other haematological non-HMCLs.

Methods. Gymnotic delivery of specific LNA-gapmeR (g#NONO) was used to silence the expression of NONO in a panel of 4 HMCLs. Dose-effect curves were obtained by Trypan Blue exclusion counts. Cell viability was assessed through CCK-8 assay.

Clonogenic potential was evaluated by methylcellulose assay. Cell cycle phases distribution and apoptosis induction were investigated by FACS analysis. PSs integrity was analyzed by confocal microscopy analysis of combined NEAT1 RNA-FISH and NONO IF. WB was used to study PSPs levels.

Results. All the tested HMCLs, albeit at different levels, showed high sensitivity to NONO silencing starting from the 3rd day of gapmeR exposure (median IC₅₀ value 6.5 µM). Growth curves retrieved from CCK-8 assay confirmed a significant reduction in the number of viable cells in samples treated with sub-cytotoxic concentration of g#NONO (5 µM) until the 7th day of exposure. Modulation in the proliferative behavior of NONO-depleted cells (NONO-KD) was confirmed by the 2-fold decreased number of colonies as compared to controls. In line with FACS results showing an increase of the % of cells distributed in the subG0/G1 phase of the cell cycle in NONO-KD samples (>10% for all HMCLs), we demonstrated apoptosis induction from the 4th day of gapmeR treatment (≈2-fold). From a molecular point of view, along with the significant downregulation of NONO (silencing efficiency >80% for all the HMCLs), we also showed a significant reduction in the expression level of the essential PS scaffold NEAT1 (50-70%, depending on the HMCL). The reduction of both NONO and NEAT1 fluorescence intensity and co-localizing signals was also confirmed by confocal microscopy analysis, demonstrating a strong PSs structure impairment. Of note WB analysis showed a 2-6-fold increase in the expression levels of two other PSPs, SFPQ and PSPC1, suggesting the presence of a compensatory mechanism between NONO and other PS elements.

Conclusion. Our results clearly demonstrate that NONO silencing in HMCLs leads to PSs structure impairment and results in an anti-proliferative and pro-apoptotic effect. Overall, a better elucidation of NONO relevance in MM could highlight it as a therapeutically valuable target for the development of novel pharmacological approaches for this incurable disease.

P104

NEXT GENERATION FLOW IN MULTIPLE MYELOMA PATIENTS: A PRELIMINARY REAL-LIFE MULTICENTER MRD HARMONIZATION EXPERIENCE

E. Saraci¹, S. Oliva¹, V. Trimarco², M. Chiarini³, N.L. Parrinello⁴, R. Zambello², I. Cordone⁵, S. Masi⁵, G. Rossi⁶, S. Marino⁴, A.M. Triolo⁴, A. Roccaro⁷, A.M. Carella⁸, F. Buccisano⁹, A. Belotti¹⁰, M.I. Consalvo¹¹, A. Romano¹², A. Tonini², S. Mercadante¹, B. Bruno¹, C. Terragna¹³, E. Zamagni¹³

¹Division of Hematology, Department of Molecular Biotechnologies and Health Sciences, University of Torino, Division of Hematology, AOU Città della Salute e della Scienza di Torino; ²Department of Medicine, Hematology and Clinical Immunology Section, Padua University School of Medicine; ³Clinical Chemistry Laboratory, Flow Cytometry Section ASST Spedali Civili di Brescia; ⁴A.O.U. Policlinico "G. Rodolico - S. Marco". Hematology unit with BMT; ⁵IRCCS Regina Elena National Cancer Institute; ⁶Department of Hematology and Stem cell Unit, Fondazione IRCCS "Casa Sollievo della Sofferenza"; ⁷ASST Spedali Civili di Brescia; ⁸Hematology Unit, IRCCS Casa Sollievo Della Sofferenza; ⁹Department of Biomedicine and Prevention, University of Rome Tor Vergata; ¹⁰Department of Hematology, ASST Spedali Civili di Brescia, Brescia, Italy; ¹¹University of Rome Tor Vergata; ¹²Division of Hematology, Azienda Policlinico-S. Marco, University of Catania; ¹³IRCCS Azienda Ospedaliero-Universitaria di Bologna, Istituto di Ematologia Seràgnoli, Italy

Introduction. Minimal residual disease (MRD) detection represents a sensitive tool to measure response in MM. The major concern

about MRD detection in real-world setting is the reproducibility of results. Therefore, a harmonized approach, according to criteria of Next generation Flow(NGF)/Next generation sequencing(NGS) established by IMWG, is warranted. The aim of this project was to create an “Italian MM MRD network” using standardized NGF and NGS-MRD approach; we report preliminary results of the NGF part.

Materials. The “NGF harmonization project” includes 7 laboratories: Brescia(L1), Catania(L2), Padova(L3), Roma 1(L4), Roma 2(L5), S. Giovanni Rotondo(L6) and Torino(L7). Standardization of all flow cytometers settings was performed by implementation of the EuroFlow Standard Operating Protocol(SOP) for instrument setup and compensation(www.euroflow.org). Bone marrow (BM) aspirates were collected from newly diagnosed MM patients treated with 4 cycles of Daratumumab, bortezomib, thalidomide, dexamethasone induction followed by autologous stem cell transplantation (ASCT) in complete-response/very-good-partial-response at day 100(+/- 15 days) after ASCT. Anonymized samples were analyzed using NGF methodology(Tube1:CD27, CD138, CD38, CD56, CD45, CD19, CD117, CD81 and Tube2:CD27, CD138, CD38, CD56, CD45, CD19, cytoplasmic κ and λ light-chain). We aimed to reach a sensitivity of at least 1×10^{-5} ; a sample was considered MRD positive when ≥ 20 mPCs were detected. Intraclass Correlation Coefficient (ICC) was performed to evaluate degree of correlation and agreement between measurements; standard deviation(SD) and Coefficient of variation(CV) to measure variability of the dataset.

Results. In stage 1 of the study, 4 laboratories performed a blinded analysis to evaluate the inter-operator variability: 100% of the participants were concordant that samples #1, #2 and #4 were MRD positive. Sample #3 was considered MRD positive by 75% of participants whereas 75% considered sample #5 as MRD negative (ICC=0.91, 95% CI 0.69-0.98, $p < 0.001$). In stage 2, 7 samples have been processed in all laboratories. The inter-laboratory correlation study showed a concordance of 100% for sample #1 and sample #3 considered as MRD positive, 100% of the participants considered sample #5 and sample #6 as MRD negative, sample #2 was considered MRD positive by 71% of participants whereas sample #4 was considered MRD negative by 86% of participants. Sample #7 was considered as not evaluable by all participants (ICC=0.61, 95% CI 0.31-0.91, $p < 0.001$)(Figure 1).

The highest difference in terms of antigen expression of mPCs was recorded for CD45 and CD27.

Conclusion. Our preliminary results demonstrate the importance of a harmonized NGF-MRD assessment to improve the accuracy and comparability of MM-MRD. Major discrepancies have been found in fresh samples vs the retrospective dataset suggesting an impact of the transportation time and sample processing on the concordance of our results.

Figure 1: Results of MRD assessment in inter-laboratory comparability study. Sample #4, #5 and #6 did not contain monoclonal plasma cells. % PC mono: % monoclonal plasma cells

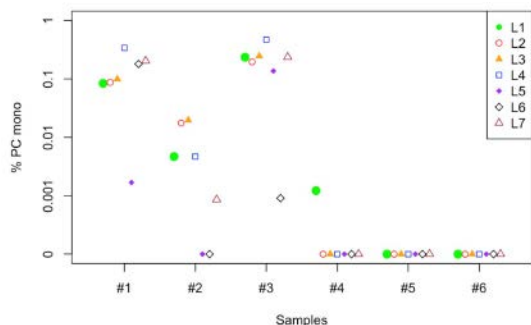


Figure 1.

P105

EVALUATION OF DARATUMUMAB EFFECT ON BIOLOGY OF MULTIPLE MYELOMA PATIENTS PLASMACELLS' BY USING NEXT GENERATION FLOW

P. Pacelli¹, E. Bestoso², D. Raspadori², F. Caroni², A. Sicuranza¹, M. Bocchia^{1,2}, A. Gozzetti^{1,2}

¹Department of Medicine, Surgery and Neuroscience, University of Siena; ²Hematology, Siena University Hospital, Italy

Introduction. Daratumumab (Dara) is an effective anti-CD38 monoclonal antibody for the treatment of Multiple Myeloma (MM) patients. Monitoring of MM Minimal Residual Disease (MRD) is possible by using Next Generation Flow (NGF), a high-sensitive and standardized technique that permits, in a rapid way, to define MRD negativity, with results that are superimposable to that of molecular techniques. We want to confirm the pivotal role of NGF for detection of MM MRD in Very Good Partial Response (VGPR) patients during consolidation therapy with Daratumumab, and to clarify the role of this drug in the clearance of MM PCs. MRD negativity confirmed at one year could be of great importance to predict clinical outcome of MM patients and to determine the efficacy of the drug.

Methods. Starting from December 2018, a multi center pilot study has been set up in Siena. MM patients in VGPR, MRD positive by NGF, were enrolled and MRD evaluation was assessed at 2 months (mos) of treatment, and every 6 mos up to 2 years. Patients negative at the first endpoint of 6 mos could stop Dara treatment, while patients still MRD positive would continue Dara up to 2 years. Percentage and median value of pathologic versus normal PCs have been measured at each timepoint.

Results. All 50 MRD+ MM patients enrolled reached the first endpoint of 6 mos of treatment; 15/50 (30%) obtained MRD negativity, of which 8/15 (53%) obtained MRD negative status already at 2 mos. 47/50 (94%), 38/50 (76%) and 33/50 (72%) patients have been evaluated at the subsequent endpoints of 12, 18 and 24 mos respectively, with 4/8 (50%) of the “early responders” patients persisting in MRD negative status up to 2 years. The high heterogeneity of response could be correlated to type of treatment, as the study seems to confirm that undergoing at least one ASCT permits to obtain a deeper response compared to non-transplantable patients. By looking at percentage of clonal vs normal PCs in patients who maintain a MRD positive status, we observed a significant decrease of pathologic MM PCs during Dara treatment, and a tendency to “stabilize” with a low percentage at longer timepoints from Dara treatment. In particular, median value of MM PCs was 0.0672 at baseline, and it decreases or stabilizes at 0.016, 0.037, 0.025, 0.029 and 0.0325 at 2, 6, 12, 18 and 24 mos respectively, while normal PCs (0.0928 at baseline) tend to decrease at the earliest stages of treatment (0.0515, 0.007, 0.001 at 2, 6 and 12 mos respectively) and then go up again at longer timepoints (0.017 and 0.065 at 18 and 24 mos respectively).

Conclusions. Daratumumab is effective as consolidation therapy in MM patients in VGPR, as it induces MRD negativity and could help “checkmate” pathologic plasma cells, that persist in MRD positive patients but with a very low tumor burden. Future investigations may be useful to reveal the role that the immune system may have in controlling the pathogenesis of MM patients and the clearance from pathologic PCs.

P106

ROLE OF FC GAMMA RECEPTORS IN MULTIPLE MYELOMA. A SINGLE CENTER SURVEY

A. Romano, D. Cambria, M.T. Cannizzaro, A. Cavallaro, V. Del Fabro, G.A. Palumbo, C. Conticello, F. Di Raimondo

Divisione di Ematologia, AOU Policlinico Rodolico San Marco; Dipartimento di Chirurgia e Specialità Medico Chirurgiche, Università degli Studi di Catania, Italy

Background. Bone erosion is one of the primary features of multiple myeloma, caused by an imbalance activation of osteoclasts and dysfunction of osteoblasts. Fc gamma receptors (FcγRs) have been implicated in osteoclastogenesis. In autoimmune diseases, the joint-deposited lupus IgG inhibited RANKL-induced osteoclastogenesis, associated to the FcγRIIa-R131 allele in African Americans and the FcγRIIIa-F176 allele in Caucasians. Daratumumab (DARA) is human anti-CD38 IgG1, high-affinity human monoclonal antibody having broad-spectrum killing activity in multiple myeloma, exerting anti-tumour activity via Fc-FcγR interaction with macrophages. Thus, we investigated a possible association between bone disease extension and polymorphism in IgG Fc receptors, FCgammaRIIa and FCgammaRIIIa and depth of early response after first two cycles of daratumumab.

Methods. We reviewed files of 109 MM (54% males, 46% females median age 65 years, range 24-81), diagnosed at Hematology Division of AOU Policlinico Rodolico, Catania, between January 2019 and August 2021, including 72 treated with daratumumab in first line. We investigated the genotyping of FCgammaRIIIa-158 and FCgammaRIIa-131 using allele-specific polymerase chain reaction (PCR) methods. Associations among FcgammaR polymorphisms and age of onset, levels of serum immunoglobulins, extension of bone disease assessed by low-dose radiation CT scan, stage and clinical outcome were analyzed.

Results. The frequencies of FCgammaRIIIa-158 were as follows V/V (32%); V/F (49%); F/F (19%). Those of the FCgammaRIIa-131 polymorphism were H/H (44%), H/R (48%), R/R (8%). Bone disease extension was not associated with FcgammaR polymorphisms. The achievement of partial response or better at first two cycles was not significantly influenced by FCgammaR polymorphisms. With a median follow up of 24 months, PFS at 18 months for patients treated with dara was 68.1%. There were no significant differences in patients carrying FCgammaRIIIa-158 (respectively V/V (n=24) 66.7%, V/F (n=35) 68.6%, F/F (n=13) 69.2%, p=0.72) or FCgammaRIIa-131 polymorphisms (respectively HH (n=32) 71.9%, HR (n=35) 65.7% and RR (n=5) 60%). Among patients carrying FCgammaRIIa-131-HH treated with a dara-based regimen (N=32) or a no-dara-containing regimen (N=16) there was no significant difference in 18-months PFS based on treatment received (71.9 vs 75%, p=0.98).

Conclusions. Taken together our results confirm that daratumumab early efficacy is independent of the FCgammaR polymorphisms. Also myeloma bone disease seems to be independent from FCgammaR polymorphisms. However, since de-sialylated IgGs binding to FcγRs with strong affinity have substantially high stimulatory effects on both murine and human osteoclasts, more data are needed to match the quality of monoclonal component before to exclude the contribution of FCgammaR polymorphisms to bone disease onset in multiple myeloma.

P107

ABSTRACT NOT PUBLISHABLE

P108

ROLE OF THE COMBINATION OF FDG PET PLUS WHOLE BODY MRI FOR STAGING NEWLY DIAGNOSED AND RELAPSED/REFRACTORY MULTIPLE MYELOMA. A PROSPECTIVE TRIAL

C. Cerchione, D. Nappi, M. Marchesini, D. Cangini, S. Ronconi, M. Ceccolini, G. Feliciani, A. Prochowski, C. Matuozzo, F. Mammoli, F. Frabetti, G. Paganelli, F. Matteucci, C. Pallotti, E. Scarpi, C. Pazzi, D. Barone, A. Romeo, G. Simonetti, G. Musuraca, G. Martinelli, A. Rossi

Hematology Unit, Istituto Romagnolo per lo Studio dei Tumori "Dino Amadori" - IRST IRCCS, Italy

Introduction. 18F-fluorodeoxyglucose (FDG) PET with CT (FDG-PET/CT) and magnetic resonance imaging (MRI) are both imaging diagnostic tools adopted in diagnosis and/or response assessment in multiple myeloma (MM). As 2016 IMWG criteria state that detection of bone lesions (myeloma defining events) is essential for diagnosis of MM (especially when CT is negative) and/or for ruling out them in patients with high risk smoldering MM (HR-SMM) and a PET/CT is one of the techniques essential for detecting the presence of bone disease in the diagnosis of MM. MR is the major diagnostic tool for identifying extra- or para-skeletal manifestations and complications, namely pathological fractures and spinal cord compression, as well as diagnostic tool for MM when > 1 lytic lesion is detected. The integration of FDG-PET/CT and WB-MRI in the diagnosis of MM may result in higher accuracy to detect bone lesion compared to them alone. This could be translated into better outcomes if early detection of myeloma defining events leads to earlier induction or re-induction treatments.

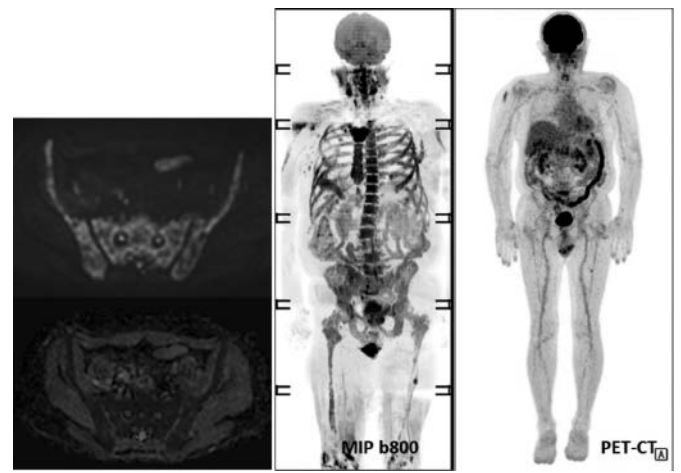


Figure 1.

Methods. In our Institution, from January 2021 to January 2023, we performed a prospective trial enrolling 73 consecutive newly diagnosed and relapsed/refractory MM (median age 63 years - range 85-35), according to IMWG, in which WB-MRI was performed according to MY-RADS criteria in combination with FDG PET/CT. 31/73 (42%) had a newly diagnosed MM, 25/73 (34%) were in follow-up after autologous stem cell transplantation and 17/73 (23%) patients were affected by relapsed/refractory MM. Subsequently, in 2 cases WB-MRI were aborted and not diagnostic so patients were excluded from the final analysis.

Results. In these 71 patients 52/71 (73%) cases of concordance of WB-MRI and 18F PET-CT, 18/71 (25%) cases of discordance. In this group 15/18 (83%) cases FDG-PET/CT was negative and WB-

MRI showed positive findings according to MYRADS criteria (5 micronodular pattern, 9 diffuse pattern e 1 focal pattern) (Figure 1 Newly diagnosed MM – diffuse pattern in WB-MRI, PET negativity), in 3/18 (17%) FDG-PET/CT was positive for focal lesions and WB-MRI was negative. IMWG criteria showed concordance with WB-MRI data in 16/18 (89%), in 2/18 (11%) case of follow-up after autologous stem cell transplantation PET-CT showed a relapsed focal lesion while WB-MRI was negative. Accuracy of WB-MRI was 69/71 (97%), whilst PET-CT was 55/71 (77%). These results are in agreement with the literature data about the ability of WB-MRI to depict diffuse and micronodular pattern of bone marrow infiltration.

Conclusions. Our preliminary results support a potential complementary role of WB-MRI and FDG PET/CT findings, on the management of patients with MM at both diagnosis and relapse. To date, there is no wide availability of WB-MRI because in concerning about costs and technical issues, but data are consistent with its possible future leading role in MM diagnostic work-up.

P109

ROLE OF THE COMBINATION OF FDG PET PLUS WHOLE BODY MRI FOR STAGING PATIENTS IN HIGH RISK SMOLDERING MYELOMA| A PROSPECTIVE TRIAL

C. Cerchione, D. Nappi, M. Marchesini, D. Cangini, S. Ronconi, M. Ceccolini, G. Feliciani, A. Prochowski, C. Matuozzo, F. Mammoli, F. Frabetti, G. Paganelli, F. Matteucci, C. Pallotti, E. Scarpi, C. Pazzi, D. Barone, A. Romeo, G. Simonetti, G. Musuraca, G. Martinelli, A. Rossi

Hematology Unit, Istituto Romagnolo per lo Studio dei Tumori “Dino Amadori” - IRST IRCCS, Italy

Introduction. According to IMWG criteria, Smoldering Multiple Myeloma (SMM) is an asymptomatic stage characterized by M-spike < 3 g/dl serum and/or bone marrow plasma cells infiltration 10-59% in absence of myeloma-defining events and organ damage. In SMM setting, it is really important to differentiate high risk SMM (HR-SMM), in which treatment could be available thanks to clinical trials. Recent evidences show the need to include in diagnostic criteria also Free light chains ratio and advanced imaging, mandatory to differentiate SMM from MM, and to better clarify the risk of progression integrating also cytogenetic and FISH. It is really important to clarify in SMM setting the best imaging in order to improve the discrimination between high risk SMM and MM. In our Institution we are currently conducting a prospective multicenter trial, based on integrated new generation imaging (PET/CT + Whole body MRI), aiming to improve patients' staging and to define its prognostic implications.

Methods. From January 2021 to January 2023, we performed a prospective trial enrolling 26 consecutive newly diagnosed high risk SMM, according to IMWG, in which WB-MRI was performed according to MY-RADS criteria in combination with FDG PET-CT (median age 56; range 36-85).

Results. Interim analysis of the comparison between WB-MRI and FDG PET-CT, showed a discordance between the two imaging modalities in 4/26 (15%) cases. In particular, in 3/26 (12%) cases WB-MRI showed bone lesions that have lead to symptomatic MM diagnosis according to IMWG criteria, while PET-CT was negative. In one case, PET-CT showed a diffuse uptake, not diagnostic for MM, while WB-MRI was negative. WB-MRI showed a 100% of accuracy in detecting SMM and MM. Therefore, WB-MRI has lead to a modification of the prognosis and treatment approach (observation in SMM vs treatment in symptomatic MM) in 3/26 patients (11%) [i]. e. Figure 1, with DWI of C2 lesion). Furthermore, in 5/23 (22%) cases of confirmed SMM WB-MRI showed a slight diffuse alteration pattern of bone marrow without any overt lytic bone lesion,

which could be a potential prognostic evidence.

Conclusions. Our preliminary results support a fundamental role of WB-MRI in combination with FDG PET/CT in the staging of patients with newly diagnosed high risk SMM, which could modify prognosis and treatment approach, improving the differentiation with symptomatic MM. In particular, combination of WB-MRI plus FDG PET/CT could be more accurate in the detection of bone lesions (myeloma defining events) than FDG PET/CT alone, being able to anticipate symptomatic MM diagnosis and consequently its treatment. Moreover, a diffuse pattern of marrow involvement could be detected in some HR-SMM patients without any overt lytic lesions! it is questionable if this group of patients is associated with a rapid progression in lytic lesions and so in symptomatic MM diagnosis. Prospective data on evolution of these patients are pending.

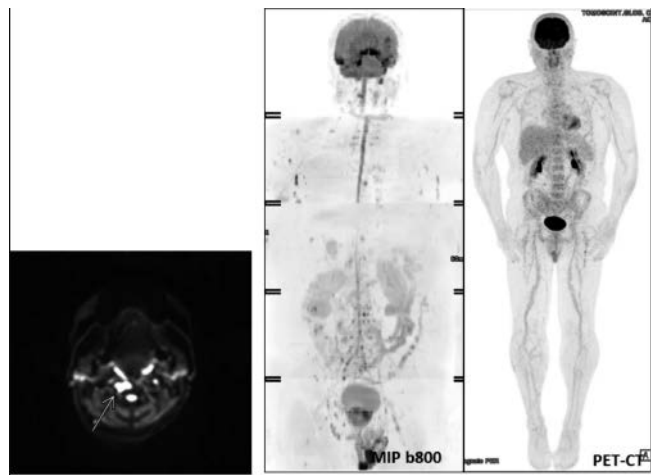


Figure 1.

P110

ABSTRACT NOT PUBLISHABLE

P111

MANAGEMENT OF OCTOGENARIAN AND FRAIL PATIENTS WITH NEWLY DIAGNOSED MULTIPLE MYELOMA, A REAL-WORLD STUDY

S. Gambarà, A. Poletti, O. La Greca, A. Cuneo*, M. Sessa*
*equally Contributed

Azienda Ospedaliero-Universitaria di Ferrara, Arcispedale Sant'Anna, Italy

Introduction. Multiple Myeloma (MM) predominantly affects the aged population. The management of elderly and frail patient is a therapeutic challenge, necessitating a balance between treatment efficacy and tolerability.

Methods. This real-world study analyzed a cohort of octogenarian patients, with newly diagnosed MM between January 2015 to August 2023. ECOG performance status, Frailty score by International Myeloma Working Group (IMWG), and Charlson Comorbidity Index (CCI) were used for patient stratification.

Results. Twenty patients with a median age of 82 years (range 80-85) were included in this analysis. The median ECOG at diagnosis was 1 (20% ECOG 0, 50% ECOG 1, 15% ECOG 2, 15% ECOG 3). All patients were classified as frail based on the IMWG Frailty Score. The median CCI was 5, indicating moderate comorbidities. High risk

cytogenetic lesions were found in 8/20 patients (40%). Treatment was initiated in 16 of the 20 patients (80%) with 12 patients (75%) receiving a 2-drug combination as first-line regimen and 4 patients (25%) receiving a 3-drug combination. Overall response rate was 56%. Median treatment duration was 19.4 months (range 7 days-31.5 months). Treatment was discontinued in 7/16 patients (44%) due to 2 infective events, 1 grade 3 neutropenia, 2 cases of deterioration of general conditions, 1 progressive disease, and 1 patient lost to follow-up. The median overall survival (OS) was 60.1 months. Patients treated with a 3-drug combination showed a median survival of 60.1 months, higher than patients treated with a 2-drug combination who showed a median survival of 14.1 months ($p=0.07$). Frailty and comorbidity did not show a significant correlation with survival outcomes. Renal insufficiency and anemia at baseline were found in 35% of the patients each, and had an impact on survival, with $p=0.046$ and $p=0.139$, respectively. Patients achieving at least a partial response to treatment had significantly better survival outcome ($p=0.002$). No significant correlation emerged between cytogenetic lesions and OS.

Conclusions. Our study reveals that patients over 80 years with MM are predominantly frail and have moderate to severe comorbidities. Overall, treatment retention was acceptable in the study population. Treatment with triple-drug regimens offered superior survival benefits, although statistical significance was not achieved. Renal function at diagnosis, as well as treatment response, emerged as important predictors for survival. Our data underscore the importance of accurate assessment of patient conditions and preexisting comorbidities to optimize the treatment regimen and improve survival in this population of elderly and frail patients. We are collecting data on a larger multicenter series and the updated results will be presented at the symposium.

Stem Cell Transplantation

P112

T-CELLS SUBSETS COUNTING BY DIGITAL PCR QUANTIFICATION OF EPIGENOTYPE MODIFICATIONS | A PILOT STUDY

G. Lia^{1,2}, M. Ferrante^{1,2}, A. Melis^{1,2}, A. Cargnino^{1,2}, A.M. Civita^{1,2}, I. Dogliotti^{1,2}, M. Borriero^{1,2}, G. Gabrielli^{1,2}, D. Drandi^{1,2}, S. Ferrero^{1,2}, B. Bruno^{1,2}, L. Giaccone^{1,2}

¹Divisione di Ematologia, AOU Città della Salute e della Scienza e Università di Torino; ²Dipartimento di Biotecnologie Molecolari e Scienze per la Salute, Università di Torino, Italy

Introduction. Flow cytometry immunophenotyping of leukocytes is an indispensable tool for the research and clinic which requires fresh and well-preserved blood samples to be performed. This requirement represents a potential limit, especially in the research setting. To cope with this problem, we developed a droplet digital polymerase chain reaction (ddPCR) assay for epigenotype analysis and counting of human naïve and memory CD4+ T-cells subsets by using genomic (gDNA) stocked materials.

Methods. gDNA was extracted by commercial kit from Peripheral Blood Mononuclear Cells (PBMC) and sorted CD4+ and CD8+ T-cells from 2 healthy subjects and 13 patients undergoing allogeneic Hematopoietic Stem Cell Transplant. Nearly 1.2 μg gDNA (range min-max 0.5-1.2 μg) was bisulfite converted (Qiagen) in 20 μl of reaction. Specific primers for differential methylation (DM) of CpG in FoxoP1, CD4, and RPP30 promoter genes were designed. Primer's optimization and probes concentration and annealing temperature were set up by RQ-PCR (ABI Prism 7900HT) using completely methylated and unmethylated human DNA template (Qiagen). Multiplex ddPCR, for CD4 and FOXOP1 methylated (HEX) and Unmethylated (FAM) targets, was performed using the QX200 Droplet Digital PCR system (Bio-Rad Laboratories). ddPCR for unmethylated RPP30 (HEX) was used as control for bisulfite efficiency. Multicolour Flow-cytometry studies (MCF) were performed by 4 to 6-colour combinations with the following monoclonal antibodies directed against CD4, CD3, CD8, CD62L, CD27, FoxP3, CD45R0, CD56, CD25, CD19; CD14 PE, CD16. Correlation between MFC and ddPCR-quantification was evaluated by Pearson's and Spearman's analysis. All reported P-values were estimated by the two-sided exact method and performed using STATA 15.1 (Stata Corp LP) and SPSS Statistics 28.0.1.0 (IBM SPSS Statistics).

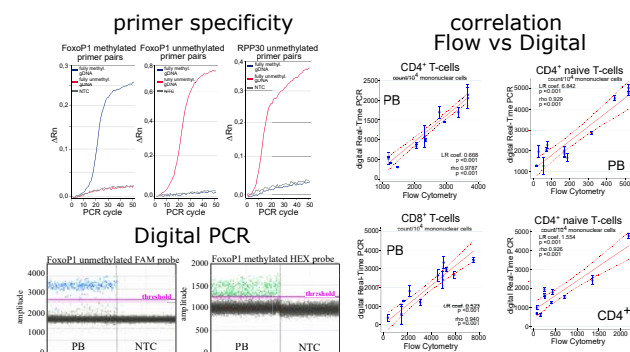


Figure 1.

Results. PCR conditions were tested on converted gDNA purified from PBMC and sorted CD4+ T cells and CD8+ T cells (Figure 1). The amplification efficiency of gene promoters for unmethylated and methylated CpG, respectively, was 0.39-0.42 for CD4; and 0.44-0.62 for FoxoP1 gene. As expected, amplification efficiency was very high (>0.95) for the control gene (RPP30). High level of correlation between MCF and ddPCR was observed in CD4+, CD8+ and naïve CD4+ T-cells (Figure 2). Pearson (rho p) and Spearman (rho s) correlation coefficient were very close to 1 (rho p and rho s, p respectively). CD4-T cells in PB (0.979-0.920 p<0.001); CD4-T cells in sorted CD4 (0.903-0.961 p<0.001); CD8-T cells in PB (0.940-0.942 p<0.001); CD8-T cells in sorted CD8 (0.884-0.839 p<0.001); naïve CD4 T-cells in PB (0.929-0.703 p≤ 0.007); naïve CD4 T-cells in sorted CD4 (0.926-0.797 p<0.001).

Conclusions. This approach has the potential to allow immunophenotyping on stored samples, which might be helpful in retrospective research studies but also in clinical setting, such as in resource-limited regions where logistical challenges pose significant obstacles.

during the entire pre- and post-HSCT hospitalisation period. At the same time, a correlation was hypothesised between the presence and state of the newly identified clones and post-HSCT immune phenomena such as T repertoire reconstitution and the onset of GVHD and GVL, in which donor alloreactive T lymphocytes are the main players. To support this hypothesis, the MRD data were supported by post-HSCT chimerism on a separate CD3+ lineage analysis.

Conclusions. This case report has allowed a cross-application of NGS technology to immunogenetics, which is emerging as a powerful and promising tool that will be able to clarify many aspects of the immunology of HSC transplantation in the future.

P113

ANALYSIS OF THE T-CELL RECEPTOR IMMUNE REPERTOIRE IN A PATIENT WITH T-CELL ACUTE LYMPHOBLASTIC LEUKAEMIA UNDERGOING ALLOGENEIC HAEMATOPOIETIC STEM CELL TRANSPLANTATION

A. Scarpa¹, E. Borotti¹, D. Ferrarese¹, S. Guidotti¹, V. Scaglia¹, A. Schiro¹, A. Rossi¹, D. Vallisa²

¹UOC Biologia dei trapianti, Ospedale "G. da Saliceto", AUSL, Piacenza; ²UOC Ematologia e CTMO, Ospedale "G. da Saliceto", AUSL, Piacenza, Italy

Introduction. Analysis of immunoglobulin and T-cell receptor (TCR) gene rearrangements by next-generation sequencing (NGS) is emerging as a highly sensitive tool for monitoring minimal residual disease in lymphoproliferative neoplasms. Its application found an interesting response in the monitoring of minimal residual disease (MRD) in a patient with T-type lymphoblastic leukaemia.

Methods. The patient underwent allogeneic haematopoietic stem cell transplantation (HSCT) in a TBI (12 Gray) + cyclophosphamide (120 mg/kg) conditioning regimen from a 10/10 unrelated donor with a permissive HLA-DPB1 mismatch. Patient and donor HLA typing was performed by NGS, including assessment of HLA-DRB3/4/5, DPA1 and DQA1 locus compatibility.

Results. MRD assessment confirmed complete remission prior to HSCT and sustained post-HSCT negativity for the TCRbeta marker identified at baseline. Analysis revealed the increasing and measurable presence of two new TCRbeta clones compared to the previous +30 days post-transplant assessment. The neoplastic origin of these two clones and the consequent development of secondary leukaemia, although possible, was immediately ruled out in the clinic. Based on current knowledge and available bioinformatic tools, several hypotheses were formulated regarding the possible reactive origin of two new clones. Using the IMGT database, we were able to identify complementarity determining regions (CDRs) The CDR3 region, responsible for the recognition and interaction with different antigenic peptides presented by MHC molecules, and the CDR1 and CDR2 regions, crucial for the interaction between the TCR and the MHC complex. The study of the CDR3 region can highlight the affinity of the TCR receptor towards infectious agents or the reactive origin of the T clone, determined by hypersensitivity to some drugs, mediated by the presence of HLA susceptibility alleles shared between donor and recipient. This first hypothesis was evaluated on the basis of the pharmacological treatment administered to the patient

Immunotherapy and Cell Therapy

P114

THE RELEASE OF ATP BY CHEMOTHERAPY-TREATED ACUTE MYELOID LEUKEMIA CELLS PROMOTES IMMUNOSUPPRESSION BY INDUCING IL-10-PRODUCING T REGULATORY CELLS VIA TOLEROGENTIC DENDRITIC CELLS

D. Ocadlikova¹, S. Sangaletti², P. Portararo², E. Adinolfi³, E. De Marchi³, A. Pegoraro³, E. Orioli³, M. Cavo^{1,4}, A. Curti⁴

¹Dipartimento di Medicina Specialistica, Diagnostica e Sperimentale, Università di Bologna; ²Fondazione IRCCS, Istituto Nazionale dei Tumori, Milano; ³Dipartimento di Scienze Mediche, Università degli Studi di Ferrara; ⁴IRCCS Azienda Ospedaliero-Universitaria di Bologna, Istituto di Ematologia "Seràgnoli", Bologna, Italy

Introduction. Some chemotherapeutic agents can induce modifications in dying tumor cells, which lead to immune system activation [immunogenic cell death). However, chemotherapy is also responsible for inducing immune tolerance. We previously demonstrated that, after binding to its most important purinergic receptor, P2X7R, chemotherapy-induced release of ATP from dying acute myeloid leukemia (AML) cells drives dendritic cells (DCs) to upregulate indoleamine 2,3-dioxygenase 1 (IDO1), which in turn induces T regulatory cells (Tregs). Our preliminary data indicated that suppressive Tregs are induced by IDO1⁺CD11c^{high} DCs and are associated with check point inhibitory receptors and ATP ectonucleotidases, such as CD39 and CD73, expression on both DCs and Tregs in a P2X7R-dependent manner. In the present work, we further investigated in a mouse AML model the mechanisms underlying ATP-driven Tregs induction after chemotherapy.

Methods. Wild-type and P2X7R KO BALB/c mice were injected with WEHI-3B AML cells. Cytarabine was administered at 9 and 11 days post AML cell injection. At sacrifice, tumors were analyzed for infiltrating T lymphocytes by flow cytometry and single-cell RNA-sequencing was used to better characterize Tregs transcriptomic profile.

Results. IL-10-producing Tregs were significantly increased after chemotherapy treatment and their frequency was higher in mice showing a reduced response to cytarabine. Of note, the enrichment in IL10⁺ Tregs was not observed in P2X7 KO model, suggesting that IL-10 production was dependent on the ATP release and subsequent catabolism. In line, CD39 and CD73 ATP ectonucleotidases were expressed on IL-10⁺ but not on IL-10⁻ Tregs. Moreover, the expression of both ectonucleotidases was associated with inhibitory immune check point receptors expression. In particular, the co-expression of CD39 and PD-1 or CD73 and ICOS was significantly increased on IL-10-producing Tregs after cytarabine treatment. The transcriptomic profile analysis of Tregs confirmed activation of genes associated with regulatory T-cell functions.

Conclusions. Our data suggest that IL10⁺ Treg-mediated immunosuppression could be established in mice escaping cytarabine treatment and that the induction of these cells could rely on ATP release by chemotherapy-treated AML cells and its subsequent catabolism. These data have implications for the full exploitation of immunogenic potential of chemotherapy effects on immune microenvironment and may help design clinical studies that combine chemotherapy with drugs targeting the ATP pathway.

P115

ABSTRACT NOT PUBLISHABLE

P116

UMG1 IS AN EFFECTIVE TARGET FOR REDIRECTED T-CELL CYTOTOXICITY IN CHRONIC LYMPHOCYTIC LEUKEMIA (CLL)

D. Caracciolo, N. Polerà, S. Signorelli, G. Juli, M. Cirillo, R. Infelise, C. Lamanna, C. Riillo, P. Tagliaferri, P. Tassone

Department of Experimental and Clinical Medicine, Magna Graecia University, Campus Salvatore Venuta, Italy

Introduction. B-cell chronic lymphocytic leukemia (B-CLL), a hematologic malignancy of mature clonal B-lymphocytes, is the most prevalent type of leukemia in Western countries. Targeted therapies, such as Bruton tyrosine kinase (BTK) and BCL-2 inhibitors have revolutionized the treatment landscape and have become the new standard of care of CLL treatment. However, the prognosis of "double refractory" patients, is still poor and, to date, limited therapeutic options are available. In this context, therapies that optimize immune function such as Bispecific T-Cell Engager (BTCE), a new class of off-the-shelf therapeutics able to recruit and trigger the T-cell toxicity against cancer cells, have the potential to overcome this clinical unmet need. We previously demonstrated potent *in vitro* and *in vivo* antitumor activity of a BTCE (UMG1/CD3ε-BTCE) directed to a novel CD43 epitope, named UMG1, highly expressed by T-cell Acute Lymphoblastic Leukemia (T-ALL) cells (Caracciolo *et al.*, JITC 2021), but not present in normal tissue except thymocytes and a small portion of T lymphocytes (<5%). Here we evaluated the expression of UMG1 and *in vitro* efficacy of UMG1/CD3ε-BTCE in B-CLL cells.

Methods. UMG1 expression was assessed by Flow Cytometry (FC) on primary cells from B-CLL patients (CD5⁺/CD19⁺). Target cells were co-cultured with healthy donor derived- peripheral blood mononuclear cells (PBMCs) labeled with viable marker in the presence of UMG1/CD3ε-BTCE or vehicle (1X PBS). T-cell cytotoxicity was evaluated by FC as 7-AAD⁺/target cells (%). Functional assays on effector cells were performed by FC analysis of T-cell activation surface markers CD69, CD25, or CD107a and IFN-γ, perforin, granzyme B and TNF-α [intracellular staining).

Results. By analyzing a set of treatment naïve primary B-CLL samples, we found that 10 out of 30 tested samples (33%) were positive for UMG1 and, among these, 13% of cases strongly expressed the epitope with more than 80% positive B-CLL cells. Interestingly, cytogenetic analysis of UMG1 positive samples reported the amplification of chromosome 12 at K-RAS, ATF1 and CDK-4 genes, suggesting a potential role of these aberrations in driving UMG1 expression. Furthermore, in a patient with pleural effusion at the diagnosis, UMG1 expression was higher in malignant pleural B-cells than in peripheral blood, indicating a potential implication of UMG1 in neoplastic B-cell migration. Next, primary B-CLL cells were cultured in the presence PBMCs from healthy donors and treated with increasing concentrations of UMG1/CD3ε-BTCE or vehicle for 72h. We observed a dose-dependent T cell-mediated cytotoxicity and release of inflammatory cytokines, which in turn led to the lysis of UMG1-positive cells but not in UMG1-negative cells.

Conclusion. Overall, UMG1 epitope is selectively expressed by a fraction of B-CLL and, therefore, UMG1-BTCE provides a novel therapeutic option as "precision oncology" approach for UMG1-positive B-CLL patients.

P117**A CASE OF RETINOPATHY AFTER CAR-T THERAPY**

A. Soravia¹, V. Simeon¹, F. Menchini², G. Di Renzo¹, F. Di Bin², J. Olivieri¹, M.L. Battista¹, G. Facchin¹, P. Lanzetta², R. Fanin¹, F. Patriarca¹

¹Department of Medicine, Hematology and Stem Cell Transplant, University of Udine; ²Department of Medicine, Ophthalmology, University of Udine, Italy

Introduction. Ocular adverse events after CAR-T cells therapy have been rarely reported and have mostly included viral infections reactivation and acute retinal necrosis. Herein, we report a case of CAR-T cell-induced eye complication leading to Acute Macular Neuroretinopathy, a rare retinal microvascular disorder.

Methods. A 64-year-old woman was diagnosed in 2021 with stage IV MCL. She received R-CHOP/R-DHAOx chemotherapy achieving CR, followed by consolidation with ASCT. Three months later, she experienced abdominal relapse that progressed during ibrutinib with bone involvement. The patient was referred to receive CAR-T cells therapy with brexucbtogene autoleucel after 1 R-BAC cycle of bridging therapy. At admission visual ability, EEG and brain MRI showed no abnormalities. Following lymphodepleting chemotherapy, CAR-T cells were administered ($0.4-2 \times 10^8$ cells/kg). The patient developed high fever ($\geq 40^\circ\text{C}$) on day 1 diagnosed as grade 1 CRS, treated on day 3 with 2 tocilizumab doses and on day 5 with dexamethasone with rapid clinical response. On day 6 she was diagnosed with grade 1 ICANS. On day 9 she experienced confusion, vertigo, slow mental processing and ocular symptoms (floaters and initial vision loss). EEG and brain MRI were normal. Anakinra was initiated on day 9 at 400 mg daily, tapered from day 12 and discontinued on day 16; dexamethasone was discontinued on day 39. Complete ocular examination, optical coherence tomography (OCT), fundus photography and fluorescein angiography were performed. OCT showed bilateral abnormal hyperreflective plaque-like lesion in retinal layers in the macular region consistent with Acute Macular Neuroretinopathy (fig. 1. 1). On day 21 the patient experienced further vision loss and scotomas, followed by a progressive improvement since day 22. To last assessment (day 60) visual acuity returned to normal in the left eye (20/20) and remained reduced in the right eye (20/25) with persistence of mild temporal paracentral scotoma. Final OCT revealed retinal abnormalities improvement (Figures 1 and 2).

IP10 and IL15 were high, while neurofilament light chain (NF-L) were normal. All cytokines showed the similar trend with a peak on day 7 and then a second elevation on day 21. NF-L levels increased later starting from day 11 with a peak on day 21 concurrently with the major visual loss.

Conclusions. This case report suggests that eye symptoms in patients with ICANS after CAR-T should be evaluated by the ophthalmologist to rule out rare retinal abnormalities. The occurrence of neuroretinopathy in parallel with CAR-T and cytokine expansions and the symptoms regression with anakinra indicates a pathogenesis similar to other well known neurological complications after CAR-T.

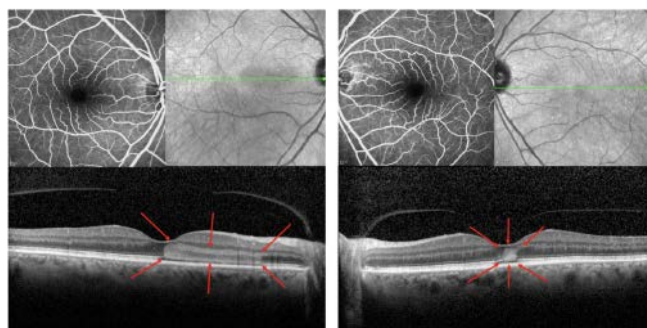
P118**ABSTRACT NOT PUBLISHABLE**

Figure 1.1 Fluorescein Angiography, Fundus Photography and Optical Coherence Tomography (OCT). OCT detects retinal abnormalities on symptoms onset (red marks).

Figure 1.2 Fluorescein Angiography, Fundus Photography and Optical Coherence Tomography (OCT). OCT detects retinal abnormalities improvement from day 22 (red marks).

Figure 1.

Results. CAR-T cell expansion started on day 7 (126/uL) and had 2 peaks on day 10 (200.73/uL) and on day 21 (95/uL), that occurred at the beginning of eye symptoms and at the time of the major visual loss, respectively. Among inflammatory cytokines, baseline IL2R α ,

Benign Hematology (Red Cell Disease Thrombosis and Hemostasis)

P119

HB MONZA. A NOVEL EXTENSIVE HBB DUPLICATION WITH PRESERVED - SUBUNIT INTERACTION AND UNSTABLE HEMOGLOBIN PHENOTYPE

I. Civettini^{1,2*}, P. Corti^{5*}, A. Zappaterra^{1,2}, A. Messina³, A. Aroldi², A. Biondi^{1,5}, F. Cavalca², V. Crippa¹, F. Crosti⁴, G.M. Ferrari⁵, F. Malighetti¹, L. Mologni¹, A. Piperno⁴, D. Ramazzotti¹, C. Scollo³, A. Zamboni⁶, F. Rossi³, C. Gambacorti-Passerini^{1,2}

*Contributed equally

¹Department of Medicine and Surgery, University of Milano-Bicocca; ²Hematology Department, Fondazione IRCCS San Gerardo dei Tintori; ³Transfusion Medicine, Fondazione IRCCS San Gerardo dei Tintori; ⁴Genetic Medicine, Fondazione IRCCS San Gerardo dei Tintori; ⁵Pediatrics, Fondazione IRCCS San Gerardo dei Tintori; ⁶Department of Chemical and Geological Science, Modena and Reggio Emilia University, Italy

Introduction. Unstable hemoglobins are variants with structural abnormalities associated with premature dissociation of heme from the globin chain. While most reported HBB variants involve changes in single of few bases, those surpassing 20 bp are rare and induce a B-Thalassemia (B-Thal). We report a family where four out of six members carry a novel mutation in the HBB gene, leading to a 23 amino acid in-frame duplication that we named Hb Monza. Despite the length of this duplication, the clinical and laboratory manifestation were consistent with an unstable variant of Hb, rather than with B-Thal phenotype.

Study design. This study endeavors to elucidate the clinical presentation of Hb Monza and to characterize its structure, evaluating the proteomic structure through 3D modeling.

Clinical Findings. During the 6-year follow-up, all the affected family members presented signs of mild chronic hemolysis. Each presented at least one acute and severe hemolytic crisis [until Hb 5.2 g/dL] triggered by infection, except the mother. HPLC revealed the presence of an anomalous hemoglobin fraction in all the affected family members. Conversely, HPLC for the remaining family members results within the expected normal range. Sequencing of HBB demonstrated an in-frame duplication of 69 bases corresponding to 23 amino acids located in exon 2 (c. 176_244dup); this was present in all patients exhibiting the abnormal fraction at HPLC. A functional validation of Hb Monza utilizing the isopropanol test confirmed the unstable nature of the variant. While long HBB mutations (>20 bp) are very rare and linked with a B-Thalassemia phenotype, Hb Monza presents as an unstable hemoglobin phenotype that is usually linked to single of few bases mutations. To understand this anomaly, a 3D model of Hb Monza was built.

3D modeling of the novel variant. The position and disordered folding of the insertion was demonstrated using SWISS-MODEL. The crystal structure of deoxy human hemoglobin (PDB 1A3N) was utilized as a template for the model generation, which was subsequently refined using the Maestro Suite (Schrodinger). The 3D-model analysis showed that the duplication is situated amidst helix E and F of hemoglobin chains; the binding of the heme group remains unaffected and the coordination of the heme group with His residues of both the E and F helix is preserved. The 23-aminoacid insertion causes a significant elongation of the EF turn, which protrudes out the wild-type conformation. The tertiary structure of the Hb β chain is scarcely affected, with a slight 2.8 Å shift of the A helix; consequently, Hb quaternary structure is also not perturbed.

Conclusions. In conclusion, our data indicate that long gene duplications can still preserve critical α - β interaction but ending in an unstable hemoglobin phenotype. Remarkably, this phenotype does not necessarily imply alterations to the key His residues typically associated with unstable hemoglobins.

P120

IRON RELEASE FROM MYELOID CELLS ENSURES THE HOMEOSTASIS OF THE HEMATOPOIETIC SYSTEM AND PREVENTS ANEMIA

L. Crisafulli^{1,2}, M. Correnti³, E. Gammella³, E. Palagano^{1,4}, C. Sobacchi^{1,2}, G. Cairo³, F. Ficara^{1,2}, S. Recalcati³

¹IRCCS Humanitas Research Hospital; ²Milan Unit, CNR-Istituto di Ricerca Genetica e Biomedica; ³University of Milan; ⁴Present CNR-Institute of Biosciences and Bioresources, Italy

Introduction. Iron is required for key physiological processes, such as oxygen transport, energy production, cell proliferation. Body iron homeostasis is primarily regulated by the erythroferrone (ERFE)-hepcidin-ferroportin (FPN) axis, which acts especially on duodenal cells and macrophages (MF) involved in iron recycling from red blood cell (RBC) breakdown. We recently showed that MF iron release is not only important at systemic levels, but can also play a role locally in neighboring proliferating cells such as in the context of skin wound healing. We asked whether this is true also in the hematopoietic system. Iron export from erythroblastic islands MF (EIM) or from other bone marrow (BM)-resident MF such as those belonging to the HSC niche, could represent promptly available local sources of iron for hematopoietic progenitors and precursors. Mild anemia was detected in three-weeks old mice with Fpn deletion in the myeloid lineage, but disappeared in young adult animals. In this study, we dissected the long-term impact of iron release from myeloid cells to hematopoietic stem cells, progenitors and precursors including erythroblasts.

Methods. Mice with LysM-Cre-dependent loss of Fpn in myeloid-cells (Fpn conditional-knockout or Fpn-cKO) and their littermate controls were aged at least until six months to analyze blood, serum, BM, liver and spleen through hemocytometer, flow cytometry, ELISA and histology.

Results. Blood analysis revealed that aged Fpn-cKO were anemic and microcytic. In line with anemia, serum iron levels were lower in Fpn-cKO mice compared to WT littermates; iron accumulated in the liver macrophages. Fpn-cKO mice also displayed thrombocytosis, in accordance with the preferential megakaryocytic commitment of megakaryocytic-erythroid progenitors in mouse models of iron deficiency. Spleen histology revealed the presence of extramedullary hematopoiesis, while BM was cytopenic. The reduction in BM cell number was mostly accounted for by reduced erythroblasts, suggesting that it was the cell population more affected by the lack of iron delivered by myeloid cells. Of note, in Fpn-cKO mice TfR1 expression was higher than in WT in virtually all the BM subpopulation analyzed, starting from hematopoietic stem cells, but more prominent along red cell development. Last, the expression of ERFE was increased in Fpn-cKO mice compared to WT.

Conclusions. Targeted Fpn deletion in myeloid cells results in the occurrence of anemia with aging, which in turn leads to multiple defects in the hematopoietic system. Compensatory mechanisms such as extramedullary hematopoiesis, increased expression of ERFE and up-regulation of TfR1 are not sufficient to fully overcome anemia. The prevalence of anemia in the elderly is an increasing public health problem, but it remains largely unexplained. A better understanding of all players involved in erythropoiesis is of crucial importance.

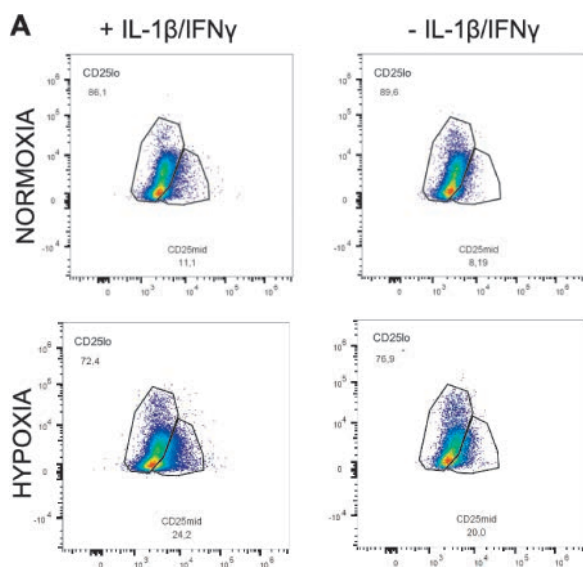
P121

EXPLORING THE IMPACT OF PRO-INFLAMMATORY CYTOKINES AND HYPOXIA ON TREG PHENOTYPE, DIFFERENTIATION, AND IMPLICATIONS IN APLASTIC ANAEMIA PATHOGENESIS

C. Tentori¹, F. Mohamed², E. Riva¹, S. Kordasti²¹Humanitas Research Hospital; ²King's College London

Background. T regulatory cells (Tregs) have emerged as pivotal orchestrators of immune homeostasis. Among these, two subsets were identified with mass cytometry by Kordasti et al (2016), the "naïve-like" CD45RA⁺ TregA and the CD95+CCR4⁺ TregB. Idiopathic aplastic anemia (AA) is an immune-mediated form of bone marrow failure. Its pathological features include elevated levels of the pro-inflammatory cytokines, notably IFN- γ and IL-1 β , in an hypoxic environment like the bone marrow. Tregs appear to be implicated in mitigating this syndrome, although their contribution to disease pathogenesis remains unidentified.

The present study aims to decipher Treg phenotype and function in the context of inflammation and hypoxia.



CD25mid frequency frequencies pre and post pro-inflammatory cytokines and hypoxia.

Figure 1.

Methods. Peripheral blood mononuclear cells (PBMCs) were isolated from the whole blood of six healthy donors. Fluorescence-assisted cell sorting (FACS) was performed to separate CD3+CD4+CD25⁺ FOXP3⁺ Treg cells from CD3+CD4+CD25lo CD127⁺ T effector cells (NonTregs). Tregs and NonTregs were cocultured at a 1/10 ratio and were left untreated or treated with pro-inflammatory cytokines IFN- γ and IL-1 β , both at a concentration of

10 ng/mL, for 96 hours. Cells were incubated in normoxia (oxygen at 20%) or experimental hypoxia (oxygen at 0.1%) and then analysed by flow cytometry to assess marker expression resulting from different environmental conditions.

Results. While there wasn't a significant overall change in Treg frequencies, there was a notable phenotypic shift from TregA to TregB, marked by a significant reduction in CD45RA expression. Upon cytometry analysis into the CD3+CD4+CD25loCD127+ Non-Tregs population, a novel population with low CD127 and higher CD25 expression (CD25 mid) was observed. All CD25mid cells expressed FOXP3. This new population appeared to originate from NonTregs and adopt a 'Tregs immune signature' in response to cytokine treatment and hypoxia. A stability assay was performed and indicated that the CD25mid population remained stable under normoxic conditions. Detailed analysis of the CD25mid subset demonstrated a significant decrease in CD127 and CD95 marker expression. Reduced CD127 expression is associated with immune activation and T cell depletion. The reduced programmed cell death leads to the accumulation of autoreactive T lymphocytes and impairs clearance of cytotoxic T cells, leading to the pronounced tissue destruction typical of AA, through persistent inflammatory responses and excessive antigen presentation.

Conclusion. Currently there's a paucity of predictive markers for conditions like AA. Deep phenotyping has the potential to shed light on immune signatures that accurately recognise AA and predict therapy response. The emergence and stability of the CD25mid subset could hold promise as a prognostic immune marker for AA patients. As it suppresses CD127 and CD95 expression, individuals with higher proportions of this subset might display heightened resistance to immunosuppressive interventions.

P122

CK1 KINASE FUNCTION IN B-LYMPHOPOIESIS

L. Quotti Tubi^{1,2}, A. Arjomand^{1,2}, A. Casellato^{1,2}, P. Macaccaro^{1,2}, K. Gianesin^{1,2}, G. Semenzato², L. Trentin¹, S. Manni^{1,2}, F. Piazza^{1,2}

¹Department of Medicine, Division of Hematology, University of Padova; ²Laboratory of Normal and Malignant Hematopoiesis and Pathobiology of Myeloma and Lymphoma, Veneto Institute of Molecular Medicine (VIMM).

Introduction. Casein Kinase 1 (CK1) is a highly-conserved monomeric serine/threonine kinase, which regulates membrane biology, signal transduction, transcription, translation, DNA damage response. Recently, CK1 α has been implicated in the biology of diffuse large B cell lymphomas. However, despite CK1 α regulates processes associated to normal and malignant blood cell development, its expression and function during hemato-lymphopoiesis are not known. We aimed to verify if CK1 α is involved in B-lymphopoiesis by using a conditional loss of function mouse model in the B-cell lineage.

Methods. Mice were generated employing a Cre/loxP system with the Cre recombinase under the control of the Mb1 early B specific promoter. FACS analysis was used to evaluate B cell differentiation, viability (AnnexinV), cell cycle (BrdU) and surface Igs. To determine IgG1 and IgG3 production, total cells from spleens were treated for 72 hours with LPS alone or with IL4. The same treatments or short exposure (5-10 minutes) to anti IgM were performed on total B cells, which were purified in negative from the spleens to evaluate the activation of signaling pathways and the expression of key factors by WB analysis.

Results. CK1 α KO mice exhibited splenic hypoplasia, with concomitant loss of mature B220⁺ CD19⁺ B-cells and increase of granulocytes/monocytes both in the spleen and the bone marrow (BM).

Moreover, B cells from KO mice presented reduction in IgD and IgM expression and increased apoptosis. This impairment started from the BM B precursors! KO mice lack pro and pre-B cells, instead heterozygous (het) mice displayed a reduction of these two populations compared to controls. Cell cycle analysis showed comparable results in pro/pre fraction of both KO and het mice compared to controls. Instead, pro and pre-B cells of het mice showed reduction in cells in S and G2/M phases. Since CK1 α KO B cells did not develop beyond the pre/pro-B stage, experiments were then focused on het mice. FACS analysis showed depletion of both transitional (T1 and T2) and of follicular B cells but expansion of marginal zone B cells. *In vitro* stimulation of total splenocytes with LPS and IL4 did not highlight differences in IgG1 or IgG3 production. At the molecular level, purified splenic B cells from het animals showed a reduction in basal expression of BCL10 and incomplete activation of P65 (S536) and AKT (S473) compared to controls. Short stimulation of B cells with anti-IgM indicated in het samples an impaired activation of ERK (T202/Y204) and AKT (S473). Next, we observed a decreased phosphorylation in IKK α/β (S176/180) and ERK after exposure to LPS and IL4.

Conclusions. We provide strong evidence of a central role for CK1 α in controlling B-cell development from the early stages to more mature steps. Further phenotypic, functional and molecular analysis are ongoing to unveil CK1 α role in the germinal center reaction, in Ig class switch as well as the process of somatic hypermutation.

P123

PRELIMINARY ANALYSIS OF ERYTHROPOIESIS AND IRON METABOLISM MARKERS IN β -THALASSEMIA PATIENTS UNDER TREATED WITH LUSPATERCEPT

S. Comit \grave{a} ¹, A.G. Grassi¹, N. Tesio¹, A. Piolatto¹, P. Falco¹, H. Kalaraiasan¹, A. Manca², J. Mula², A. Palermi², C. Gaglioti², A. Brusco,¹ A. D'avolio², G.B. Ferrero¹, A. Roetto¹

¹Department of Clinical and Biological Sciences, University of Turin; ²Department of Medical Sciences, University of Turin, Italy

Introduction. β -thalassemia (beta-thal), is a very common hematological disease due to mutations in the gene that codifies for haemoglobin beta chain (HBB) and induces chronic anemia and iron overload complications. Luspatercept, a novel erythroid maturation agent, has shown promising results in treating β -thal, but its biological mechanisms and impact on iron metabolism remain unclear. A cross-sectional observational study was set up to better characterize the response to Luspatercept in β -thal patients by evaluating biochemical markers of erythropoiesis and iron metabolism in both Non Transfusion Dependent (NTDT) and Transfusion Dependent (TDT) beta-thal patients treated with common care (CC, blood transfusions and iron chelating therapy, as needed) and CC plus Luspatercept. This preliminary biochemical analysis reports the results on the he cytokine erythropoietin (Epo), that plays a crucial stimulant for erythropoiesis, the experimental biomarker of ineffective erythropoiesis GDF15, and on the main systemic iron availability regulator Heparidin, measured in all the subjects' serum.

Methods. Among the 51 subjects participating at the research, β -thal trait carriers and healthy volunteers served as controls. NTDT and TDT subjects were selected among the patients followed up at San Luigi Gonzaga University Hospital Hemoglobinopathies Center. β -thalassemia carriers were selected among parents of TDT patients and were determined to be carriers based on the results of whole blood and hemoglobin electrophoresis. The healthy subjects' control group included individuals who did not have a history of transfusion, did not show any signs of hemolytic anemia, and did not have a

chronic disease. Red and white blood cells, circulating erythrocytes, plasma and serum hawere isolated from Pperipheral blood mononuclear cells (PBMC) of all the subjects enrolled in the study

Results. Serological assessments evidenced that baseline erythropoietin (Epo) and GDF15 levels were considerably higher in TDT (p=0.004; p=0.043) and NTDT (p0.001; p=0.012) patients treated with Luspatercept compared to CC patients. Baseline Heparidin levels in Luspatercept-treated NTDT patients were substantially higher than in CC-treated NTDT patients (p=0.029), although the baseline heparidin-to-ferritin ratio was significantly lower (p=0.014). Furthermore, heparidin levels in NTDT patients were considerably lower (p=0.040) seven days following Luspatercept therapy compared to baseline.

Conclusions. These serological data show that Luspatercept may operate on erythropoietin-dependent erythroid proliferation, generating higher erythropoietic stress, as seen by raised GDF15 levels, and may lower heparidin as a result of increased erythropoiesis. They strengthen the hypothesis that erythropoietic and iron metabolism pathways are deeply involved in patient's response to Luspatercept and spur to further characterize the main molecular players involved in this response.

Susceptibility and Pathogenesis of Hematologic Malignancies

P124

IMBALANCE OF THE GUT MICROBIOME IN MYELOID NEOPLASMS AND ITS CORRELATION WITH CLINICAL AND GENOMIC FEATURES

A. Campagna², T. Portlock¹, F. Viviani², M. Zampini², F. Ficara^{2,6}, L. Crisafulli^{2,6}, M. Ubezio², A. Russo², G. Todisco², E. Torre³, E. Saba², R. Antunes Dos Reis³, M. Uhlen¹, C.N. Harrison⁴, S. Kordasti⁵, M.G. Della Porta², S. Shoaie⁵

¹Science for Life Laboratory, Royal Institute of Technology (KTH); ²IRCCS Humanitas Research Hospital; ³Comprehensive Cancer Centre, King's College London; ⁴Guy's and St. Thomas' NHS Foundation Trust; ⁵King's College London; ⁶Milan Unit CNR-Istituto di Ricerca Genetica e Biomedica, Italy

Introduction. Increasing evidence suggests the role of gut microbiome on carcinogenesis and therapy response. Here, we analyzed gut microbial species and function in patients with acute myeloid leukemia (AML), myelodysplastic neoplasms (MDS) and myeloproliferative neoplasms (MPN).

Methods. Fecal samples were collected from 337 patients with MDS, MPN and AML at Humanitas Research Hospital, Milan. Extracted DNA samples were sequenced (Illumina Novaseq 6000) and quality-trimmed data mapped against Integrated Gut Catalog using METEOR pipeline. Human contaminant sequences were removed, and gene count tables were normalized according to the FPKM strategy using MOMR normFreqRPKM function.

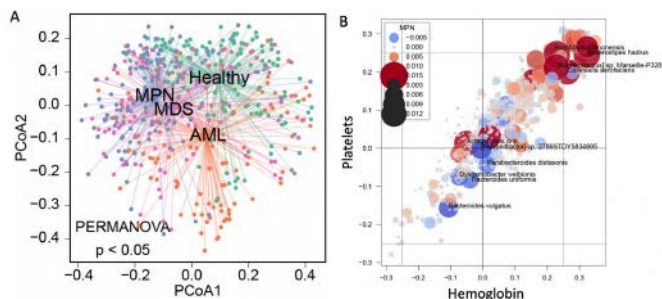


Figure 1.

Results. Overall 138 AML, 93 MPN and 106 MDS patients were included. We observed lower richness and diversity in AML compared to MDS or MPN. Principal Coordinates Analysis revealed significant differences in gut microbiomes between disease groups (PERMANOVA $R^2=7.38$, $p<0.001$) (Figure 1A). AML and MDS shared 7 depleted species, including 3 MetaGenomic Species for *F. prausnitzii*. Random forest classification modelling discriminated AML, MDS and MPN patients (AUCROC=0.91, 0.89, 0.85, MDS, AML, MPN respectively), with primary distinctions associated with increased levels of pro-inflammatory species. We further explored mutation-specific microbiome signatures using Shannon diversity; JAK2 mutated MPN had greater diversity than MDS or AML ($\log_2(\text{MPN}/\text{AML})=0.28$, $p=7.7e-12$, $\log_2(\text{MPN}/\text{MDS})=0.12$, $p=1.3e-9$); MDS with SF3B1 mutation differ significantly from those with TP53 mutation ($\log_2(\text{SF3B1}/\text{TP53})=0.23$, $p=0.03$). Correlation analysis with blood indices in AML and MDS showed that two depleted signature, butyrate-producing species like *F. prausnitzii*,

correlated positively with platelets (Plt) ($\rho=0.17$, $q=0.001$) and haemoglobin (H[b]) ($\rho=0.23$, $q=1.7e-5$) while enriched species such as *Erysipiclostridium ramosum* had a negative correlation with Hb ($\rho=-0.23$, $q=1.26e-5$) and Plt ($\rho=-0.17$, $q=0.002$). The pattern was reversed in MPN, with depleted species such as *Flavonifractor plautii* negatively correlated with Hb ($\rho=-0.15$, $p=0.004$) and Plt ($\rho=-0.19$, $q=0.4e-3$) (Figure 1B). We then compared microbiome signatures at diagnosis and relapse in 94 MDS/AML treated with hypomethylating agents; samples collected at relapse showed significantly reduced taxonomic abundances ($p<0.001$). Finally, evaluating the incidence of infections in 133 MDS/AML receiving disease-modifying treatment, we found that patients who developed a severe infection had a reduced taxonomic abundance of the gut microbiome (assessed at diagnosis) compared to the others ($p<0.001$).

Conclusion. Our study reveals striking correlations between the gut microbiome and the clinical and genetic features of AML, MDS and MPN. Further investigation of the complex interplay between the gut microbiome, genetic mutations and clinical features in these diseases could potentially lead to the development of microbiome-targeted therapies.

P125

NEXT GENERATION SEQUENCING (NGS) DETECTS POSSIBLE GERMLINE VARIANTS IN MYELOID NEOPLASMS

E. Ronda¹, E. Borotti¹, E. Follini², L. Pochintesta², G. Roti³, D. Vallisa², A. Rossi¹

¹UOC Biologia dei trapianti diagnostica molecolare e manipolazione cellule staminali emopoietiche AUSL di Piacenza; ²UOC Ematologia AUSL di Piacenza; ³Dipartimento di Medicina e Chirurgia Università di Parma, UOC Ematologia e CTMO, Italy

Introduction. The assessment of hereditary predisposition to hematopoietic neoplasms has become more common in clinical practice. Many genes responsible for these conditions are frequently subject to somatic mutations in sporadic hematological diseases, and they are regularly screened at the time of onset. Therefore, recognizing a germline condition based on the results of a somatic test is the initial step in appropriately managing these patients.

Methods. We present the results of NGS analysis using the Ampliseq Myeloid Panel-Illumina, conducted from January 2021 to September 2023 at our center. Our cohort comprises 279 patients (age 20-88 years, median 70y) diagnosed with acute myeloid leukemia (AML 75), myelodysplastic syndrome (MDS 138), and chronic myeloproliferative neoplasms (MPN 66), who were recruited by the Hematology Units of A. U. S. L. Piacenza and A. O. U. Parma. Panel sequencing with average coverage between 1560X and 12500X (mean 7700X). Variant interpretation was carried out in accordance with the guidelines provided by the American College of Medical Genetics and Genomics/Association for Molecular Pathology.

Results. Among the analyzed patients, 91% of AML patients, 74% of MDS patients and 77% of MPN patients exhibited at least one somatic variant in the studied genes. *TET2*, *DNMT3A*, *SRSF2*, *JAK2*, *TP53*, *ASXL1*, *NPM1*, *STAG2*, *SF3B1*, *RUNX1*, *IDH2*[i] and *FLT3* genes were enriched in variants compared to other genes. Notably, 81 patients carried variants in genes associated with hereditary disorders, showing allele frequencies consistent with germline origin (ranging from 40-60% or 90%). The genes implicated, in order of prevalence, are as follows: *TET2*, *JAK2*, *RUNX1*, *TP53*, *CALR*, *NRAS*, *CEBPA*, *NF1*, *WT1*, *ETV6*, *KRAS*, *GATA2*, *RB1*, *CBL1*, *CSF3R*, *MPL1*, and *MYD88*. Particularly, variants detected in *TP53*, *RUNX1*, and *GATA2* were predominantly classified as class 4 and 5. Additionally, among these suspected germline variants, somatic hot spots were observed in variants within *KRAS* (five AML and MDS

patients), *NRAS* (three myelofibrosis and polycythemia vera patients), and *MPL* (one patient with myelofibrosis). It is worth mentioning that one class 5 variant in the *TP53* gene, along with two class 4 variants in *ETV6* and *NFI*, were confirmed in remission analyses as well with allele frequency like to heterozygosity, suggesting the possible germinal origin.

Conclusions. The clinical significance of variants in patients during remission is noteworthy, even when they haven't been confirmed in alternative tissue. Notably, there is a high incidence of variants within the *TET2* gene, suggesting that germline variants or their combination with somatic alterations could constitute complex predisposing factors for the development of myeloid neoplasms. This data serves as a proof-of-concept study, emphasizing that the management of patients at risk of hereditary myeloid malignancies is a significant challenge, beginning with the accurate reporting and interpretation of genetic variants.

Author Index

- Abbenante, M. 79
 Abeltino, M. 66
 Abrisqueta, P. 49
 Abruzzese, E. 40, 42
 Accorsi Buttini, E. 40, 43, 67, 68
 Adamo, F.M. 51
 Adès, L. 9
 Adinolfi, E. 116
 Agnelli, L. 20, 21, 44
 Agolini, E. 103
 Agostinelli, C. 3, 5, 37
 Agostini, A. 64
 Aguenouz, M. 108
 Aimo, A. 109
 Al Deeban, B. 50
 Albicocco Giovinati, L. 81
 Albiero, M. 48
 Aldridge, F. 56
 Aleo, E. 20
 Alesi, V. 103
 Alessandria, B. 36
 Aletti, F. 4
 Alfò, M. 82
 Alma, E. 99, 100
 Almasri, M. 10, 13, 35, 50
 Alviano, F. 3
 Amadori, S. 84
 Amato, C. 9, 69
 Amodio, N. 26
 Amoresano, A. 105
 Amorini, A.M. 61
 Andorno, A. 35
 Andresen, V. 30
 Angelini, D.F. 7, 32
 Angelini, S. 71
 Angelucci, E. 26
 Angotzi, F. 49, 100
 Annunziato, F. 33
 Ansuinelli, M. 18
 Antonioli, E. 28
 Antunes Dos Reis, R. 121
 Aparo, A. 97
 Aquilina, C. 29, 107, 108
 Aquino, S. 26, 106
 Arcaini, L. 37
 Arcaleni, R. 51
 Arcari, A. 13, 93, 95
 Arciprete, F. 40
 Arena, V. 34, 82
 Argentati, C. 47
 Argnani, L. 52
 Arienzo, F. 64
 Arjomand, A. 119
 Armando, F. 66
 Armenio, M. 23
 Armuzzi, S. 20, 21
 Arniani, S. 16, 19
 Aroldi, A. 118
 Arpinati, M. 86, 87
 Arshadi, A. 64
 Ascani, S. 97
 Asti, G. 11, 24, 25
 Atene, C.G. 52, 93
 Athanasiadou, A. 49
 Atharina Zoldan, K. 9
 Attardi, E. 31, 85
 Attucci, I. 28
 Atzeni, G. 86
 Audisio, E. 34, 79
 Awada, H. 31
 Bacchiarri, F. 28
 Badii, F. 41
 Bakaks, A. 100
 Baldini, L. 36
 Baldoni, S. 45, 46, 51, 63
 Balducci, S. 67
 Balduini, A. 40
 Baliakas, P. 49
 Ballerini, F. 13
 Balliu, M. 39, 40, 59
 Balzarotti, M. 13
 Bandinelli, S. 69
 Bandini, C. 28
 Bandini, L. 63, 74, 86, 87
 Banella, C. 75
 Baran-marszak, F. 49
 Baratè, C. 66, 71, 94
 Barbieri, M. 19, 110
 Barbui, T. 12, 62
 Bardelli, V. 15, 16, 19
 Bardini, M. 16
 Barilà, G. 53, 91, 92, 93
 Barone, D. 112, 113
 Barone, M. 86, 87
 Barosi, G. 62
 Bartalucc, N. 40
 Bartalucci, N. 39
 Basilico, C. 81
 Bassan, R. 18
 Bassi, L. 64
 Basso, M. 85
 Battista, M.L. 117
 Bazzoni, F. 53, 93
 Beacci, D. 19
 Becherini, P. 26, 27, 106
 Beghini, A. 81
 Beldinanzi, M. 18, 78
 Bellesi, S. 99, 100
 Bellia, M. 10, 50
 Bellini, M. 12
 Bellisario, F. 99, 100
 Bellomario, V. 78
 Bellotti, A. 26, 106
 Belotti, A. 110
 Beltrami, G. 34
 Bencini, S. 33
 Benedetti, E. 71, 94
 Benelli, R. 102
 Benevolo, G. 12
 Benjamin, R. 56
 Bergonzini, G. 88
 Berliner, M. 37
 Bermema, A. 44
 Bernabei, D. 52, 88, 93
 Bernardi, M. 9, 20, 29, 81
 Bernardi, S. 40, 43, 67, 68
 Berno, T. 98
 Berrocal, J.C. 9
 Bertesi, M. 39, 41, 60
 Bertuglia, G. 106
 Bertuzzi, C. 3
 Bestoso, E. 28, 111
 Bettelli, F. 52, 88
 Betti, S. 12
 Bezzi, D. 21
 Bianchi, B. 37
 Bianchi, E. 39, 41, 60
 Biancotti, R. 61
 Bicchieri, M. 11, 24, 25
 Bielli, P. 23
 Bigerna, B. 30, 47
 Binotto, G. 61
 Biondi, A. 16, 118
 Bittolo, T. 35, 36
 Boaro, M.P. 48
 Boccadoro, M. 106
 Bocchia, M. 18, 28, 34, 42, 66, 95, 104, 111
 Bocchicchio, M.T. 74
 Boccomini, C. 13
 Bochenkova, E. 68
 Bochicchio, M.T. 34, 79, 84
 Boga, C. 75
 Boldorini, R. 35
 Boldyreff, B. 48
 Bolis, M. 28
 Bolli, N. 11, 19, 22, 28, 58, 106, 110
 Bomben, R. 13, 35, 36
 Bonaldi, L. 49
 Bonati, A. 66
 Bonetto, G. 98
 Bonifacio, M. 12, 58, 66, 79
 Bono, C. 36, 66, 94
 Bonomini, S. 64
 Bonuomo, V. 23
 Bonvicini, C. 40
 Borlenghi, E. 18, 81
 Borotti, E. 57, 89, 90, 93, 95, 115, 121
 Borriero, M. 114
 Borsani, G. 43
 Borsellino, B. 31
 Borsi, E. 20, 21
 Bortoluzzi, S. 39, 49, 51, 53, 91
 Bosch, F. 49
 Botta, C. 29, 107, 108
 Botti, A. 107
 Bracco, E. 23
 Bracischi, A. 71
 Branca, A. 98
 Brando, B. 81
 Breccia, M. 40, 42
 Bresciani, P. 52, 88
 Brindisi, M. 59
 Broccoli, A. 52
 Bruna, R. 13, 35
 Brunak, S. 108

- Brunati, A.M. 94
 Brunetti, L. 19, 80
 Bruno, B. 36, 106, 110, 114
 Bruno, S. 55, 58, 67, 75
 Brunori, M. 101
 Bruscazzin, A. 35
 Brusco, A. 120
 Bruzzone, S. 26, 27
 Buccisano, F. 33, 82, 110
 Bucelli, C. 12
 Buda, G. 28, 71, 107, 109
 Bulian, P. 35
 Bullinger, L. 13
 Buratin, A. 49, 51, 53
 Burattin, A. 91
 Burroughs Garcia, J. 20, 21
 Buson, E. 53, 91, 92, 93
 Bussolati, O. 27
 Buzzatti, E. 85
- Caccamo, N. 29, 107, 108
 Cacciola, E. 12
 Cafarelli, C. 42
 Caflisch, A. 68
 Cagnetta, A. 106
 Caicci, F. 52
 Caira, M. 89
 Cairo, G. 118
 Cairolì, R. 81
 Calabresi, L. 40
 Calabretto, G. 51, 53, 91, 92, 93
 Calacci, C. 103
 Calandrelli, M. 101
 Caldarelli, N. 35, 44
 Calice, G. 102
 Caliendo, C. 90
 Califano, C. 34, 90
 Calomino, N. 104
 Caltabiano, R. 62
 Calvani, M. 75
 Cama, A. 45
 Camaioni, E. 71
 Camarda, G. 29
 Cambò, B. 15, 64
 Cambria, D. 105, 112
 Campagna, A. 11, 24, 25, 121
 Campana, F. 100
 Campelo, M.D. 11
 Candi, V. 28
 Candoni, A. 52, 79, 88
 Cangini, D. 84, 112, 113
 Cannizzaro, M.T. 112
 Canovas Nunes, S. 48
 Cantafio Gallo, M.E. 26
 Cantoni, A.M. 66
 Canzonieri, V. 35
 Caparello, M.C. 71
 Capasso, G. 91, 94, 100
 Capirossi, G. 17, 74
 Caponi, L. 107
 Caporale, R. 33
 Cappellini, A. 70
- Capria, S. 34
 Capurro, M. 46, 47
 Caracciolo, D. 116
 Caramella, M. 12
 Cardinali, D. 18, 78
 Cardinali, V. 73
 Carella, A.M. 110
 Carella, M. 64
 Cargnino, A. 114
 Caridi, M. 83
 Carioli, G. 12
 Carlet, M. 16
 Carli, G. 12
 Carlini, G. 24, 25
 Carniti, C. 35, 44
 Carobbio, A. 12
 Carollo, C. 88
 Caroni, F. 28, 111
 Caroprese, J. 33
 Carpi, F. 37
 Carrabba, M. 4
 Carrabba, M.G. 9, 34
 Carraro, M. 98
 Carraro, S. 99
 Carretta, C. 39, 41, 60
 Carrozzo, F. 75
 Carsana, E. 4
 Caruana, I. 45
 Casalini, I. 70
 Casarini, L. 41
 Cascavilla, N. 12
 Casellato, A. 119
 Cassano, R. 109
 Cassari, M. 69
 Castagnetti, F. 42, 67
 Castellani, G. 11, 24, 25
 Castellano, G. 11, 19
 Castellino, C. 13, 35
 Catalano, G. 32
 Catani, L. 52, 59, 86
 Catitti, G. 45
 Cattaneo, A. 11
 Cattaneo, C. 34, 79
 Cavalca, F. 118
 Cavallari, M. 79
 Cavallaro, A. 112
 Cavalleri, A. 40, 43, 67, 68
 Cavallini, C. 97
 Cavallo, F. 13
 Cavarretta, C.A. 49
 Cavo, M. 20, 21, 55, 58, 67, 70, 74, 86, 87, 116
 Cazzaniga, G. 16
 Cea, M. 26, 27, 106
 Ceccato, J. 98, 99
 Ceccolini, M. 84, 112, 113
 Cefalo, M.G. 85
 Cellini, A. 49, 100
 Cencini, E. 36, 104
 Ceneri, E. 70
 Centurioni, R. 36
 Cerchione, C. 84, 112, 113
 Cerrano, M. 34, 67
- Cerullo, V. 4
 Cesaro, B. 68
 Chamuleau, M. 103
 Chandra, N. 26
 Chapuis, N. 9
 Chatzikonstantinou, T. 49
 Chavez, J.C. 103
 Chedere, A. 26
 Chiappella, A. 35, 44
 Chiaramonte, R. 22
 Chiaretti, S. 18, 78, 79
 Chiarini, M. 110
 Chiarucci, M. 101
 Chignola, R. 97
 Chirumbolo, G. 86
 Chiu, M. 27
 Chiusolo, P. 58
 Ciarrocchi, A. 22, 28, 97, 110
 Ciaurro, V. 81
 Ciavarella, S. 37
 Ciceri, F. 9, 12, 19
 Ciciarello, M. 55
 Cidonio, G. 77
 Cilloni, D. 23, 77, 79
 Cimino, G. 83
 Cimminiello, M. 16
 Cinetto, F. 99
 Ciofini, S. 28, 95
 Ciolli, G. 33
 Ciotti, G. 85
 Cipriani, M. 31
 Cipriani, S. 72, 73, 76, 81, 83
 Cirillo, M. 116
 Cisneros, A. 78
 Civettini, I. 118
 Civita, A.M. 36, 114
 Cocco, L. 70
 Codeluppi, N. 89, 90
 Cola, M. 78
 Colaci, E. 52, 88
 Colasante, C. 39
 Colla, S. 32
 Colombatti, R. 48
 Colombo, F. 110
 Colombo, F.S. 48
 Coluccio, V. 88
 Colugnat, I. 41
 Comità, S. 120
 Consagra, A. 9, 69
 Consalvo, M.I. 33, 110
 Conte, B. 52, 88, 93
 Conte, L. 56
 Conti, C. 85
 Conticello, C. 108, 109, 112
 Coppola, P. 52
 Cordone, I. 110
 Corradi, A. 66
 Corradi, G. 45, 46, 55
 Corradini, G. 52, 88, 93
 Corradini, P. 13, 35, 44
 Correnti, M. 118
 Corsale, A.M. 29, 107, 108
 Cortellazzi, P. 89, 90

- Cortellino, S. 105
Corti, P. 118
Cosentino, C. 10, 13, 35, 50
Cotugno, F. 34
Craparotta, I. 28
Craviotto, L. 64
Crea, E. 85
Crippa, V. 118
Crisafulli, L. 48, 59, 118, 121
Cristiano, A. 23
Cristiano, G. 6, 70, 74, 86, 87
Cristinelli, C. 37
Crocioni, M. 19
Cross, N.C.P. 58
Crosti, F. 118
Crupi, F. 33
Crupi, R. 95
Cucci, R. 62, 63, 84
Cuneo, A. 49, 113
Cuoghi, A. 52, 88
Curti, A. 6, 34, 55, 70, 74, 86, 87, 116
Curti, N. 24, 25
Curto-Garcia, N. 42
- D'adda, M. 42
D'agnolo, M. 48
D'agostino, F. 96
D'agostino, M. 106
D'agostino, S. 102
D'alfonso, G. 42
D'alò, F. 99, 100
D'amico, S. 4, 11, 24, 25
D'auria, F. 102
D'avolio, A. 120
D'Innocenzo, S. 99, 100
Da Vià, M.C. 11, 19
Dall'olio, D. 11, 24, 25
Dall'olio, L. 11, 24, 25
Dalla Palma, B. 20, 21
DallaPalma, A.B. 27, 29
Damiani, D. 58
Danesin, N. 98
Daniele, A. 96
Dargenio, M. 16
Davies, A. 103
Davis, Z. 49
De Fabritiis, P. 79
De Falco, F. 51
De Giorgi, F. 71
De Haro, N. 78
De Magistris, C. 11, 19
De Marchi, E. 116
De Marinis, E. 32
De Matteis, G. 58
De Paoli, F. 37
De Pourcq, S.J.M. 9, 69, 70
De Propriis, M. 79
De Santis, S. 58, 67
De Simone, G. 48
De Stefano, A. 70
De Stefano, V. 12, 62
De Vito, R. 103
- Deambrogi, C. 35
Debbia, G. 52, 93
Defina, M. 16, 42
Defrancesco, I. 37
Dei Tos, A.P. 61
Del Bianco, P. 98
Del Boccio, P. 45
Del Buono, N. 37
Del Fabro, V. 108, 109, 112
Del Giudice, I. 13, 35, 36, 78
Del Giudice, M.L. 28, 107, 109
Del Monaco, V. 20
Del Papa, B. 51
Del Principe, M.I. 85
Dell'aquila, M. 64
Della Porta, M. 24, 25
Della Porta, M.G. 11, 31, 34, 59, 89, 121
Della Starza, I. 18, 36, 78, 79
Dello Sbarba, P. 66
Derus, N.R. 24, 25
Desantis, V. 21
Di Bin, F. 117
Di Buduo, C. 40
Di Camillo, B. 81
Di Chio, M.C. 34
Di Francesco, B. 45, 46
Di Ianni, M. 45, 46, 63
Di Liddo, R. 85
Di Micco, R. 4
Di Napoli, A. 5
Di Nolfo, F. 101
Di Raimondo, F. 26, 61, 62, 108, 105, 109, 112
Di Renzo, G. 117
Di Renzo, N. 36
Di Rocco, A. 13, 35
Di Simone, M. 29, 107, 108
Di Trani, M. 18, 78
Dicataldo, M. 86
Dickinson, M. 103
Dieli, F. 29, 107, 108
Diez Campelo, M. 9
Diez-campelo, M. 24, 25
Dillon, R. 13
Divona, M. 7, 32, 77, 82, 85
Divona, M.D. 84
Dodero, A. 35
Dogliotti, I. 114
Döhner, H. 13
Döhner, K. 13
Donati, B. 97
Dondolin, R. 10, 35, 50
Donnini, S. 72, 73, 76, 81, 83
Donofrio, G. 21, 29
Doriguzzi Breatta, E. 48
Dorillo, E. 51
Doubek, M. 49
Dragomir, A. 104
Drandi, D. 36, 114
Dulcamare, I. 105, 108
Duminuco, A. 42, 62
Dunn, R. 56
Durmaz, A. 31
Duschosal, M. 26, 106
- Eberini, I. 22
Eccher, A. 88
Edmin, M. 109
Eichhorst, B. 49
Elena, C. 58
Elia, L. 78
Emiliani, C. 47
Enderti, A. 39, 40
Endri, M. 17, 74
Enzo, E. 41
Erol, G. 47
Erratico, S. 22, 110
Errichiello, S. 58, 84
Espinet, B. 49
Esposito, A. 51
Esposito, F. 37
Esposito, L. 96
Evangelista, A. 13
- Fabbiani, L. 39
Fabbiano, G. 19, 22, 110
Fabbri, A. 104
Fabbricatore, C. 90
Fabi, B. 45, 46, 63
Fabiani, E. 23, 32, 63
Fabiano, V. 61
Fabris, S. 11, 19, 58
Facchetti, F. 30
Facchin, G. 117
Facco, M. 49, 51, 53, 91, 92, 93, 100
Facella, F. 71, 94
Fadini, G.P. 48
Faggiano, M.V. 103
Falco, P. 120
Falconi, G. 2, 23
Falini, B. 30, 46, 47, 73, 80, 84
Fanin, R. 58, 117
Fardella, E. 35
Farina, M. 40, 43, 67, 68
Fasano, L. 33
Fatica, A. 68
Favasuli, V.K. 110
Faz, P. 34
Fazi, F. 68, 77
Fazi, P. 63, 79, 84
Federico, M. 36
Feliciani, G. 112, 113
Fenau, P. 11, 24
Fenauz, P. 25
Fenoglio, D. 27
Feola, S. 4
Fernandez Rodriguez, G. 68
Ferrante, M. 36, 114
Ferrara, F. 18, 79
Ferrarese, D. 90, 115
Ferrari, A. 17, 66, 73, 74, 79, 84, 93
Ferrari, G.M. 118
Ferrarini, I. 13, 53, 92, 97
Ferraro, R.M. 67, 68
Ferreri, A.J.M. 103
Ferreri, C. 101
Ferrero, G.B. 120

- Ferrero, S. 13, 36, 114
 Ferretti, V.V. 37
 Ferrigno, J. 61
 Ferrucci, L. 69
 Fianchi, L. 5
 Ficara, F. 48, 59, 118, 121
 Filhol, O. 48
 Finazzi, M.C. 12
 Finelli, C. 70
 Finsinger, P. 89
 Fiori, S. 13
 Flinn, I.W. 103
 Foà, R. 18, 35, 49, 78
 Foca, F. 59
 Fogli, M. 70
 Follini, E. 89, 90, 121
 Follo, M.Y. 70
 Fong Ng, J. 27
 Fontenay, M. 9
 Fonzi, E. 17, 74
 Forghieri, F. 52, 88
 Forte, D. 52, 74, 86
 Frabetti, F. 59, 112, 113
 Fracchiolla, N. 79
 Fragliasso, V. 28, 97
 Franceschi, V. 21, 29
 Franceschini, M. 104
 Franciosa, M. 66
 Fraticelli, S. 37
 Fregnani, A. 48, 98
 Freilone, R. 34
 Frezzato, F. 49, 91, 94, 100
 Frigeni, M. 34
 Frusteri, C. 92
 Fulciniti, M. 27
 Fumagalli, M. 17, 74, 81
 Furlan, D. 37
 Furstenau, M. 49
 Fusco, S. 4
- Gabrielli, G. 114
 Gaffo, E. 39, 49, 51, 53
 Gagliardi, A. 80
 Gaglioti, C. 120
 Gaidano, F. 50
 Gaidano, G. 10, 13, 35
 Gaidano, V. 74
 Galasso, M. 53, 97
 Galieni, P. 28, 71
 Galimberti, S. 13, 17, 28, 36, 42, 66, 67, 71, 74, 94, 107, 109
 Gallingani, I. 98
 Gallo, A. 26
 Galossi, E. 2, 23
 Gambacorti-Passerini, C. 66, 118
 Gambara, S. 113
 Gambarelli, G. 97
 Gambino, S. 53, 97
 Gammella, E. 118
 Ganino, L. 26
 Gargano, G. 37
 Garibotto, M. 26
- Garofano, F. 29, 107, 108
 Garonzi, M. 20
 Garuffo, L. 40, 43, 67, 68
 Gasparini, V.R. 51, 53, 91, 92
 Gattei, V. 35, 36
 Gatti, A. 81
 Gelli, E. 26
 Genovese, E. 39, 41
 Genovese, S. 103
 Genovesi, D. 109
 Gentile, M. 26, 32
 Gentili, M. 46, 47
 Gentner, B. 9
 Genuardi, E. 36
 Geraci, C. 51
 Gesullo, F. 12, 58, 62
 Ghanej, J. 10, 50
 Ghelli Luserna Di Rorà, A. 17, 74, 75
 Gherli, A. 32
 Ghetti, M. 75, 84
 Ghia, P. 49
 Ghirardi, A. 12
 Giaccone, L. 34, 114
 Giacobbi, F. 52, 88, 93
 Giaimo, M. 15, 64
 Giallongo, C. 26, 61, 62, 105, 108
 Giallongo, S. 61, 62, 108
 Gianelli, U. 62
 Giancesin, K. 119
 Gianfaldoni, G. 33
 Giannandrea, D. 22
 Giannetti, K. 4
 Giannini, B. 17, 74
 Giannini, M.B. 84
 Giannone, S. 109
 Giannotta, C. 106
 Giansanti, A. 56
 Gigli, F. 79
 Giglio, F. 16, 17, 19, 74
 Gigliotta, E. 29, 107
 Gilioli, A. 52, 88
 Gilioli, D. 4
 Gini, G. 13
 Gionfriddo, I. 72, 73, 76, 81, 83
 Giordano, C. 64, 96
 Giordano, G. 59
 Giorgetti, G. 26, 27, 106
 Giorgis, M. 68
 Giugliano, E. 84
 Giugno, R. 97
 Giuliani, N. 20, 21, 27, 29
 Giusti, D. 52, 88
 Gjertsen, B.T. 30
 Glaß, B. 103
 Glogovitis, I. 39
 Gobbi, M. 47
 Gonella, F. 56
 González, T. 64
 Goodell, M. 80
 Gottardi, E. 84
 Gottardo, M. 85
 Gotti, M. 37
 Gozzetti, A. 28, 95, 104, 111
- Granada, I. 78
 Grassi, A.G. 120
 Grassi, S. 94
 Greco, R. 81
 Gregori, S. 4
 Grillo, G. 79, 81
 Grondelli, M.C. 24, 25
 Gualberti, G. 89
 Gualtieri, G. 99
 Guardalupi, F. 45, 46
 Guarini, A. 37
 Guarnera, L. 13
 Guerri, V. 94
 Guerrini, F. 36, 66, 94
 Guglielmelli, P. 12, 33, 39, 40, 41, 58, 59, 60, 62, 63
 Gugliotta, G. 42, 67
 Guidi, A. 20
 Guidotti, S. 90, 115
 Gulla, A. 108
 Gundry, M. 80
 Guolo, F. 26, 34, 106
 Gurnari, C. 2, 7, 13, 31, 85
 Gurrieri, C. 48, 98
- Haferlach, C. 49
 Haferlach, T. 11, 23, 24, 25
 Hajrullaj, H. 23
 Harrison, C. 42
 Harrison, C.N. 121
 Hernández-rivas, J.M. 13, 64
 Herrera, M. 108
 Hohaus, S. 13, 99, 100
 Hutter, S. 23
- Iacobucci, I. 2
 Iacovelli, C. 100
 Iaiza, A. 68
 Iannozzi, N.T. 20, 21, 27, 29
 Ielo, C. 40
 Ilariucci, F. 93
 Imovilli, A. 17, 74
 Infelise, R. 116
 Intermesoli, T. 42
 Irene Grifoni, F. 58
 Isidori, A. 101
 Isidori, R. 64
 Itri, F. 23, 77
 Iuliano, F. 42
 Iurlo, A. 12, 67
 Izzo, B. 58, 84
- Jacobson, C.A. 103
 Javadpoor, A. 77
 Jeremias, I. 16
 Jonnalagadda, S. 44
 Jottini, S. 66
 Juli, G. 116

- Kalaraiasan, H. 120
 Kalashnikova, O. 49
 Kanapari, A. 20, 21
 Kang, J. 103
 Kaplan, A. 103
 Kater, A. 49
 Kleidon, A. 56
 Klein, F. 16
 Kleissle, S. 72
 Kogila, S. 10, 50
 Kordasti, S. 11, 24, 25, 42, 69, 119, 121
 Kosmider, O. 9
 Krampera, M. 53, 58, 81, 97
 Kreuzer, K.A. 49
 Kubasch, A. 9
 Kubasch, A.S. 11, 24, 25
- L'abbate, A. 64
 La Barba, G. 63
 La Greca, O. 113
 La Sala, E. 13
 La Spina, E. 62, 105, 108
 La Starza, R. 15, 16, 19, 32
 Ladetto, M. 13, 36
 Ladiana, R. 99
 Ladisa, F. 26, 27, 106
 Lamanna, C. 116
 Lancellotti, C. 88
 Landi, S. 71
 Lanino, L. 11, 24, 25
 Lanuti, P. 45, 46
 Lanzetta, P. 117
 Lapietra, G. 78
 Larocca, A. 106
 Larocca, L.M. 100
 Latagliata, R. 23, 64
 Laurenzi, T. 22
 Lazic, T. 37
 Lazzarino, G. 61
 Lazzaroni, F. 11, 19
 Le Anh Luong, 56
 Ledda, L. 17, 74, 75
 Lehmann, S. 13
 Lema Fernandez, A.G. 16, 19
 Lemoli, R.M. 26, 27, 34, 79, 106
 Leonard, G. 52, 88, 93
 Leoncin, M. 16
 Leoni, A. 40, 43, 67, 68
 Lessi, F. 98
 Leutner, M. 35
 Li Volti, G. 61, 62, 108
 Lia, G. 114
 Libera, L. 37
 Liberati, A.M. 28
 Librale, F. 20, 21
 Liccardo, F. 77
 Lico, A. 34, 79
 Lindfors Rossi, E.L. 82
 Lionetti, M. 11, 19
 Liscano, E. 56
 Lisi, D. 96
 Lisignoli, G. 20
- Liso, A. 62
 Liturri, M. 59
 Ljevar, S. 35
 Lo Celso, C. 4
 Lo Schiavo, F. 17, 74
 Locatelli, F. 85
 Lolli, M. 68
 Lombardi, G. 66
 Lombardo, A. 28
 Lomi, M. 40
 Lonati, S. 11, 19
 Longetti, E. 46, 47
 Longhitano, L. 61, 62, 108
 Loscocco, F. 101
 Loscocco, G.G. 12
 Loseto, G. 37
 Losi, L. 39
 Lovato, E. 53, 92
 Lovato, O. 53, 97
 Lovisa, F. 98
 Lucchesi, A. 59
 Luciano, L. 42
 Lucioni, M. 37
 Luminari, S. 36
 Lunghi, F. 12
 Lunghi, M. 42, 79
 Lunghi, P. 66
 Lungu, O. 20, 21, 27, 29
 Luppi, M. 39, 41, 52, 60, 88, 93
- Macaccaro, P. 119
 Maccaferri, M. 39, 41, 52, 60, 88, 93
 Maccari, C. 33
 Maciejewski, J.P. 31
 Maeda, A. 11, 19
 Maffei, R. 52, 88, 93
 Maffeo, B. 23, 77
 Magagnotto, C. 58
 Maggioni, G. 11, 24, 25
 Magliano, G. 81
 Magni, M. 35, 44
 Mahmoud, A. 35
 Mai, A. 68
 Maiolo, E. 99, 100
 Malafronte, R. 99, 100
 Malagola, M. 40, 42, 43, 67, 68
 Malato, A. 42
 Malcovati, L. 1
 Malferà, G. 90
 Malgieri, S. 89
 Malighetti, F. 118
 Mallardo, M. 96
 Mallegni, F. 31, 85
 Mallia, S. 97
 Mallo, M. 78
 Maloney, D.G. 103
 Maltoni, F. 52
 Mamelì, M.G. 51
 Mammoli, F. 112, 113
 Manaresi, N. 20
 Manca, A. 120
 Mancini, M. 58, 67
- Mancini, V. 81
 Mancuso, K. 21
 Mancuso, S. 36
 Mandato, E. 48
 Manferdini, C. 20
 Manfredini, R. 39, 41, 60
 Mangolini, V. 40
 Manicardi, V. 28, 97
 Mannarella, C. 36
 Mannelli, F. 33, 58
 Manni, S. 48, 91, 93, 98, 99, 100, 119
 Mansueto, G. 102
 Manzoli, L. 70
 Manzotti, G. 28
 Marafioti, T. 30
 Marasca, R. 52, 88, 93
 Maravalle, D. 71
 Marchesini, M. 32, 84, 112, 113
 Marchetti, A. 19
 Marchica, V. 20, 21, 29
 Marconi, G. 34, 74, 79, 84
 Marcotulli, M. 77
 Marella, A. 11, 19
 Marietta, M. 88
 Marini, S. 23
 Marino, M.R. 79
 Marino, S. 109, 110
 Mariotti, B. 53, 93
 Maroto-martin, E. 27
 Marra, A. 30
 Marrassi, A. 75
 Marrasso, P. 3
 Marsili, G. 34, 82
 Martarelli, N. 46, 47
 Martella, M. 48
 Martelli, M. 35
 Martelli, M.P. 30, 46, 72, 73, 76, 81, 83
 Martello, M. 20, 21
 Martinelli, G. 17, 34, 59, 66, 74, 79, 84, 112, 113
 Martinelli, S. 41, 52, 88, 93
 Martines, A. 49
 Martino, G. 73, 83, 97
 Martino, S. 47
 Martinuzzi, C. 26, 27
 Martucci, L. 103
 Marzocchi, G. 20
 Masciarelli, S. 68, 77
 Masciulli, A. 12
 Masi, S. 110
 Massaia, M. 106
 Mastaglio, S. 16, 19
 Matarazzo, M. 78
 Matera, A. 11, 19
 Matis, S. 102
 Mattei, A. 84
 Mattei, D. 79
 Mattei, G. 75
 Mattei, M. 7
 Matteucci, F. 112, 113
 Mattioli, F. 71
 Mattioli, S. 71
 Mattiuz, G. 9, 69

- Matuozzo, C. 112, 113
 Maura, F. 106
 Maurillo, L. 82
 Mauro, F.R. 49
 Mavilia, F. 94
 Mazzacane, A. 37
 Mazzanti, G. 77
 Mazzerà, L. 66
 Mazzocchetti, G. 20, 21
 Mecca, M. 105
 Mecucci, C. 15, 16, 19, 32
 Meddi, E. 85
 Mehari Sium, A. 50
 Melis, A. 114
 Melle, F. 13, 35
 Menchini, F. 117
 Meraviglia, S. 29, 107, 108
 Mercadante, S. 110
 Mercalli, F. 35
 Merelli, I. 4
 Mereu, E. 28
 Merli, A. 13
 Merli, F. 13
 Merli, M. 37
 Merlo, R. 39
 Mesini, N. 52, 93
 Messerotti, A. 52, 88, 93
 Messina, A. 118
 Messina, M. 15, 18, 62, 63, 79, 84
 Metelli, M.R. 94
 Meunier, M. 9
 Mezzasoma, F. 73, 81
 Mianulli, A.M. 17, 74
 Miao, H. 103
 Micheletti, G. 75
 Micucci, G. 59
 Migliaccio, A.R. 40
 Mignani, L. 43
 Milano, F. 72, 73, 76, 81, 83
 Miller, C. 49
 Minetto, P. 34
 Minnella, G. 58
 Minotti, C. 34
 Mirabile, M. 41, 60
 Mirandola, P. 29
 Mohamed, F. 119
 Mohamed, S. 16
 Mohamedali, A. 56
 Moia, R. 10, 13, 35, 50
 Mologni, L. 118
 Molteni, A. 81
 Monaldi, C. 58, 67
 Mondelli, P. 37
 Montanaro, A. 15, 32
 Monti, E. 43
 Mora, B. 12, 37, 39, 41
 Moraca, A. 23, 77
 Morandini, P. 24, 25
 Morelli, F. 102
 Morelli, G. 58
 Morello, E. 40, 43, 67, 68
 Morena, F. 47
 Moretti, F. 31
 Moretti, L. 51
 Moron Dalla Tor, L. 15, 32
 Morschhauser, F. 103
 Morselli, M. 52, 88
 Morsia, E. 63
 Mosca, E. 11
 Motta, G. 3, 13, 35
 Mouawad, N. 91, 94, 100
 Mouhssine, S. 10, 35, 50
 Mozzo, V. 53
 Mula, J. 120
 Mullai, R. 58
 Munshi, N.C. 27
 Murineddu, M. 36
 Musolino, C. 12
 Mussolin, L. 98
 Musuraca, G. 13, 59, 84, 112, 113
 Mutti, S. 40, 43, 67, 68

 Nabergoj, M. 48
 Nabki, J. 50
 Nadarajah, N. 23
 Nahimana, A. 26, 27, 106
 Naldini, M.M. 9
 Nanni, C. 21
 Nanni, J. 6, 34, 55, 74, 79, 87
 Napolitano, M. 59
 Napolitano, R. 75
 Nappi, D. 84, 112, 113
 Nardelli, C. 16, 19
 Nardoza, A.M. 85
 Narimanfar, G. 52
 Nasillo, V. 52, 88, 93
 Naso, S. 16
 Nassi, L. 37
 Nasuto, M.I. 64
 Natoni, F. 64
 Nencioni, A. 26
 Neri, A. 19, 22, 26, 28, 97, 105, 110
 Neri, G. 37
 Nervi, C. 32
 Neuenschwander, M. 72, 76
 Neumann, B. 76
 Nexha, E. 85
 Nguyen-khac, F. 49
 Nigro, E. 96
 Nikitsenka, K. 88
 Nikolajeva, O. 103
 Noguera, N.I. 32
 Norata, M. 84
 Norfo, R. 39, 41, 60
 Novella, E. 88
 Novelli, A. 103
 Nucciarelli, D. 89

 Ocadlikova, D. 116
 Occhini, U. 28
 Olimpico, F. 75
 Oliva, S. 110
 Olivieri, A. 79
 Olivieri, J. 117

 Onorato, A. 23
 Opinto, G. 37
 Orioli, E. 116
 Orlando, C. 9
 Orlando, S. 84
 Orofino, G. 9
 Orsi, S. 49, 51, 91
 Orsucci, L. 35
 Oscier, D. 49
 Oteri, R. 108
 Ottaviani, E. 63, 74, 84, 86, 87
 Ottomano, A. 88
 Ottone, T. 2, 7, 32, 77, 82, 84, 85

 Pacelli, P. 28, 111
 Padiglioni, E. 72, 76, 81, 83
 Pagan, A. 90
 Paganelli, G. 112, 113
 Paganelli, M. 17, 74
 Pagano, L. 58
 Pagano, M.A. 94
 Pagliaro, L. 15, 32
 Paiva, B. 29
 Palagano, E. 118
 Palandri, F. 12
 Palazzolo, L. 22
 Palermi, A. 120
 Pallotti, C. 112, 113
 Palmieri, R. 33, 82
 Palumbo, G.A. 61, 62, 105, 108, 109, 112
 Palumbo, O. 64
 Paluzzi, M. 92
 Panagiotidis, P. 49
 Pancani, F. 33
 Pane, F. 12, 62, 84, 96
 Pantani, L. 20, 21
 Panuzzo, C. 23, 77
 Paolini, A. 52, 88, 93
 Paolini, S. 70
 Paolini, S. 70, 74
 Papayanidis, C. 16
 Papayannidis, C. 6, 17, 34, 58, 74, 79, 87
 Pappagallo, S.A. 37
 Paradiso, I.V. 33
 Parenti, S. 39, 41, 60
 Paris, F. 3
 Parisi, S. 70
 Parisi, S. 70, 74
 Park, S. 9
 Parrinello, N.L. 108, 109, 110
 Pascale, M. 2
 Pasciolla, C. 17, 19, 74
 Pasha, A. 75
 Pasquini, A. 33
 Passamonti, F. 11, 19, 39, 41, 62
 Passerini, L. 4
 Patriarca, A. 12, 42
 Patriarca, F. 117
 Patuelli, A. 86
 Paulli, M. 37
 Pavone, V. 13

- Pazzi, C. 112, 113
 Peccatori, J. 9
 Peccia, K. 95
 Pedrazzi, F. 39, 41, 60
 Pegoraro, A. 116
 Peli, A. 66
 Pepperkok, R. 76
 Perbellini, O. 53
 Perez, C. 29
 Pergolizzi, B. 23, 77
 Perriello, V. 30
 Perriello, V.M. 46, 47
 Perris, R. 66
 Perrotta, I. 26
 Peruzzi, B. 33
 Peruzzi, S. 80
 Pesavento, M. 98
 Pessina, C. 41
 Pessina, G. 64
 Petrucci, M.T. 35
 Pettine, L. 11, 19
 Pezzoni, V. 71
 Piacente, F. 26
 Pianigiani, G. 80
 Piazza, F. 13, 48, 98, 99, 100, 119
 Piazza, M. 99
 Picardi, M. 96
 Piccini, M. 16, 18, 19, 33
 Picciocchi, A. 85
 Pichino, S. 105
 Picciocchi, A. 13, 18, 31, 34, 42, 62, 63, 79, 82, 84
 Pieraccioli, M. 23
 Pieragostino, D. 45
 Pierangeli, S. 72, 73, 76, 81, 83
 Pierini, V. 16, 19
 Pietra, D. 58
 Pietrantuono, G. 102
 Pilato, F. 52, 88, 93
 Pileri, S. 13, 35
 Pileri, S.A. 37
 Pinto, A. 35
 Pinto, G. 105
 Pioggia, S. 11, 19
 Piolatto, A. 120
 Pioli, V. 52, 88, 93
 Piperno, A. 118
 Piro, A. 45
 Pistis, I. 20, 21
 Pitisci, A. 103
 Piva, R. 28
 Pizzi, M. 48, 61, 98, 100
 Pizzuti, V. 3
 Plano, F. 29
 Platzbecker, U. 9, 11, 13, 24, 25
 Plevova, K. 49
 Pochintesta, L. 89, 90, 121
 Poggi, A. 102
 Poggiaspalla, M. 59
 Polerà, N. 116
 Poletti, A. 20, 21, 113
 Polito, F. 108
 Polverelli, N. 40, 43, 67, 68
 Porretti, L. 110
 Portararo, P. 116
 Portlock, T. 121
 Poscente, M. 64
 Potenza, L. 39, 41, 52, 60, 88
 Pott, C. 36
 Pozzi, G. 29
 Pravato, S. 91
 Prezioso, L. 64
 Prochowski, A. 112, 113
 Procopio, S. 16
 Pruneri, G. 21
 Puccetti, L. 28
 Puccini, B. 13
 Puccio, N. 19, 22, 28, 97, 110
 Pugliese, N. 96
 Puiggros, A. 49
 Punta, M. 9
 Quadalti, C. 81
 Quaglia, F.M. 53, 97
 Quaini, F. 32
 Quinti, E. 33
 Quotti Tubi, L. 48, 98, 100, 119
 Raddi, M.G. 9, 69
 Radeghieri, A. 40
 Radici, V. 40, 43, 67, 68
 Ragaini, S. 36
 Raimondi, V. 20, 21, 27, 29
 Ramazzotti, D. 118
 Rambaldi, A. 12, 18, 79
 Rampazzo, E. 51, 53, 91, 92, 93
 Ranalli, P. 63
 Ranieri, R. 72, 76, 81, 83
 Ranucci, G. 85
 Rapezzi, D. 12
 Rasi, S. 10, 35, 50
 Raspadori, D. 28, 66, 111
 Ratti, S. 70
 Ravera, S. 26
 Re, A. 13, 35
 Re, F. 43
 Recalcati, S. 118
 Rege Cambrin, G. 42
 Restuccia, F. 56
 Ribera, J. 78
 Ribera, J.M. 78
 Riboni, R. 37
 Ricca, M. 66
 Ricci, F. 66, 71, 94
 Ricci, S. 20, 27
 Ricco, A. 12
 Rich, E.S. 103
 Rigamonti, A. 44
 Righi, S. 3
 Rigodanza, L. 9, 69
 Rigolin, G.M. 49
 Riillo, C. 116
 Rina, I. 71
 Rinaldi, A. 64
 Ripamonti, A. 66
 Riva, E. 11, 59, 119
 Riva, G. 52, 88, 93
 Riva, M. 81
 Rizzello, I. 20, 21
 Rizzo, E. 37
 Robustelli, V. 87
 Roccaro, A. 110
 Rocco, S. 77
 Roetto, A. 120
 Rogers, K.A. 49
 Romagnoli, S. 39, 40
 Romano, A. 56, 61, 62, 105, 107, 108, 109, 110, 112
 Romeo, A. 112, 113
 Rompietti, C. 51
 Roncaglia, E. 49, 53
 Roncati, L. 88
 Ronchetti, D. 19, 22, 28, 110
 Ronconi, S. 84, 112, 113
 Ronda, E. 57, 89, 90, 121
 Rondoni, M. 17, 34, 74
 Rontautoli, S. 39, 41, 60
 Rosamilio, R. 90
 Rosati, E. 51
 Rosellini, S. 34
 Rosseto, A. 47
 Rossetti, E. 66
 Rossi, A. 57, 89, 90, 93, 95, 112, 113, 115, 121
 Rossi, A. Russo 42
 Rossi, D. 35
 Rossi, E. 12
 Rossi, F. 118
 Rossi, F.G. 13, 35
 Rossi, G. 110
 Rossi, M. 3, 34
 Rossi, R. 46, 47
 Roti, G. 15, 32, 51, 64, 93, 121
 Rotili, D. 68
 Rotolo, C. 29
 Rotunno, G. 33, 63
 Rovatti, P.E. 9
 Rovida, E. 66
 Ruggeri, E. 91, 94, 100
 Ruggeri, L. 45, 46, 83
 Ruggieri, M. 28
 Rumi, E. 12
 Ruocco, V. 49
 Rupoli, S. 63
 Russell, N.H. 13
 Russo, A. 24, 25, 121
 Russo, D. 40, 42, 43, 67, 68
 Russo, F. 93
 Russo, S. 4, 103
 Rutella, S. 74
 Sa, I. 56
 Saba, E. 59, 121
 Sabattini, E. 3, 5, 37
 Sabino, M. 73, 81
 Sacchi, M.V. 13

- Saggin, L. 98
 Saglio, G. 84
 Sala, C. 11, 24, 25
 Salehi, M. 35
 Salutari, P. 16, 17, 74, 79
 Salvatorelli, L. 62
 Salves, C. 74
 Salvesi, C. 17
 Sammarelli, G. 20, 21, 64
 Sammartano, V. 28, 42
 Sannuri, P. 94
 Sangaletti, S. 116
 Sanguedolce, F. 97
 Sanna, A. 9
 Sansone, A. 101
 Santafè, E. 78
 Santagati, M. 107
 Santaolalla, A. 42
 Santini, V. 9, 11, 24, 25, 69
 Santo, I. 66, 71
 Santoni, A. 28
 Santoro, A. 4, 11, 24, 25, 63, 84
 Santoro, M. 29
 Saraci, E. 106, 110
 Sargentini, V. 85
 Sartor, C. 6, 58, 74, 87
 Sauta, E. 11, 24, 25, 97
 Savevski, V. 11, 24, 25
 Savi, A. 23, 31, 85
 Scaffidi, L. 12, 58
 Scaglia, V. 95, 115
 Scandura, G. 105, 108
 Scapinello, G. 98
 Scappini, B. 33
 Scard, S. 46
 Scarfò, L. 49
 Scarmozzino, F. 98
 Scarpa, A. 90, 93, 95, 96, 115
 Scarpi, E. 112, 113
 Scattoni, A. 37
 Schavgoulidze, A. 27
 Schena, A. 57
 Schiaffini, G. 100
 Schiavone, M.L. 48
 Schiro, A. 89, 90, 115
 Schoepf, B. 103
 Schupp, M. 103
 Scialolacci, S. 73
 Scialdone, A. 80
 Sciarra, R. 13, 37
 Scita, M. 20, 21, 27, 29
 Sciumè, M. 58
 Scollo, C. 118
 Scopetti, M. 11, 19
 Scuderi, E. 105
 Scuderi, G. 109
 Scupoli, M.T. 53, 66, 97
 Sebert, M. 9
 Secomandi, E. 10, 50
 Segreto, R. 64
 Semenzato, G. 48, 51, 53, 91, 92, 93, 99, 119
 Serafin, A. 49
 Serio, B. 34
 Serpico, S. 105
 Serra, M. 7
 Servilli, C. 74
 Sessa, F. 37
 Sessa, M. 113
 Severin, F. 91
 Sgambato, A. 105
 Shahani, S. 103
 Shekarkar Azgomi, M. 29, 107, 108
 Shoaie, S. 121
 Sica, S. 16
 Sicuranza, A. 28, 42, 66, 104, 111
 Signorelli, S. 116
 Signori, L. 33
 Sijoni, L. 71
 Silva Barcelos, E.C. 51
 Silvestri, S. 72, 73, 81
 Silvestrini, G. 7, 23, 31
 Silvestris, I. 19, 22, 110
 Simeon, V. 117
 Simeone, P. 45
 Simoncini, E. 32
 Simonetti, G. 17, 34, 59, 74, 75, 79, 84, 112, 113
 Simoni, M. 41
 Sini, D. 85
 Siragusa, S. 12, 29, 79, 107, 108
 Sobacchi, C. 48, 118
 Soddu, S. 79, 84
 Solé, F. 78
 Solimando, A. 21
 Solimando, A.G. 64
 Solli, V. 20, 21
 Soncini, D. 26, 27, 106
 Soravia, A. 117
 Sorcini, D. 30, 51, 73
 Sorgiovanni, I. 94
 Soscia, R. 35, 36, 78
 Soverini, S. 58, 63, 67
 Speciale, M. 29, 107, 108
 Sperduti, S. 41
 Sperotto, A. 85
 Spina, M. 35
 Spinello, Z. 48
 Spinozzi, G. 72, 73, 76, 81
 Sportoletti, P. 30, 51, 73
 Squarzoni, S. 55
 Staderini, M. 28
 Stamatopoulos, K. 49
 Starza, I. D. 35
 Statuto, T. 102
 Stefanucci, M.R. 81
 Stefoni, V. 35, 36
 Stella, A. 47, 51, 73
 Storlazzi, C.T. 64
 Storti, P. 20, 21, 27, 29
 Strazimiri, A. 58
 Strina, D. 48, 59
 Sureda, A. 103
 Surra, F. 56
 Susani, L. 59
 Tabanelli, V. 13, 37
 Tacchetti, P. 21
 Taccini, A.C. 67
 Tagliaferri, P. 116
 Tagliafico, E. 39, 41, 52, 60, 88, 93
 Taiana, E. 19, 22, 28, 110
 Talotta, D. 10
 Talotta, D. 13, 35, 50
 Tamagnini, I. 97
 Tameni, A. 97
 Tanasi, I. 58
 Tancredi, G. 94
 Tani, M. 13
 Tanturli, M. 69
 Tarantino, D. 39, 40
 Tarullo, M. 68
 Tassone, P. 116
 Taurisano, B. 20, 21
 Tausch, E. 49
 Tavella, T. 4
 Tavernari, L. 39, 41, 60
 Tedone, E. 34
 Tees, M. 103
 Tenedini, E. 41
 Tentori, C. 119
 Tentori, C.A. 11, 24, 25
 Teramo, A. 51, 53, 91, 92, 93
 Terol, M.J. 49
 Terracciano, M. 20
 Terragna, C. 20, 21, 110
 Terzi Di Bergamo, L. 35
 Tesio, N. 120
 Testoni, N. 20, 74, 87
 Thomas, I. 13
 Tiacci, E. 30, 46, 47
 Tibullo, D. 26, 61, 62, 105, 108
 Tini, V. 72, 76, 81
 Tini, V. 73
 Tiribelli, M. 58
 Tischler, C. 76
 Tisi, M.C. 13
 Tocci, D. 28, 95
 Todaro, G. 20, 21, 64
 Todisco, E. 16, 81
 Todisco, G. 24, 25, 121
 Tofacchi, E. 9, 69
 Toffalori, C. 9
 Tognoni, G. 12
 Tolomeo, D. 64
 Tondo, A. 75
 Tonini, A. 91, 110
 Torcasio, R. 26
 Torelli, T. 20, 44
 Tornese, M. 11
 Torre, E. 42, 121
 Torrente, Y. 22, 110
 Torricelli, F. 19
 Torricelli, F. 28, 97
 Toscani, D. 20, 21, 27, 29
 Toscano, A. 99, 100
 Tosetto, A. 88
 Tosoni, L. 58
 Tragni, K. 15
 Traini, V. 19, 22, 110

- Trapè, G. 64
 Trappolini, S. 19
 Travaglini, S. 7, 32, 75, 77
 Travaglino, E. 24
 Traverso, I. 27, 106
 Trenta, F. 43
 Trenti, T. 52, 88, 93
 Trentin, L. 48, 49, 51, 53, 61, 91, 92, 93, 94, 98, 99, 100, 119
 Trimarco, V. 91, 92, 93, 110
 Triolo, A. 109
 Triolo, A.M. 110
 Tropea, E. 61
 Trubini, S. 57
 Truffelli, D. 26, 106
 Tur, L. 13
 Turrini, M. 81
 Tusa, I. 66

 Ubezio, M. 11, 24, 25, 81, 121
 Ubiali, A. 57
 Uccella, S. 37
 Uddin Dekha, J. 98
 Uhlen, M. 121
 Uras, C.R.M. 27
 Usai, S.V. 35

 Vago, L. 4, 9, 81
 Valentino, I. 26
 Valenzuela, M. 23
 Valiente, A. 49
 Vallisa, D. 57, 89, 90, 93, 95, 115, 121
 Valsecchi, L. 16
 Valvano, L. 102
 Vanderwert, F. 12, 33
 Vannucchi, A. 59
 Vannucchi, A.M. 12, 28, 33, 39, 40, 41, 58, 60, 62, 63
 Varraso, C. 37
 Vassoughi, R. 47
 Vegliante, M.C. 37
 Venditti, A. 31, 32, 33, 34, 82, 85

 Vento, F. 32
 Vergaro, G. 109
 Veronese, S.M. 81
 Vesch, S. 45
 Veschi, S. 45
 Vescovini, R. 20, 21, 29
 Vespa, S. 45
 Vianelli, N. 12
 Vianello, F. 48, 98, 99
 Vicario, N. 108
 Vicenzetto, C. 53, 92
 Viglietto, G. 26
 Vigliotta, I. 20, 21
 Vignetti, M. 13, 34, 62, 63, 79, 84
 Vilella, R. 102
 Villani, O. 102
 Villanova, I. 45, 46
 Villaverde Ramiro, A. 13
 Villena, M.C. 78
 Vincenzi, A. 96
 Vinchesi, M.C. 75
 Vinti, L. 103
 Visani, G. 101
 Visco, C. 13, 53, 66, 97
 Visconte, V. 31
 Visentin, A. 49, 91, 94, 98, 100
 Vit, F. 35
 Vitale, E. 97
 Vitulo, N. 48
 Viviani, F. 121
 Volkava, K. 55
 Volpicelli, P. 89
 Von Kries, J.P. 72, 76
 Voso, M.T. 2, 7, 13, 23, 31, 32, 63, 77, 82, 84, 85
 Votto, A. 66
 Vucinic, V. 42
 Vullo, C. 29, 107

 Westin, J.R. 103
 Woyach, J.A. 49

 Xhahysa, B. 40, 43, 67, 68
 Xin Hjaltelin, J. 108
 Xue, A. 103

 Yami, A. 98
 Zaccaria, G. 37

 Zacheo, I. 84
 Zamagni, E. 20, 21, 110
 Zambello, R. 51, 53, 91, 92, 93, 98, 110
 Zambon, A. 118
 Zampini, M. 11, 24, 25, 59, 121
 Zamponi, R. 15, 32
 Zanelli, M. 97
 Zangari, A. 4
 Zangrandi, A. 57
 Zanirato, G. 35, 44
 Zannetti, B.A. 34
 Zannier, M.E. 58
 Zannoni, L. 70, 74, 87
 Zanotti, R. 58
 Zappasodi, P. 16, 18, 79, 81
 Zappaterra, A. 118
 Zatta, I. 49
 Zaza, A. 32
 Zeidan, A.M. 24, 25
 Zerbi, C. 37
 Zhao, L. 24, 25
 Zibellini, S. 37
 Ziccheddu, B. 106
 Zingarelli, F. 74, 87
 Zingariello, M. 40
 Zinzani, P.L. 52
 Zizioli, D. 43
 Zocca, L. 75
 Zocchi, M.R. 102
 Zoletto, S. 61
 Zuppelli, T. 108